Dental and Medical Problems

BIMONTHLY ISSN 1644-387X (PRINT) ISSN 2300-9020 (ONLINE) www.dmp.umw.edu.pl

2026, Vol. 63, No. 5 (September–October)

Impact Factor (IF) – 4.3
Ministry of Science and Higher Education – 70 pts



Wroclaw Medical University

Dental and Medical Problems

ISSN 1644-387X (PRINT) ISSN 2300-9020 (ONLINE) www.dmp.umw.edu.pl

Dental and Medical Problems is an international, peer-reviewed, open access journal covering all aspects of oral sciences and related fields of general medicine, published bimonthly by Wroclaw Medical University.

BIMONTHLY
2026, Vol. 63, No. 5
(September–October)

Editor-in-Chief
Mieszko Więckiewicz

Deputy Editor
Helena Martynowicz

Thematic Editors
Marek Niedoszytko (Allergology, Immunology and Oral Health)
Jan Biegus (Cardiovascular Diseases and Oral Health)
Katarzyna Skośkiewicz-Malinowska (Conservative Dentistry and Endodontics)
Krzysztof Dowgierd (Cranio-Maxillofacial Surgery)
Grzegorz Trybek (Oral Surgery and Dental Implantology)
Klaus Boening (Dental Materials)
Katarzyna Neubauer (Gastroenterology (including microbiome and dietetics))
Robert Śmigiel (Genetics and Oral Health)
Mariusz Kusztal (Internal Medicine and Oral Health)
Paweł Gać (Medical and Dentomaxillofacial Imaging)
Błażej Misiak (Mental Health)
Agata Czajka-Jakubowska (Orthodontics)
Helena Martynowicz (Sleep Medicine and Dental Sleep Medicine)
Alona Emodi-Perlman (Orofacial Pain and Headache)
Piotr Donizy (Oral and Maxillofacial Pathology)
Anna Paradowska-Stolarz (Pediatric Dentistry)
Kinga Grzech-Leśniak (Periodontology and Laser Therapy)
Monika Łukomska-Szymańska (Prosthodontics)
Ilona Dekkers (Public Health and Clinical Epidemiology)
Aleksandra Butrym (Oncology and Hematology Related to Oral Health)
Cyprian Olchowy (Novel Technologies in Medicine and Telemedicine)

Editorial Office
Marcinkowskiego 2–6
50-368 Wrocław, Poland
Tel.: +48 71 784 12 05
E-mail: dental@umw.edu.pl

Publisher
Wroclaw Medical University
Wybrzeże L. Pasteura 1
50-367 Wrocław, Poland

Online edition is the original version of the journal

International Advisory Board
Gilles Lavigne (Canada)
Richard Ohrbach (USA)
Frank Lobbezoo (the Netherlands)
Susan Armijo-Olivo (Germany)
Takafumi Kato (Japan)
Ephraim Winocur (Israel)
Daniele Manfredini (Italy)
Praveen Ravindra Arany (USA)
Marc Schmitter (Germany)
Cibele Dal Fabbro (Brazil)
Zeev Ormianer (Israel)
Julita Kulbacka (Poland)
Akira Aoki (Japan)
Gustavo Fernandes (USA)
Marta Waliszewska-Prosół (Poland)
Oliver Schierz (Germany)
Małgorzata Krzystek-Korpacka (Poland)
Luca Testarelli (Italy)
Robert Skomro (Canada)
Isabel Moreno-Hay (USA)
Muhammad Sohail Zafar (UAE)
Gaetano Isola (Italy)
Agata Sebastian (Poland)
Xin Xiong (China)
Maciej Patrzyk (Germany)
João Paulo Mendes Tribst (the Netherlands)
Agata Gabryelska (Poland)
Kültigin Türkmen (Turkey)
Inae Caroline Gadotti (USA)
Antonino Lo Giudice (Italy)
Boyapati Ramanarayana (India)
Kamil Jurczyszyn (Poland)
Abdul Samad Khan (Saudi Arabia)
Mansur Rahnama-Hezavah (Poland)
Carlos Nemcovsky (Israel)
Ingrid Różyło-Kalinowska (Poland)
Tommaso Castroflorio (Italy)
Hagay Slutzky (Israel)
Maciej Dobrzyński (Poland)
Giuseppe Minervini (Italy)
Katarzyna Kresse-Walczak (Germany)
Javier Labad (Spain)
Ahmed Moustafa (Australia)
Magdalena Osiewicz (the Netherlands)
Anita Hryncewicz-Gwóźdź (Poland)
Miguel Meira e Cruz (Portugal)
Paweł Dąbrowski (Poland)

Manuscript editing
Joanna Gudarowska
Jolanta Prazeres

Editorial Policy

During the review process, the Editorial Board conforms to the "Uniform Requirements for Manuscripts Submitted to Biomedical Journals: Writing and Editing for Biomedical Publication" approved by the International Committee of Medical Journal Editors (http://www.icmje.org/). Journal accepts only original papers and all kinds of reviews (narrative review, systematic review, systematic review and meta-analysis, etc.). Experimental studies must include a statement that the experimental protocol and informed consent procedure were in compliance with the Helsinki Convention and were approved by an ethics committee.

Indexed in: PubMed/MEDLINE, Web of Science, Clarivate Journal Citation Report, Scopus, ICI Journals Master List, DOAJ, WorldCat, Embase, Polska Bibliografia Naukowa, EBSCO, Crossref, CLOCKSS

Typographic design: Monika Kolęda, Piotr Gil
Cover: Monika Kolęda
DTP: Adam Barg
Printing and binding: Agencja Wydawnicza "ARGI" s.c.

Dental
and Medical Problems

BIMONTHLY 2026, Vol. 63, No. 5 (September–October)

ISSN 1644-387X (PRINT)
ISSN 2300-9020 (ONLINE)
www.dmp.umw.edu.pl

Contents

Editorials

1087 Bartosz Szmyd, Rafał Wójcik, Agata Gabryelska
Non-invasive functional neurosurgery revisited: The emerging role of MRgFUS in neuropsychiatric disorders

1091 Marcin Mikulewicz
Validation and reporting standards for dental artificial intelligence: Lessons from materials biosafety

Original papers

1095 Daya Masri, Ehud Jonas, Gal Avishai, Hiba Masri-Iraqi, Adrian Kahn, Liat Chaushu
Impact of glycemic control on early implant failure: A retrospective cohort study

1107 Jakub Hadzik, Marzena Dominiak
Peri-implant soft tissue thickness following connective tissue grafting or volume-stable collagen matrix augmentation: A randomized controlled trial

1121 Ronald Wigler, Nuphar Blau-Venezia, Tomer Goldberger
Comparative efficacy of supplementary techniques, with and without a solvent, for removing root filling remnants from canal irregularities: An in vitro study

1127 Marcelo Araripe Loureiro, Adan Lucas Pantoja de Santana, Nélio Jorge Veiga, Renata Tolêdo Alves, Gustavo Vicentis de Oliveira Fernandes, Anna Carolina Volpi Mello-Moura
Malocclusions and their impact on quality of life in children from disadvantaged socioeconomic conditions: A cross-sectional observational study

1137 Agata Izabela Cieślik, Wioletta Nowaczewska, Paweł Dąbrowski, Tomasz Dzieńkowski, Joanna Wysocka
Ante-mortem tooth loss (AMTL) and dentoalveolar pathologies in the 11th–15th-century Gródek on the Bug River skeletal collection: Patterns and implications

1147 Jan Liska, Veronika Liskova, Nikoleta Molnarova, Ondrej Topolcan, Jan Netolicky, Pavel Andrle, Lucie Nechutna, Lukas Hauer, Denisa Kacerovska
Risk of malignant transformation in oral lichen planus and oral lichen planus with dysplasia: A retrospective clinical study of 435 histologically verified cases

1155 Elham Saberian, Adriána Petrášová, Andrej Jenča Jr., Janka Jenčová, Kimia Shirali, Andrej Jenča, Mieszko Adam Więckiewicz, Hadi Zare-Zardini, Meysam Ebrahimi Far
Oral microbiota diversity and composition in patients with oral lichen planus: An observational molecular analysis study

1167 Christoph Matthias Schoppmeier, Malin Janson, Michael Jochen Wicht, Max von Kohout, Anna Greta Barbe
Color atlas of resin-infiltrated white spot lesions: Data on aesthetic stability following resin infiltration, bleaching and re-bleaching

1179 María Pelechá-Salvador, Sandra López-Domènech, Cecilia Fabiana Márquez-Arrico, Meylin Fernández-Reyes, Laura Perea-Galera, Jonathan Hermenejildo, Carlos Morillas, Pablo Fernández-Collazo, Javier Silvestre-Rangil, Víctor Manuel Víctor, Francisco Javier Silvestre, Milagros Rocha
Endoplasmic reticulum stress in women with polycystic ovary syndrome and gingivitis: A case–control study of metabolic–periodontal interplay

1189 Emőke Márta Takács, Ibolya Süveges, Szilvia Ambrus, Péter Schmidt, Bálint Jász, Péter Hermann, Szandra Körmendi, Máté Jász
Does the prevalence of temporomandibular disorders increase as a result of tooth loss or prosthodontic rehabilitation? A national representative cross-sectional study

1199 Efsun Somay, Erkan Topkan, Sibel Bascil, Sukran Senyurek, Duriye Ozturk, Nilufer Kılıc Durankuş, Ugur Selek
Predicting osteoradionecrosis in nasopharyngeal carcinoma: The role of the GLUCAR index

1209 Luis Eduardo Almeida, Matthew Beck, Olivia Kraft, Samuel Zammuto, Flavio de Alcantara Camejo, Maria Maddalena Marrapodi, Gabriele Cervino, Andrea Doetzer, Giuseppe Minervini
Immunohistochemical expression of GRP78 in temporomandibular joint dysfunction

1215 Walla Samara, Omid Moztarzadeh, Mohammad Najeh Samara, Lukas Hauer, Jan Pernicky
Incidental detection of carotid artery calcification on CBCT: A retrospective analysis of 890 scans (108 cases)

1225 Dorota Pylińska-Dąbrowska, Hanna Kujawska-Danecka, Kacper Jagiełło, Małgorzata Mossakowska, Tomasz Roman Zdrojewski
Correlation of dental status and denture use with functional disability (VES-13) and frailty syndrome (Fried phenotype) in Polish older adults: A cross-sectional study

1233 Rafał Pokrowiecki, Caner Bakici, Anna Lipowicz, Barbora Sufliarsky, Krzysztof Dowgierd
Frontal sinus morphology and surgical implications in forehead feminization: A radiographic and 3D anthropometric study

1243 Hadi Zare-Zardini, Elham Saberian, Andrej Jenča Jr., Adriána Petrášová, Janka Jenčová, Andrej Jenča, Eliška Kubíková, Tetyana Pyndus, Mieszko Adam Więckiewicz
HAp–ZrO_2–AgNP-reinforced polystyrene dental nanocomposites: Antibacterial, antiplaque and self-cleaning properties

1259 Liat Chaushu, Shiri Lapides, Gal Avishai, Aya Vituri, Sigalit Blumer
Factors affecting the duration of hospitalization due to odontogenic abscesses in children

1267 Helena Martynowicz, Małgorzata Trocha, Karol Marschollek, Piotr Macek, Wiktor Trzepietowski, Jakub Przegrałek, Katarzyna Madziarska, Mieszko Więckiewicz
Interactions between sleep parameters and heart rate variability in temporomandibular disorders

1277 Adam Lubojański, Katarzyna Szyszka, Bartosz Mielan, Magdalena Pajączkowska, Joanna Nowicka, Magdalena Ziąbka, Adam Watras, Rafal Jakub Wiglusz, Maciej Dobrzyński
Antibacterial and antifungal properties of compomer materials modified with silver nanoparticles and copper oxide, with determination of their cytotoxicity

Reviews

1289 Kinga Grzech-Leśniak, Paolo Vescovi, Georgios Romanos, Rafał Wiench, Jakub Fiegler-Rudol, Ilaria Giovannacci, Janina Golob Deeb, Zuzanna Grzech-Leśniak, Jacek Matys, Aldo Brugnera Junior, Mariusz Szuta, Sajee Sattayut, Praveen Arany, Marco Meleti, Maha Taalab, Josep Arnabat-Dominguez, Alessandro Del Vecchio, Jamil Awad Shibli, Maciej Misiołek, Octavi Camps-Font, Akira Aoki, Umberto Romeo, Samir Nammour
Laser-based management of oral leukoplakia: A narrative review by a study group of the World Federation for Laser Dentistry (WFLD)

1303 Ganiga Channaiah Shivakumar, Nishath Sayed Abdul, Mahesh Shenoy, Abdullah Abdulaziz Saeidi, Vincenzo Ronsivalle, Hande Uzunçıbuk, Gabriele Cervino, Maria Maddalena Marrapodi, Giuseppe Minervini
Efficacy of systemic enzyme therapy as an anti-inflammatory agent when used as monotherapy or in combination with NSAIDs: A systematic review

1313 Oliwier Wojciech Pioterek, Katarzyna Majka, Jakub Goździewicz, Wiktoria Taurogińska, Barbara Parol, Daria Pozdniakowa, Albert Synal, Aleksander Sowiński, Martyna Piskorz, Mateusz Drążyk, Mateusz Mazurek, Michał Tulski, Zygmunt Domagała, Maciej Dobrzyński, Paweł Dąbrowski
Accuracy and reproducibility of photogrammetric measurements in dentistry: A systematic review

1331 Mehmood Asghar, Ros Anita Omar, Rosiyah Yahya, Adrian Ujin Yap, Muhammad Amber Fareed
Silver diamine fluoride for the treatment of dental caries: A comprehensive review of the literature

1347 Bacem Othman, Omid Moztarzadeh, Lukas Hauer
Subsite-resolved molecular and epigenetic characterization of oral tongue squamous cell carcinoma: A systematic review and in silico genome-wide DNA methylation analysis

Editorial

Non-invasive functional neurosurgery revisited: The emerging role of MRgFUS in neuropsychiatric disorders

Bartosz Szmyd[1,2,A–F], Rafał Wójcik[1,E,F], Agata Gabryelska[3,A,E,F]

[1] Department of Neurosurgery and Neuro-Oncology, Medical University of Lodz, Poland
[2] Department of Pediatrics, Oncology and Hematology, Medical University of Lodz, Poland
[3] Department of Sleep Medicine and Metabolic Disorders, Medical University of Lodz, Poland

A – research concept and design; B – collection and/or assembly of data; C – data analysis and interpretation; D – writing the article; E – critical revision of the article; F – final approval of the article

Dental and Medical Problems, ISSN 1644-387X (print), ISSN 2300-9020 (online) *Dent Med Probl*. 2026;63(5):1087–1090

Address for correspondence
Agata Gabryelska
E-mail: agata.gabryelska@gmail.com

Funding sources
None declared

Conflict of interest
None declared

Acknowledgements
None declared

Received on May 24, 2026
Reviewed on June 17, 2026
Accepted on July 13, 2026

Published online on October 6, 2026

Cite as
Szmyd B, Wójcik R, Gabryelska A. Non-invasive functional neurosurgery revisited: The emerging role of MRgFUS in neuropsychiatric disorders. *Dent Med Probl*. 2026;63(5):1087–1090. doi:10.17219/dmp/225910

DOI
10.17219/dmp/225910

Copyright
Copyright by Author(s)
This is an article distributed under the terms of the Creative Commons Attribution 3.0 Unported (CC BY 3.0) (https://creativecommons.org/licenses/by/3.0/)

Keywords: MRgFUS, functional neurosurgery, deep brain stimulation, neuropsychiatric disorders

Magnetic resonance-guided focused ultrasound (MRgFUS) represents a conceptual shift in functional neurosurgery by integrating non-invasive precision lesioning and potential neuromodulation within a single, circuit-based platform for refractory neuropsychiatric disorders, although its clinical implementation requires controlled evidence, refined patient selection, and careful consideration of ethical and social perceptions.

Classical neurosurgery is fundamentally oriented toward removing or neutralizing pathological substrates that exert mechanical or hemodynamic effects on the nervous system. The therapeutic objective is primarily the restoration of structural integrity and physiological flow dynamics, for example through tumor resection, hematoma evacuation or aneurysm clipping. In contrast, functional neurosurgery represents a distinct conceptual framework. Rather than eliminating the pathological substrate itself, it aims to modify the way neural circuits operate. The therapeutic target is often a dysfunctional circuit rather than a mass lesion requiring removal. Clinical benefits are achieved by modulating aberrant activity within specific circuits, often without directly removing or otherwise eliminating the underlying anatomical substrate.

This distinction reflects a broader conceptual shift in neuroscience from localizationist to network-based models. Within this framework, functional neurosurgery has become an established standard of care for selected neurological disorders, most notably Parkinson's disease, essential tremor and dystonia. In these conditions, the modulation of well-characterized motor circuits can produce robust and reproducible clinical benefits.

At the same time, the field is rapidly expanding beyond its classical neurological indications. Advanced clinical investigations, including phase II–III studies, are exploring its potential in treatment-resistant depression, chronic pain syndromes, Tourette syndrome, and spasmodic dysphonia, with the emerging data also regarding Alzheimer's disease. In parallel, a growing body of preclinical and early-phase clinical research is extending the scope of functional neurosurgery into psychiatric and neurobehavioral domains, including schizophrenia, addiction, tinnitus, disorders of consciousness, obesity and anorexia nervosa, and Huntington's disease.[1] The frequent overlap among pain, sleep disturbances and

mental health symptoms further underscores the need for the interdisciplinary assessment and management of patients with complex neuropsychiatric conditions.[2–4]

These indications highlight the expanding interface between functional neurosurgery and psychiatry, providing the foundation for what is now termed interventional neuropsychiatry. The evolution of functional neurosurgery has been driven by successive technological advances, each seeking to optimize the balance between precision, invasiveness and reversibility.

Early stereotactic lesioning techniques, such as radiofrequency ablation (RFA), offered simplicity and cost-effectiveness, but at the expense of irreversibility and the need for invasive surgical access. The introduction of deep brain stimulation (DBS) marked a paradigm shift toward adjustable and partially reversible neuromodulation, with the additional advantages of bilateral applicability and a strong evidence base. However, these benefits come with the burden of hardware implantation, infection risk and long-term device management. More recent approaches, such as laser interstitial thermal therapy (LITT), have improved intraoperative precision through magnetic resonance imaging (MRI)-based thermometry, yet remain invasive and resource-intensive.

A key advantage of DBS, particularly in Parkinson's disease, is the possibility of intraoperative neurophysiological recording, including microelectrode recording (MER), which enables real-time functional target verification and the refinement of lead placement. This electrophysiological feedback has historically been considered an important contributor to the precision of DBS targeting and, potentially, to its clinical efficacy in well-characterized motor circuits. In contrast, magnetic resonance-guided focused ultrasound (MRgFUS) combines focused ultrasound energy with MRI-based anatomical targeting and treatment monitoring, but does not provide intraoperative neuronal recording. In its clinically established ablative form, MRgFUS uses high-intensity focused ultrasound (HIFU) to induce focal tissue heating and coagulative necrosis. Magnetic resonance imaging provides high-resolution anatomical guidance and quantitative thermometry, enabling controlled energy delivery while limiting the exposure of the surrounding tissues.

The clinical relevance of intraoperative electrophysiological mapping in neuropsychiatric interventions remains uncertain. Unlike movement disorders, in which well-characterized electrophysiological signatures can inform target localization, psychiatric disorders involve distributed and heterogeneous network dysfunction, and validated intraoperative biomarkers of treatment-relevant circuit engagement are currently lacking. Moreover, MER is not consistently incorporated into DBS procedures for psychiatric indications, and there is currently no clear evidence that its use improves clinical outcomes in this setting. However, this does not imply that intraoperative neurophysiology has no potential value. Advances in physiology-guided neuromodulation, closed-loop stimulation and adaptive DBS may make electrophysiological recordings increasingly relevant for identifying pathological network states, refining targets and personalizing treatment. The absence of intraoperative neuronal recording in MRgFUS should therefore be regarded as a potential limitation, although its clinical significance has yet to be established.

In light of these considerations, technologies that do not rely on intraoperative electrophysiology, such as MRgFUS, may be particularly well suited to certain network-based neuropsychiatric interventions. By enabling incisionless, image-guided energy delivery, MRgFUS combines the spatial precision of stereotactic techniques with a fundamentally non-invasive approach. Real-time MRI thermometry enables continuous monitoring of tissue temperature and the control of energy delivery, while immediate clinical feedback, such as tremor suppression, can provide the functional confirmation of target engagement during the procedure.

Focused ultrasound has 2 conceptually distinct applications in functional neurosurgery, although they are currently at different stages of development. As noted above, HIFU is already used clinically to create precise, irreversible thermal lesions through focal heating and coagulative necrosis. By contrast, low-intensity focused ultrasound (LIFU) uses lower-intensity, typically pulsed sonication to produce predominantly mechanical neuromodulatory effects while minimizing tissue heating, and remains largely investigational. The reversible and non-ablative effects of LIFU make it an attractive potential research tool for transiently perturbing candidate neural networks and assessing their therapeutic relevance before irreversible lesioning is considered. This application should, however, be clearly distinguished from the current clinical use of ablative HIFU. The use of LIFU for neuromodulation and target validation will require standardized stimulation protocols, reproducible biomarkers of circuit engagement, and demonstration of efficacy and safety in controlled clinical studies.[5]

The emerging clinical evidence increasingly supports the feasibility and therapeutic potential of MRgFUS in neuropsychiatric disorders. Early proof-of-concept studies in treatment-refractory obsessive-compulsive disorder (OCD) demonstrated that bilateral MRgFUS capsulotomy can achieve meaningful symptom reduction, with improvement in OCD, depression and anxiety symptoms, and an overall favorable safety profile, notably without the evidence of persistent neurocognitive impairment.[6,7] These findings are further supported by subsequent studies reporting sustained clinical benefits without significant cognitive deterioration, with some patients even demonstrating improvement in specific domains of executive function.[8]

More recent prospective data extend these observations, indicating that MRgFUS capsulotomy maintains

a favorable safety profile over long-term follow-up, with clinically meaningful response rates, particularly in OCD, although outcomes in major depressive disorder (MDD) appear more variable, and may depend on lesion location and the extent of network engagement.[9] This greater variability may partly reflect the marked clinical and neurobiological heterogeneity of MDD, which may encompass distinct depressive biotypes characterized by different patterns of network dysfunction and, consequently, different optimal therapeutic targets. Importantly, the emerging connectomic analyses suggest that treatment efficacy is closely related to the precise engagement of specific fronto-striatal networks, reinforcing the concept of a network-targeted intervention rather than purely anatomical lesioning.[10]

From a broader perspective, MRgFUS may offer potential advantages by avoiding surgical incisions, implanted hardware, and some of the complications associated with open procedures. However, its overall risk–benefit ratio and cost-effectiveness remain uncertain, and cannot be generalized across healthcare settings. These assessments depend on procedural and infrastructure costs, the choice of comparator treatment, reimbursement structures, the complication and retreatment rates, and the durability of clinical benefits. Long-term comparative and health-economic studies are therefore needed before firm conclusions can be drawn.[11]

Importantly, the strength of evidence differs substantially across these indications. Among the psychiatric applications of MRgFUS, OCD currently has the most developed clinical evidence, including prospective studies of ablative capsulotomy. Evidence for MDD is more limited and outcomes appear more variable, whereas reports regarding addiction remain preliminary. For schizophrenia, obesity, anorexia nervosa, tinnitus, and several other neurobehavioral conditions, the available evidence is still sparse and largely limited to preclinical studies, feasibility investigations, or early proof-of-concept reports. These indications should therefore be regarded as being at different stages of clinical development rather than as comparable emerging applications.

Despite these encouraging results, the current evidence remains limited. Most studies of MRgFUS in psychiatric disorders have included small and highly selected patient populations, and have been conducted at only a few specialized centers. Many were uncontrolled, open-label or proof-of-concept studies. The studies also differ in patient selection, treatment targets, lesion location and size, outcome measures, and follow-up duration, which makes direct comparisons difficult. Large, multicenter randomized controlled trials (RCTs) are still lacking for most psychiatric indications. Magnetic resonance-guided focused ultrasound should therefore be viewed as promising but still investigational treatment rather than an established option in neuropsychiatric care.

Taken together, the available studies suggest that MRgFUS may become a useful platform for circuit-based interventions in selected neuropsychiatric disorders. However, the evidence remains preliminary, and larger controlled studies are needed to establish its safety, clinical effectiveness, the durability of treatment effects, and generalizability.

Against this historical and technological backdrop, the broader focused ultrasound platform represents more than a technical refinement, encompassing both the established ablative applications and the emerging approaches to non-ablative neuromodulation. Although the feasibility of MRgFUS has been demonstrated for selected indications, important questions remain regarding efficacy, the durability of benefits, optimal targeting, patient selection, and comparative effectiveness. Particular attention should also be paid to its social perception in light of the historical legacy of psychosurgery, including lobotomy, which may continue to shape attitudes toward the emerging neuropsychiatric interventions.

Ethics approval and consent to participate

Not applicable.

Data availability

Not applicable.

Consent for publication

Not applicable.

Use of AI and AI-assisted technologies

During the preparation of this manuscript, the authors used ChatGPT (OpenAI) for English-language editing and to assist in drafting and refining the summary. The authors reviewed and edited all AI-assisted content and take full responsibility for the final content of the manuscript.

ORCID iDs

Bartosz Szmyd https://orcid.org/0000-0002-4051-0887
Rafał Wójcik https://orcid.org/0000-0002-5688-738X
Agata Gabryelska https://orcid.org/0000-0002-4430-6488

References

1. Wang F, Paerhati H, Lin Z, Liu S, Sun B, Li D. Treatment of alcohol use disorder via magnetic resonance-guided focused ultrasound ablation surgery. *Addict Sci Clin Pract*. 2026;21(1):18. doi:10.1186/s13722-025-00644-0
2. Zieliński G, Ginszt M, Ginszt A, Wójcicki M, Litko-Rola M, Wieckiewicz M. Meta-analysis of the global prevalence of oral and facial pain. *Dent Med Probl*. 2026;63(1):219–231. doi:10.17219/dmp/214956
3. Meira e Cruz M, Santos I, Salles C, Rocha I, Gozal D, Ettlin DE. Sleep-related respiratory impairment and psychosocial stress in patients with persistent orofacial pain: A cross-sectional exploratory study. *Dent Med Probl*. 2026;63(1):73–86. doi:10.17219/dmp/195283
4. Pitułaj A, Kiejna A, Dominiak M. Negative synergy of mental disorders and oral diseases versus general health. *Dent Med Probl*. 2019;56(2):197–201. doi:10.17219/dmp/105253
5. Lee S, Chang JW. From ablation to neuromodulation platform: The evolving role of magnetic resonance-guided focused ultrasound in functional neurosurgery. *J Clin Neurol*. 2026;22(1):17–41. doi:10.3988/jcn.2025.0563

6. Jung HH, Kim SJ, Roh D, et al. Bilateral thermal capsulotomy with MR-guided focused ultrasound for patients with treatment-refractory obsessive-compulsive disorder: A proof-of-concept study. *Mol Psychiatry*. 2015;20(10):1205–1211. doi:10.1038/mp.2014.154
7. Kim SJ, Roh D, Jung HH, Chang WS, Kim CH, Chang JW. A study of novel bilateral thermal capsulotomy with focused ultrasound for treatment-refractory obsessive-compulsive disorder: 2-year follow-up. *J Psychiatry Neurosci*. 2018;43(5):327–337. doi:10.1503/jpn.170188
8. Davidson B, Hamani C, Meng Y, et al. Examining cognitive change in magnetic resonance-guided focused ultrasound capsulotomy for psychiatric illness. *Transl Psychiatry*. 2020;10(1):397. doi:10.1038/s41398-020-01072-1
9. Hamani C, Davidson B, Rabin JS, et al. Long-term safety and efficacy of focused ultrasound capsulotomy for obsessive-compulsive disorder and major depressive disorder. *Biol Psychiatry*. 2025;97(7):698–706. doi:10.1016/j.biopsych.2024.08.015
10. Germann J, Elias GJ, Neudorfer C, et al. Potential optimization of focused ultrasound capsulotomy for obsessive compulsive disorder. *Brain*. 2021;144(11):3529–3540. doi:10.1093/brain/awab232
11. Kumar KK, Bhati MT, Ravikumar VK, Ghanouni P, Stein SC, Halpern CH. MR-guided focused ultrasound versus radiofrequency capsulotomy for treatment-refractory obsessive-compulsive disorder: A cost-effectiveness threshold analysis. *Front Neurosci*. 2019;13:66. doi:10.3389/fnins.2019.00066

Editorial

Validation and reporting standards for dental artificial intelligence: Lessons from materials biosafety

Marcin Mikulewicz[A–F]

Division of Facial Developmental Defects, Department of Maxillofacial Orthopaedics and Orthodontics, Faculty of Dentistry, Wroclaw Medical University, Poland

A – research concept and design; B – collection and/or assembly of data; C – data analysis and interpretation;
D – writing the article; E – critical revision of the article; F – final approval of the article

Dental and Medical Problems, ISSN 1644-387X (print), ISSN 2300-9020 (online) *Dent Med Probl*. 2026;63(5):1091–1094

Address for correspondence
Marcin Mikulewicz
E-mail: marcin.mikulewicz@umw.edu.pl

Funding sources
None declared

Conflict of interest
None declared

Acknowledgements
None declared

Received on July 10, 2026
Reviewed on July 13, 2026
Accepted on July 16, 2026

Published online on September 24, 2026

Keywords: dentistry, artificial intelligence, biocompatible materials

Extending dentistry's rigorous biomaterial-biosafety validation principles to artificial-intelligence (AI) treatment-planning tools requires prospective and external validation, clearly defined clinical indications, and post-deployment performance monitoring.

An orthodontic archwire cannot enter a patient's mouth until it has cleared a defined evidentiary gate. Its corrosion behavior and ion-release profile are quantified under standardized immersion conditions, benchmarked against the International Organization for Standardization (ISO) biocompatibility expectations, and reported in the literature, with the element-specific concentrations measured using techniques such as inductively coupled plasma optical emission spectrometry (ICP-OES).[1,2] A clinician selecting that wire can, in principle, trace its safety profile to reproducible measurements. The same cannot be said of the algorithm that increasingly helps determine how that wire will be used.

Dentistry has spent decades building a mature, quantitative paradigm for the biosafety of what it places in the patient – alloys, resins and ceramics – yet it is adopting artificial intelligence (AI) into what it decides for the patient with comparatively little validation, transparency or regulatory scaffolding. A discipline that would never accept an uncharacterized biomaterial is, in parallel, accepting largely uncharacterized decision tools. *Dental and Medical Problems* is a natural venue to identify this inconsistency and propose a corrective framework.

Two standards of evidence, one discipline

The biomaterials side of the ledger is well developed. A systematic synthesis of in vitro ion-release studies established, more than a decade ago, that the doses released from fixed appliances generally fell well below toxic thresholds, while also exposing the methodological limits of static immersion models that ignore biofilm, salivary dynamics and pH variation.[2] Comparative ICP-OES work continues to refine this picture – for example, showing that nickel-titanium and chromium-cobalt wires release significantly more nickel and chromium than stainless steel, with direct relevance to allergy risk.[1] The same measurement culture extends beyond wrought alloys – surface-engineered implant coatings are screened by combined physicochemical characterization, corrosion and cytocompatibility testing before any clinical claim is made,[3] and where static

Cite as
Mikulewicz M. Validation and reporting standards for dental artificial intelligence: Lessons from materials biosafety. *Dent Med Probl.* 2026;63(5):1091–1094. doi:10.17219/dmp/226044

DOI
10.17219/dmp/226044

Copyright
Copyright by Author(s)
This is an article distributed under the terms of the Creative Commons Attribution 3.0 Unported (CC BY 3.0) (https://creativecommons.org/licenses/by/3.0/)

immersion falls short, pulp-capping materials are taken into in vivo tissue-reaction testing by subcutaneous implantation, with the biological response assessed directly rather than inferred.[4] Whatever its imperfections, this is a culture of measurement: defined media, defined exposure, element-level quantification, and explicit acknowledgment of what the model does not capture.

The AI side looks different. The critical appraisals of AI across dental medicine repeatedly identify the same weaknesses – inconsistent data quality, the risk of bias, opacity, and limited clinical validation – which together undermine study quality and impede safe integration into routine care.[5] In teleorthodontics specifically, a scoping review found real-world deployment narrowly concentrated in commercial monitoring platforms, with variable repeatability of clinical decisions and limited independent validation; its conclusion was that AI should function as a complementary tool and never as a substitute for clinical judgement.[6] A recent *Dental and Medical Problems* editorial reaches a similar conclusion from a broader vantage point – AI as an adjunct rather than a replacement, with its promise contingent on validation, standardization and clinician training.[7] That is the same "assistant, not replacement" position the orthodontic community has reached elsewhere – sound as a principle, but not yet operationalized as an evidentiary requirement.

Adoption is outrunning preparation

The disconnect is not theoretical. A survey of postgraduate orthodontic programs in North America with an accreditation process found that more than half had introduced or planned to introduce AI training, yet most had no organized AI training, and about three quarters did not encourage residents to use AI for clinical patient care, research or teaching.[8] In other words, the technology is entering educational programs faster than curricula, oversight, and competency statements are being developed to govern its use. Adoption is preceding instruction – the inverse of how the profession introduced, for example, cone-beam imaging or new bonding systems.

Other branches of medicine have already articulated what a serious answer looks like. In cardiovascular device innovation, expert consensus frames the legitimate lifecycle as an early feasibility study, followed by randomized comparison with the accepted standard of care where one exists, and then post-market real-world evidence – while explicitly noting that regulatory standards and pathways for machine-learning applications remain under development.[9] Dentistry rarely subjects an AI planning aid to anything resembling that sequence. We would not adopt a new luting cement on the basis of a retrospective case series and a favorable impression; we should be equally reluctant to adopt a treatment-planning model on less.

Toward a biosafety frame for algorithms

The constructive move is to borrow the logic the profession already trusts. "Biosafety" in dental materials is not a single test, but a layered expectation: characterize the agent, define exposure conditions, quantify outputs, declare limitations, and report reproducibly. An analogous minimum set for an AI-driven dental tool is not exotic. It would characterize the tool along the same axes we already apply to a biomaterial – what it is, how it performs under realistic conditions, how it fails, and where it may be used – which the checklist below sets out concretely (Fig. 1).

A static alloy is characterized once, and thereafter behaves as characterized; a learning algorithm is a moving target – retrained, updated, and liable to drift as it encounters populations unlike those on which it was developed. Yet this disanalogy sharpens rather than defeats the frame, for materials science has never assumed that characterization at time zero is sufficient: it fatigue-tests materials over their projected service life and mandates post-market surveillance precisely, as performance can change under use. The algorithmic counterpart is neither exotic nor unattainable – versioned revalidation tied to each model update, coupled with continuous monitoring of real-world performance, simply extends to software the post-market-surveillance logic that cardiovascular consensus already applies to algorithmic change.[9]

Framed this way, the recurring "assistant, not replacement" formula stops being a reassurance and becomes a specification: an assistant whose reliability is characterized to the same standard we demand of the materials it helps deploy. This is also where a journal spanning dentistry and general medicine has a distinctive contribution to make. The validation problem is shared across radiology, cardiology and dentistry; in cardiology, for instance, AI for heart-failure diagnosis and risk stratification remains constrained by overfitting, limited external validation and limited explainability – the very barriers that impede routine deployment.[10] The materials-science culture of quantified biosafety, by contrast, is comparatively specific to dentistry. Translating the second into a template for the first is a genuinely cross-disciplinary task, and it is the kind of contribution the journal's broadened article types can accommodate, with perspectives, comments and guidelines now included alongside editorials.[11]

Concretely, this journal could ask any submission describing an AI-driven dental tool to report 5 things (Fig. 1):

1. Specify the composition and representativeness of the training population, including the settings and demographics from which it was drawn (the analog of declaring alloy composition).
2. Report prospective and, where feasible, external validation against outcomes in deployment-relevant populations, rather than retrospective performance on held-out data alone (the analog of in vivo rather than bench testing).

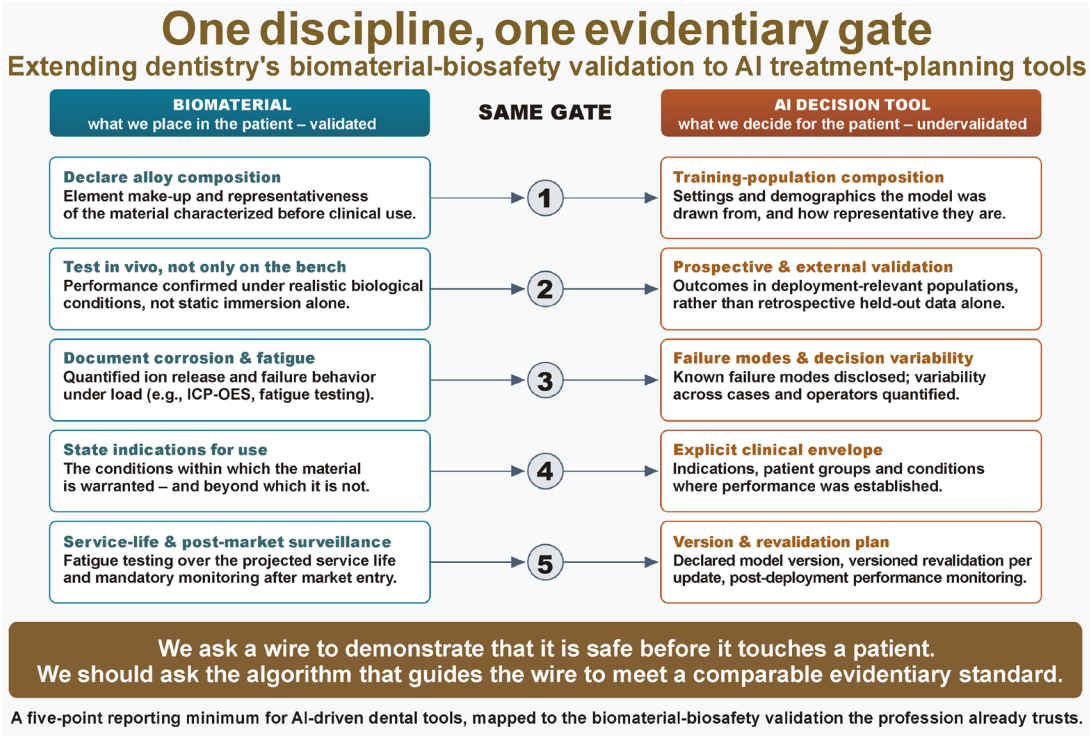

Fig. 1. Artificial intelligence (AI) biosafety

One discipline, one evidentiary gate. The five-point reporting minimum proposed for AI-driven dental tools (right), with each item mapped to the corresponding element of the biomaterial-biosafety validation the profession already applies (left).
ICP-OES – inductively coupled plasma optical emission spectrometry.

3. Disclose known failure modes and quantify decision variability across cases and operators (the analog of documented corrosion and fatigue behavior).
4. State the clinical envelope explicitly – the indications, patient groups and conditions within which performance was established, and beyond which the tool is not warranted (the analog of indications for use).
5. Declare a model version and a plan for versioned revalidation and post-deployment performance monitoring (the analog of service-life fatigue testing and post-market surveillance).

None of this is an argument against AI in dentistry; the case for its diagnostic and workflow value is strong and growing. It is an argument against a double standard. We ask a wire to demonstrate that it is safe before it touches a patient. We should ask the algorithm that guides the wire to meet a comparable evidentiary standard. Closing that gap – conceptually, and eventually through reporting and validation expectations that editors and reviewers can enforce – is a concrete, near-term agenda that this journal is well placed to lead.

Ethics approval and consent to participate

Not applicable.

Data availability

Not applicable.

Consent for publication

Not applicable.

Use of AI and AI-assisted technologies

The author declares that no generative artificial intelligence (AI) or AI-assisted technologies were used in the preparation of this manuscript.

ORCID iD

Marcin Mikulewicz https://orcid.org/0000-0001-5754-0284

References

1. Mikulewicz M, Suski P, Tokarczuk O, Warzyńska-Maciejewska M, Pohl P, Tokarczuk B. Metal ion release from orthodontic archwires: A comparative study of biocompatibility and corrosion resistance. *Molecules*. 2024;29(23):5685. doi:10.3390/molecules29235685
2. Mikulewicz M, Chojnacka K. Release of metal ions from orthodontic appliances by in vitro studies: A systematic literature review. *Biol Trace Elem Res*. 2011;139(3):241–256. doi:10.1007/s12011-010-8670-9
3. Biju D, Arumugam P, Kannan S, et al. Development, characterization, and biocompatibility and corrosion analyses of a silver-decorated graphene oxide and chitosan surface coating for titanium dental implants: A preliminary report. *Dent Med Probl*. 2024;61(4):627–632. doi:10.17219/dmp/187107
4. Rady D, El Moshy S, Yousry YM, Ramadan M, Radwan IA. Biocompatibility of NeoPUTTY™ versus TheraCal PT® and TheraCal LC® pulp-capping materials, and tissue reaction following subcutaneous implantation in rats: Histological and molecular investigation. *Dent Med Probl*. 2026;63(1):131–143. doi:10.17219/dmp/168627

5. Sitaras S, Tsolakis IA, Gelsini M, et al. Applications of artificial intelligence in dental medicine: A critical review. *Int Dent J*. 2025;75(2):474–486. doi:10.1016/j.identj.2024.11.009
6. Polizzi A, Serra S, Leonardi R, Isola G. Clinical applications of artificial intelligence in teleorthodontics: A scoping review. *Medicina (Kaunas)*. 2025;61(7):1141. doi:10.3390/medicina61071141
7. Paradowska-Stolarz AM. AI in modern dentistry: Hype, hope, or real transformation? *Dent Med Probl*. 2025;62(6):1013–1016. doi:10.17219/dmp/211356
8. Hanenkrath J, Park JH, Bay C. Training, use, and modifications related to artificial intelligence in postgraduate orthodontic programs in North America. *Am J Orthod Dentofacial Orthop*. 2025;167(1):89–94.e2. doi:10.1016/j.ajodo.2024.09.008
9. Windecker S, Gilard M, Achenbach S, et al. Device innovation in cardiovascular medicine: A report from the European Society of Cardiology Cardiovascular Round Table. *Eur Heart J*. 2024;45(13):1104–1115. doi:10.1093/eurheartj/ehae069
10. Resch J, Lelonek M. The role of artificial intelligence in the diagnosis, risk stratification, and treatment of heart failure: A narrative review [published online as ahead of print July 3, 2026]. *Adv Clin Exp Med*. doi:10.17219/acem/218578
11. Więckiewicz M, Martynowicz H. Journal Impact Factor and highly cited papers: The beginning of a new era in *Dental and Medical Problems*. *Dent Med Probl*. 2023;60(4):541–542. doi:10.17219/dmp/176039

Original paper

Impact of glycemic control on early implant failure: A retrospective cohort study

Daya Masri[1,2,A–F*], Ehud Jonas[1,2,A,C–F*], Gal Avishai[1,2,A,E,F], Hiba Masri-Iraqi[3,A,E,F], Adrian Kahn[2,A,E,F], Liat Chaushu[4,A,E,F]

[1] Department of Oral and Maxillofacial Surgery, Rabin Medical Center, Petah Tiqwa, Israel
[2] Department of Oral and Maxillofacial Surgery, The Maurice and Gabriela Goldschleger School of Dental Medicine, Tel Aviv University, Israel
[3] Department of Endocrinology, Rabin Medical Center, Petah Tiqwa, Israel
[4] Department of Periodontology and Implant Dentistry, The Maurice and Gabriela Goldschleger School of Dental Medicine, Tel Aviv University, Israel
*These authors contributed equally to this work.

A – research concept and design; B – collection and/or assembly of data; C – data analysis and interpretation;
D – writing the article; E – critical revision of the article; F – final approval of the article

Dental and Medical Problems, ISSN 1644-387X (print), ISSN 2300-9020 (online) *Dent Med Probl*. 2026;63(5):1095–1105

Address for correspondence
Ehud Jonas
E-mail: ehudjonas@gmail.com

Funding sources
None declared

Conflict of interest
None declared

Acknowledgements
The graphical abstract was designed using resources from Flaticon (https://www.flaticon.com).

Received on February 7, 2025
Reviewed on April 19, 2025
Accepted on May 4, 2025

Published online on October 30, 2026

Abstract

Background. The impact of diabetes mellitus (DM), as reflected by glycemic control, on dental implant outcomes remains debated. Specifically, there is a critical gap in our understanding of the impact of uncontrolled DM on early implant failure (EIF), despite the potential benefits of implant dentistry for these patients.

Objectives. The aim of the present study was to investigate the impact of glycemic control on EIF in patients with DM.

Material and methods. A retrospective analysis of electronic medical records (EMRs) was conducted over a 5-year period at a tertiary referral center. Data from 100 patients with 427 implants were collected, including demographic characteristics, systemic conditions, the glycated hemoglobin (HbA1c) values, procedural details, and implant-related variables. Statistical analyses were performed to assess the associations between glycemic control, the study variables and EIF, with statistical significance set at $p < 0.05$.

Results. Uncontrolled DM (HbA1c > 8%) was observed in 17 patients and was not a significant predictor of EIF. However, it was associated with a greater need for bone augmentation (90.8% vs. 45.0%), the placement of longer implants (11.8 mm vs. 11.4 mm), a higher proportion of implants placed in the anterior maxilla (22.4% vs. 11.1%), and younger patient age (62.8 years vs. 67.8 years). The EIF rates were higher for implants placed in augmented bone and lower for implants placed in the anterior and premolar regions of the maxilla.

Conclusions. This study indicates that, although uncontrolled DM may present certain challenges in implant dentistry, including a younger age at implant placement, an increased need for bone augmentation, and a preference for specific implant sites, it does not significantly affect the EIF rates.

Keywords: risk factor, implant, glycemic control, diabetes, early implant failure

Cite as
Masri D, Jonas E, Avishai G, Masri-Iraqi H, Kahn A, Chaushu L. Impact of glycemic control on early implant failure: A retrospective cohort study. *Dent Med Probl.* 2026;63(5):1095–1105. doi:10.17219/dmp/204640

DOI
10.17219/dmp/204640

Copyright
Copyright by Author(s)
This is an article distributed under the terms of the Creative Commons Attribution 3.0 Unported (CC BY 3.0) (https://creativecommons.org/licenses/by/3.0/)

Highlights

- Uncontrolled diabetes mellitus (DM) did not significantly impact the early implant failure (EIF) rates.
- Uncontrolled DM was associated with a younger age at implant placement.
- Uncontrolled DM was associated with an increased need for bone augmentation.
- This study suggests uncontrolled DM is not an absolute contraindication to implant therapy.

Introduction

Diabetes mellitus (DM) is a common metabolic disorder that may lead to adverse oral health outcomes, including microvascular disease, delayed wound healing, functional alterations in the salivary glands, periodontitis, changes in the oral microbiota, and an impaired response to infection.[1–3]

Dental implants have become a popular treatment option for missing teeth, offering a stable and esthetic solution.[4–10] The influence of DM on implant dentistry has been debated for many years. While some studies have considered dental implant placement in patients with DM a relative contraindication,[11] others have reported that implant survival and osseointegration remain predictable and comparable to those in healthy individuals.[1,4,12,13] These studies have also highlighted the potential negative effects of hyperglycemia and uncontrolled hemoglobin A1c (HbA1c) levels on implant therapy outcomes.[4,13,14]

Glycemic control is a crucial factor in the management of patients with DM. Adequate control of blood glucose and HbA1c levels may help prevent microvascular and macrovascular complications, wound infections, and impaired bone formation.[14–16] Poor glycemic control has been suggested to compromise osseointegration. For example, Oates et al. conducted a prospective clinical study demonstrating that, in patients with type 2 diabetes mellitus (T2DM), poor glycemic control (HbA1c ≥ 8.1%) was associated with reduced initial implant stability and prolonged healing following implant placement.[17] However, after 16 weeks, implant stability was comparable to that in patients without DM, suggesting that successful osseointegration is achievable, although healing may take longer.[17] Other studies have reported that glycemic control does not significantly affect implant success.[1,18] Escow and Oates conducted a 2-year observational study involving patients with poorly controlled T2DM (HbA1c levels ranging from 6.3% to 13.1%) and found that elevated glycemic levels did not significantly affect the implant survival rates, challenging the prevailing notion that strict glycemic control is essential for early implant success.[18]

Although the influence of DM on dental implant outcomes has been investigated in previous studies, an important limitation remains in the current literature. Many studies have excluded patients with uncontrolled DM, despite the ongoing debate on the impact of glycemic control on early implant failure (EIF).[19–21] This exclusion creates a significant knowledge gap regarding the effect of uncontrolled DM on implant outcomes, particularly during the early stages of healing.

Traditionally, some oral surgeons have considered uncontrolled DM a relative contraindication to implant placement.[11] This is particularly relevant for patients who struggle to achieve adequate glycemic control, as they may be denied access to implant therapy based on limited evidence. Implant-supported prostheses offer potential benefits for patients with DM, particularly those who are partially or completely edentulous. By restoring masticatory function, dental implants may facilitate healthier dietary choices and potentially improve glycemic control. These benefits may, in turn, contribute to an improved quality of life (QoL), enhanced self-image, and better overall health outcomes in these patients.[22,23]

The evolving understanding of DM management, the limited evidence supporting the contraindication of implant therapy in patients with uncontrolled DM, and the growing emphasis on holistic, patient-centered care necessitate a re-evaluation of this approach.

Therefore, the aim of the present study was to assess the impact of glycemic control on EIF in patients with DM. The null hypothesis was that glycemic control is not a significant risk factor for EIF in patients with DM.

Material and methods

A retrospective cohort study, conducted in accordance with the STROBE (Strengthening the Reporting of Observational Studies in Epidemiology) guidelines for observational research, was performed at the Department of Oral and Maxillofacial Surgery, Rabin Medical Center, Petah Tiqwa, Israel, between January 2013 and December 2018. The study complied with the Declaration of Helsinki and its subsequent amendments, and received ethical approval (No. 0674-19-RMC). Written informed consent was obtained from all participants included in the study.

Patients were eligible for inclusion if they were older than 18 years, had undergone implant dentistry treatment, were treated consecutively during the study period, and had available HbA1c measurements obtained within the 3 months preceding implant placement. Patients with incomplete documentation were excluded from the study.

Surgical protocol

Preoperative radiological assessment was performed using cone-beam computed tomography (CBCT). All bone augmentation and implant placement procedures were performed by well-trained oral and maxillofacial surgeons with a minimum of 10 years of clinical experience. Implant placement began with a mid-crestal incision, followed by the elevation of a full-thickness flap. When the available bone volume was insufficient to accommodate an implant with a diameter of ≥3.3 mm and a length of ≥8 mm, or when augmentation was indicated for esthetic reasons, bone augmentation was performed using one of the following bone substitutes or a collagen membrane prior to implant placement:

– xenogeneic bone substitute (Bio-Oss; Geistlisch Pharma, Wolhusen, Switzerland);
– allogeneic bone substitute (OraGraft®; LifeNet Health, Virginia Beach, USA);
– collagen membrane (Ossix® Plus; Datum Dental Ltd., Lod, Israel).

When adequate primary implant stability could be achieved, implants were placed, with simultaneous bone augmentation when indicated, according to the implant manufacturer's protocol and using the dedicated surgical bur set. Upon discharge, patients were prescribed antibiotics (amoxicillin 500 mg 3 times daily for 5 days, or clindamycin 300 mg 3 times daily for 7 days in patients with a penicillin allergy), a chlorhexidine mouth rinse and an analgesic regimen.

Data collection

Clinical data were collected using the Chameleon Electronic Medical Records (EMR) system, while medical histories were retrieved from the Ofek EMR system. The Ofek EMR system provides comprehensive access to patients' medical histories across all Clalit Health Services hospitals and community clinics in Israel. The available information includes diagnoses, medications, complete blood counts (CBCs), histopathology results, and other clinically relevant data. By centralizing this information, the Ofek EMR system helps minimize the risk of disclosure and reporting biases. Data collection was performed independently by D.M. and E.J. Any discrepancies were discussed until a consensus was reached.

Demographic characteristics included patients' gender and age at the time of the procedure. In addition, systemic conditions, HbA1c levels, and the smoking status were recorded.

Patients were stratified into 3 groups according to HbA1c levels[17,18]: non-diabetic (HbA1c < 6.5%); controlled DM (HbA1c between 6.5% and 8%); and uncontrolled DM (HbA1c > 8%).

The following variables were taken into consideration:

– span length: short-span partial edentulism (≤2 missing teeth); long-span partial edentulism (>2 missing teeth; and total edentulism;
– implant:
  • brand;
  • length;
  • diameter;
  • location in the maxilla or the mandible, and in particular regions: anterior (central incisor to canine); premolar (first and second premolars); and posterior (first and second molars);
– number of implants per patient;
– need for bone augmentation (yes/no); and
– EIF defined as implant removal ≤1 year after permanent rehabilitation – primary outcome variable.

Statistical analysis

The data were analyzed using IBM SPSS Statistics, v. 25.0 (IBM Corp., Armonk, USA). Descriptive statistics were used to summarize continuous variables as means and standard deviations ($M \pm SD$) and categorical variables as frequencies. Comparisons among the 3 groups (patients without DM, patients with controlled DM, and patients with uncontrolled DM) were performed using the Kruskal–Wallis test for continuous variables and the χ^2 test for categorical variables.

To account for multiple implants within the same patient and the resulting within-patient correlation, a generalized estimating equations (GEE) model was used to estimate the risk of EIF. The GEE model accounted for subject-level clustering, binomial distribution and exchangeable correlation. Multicollinearity was assessed using the variance inflation factor (VIF). Variables with univariate p-values <0.1 and no evidence of multicollinearity were included in the multivariable models – multivariable GEE at the implant level and multivariable logistic regression at the patient level. Statistical significance was set at $p \leq 0.05$.

Results

Descriptive statistics

Cohort patient level

At the patient level (Table 1), the cohort ($N = 100$) comprised 40% males and 60% females. The mean age was 67.1 ±11.5 years, and 6% of the patients were smokers. Sixty-one percent of the patients received Zimmer implants (Zimmer Biomet TMT, Parsippany, USA; a microtextured (MTX) surface, treated by grit-blasting with hydroxyapatite, followed by washing with non-etching acid and distilled water), 26% received MIS implants (MIS Implants

Table 1. Demographic and baseline clinical characteristics of the cohort at the patient level ($N = 100$)

Variable	Subgroup	Characteristic
Gender	M	40 (40.0)
	F	60 (60.0)
Age [years]	–	67.1 ±11.5
Smoking	–	6 (6.0)
HbA1c level prior to implantation [%]	–	7.1 ±1.1
	non-diabetic	37 (37.0)
	controlled DM	46 (46.0)
Glycemic control	uncontrolled DM	17 (17.0)
	Ditron	13 (13.0)
	MIS	26 (26.0)
Implant brand	Zimmer	61 (61.0)
	short-span partial edentulism	49 (49.0)
	long-span partial edentulism	32 (32.0)
Span length	complete edentulism	19 (19.0)
Number of implants per patient	–	4.3 ±2.9
Bone augmentation	–	51 (51.0)
EIF	–	12 (12.0)

Data presented as mean ± standard deviation ($M \pm SD$), or as number (percentage) (n (%)).
M – male; F – female; HbA1c – hemoglobin A1c; DM – diabetes mellitus; EIF – early implant failure.

Technologies Ltd., Karmiel, Israel; a sandblasted and acid-etched surface), and the remainder received Ditron implants (MPI (Molecular Precision Implant); Ditron Dental, Ashkelon, Israel; a blasted and thermally acid-etched endosseous surface). The mean number of implants per patient was 4.3 ±2.9. Most of the cohort (51%) required bone augmentation.

The mean HbA1c level in the entire cohort was 7.10 ±1.08%. Seventeen percent of the patients were classified as having uncontrolled DM (HbA1c > 8%), 46% as having controlled DM (HbA1c 6.5–8%), and 37% as non-diabetic (HbA1c < 6.5%). Twelve patients had at least one EIF.

Cohort implant level

All data were likewise analyzed at the implant level ($N = 427$) (Table 2). Most implants (58.8%) were Zimmer implants, with 15–20% distributed across each sextant. Twenty-three percent of the implants were placed in patients with uncontrolled DM. The overall incidence of EIF was 2.8% at the implant level.

Table 2. Demographic and baseline clinical characteristics of the cohort at the implant level ($N = 427$)

Variable	Subgroup	Characteristic
Age [years]	–	66.6 ±10.8
Smoking	–	14 (3.3)
Glycemic control	non-diabetic	158 (37.0)
	controlled DM	171 (40.0)
	uncontrolled DM	98 (23.0)
Implant brand	Ditron	63 (14.8)
	MIS	113 (26.5)
	Zimmer	251 (58.8)
Implant length [mm]	–	11.5 ±1.5
Implant diameter [mm]	–	3.8 ±0.3
Implant location	anterior maxilla	58 (13.6)
	premolar maxilla	86 (20.1)
	posterior maxilla	66 (15.5)
	anterior mandible	76 (17.8)
	premolar mandible	70 (16.4)
	posterior mandible	71 (16.6)
Bone augmentation	–	228 (53.4)
EIF	–	12 (2.8)

Data presented as $M \pm SD$, or as n (%).

Statistical analysis

Univariate analyses

At the implant level (Table 3), uncontrolled DM was associated with a substantially higher need for bone augmentation (90.8%) as compared to the controlled DM group (45.0%) and non-diabetic individuals (39.2%). The younger mean age (62.8 ±12.2 years) and female predominance (63.3%) in the poorly controlled DM group were statistically significant. Differences were also observed in implant location, with a higher proportion of implants placed in the anterior maxilla among patients with uncontrolled DM. In addition, implants were significantly longer in this group. Notably, no significant differences were found between the non-diabetic, controlled DM and uncontrolled DM groups.

At the patient level (Table 4), the prevalence of bone augmentation was significantly associated with glycemic control, with a higher need among patients with uncontrolled DM (82.4%) than among those with controlled DM (45.7%) or non-diabetic individuals (43.2%). The number of implants per patient also differed between the groups ($p < 0.1$), reflecting the greater extent of tooth loss in patients with uncontrolled DM.

Table 3. Univariate tests at the implant level to assess the influence of glycemic control on the study variables

Variable	Subgroup	Non-diabetic (*n* = 158)	Controlled DM (*n* = 171)	Uncontrolled DM (*n* = 98)	Statistical analysis		
					Kruskal–Wallis test	χ^2 test	*p*-value
Gender	M	42 (26.6)	73 (42.7)	36 (36.7)	–	9.42	0.009***
	F	116 (73.4)	98 (57.3)	62 (63.3)			
Age [years]	–	67.6 ±10.8	67.8 ±9.6	62.8 ±12.2	13.23	–	0.001***
HbA1c level prior to implantation [%]	–	6.1 ±0.3	7.2 ±0.9	9.1 ±0.4	373.10	–	<0.001***
Implant length [mm]	–	11.3 ±1.7	11.4 ±1.5	11.8 ±1.4	10.49	–	0.007***
Implant diameter [mm]	–	3.9 ±0.3	3.8 ±0.4	3.8 ±0.2	1.61	–	0.142
Implant location	anterior maxilla	17 (10.8)	19 (11.1)	22 (22.4)	–	9.60	0.047**
	premolar maxilla	36 (22.8)	29 (17.0)	21 (21.4)	–	1.90	0.394
	posterior maxilla	29 (18.4)	25 (14.6)	12 (12.2)	–	1.90	0.391
	anterior mandible	21 (13.3)	36 (21.1)	19 (19.4)	–	3.60	0.165
	premolar mandible	28 (17.7)	25 (14.6)	17 (17.3)	–	0.66	0.719
	posterior mandible	27 (17.1)	37 (21.6)	7 (7.1)	–	9.48	0.009***
Bone augmentation	–	62 (39.2)	77 (45.0)	89 (90.8)	–	72.70	<0.001***
EIF	–	5 (3.2)	3 (1.8)	4 (4.1)	–	1.35	0.509

Data presented as *M* ±*SD*, or as *n* (%).
* $p < 0.1$; ** $p < 0.05$; *** $p < 0.01$.

Table 4. Univariate tests at the patient level to assess the influence of glycemic control on the study variables

Variable	Subgroup	Non-diabetic (*n* = 37)	Controlled DM (*n* = 46)	Uncontrolled DM (*n* = 17)	Statistical analysis		
					Kruskal–Wallis test	χ^2 test	*p*-value
Gender	M	11 (29.7)	22 (47.8)	7 (41.2)	–	2.81	0.245
	F	26 (70.3)	24 (52.2)	10 (58.8)			
Age [years]	–	67.6 ±11.6	68.6 ±10.2	62.4 ±13.9	2.92	–	0.231
HbA1c level prior to implantation [%]	–	6.1 ±0.4	7.2 ±0.4	8.9. ±0.9	84.09	–	<0.001***
Span length	short-span partial edentulism	20 (54.1)	26 (56.5)	3 (17.6)	–	10.00	0.125
	long-span partial edentulism	10 (27.0)	13 (28.3)	9 (52.9)			
	complete edentulism	7 (18.9)	7 (15.2)	5 (29.4)			
Number of implants per patient	–	4.3 ±2.9	3.8 ±2.4	5.8 ±3.8	4.73	–	0.094*
Bone augmentation	–	16 (43.2)	21 (45.7)	14 (82.4)	–	8.10	0.017**
EIF	–	5 (13.5)	3 (6.5)	4 (23.5)	–	3.52	0.171

Data presented as *M* ±*SD*, or as *n* (%).
* $p < 0.1$; ** $p < 0.05$; *** $p < 0.01$.

Analyses were performed at both the implant and patient levels to identify risk factors for EIF. These analyses revealed that implant placement in the augmented bone was a significant risk factor for EIF. Notably, no EIF events occurred among implants placed in the anterior or premolar regions of the maxilla, suggesting a lower risk of failure at these sites. Conversely, implants placed in the anterior mandible had significantly higher odds of EIF (*OR* = 3.46). Implants placed in the posterior maxilla showed a borderline statistically significant increase in the odds of failure (*OR* = 2.85; $p = 0.085$) (Tables 5 and 6).

Table 5. Univariate generalized estimating equations (GEE) analysis at the implant level to assess risk factors for early implant failure (EIF)

Variable	Subgroup	*OR*	95% *CI*	*p*-value
Gender	F	1	–	–
	M	2.62	0.82–8.41	0.105
Age	–	1.01	0.97–1.05	0.680
Smoking	–	2.82	0.35–22.76	0.330
HbA1c level prior to implantation	non-diabetic (healthy)	1	–	–
	controlled DM	0.54	0.13–2.30	0.410
	uncontrolled DM	1.30	0.33–5.06	0.700
ASA classification	ASA 2	1	–	–
	ASA 3	1.82	0.57–5.83	0.310
Hypertension	–	0.75	0.24–2.33	0.620
Hyperlipidemia	–	0.64	0.17–2.41	0.520
Osteoporosis	–	2.34	0.58–9.55	0.230
CVA	–	2.89	0.68–12.41	0.150
Implant brand	Ditron	1	–	–
	MIS	0.27	0.02–3.06	0.290
	Zimmer	1.13	0.25–5.20	0.870
Implant length	–	1.12	0.76–1.66	0.550
Implant diameter	–	1.88	0.48–7.40	0.360
Implant location	anterior maxilla	0[a]	0	0
	premolar maxilla	0[a]	0	0
	posterior maxilla	2.85	0.86–9.42	0.085*
	anterior mandible	3.46	1.10–10.91	0.033**
	premolar mandible	1.02	0.22–4.76	0.970
	posterior mandible	0.44	0.06–3.54	0.440
Bone augmentation	–	10.04	1.33–76.03	0.020**

OR – odds ratio; *CI* – confidence interval; ASA – American Society of Anesthesiology; CVA – cerebrovascular accident; [a] no failures occurred in these subgroups; * $p < 0.1$; ** $p < 0.05$; *** $p < 0.01$.

Table 6. Univariate statistical analysis at the patient level to assess risk factors for early implant failure (EIF)

Variable	Subgroup	Failure ($n = 12$)	Success ($n = 88$)	Statistical analysis		
				Kruskal–Wallis test	χ^2 test	*p*-value
Gender	M	7 (58.3)	33 (37.5)	–	1.14	0.280
	F	5 (41.7)	55 (62.5)			
Age	–	67.5 ±7.93	67.1 ±11.9	0	–	0.980
Smoking	–	1 (8.3)	5 (5.7)	–	0	1.000
ASA classification	ASA 2	5 (41.7)	51 (58.0)	–	0.57	0.450
	ASA 3	7 (58.3)	37 (42.0))			
Hypertension	–	7 (58.3)	54 (61.4)	–	0	1.000
Hyperlipidemia	–	3 (25.0)	32 (36.4)	–	0.20	0.650
Osteoporosis	–	2 (16.7)	11 (12.5)	–	0	1.000
CVA	–	2 (16.7)	7 (8.0)	–	0.20	0.650
Span length	short-span partial edentulism	6 (50.0)	43 (48.9)	–	3.97	0.140
	long-span partial edentulism	6 (50.0)	26 (30.0)			
	complete edentulism	0 (0.0)	19 (21.6)			
Number of implants per patient	–	3.5 ±2.1	4.4 ±3.0	0.72	–	0.400
Bone augmentation	–	11 (91.7)	40 (45.5)	–	7.27	0.007***

Data presented as *M* ±*SD*, or as *n* (%).
* $p < 0.1$; ** $p < 0.05$; *** $p < 0.01$.

Multivariable analysis for EIF

Similar to the univariate analysis, the implant-level multivariable GEE model showed that implantation in augmented bone was a significant risk factor for EIF (*OR* = 17.48). Implants placed in the anterior and premolar regions of the maxilla had a significantly lower risk of failure, with no occurrences of EIF observed in these regions (Table 7).

The patient-level model showed that, after controlling for potential confounders, there was no statistically significant difference between the controlled and uncontrolled DM groups (Table 8).

Table 9 illustrates the characteristics of EIF. Notably, 11 of the 12 patients who experienced EIF in this study had augmented bone.

Table 7. Multivariable generalized estimating equations (GEE) model to predict early implant failure (EIF) at the implant level

Variable	Subgroup	*OR*	95% *CI*	*p*-value
Implant location	anterior maxilla	0	0	0[a]
	premolar maxilla	0	0	0[a]
	posterior maxilla	2.56	0.59–11.21	0.210
	anterior mandible	5.33	0.88–14.69	0.090*
Bone augmentation	–	17.48	2.27–34.20	0.002***

[a] no failures occurred in these subgroups; * $p < 0.1$; ** $p < 0.05$; *** $p < 0.01$. Adjusted for age, smoking, hypertension, and hyperlipidemia.

Table 8. Multivariable logistic regression model to predict early implant failure (EIF) at the patient level

Variable	*OR*	95% *CI*	*p*-value
Controlled DM	0.41	0.18–2.67	0.350
Uncontrolled DM	1.35	0.34–3.66	0.960
Bone augmentation	13.24	3.46–96.33	0.013**

* $p < 0.1$; ** $p < 0.05$; *** $p < 0.01$. Adjusted for age, smoking, hypertension, and hyperlipidemia.

Discussion

Achieving successful osseointegration and long-term implant stability is a primary goal in implant dentistry. Various factors can influence implant outcomes, including systemic conditions such as diabetes.[24] Currently, the evidence regarding the impact of uncontrolled DM on EIF remains limited, primarily because individuals with poorly controlled DM are often excluded from clinical studies.[19–21] This study sought to address this gap by analyzing a substantial cohort of patients with varying levels of glycemic control, providing valuable insights into the impact of DM on dental implant outcomes, particularly among patients with uncontrolled DM. The results revealed several significant differences among non-diabetic patients and those with controlled and uncontrolled DM.

Table 9. Characteristics of failed implants at the patient level

No.	Age [years]	HbA1c level prior to implantation [%]	Span length	Implant brand	Implant length [mm]	Implant diameter [mm]	Implant location	Pristine/ augmented bone
1	64	6.8[2]	long-span partial edentulism	Zimmer	11.5	3.7	anterior mandible	pristine
2	68	8.2[3]	short-span partial edentulism	Ditron	11.5	4.1	anterior mandible	augmented
3	69	8.0[2]	short-span partial edentulism	Zimmer	11.5	3.7	posterior maxilla	augmented
4	61	8.6[3]	long-span partial edentulism	Zimmer	13.0	3.75	anterior mandible	augmented
5	52	7.9[2]	long-span partial edentulism	Zimmer	13.0	5.0	posterior maxilla	augmented
6	64	11.3[3]	long-span partial edentulism	Ditron	13.0	3.7	posterior maxilla	augmented
7	65	9.5[3]	long-span partial edentulism	Zimmer	11.5	3.7	premolar mandible	augmented
8	81	5.8[1]	short-span partial edentulism	Zimmer	11.5	3.75	anterior mandible	augmented
9	76	5.8[1]	long-span partial edentulism	Zimmer	8.0	4.2	posterior mandible	augmented
10	64	6.2[1]	short-span partial edentulism	MIS	13.0	3.75	anterior mandible	augmented
11	68	6.2[1]	short-span partial edentulism	Zimmer	10.0	3.75	premolar mandible	augmented
12	78	6.3[1]	short-span partial edentulism	Zimmer	13.0	3.75	posterior maxilla	augmented

[1] non-diabetic; [2] controlled DM; [3] uncontrolled DM.

Osseointegration is the biological process through which a direct interface forms between bone and an implant.[25] Dental implants rely on this process for their initial success; therefore, any disruption may increase the risk of EIF.[4] Prolonged hyperglycemia has been associated with several mechanisms that may impair osseointegration and contribute to EIF. These include the tissue damage resulting from insulin-independent glucose uptake by endothelial cells, endothelial dysfunction and vascular impairment. Additionally, hyperglycemia may impair polymorphonuclear leukocyte migration and phagocytosis while enhancing the inflammatory response to microbial stimuli.[4] These alterations may compromise angiogenesis and disrupt the inflammatory response, both of which are essential for successful osseointegration. Furthermore, in the context of hyperglycemia, the formation of advanced glycation end products (AGEs) is of particular concern. These compounds result from non-enzymatic reactions between sugars and proteins or lipids, a process accelerated by elevated glucose levels. The accumulation of AGEs has been associated with impaired osteoblast differentiation and function, alterations in bone matrix formation and quality, and compromised angiogenesis, all of which are critical for bone healing around implants.[26–33] By directly affecting bone cells and the structural integrity of bone tissue, AGEs may further compromise the achievement of successful osseointegration in individuals with hyperglycemia.[34]

The statistical analysis revealed that neither the DM status nor glycemic control was a statistically significant risk factor for EIF at either the patient or implant level. This finding is consistent with several previous studies. Ghiraldini et al. found no significant differences in implant stability 3 months after implantation between patients with well-controlled (HbA1c < 8%) and poorly controlled (HbA1c > 8.1%) DM.[35] Oates et al. similarly demonstrated that patients with poorly controlled DM did not exhibit significantly reduced implant stability at 16 weeks after implantation.[17] Shi et al. conducted a meta-analysis to assess the association between poorly controlled DM and EIF. Their findings did not demonstrate a significant difference in the implant failure rates between patients with controlled and uncontrolled DM.[36]

Patients with uncontrolled DM were notably younger, highlighting the potential oral health implications of poor glycemic control, which is associated with an increased risk of periodontitis and tooth loss. These patients may experience tooth loss at an earlier age, leading to the need for implant therapy at a younger age.[37] This finding is consistent with the existing literature, as several studies have reported an association between better glycemic control and an older age.[38,39] This observation underscores the importance of effective diabetes management from an early age to help delay or potentially prevent tooth loss and other oral health complications.

Consistent with previous studies, we found that the dental status of patients with uncontrolled DM prior to implant placement was significantly compromised.[14] A higher proportion of patients with poorly controlled DM required bone augmentation procedures. Type 2 DM may exacerbate the host inflammatory response to oral plaque, thereby aggravating bone resorption associated with periodontitis and peri-implantitis.[39–45] Patients with DM exhibit increased levels of pro-inflammatory cytokines in bone tissues, including interleukin (IL)-1β, IL-6, and tumor necrosis factor alpha (TNF-α).[46–49] Consequently, increased osteoclast activity may lead to greater bone resorption. Previous studies have also reported that good glycemic control improves osteoclast function, and helps prevent periodontal bone loss and tooth loss.[50,51] These findings are consistent with previous research, as well as with the results of the present study, which indicate a higher prevalence of EIF in patients with augmented bone.[22,52,53] This evidence underscores the importance of preserving natural bone and preventing bone loss associated with periodontal disease. Additionally, a significant difference was observed in the mean implant length between the 3 groups, with patients with well-controlled DM receiving shorter implants, on average, than those with poorly controlled DM. This difference may be attributable to the additional bone volume gained through the augmentation procedures, which may have allowed the placement of longer implants.

The results also revealed significant differences in implant location between patients with controlled and uncontrolled DM. Uncontrolled DM was associated with a higher likelihood of implants being placed in the anterior maxilla, whereas controlled DM was more frequently associated with implant placement in the mandibular molar region. These findings highlight the importance of considering anatomical factors when evaluating implant placement patterns in patients with DM. They may also reflect more pronounced bone resorption and periodontal damage in the anterior maxilla among patients with uncontrolled DM, although this interpretation requires further investigation. To the best of our knowledge, no previous studies have specifically reported differences in implant location according to glycemic control. However, these findings are supported by a previous study conducted in healthy individuals.[54]

Another finding regarding implant location was the lower incidence of EIF in implants placed in the anterior and premolar regions of the maxilla, compared with the higher incidence observed in the anterior mandible. This difference may be attributed to the superior vascular supply of the maxilla as compared to the mandible, which may promote osseointegration.[55] The relatively limited vascular supply in the anterior mandible may, in turn, contribute to the higher EIF rates observed in this region.[55] We hypothesize that this anatomical factor may be particularly relevant in patients with DM, who often experience microvascular damage.[1] Impaired blood flow could further compromise osseointegration in areas with inherently

limited vascularity, such as the anterior mandible, potentially increasing the risk of EIF. Further studies are needed to investigate this proposed mechanism.

The results of this study call for a reevaluation of the current approach to treating patients with uncontrolled DM who require dental implant therapy. Although achieving optimal glycemic control remains the ideal goal, this is not always attainable, particularly in individuals with complex health conditions or socioeconomic barriers.[56] Despite numerous studies investigating implant outcomes in patients with DM, definitive evidence regarding its independent negative impact on EIF remains inconclusive.[17–20,35,36,51,57] In fact, some studies suggest that implant therapy in patients with DM may indirectly contribute to improved glycemic control. The restoration of masticatory function through implant-supported prostheses may facilitate healthier dietary choices and improve overall health, potentially contributing to a reduction in the HbA1c levels.[22]

Furthermore, the improvement in QoL associated with implant therapy, both functionally and psychologically, is substantial and should not be underestimated.[58] The ability to eat comfortably, speak clearly and smile confidently can have a profound impact on a patient's overall well-being. Denying these benefits solely on the basis of uncontrolled DM may represent an overly restrictive approach. Our findings suggest that, although uncontrolled DM may present certain challenges in implant dentistry, including a potentially higher risk of peri-implantitis and consequently reduced implant survival, it should not be considered an absolute contraindication to implant therapy. Instead, treatment decisions should be individualized, taking into account the patient's overall health status, degree of glycemic control, and risk factors for implant complications.

Limitations

The limitations of this study stem primarily from its retrospective design and the involvement of multiple operators, which may have introduced variability in data recording and surgical techniques, thereby limiting the generalizability of the findings. Although this study represents one of the larger investigations of diabetic patients undergoing implant therapy, a larger sample size may help identify additional statistically significant predictors and subtle differences in implant failure risk, as suggested by the wide confidence intervals observed in our analyses. Additionally, data on medication use were unavailable. It is possible that antidiabetic medications may influence implant outcomes and potentially reduce the EIF rates in these patients.

Another potential limitation is the possibility of selection bias. Previous studies have raised concerns regarding the oral complications associated with chronic hyperglycemia, including periodontitis, hyposalivation, impaired inflammatory responses, and potentially EIF. These concerns may have prompted clinicians to adopt a more cautious approach when treating patients with uncontrolled DM. Consequently, such patients may have been advised to improve their glycemic control before undergoing the implant placement or bone augmentation procedures. This selection process could have reduced the observed risk of implant failure, even among patients with elevated HbA1c levels.

Lastly, although the HbA1c levels were measured within 3 months before implant placement, fluctuations in glycemic control over time were not accounted for. This may have resulted in the misclassification of the patients' glycemic status and potentially influenced the observed associations between glycemic control and EIF.

Conclusions

This study indicates that, although uncontrolled DM may present certain challenges in implant dentistry, including a younger age at implant placement, an increased need for bone augmentation, and a preference for specific implant sites, it does not significantly affect the EIF rates.

Ethics approval and consent to participate

The research adhered to the ethical standards outlined in the Declaration of Helsinki, and received approval from the institutional review board at Rabin Medical Center, Petah Tiqwa, Israel (No. 0674-19-RMC). All study participants provided written informed consent prior to their inclusion.

Data availability

The datasets supporting the findings of the current study are available from the corresponding author on reasonable request.

Consent for publication

Not applicable.

Use of AI and AI-assisted technologies

Not applicable.

ORCID iDs

Daya Masri https://orcid.org/0000-0002-3808-8664
Ehud Jonas https://orcid.org/0000-0001-8780-6979
Gal Avishai https://orcid.org/0000-0001-5111-8496
Hiba Masri-Iraqi https://orcid.org/0000-0002-0889-8025
Adrian Kahn https://orcid.org/0000-0002-4804-3099
Liat Chaushu https://orcid.org/0000-0002-5755-7526

References

1. Chrcanovic BR, Albrektsson T, Wennerberg A. Diabetes and oral implant failure: A systematic review. *J Dent Res*. 2014;93(9):859–867. doi:10.1177/0022034514538820
2. Khader YS, Dauod AS, El-Qaderi SS, Alkafajei A, Batayha WQ. Periodontal status of diabetics compared with nondiabetics: A meta-analysis. *J Diabetes Complications*. 2006;20(1):59–68. doi:10.1016/j.jdiacomp.2005.05.006
3. Blumer S, Eliasi H, Peretz B, Kharouba J, Jonas E. Knowledge and decision-making among Israeli dentists treating young patients with type 1 diabetes mellitus: A cross-sectional survey. *J Clin Pediatr Dent*. 2022;46(3):225–232. doi:10.17796/1053-4625-46.3.9
4. Javed F, Romanos GE. Impact of diabetes mellitus and glycemic control on the osseointegration of dental implants: A systematic literature review. *J Periodontol*. 2009;80(11):1719–1730. doi:10.1902/jop.2009.090283
5. Nissan J, Zenziper E, Rosner O, Kolerman R, Chaushu L, Chaushu G. The effect of mucosal cuff shrinkage around dental implants during healing abutment replacement. *J Oral Rehabil*. 2015;42(10):774–778. doi:10.1111/joor.12315
6. Nissan J, Snir D, Rosner O, Kolerman R, Chaushu L, Chaushu G. Reliability of retrievable cemented implant-supported prostheses. *J Prosthet Dent*. 2016;115(5):587–591. doi:10.1016/j.prosdent.2015.10.013
7. Kolerman R, Qahaz N, Barnea E, et al. Allograft and collagen membrane augmentation procedures preserve the bone level around implants after immediate placement and restoration. *Int J Environ Res Public Health*. 2020;17(4):1133. Published 2020 Feb 11. doi:10.3390/ijerph17041133
8. Esteves Fernandes PR, Pelaez Otero AI, Hasse Fernandes JC, Nassani LM, Castilho RM, Fernandes GVdO. Clinical performance comparing titanium and titanium-zirconium or zirconia dental implants: A systematic review of randomized controlled trials. *Dent J (Basel)*. 2022;10(5):83. doi:10.3390/dj10050083
9. Remísio MJdS, Borges T, Castro F, Gehrke SA, Hasse Fernandes JC, Fernandes GVdO. Histologic osseointegration level comparing titanium and zirconia dental implants: Meta-analysis of preclinical studies. *Int J Oral Maxillofac Implants*. 2023;38(4):667–680. doi:10.11607/jomi.10142
10. Shrivastava D, Quadri SA, Alshadidi AA, et al. Clinical assessment of the relationship of dental implant materials (titanium and zirconia) and peri-implantitis: A systematic review. *J Maxillofac Oral Surg*. 2025;24(4):1010–1028. doi:10.1007/s12663-024-02409-9
11. Samara W, Moztarzadeh O, Hauer L, Babuska V. Dental implant placement in medically compromised patients: A literature review. *Cureus*. 2024;16(2):e54199. doi:10.7759/cureus.54199
12. Michaeli E, Weinberg I, Nahlieli O. Dental implants in the diabetic patient: Systemic and rehabilitative considerations. *Quintessence Int*. 2009;40(8):639–645. PMID:19639088.
13. Wagner J, Spille JH, Wiltfang J, Naujokat H. Systematic review on diabetes mellitus and dental implants: An update. *Int J Implant Dent*. 2022;8(1):1. doi:10.1186/s40729-021-00399-8
14. Tan SJ, Baharin B, Nabil S, Mohd N, Zhu Y. Does glycemic control have a dose–response relationship with implant outcomes? A comprehensive systematic review and meta-analysis. *J Evid Based Dent Pract*. 2021;21(2):101543. doi:10.1016/j.jebdp.2021.101543
15. Guarnieri R, Reda R, Zanza A, Miccoli G, Di Nardo D, Testarelli L. Can peri-implant marginal bone loss progression and a-MMP-8 be considered indicators of the subsequent onset of peri-implantitis? A 5-year study. *Diagnostics (Basel)*. 2022;12(11):2599. doi:10.3390/diagnostics12112599
16. Guarnieri R, Reda R, Di Nardo D, Miccoli G, Zanza A, Testarelli L. Clinical, radiographic, and biochemical evaluation of two-piece versus one-piece single implants with a laser-microgrooved collar surface after 5 years of functional loading. *Clin Implant Dent Relat Res*. 2022;24(5):676–682. doi:10.1111/cid.13118
17. Oates TW, Dowell S, Robinson M, McMahan CA. Glycemic control and implant stabilization in type 2 diabetes mellitus. *J Dent Res*. 2009;88(4):367–371. doi:10.1177/0022034509334203
18. Eskow CC, Oates TW. Dental implant survival and complication rate over 2 years for individuals with poorly controlled type 2 diabetes mellitus. *Clin Implant Dent Relat Res*. 2017;19(3):423–431. doi:10.1111/cid.12465
19. Chae SW, Kim YS, Kim WK, Lee YK, Kim SH. Effect of glycemic control on the incidence of dental implant complications in diabetic patients. *J Implant Appl Sci*. 2023;27(4):163–173. doi:10.32542/implantology.2023019
20. Tang D, Wang E, Xu Y, et al. Is hyperglycemia the only risk factor for implant in type 2 diabetics during the healing period? *Oral Dis*. 2021;27(6):1551–1563. doi:10.1111/odi.13685
21. De Angelis P, Manicone PF, Gasparini G, et al. The effect of controlled diabetes and hyperglycemia on implant placement with simultaneous horizontal guided bone regeneration: A clinical retrospective analysis. *Biomed Res Int*. 2021;2021:9931505. doi:10.1155/2021/9931505
22. Masri D, Masri-Iraqi H, Nissan J, et al. On the association between implant-supported prosthesis and glycemic control (HbA1c values). *Int J Environ Res Public Health*. 2022;19(11):6923. doi:10.3390/ijerph19116923
23. Masri D, Masri-Iraqi H, Naishlos S, Weinberg E, Reiser V, Chaushu L. Implant-supported prosthesis is a viable treatment alternative for American Society of Anesthesiology physical status 3 individuals – a retrospective cohort study. *J Clin Med*. 2022;11(7):2002. doi:10.3390/jcm11072002
24. Jonas E, Masri D, Avishai G, Masri-Iraqi H, Chaushu G, Chaushu L. The impact of antiplatelet and anticoagulant medications on early implant failure following sinus floor augmentation: A retrospective cohort analysis. *Clin Implant Dent Relat Res*. 2024;26(5):1046–1055. doi:10.1111/cid.13369
25. Albrektsson T, Brånemark PI, Hansson HA, Lindström J. Osseointegrated titanium implants. Requirements for ensuring a long-lasting, direct bone-to-implant anchorage in man. *Acta Orthop Scand*. 1981;52(2):155–170. doi:10.3109/17453678108991776
26. Park SY, Choi KH, Jun JE, Chung HY. Effects of advanced glycation end products on differentiation and function of osteoblasts and osteoclasts. *J Korean Med Sci*. 2021;36(37):e239. doi:10.3346/jkms.2021.36.e239
27. Jia T, Wang YN, Zhang D, Xu X. 1α,25-dihydroxyvitamin D3 promotes osseointegration of titanium implant via downregulating AGEs/RAGE pathway in T2DM. *Endocr Connect*. 2018;7(11):1186–1195. doi:10.1530/EC-18-0241
28. Phimphilai M, Pothacharoen P, Kongtawelert P. Age-influenced receptors of advanced glycation end product overexpression associated with osteogenic differentiation impairment in patients with type 2 diabetes. *Front Endocrinol (Lausanne)*. 2021;12:726182. doi:10.3389/fendo.2021.726182
29. Phimphilai M, Pothacharoen P, Chattipakorn N, Kongtawelert P. Receptors of advanced glycation end product (RAGE) suppression associated with a preserved osteogenic differentiation in patients with prediabetes. *Front Endocrinol (Lausanne)*. 2022;13:799872. doi:10.3389/fendo.2022.799872
30. Marin C, Luyten FP, Van der Schueren B, Kerckhofs G, Vandamme K. The impact of type 2 diabetes on bone fracture healing. *Front Endocrinol (Lausanne)*. 2018;9:6. doi:10.3389/fendo.2018.00006
31. Stirban A, Gawlowski T, Roden M. Vascular effects of advanced glycation endproducts: Clinical effects and molecular mechanisms. *Mol Metab*. 2013;3(2):94–108. doi:10.1016/j.molmet.2013.11.006
32. Asadipooya K, Uy EM. Advanced glycation end products (AGEs), receptor for AGEs, diabetes, and bone: Review of the literature. *J Endocr Soc*. 2019;3(10):1799–1818. doi:10.1210/js.2019-00160
33. Yamamoto M, Sugimoto T. Advanced glycation end products, diabetes, and bone strength. *Curr Osteoporos Rep*. 2016;14(6):320–326. doi:10.1007/s11914-016-0332-1
34. Cosola S, Butera A, Zergaw AH, et al. Glycemic control and implant stability in patients with type II diabetes: Narrative review. *Healthcare (Basel)*. 2025;13(5):449. doi:10.3390/healthcare13050449
35. Ghiraldini B, Conte A, Casarin RC, et al. Influence of glycemic control on peri-implant bone healing: 12-month outcomes of local release of bone-related factors and implant stabilization in type 2 diabetics. *Clin Implant Dent Relat Res*. 2016;18(4):801–809. doi:10.1111/cid.12339
36. Shi Q, Xu J, Huo N, Cai C, Liu H. Does a higher glycemic level lead to a higher rate of dental implant failure? A meta-analysis. *J Am Dent Assoc*. 2016;147(11):875–881. doi:10.1016/j.adaj.2016.06.011
37. Genco RJ, Graziani F, Hasturk H. Effects of periodontal disease on glycemic control, complications, and incidence of diabetes mellitus. *Periodontol 2000*. 2020;83(1):59–65. doi:10.1111/prd.12271

38. Berkowitz SA, Meigs JB, Wexler DJ. Age at type 2 diabetes onset and glycaemic control: Results from the National Health and Nutrition Examination Survey (NHANES) 2005–2010. *Diabetologia*. 2013;56(12):2593–2600. doi:10.1007/s00125-013-3036-4
39. Shamshirgaran SM, Mamaghanian A, Aliasgarzadeh A, Aiminisani N, Iranparvar-Alamdari M, Ataie J. Age differences in diabetes-related complications and glycemic control. *BMC Endocr Disord*. 2017;17(1):25. doi:10.1186/s12902-017-0175-5
40. Andriankaja OM, Barros SP, Moss K, et al. Levels of serum interleukin (IL)-6 and gingival crevicular fluid of IL-1beta and prostaglandin E(2) among non-smoking subjects with gingivitis and type 2 diabetes. *J Periodontol*. 2009;80(2):307–316. doi:10.1902/jop.2009.080385
41. Chaushu L, Tal H, Sculean A, Fernández-Tomé B, Chaushu G. Peri-implant disease affects systemic complete blood count values – an experimental in vivo study. *Clin Oral Investig*. 2020;24(12):4531–4539. doi:10.1007/s00784-020-03318-0
42. Chaushu L, Tal H, Sculean A, Fernández-Tomé B, Chaushu G. Effects of peri-implant infection on serum biochemical analysis. *J Periodontol*. 2021;92(3):436–445. doi:10.1002/JPER.20-0048
43. Chaushu L, Weinreb M, Beitlitum I, Moses O, Nemcovsky CE. Evaluation of a topical herbal patch for soft tissue wound healing: An animal study. *J Clin Periodontol*. 2015;42(3):288–293. doi:10.1111/jcpe.12372
44. Lo Bianco L, Montevecchi M, Ostanello M, Checchi V. Recognition and treatment of peri-implant mucositis: Do we have the right perception? A structured review. *Dent Med Probl*. 2021;58(4):545–554. doi:10.17219/dmp/136359
45. Fernandes GVdO, Martins BGdS, Fraile JF. Revisiting peri-implant diseases in order to rethink the future of compromised dental implants: Considerations, perspectives, treatment, and prognosis. *Dent Med Probl*. 2024;61(5):637–640. doi:10.17219/dmp/187215
46. Graves DT, Cochran D. The contribution of interleukin-1 and tumor necrosis factor to periodontal tissue destruction. *J Periodontol*. 2003;74(3):391–401. doi:10.1902/jop.2003.74.3.391
47. Graves D. Cytokines that promote periodontal tissue destruction. *J Periodontol*. 2008;79(Suppl 8):1585–1591. doi:10.1902/jop.2008.080183
48. Cochran DL. Inflammation and bone loss in periodontal disease. *J Periodontol*. 2008;79(Suppl 8):1569–1576. doi:10.1902/jop.2008.080233
49. Al-Askar M, Ajlan S, Alomar N, Al-Daghri NM. Clinical and radiographic peri-implant parameters and whole salivary interleukin-1β and interleukin-6 levels among type-2 diabetic and nondiabetic patients with and without peri-implantitis. *Med Princ Pract*. 2018;27(2):133–138. doi:10.1159/000488032
50. Araujo MG, Lindhe J. Peri-implant health. *J Clin Periodontol*. 2018;45(Suppl 20):S230–S236. doi:10.1111/jcpe.12952
51. Taylor GW, Burt BA, Becker MP, Genco RJ, Shlossman M. Glycemic control and alveolar bone loss progression in type 2 diabetes. *Ann Periodontol*. 1998;3(1):30–39. doi:10.1902/annals.1998.3.1.30
52. Chatzopoulos GS, Wolff LF. Dental implant failure and bone augmentation: A retrospective study. *J Clin Exp Dent*. 2023;15(3):e195–e204. doi:10.4317/jced.60171
53. Alshiddi IF. Survival rate and clinico-radiographic parameters around narrow-diameter dental implants for fixed dental prostheses in the posterior regions: A systematic review. *Dent Med Probl*. 2023;60(2):345–353. doi:10.17219/dmp/140757
54. Olate S, Negreiros Lyrio MC, de Moraes M, Mazzonetto R, Fernandes Moreira RW. Influence of diameter and length of implant on early dental implant failure. *J Oral Maxillofac Surg*. 2010;68(2):414–419. doi:10.1016/j.joms.2009.10.002
55. Tsaï GE, Volkov SI, Lavrent'ev PA, Lavrent'ev AA. Blood supply topographic features in maxilla and mandible [in Russian]. *Stomatologiia (Mosk)*. 2015;94(1):7–10. doi:10.17116/stomat20159417-10
56. Qaseem A, Wilt TJ, Kansagara D, et al. Hemoglobin A1c targets for glycemic control with pharmacologic therapy for nonpregnant adults with type 2 diabetes mellitus: A guidance statement update from the American College of Physicians. *Ann Intern Med*. 2018;168(8):569–576. doi:10.7326/M17-0939
57. Oates Jr. TW, Galloway P, Alexander P, et al. The effects of elevated hemoglobin A(1c) in patients with type 2 diabetes mellitus on dental implants: Survival and stability at one year. *J Am Dent Assoc*. 2014;145(12):1218–1226. doi:10.14219/jada.2014.93
58. Sargozaie N, Moeintaghavi A, Shojaie H. Comparing the quality of life of patients requesting dental implants before and after implant. *Open Dent J*. 2017;11:485–491. doi:10.2174/1874210601711010485

Original paper

Peri-implant soft tissue thickness following connective tissue grafting or volume-stable collagen matrix augmentation: A randomized controlled trial

Jakub Hadzik[1,2,A–F], Marzena Dominiak[1,A,F]

[1] Department of Dental Surgery, Faculty of Dentistry, Wroclaw Medical University, Poland
[2] Wroclaw Medical Innovation Center (MCIW), Poland

A – research concept and design; B – collection and/or assembly of data; C – data analysis and interpretation;
D – writing the article; E – critical revision of the article; F – final approval of the article

Dental and Medical Problems, ISSN 1644-387X (print), ISSN 2300-9020 (online) *Dent Med Probl.* 2026;63(5):1107–1120

Address for correspondence
Jakub Hadzik
E-mail: jakub.hadzik@umw.edu.pl

Funding sources
This investigator-initiated clinical trial, with Jakub Hadzik as the principal study investigator, was financially supported by Geistlich Pharma AG (Wolhusen, Switzerland).

Conflict of interest
None declared

Acknowledgements
The authors would like to acknowledge the clinical support provided by the clinical staff involved in the conduct of the study, with special thanks to Sabina Wojciechowska and Iwona Kochel (Wroclaw Medical Innovation Center, Poland) for assistance with the clinical measurements performed according to the study protocol. The authors also acknowledge the statistical assistance in data analysis provided by Krzysztof Kujawa (Statistical Analysis Center, Wroclaw Medical University, Poland). The authors additionally thank the staff of the Wroclaw Medical Innovation Center for their organizational and technical assistance during the clinical trial.

Received on April 10, 2026
Reviewed on May 17, 2026
Accepted on May 22, 2026

Published online on June 29, 2026

Cite as
Hadzik J, Dominiak M. Peri-implant soft tissue thickness following connective tissue grafting or volume-stable collagen matrix augmentation: A randomized controlled trial. *Dent Med Probl.* 2026;63(5):1107–1120. doi:10.17219/dmp/222370

DOI
10.17219/dmp/222370

Copyright
Copyright by Author(s)
This is an article distributed under the terms of the Creative Commons Attribution 3.0 Unported (CC BY 3.0) (https://creativecommons.org/licenses/by/3.0/)

Abstract

Background. Peri-implant soft tissue thickness (STT) is considered as an important factor influencing marginal bone stability and esthetic outcomes; however, the effectiveness of different augmentation materials and the impact of augmentation timing remain unclear.

Objectives. The aim of this study was to compare changes in peri-implant SST following augmentation with a subepithelial connective tissue graft (CTG) or a volume-stable collagen matrix (VCMX) vs. non-augmented control sites, and to explore the potential influence of augmentation timing.

Material and methods. In this randomized controlled clinical trial (RCT), 36 patients with 40 implant sites in the esthetic zone were allocated to the CTG ($n = 16$), VCMX ($n = 16$) or non-augmented control ($n = 8$) groups. Within the CTG and VCMX groups, implant sites were further subdivided according to augmentation timing (staged vs. simultaneous), with each subgroup consisting of 8 implant sites. Soft tissue augmentation was performed either prior to implant placement or simultaneously with implant insertion. Soft tissue thickness was assessed using standardized ultrasonographic measurements at baseline (T0), 3 months (T1) and 12 months (T2). Marginal bone loss (MBL) and complications were recorded as secondary outcomes.

Results. Both augmentation methods resulted in significantly greater SST as compared to non-augmented sites ($p < 0.001$). At T2, CTGs tended to achieve greater final thickness than the collagen matrix (a difference of 0.3–0.6 mm in the final SST). All augmented sites exceeded 2 mm mucosal thickness. No statistically significant differences related to augmentation timing were detected. Marginal bone loss was low and comparable among the groups, and no biological or technical complications were observed.

Conclusions. Soft tissue augmentation results in clinically relevant and stable increases in peri-implant tissue thickness. Connective tissue grafts tended to provide greater final thickness, whereas the collagen matrix may represent a reliable and less invasive alternative. No statistically significant influence of augmentation timing on the final STT outcomes was detected over 12 months.

Keywords: randomized controlled trial, peri-implant soft tissue, soft tissue augmentation, connective tissue graft, collagen matrix

Highlights

- Peri-implant soft tissue augmentation significantly increased tissue thickness as compared to non-augmented sites.
- Connective tissue grafts achieved greater final soft tissue thickness than the volume-stable collagen matrix.
- Both augmentation methods resulted in stable soft tissue thickness after 12 months.
- Augmentation timing did not influence the final peri-implant soft tissue thickness outcomes.
- Volume-stable collagen matrix represents a less invasive alternative with clinically relevant outcomes.

Introduction

Adequate peri-implant soft tissue dimensions play a crucial role in achieving the long-term stability of dental implants. Proper soft tissue quality facilitates predictable primary wound closure during bone augmentation procedures and supports the maintenance of stable peri-implant tissues over time.[1–3] Moreover, sufficient soft tissue volume is essential for the development of a favorable emergence profile of implant-supported restorations, thereby contributing to satisfactory functional and esthetic treatment outcomes.[4,5]

Peri-implant soft tissue thickness (SST) has been identified as a key determinant of crestal bone stability and long-term implant survival,[6–8] as further emphasized in the 2024 Academy of Osseointegration/American Academy of Periodontology (AO/AAP) reports highlighting the clinical relevance of peri-implant soft tissue dimensions and keratinized mucosa.[9] Moreover, the most recent 2026 Global Consensus for Clinical Guidelines (GCCG) initiatives have identified marginal bone loss (MBL) and peri-implant tissue conditions as core outcome domains in implant dentistry.[10] In particular, insufficient peri-implant mucosal dimensions have been associated with increased plaque accumulation, inflammation and MBL.[11] Evidence indicates that a mucosal thickness below 2 mm predisposes implant sites to additional crestal bone remodeling during the re-establishment of peri-implant biological width, potentially compromising implant longevity.[12] Furthermore, reduced peri-implant SST has been linked to an increased risk of biological complications.[13,14]

Consequently, interventions aimed at augmenting peri-implant mucosal thickness at the sites presenting with a thin soft tissue phenotype are indicated to optimize esthetic outcomes and maintain peri-implant health. Recent evidence also shows that hard and/or soft tissue grafting associated with immediate implant placement may help reduce peri-implant tissue loss, and improve mid-facial mucosa stability and facial bone thickness.[15]

Autogenous soft tissue grafting

Current scientific evidence supports the use of autogenous subepithelial connective tissue grafts (CTGs) as the grafting material of choice for peri-implant mucosal thickness augmentation. Connective tissue grafts are still considered the reference standard for peri-implant soft tissue augmentation due to their predictable clinical performance and long-term stability.[12] Various surgical techniques employing CTG have been described, enabling reliable increases in soft tissue volume and favorable peri-implant tissue outcomes.

Despite their effectiveness, autogenous grafting procedures are associated with increased surgical complexity, donor-site morbidity and postoperative discomfort. Therefore, the selection of a soft tissue augmentation approach should balance the expected clinical benefits against patient-related morbidity, particularly in cases requiring multiple or staged surgical interventions.

Biomaterials as soft tissue substitutes

To improve peri-implant soft tissue conditions, various biomaterials have been introduced as alternatives to autogenous grafts. These biomaterials can be broadly classified according to their origin into allogeneic, xenogeneic and synthetic soft tissue substitutes. Among these categories, xenogeneic collagen-based matrices represent the most extensively investigated group of soft tissue substitutes in implant dentistry.[16]

Collagen matrices are designed to provide a three-dimensional (3D) scaffold supporting soft tissue integration and early volume stabilization while reducing surgical invasiveness and patient morbidity. Depending on their structural characteristics, collagen matrices may be further distinguished into native (non-cross-linked) matrices and cross-linked, volume-stable matrices, which differ in degradation behavior, mechanical properties and the capacity to maintain soft tissue volume over time.[17,18]

Although collagen-based substitutes can achieve satisfactory clinical outcomes, the magnitude of soft tissue volume gain is generally lower as compared to subepithelial CTGs.[2,19,20] Moreover, substantial heterogeneity exists among the available studies with respect to surgical protocols, follow-up periods, outcome definitions, and the methods used for SST assessment, limiting data comparability and evidence-based interpretation.

Timing of soft tissue augmentation in implant therapy

In addition to the choice of the augmentation material, the timing of soft tissue augmentation in relation to implant placement represents a critical clinical decision. Soft tissue augmentation may be performed either prior to implant placement as a staged procedure or simultaneously with implant insertion. Both approaches are commonly applied in clinical practice; however, their potential influence on peri-implant SST and long-term tissue stability has not been consistently clarified.

The available studies addressing the timing of soft tissue augmentation are characterized by substantial heterogeneity with respect to the study design, surgical protocols and outcome assessment methods. This lack of direct comparative clinical evidence represents an important gap in the current literature.

Aim of the study

The primary aim of this randomized controlled clinical trial (RCT) was to evaluate changes in peri-implant SST following augmentation with either a subepithelial CTG or a volume-stable collagen matrix (VCMX) (Fibro-Gide®), in comparison with non-augmented control sites, in the esthetic zone.

A secondary, exploratory aim was to assess the influence of augmentation timing. Additionally, the relationship between SST and MBL over a 12-month follow-up period was investigated.

Material and methods

Study design

This study was designed as a prospective, investigator-initiated RCT, conducted to evaluate the influence of the soft tissue augmentation material and to explore the potential influence of augmentation timing on peri-implant soft and hard tissue outcomes in the esthetic zone. The trial compared the peri-implant soft tissue augmentation performed using an autogenous subepithelial CTG or VCMX with non-augmented control sites.

The study protocol was reviewed and approved by the Bioethics Committee at Wroclaw Medical University, Poland (approval No. KB-863/2021; October 28, 2021), and the trial was conducted in accordance with the principles of the Declaration of Helsinki and the Good Clinical Practice guidelines. All participants were informed about the nature and objectives of the study, and provided written informed consent prior to enrollment. Patients were not involved in the design, conduct or reporting of the study. The trial was registered at ClinicalTrials.gov (NCT07324187).

Study population and eligibility criteria

Patients requiring single-tooth implant rehabilitation in the esthetic zone (incisors, canines or premolars) of the maxilla or the mandible were consecutively screened for eligibility. Adult patients aged 18–60 years, presenting with single-tooth edentulism or bilateral two-tooth edentulism in separate quadrants, with natural teeth adjacent to each implant site, were eligible for inclusion.

Eligible implant sites were required to present a minimum buccolingual bone width of 6.0 mm, as assessed by cone-beam computed tomography (CBCT), a baseline SST between 0.5 and 2.5 mm, and a minimum height of keratinized tissue of 2.0 mm. Adequate oral hygiene was mandatory and was defined as an approximal plaque index (API) below 25%.

Exclusion criteria included local and systemic conditions that could interfere with soft or hard tissue healing. Local exclusion criteria comprised previous bone augmentation at the intended implant site, severe periodontal disease, bruxism, and smoking. Systemic exclusion criteria included uncontrolled diabetes mellitus, metabolic disorders, a history of head and neck radiotherapy, previous bisphosphonate therapy, bleeding disorders, and other systemic conditions known to impair wound healing.

Patients presenting with a tooth at the intended implant site were eligible only after tooth extraction followed by unassisted socket healing for a minimum of 4 months. No ridge preservation or bone augmentation procedures were performed at extraction sites. Final eligibility was confirmed by CBCT after healing to ensure that baseline bone conditions reflected natural post-extraction healing.

A total of 36 patients fulfilling all eligibility criteria were enrolled. Overall, 40 dental implants were placed, as 4 patients received implants at 2 separate sites; in these cases, implants were located in different quadrants or in the opposing jaws, and were never placed adjacent to each other. Each implant site was therefore treated as an independent experimental unit for statistical analysis.

Randomization and study groups

After the confirmation of eligibility, implant sites were randomly allocated to one of 3 study groups according to the type of soft tissue augmentation protocol. Randomization was performed prior to the surgical intervention, using sealed, opaque allocation cards prepared by a team member not involved in patient recruitment or treatment, ensuring allocation concealment.

Based on the augmentation material, implant sites were assigned to one of the following groups: group G1 (CTG group), in which peri-implant soft tissue augmentation was performed using an autogenous subepithelial CTG (n = 16 implant sites); group G2 (VCMX group), in which peri-implant soft tissue augmentation was performed using VCMX (Fibro-Gide; Geistlich Pharma AG (Wolhusen,

Switzerland) (n = 16 implant sites); and group G3 (control group), in which implants were placed without soft tissue augmentation (n = 8 implant sites).

Within G1 and G2, implant sites were further allocated according to the timing of soft tissue augmentation. In the two-stage protocol, soft tissue augmentation was performed 3 months prior to implant placement (G1A and G2A; n = 8 implant sites per augmentation material), whereas in the one-stage protocol, soft tissue augmentation was performed simultaneously with implant insertion (G1B and G2B; n = 8 implant sites per augmentation material). This was a three-arm, parallel, exploratory RCT with a 2:2:1 allocation ratio, applied to increase the number of observations in the intervention groups, while maintaining a reference control group (Fig. 1). This approach was consistent with the exploratory design of the study, with a focus on effect size estimation within the intervention groups rather than confirmatory comparisons with the control group.

Surgical and prosthetic procedures

Due to the nature of surgical interventions, neither participants nor operators were blinded to group allocation. All surgical and prosthetic procedures were performed by the same experienced clinician to ensure procedural consistency throughout the study.

Soft tissue augmentation procedures

Depending on group allocation, peri-implant soft tissue augmentation was performed using either an autogenous subepithelial CTG or VCMX.

In the CTG groups, subepithelial CTGs were harvested from the palatal donor site, using a standardized surgical technique. After de-epithelialization, the grafts were adapted to the recipient site and fully covered by the repositioned mucosal flap.

In the VCMX groups, the Fibro-Gide VCMX with a standardized thickness of 3 mm was trimmed to fit the recipient site and placed according to the manufacturer's recommendations. The matrix was completely covered by the mucosal flap to allow submerged healing.

In the two-stage protocol, soft tissue augmentation was performed as a standalone procedure 3 months prior to implant placement. In the one-stage protocol, soft tissue augmentation and implant placement were performed simultaneously during the same surgical session.

Implant placement

Implant placement was performed following prosthetically driven planning, using a standardized crestal incision along the edentulous ridge in all study groups. Implant positioning was guided by a surgical template (Simplant®; Dentsply Sirona, Charlotte, USA) to ensure prosthetically driven 3D implant placement. All implants were placed at the crestal level or up to a maximum of 0.5 mm subcrestally relative to the buccal bone plate, under direct visual control.

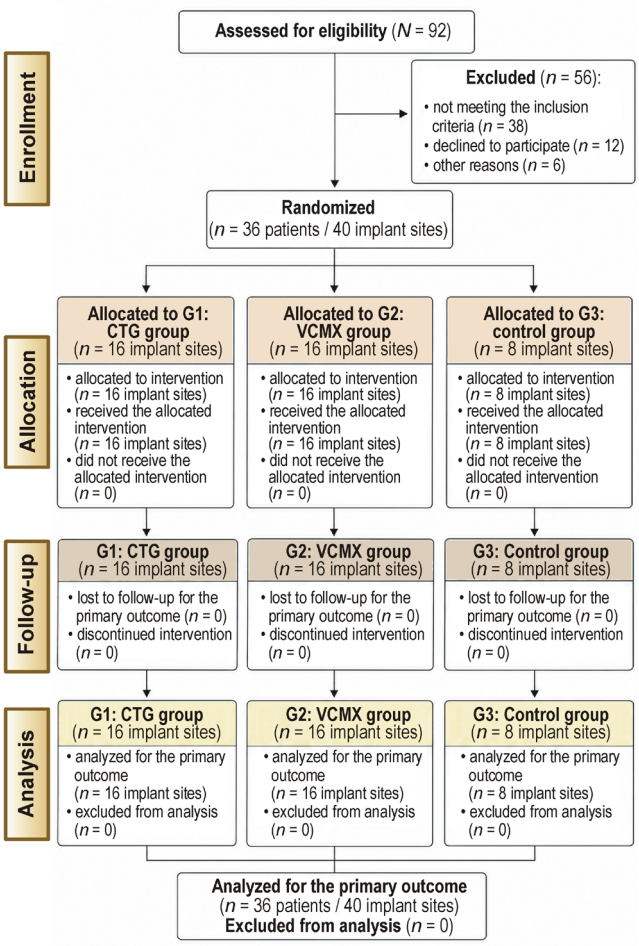

Fig. 1. CONSORT (Consolidated Standards of Reporting Trials) flow diagram illustrating patient recruitment, randomization, allocation to the study groups, follow-up, and analysis in the present randomized controlled clinical trial (RCT)

CTG – connective tissue graft; VCMX – volume-stable collagen matrix.

A minimally invasive flap approach was applied at sites without soft tissue augmentation, allowing implant insertion and submerged healing. At the sites allocated to simultaneous soft tissue augmentation (the one-stage protocol), implant placement was combined with a split-thickness flap preparation on the buccal aspect to enable the insertion of the CTG or VCMX, and to allow the complete coverage of the augmented area.

All implants were placed according to the manufacturer's surgical guidelines, using the same implant system (Astra Tech Implant System EV; Dentsply Sirona). Implants with diameters of 3.6 mm and 4.2 mm and lengths ranging from 8 to 11 mm were used, selected according to site-specific anatomical conditions.

All implants were placed using the submerged healing protocol. After a healing period of 3 months, the implants were surgically uncovered and standard healing abutments were placed for soft tissue conditioning.

Prosthetic rehabilitation

Following soft tissue conditioning, definitive prosthetic rehabilitation was performed. Implant positions were recorded using the digital impressions obtained with an intraoral scanner (Primescan®; Dentsply Sirona), and customized abutments were fabricated (Atlantis®; Dentsply Sirona).

The final restorations consisted of single-unit full-contour zirconia (ZrO_2) crowns with individualized characterization, which were screw-retained on the customized abutments. All restorations were delivered according to standard clinical protocols to ensure the appropriate occlusion, emergence profile and esthetic integration.

All surgical and prosthetic procedures were performed by a single clinician who was also involved in the study design, to ensure procedural consistency and reduce operator-related variability, in accordance with a standardized study protocol.

Figure 2 presents the study timeline for all groups.

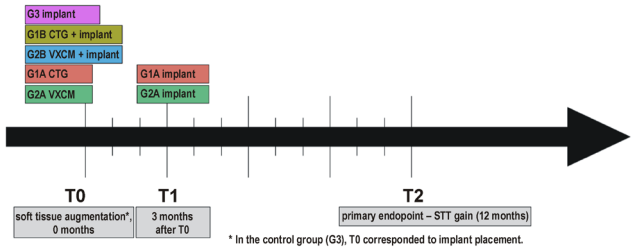

Fig.2. Schematic illustration of group allocation, the timing of soft tissue augmentation and implant placement, and outcome assessment

Patients were allocated to 3 groups: G1 (a subepithelial CTG); G2 (VCMX); and G3 (control, no soft tissue augmentation). In the two-stage protocol (G1A and G2A), soft tissue augmentation was performed at baseline (T0), followed by implant placement 3 months later (T1). In the one-stage protocol (G1B and G2B), soft tissue augmentation and implant placement were performed simultaneously at T0. In the control group (G3), implant placement corresponded to T0. Soft tissue thickness (STT) was assessed at T0, T1 and at the 12-month follow-up (T2), which represented the primary endpoint of the study.

Outcome measures

The primary and secondary outcome measures were defined a priori, while the analyses related to augmentation timing were considered exploratory. Ultrasonographic and radiographic assessments were performed by an independent examiner who was blinded to group allocation and the type of augmentation material used.

Primary outcome

The primary outcome of the study was peri-implant STT in the esthetic zone. Soft tissue thickness was assessed longitudinally, using a standardized, non-invasive ultrasonic measurement protocol, and served as the main parameter for evaluating the effects of the augmentation material and the potential influence of augmentation timing.

Primary outcome analyses included the absolute STT values at the 12-month follow-up, as well as changes in STT over time relative to baseline.

Secondary outcomes

The secondary outcomes of the study included the following: MBL around the dental implants, assessed radiographically over the observation period; implant survival, defined as the presence of clinically functional implants throughout follow-up; and biological complications, including peri-implant mucositis and peri-implantitis, diagnosed according to the established clinical and radiographic criteria. In addition, prosthetic complications, including the abutment- or crown-related technical events occurring during the follow-up period, were recorded. Implant stability was assessed using the resonance frequency analysis (RFA). The implant stability quotient (ISQ) values were recorded at implant placement and prior to the delivery of the definitive prosthetic restoration, using a handheld RFA device.

Soft tissue thickness measurements

Peri-implant STT was assessed using a standardized, non-invasive ultrasonic measurement method and served as the primary outcome of the study. All longitudinal STT measurements were performed using an ultrasonic device (Pirop®; Echo-Son, Puławy, Poland) according to the manufacturer's instructions.

Soft tissue thickness was assessed at 3 predefined measurement points along the implant axis. The crestal measurement point (P1) was located at the crest of the alveolar ridge, corresponding to the future implant emergence profile. This point was accessible only during surgical procedures, and was therefore assessed exclusively at baseline (T0) and during the pre-prosthetic phase (T1). Longitudinal analyses focused on 2 buccal measurement points that remained accessible throughout the entire observation period. Measurement point P2 was positioned buccally at the midline connecting the cementoenamel junctions (CEJs) of the adjacent teeth, along the implant axis. Measurement point P3 was located buccally at the mucogingival junction (MGJ), along the same axis. These 2 points were used for all longitudinal STT analyses (Fig. 3).

Soft tissue thickness was measured at baseline (T0), at 3 months (T1) and at the 12-month follow-up (T2), which represented the primary endpoint of the study. In the augmentation groups, baseline (T0) corresponded to the time of soft tissue augmentation, performed either as a standalone procedure in the two-stage protocol or simultaneously with implant placement in the one-stage protocol. In the control group, implant placement served as baseline (T0).

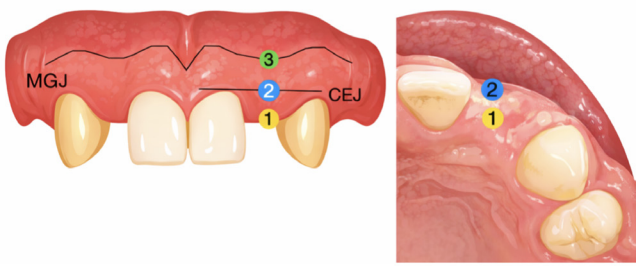

Fig. 3. Schematic illustration of the peri-implant soft tissue thickness (STT) measurement points (P1–P3) in the esthetic zone

CEJ – cementoenamel junction; MGJ – mucogingival junction.

Longitudinal changes in SST were calculated relative to baseline (T0) for each implant site, allowing the evaluation of within-site STT changes over time according to the assigned treatment pathway.

The ultrasonic measurement method used in the present study has previously been validated against direct measurements performed after the crestal incision and against the clinical measurements obtained using a millimeter-scaled periodontal probe.[21] Prior to the study, the examiner underwent calibration for the ultrasonic measurement protocol to ensure measurement consistency (Fig. 4).

Radiographic assessment of marginal bone loss

Radiographic evaluation was performed to assess MBL around the dental implants. Standardized intraoral periapical radiographs were obtained using the long-cone paralleling technique with individualized positioning devices to ensure reproducible imaging conditions.

Baseline radiographs were acquired immediately after implant placement and served as the reference for the subsequent measurements. Follow-up radiographs were obtained at the 12-month evaluation. Marginal bone loss was defined as the vertical change in the crestal bone level between baseline and the 12-month follow-up.

Radiographic images were calibrated using the known length of the implant fixture. Measurements were performed using dedicated imaging software, and the vertical distance from the implant shoulder to the first bone-to-implant contact was recorded on both the mesial and distal aspects of each implant. The mean of the mesial and distal measurements was calculated and used for statistical analysis.



Fig. 4. Representative ultrasonographic measurement of peri-implant soft tissue thickness (STT), performed at measurement point P1 during the pre-prosthetic phase (T1)

The ultrasound probe was positioned perpendicular to the mucosal surface in the peri-implant region according to the standardized measurement protocol.

Handling of correlated data

In patients receiving 2 implants, implant sites were treated as separate experimental units. To account for within-patient dependency, the applied non-parametric repeated-measures models incorporated subject-level clustering, using resampling-based procedures. This approach explicitly accounts for clustering at the subject level and allows valid statistical inference without assuming independence of observations.

Statistical analysis

No formal a priori sample size calculation was performed. The sample size was determined pragmatically based on feasibility. The present study should therefore be considered exploratory with respect to effect size estimation, in line with recent methodological recommendations emphasizing transparent reporting and interpretation of effect sizes and sample size considerations in dental research.[22] Although designed as an RCT, the study should be interpreted as exploratory due to the absence of a formal sample size calculation, and the findings should therefore be interpreted as hypothesis-generating rather than confirmatory.

No missing data was observed for the presented outcomes. Statistical analyses were performed at the implant site level. In patients receiving 2 implants, implant sites were treated as separate experimental units, and within-subject dependency was accounted for in the applied statistical models using a resampling-based non-parametric approach (MANOVA.RM).

Due to non-normal data distribution and small subgroup sizes, non-parametric statistical methods were applied. Quantitative variables are presented as medians (*Me*) with interquartile ranges (*IQR*) (Q1–Q3), and categorical variables as frequencies and percentages.

Longitudinal changes in peri-implant STT were analyzed using a non-parametric repeated-measures analysis based on ANOVA-type statistics (ATS), evaluating the associations between the treatment group, time, and their interaction. In addition, a multivariate non-parametric repeated-measures analysis for combined STT measurements at points P2 and P3 was performed using a resampling-based modified ANOVA-type statistic (MATS) with wild bootstrap inference.

Post hoc between-group and within-group comparisons were performed using the Wilcoxon rank-sum test and the Wilcoxon signed-rank test, respectively, with the Benjamini–Hochberg correction applied to control the false discovery rate.

Marginal bone loss was compared between the groups using the Kruskal–Wallis test.

All statistical tests were two-tailed, and the level of statistical significance was set at $p < 0.05$. All analyses were conducted using the R statistical computing environment (R Foundation for Statistical Computing, Vienna, Austria).

Results

Study population

A total of 36 patients (40 implant sites) were included in the final analysis. Patient recruitment, allocation, follow-up, and analysis are presented in the CONSORT (Consolidated Standards of Reporting Trials) flow diagram (Fig. 1). No patients or implant sites were lost to follow-up during the 12-month observation period. Patient recruitment was conducted between April 2022 and October 2024. The last follow-up visit of the final enrolled patient took place in October 2025. The trial was completed as planned after the recruitment of the predefined number of implant sites, with no premature termination. Implant sites were allocated to 3 study groups: G1 (CTG; $n = 16$); G2 (VCMX; $n = 16$); and G3 (control; $n = 8$). In patients receiving 2 implants, implant sites were located in different quadrants or the opposing jaws, and were treated as independent experimental units.

Baseline demographic characteristics are summarized in Table 1. The analysis was conducted at the implant-site level ($n = 40$). The median age of the study population was 35 (*IQR*: 31.75–45.25) years, with comparable distribution across the groups.

Primary outcome – peri-implant soft tissue thickness (STT)

At 12 months, the absolute difference in STT between the CTG and VCMX groups ranged from approx. 0.3 to 0.6 mm.

Subgroup analysis of STT at the crestal point (P1)

At the crestal measurement point (P1), peri-implant STT was assessed exclusively during the pre-prosthetic period, at baseline (T0) and at the 3-month follow-up (T1). The non-parametric repeated-measures analysis demonstrated a statistically significant main effect of time ($p < 0.001$) and a significant time × group interaction ($p < 0.001$), whereas the main effect of group was not statistically significant ($p = 0.27$).

At baseline (T0), no statistically significant differences in crestal STT were observed between the study subgroups, indicating comparable baseline conditions. The median STT values at T0 were 2.06 (1.17–2.30) mm in G1A, 2.07 (1.82–2.36) mm in G1B, 2.30 (1.50–2.75) mm in G2A, 2.08 (1.79–2.19) mm in G2B, and 2.13 (1.64–2.40) mm in the control group (G3). Post hoc analyses confirmed the absence of statistically significant between-group differences at baseline.

At the pre-prosthetic follow-up (T1), increases in STT were observed in all augmentation subgroups (G1A, G1B, G2A, and G2B), whereas no increase was observed in the control group (G3). The median STT increased from 2.06 (1.17–2.30) mm to 2.77 (2.05–3.14) mm in the two-stage CTG subgroup (G1A), from 2.07 (1.82–2.36) mm to 3.04 (2.75–3.13) mm in the one-stage CTG subgroup (G1B), and from 2.08 (1.79–2.19) mm to 2.69 (2.20–3.26) mm in the one-stage VCMX subgroup (G2B). In contrast, the median STT in the two-stage VCMX subgroup (G2A) remained unchanged (2.30 (1.50–2.75) mm at T0 vs. 2.30 (2.09–2.65) mm at T1), while a slight numerical decrease was observed in the control group (from 2.13 (1.64–2.40) mm to 1.88 (1.49–2.31) mm) (Fig. 5).

After adjustment for multiple testing, a statistically significant between-group difference at T1 was identified exclusively between the one-stage CTG subgroup (G1B) and the control group (G3). Within-group post hoc analyses demonstrated statistically significant increases in STT from T0 to T1 in both CTG subgroups and in the one-stage VCMX (G2B) subgroup, whereas changes in the two-stage VCMX subgroup (G2A) and in the control group (G3) were not statistically significant (Table 2).

Longitudinal STT analysis at measurement points P2 and P3 (primary endpoint)

At measurement points P2 and P3, peri-implant STT was assessed longitudinally at baseline (T0), at 3 months (T1) and at the 12-month follow-up (T2). A multivariate non-parametric repeated-measures analysis demonstrated statistically significant main effects of time and group, as well as a significant time × group interaction (all $p < 0.001$; MANOVA.RM with wild bootstrap MATS).

Table 1. Baseline demographic characteristics

Variable		G1 (CTG) $n = 16$	G2 (VCMX) $n = 16$	G3 (control) $n = 8$	Total $N = 40$
Age [years] *Me* (*IQR*)		34.0 (32.0–43.6)	34.5 (32.5–44.3)	39.5 (28.3–49.5)	35.0 (31.8–45.3)
Sex *n* (%)	M	8 (50.0)	10 (62.5)	5 (62.5)	23 (57.5)
	F	8 (50.0)	6 (37.5)	3 (37.5)	17 (42.5)

Me – median; *IQR* – interquartile range; M – male; F – female.

Table 2. Peri-implant soft tissue thickness (STT) [mm] at the crestal measurement point (P1)

Groups	T0	T1	Δ T1–T0	*p*-value (within-group)
G1A (CTG, two-stage)	2.06 (1.17–2.30)	2.77 (2.05–3.14)	+0.71	0.026*
G1B (CTG, one-stage)	2.07 (1.82–2.36)	3.04 (2.75–3.13)	+0.97	0.026*
G2A (VCMX, two-stage)	2.30 (1.50–2.75)	2.30 (2.09–2.65)	0.00	NS
G2B (VCMX, one-stage)	2.08 (1.79–2.19)	2.69 (2.20–3.26)	+0.61	0.026*
G3 (control)	2.13 (1.64–2.40)	1.88 (1.49–2.31)	–0.25	NS

Data presented as *Me* (*IQR*).
* statistically significant; NS – non-significant. Within-group comparisons between baseline (T0) and the pre-prosthetic follow-up (T1) were performed using the Wilcoxon signed-rank test. Between-group post hoc comparisons at T1 were adjusted for multiple testing using the Benjamini–Hochberg procedure.

Across all augmentation subgroups (CTG and VCMX), a statistically significant increase in STT was observed between T0 and T1 at both measurement points.

At measurement point P2, the median STT values increased in the CTG subgroups from 0.88 (0.70–1.10) mm in G1A and 0.75 (0.61–0.87) mm in G1B at baseline to 2.51 (2.30–3.26) mm and 2.00 (1.70–2.34) mm at T1, respectively. In the VCMX subgroups, the median STT increased from 0.66 (0.60–1.14) mm in G2A and 0.74 (0.59–0.91) mm in G2B at T0 to 1.80 (1.60–2.80) mm and 2.21 (2.00–2.49) mm at T1, respectively.

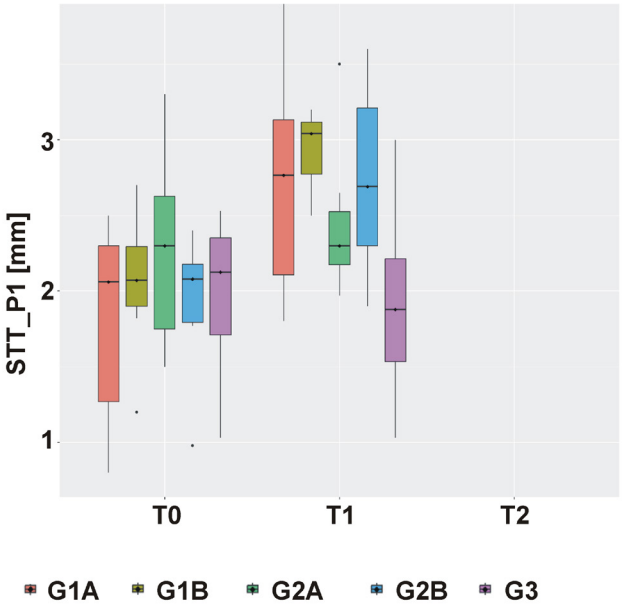

Fig. 5. Peri-implant soft tissue thickness (STT) at the crestal measurement point (P1) – subgroup analysis

The X axis represents the assessment time points (baseline (T0) and pre-prosthetic follow-up (T1)), and the Y axis represents peri-implant STT expressed in millimeters. Boxplots illustrate the STT values at P1 in the study subgroups: G1A (CTG, two-stage); G1B (CTG, one-stage); G2A (VCMX, two-stage); G2B (VCMX, one-stage), and the control group without soft tissue augmentation (G3). Boxes represent median values and interquartile ranges (*Me* (*IQR*)), with whiskers indicating data dispersion and dots representing individual measurements.

A comparable pattern was observed at measurement point P3, where the median STT values increased from the baseline levels of approx. 0.5–0.8 mm to approx. 1.7–2.5 mm at T1 in all augmentation subgroups.

In contrast, the control group (G3) demonstrated no statistically significant changes in STT at either P2 or P3, with the median values remaining close to baseline at all time points. Post hoc analyses revealed statistically significant differences between all augmentation groups and the control group already at T1.

In the CTG subgroups, the STT values remained stable between T1 and T2. At P2, the median STT values at T2 amounted to 2.75 (2.30–3.00) mm in G1A and 2.40 (2.20–2.51) mm in G1B. At P3, the median STT values at T2 were 2.00 (1.89–2.70) mm and 2.20 (1.82–2.49) mm, respectively.

In the VCMX subgroups, changes between T1 and T2 differed according to augmentation timing. At P2, the median STT at T2 amounted to 2.33 (1.90–2.58) mm in the two-stage subgroup (G2A), whereas in the one-stage subgroup (G2B), the median STT decreased from 2.21 (2.00–2.49) mm at T1 to 1.83 (1.30–2.13) mm at T2. At P3, the median STT values at T2 were 1.80 (1.37–2.53) mm in G2A and 1.55 (1.42–1.83) mm in G2B.

At the 12-month follow-up (T2), the STT values in all augmentation subgroups remained significantly higher than in the control group at both measurement points. Between-group comparisons at T2 demonstrated higher STT values in the CTG subgroups as compared to the VCMX subgroups in several comparisons, whereas other CTG–VCMX comparisons did not reach statistical significance.

The data is presented in Fig. 6 and 7, and in Table 3.

Secondary outcomes

Implant stability

Implant stability was assessed using RFA. The median ISQ values were high at implant placement and remained stable prior to prosthetic loading, indicating adequate

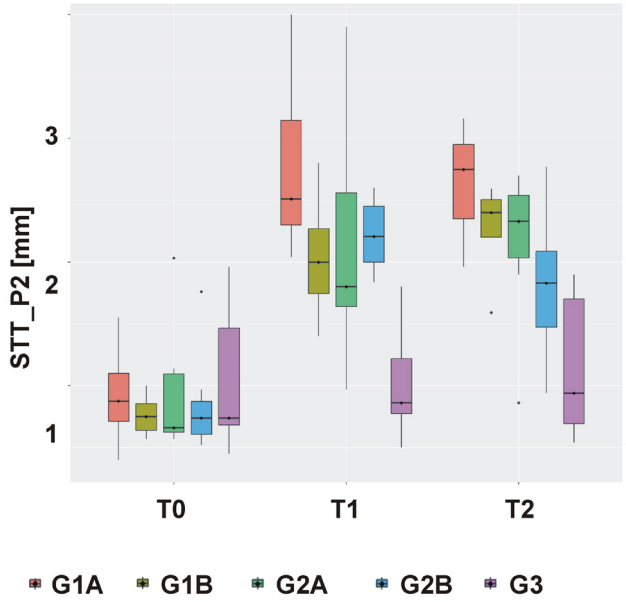

Fig. 6. Peri-implant soft tissue thickness (STT) at measurement point P2 – longitudinal subgroup analysis

The X axis represents the assessment time points (baseline (T0), 3 months (T1) and 12 months (T2)), and the Y axis represents peri-implant STT expressed in millimeters. Boxplots illustrate the STT values at P2 in the study subgroups: G1A (CTG, two-stage); G1B (CTG, one-stage); G2A (VCMX, two-stage); G2B (VCMX, one-stage), and the control group without soft tissue augmentation (G3). Boxes represent median values and interquartile ranges (*Me* (*IQR*)), with whiskers indicating data dispersion and dots representing individual measurements.

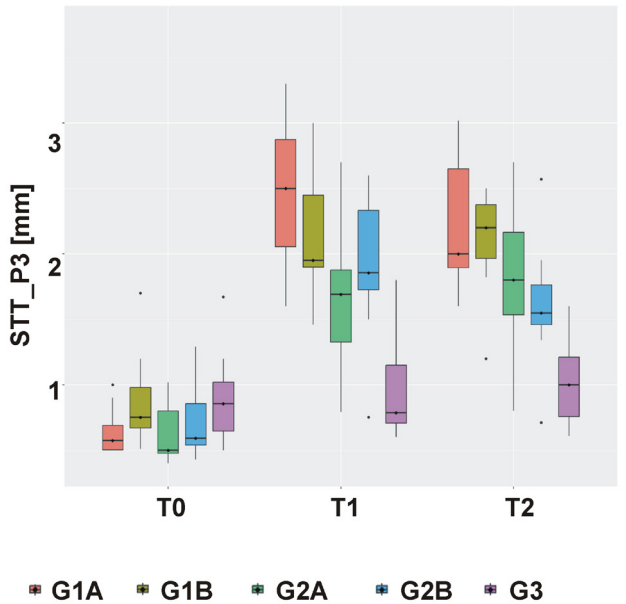

Fig. 7. Peri-implant soft tissue thickness (STT) at measurement point P3 – longitudinal subgroup analysis

The X axis represents the assessment time points (baseline (T0), 3 months (T1) and 12 months (T2)), and the Y axis represents peri-implant STT expressed in millimeters. Boxplots illustrate the STT values at P2 in the study subgroups: G1A (CTG, two-stage); G1B (CTG, one-stage); G2A (VCMX, two-stage); G2B (VCMX, one-stage), and the control group without soft tissue augmentation (G3). Boxes represent median values and interquartile ranges (*Me* (*IQR*)), with whiskers indicating data dispersion and dots representing individual measurements.

Table 3. Peri-implant soft tissue thickness (STT) [mm] at points P2 and P3

Point	Group	T0	T1	T2	Significance summary
P2	G1A (CTG, two-stage)	0.88 (0.70–1.10)	2.51 (2.30–3.26)	2.75 (2.30–3.00)	† T0–T1 † T0–T2 * T1 * T2
P2	G1B (CTG, one-stage)	0.75 (0.61–0.87)	2.00 (1.70–2.34)	2.40 (2.20–2.51)	† T0–T1 † T0–T2 * T1 * T2
P2	G2A (VCMX, two-stage)	0.66 (0.60–1.14)	1.80 (1.60–2.80)	2.33 (1.90–2.58)	† T0–T1 † T0–T2 * T2
P2	G2B (VCMX, one-stage)	0.74 (0.59–0.91)	2.21 (2.00–2.49)	1.83 (1.30–2.13)	† T0–T1 † T0–T2 * T1 * T2
P2	G3 (control)	0.74 (0.66–1.54)	0.86 (0.75–1.40)	0.94 (0.69–1.74)	NS
P3	G1A (CTG, two-stage)	0.58 (0.50–0.69)	2.50 (2.05–2.93)	2.00 (1.89–2.70)	† T0–T1 † T0–T2 * T1 * T2
P3	G1B (CTG, one-stage)	0.75 (0.63–1.20)	1.95 (1.90–2.60)	2.20 (1.82–2.49)	† T0–T1 † T0–T2 * T1 * T2
P3	G2A (VCMX, two-stage)	0.50 (0.45–1.00)	1.69 (1.25–1.90)	1.80 (1.37–2.53)	† T0–T1 † T0–T2 * T1 * T2
P3	G2B (VCMX, one-stage)	0.59 (0.54–0.98)	1.86 (1.65–2.34)	1.55 (1.42–1.83)	† T0–T1 † T0–T2 * T1 * T2
P3	G3 (control)	0.86 (0.63–1.08)	0.79 (0.71–1.20)	1.00 (0.72–1.24)	NS

Data presented as *Me* (*IQR*).
* statistically significant difference vs. the control group (G3); † significant within-group change vs. T0; NS – non-significant (Benjamini–Hochberg correction).

primary and secondary implant stability across all study groups. All implants reached ISQ values considered suitable for prosthetic loading.

Marginal bone loss

Radiographic evaluation demonstrated low MBL values across the study population during the 12-month follow-up period. When all implants were analyzed collectively, the median MBL was 0.2 (0.0–0.6) mm, with a maximum observed value of 1.5 mm.

The analysis of the main study groups revealed low median MBL values in all groups, amounting to 0.1 mm in the CTG group (G1), 0.5 mm in the VCMX group (G2) and 0.3 mm in the control group (G3). Subgroup analysis stratified by the augmentation material and timing similarly demonstrated low MBL values, with median bone loss not exceeding 0.7 mm in any subgroup.

Intergroup comparison using the Kruskal–Wallis rank-sum test revealed no statistically significant differences in MBL between the analyzed subgroups (χ^2 = 3.88; df = 4; p = 0.42).

Biological and prosthetic complications

Biological and prosthetic complications were assessed at each follow-up visit, using the predefined clinical and radiographic criteria. No biological complications, including peri-implant mucositis or peri-implantitis, were observed at any implant site during the 12-month follow-up period. Similarly, no prosthetic complications, such as abutment loosening, screw fracture or crown-related technical events, were recorded throughout the observation period.

Discussion

Principal findings

The principal finding of this RCT was that peri-implant soft tissue augmentation was associated with a significant and clinically relevant increase in STT as compared to non-augmented control sites, irrespective of the augmentation material used. While both augmentation approaches were associated with increased SST, subepithelial CTGs tended to achieve significantly higher final peri-implant SST than VCMX, with differences in the range of approx. 0.3–0.6 mm at the 12-month follow-up.

Importantly, no statistically significant differences related to augmentation timing were detected in either the CTG or the VCMX groups with respect to the final STT outcomes.

Taken together, these findings suggest that while CTG appeared to be associated with a greater and more stable increase in peri-implant STT, VCMX may provide a clinically meaningful alternative capable of improving soft tissue conditions as compared to non-augmented sites.

Comparison with previous studies

Recent systematic reviews and RCTs provide a consistent clinical framework for the present findings. A recent systematic review and meta-analysis by Ramanauskaite et al. demonstrated that autogenous CTGs provide greater mucosal thickness gain as compared to soft tissue substitutes, while differences in patient-reported esthetic outcomes appear to be less pronounced.[23] In a network meta-analysis, Tommasato et al. ranked CTGs as the most effective approach for increasing peri-implant STT, while VCMXs, including Fibro-Gide, achieved slightly lower but clinically relevant thickness gains with reduced patient morbidity.[12] Similarly, a meta-analysis by Ríos-Osorio et al. demonstrated that the reported inferiority of collagen matrices was primarily driven by non-cross-linked materials, whereas volume-stable cross-linked matrices achieved mucosal thickness gains comparable to CTG, with pooled intergroup differences close to zero.[2] This pattern appears consistent with the present findings, in which CTG tended to achieve greater final STT than VCMX, while both modalities resulted in clinically meaningful tissue augmentation.

Long-term randomized clinical data further supports these observations. In a 5-year follow-up study, Thoma et al. reported STT gains of approx. 0.5–0.6 mm for both CTG and VCMX, with no clinically relevant intergroup differences in volumetric outcomes.[24] Using ultrasonographic measurements, the present study showed a comparable order of magnitude of soft tissue augmentation, despite differences in the study design, augmentation timing and assessment methodology.

In contrast, a large multicenter RCT by Hämmerle et al. reported inconclusive evidence regarding the non-inferiority of VCMX as compared to CTG for crestal mucosal thickness, with differences of approx. 0.5 mm favoring CTG.[25] Notably, these differences appear consistent with the magnitude of intergroup differences observed in the present study, and may be partly explained by variations in the anatomical focus and outcome assessment. Nevertheless, comparisons between studies should be interpreted cautiously due to differences in the study design, augmentation timing protocols and outcome assessment methodologies.

Differences between autogenous grafts and collagen matrices may be explained by distinct patterns of vascularization and remodeling, as CTGs demonstrate greater vascular integration, whereas VCMXs are characterized by reduced perfusion and a denser connective tissue architecture, as demonstrated in both preclinical and human histological studies.[26–28]

Preclinical and histological studies provide a biological rationale for the clinically observed behavior of VCMXs. Experimental investigations demonstrated rapid vascularization, progressive tissue integration and greater volumetric stability of VCMXs in comparison with non-cross-linked collagen matrices, accompanied by the absence of a chronic foreign-body reaction. These observations have been consistently reported in preclinical models by Caballe-Serrano et al.,[27] Naenni et al.[28] and Imber et al.,[29] supporting the favorable biological performance of VCMXs.

Importantly, human histological data reported by Smirani et al. showed that the sites augmented with Fibro-Gide exhibited a denser connective tissue architecture with reduced vascularization as compared to CTG, despite achieving comparable clinical soft tissue dimensions.[26] Collectively, these findings support the present clinical observations and suggest distinct remodeling patterns rather than differences in the magnitude of the achieved clinical effect.

Timing of soft tissue augmentation

Despite extensive research on peri-implant soft tissue augmentation, the influence of augmentation timing has not been systematically investigated. Previous clinical trials applied augmentation either at implant placement or at later surgical stages, without formally comparing timing-related effects.

Limited randomized evidence by Hadzik et al.[30] and Puzio et al.[31,32] suggests more pronounced and stable increases in SST when augmentation is performed prior to implant placement, using CTGs or a non–volume-stable collagen matrix. However, these findings cannot be directly extrapolated to volume-stable cross-linked collagen matrices due to fundamental differences in material properties and remodeling behavior.

In the present TCT, augmentation timing was prospectively evaluated for both CTG and VCMX, using standardized ultrasonographic measurements. While timing appeared to influence early remodeling patterns, the final peri-implant STT values exceeded 2 mm in all augmented sites, and were comparable between the one-stage and two-stage protocols. These findings should be interpreted with caution, as the study may be underpowered to detect small but clinically relevant differences. Within these limitations, the absence of statistical significance should not be interpreted as the evidence of equivalence. These findings suggest that augmentation timing may affect early healing dynamics, whereas long-term soft tissue dimensions may be less dependent on the surgical stage at which augmentation is performed.

Hard tissue stability and safety

Peri-implant hard tissue stability appeared to be preserved regardless of the augmentation modality or timing, with stable marginal bone levels observed across all groups. This finding is of particular clinical relevance, as MBL and peri-implant tissue conditions have been identified as core outcome domains in contemporary consensus frameworks for implant dentistry.[10] These findings are consistent with long-term clinical observations indicating that inadequate peri-implant soft tissue conditions, including insufficient keratinized mucosa, are associated with an increased risk of peri-implant disease and greater MBL over time.[33] No statistically significant association between STT and MBL was detected. Importantly, following soft tissue augmentation, all augmented study sites exhibited a peri-implant mucosal thickness exceeding 2 mm.

The clinical relevance of achieving an adequate SST has been previously highlighted by Linkevicius et al., who demonstrated significantly greater MBL around the implants placed at sites with a mucosal thickness ≤2 mm.[13,34] Similarly, a recent systematic review and network meta-analysis by Tommasato et al. reported that both keratinized mucosa width ≥2 mm and STT > 2 mm were associated with reduced inflammation, recession and peri-implant bone loss, suggesting a protective role of increased soft tissue dimensions.[12] However, despite this growing body of evidence, no clear consensus exists regarding a definitive threshold, and the 2-mm value should not be interpreted as a strict biological cutoff, but rather as a clinically derived reference point reflecting a transition toward more favorable tissue stability conditions. In this context, the absence of significant differences in MBL observed in the present study may partly be explained by the achievement of a sufficiently thick peri-implant soft tissue envelope across the augmented treatment groups, thereby minimizing the influence of the baseline tissue thickness on bone-level changes.

In addition, no biological or technical complications, implant losses, or adverse tissue reactions were recorded, supporting the clinical safety of the applied augmentation procedures within the limitations of the present follow-up period.

Clinical implications

The present findings suggest that both autogenous CTGs and xenogeneic VCMXs may be considered clinically viable options for peri-implant soft tissue augmentation when the primary clinical objective is to achieve an adequate final STT. From a clinical perspective, the choice of the augmentation modality may therefore also be guided by patient-related factors, surgical morbidity and operator preference rather than by the expectations of differences in long-term soft tissue dimensions, which is consistent with the reports highlighting variability in clinicians' knowledge, awareness and decision-making regarding peri-implant soft and hard tissue management.[35] Although patient-reported outcomes and esthetic perception may also contribute to clinical decision-making, the present study was primarily designed to evaluate biological and dimensional peri-implant soft tissue outcomes. The observed intergroup difference in STT between CTG and VCMX (0.3–0.6 mm) may nevertheless be clinically relevant in specific clinical scenarios, particularly at sites with an initially thin soft tissue phenotype.

Furthermore, as augmentation timing primarily influenced early healing dynamics, without statistically significant differences in the final STT being detected, clinicians may consider individualizing the sequencing of soft tissue augmentation according to the clinical situation, surgical workflow and prosthetic requirements. Importantly, achieving a peri-implant STT exceeding clinically relevant thresholds appears sufficient to maintain peri-implant hard tissue stability, supporting a pragmatic and patient-centered approach to soft tissue management. Emerging evidence indicates that genetic and epigenetic factors may modulate the peri-implant tissue response, bone remodeling and implant success. These observations support the future development of personalized, genomics-based approaches in implant therapy aimed at improving treatment predictability and long-term outcomes.[36] These findings

are aligned with the 2026 GCCG,[10] representing the first globally developed evidence-based guideline framework in implant dentistry, which emphasizes standardized outcome domains and peri-implant tissue management strategies.[37,38]

Representative clinical cases illustrating soft tissue changes following augmentation with CTG and VCMX are presented in Fig. 8.

Limitations

Several limitations of the present study should be acknowledged. Patient-reported outcome measures (PROMs) and esthetic outcomes were not included among the predefined study endpoints. First, the sample size was limited and no formal a priori sample size calculation was performed, which might affect the statistical power and increase the risk of type II error, particularly in subgroup analysis related to augmentation timing. Second, the trial was conducted at a single clinical center and all surgical procedures were performed by a single operator, which might limit the external generalizability of the findings. In addition, due to the nature of the interventions, operator blinding was not feasible, which might introduce potential bias. Third, the follow-up period was limited to 12 months; therefore, potential long-term differences in soft tissue behavior beyond this observation period cannot be excluded. Finally, soft tissue assessment was based on ultrasonographic measurements at the predefined points, which did not permit a comprehensive volumetric analysis of peri-implant soft tissue changes. Although this approach provided standardized and reproducible measurements of STT, it might not fully capture the 3D volumetric and contour alterations of peri-implant soft tissues.

Conclusions

Peri-implant soft tissue augmentation was associated with a significant and clinically relevant increase in STT as compared to non-augmented control sites. While subepithelial CTGs tended to achieve greater final STT than VCMX, both approaches provided clinically meaningful improvement in peri-implant soft tissue dimensions.

The timing of soft tissue augmentation, performed either prior to implant placement or simultaneously with implant insertion, was not associated with statistically significant differences in the final STT outcomes within the limitations of this exploratory study and the 12-month follow-up, despite differences in early remodeling patterns. Moreover, stable marginal bone levels, and the absence of biological or technical complications support the short-term clinical safety of both augmentation modalities and protocols.

Within the limitations of the present study, VCMXs may represent a reliable alternative to autogenous CTGs for peri-implant soft tissue augmentation, potentially allowing clinicians to individualize treatment strategies based on clinical conditions and patient-related factors.

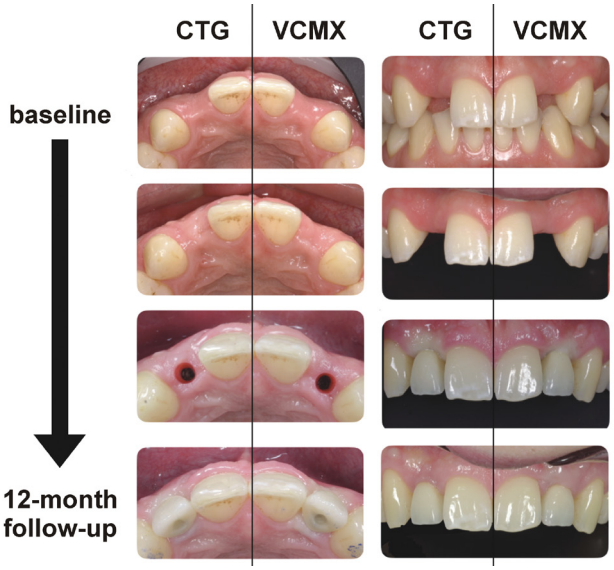

Fig. 8. Representative clinical cases illustrating peri-implant soft tissue augmentation using a subepithelial connective tissue graft (CTG) and a volume-stable collagen matrix (VCMX)

Standardized intraoral photographs are presented at baseline and after 12-month follow-up.

Trial registration

The trial was registered at ClinicalTrials.gov (NCT07324187).

Ethics approval and consent to participate

This randomized controlled clinical trial was approved by the Bioethics Committee at Wroclaw Medical University, Poland (approval No. KB-863/2021; October 28, 2021), and conducted in accordance with the Declaration of Helsinki and the Good Clinical Practice guidelines. Written informed consent was obtained from all participants prior to enrollment in the study.

Data availability

The datasets supporting the findings of the current study are available from the corresponding author on reasonable request.

Consent for publication

Not applicable.

Use of AI and AI-assisted technologies

The original data was not generated, processed or analyzed using AI technologies. The authors take full responsibility for the content of the manuscript.

ORCID iDs

Jakub Hadzik https://orcid.org/0000-0002-2353-3198
Marzena Dominiak https://orcid.org/0000-0001-8943-0549

References

1. Sun TC, Chang TK. Soft tissue management around dental implant in esthetic zone – the current concepts and novel techniques. *J Dent Sci*. 2024;19(3):1348–1358. doi:10.1016/j.jds.2024.03.003
2. Ríos-Osorio N, Orozco-Agudelo M, Cespedes-Moreno I, et al. Comparative outcomes of xenogeneic collagen matrices and autogenous graft-based techniques to increase mucosal thickness and keratinised mucosa width at implant sites: Are autologous grafts still the gold standard? A systematic review and meta-analysis of randomised clinical trials. *J Periodontal Implant Sci*. 2026;56(2):87–118. doi:10.5051/jpis.2500260013
3. Ravidà A, Arena C, Tattan M, et al. The role of keratinized mucosa width as a risk factor for peri-implant disease: A systematic review, meta-analysis, and trial sequential analysis. *Clin Implant Dent Relat Res*. 2022;24(3):287–300. doi:10.1111/cid.13080
4. Bassetti M, Kaufmann R, Salvi GE, Sculean A, Bassetti R. Soft tissue grafting to improve the attached mucosa at dental implants: A review of the literature and proposal of a decision tree. *Quintessence Int*. 2015;46(6):499–510. doi:10.3290/j.qi.a33688
5. Thoma DS, Mühlemann S, Jung RE. Critical soft-tissue dimensions with dental implants and treatment concepts. *Periodontol 2000*. 2014;66(1):106–118. doi:10.1111/prd.12045
6. Eroglu ZT, Sen DO, Oncu E. Association of peri-implant keratinized mucosa width and mucosal thickness with early bone loss: A cross-sectional study. *J Clin Med*. 2024;13(7):1936. doi:10.3390/jcm13071936
7. Bajaj V, Kolte AP, Kolte R, Bawankar PV. Comparative evaluation of immediate implant placement and provisionalization (IIPP) with and without a concentrated growth factor-enriched bone graft: A randomized controlled trial. *Dent Med Probl*. 2025;62(3):449–459. doi:10.17219/dmp/170045
8. Dulinska-Litewka J, Wilisowski D, Felkle D. Influence of the soft tissue thickness and the levels of vitamin D3 as important factors in bone preservation around the dental implant platform: A retrospective observational study. *Dent Med Probl*. 2025;62(3):499–504. doi:10.17219/dmp/179004
9. Wang HL, Avila-Ortiz G, Monje A, et al.; AO/AAP Consensus Participants. AO/AAP consensus on prevention and management of peri-implant diseases and conditions: Summary report. *J Periodontol*. 2025;96(6):519–541. doi:10.1002/JPER.25-0270
10. Brunello G, Lin GH, Kopp I, et al. 1st Global Consensus for Clinical Guidelines: Identifying a core outcome set for implant dentistry in edentulous maxilla rehabilitation. *Clin Oral Implants Res*. 2026;37(Suppl 30):S108–S120. doi:10.1111/clr.70075
11. Sanz M, Schwarz F, Herrera D, et al. Importance of keratinized mucosa around dental implants: Consensus report of group 1 of the DGI/SEPA/Osteology Workshop. *Clin Oral Implants Res*. 2022;33(Suppl 23):47–55. doi:10.1111/clr.13956
12. Tommasato G, Del Fabbro M, Oliva N, et al. Autogenous graft versus collagen matrices for peri-implant soft tissue augmentation. A systematic review and network meta-analysis. *Clin Oral Investig*. 2024;28(5):300. doi:10.1007/s00784-024-05684-5
13. Linkevicius T, Apse P, Grybauskas S, Puisys A. The influence of soft tissue thickness on crestal bone changes around implants: A 1-year prospective controlled clinical trial. *Int J Oral Maxillofac Implants*. 2009;24(4):712–719. PMID:19885413.
14. Fernandes GVdO, Martins BGdS, Fraile JF. Revisiting peri-implant diseases in order to rethink the future of compromised dental implants: Considerations, perspectives, treatment, and prognosis. *Dent Med Probl*. 2024;61(5):637–640. doi:10.17219/dmp/187215
15. Rondone EM, Leitão-Almeida B, Pereira MS, Fernandes GVO, Borges T. The use of tissue grafts associated with immediate implant placement to achieve better peri-implant stability and efficacy: A systematic review and meta-analysis. *J Clin Med*. 2024;13(3):821. doi:10.3390/jcm13030821
16. Mounssif I, Bentivogli V, Rendón A, et al. Peri-implant soft tissue augmentation with connective tissue graft substitutes. *Appl Sci*. 2025;15(18):10178. doi:10.3390/app151810178
17. Ibrahim A, Saymeh R. Alveolar ridge preservation with Fibro-Gide or connective tissue graft: A randomized controlled trial of soft and hard tissue changes. *Clin Exp Dent Res*. 2024;10(4):e929. doi:10.1002/cre2.929
18. Thoma DS, Gasser TJ, Jung RE, Hämmerle CH. Randomized controlled clinical trial comparing implant sites augmented with a volume-stable collagen matrix or an autogenous connective tissue graft: 3-year data after insertion of reconstructions. *J Clin Periodontol*. 2020;47(5):630–639. doi:10.1111/jcpe.13271
19. Miguel MM, Mathias-Santamaria IF, Kopereck MS, Martins TM, Nunes MP, Santamaria MP. A volume-stable collagen matrix (VCMX) to treat single gingival recessions associated with partially restored noncarious cervical lesions: A case series. *Int J Periodontics Restorative Dent*. 2025;45(1):21–29. doi:10.11607/prd.6924
20. Naenni N, Bienz SP, Benic GI, Jung RE, Hämmerle CH, Thoma DS. Volumetric and linear changes at dental implants following grafting with volume-stable three-dimensional collagen matrices or autogenous connective tissue grafts: 6-month data. *Clin Oral Investig*. 2018;22(3):1185–1195. doi:10.1007/s00784-017-2210-3
21. Hadzik J, Kubasiewicz-Ross P, Kujawa K, Gedrange T, Dominiak M. Methodological validation of the PIROP ultrasound-based system for measuring peri-implant soft tissue thickness in a clinical setting. *J Clin Med*. 2026;15(4):1581. doi:10.3390/jcm15041581
22. Zieliński G, Więckiewicz M. New effect size and sample size guidelines in dentistry. *Dent Med Probl*. 2025;62(5):907–917. doi:10.17219/dmp/210478
23. Ramanauskaite A, Sadilina S, Schwarz F, Cafferata EA, Strauss FJ, Thoma DS. Soft-tissue volume augmentation during early, delayed, and late dental implant therapy: A systematic review and meta-analysis on professionally determined esthetics and self-reported patient satisfaction on esthetics. *Periodontol 2000*. 2025. doi:10.1111/prd.12628
24. Thoma DS, Gasser TJ, Hämmerle CH, Strauss FJ, Jung RE. Soft tissue augmentation with a volume-stable collagen matrix or an autogenous connective tissue graft at implant sites: Five-year results of a randomized controlled trial post implant loading. *J Periodontol*. 2023;94(2):230–243. doi:10.1002/JPER.22-0226
25. Hämmerle CH, Jepsen K, Sailer I, et al. Efficacy of a collagen matrix for soft tissue augmentation after implant placement compared to connective tissue grafts: A multicenter, noninferiority, randomized controlled trial. *Clin Oral Implants Res*. 2023;34(9):999–1013. doi:10.1111/clr.14127
26. Smirani R, Strauss FJ, Hitz S, Jung RE, Kraus R, Thoma DS. Tissue integration and vascularization of volume collagen matrices and connective tissue grafts following peri-implant soft tissue augmentation: A secondary histological analysis. *Swiss Dent J*. 2025;135(2):37–42. doi:10.61872/sdj-2025-02-04
27. Caballé-Serrano J, Zhang S, Ferrantino L, Simion M, Chappuis V, Bosshardt DD. Tissue response to a porous collagen matrix used for soft tissue augmentation. *Materials (Basel)*. 2019;12(22):3721. doi:10.3390/ma12223721
28. Naenni N, Walter P, Hämmerle CH, Jung RE, Thoma DS. Augmentation of soft tissue volume at pontic sites: A comparison between a cross-linked and a non-cross-linked collagen matrix. *Clin Oral Investig*. 2021;25(3):1535–1545. doi:10.1007/s00784-020-03461-8
29. Imber JC, Roccuzzo A, Stähli A, et al. Immunohistochemical evaluation of periodontal regeneration using a porous collagen scaffold. *Int J Mol Sci*. 2021;22(20):10915. doi:10.3390/ijms222010915
30. Hadzik J, Błaszczyszyn A, Gedrange T, Dominiak M. Soft-tissue augmentation around dental implants with a connective tissue graft (CTG) and xenogeneic collagen matrix (CMX) – 5-year follow-up. *J Clin Med*. 2023;12(3):924. doi:10.3390/jcm12030924
31. Puzio M, Hadzik J, Błaszczyszyn A, Gedrange T, Dominiak M. Soft tissue augmentation around dental implants with connective tissue graft (CTG) and xenogenic collagen matrix (XCM). 1-year randomized control trail. *Ann Anat*. 2020;230:151484. doi:10.1016/j.aanat.2020.151484
32. Puzio M, Błaszczyszyn A, Hadzik J, Dominiak M. Ultrasound assessment of soft tissue augmentation around implants in the aesthetic zone using a connective tissue graft and xenogeneic collagen matrix – 1-year randomised follow-up. *Ann Anat*. 2018;217:129–141. doi:10.1016/j.aanat.2017.11.003

33. Roccuzzo A, Imber JC, Stähli A, et al. Role of keratinized mucosa on the risk of peri-implant diseases and soft tissue dehiscence in the posterior mandible – a 20-year prospective cohort study. *J Periodontal Res*. 2025;60(12):1212–1221. doi:10.1111/jre.70018
34. Linkevicius T, Apse P, Grybauskas S, Puisys A. Influence of thin mucosal tissues on crestal bone stability around implants with platform switching: A 1-year pilot study. *J Oral Maxillofac Surg*. 2010;68(9):2272–2277. doi:10.1016/j.joms.2009.08.018
35. Raghavendra Vamsi A, Shenoy SB, Chandran T. Implant practitioners' knowledge, awareness and attitudes regarding soft and hard tissue considerations at a single implant site: A questionnaire study. *Dent Med Probl*. 2023;60(3):427–435. doi:10.17219/dmp/146875
36. Prabhu SS, Narayana A, Krishnamoorthy G. Genomics in dental implantology: The role of genetic and epigenetic factors in dental implant failure – a narrative review. *Dent Med Probl*. 2025;62(5):977–986. doi:10.17219/dmp/207334
37. Pala K, Neugebauer J, Buser D, et al. Consensus report of Group 2 of the 1st Global Consensus for Clinical Guidelines for the Rehabilitation of the Edentulous Maxilla: Zygomatic, standard-length, and short implant-supported prostheses. *Clin Oral Implants Res*. 2026;37(Suppl 30):S49–S67. doi:10.1111/clr.70081
38. Brunello G, Strauss FJ, Milinkovic I, Kopp I, Schwarz F, Wang HL. 1st Global Consensus for Clinical Guidelines for the Rehabilitation of the Edentulous Maxilla: A single-round survey on sinus lift and alveolar bone augmentation techniques. *Clin Oral Implants Res*. 2026;37(Suppl 30):S166–S187. doi:10.1111/clr.70018

Original paper

Comparative efficacy of supplementary techniques, with and without a solvent, for removing root filling remnants from canal irregularities: An in vitro study

Ronald Wigler[A–F], Nuphar Blau-Venezia[C,E], Tomer Goldberger[C,E,F]

Department of Endodontics, The Maurice and Gabriela Goldschleger School of Dental Medicine, Tel Aviv University, Israel

A – research concept and design; B – collection and/or assembly of data; C – data analysis and interpretation;
D – writing the article; E – critical revision of the article; F – final approval of the article

Dental and Medical Problems, ISSN 1644-387X (print), ISSN 2300-9020 (online) *Dent Med Probl*. 2026;63(5):1121–1126

Address for correspondence
Ronald Wigler
E-mail: dr.wigler@gmail.com

Funding sources
None declared

Conflict of interest
None declared

Acknowledgements
None declared

Received on March 26, 2025
Reviewed on May 2, 2025
Accepted on May 22, 2025

Published online on October 30, 2026

Abstract

Background. The complete removal of the filling material from the root canal system is essential for effective cleaning and disinfection during retreatment procedures. However, due to the anatomical complexity of the root canal system and the limitations of conventional instruments, achieving complete removal remains a significant challenge.

Objectives. The aim of the study was to assess the efficacy of supplementary techniques, with and without the use of a solvent, for removing the filling material from artificial, standardized grooves in the apical third of root canals.

Material and methods. A total of 120 incisors with single root canals were prepared to size 40/0.04. After longitudinal splitting, standardized grooves were created in the apical third of one half of each root. The grooves were filled with a sealer and gutta-percha, and the roots were then reassembled. The specimens were randomly allocated to 2 control groups ($n = 6$) and 6 experimental groups ($n = 18$), according to the removal technique used: passive ultrasonic irrigation (PUI); XP-endo Finisher (XP); or XP-endo Finisher R (XPR), each tested with or without a solvent. Filling material remnants were assessed using a 4-grade scoring system.

Results. Passive ultrasonic irrigation consistently failed to remove the filling material from the grooves, irrespective of solvent use, and yielded significantly poorer scores than all XP and XPR groups ($p < 0.001$). Without a solvent, neither XP nor XPR achieved the complete removal of the filling material, and no significant difference was observed between the 2 instruments ($p = 0.195$). However, both instruments demonstrated significantly improved cleaning efficacy when used with a solvent ($p < 0.001$), with no significant difference between the 2 methods ($p = 0.708$).

Conclusions. The use of a solvent significantly improves the efficacy of the XP and XPR instruments in removing the filling material from grooves in the apical third of root canals. Both systems exhibited comparable effectiveness, whereas PUI proved ineffective in cleaning the grooves. These findings highlight the critical role of solvents in enhancing cleaning efficacy during retreatment procedures.

Keywords: solvent, passive ultrasonic irrigation, gutta-percha removal, XP-endo Finisher, XP-endo Finisher R

Cite as
Wigler R, Blau-Venezia N, Goldberger T. Comparative efficacy of supplementary techniques, with and without a solvent, for removing root filling remnants from canal irregularities: An in vitro study. *Dent Med Probl.* 2026;63(5):1121–1126. doi:10.17219/dmp/205470

DOI
10.17219/dmp/205470

Copyright
Copyright by Author(s)
This is an article distributed under the terms of the Creative Commons Attribution 3.0 Unported (CC BY 3.0) (https://creativecommons.org/licenses/by/3.0/)

Highlights

- The study evaluated the efficacy of XP-endo Finisher (XP), XP-endo Finisher R (XPR) and passive ultrasonic irrigation (PUI) in removing the filling material from apical grooves.
- Solvent use significantly improved the cleaning efficacy of both the XP and XPR instruments.
- Passive ultrasonic irrigation was ineffective in removing the filling material from apical grooves, regardless of solvent use.
- XP and XPR demonstrated comparable effectiveness when used with a solvent.
- The study emphasizes the clinical relevance of solvents in enhancing retreatment cleaning efficacy, particularly in challenging apical areas of root canals.

Introduction

Post-treatment endodontic diseases often stem from persistent or secondary intraradicular infections.[1] The cornerstone of successful retreatment is the complete removal of the contaminated filling material and thorough disinfection of the root canal system.[2–4] However, the complex anatomy of root canals and the limitations of conventional instruments often make the complete removal of the filling material challenging, if not impossible.[5] Although most specially designed instruments and techniques can remove the majority of the filling material from the main canal, none can ensure a completely filling-free root canal system.[5–8] Consequently, the remnants of the filling material may cover the areas harboring residual infection.[7,9] Several supplementary finishing techniques have been proposed to address this problem.[10] Passive ultrasonic irrigation (PUI), a widely researched supplementary technique, has been reported to significantly reduce the amount of residual filling material, although complete removal remains elusive.[3,11–13]

XP-endo Finisher (XP) and XP-endo Finisher R (XPR) (FKG Dentaire, La Chaux-de-Fonds, Switzerland) are supplementary instruments made of a nickel-titanium (NiTi) shape-memory alloy and have no taper. They have core sizes of 25 and 30, respectively, and are designed to clean complex canal morphologies and hard-to-reach areas. XP-endo Finisher R was specifically designed for retreatment procedures, in which it is used as a final step in the removal of the filling material. According to the manufacturer (FKG Dentaire), XPR features enhanced expansion capability, allowing its semi-active tip to effectively scrape the canal walls and remove the filling material from challenging locations. Due to its innovative design, the instrument is able to reach and clean areas that are typically difficult to access during root canal retreatment. Several studies have supported the manufacturer's claims, reporting a significant reduction in residual gutta-percha, following the use of XPR.[2–5,10] However, recent studies comparing XP and XPR have demonstrated comparable efficacy, although neither instrument achieved complete canal clearance.[2,3] The researchers noted that they had deviated from the manufacturer's instructions by omitting solvent use and concluded that further investigations should assess the efficacy of XP and XPR with and without solvents.[2,3] Solvents have been recommended when gutta-percha is difficult to remove because of its close adherence to the canal walls.[14]

The present study aimed to assess the efficacy of XP, XPR and PUI, with and without solvent use, in removing the filling material from artificial, standardized grooves in the apical third of root canals. The researchers hypothesized that there would be no significant differences in efficacy among XP, XPR and PUI, regardless of solvent use.

Material and methods

The study was approved by the Institutional Ethics Committee (IEC approval No. 170.19) at Tel Aviv University, Israel, and adhered to the ethical guidelines outlined in the Declaration of Helsinki.

The study utilized 120 intact human mandibular incisors, each measuring at least 19 mm in length, with fully developed apices and no evidence of apical resorption. The teeth were randomly selected from a pool of recently extracted specimens. Each specimen was secured in a ProTrain endodontic platform (Simit Dental, Mantova, Italy) and radiographically examined in buccal and proximal views to assess the degree of canal curvature, and confirm the presence of a single oval canal configuration, as defined by De-Deus et al.[15,16] Only teeth exhibiting minimal canal curvature (angle <5°) were selected for inclusion in the study.

The researchers prepared access cavities and verified canal patency using a No. 10 K-file (Mani Inc., Utsunomiya, Japan). Canal lengths were determined under a dental operating microscope (Karl Kaps, Asslar, Germany) by advancing the file until its tip became visible at the apical foramen. To standardize the tooth length, the incisal edges were horizontally trimmed to achieve a uniform length of 18 mm, resulting in a working length (WL) of 17 mm.

The specimens were secured in plexiglass tubes using silicone impression material (Coltène/Whaledent, Langenau, Germany). Root canal preparation was performed using the 2Shape instruments (Micro-Mega, Besançon, France) up to size 40/0.04. Between each instrument, the canals were irrigated with 5 mL of 4% NaOCl. Upon completion of the preparation, a final rinse was performed using 5 mL

of 17% ethylenediaminetetraacetic acid (EDTA), followed by 5 mL of 4% NaOCl. The canals were then dried with paper points. The teeth were subsequently removed from the impression material, and 2 longitudinal grooves were carefully made using a diamond disc (HORICO, Berlin, Germany), taking care not to penetrate the root canals. Finally, the specimens were split into two halves using a chisel.

A groove measuring 3 × 0.2 × 0.5 mm (length/width/depth) was created in the apical third of one half of each root, 2 mm from the apex, using a size 20 ultrasonic stainless-steel file (Mani Inc.), following the well-established groove-creation protocol.[17–19] Debris was removed from the grooves using a toothbrush.

AH Plus sealer (Dentsply Sirona, Ballaigues, Switzerland) was mixed to a homogeneous consistency and applied using paper points under magnification (Karl Kaps).[20] Excess sealer was removed with paper points until a thin, homogeneous layer was obtained. Thermoplastic gutta-percha was then injected into the grooves under magnification using a root canal filling system (SuperEndo β; B&L Biotech USA Inc., Fairfax, USA) and condensed with hand pluggers (Dentsply Sirona). Excess material was removed using a heat carrier plugger (SuperEndo α; B&L Biotech USA Inc.) until a uniform filling corresponding to the dimensions of the grooves was obtained. This technique was intended to simulate a clinical situation in which the filling material remains within a recess in the apical third of the root canal, following its removal from the main canal system.

The root halves were reassembled using a flowable composite (3M ESPE, Seefeld, Germany), which was applied to their external surfaces. The reconstructed specimens were then reinserted into the plexiglass tube molds. The access cavities were sealed using cotton pellets and Cavit™ (3M ESPE). Finally, the specimens were stored under controlled conditions at 37°C and 100% relative humidity to allow the sealer to set.

One week later, the specimens were randomly divided into 8 groups. Six experimental groups, each consisting of 18 samples, were established according to the supplementary removal technique and the use of a solvent: XP and XPR, each with and without a solvent; and PUI, with and without a solvent. Two additional control groups, each comprising 6 samples, were also included. In the positive control group, gutta-percha was applied, but not removed, whereas in the negative control group, gutta-percha was not applied. This grouping strategy enabled a comprehensive evaluation of the different removal techniques under various conditions.

Gutta-percha removal procedure

All attempts to remove gutta-percha were performed with the plexiglass tubes immersed in a digital water bath maintained at 37°C to simulate body temperature conditions.

A torque-controlled motor (Dentsply Sirona) was used to operate the XP and XPR instruments at 1,000 rpm and a torque of 1 N·cm. In the PUI groups, an ultrasonic unit (Satelec P5 Newtron; Acteon Group, Norwich, UK) was used to operate a size 20 Irrisafe instrument at 30% power.

The canals were filled with 0.1 mL of chloroform in the solvent groups and with 4% NaOCl solution in the groups without a solvent. After 2 min, the XP and XPR instruments were inserted to WL, whereas the IrriSafe instrument was inserted to a depth of 1 mm short of WL. All instruments were operated or activated for 30 s using slow in-and-out movements.

The root canals were then irrigated for 30 s with 4% NaOCl solution using a syringe fitted with a 30-gauge needle (NaviTip; Ultradent, South Jordan, USA), inserted to a depth of 1 mm short of WL, with an estimated flow rate of 5 mL/min. The same instrumentation and activation protocol was repeated twice more – the first cycle was followed by 15 s of irrigation with 17% EDTA solution, and the second by a final rinse with 5 mL of 4% NaOCl solution. Any debris adhering to the XP or XPR instruments was removed between the irrigation cycles using gauze soaked in alcohol.

In the PUI groups, care was taken to maintain the IrriSafe instrument in a central position within the canal to minimize contact with the canal walls, which could dampen its oscillatory motion.[21] Each instrument was used in a single canal and then discarded.

Cleaning efficacy assessment

After treatment completion and drying of the canals with paper points, the specimens were disassembled to evaluate the removal of the filling material from the grooves. A microscope (Karl Kaps), set at ×25 magnification and coupled with a digital camera (Sony Alpha A6000; Sony Inc., New York, USA), was used to capture images of the grooves before filling material application and after its removal. To prevent the evaluators from identifying the specimens, the photographs were coded. Two endodontic specialists independently assessed the amount of filling material remaining in the grooves using a 4-point grading scale (Fig. 1).[22] Score 0 indicated a groove entirely devoid of filling material. Score 1 represented traces of the filling material covering less than half of the groove area. Score 2 denoted traces of the filling material covering more than half of the groove area. Score 3 indicated a groove completely filled with the filling material.

Statistical analysis

Statistical analysis was performed using the Statistical Analysis Program (SAS®) 9.4 (SAS Institute, Cary, USA). Kappa coefficients were calculated to assess intraobserver and interobserver reliability. Differences in filling material scores among the groups were analyzed using

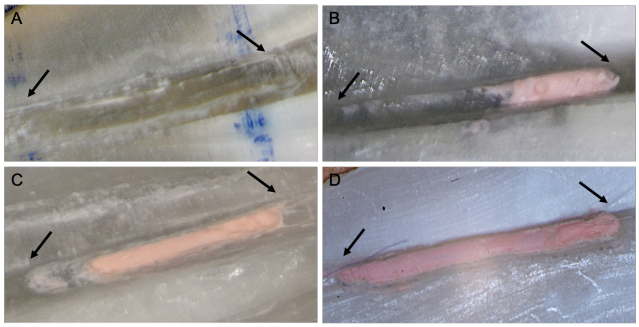

Fig. 1. Scoring system designed to evaluate the removal of the filling material from an artificial groove

A – score 0: the entire groove is empty; B – score 1: the filling material is present in less than half of the groove area; C – score 2: the filling material covers more than half of the groove area; D – score 3: the groove is completely filled with the filling material.
Black arrows indicate the coronal and apical ends of the grooves.

the Kruskal–Wallis test, followed by post hoc pairwise comparisons using the Dwass–Steel–Critchlow–Fligner (DSCF) test. Statistical significance was set at $p \leq 0.05$.

A sample size of 18 teeth per group provided 85% statistical power at a 5% significance level to detect an 8% difference among the supplementary techniques.

Results

The intraobserver and interobserver differences in scoring did not exceed one score point. The kappa coefficients were 0.928 for the first observer, 0.938 for the second observer, and 0.967 for interobserver agreement.

The distribution of scores for filling material removal from the grooves is presented in Fig. 2. The results showed that PUI failed to remove the filling material from the grooves, consistently receiving a score of 3, regardless of solvent use. The PUI scores differed significantly from those of all XP and XPR groups ($p < 0.001$).

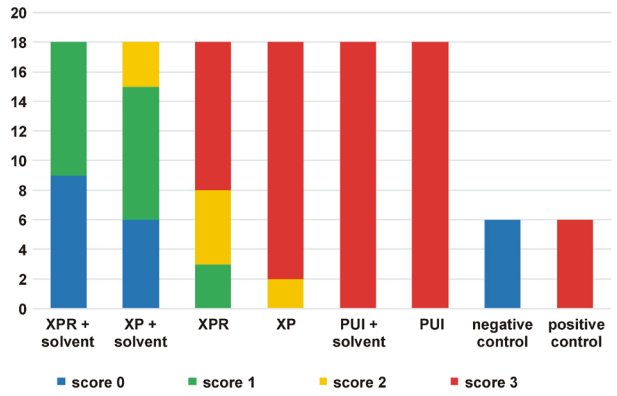

Fig. 2. Distribution of scores for filling material removal from the grooves in the experimental and control groups

XPR – XP-endo Finisher R; XP – XP-endo Finisher; PUI – passive ultrasonic irrigation.

In the XP group, 88.9% of the grooves were completely filled with the filling material (score 3), and all specimens (100%) exhibited the filling material covering more than 50% of the groove area (scores 2 and 3). Similarly, more than 50% of the grooves in the XPR group remained completely filled with the filling material (score 3), while 83.3% of the specimens exhibited the filling material covering more than 50% of the groove area (scores 2 and 3). Thus, in the absence of a solvent, neither the XP nor the XPR technique was able to completely remove the filling material from the artificial, standardized grooves. No significant difference was observed between the 2 techniques ($p = 0.195$).

In contrast, when a solvent was used, the grooves were completely free of the filling material (score 0) in 33.3% and 50% of the specimens treated with the XP and XPR instruments, respectively. Furthermore, 83.3% and 100% of the specimens in the XP and XPR groups, respectively, exhibited the filling material covering less than 50% of the groove area (scores 0 and 1). These results demonstrate that both the XP and XPR instruments removed significantly more filling material from the artificial, standardized grooves in the presence of a solvent ($p < 0.001$), with no significant difference between the 2 techniques ($p = 0.708$).

Discussion

The primary objectives of successful endodontic retreatment are to remove the filling material, followed by thorough shaping and cleaning of the root canal space.[2] Despite advances in retreatment techniques, achieving root canals entirely free of the filling material remains an elusive goal, as demonstrated by numerous studies.[2,23–26] The present study aimed to assess the efficacy of supplementary instruments (XP, XPR and PUI), with and without the use of a solvent, in removing the filling material from grooves in the apical third of root canals. The study design, which incorporated an artificial groove model, provided a controlled environment that allowed standardization of the groove size and location, and the filling material volume while simulating complex root canal anatomy.

XPR, a variant of XP featuring a size 30 tip, incorporates an innovative design that, according to the manufacturer (FKG Dentaire), enhances its ability to effectively scrape the canal walls and remove the filling material from difficult-to-access areas. This claim is supported by a study conducted by Machado et al., which demonstrated that the additional use of XPR significantly reduced the volume of residual filling material during retreatment with various instruments.[5] Similarly, Silva et al. evaluated the efficacy of XP and XPR in oval canals, and found that both instruments were effective in removing the residual filling material from straight oval-shaped canals.[2] Despite differences in the core diameter and the tip angle, which could potentially make XPR more effective than XP in removing the filling material, the authors found no

significant differences in the efficacy of the 2 supplementary instruments.[2] It should be noted, however, that none of the instruments investigated in these studies was able to completely remove the residual filling material.[2,3] Notably, neither study involved the use of solvents, despite their recommendation by the manufacturer (FKG Dentaire).

The results of the present study confirm that neither XP nor XPR was able to completely remove the filling material from the grooves. However, the efficacy of both XP and XPR in removing the filling material was significantly improved by the use of a solvent, with a similar effect observed for both instruments. Notably, regardless of solvent use, PUI failed to remove the filling material from the grooves, and was significantly less effective than XP and XPR. Therefore, the null hypothesis was rejected.

A recently published study reported that XPR and PUI, when used in combination with a solvent, were similarly effective in removing the residual filling material from root canals.[27] The discrepancy between these findings and those of the present study may be attributed to differences in the study objectives. While the previous study focused on cleaning efficacy within the main root canal system, the present study specifically investigated the removal of the filling material from irregular areas. In this context, XP and XPR demonstrated the ability to reach and mechanically dislodge the filling material from the canal walls, particularly in irregular areas. In contrast, PUI relies primarily on fluid dynamics to access such areas.[28,29] Passive ultrasonic irrigation employs a non-cutting stainless-steel tip designed to oscillate freely within the root canal without contacting its walls, thereby maximizing its effectiveness and preventing the restriction of its movement.[28,29] Its cleaning mechanism is based on cavitation and acoustic microstreaming, which enhance the ability of the irrigant to remove debris.[27,28] However, unlike XP and XPR, which directly engage with the filling material, the indirect action of PUI may limit its ability to effectively remove remnants from complex or irregular spaces, such as artificial grooves.

A previous study demonstrated that 3 cycles of PUI combined with chloroform resulted in significantly fewer gutta-percha remnants in simulated uninstrumented areas than the use of NaOCl, chloroform and paper points.[22] In the present study, only one cycle of solvent application was performed to replicate the manufacturer's recommended protocol for XPR. This methodological difference may help explain the discrepancy between the findings of the 2 studies. Multiple solvent-assisted activation cycles may facilitate more effective filling material removal, whereas a single cycle, following the manufacturer's recommendations, may limit the cleaning efficacy of supplementary techniques. Future studies should investigate the effectiveness of multiple solvent-assisted activation cycles in removing the filling material from irregular root canal areas.

According to a systematic review by Rossi-Fedele and Aly Ahmed, solvents may facilitate the penetration of the file into root canals when used during the initial stages of retreatment, but may hinder cleaning efficacy.[30] In contrast, when used after instrumentation, solvents may enhance the removal of the root filling material, thereby reducing the amount of residual material. Therefore, it is not surprising that solvent use in the present study improved the ability of XP and XPR to remove the filling material from the artificial grooves.

Limitations

One potential limitation of the present study is that different activation times were not investigated. Although the study protocol followed the manufacturer's recommendations, the recommended activation time proved insufficient to completely remove the filling material from all the grooves. Since clinicians cannot control the frequency with which the XP and XPR instruments contact the residual filling material in irregular areas within the recommended working time, longer activation periods may provide more opportunities for mechanical contact, potentially resulting in improved cleaning outcomes. Therefore, future studies should investigate the effects of extended activation times on cleaning efficacy.

Conclusions

The use of a solvent significantly improved the efficacy of the XP and XPR instruments in removing the filling material from the grooves located in the apical third of root canals. Both instruments demonstrated comparable effectiveness, whereas PUI was ineffective in removing the filling material from the grooves, regardless of solvent use. These findings highlight the importance of solvent use in conjunction with XP and XPR to improve cleaning of irregular areas within the root canal system. However, the potential clinical benefits of this approach remain to be established. Future studies should investigate the effects of extended activation times and multiple solvent-assisted cycles to further optimize the cleaning efficacy of these techniques.

Ethics approval and consent to participate

The study was approved by the Institutional Ethics Committee (IEC approval No. 170.19) at Tel Aviv University, Israel.

Data availability

The datasets supporting the findings of the current study are available from the corresponding author on reasonable request.

Consent for publication

Not applicable.

Use of AI and AI-assisted technologies

Not applicable.

ORCID iDs

Ronald Wigler https://orcid.org/0000-0002-3522-2194
Nuphar Blau-Venezia https://orcid.org/0000-0001-8950-582X
Tomer Goldberger https://orcid.org/0000-0002-8173-5804

References

1. Siqueira JF Jr. Aetiology of root canal treatment failure: Why well-treated teeth can fail. *Int Endod J*. 2001;34(1):1–10. doi:10.1046/j.1365-2591.2001.00396.x
2. Silva EJ, Belladonna FG, Zuolo AS, et al. Effectiveness of XP-endo Finisher and XP-endo Finisher R in removing root filling remnants: A micro-CT study. *Int Endod J*. 2018;51(1):86–91. doi:10.1111/iej.12788
3. De-Deus G, Belladonna FG, Zuolo AS, et al. XP-endo Finisher R instrument optimizes the removal of root filling remnants in oval-shaped canals. *Int Endod J*. 2019;52(6):899–907. doi:10.1111/iej.13077
4. De-Deus G, Belladonna FG, de Siqueira Zuolo A, et al. 3-dimensional ability assessment in removing root filling material from pair-matched oval-shaped canals using thermal-treated instruments. *J Endod*. 2019;45(9):1135–1141. doi:10.1016/j.joen.2019.06.003
5. Machado AG, Guilherme BP, Provenzano JC, et al. Effects of preparation with the Self-Adjusting File, TRUShape and XP-endo Shaper systems, and a supplementary step with XP-endo Finisher R on filling material removal during retreatment of mandibular molar canals. *Int Endod J*. 2019;52(5):709–715. doi:10.1111/iej.13039
6. Hammad M, Qualtrough A, Silikas N. Three-dimensional evaluation of effectiveness of hand and rotary instrumentation for retreatment of canals filled with different materials. *J Endod*. 2008;34(11):1370–1373. doi:10.1016/j.joen.2008.07.024
7. Alves FR, Marceliano-Alves MF, Sousa JC, Silveira SB, Provenzano JC, Siqueira JF Jr. Removal of root canal fillings in curved canals using either reciprocating single- or rotary multi-instrument systems and a supplementary step with the XP-Endo Finisher. *J Endod*. 2016;42(7):1114–1119. doi:10.1016/j.joen.2016.04.007
8. Azim AA, Wang HH, Tarrosh M, Azim KA, Piasecki L. Comparison between single-file rotary systems: Part 1 – efficiency, effectiveness, and adverse effects in endodontic retreatment. *J Endod*. 2018;44(11):1720–1724. doi:10.1016/j.joen.2018.07.022
9. Vieira AR, Siqueira JF Jr., Ricucci D, Lopes WS. Dentinal tubule infection as the cause of recurrent disease and late endodontic treatment failure: A case report. *J Endod*. 2012;38(2):250–254. doi:10.1016/j.joen.2011.10.019
10. Campello AF, Almeida BM, Franzoni MA, et al. Influence of solvent and a supplementary step with a finishing instrument on filling material removal from canals connected by an isthmus. *Int Endod J*. 2019;52(5):716–724. doi:10.1111/iej.13047
11. Cavenago BC, Ordinola-Zapata R, Duarte MA, et al. Efficacy of xylene and passive ultrasonic irrigation on remaining root filling material during retreatment of anatomically complex teeth. *Int Endod J*. 2014;47(11):1078–1083. doi:10.1111/iej.12253
12. Bernardes RA, Duarte MA, Vivan RR, Alcalde MP, Vasconcelos BC, Bramante CM. Comparison of three retreatment techniques with ultrasonic activation in flattened canals using micro-computed tomography and scanning electron microscopy. *Int Endod J*. 2016;49(9):890–897. doi:10.1111/iej.12522
13. Silveira SB, Alves FR, Marceliano-Alves MF, et al. Removal of root canal fillings in curved canals using either Mani GPR or HyFlex NT followed by passive ultrasonic irrigation. *J Endod*. 2018;44(2):299–303.e1. doi:10.1016/j.joen.2017.09.012
14. Dotto L, Sarkis-Onofre R, Bacchi A, Rocha Pereira GK. The use of solvents for gutta-percha dissolution/removal during endodontic retreatments: A scoping review. *J Biomed Mater Res B Appl Biomater*. 2021;109(6):890–901. doi:10.1002/jbm.b.34753
15. Iqbal MK, Firic S, Tulcan J, Karabucak B, Kim S. Comparison of apical transportation between ProFile and ProTaper NiTi rotary instruments. *Int Endod J*. 2004;37(6):359–364. doi:10.1111/j.1365-2591.2004.00792.x
16. De-Deus G, Reis C, Beznos D, Gruetzmacher de Abranches AM, Coutinho-Filho T, Paciornik S. Limited ability of three commonly used thermoplasticized gutta-percha techniques in filling oval-shaped canals. *J Endod*. 2008;34(11):1401–1405. doi:10.1016/j.joen.2008.08.015
17. Lee SJ, Wu MK, Wesselink PR. The effectiveness of syringe irrigation and ultrasonics to remove debris from simulated irregularities within prepared root canal walls. *Int Endod J*. 2004;37(10):672–678. doi:10.1111/j.1365-2591.2004.00848.x
18. Van der Sluis LW, Versluis M, Wu MK, Wesselink PR. Passive ultrasonic irrigation of the root canal: A review of the literature. *Int Endod J*. 2007;40(6):415–426. doi:10.1111/j.1365-2591.2007.01243.x
19. Wigler R, Dvir R, Weisman A, Matalon S, Kfir A. Efficacy of XP-endo Finisher files in the removal of calcium hydroxide paste from artificial standardized grooves in the apical third of oval root canals. *Int Endod J*. 2017;50(7):700–705. doi:10.1111/iej.12668
20. Álvarez-Vásquez JL, Erazo-Guijarro MJ, Domínguez-Ordoñez GS, Ortiz-Garay ÉM. Epoxy resin-based root canal sealers: An integrative literature review. *Dent Med Probl*. 2024;61(2):279–291. doi:10.17219/dmp/156654
21. Jiang LM, Verhaagen B, Versluis M, Langedijk J, Wesselink P, Van der Sluis LW. The influence of the ultrasonic intensity on the cleaning efficacy of passive ultrasonic irrigation. *J Endod*. 2011;37(5):688–692. doi:10.1016/j.joen.2011.02.004
22. Garcia A, Fernandez R, Arias A, De Gregorio C. Efficacy of different irrigation protocols for removing gutta-percha and sealer remnants in artificial un-instrumented areas. *Eur Endod J*. 2017;2(1):1–6. doi:10.5152/eej.2017.16033
23. Imura N, Zuolo ML, Ferreira MO, Novo NF. Effectiveness of the Canal Finder and hand instrumentation in removal of gutta-percha root fillings during root canal retreatment. *Int Endod J*. 1996;29(6):382–386. doi:10.1111/j.1365-2591.1996.tb01402.x
24. Bramante CM, Fidelis NS, Assumpção TS, et al. Heat release, time required, and cleaning ability of MTwo R and ProTaper universal retreatment systems in the removal of filling material. *J Endod*. 2010;36(11):1870–1873. doi:10.1016/j.joen.2010.08.013
25. Zuolo AS, Mello JE Jr., Cunha RS, Zuolo ML, Bueno CE. Efficacy of reciprocating and rotary techniques for removing filling material during root canal retreatment. *Int Endod J*. 2013;46(10):947–953. doi:10.1111/iej.12085
26. De Siqueira Zuolo A, Zuolo ML, da Silveira Bueno CE, Chu R, Cunha RS. Evaluation of the efficacy of TRUShape and Reciproc file systems in the removal of root filling material: An ex vivo micro-computed tomographic study. *J Endod*. 2016;42(2):315–319. doi:10.1016/j.joen.2015.11.005
27. Ferreira I, Babo PS, Braga AC, Lopes MA, Gomes ME, Pina-Vaz I. Supplementary solvent irrigation efficacy on filling remnants removal comparing XP-endo Finisher R vs IrriSafe. *Sci Rep*. 2021;11(1):12659. doi:10.1038/s41598-021-92175-2
28. Gu LS, Kim JR, Ling J, Choi KK, Pashley DH, Tay FR. Review of contemporary irrigant agitation techniques and devices. *J Endod*. 2009;35(6):791–804. doi:10.1016/j.joen.2009.03.010
29. Căpută PE, Retsas A, Kuijk L, Chávez de Paz LE, Boutsioukis C. Ultrasonic irrigant activation during root canal treatment: A systematic review. *J Endod*. 2019;45(1):31–44.e13. doi:10.1016/j.joen.2018.09.010
30. Rossi-Fedele G, Aly Ahmed HM. Assessment of root canal filling removal effectiveness using micro-computed tomography: A systematic review. *J Endod*. 2017;43(4):520–526. doi:10.1016/j.joen.2016.12.008

Original paper

Malocclusions and their impact on quality of life in children from disadvantaged socioeconomic conditions: A cross-sectional observational study

Marcelo Araripe Loureiro[1,A–F], Adan Lucas Pantoja de Santana[2,A–F], Nélio Jorge Veiga[1,3,B–F], Renata Tolêdo Alves[1,A–F], Gustavo Vicentis de Oliveira Fernandes[3,4,A,C–F], Anna Carolina Volpi Mello-Moura[1,3,A–F]

[1] Faculty of Dental Medicine, Catholic University of Portugal, Viseu, Portugal
[2] School of Dentistry, Federal University of Pará, Belém, Brazil
[3] Center for Interdisciplinary Research in Health, Catholic University of Portugal, Viseu, Portugal
[4] Department of Periodontics, Bitonte College of Dentistry, Northeast Ohio Medical University (NEOMED), Rootstown, USA

A – research concept and design; B – collection and/or assembly of data; C – data analysis and interpretation; D – writing the article; E – critical revision of the article; F – final approval of the article

Dental and Medical Problems, ISSN 1644-387X (print), ISSN 2300-9020 (online) *Dent Med Probl*. 2026;63(5):1127–1136

Address for correspondence
Gustavo Vicentis de Oliveira Fernandes
E-mail: gustfernandes@gmail.com

Funding sources
None declared

Conflict of interest
None declared

Acknowledgements
None declared

Received on March 12, 2025
Reviewed on May 17, 2025
Accepted on May 25, 2025

Published online on October 30, 2026

Abstract

Background. Malocclusion is characterized by dental and facial alterations that may impair the proper functioning of the stomatognathic system. Its prevalence and characteristics vary across populations, and are associated with socioeconomic conditions and deleterious oral habits.

Objectives. This study investigated the prevalence of malocclusion and its associations with sociodemographic characteristics, deleterious oral habits, and oral health-related quality of life (OHRQoL) among Portuguese children.

Material and methods. Children aged 3–12 years who participated in the "Ser Criança" project were included in the study. Sociodemographic data, deleterious oral habits and OHRQoL were assessed using the Early Childhood Oral Health Impact Scale – Portuguese version (ECOHIS-Pt) instruments or Parental-Caregiver Perceptions Questionnaire – Portuguese version (P-CPQ-Pt), as appropriate. Clinical data were obtained through the direct examination of the children. The malocclusions assessed included: (1) anterior open bite; (2) overbite; (3) overjet; (4) anterior crossbite; and (5) unilateral and bilateral posterior crossbite. Descriptive analyses and group comparisons were performed using Pearson's χ^2 test and the independent-samples *t* test, with statistical significance set at $p < 0.05$.

Results. A total of 63 children were included in the study. Most were female, aged 6–12 years, and came from families with an income above the minimum wage. Pacifier use and bottle-feeding were the most prevalent deleterious oral habits. Overbite and unilateral posterior crossbite were the most frequently observed malocclusions. Among children aged 3–5 years, anterior open bite was associated with OHRQoL. In the 6–12-year-old group, malocclusions such as overbite, anterior crossbite and unilateral posterior crossbite showed significant associations with OHRQoL.

Conclusions. Malocclusions were moderately prevalent among the children, with overbite and unilateral posterior crossbite being the most common. No significant associations were found between malocclusion and sex, age or family income. However, pacifier use was significantly associated with unilateral posterior crossbite. Regarding the relationships between malocclusion and OHRQoL, anterior open bite in the 3–5-year-old group was associated with the family impact subscale. Among children aged 6–12 years, significant associations were found between: (1) overbite and the functional limitations and family impact subscales; (2) anterior crossbite and the functional limitations and emotional well-being subscales; and (3) unilateral posterior crossbite and the emotional well-being subscale.

Keywords: malocclusion, epidemiology, quality of life, oral health, questionnaires

Cite as
Loureiro MA, Santana ALPd, Veiga NJ, Alves RT, Fernandes GVdO, Mello-Moura ACV. Malocclusions and their impact on quality of life in children from disadvantaged socioeconomic conditions: A cross-sectional observational study. *Dent Med Probl.* 2026;63(5):1127–1136. doi:10.17219/dmp/205536

DOI
10.17219/dmp/205536

Copyright
Copyright by Author(s)
This is an article distributed under the terms of the Creative Commons Attribution 3.0 Unported (CC BY 3.0) (https://creativecommons.org/licenses/by/3.0/)

Highlights

- Malocclusions were common among children, with overbite and unilateral posterior crossbite being the most frequently observed.
- No significant associations were found between malocclusion and demographic or socioeconomic factors.
- Pacifier use was significantly associated with unilateral posterior crossbite.
- Specific malocclusions were associated with impaired oral health-related quality of life (OHRQoL), particularly in terms of functional limitations, emotional well-being and family impact.

Introduction

Smile esthetics play a significant role in an individual's life, influencing psychological well-being and social interactions. The visual appeal of a smile is often associated with perceived attractiveness, which, in turn, can affect self-esteem and self-confidence.[1,2] Research indicates that individuals with malocclusion may experience social discrimination or diminished self-esteem, potentially compromising their overall oral health-related quality of life (OHRQoL).[3,4] Malocclusion, characterized by improper tooth alignment, can lead to functional difficulties and esthetic concerns, prompting individuals to seek orthodontic treatment to improve their appearance and quality of life (QoL).[5–8]

The Index of Orthodontic Treatment Need (IOTN) is a standardized index used to assess the need for orthodontic treatment, providing a structured approach to identifying individuals who would benefit most from orthodontic care.[8] The IOTN incorporates esthetic and clinical components, offering insight into the relationship between dental esthetics and treatment need.[8] Other factors indicating an increased need for orthodontic treatment include functional impairment and the psychological effects of dental esthetics. Furthermore, malocclusion has been reported to affect not only oral functions, such as chewing and speech, but also psychosocial well-being, thereby increasing the perceived need for orthodontic treatment.[8,9]

Further studies have shown that sociodemographic variables, including age, sex and socioeconomic status, may influence the perception of malocclusion and the perceived need for orthodontic treatment.[8] Adolescents often experience greater pressure to conform to societal expectations regarding physical appearance, making esthetic considerations an important factor in their treatment decisions.[10] Thus, the relationship between orthodontic treatment, smile esthetics, and overall life satisfaction represents an important area of investigation, as these factors may collectively influence public health and individual health-related behaviors.[8]

Malocclusion is characterized by dental and facial alterations that may impair the proper functioning of the stomatognathic system, and may necessitate orthodontic treatment.[11] According to the World Health Organization (WHO), malocclusion is considered the 3rd most prevalent oral health problem worldwide, following dental caries and periodontal disease.[12] Studies conducted worldwide have investigated the prevalence of malocclusion and occlusal trauma across different populations and settings.[13,14]

A systematic review reported that Angle's Class I is the most prevalent malocclusion worldwide, with prevalence estimates ranging from 31% to 96.6%.[15] Angle's Class II has a global average prevalence of 19.6%, although considerable variation has been observed across populations, with estimates ranging from 1.6% to 63%. In contrast, Angle's Class III is less common, with a global average prevalence of 5.9% and estimates ranging from 0.7% to 19.9%.[15] The distribution of malocclusion classes also varies considerably across geographical regions. Class I malocclusion and anterior open bite are more prevalent in Africa, whereas Class II malocclusion is more common among Caucasian populations, particularly in Europe.[15,16] These findings highlight the geographical variation in the prevalence and distribution of malocclusion across different populations.

Oral health-related quality of life is a multidimensional concept that subjectively assesses the impact of oral health on functional and emotional well-being, expectations, satisfaction with care, and self-perception. This biopsychosocial approach has gained prominence in pediatric dentistry and orthodontics, recognizing that dental treatment extends beyond the management of oral conditions to encompass patients' overall well-being.[17] The impact of malocclusion on the OHRQoL of children and adolescents has been investigated in recent studies.[18] Understanding this relationship requires acknowledging that malocclusion affects not only patients' physical condition, but also their subjective perception of oral health and well-being.[19,20]

Therefore, contemporary dentistry extends beyond the traditional paradigm focused solely on oral diseases to embrace a broader biopsychosocial perspective that considers the patient's overall well-being. Another systematic review examined the association between malocclusion, orthodontic treatment need and OHRQoL, identifying a modest and variable relationship among these factors.[21] The findings highlight the importance of standardized assessment methods in improving the consistency of results and facilitating comparisons across studies.

In this context, 2 validated instruments, the Portuguese versions of the Parental-Caregiver Perceptions Questionnaire (P-CPQ-Pt) and the Early Childhood Oral Health Impact Scale (ECOHIS-Pt), have been used to assess OHRQoL in Portuguese-speaking populations. The P-CPQ-Pt is a parent-reported questionnaire designed to assess the perceived impact of oral health conditions on children aged 6–12 years, covering domains such as oral symptoms, functional limitations, emotional well-being, social well-being, and family impact. The ECOHIS-Pt, in contrast, is designed for younger children, typically under 6 years of age, and comprises both child and family impact sections, addressing the effects of oral health conditions on children's daily lives, as well as the emotional and financial burden on their caregivers. Both instruments have been culturally adapted and linguistically validated for use in Portugal, supporting reliable and contextually appropriate assessments of the impact of oral health on QoL. Their application provides a more comprehensive understanding of how oral health affects children's QoL, thereby supporting the development of targeted public health interventions and treatment strategies.

Malocclusion varies considerably across populations, and is associated with socioeconomic conditions and deleterious oral habits.[22,23] The prevalence of malocclusion highlights the need to strengthen oral health literacy.[24,25] Effective oral health education can empower families to recognize dental problems at an early stage and seek appropriate treatment, thereby helping to reduce socioeconomic disparities in children's access to oral healthcare and promoting their overall well-being.

Thus, the present study aimed to address a gap in the literature by investigating the prevalence of malocclusion among children from low socioeconomic backgrounds. Additionally, it examined the associations between sociodemographic characteristics and OHRQoL, with the aim of informing the development of effective strategies to promote oral health in this population.

Material and methods

This observational study was conducted between June 2022 and January 2023, and followed the Strengthening the Reporting of Observational Studies in Epidemiology (STROBE) guidelines. The study was approved by the Ethics Committee of the Catholic University of Portugal, Viseu, Portugal (No. 30/2019). This project involved a collaboration between the Faculty of Dental Medicine of the Catholic University of Portugal, Viseu, Portugal, and the Social, Educational and Cultural Association of Viseu, Portugal. The partnership aimed to promote oral health and oral health literacy among disadvantaged populations in Portugal. The collaboration was formalized through a cooperation protocol between the institutions.

Eligibility criteria

Participants were selected using a convenience sampling method based on the availability and accessibility of the families participating in the social project "Ser Criança". The project was established through a partnership between the Faculty of Dental Medicine of the Catholic University of Portugal, Viseu, Portugal, and the Social, Educational and Cultural Association of Viseu, Portugal, and targeted populations experiencing socioeconomic disadvantage. Eligible families were characterized by an annual household income at or slightly above the minimum wage, regardless of whether they accessed public schools or community centers.

Healthy children in either the primary dentition stage (3–5 years of age) or the mixed dentition stage (6–12 years of age), regardless of sex, were eligible for inclusion, provided that their parents or legal guardians provided written informed consent to participate. Children with severe systemic or cognitive impairment, significant behavioral difficulties, or those who refused to participate or undergo clinical examinations were excluded. Children whose parents or legal guardians did not provide written informed consent or who were not fluent in Portuguese were also excluded.

Data collection

Data collection was conducted by a single experienced clinician and researcher, in the presence of the interviewees and before the children's clinical examinations. Sociodemographic data, including name, age, sex, and family income, were recorded, together with information on non-nutritive sucking habits, such as thumb-sucking, pacifier use and bottle-feeding, among others.

Oral health-related quality of life was assessed using 2 adapted and validated instruments – P-CPQ-Pt and ECOHIS-Pt, the latter designed for preschool-aged children.[26–28] Both instruments were adapted in a study by Ferreira.[29] The adaptations included modifications to the response scales to better reflect the cultural context of the study population and ensure an appropriate assessment of the impact of oral health on children's QoL.

The P-CPQ-Pt includes 2 global questions asking parents to rate their child's oral health: "How do you evaluate the health of your child's teeth, lips, jaws, and mouth?" (response options: "excellent"; "very good"; "good"; "fair"; and "poor") and "To what extent is your child's well-being affected by the condition of their teeth, lips, mouth, and jaws?" (response options: "not at all"; "very little"; "some"; "a lot"; and "very much").

The P-CPQ-Pt consists of 47 items divided into 5 subscales: oral symptoms (6 items); functional limitations (8 items); emotional well-being (8 items); social well-being (11 items); and family impact (14 items). The questions refer to the frequency of events experienced by the child during the previous 3 months. Responses are recorded

using a 5-point Likert-type scale: "never" (score 0); "once or twice" (score 1); "sometimes" (score 2); "often" (score 3); and "nearly every day" (score 4). The total score is calculated by summing the response codes, with possible scores ranging from 0 to 188.

The ECOHIS-Pt comprises 2 sections: the child impact section, consisting of 9 items addressing the impact of dental problems and dental treatment on children's daily activities and well-being; and the family impact section, consisting of 4 items evaluating the impact of children's dental problems and treatment on family members. The response options are "never/hardly ever", "occasionally/often/very often", and "don't know".

The child impact section:

- How often has your child experienced pain in the teeth, mouth, or jaws because of dental problems or dental treatment?
- How often has your child had difficulty drinking hot or cold beverages because of dental problems or dental treatment?
- How often has your child had difficulty eating certain foods because of dental problems or dental treatment?
- How often has your child had difficulty pronouncing words because of dental problems or dental treatment?
- How often has your child missed preschool, daycare or school because of dental problems or dental treatment?
- How often has your child had difficulty sleeping because of dental problems or dental treatment?
- How often has your child been irritable or frustrated because of dental problems or dental treatment?
- How often has your child avoided smiling or laughing because of dental problems or dental treatment?
- How often has your child avoided talking because of dental problems or dental treatment?

The family impact section:

- How often have you or another family member felt upset because of your child's dental problems or dental treatment?
- How often have you or another family member felt guilty because of your child's dental problems or dental treatment?
- How often have you or another family member taken time off work because of your child's dental problems or dental treatment?
- How often have your child's dental problems or dental treatment had a financial impact on your family?

Responses to the ECOHIS-Pt are coded as follows: 0 ("never"); 1 ("hardly ever"); 2 ("occasionally"); 3 ("often"); 4 ("very often"); and 5 ("don't know"). The total scores were calculated by summing the response codes separately for child impact and family impact sections, yielding possible score ranges of 9–45 and 4–20, respectively.

Following data collection from the parents/legal guardians and the assessment of oral health literacy among the children, clinical examinations of the oral cavity were performed. The examinations were conducted individually in adapted rooms, with the children positioned in a supine position on appropriate examination tables. The examiners used personal protective equipment (PPE) and clinical examination instruments, including a flashlight (Orascoptic Spark TruColor™ Cordless Headlight System; Orascoptic, Madison, USA), wooden spatulas, disposable clinical kits, and gauze compresses. Each child was examined by a single operator, assisted by a recorder who documented the type of dentition and the presence or absence of malocclusions. The same assessment criteria were applied to children with primary and mixed dentition. The evaluation of occlusal parameters followed the protocols described by Baume et al.[30] and Bjoerk et al.[31]

The investigated malocclusions included: (1) anterior open bite; (2) overbite, characterized by excessive vertical overlap of the upper incisors over the lower incisors; (3) overjet; (4) anterior crossbite; and (5) unilateral or bilateral posterior crossbite. Each condition was recorded dichotomously as present or absent.

The Baume classification was used to describe the morphology of the primary dental arches according to the presence or absence of interdental spacing.[30] Two arch types were identified: Type I, characterized by open or spaced primary dental arches (physiological spacing); and Type II, characterized by closed or non-spaced dental arches. Although this classification is not a conventional index for assessing malocclusion severity or orthodontic treatment need, it provides valuable information about early occlusal development and potential risk factors for crowding in the permanent dentition.

Bjoerk et al. classified dental anomalies into 2 main categories: (a) dental anomalies, including tooth anomalies, abnormal eruption and the misalignment of individual teeth; and (b) occlusal anomalies, involving deviations in the positional relationships between the upper and lower dental arches in the 3 spatial planes.[31] These classifications provide a framework for identifying dental and occlusal deviations, and assessing their potential implications for subsequent occlusal development.

When conditions requiring urgent intervention were identified during the clinical examination, such as the reported pain or signs of infection, the child was promptly referred to the Department of Pediatric Dentistry at the Catholic University of Portugal, Viseu, Portugal, for appropriate treatment.

Occlusion was also assessed by examining the molar relationship, which was classified according to Angle's classification as follows: Class I, in which the mesiobuccal cusp of the maxillary first permanent molar aligns with the buccal groove of the mandibular first permanent molar; Class II, in which the mesiobuccal cusp of the maxillary first permanent molar is positioned anteriorly to the buccal groove of the mandibular first permanent molar; and Class III, in which the mesiobuccal cusp of the maxillary first permanent molar is positioned posteriorly to the buccal groove of the mandibular first permanent molar.

In the primary dentition, the sagittal relationship between the second primary molars was classified according to the terminal plane relationship as follows: (1) a flush terminal plane, in which the distal surfaces of the maxillary and mandibular second primary molars are aligned in the same vertical plane; (2) a mesial step, in which the distal surface of the mandibular second primary molar is positioned mesially to that of the maxillary second primary molar; and (3) a distal step, in which the distal surface of the mandibular second primary molar is positioned distally to that of the maxillary second primary molar.

The dental arch form was assessed visually, and classified as either non-spaced arches, characterized by the absence of significant spacing between the anterior teeth, or spaced arches, characterized by the presence of interdental spaces or diastemas between the anterior teeth.

Statistical analysis

The data were organized and tabulated for subsequent statistical analysis using IBM SPSS Statistics, v. 28.0.1.0 (IBM Corp., Armonk, USA). Descriptive statistics included the calculation of absolute and relative frequencies for the variables under study. Inferential analyses were performed using Pearson's χ^2 test to compare proportions, and examine the associations between malocclusion, sociodemographic characteristics and deleterious oral habits. Additionally, the mean scores for the subscales and total scores of the P-CPQ-Pt and ECOHIS-Pt instruments were calculated to assess the association between malocclusion and OHRQoL. Group comparisons were performed using the independent-samples *t* test, with statistical significance set at 5% ($p < 0.05$).

Results

A total of 74 children, accompanied by their guardians, initially participated in a structured educational intervention focused on oral health literacy, and were subsequently screened for eligibility for the study. Following the initial data screening, 11 children were excluded – 6 did not meet the age criteria, 1 declined to undergo the examination, and 4 due to incomplete or incorrectly completed OHRQoL instruments. This resulted in a final sample of 63 children.

Most participants were female (n = 36; 57.1%), while 27 were male (42.9%). The predominant age group was 6–12 years (n = 41; 65.1%; mean age: 9.07 years), whereas 34.9% of the participants were aged 3–5 years (n = 22; mean age: 4.05 years). Regarding family income, 62.0% reported earnings above the minimum wage, while 30.1% reported income at or below the minimum wage. Income information was not provided by 7.9% of the participants.

Data on oral habits revealed that pacifier use and bottle-feeding were the most prevalent, each reported in more than 25% of the sample. Thumb-sucking was reported by more than 20% of the children. Of the total sample, 32 children were in the deciduous dentition stage and 31 were in the mixed dentition stage. Among children with deciduous dentition, Baume's Type I arch and a mesial step molar relationship were the most common findings, whereas Angle's Class I was predominant among those with mixed dentition. In the overall sample (N = 63), overbite and unilateral posterior crossbite were the most frequently observed malocclusions.

Among children with deciduous dentition (n = 32), the terminal plane relationships were distributed as follows: a flush terminal plane in 6 children (18.8%); a mesial step in 21 children (65.6%); and a distal step in 5 children (15.6%). Regarding the arch form, 28 children (87.5%) had open arches with spacing (Baume's Type I), whereas 4 children (12.5%) had closed arches without spacing (Baume's Type II).

Among children with mixed dentition (n = 31), the molar relationships, according to Angle's classification, were distributed as follows: Class I in 17 children (54.8%); Class II in 10 children (32.3%); and Class III in 4 children (12.9%). Regarding the arch form, 17 children (54.8%) had open arches with spacing, while 14 (45.2%) had closed arches without spacing.

Table 1 presents the OHRQoL scores of children aged 3–5 years (n = 22), assessed using the ECOHIS-Pt, which indicated good QoL in this age group. Among children aged 6–12 years (n = 41), the mean subscale scores were also close to the minimum values, indicating good QoL, as shown in Table 2.

Table 1. Oral health-related quality of life (OHRQoL) assessed by Early Childhood Oral Health Impact Scale – Portuguese version (ECOHIS-Pt) in children aged 3–5 years (n = 22)

ECOHIS-Pt scale	min	max	*M* ±*SD*
Child impact subscale (items: 1–9; points: 9–45)	9	15	10.09 ±1.82
Family impact subscale (items: 10–13; points: 4–20)	4	7	4.36 ±0.95
Total (items: 1–13; points: 13–65)	13	21	14.59 ±2.13

min – minimum; max – maximum; *M* – mean; *SD* – standard deviation.

Table 2. Oral health-related quality of life (OHRQoL) assessed by Parental-Caregiver Perceptions Questionnaire – Portuguese version (P-CPQ-Pt) in children aged 6–12 years (n = 41)

P-CPQ-Pt scale	min	max	*M* ±*SD*
Oral symptoms subscale (items: 1–6; points: 0–24)	0	11	3.98 ±2.78
Functional limitations subscale (items: 7–14; points: 0–32)	0	18	4.22 ±4.28
Emotional well-being subscale (items: 15–22 points: 0–32)	0	12	2.29 ±3.24
Social well-being subscale (items: 23–33; points: 0–44)	0	16	1.95 ±3.39
Family impact subscale (items: 34–47; points: 0–56)	0	24	3.46 ±5.81
Total (items: 1–47; points: 0–188)	0	62	16.12 ±14.86

The analysis of the associations between malocclusion and other variables revealed no statistically significant differences according to sex, age, or family income, as shown in Table 3. However, a history of pacifier use was significantly associated with the presence of unilateral posterior crossbite ($p = 0.047$), as shown in Table 4.

When evaluating the associations between OHRQoL and malocclusion (Table 5), anterior open bite in children aged 3–5 years was associated with the family impact subscale. Among children aged 6–12 years, overbite was associated with the functional limitations and family impact subscales, whereas anterior crossbite was associated with the functional limitations and emotional well-being subscales. Additionally, unilateral posterior crossbite was associated with the emotional well-being subscale.

Table 3. Associations between malocclusion and sociodemographic variables

Malocclusion	Sociodemographic variables (*p*-value)		
	sex	age	family income
Deciduous arch type	0.647	0.333	0.948
Deciduous molar relationship	0.323	0.314	0.493
Permanent molar relationship	0.265	0.982	0.286
Anterior open bite	0.710	0.666	0.375
Overbite	0.787	0.423	0.087
Overjet	0.842	0.190	0.968
Anterior crossbite	0.275	0.331	0.758
Unilateral posterior crossbite	0.190	0.837	0.943
Bilateral posterior crossbite	0.244	0.071	a

a – the variable is a constant. Pearson's χ^2 test for the comparison of proportions ($p < 0.05$).

Discussion

Although several studies have assessed the Portuguese population,[14,32,33] the present study specifically investigated the prevalence of malocclusions among Portuguese children. The findings revealed a moderate overall prevalence, with no significant associations with demographic, socioeconomic, or deleterious oral habit variables. However,

Table 4. Associations between malocclusion and deleterious oral habits

Malocclusion	Deleterious oral habits (*p*-value)			
	thumb-sucking	pacifier use	bottle-feeding	other
Deciduous arch type	0.823	0.291	0.286	0.282
Deciduous molar relationship	0.215	0.703	0.517	0.430
Permanent molar relationship	0.500	0.882	0.653	0.751
Anterior open bite	0.503	0.639	0.606	0.678
Overbite	0.292	0.100	0.352	0.301
Overjet	0.054	0.715	0.715	0.929
Anterior crossbite	0.431	0.978	0.978	0.591
Unilateral posterior crossbite	0.367	0.047*	0.910	0.901
Bilateral posterior crossbite	0.793	0.556	0.556	0.398

* statistically significant. Pearson's χ^2 test for the comparison of proportions ($p < 0.05$).

Table 5. Association between malocclusion and oral health-related quality of life (OHRQoL)

Malocclusion	OHRQoL (*p*-value)								
	ECOHIS-Pt scores			P-CPQ-Pt scores					
	S1	S2	T	S1	S2	S3	S4	S5	T
Deciduous arch type	0.470	0.347	0.308	0.469	0.614	0.737	0.833	0.445	0.721
Deciduous molar relationship	0.769	0.473	0.684	0.919	0.017*	0.884	0.986	0.233	0.412
Permanent molar relationship	0.237	0.864	0.521	0.897	0.737	0.834	0.979	0.964	0.884
Anterior open bite	0.407	0.054*	0.815	0.369	0.817	0.797	0.186	0.145	0.612
Overbite	0.386	0.106	0.261	0.456	0.015*	0.235	0.085	0.014*	0.045
Overjet	0.196	0.103	0.456	0.827	0.446	0.243	0.762	0.135	0.742
Anterior crossbite	a	a	a	0.965	0.017*	0.003*	0.111	0.914	0.201
Unilateral posterior crossbite	a	a	a	0.091	0.247	0.030*	0.140	0.379	0.121
Bilateral posterior crossbite	a	a	a	a	a	a	a	a	a

ECOHIS-Pt – Early Childhood Oral Health Impact Scale – Portuguese version: S1 – child impact subscale score ; S2: family impact subscale score; T: total score.
P-CPQ-Pt – Parental-Caregiver Perceptions Questionnaire – Portuguese version: S1 – oral symptoms subscale score; S2 – functional limitations subscale score; S3 – emotional well-being subscale score; S4 – social well-being subscale score; S5 – family impact subscale score; T: total score.
a – cannot be calculated, since one of the groups was empty. * statistically significant. Independent-samples *t* test ($p < 0.05$).

specific associations with OHRQoL were identified, particularly among preschool- and school-aged children.

The most frequently observed malocclusions in the deciduous and mixed dentition stages were overbite and unilateral posterior crossbite, affecting a considerable proportion of the children assessed. The prevalence of Class II malocclusion was moderate and consistent with the global estimates reported by Alhammadi et al., who found prevalences of 23% in mixed dentition and 19.56% in permanent dentition.[22] These figures fall within the range reported across different populations. However, the prevalence observed in the present study was slightly lower than the global average reported for Caucasian populations, in which Class II malocclusion is more prevalent, as described by Cenzato et al.[23] Overall, these findings are consistent with the international distribution of malocclusions, in which Class I is the most prevalent, followed by Class II and Class III.

This study contributes to a better understanding of occlusal characteristics in Portuguese children and highlights the importance of considering specific QoL-related factors when planning orthodontic interventions.[34] It also provides evidence that variations in malocclusion prevalence may be attributed to differences in population demographics and the assessment criteria employed.[35] No significant associations were found between malocclusion and the demographic or socioeconomic characteristics of the participants ($p > 0.05$), which is consistent with previous research indicating that malocclusion affects children regardless of sex, age, the educational level, or family income.[36] Although this association was not confirmed in the present study, the literature suggests that unfavorable demographic and socioeconomic conditions may contribute to the development of deleterious oral habits, potentially compromising OHRQoL.[36,37]

Oral health literacy plays a crucial role in promoting effective oral health practices, particularly in socioeconomically vulnerable communities. Collaboration between universities and communities is essential for implementing educational programs and epidemiological screenings aimed at identifying and reducing oral health disparities. These initiatives not only improve knowledge on dental prevention and treatment, but also strengthen community ties by providing targeted and accessible health services.[38] Epidemiological screenings generate reliable data on the prevalence of oral conditions, enabling health authorities to develop and implement effective interventions to improve oral health and overall well-being.[39]

The prevalence of deleterious oral habits, including pacifier use, bottle-feeding and thumb-sucking, was investigated in this study, and was found to vary across different age groups and populations. Previous studies have demonstrated associations between these habits and certain malocclusions. For example, a systematic review found that pacifier-sucking was associated with the development of anterior open bite and posterior crossbite, indicating a potential impact on orofacial structures.[40] Additionally, research has shown that prolonged pacifier use and thumb-sucking are associated with malocclusions such as anterior open bite and increased overjet.[39] However, in the present study, despite variations in the prevalence of oral habits, no significant associations between these habits and specific malocclusions were identified, except for the association between pacifier use and unilateral posterior crossbite. This finding should be interpreted in light of the literature, which highlights the need for further well-designed studies to conclusively evaluate the effects of non-nutritive oral habits on occlusal characteristics.[40]

Oral health-related quality of life in children, assessed using the P-CPQ and ECOHIS instruments validated for the Portuguese language, revealed significant associations between malocclusions and functional limitations, emotional well-being and family impact, particularly in cases of anterior malocclusions. These findings highlight the potential importance of early orthodontic assessment and intervention in improving children's oral health and overall QoL, as well as that of their families.

Another useful instrument that was not employed in the present study is the Malocclusion Impact Questionnaire (MIQ), which was specifically developed and validated to assess the impact of malocclusion on the QoL of children and adolescents. Research has highlighted the need for malocclusion-specific assessment tools, as generic OHRQoL measures may fail to capture the unique challenges experienced by individuals with malocclusion.[41,42] The MIQ was developed through qualitative research that prioritized the perspectives of the affected individuals, allowing the inclusion of items that reflect the experiences and concerns of young patients in the UK and other cultural contexts.[41–43] Therefore, the MIQ may be a valuable instrument to consider in future studies.

In Brazil, studies have reported a high prevalence of malocclusion, with environmental factors, including socioeconomic status and oral habits, playing an important role.[44] Evidence suggests that children from lower socioeconomic backgrounds have a higher prevalence of malocclusion, with Class II and Class III malocclusions being particularly common in these populations.[44,45] Studies involving Brazilian preschool children have shown that, although malocclusion is highly prevalent, it is not necessarily significantly associated with children's OHRQoL. However, other studies have reported that severe malocclusions negatively affect QoL, highlighting the need for targeted oral health interventions in socioeconomically vulnerable populations.[46]

Evidence from Portugal also contributes to this discussion, as studies have demonstrated an association between socioeconomic factors and malocclusion prevalence.[47] Portuguese children from lower socioeconomic backgrounds presented poorer oral health outcomes, potentially resulting in worse OHRQoL.[47] The consequences of malocclusion may also extend to psychosocial well-being, further emphasizing the importance of systematic public health initiatives aimed at reducing these disparities.[45]

In Zambia, studies have reported a high prevalence of malocclusion among children, reflecting the patterns observed in other European countries and suggesting possible geographical variations associated with socioeconomic factors.[48] Importantly, the study identified significant associations between malocclusion severity and several health-related QoL measures, reinforcing the need for further research into these relationships.[48] Children with more severe malocclusions reported greater negative impacts on their QoL, consistent with findings from studies conducted in Brazil, which have also highlighted concerns regarding inadequate access to dental care among lower socioeconomic groups.[45]

Systematic reviews have further emphasized that malocclusion prevalence across different countries is influenced by environmental and behavioral factors, including access to dental care and deleterious oral habits, which may be more prevalent in socioeconomically disadvantaged populations.[49,50] Understanding the complex relationships between socioeconomic status, malocclusion prevalence, and QoL is therefore essential for developing targeted public health strategies and reducing oral health inequalities.

Limitations

This study has several limitations. First, its observational design did not include any therapeutic interventions. Second, the sample size was relatively small, as the inclusion of participants depended on the voluntary participation of children enrolled in the social project. The limited sample size raises concerns regarding the generalizability of the findings, which should therefore be interpreted with caution. Furthermore, the study was geographically restricted to Viseu, Portugal, and did not include larger and more densely populated cities, such as Porto and Lisbon, limiting the representativeness of the sample.

Another important limitation was the delay in study implementation. Although approval to initiate the study was obtained in late 2019, the COVID-19 pandemic postponed its implementation until 2022–2023. The pandemic also generated widespread insecurity among the target population, with families primarily seeking dental care for urgent needs, further hindering participant recruitment and study progress.[32]

Despite these limitations, particularly the use of a convenience sample, the findings provide valuable information to guide future intervention strategies. They highlight the need for an integrated approach that considers not only the correction of malocclusions, but also the broader range of factors influencing children's QoL.

Conclusions

Within the limitations of this study, malocclusions were found to be prevalent among the children, with overbite and unilateral posterior crossbite being the most frequently observed. No significant associations were found between malocclusion and sex, age or family income. However, pacifier use was significantly associated with unilateral posterior crossbite. Regarding the associations between QoL and malocclusion, anterior open bite in children aged 3–5 years was associated with the family impact subscale. Among children aged 6–12 years, the following associations were identified: (1) overbite with the functional limitations and family impact subscales; (2) anterior crossbite with the functional limitations and emotional well-being subscales; and (3) unilateral posterior crossbite with the emotional well-being subscale.

Ethics approval and consent to participate

The study was approved by the Ethics Committee of the Catholic University of Portugal, Viseu, Portugal (No. 30/2019). This project involved a collaboration between the Faculty of Dental Medicine of the Catholic University of Portugal, Viseu, Portugal, and the Social, Educational and Cultural Association of Viseu, Portugal. All parents/caregivers signed the informed consent form.

Data availability

The datasets supporting the findings of the current study are available from the corresponding author on reasonable request.

Consent for publication

Not applicable.

Use of AI and AI-assisted technologies

Not applicable.

ORCID iDs

Marcelo Araripe Loureiro https://orcid.org/0000-0002-0561-6096
Adan Lucas Pantoja de Santana https://orcid.org/0000-0002-9773-5120
Nélio Jorge Veiga https://orcid.org/0000-0001-6288-0435
Renata Tolêdo Alves https://orcid.org/0000-0003-3531-1186
Gustavo Vicentis de Oliveira Fernandes https://orcid.org/0000-0003-3022-4390
Anna Carolina Volpi Mello-Moura https://orcid.org/0000-0002-9420-1721

References

1. Cunha J, Fernandes GVO, Fernandes JCH, Lopes PC, Rio R. The interference of age and gender on smile characterization analyzed on six parameters: A clinical-photographic pilot study. *Medicina*. 2023;59(3):595. doi:10.3390/medicina59030595
2. Chrapla P, Paradowska-Stolarz A, Skoskiewicz-Malinowska K. Subjective and objective evaluation of the symmetry of maxillary incisors among residents of southwest Poland. *Symmetry*. 2022;14(6):1257. doi:10.3390/sym14061257
3. Pio Pennacchio BF, Giorgio RV, Cardarelli F, et al. AMCOP bioactivators: An innovative solution in interceptive orthodontics for the treatment of malocclusions and orofacial dysfunctions. *Oral Implantol*. 2024;16(3,S1):162–175. doi:10.11138/oi163.1suppl162-175

4. Palermo A, Cazzato G, Di Noia A, et al. Comparative effectiveness of orthopedic devices for treating skeletal class III malocclusion in growing patients. *Oral Implantol*. 2024;16(3,S1):612–634. doi:10.11138/oi163.1suppl612-634
5. Palermo A, Ferrante L, Cazzato G, et al. Transverse skeletal deficiencies in orthodontics: Etiology, consequences and treatment approaches. *Oral Implantol*. 2024;16(3,S1):595–611. doi:10.11138/oi163.1suppl595-611
6. Partouche AJ, Castro F, Baptista AS, Costa LG, Fernandes JCH, Fernandes GVdO. Effects of multibracket orthodontic treatment versus clear aligners on periodontal health: An integrative review. *Dent J (Basel)*. 2022;10(10):177. doi:10.3390/dj10100177
7. Farsoun CF, Castro F, Farsoun A, Farsoun J, Fernandes JCH, Fernandes GVdO. Gingival recession in canines orthodontically aligned: A narrative review. *Rev Flum Odontol*. 2023;3(62):100–121. doi:10.22409/ijosd.v3i62.57027
8. Barrera-Chaparro JP, Plaza-Ruíz SP, Parra KL, et al. Orthodontic treatment need, the types of brackets and the oral health-related quality of life. *Dent Med Probl*. 2023;60(2):287–294. doi:10.17219/dmp/151577
9. Shyagali T, Kubavat A, Bhayya D. Evaluation of the personality traits in subjects in need of orthodontic treatment using the Big Five model: A cross-sectional questionnaire-based study. *Dent Med Probl*. 2025;62(1):49–56. doi:10.17219/dmp/165799
10. Kahn S, de Pinho Reis Rodrigues WJ, Dias AT, Resende R, Fernandes JCH, Fernandes GVO. Crown lengthening surgery in the esthetic area for optimized results: A review with surgical recommendations. *Surgeries*. 2024;5(4):1043–1055. doi:10.3390/surgeries5040084
11. Alhammadi MS, Halboub E, Fayed MS, Labib A, El-Saaidi C. Global distribution of malocclusion traits: A systematic review. *Dental Press J Orthod*. 2018;23(6):40.e1-40.e10. doi:10.1590/2177-6709.23.6.40.e1-10.onl
12. World Health Organization (WHO). *Oral Health Surveys: Basic Methods*. 5th ed. Geneva, Switzerland: World Health Organization; 2013.
13. Senos Tróia PMBP, Spuldaro TR, Barroso da Fonseca PA, Fernandes GVdO. Presence of gingival recession or noncarious cervical lesions on teeth under occlusal trauma: A systematic review. *Eur J Gen Dent*. 2021;10:50–59. doi:10.1055/s-0041-1732781
14. Marcelino V, Baptista S, Marcelino S, et al. Occlusal changes with clear aligners and the case complexity influence: A longitudinal cohort clinical study. *J Clin Med*. 2023;12(10):3435. doi:10.3390/jcm12103435
15. Chen H, Lin L, Chen J, Huang F. Prevalence of malocclusion traits in primary dentition, 2010–2024: A systematic review. *Healthcare (Basel)*. 2024;12(13):1321. doi:10.3390/healthcare12131321
16. Lombardo G, Vena F, Negri P, et al. Worldwide prevalence of malocclusion in the different stages of dentition: A systematic review and meta-analysis. *Eur J Paediatr Dent*. 2020;21(2):115–122. doi:10.23804/ejpd.2020.21.02.05
17. De Ridder L, Aleksieva A, Willems G, Declerck D, de Llano-Pérula MC. Prevalence of orthodontic malocclusions in healthy children and adolescents: A systematic review. *Int J Environ Res Public Health*. 2022;19(12):7446. doi:10.3390/ijerph19127446
18. Göranson E, Sonesson M, Naimi-Akbar A, Dimberg L. Malocclusions and quality of life among adolescents: A systematic review and meta-analysis. *Eur J Orthod*. 2023;45(3):295–307. doi:10.1093/ejo/cjad009
19. Liu Z, McGrath C, Hägg U. The impact of malocclusion/orthodontic treatment need on the quality of life: A systematic review. *Angle Orthod*. 2009;79(3):585–591. doi:10.2319/042108-224.1
20. Kragt L, Dhamo B, Wolvius EB, Ongkosuwito EM. The impact of malocclusions on oral health-related quality of life in children – a systematic review and meta-analysis. *Clin Oral Investig*. 2016;20(8):1881–1894. doi:10.1007/s00784-015-1681-3
21. Brondani MA, MacEntee MI. Thirty years of portraying oral health through models: What have we accomplished in oral health-related quality of life research? *Qual Life Res*. 2014;23(4):1087–1096. doi:10.1007/s11136-013-0541-3
22. Erratum. *Dental Press J Orthod*. 2019;24(3):113. doi:10.1590/2177-6709.24.3.113.err
23. Cenzato N, Nobili A, Maspero C. Prevalence of dental malocclusions in different geographical areas: Scoping review. *Dent J (Basel)*. 2021;9(10):117. doi:10.3390/dj9100117
24. Dovigo G, Pessoa MN, dos Santos PR, Scudeler Vedovello SA, Marcantonio E. Evaluation of quality of life related to the health of children and their families and associated factors [in Portuguese]. *Rev Odontol UNESP*. 2021;50:e20210048. doi:10.1590/1807-2577.04821
25. Sischo L, Broder HL. Oral health-related quality of life: What, why, how, and future implications. *J Dent Res*. 2011;90(11):1264–1270. doi:10.1177/0022034511399918
26. Goursand D, Paiva SM, Zarzar PM, et al. Cross-cultural adaptation of the Child Perceptions Questionnaire 11-14 (CPQ11-14) for the Brazilian Portuguese language. *Health Qual Life Outcomes*. 2008;6:2. doi:10.1186/1477-7525-6-2
27. de Souza Barbosa T, Duarte Gavião MB. Validation of the Parental-Caregiver Perceptions Questionnaire: Agreement between parental and child reports. *J Public Health Dent*. 2012;75(4):255–264. doi:10.1111/j.1752-7325.2012.00371.x
28. Pentapati KC, Chenna D, Kumar VS, Kumar N, Pai M, Kumar S. Early Childhood Oral Health Impact Scale (ECOHIS) questionnaire: Reliability generalization meta-analysis of Cronbach's alpha. *BMC Oral Health*. 2025;25(1):947. doi:10.1186/s12903-025-06342-2
29. Ferreira NF. Association between oral condition in a population of Portuguese children and quality of life [Master's thesis]. Lisbon, Portugal: Catholic University of Portugal; 2024. http://hdl.handle.net/10400.14/46077. Accessed November 6, 2026.
30. Baume LJ, Horowitz HS, Summers CJ, et al. A method for the measurement of occlusal characteristics (developed for the Commission on Classification and Statistics of the FDI, (COCSTOC) Study Group 2 on dentofacial abnormalities, 1969–72) [in Spanish]. *Int Dent J*. 1974;24(1):90–97. PMID:4525548.
31. Bjoerk A, Krebs A, Solow B. A method for epidemiological registration of malocclusion. *Acta Odontol Scand*. 1964;22:27–41. doi:10.3109/00016356408993963
32. Dos Santos Gonçalves RM, Fernandes GVO, Fernandes JCH, Seabra M, Figueiredo A. Impact of COVID-19 on Portuguese dental students: A cohort study. *Healthcare (Basel)*. 2023;11(6):818. doi:10.3390/healthcare11060818
33. Silva CF, Fernandes GVdO, Fernandes JCH, Fialho J, Correia A, Figueiredo C. Sexual dimorphism in the mandible in a Portuguese population – predicting the gender for forensic purpose: A pilot study. *Rev Flum Odontol*. 2025;2(67):171–185. doi:10.22409/ijosd.v2i67.62521
34. Alves H, Raposo R, Sato S, Slavicek R. Three-dimensional study of different skeletal craniofacial patterns from the eighteenth to the twenty-first century in a Portuguese population. *Cranio*. 2022;40(3):274–281. doi:10.1080/08869634.2020.1721138
35. Moghaddam LF, Vettore MV, Bayani A, et al. The association of oral health status, demographic characteristics and socioeconomic determinants with oral health-related quality of life among children: A systematic review and meta-analysis. *BMC Pediatr*. 2020;20(1):489. doi:10.1186/s12887-020-02371-8
36. de Paula JS, Gonçalves Leite IC, de Almeida AB, Bovi Ambrosano GM, Mialhe FL. The impact of socioenvironmental characteristics on domains of oral health-related quality of life in Brazilian schoolchildren. *BMC Oral Health*. 2013;13:10. doi:10.1186/1472-6831-13-10
37. Machado SCS, Manzanares-Céspedes MC, Ferreira-Moreira J, Ferreira-Pacheco JJ, Rompante PAMA, Ustrell-Torrent JM. A sample of non-nutritive sucking habits (pacifier and digit) in Portuguese children and its relation with the molar classes of angle. *J Clin Exp Dent*. 2018;10(12):e1161–e1166. doi:10.4317/jced.55284
38. Northridge ME, Kumar A, Kaur R. Disparities in access to oral health care. *Ann Rev Public Health*. 2020;41:513–535. doi:10.1146/annurev-publhealth-040119-094318
39. Ling HTB, Sum MH, Zhang L, et al. The association between nutritive, non-nutritive sucking habits and primary dental occlusion. *BMC Oral Health*. 2018;18(1):145. doi:10.1186/s12903-018-0610-7
40. Sadoun C, Templier L, Alloul L, et al. Effects of non-nutritive sucking habits on malocclusions: A systematic review. *J Clin Pediatr Dent*. 2024;48(2):4–18. doi:10.22514/jocpd.2024.029
41. Benson PE, Gilchrist F, Farella M. The Malocclusion Impact Questionnaire (MIQ): Cross-sectional validation in a group of young people seeking orthodontic treatment in New Zealand. *Dent J (Basel)*. 2019;7(1):24. doi:10.3390/dj7010024

42. Tassi A, Tan J, Piplani B, Longmire NM, Wong Riff KW, Klassen AF. Establishing content validity of an orthodontic subset of the FACE-Q Craniofacial Module in children and young adults with malocclusion. *Orthod Craniofac Res*. 2021;24(4):553–560. doi:10.1111/ocr.12474
43. Hope B, Zaror C, Sandoval P, Garay M, Streiner DL. Cross-cultural adaptation and validation in Spanish of the Malocclusion Impact Questionnaire (MIQ). *Health Qual Life Outcomes*. 2020;18(1):146. doi:10.1186/s12955-020-01385-1
44. Normando TS, Feio Barroso RF, Normando D. Influence of the socio-economic status on the prevalence of malocclusion in the primary dentition. *Dental Press J Orthod*. 2015;20(1):74–78. doi:10.1590/2176-9451.20.1.074-078.oar
45. Dutra SR, Pretti H, Martins MT, Bendo CB, Vale MP. Impact of malocclusion on the quality of life of children aged 8 to 10 years. *Dental Press J Orthod*. 2018;23(2):46–53. doi:10.1590/2177-6709.23.2.046-053.oar
46. Sousa RV, Clementino MA, Gomes MC, Martins CC, Granville-Garcia AF, Paiva SM. Malocclusion and quality of life in Brazilian preschoolers. *Eur J Oral Sci*. 2014;122(3):223–229. doi:10.1111/eos.12130
47. Pimenta C, Esperancinha C, Bernardo M, Mendes S. Malocclusion in primary dentition: A cross-sectional study in a Lisbon population. *Rev Portug Estomatol Med Dent Cir Maxilofac*. 2023;64(1):28–34. doi:10.24873/j.rpemd.2023.03.1048
48. Anthony SN, Zimba K, Balakrishnan S. Impact of malocclusions on the oral health-related quality of life of early adolescents in Ndola, Zambia. *Int J Dent*. 2018;2018:7920973. doi:10.1155/2018/7920973
49. Elelmi Y, Guetat R, Ben Salem MK, et al. Association between malocclusion and dental caries experience in the primary dentition. *Saudi J Oral Dent Res*. 2020;5(1):71–75. doi:10.36348/sjodr.2020.v05i01.012
50. Todor BI, Scrobotă I, Todor L, Lucan AI, Vaida L. Environmental factors associated with malocclusion in children population from mining areas, western Romania. *Int J Env Res Public Health*. 2019;16(18):3383. doi:10.3390/ijerph16183383

Original paper

Ante-mortem tooth loss (AMTL) and dentoalveolar pathologies in the 11th–15th-century Gródek on the Bug River skeletal collection: Patterns and implications

Agata Izabela Cieślik[1,A–D], Wioletta Nowaczewska[2,D–F], Paweł Dąbrowski[3,D–F], Tomasz Dzieńkowski[4,E,F], Joanna Wysocka[1,C–F]

[1] Department of Anthropology, Ludwik Hirszfeld Institute of Immunology and Experimental Therapy, Polish Academy of Sciences, Wroclaw, Poland
[2] Department of Human Biology, University of Wrocław, Poland
[3] Division of Anatomy, Department of Human Morphology and Embryology, Wroclaw Medical University, Poland
[4] Institute of Archaeology, Maria Curie-Skłodowska University in Lublin, Poland

A – research concept and design; B – collection and/or assembly of data; C – data analysis and interpretation;
D – writing the article; E – critical revision of the article; F – final approval of the article

Dental and Medical Problems, ISSN 1644-387X (print), ISSN 2300-9020 (online) *Dent Med Probl*. 2026;63(5):1137–1145

Address for correspondence
Agata Izabela Cieślik
E-mail: agata.cieslik@hirszfeld.pl

Funding sources
None declared

Conflict of interest
None declared

Acknowledgements
None declared

Received on May 26, 2025
Reviewed on June 11, 2025
Accepted on July 21, 2025

Published online on October 30, 2026

Abstract

Background. Oral health is one of the most important aspects of general well-being, and early tooth loss is associated with an increased risk of complications and mortality. These effects were even more pronounced in historical populations due to the limited effectiveness of the available treatment options.

Objectives. The primary aim of the present study was to investigate the prevalence of ante-mortem tooth loss (AMTL) and periapical lesions in a historical population from Gródek on the Bug River (Lublin Voivodeship), dating from the 11th to the 15th century, as valuable indicators of the population's general health.

Material and methods. The study sample consisted of skulls of adult individuals whose permanent teeth had completed the eruption process ($N = 156$). A novel 6-stage classification system (0–5) for quantifying the severity of AMTL, accompanied by descriptive labels ranging from 'none' to 'total', was proposed to improve methodological consistency in paleoanthropological research. Periapical lesions were assessed macroscopically, with lesions smaller than 3 mm classified as granulomas.

Results. Out of the 156 examined skulls, only 9 (5.8%) retained their full dentition until death, while the remaining individuals had experienced tooth loss during their lifetimes. Nearly 2/3 of the examined skulls showed considerable AMTL. A considerable proportion (32%) of the individuals from the historical population of Gródek on the Bug River exhibited severe, potentially life-threatening periapical lesions resulting from oral health complications.

Conclusions. Ante-mortem tooth loss is a common consequence of poor oral hygiene and inadequate diet in historical populations. However, AMTL is a more complex phenomenon, as its consequences can have a substantial and long-term negative impact on general health. The observed patterns of AMTL may reflect difficulties in maintaining oral health, with potential implications for broader health and dietary conditions.

Keywords: periapical granuloma, periapical cyst, paleopathology, ante mortem tooth loss (AMTL)

Cite as
Cieślik AI, Nowaczewska W, Dąbrowski P, Dzieńkowski T, Wysocka J. Ante-mortem tooth loss (AMTL) and dentoalveolar pathologies in the 11th–15th-century Gródek on the Bug River skeletal collection: Patterns and implications. *Dent Med Probl.* 2026;63(5):1137–1145. doi:10.17219/dmp/208468

DOI
10.17219/dmp/208468

Copyright
Copyright by Author(s)
This is an article distributed under the terms of the Creative Commons Attribution 3.0 Unported (CC BY 3.0) (https://creativecommons.org/licenses/by/3.0/)

Highlights

- Oral health was assessed in 156 adult skulls from medieval Gródek on the Bug River.
- A novel 6-stage ante-mortem tooth loss (AMTL) classification system with descriptive severity labels was proposed.
- Approximately ⅔ of individuals exhibited substantial AMTL, reflecting chronic oral diseases, likely associated with poor oral hygiene and inadequate nutrition.
- Periapical lesions were identified in approximately ⅓ of skulls, indicating a considerable burden of untreated oral infections with potentially serious health consequences.

Introduction

Oral health is one of the most important aspects of general well-being and depends on the proper functioning of all components of the stomatognathic system (SS). The SS comprises the teeth and periodontium (dentoalveolar system), the articulatory and occlusal systems of the upper and lower dental arches (dento-dental system), functionally interconnected temporomandibular joints (TMJs) (joint complex), as well as the facial bones, soft tissues, and the organs of the oral cavity and face. The proper structure and functioning of these components are essential for several critical processes, including the sucking reflex, articulation, mastication, and the initial stages of food digestion.[1–3]

The SS is structurally and functionally complex, and is therefore susceptible to various forms of damage and dysfunction. While modern dentistry can effectively treat or mitigate the consequences of many such conditions, diseases and disorders affecting the SS in historical populations often had serious health implications due to the limited medical knowledge and therapeutic options available at the time.

Ante-mortem tooth loss (AMTL) in historical populations most commonly resulted from the interplay of dietary habits, cultural practices and environmental factors. Dietary and nutritional factors played a significant role in AMTL. For instance, the consumption of tough and unprocessed foods led to increased dental wear, which was a major contributor to tooth loss.[4] Conversely, a diet consisting of soft, highly processed foods rich in carbohydrates may have promoted the development of extensive carious lesions, leading to pulp exposure, abscess formation, and ultimately tooth loss.[5,6] Smith and Betsinger demonstrated that, in prehistoric Tennessee, the transition to maize agriculture was associated with changes in AMTL patterns, suggesting that dietary carbohydrates and nutritional deficiencies may have contributed to tooth loss.[7] Poor oral hygiene also contributed significantly to AMTL in historical populations. The substantial accumulation of dental calculus could lead to the inflammation of the periodontal tissues, potentially resulting in tooth loosening and eventual loss. Cases of AMTL resulting from trauma are less frequently reported in the literature, although traumatic injuries could undoubtedly cause serious complications within the SS.[4,8] Finally, teeth could also be lost during an individual's lifetime as a result of deliberate practices. Dental ablation for esthetic or cultural (ritual or symbolic) reasons was a recognized cause of AMTL in certain populations, including Hawaiians and prehistoric populations in Africa, China and Japan.[9–11]

One of the most serious dental pathologies observed in historical populations and contributing to AMTL was the development of periapical lesions and inflammatory apical cysts resulting from bacterial infections of the root canal system. The incidence of periapical lesions and the mortality associated with dental infections in historical populations were considerably higher than today, with dental diseases representing an important cause of death. Historical records indicate that, in the early 17th century, "teeth" were consistently listed as the 5th or 6th leading cause of death in London.[12] This finding highlights the potentially severe consequences of untreated dental infections, which could lead not only to AMTL, but also to systemic complications and death. This is further supported by case studies of prehistoric populations, demonstrating that oral abscesses could result in life-threatening conditions.[13]

The primary aim of the present study was to investigate the prevalence of AMTL in a historical population from Gródek on the Bug River (Lublin Voivodeship), dating from the 11th to the 15th century, in order to characterize oral health patterns within this medieval community. The study also examined the occurrence of periapical bone destruction in this population, assessing the frequency and severity of these pathological lesions as indicators of dental health status. From a methodological perspective, we propose a comprehensive 6-stage classification system (0–5) for AMTL, accompanied by descriptive labels, to provide a standardized approach to quantifying the severity of tooth loss in paleoanthropological studies.

Material and methods

The stronghold at Gródek on the Bug River (Polish: *Gródek nad Bugiem*) forms part of a large medieval settlement complex situated near the confluence of the Huczwa and Bug Rivers, close to the present-day eastern border of Poland. Initially, the settlement at Gródek on the Bug River was dated to the 12th–15th centuries. However, recent

research using radiocarbon (^{14}C) dating has shown that the cemetery is older, establishing the 11th–15th centuries as a more reliable chronological framework for its use.[14]

The skeletal material was excavated during the 1952–1955 field seasons, and the preliminary results of anthropological analyses involving 303 individuals (170 males and 133 females) were published by Belniak et al.[15] Currently, the osteological collection from Gródek on the Bug River is less numerous than it was in the 1950s, owing to the damage caused by the flood that affected Wroclaw in 1997. The remains of 197 individuals are currently housed at the Department of Anthropology, Ludwik Hirszfeld Institute of Immunology and Experimental Therapy, Polish Academy of Sciences, in Wroclaw, Poland. Skulls in relatively good condition constitute the largest part of this osteological collection (191 out of 197 individuals).[16]

Long-term archaeological research conducted at this site has revealed numerous artifacts providing valuable insights into the everyday lives of the inhabitants of medieval Gródek on the Bug River. Clusters of graves containing similar grave goods, such as buttons and fabric fragments, sometimes interwoven with a gold thread, have been identified in the eastern part of the cemetery. The concentration of graves, both with and without grave goods, in this area is particularly intriguing and may suggest that this part of the cemetery was established earlier than the others. It is possible that this area once constituted the central part of the cemetery, where individuals from the wealthiest and most prominent families were buried.[17] These findings may indicate social stratification within the medieval community of Gródek on the Bug River, particularly given that some graves contained silk textiles and fabrics incorporating gold or gilded silver threads, which would have been affordable only to the most affluent members of society.[18]

The study sample consisted of 156 adult skulls from individuals whose permanent teeth had completed the eruption process. An essential criterion for inclusion in the study was the good state of preservation of both the skulls and the anatomical structures of the SS. Sex and age at death were estimated based on cranial features.[19–21] The biological age categories followed the classification proposed by Martin and Saller.[22] The sample was divided into 2 age groups: younger adults (*juvenis*, including only individuals with their third molars erupted, and *adultus*) and older adults (*maturus* and *senilis*).

For each individual in the examined sample, AMTL was documented by identifying the specific tooth positions (incisors, canines, premolars, and molars) in both the maxilla and the mandible, based on visible evidence of healing in the alveolar sockets. The 6-point classification scale developed for this study was used to assess the severity of AMTL, taking into account various functional aspects of tooth loss (Table 1).

Kennedy's classification served as the initial methodological framework for this study.[23] However, this system focuses on patterns of partial edentulism relevant to prosthetic rehabilitation and does not account for individual tooth losses. Our approach differs fundamentally, as it examines all patterns of tooth loss in the Gródek population as indicators of the oral health challenges faced by this historical community. Consequently, documenting single-tooth losses, multiple-tooth losses, and losses involving functional tooth groups is essential for a comprehensive assessment of dental pathology.

Table 1. Six-point classification scale to assess the severity of ante-mortem tooth loss (AMTL) in the Gródek on the Bug River population (11th–15th centuries)

Stage	Descriptive label	Criterion
0	none	no AMTL observed
I	mild	loss of 1–4 teeth in different parts of the dentoalveolar processes
II	moderate	loss of 5–8 teeth in different parts of the dentoalveolar processes
III	severe	unilateral loss of at least 3 adjacent teeth
IV	extensive	bilateral loss of at least 3 adjacent teeth within the dental arch of the maxilla or/and the mandible
V	total	edentulism

Periapical lesions were examined macroscopically according to the criteria proposed by Dias et al.[24] Lesions with a maximum intraosseous diameter of less than 3 mm were classified as periapical granulomas, whereas those exceeding this threshold were classified as apical periodontal cysts.

To determine whether sex or age at death influenced the severity of tooth loss, the Mann–Whitney *U* test was used to compare the groups, and the effect size was calculated.

Results

Of the 156 examined skulls, only 9 (5.8%) retained their full dentition until death, while the remaining individuals had experienced tooth loss during their lifetimes. Nearly ⅓ of the examined skulls showed a degree of AMTL corresponding to the first category of the classification scale, whereas the remaining individuals exhibited more significant tooth loss, including patterns that would have required prosthetic rehabilitation (Table 2).

Table 2. Tooth loss according to the 6-point classification scale

AMTL stage	Younger adults	Older adults	Total
0	9 (12)	0 (0)	9 (6)
I	33 (44)	15 (18)	48 (31)
II	14 (19)	21 (26)	35 (22)
III	9 (12)	22 (27)	31 (20)
IV	10 (13)	20 (25)	30 (19)
V	0 (0)	3 (4)	3 (2)
Total	75 (100)	81 (100)	156 (100)

Data presented as number (percentage) (*n* (%)).
AMTL – ante-mortem tooth loss.

The initial study group consisted of 156 individuals; however, 4 juveniles and one individual who died at a senile age were excluded from the statistical analysis, as they did not meet the inclusion criteria. The final sample included in the statistical analysis comprised 151 skulls (92 male and 59 female). Seventy-one individuals were classified as young adults, while the remaining 80 were classified as older adults. Ante-mortem tooth loss was found to be significantly more severe in older adults than in younger adults (medium effect size; $r = 0.36$). No significant differences in AMTL were observed between male and female individuals (Table 3).

No sex-related differences in AMTL were observed within either the younger or older age groups. This may suggest that the factors influencing AMTL in this population affected males and females similarly across the examined age categories (Table 4).

A considerable proportion of the individuals from the historical population of Gródek on the Bug River ($n = 50$; 32%) exhibited periapical lesions, some of which were potentially life-threatening complications of oral disease (Supplementary material S1, available on request from the corresponding author). Most of these lesions (46 out of 50; 92%) were classified as granulomas, measuring no more than 3 mm in diameter. An example of an extensive lesion was observed in the cranium of an adult male (specimen No. 10; Fig. 1). The specimen was generally well preserved. However, most of its dentition had been lost ante mortem, particularly in the maxilla. The teeth extending from the left maxillary lateral incisor to the left maxillary third molar were missing, along with the left part of the maxillary body, and signs of extensive bone remodeling were evident (Fig. 1C and 1D). On the right side, further evidence of AMTL was observed, mainly affecting the premolars and molars. The missing teeth in the maxillary alveolar processes corresponded to those missing from the mandible (Fig. 1A and 1B).

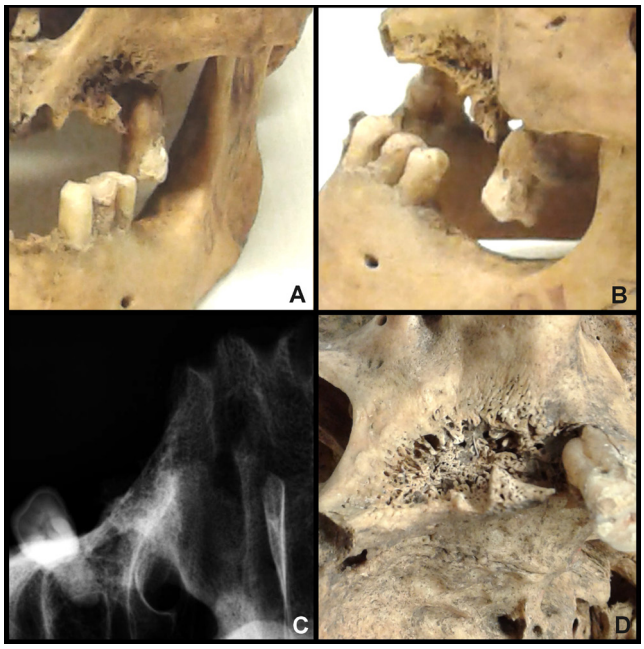

Fig. 1. Anterior (A) and lateral (B) views of skull No. 10 (male, *adultus*), showing extensive ante-mortem tooth loss (AMTL) in both the maxillary and mandibular dental arches. Note the extensive bone remodeling within the alveolus (C and D)

Table 3. Comparison of the ante-mortem tooth loss (AMTL) stage between the examined sex and age categories

Category		AMTL stage			*Z*	*p*-value	*r*
		mean rank	*Me*	*IQR*			
Sex	M ($n = 92$)	79.27	2.00	2.75	−1.18	0.237	0.10
	F ($n = 59$)	70.90	2.00	2.00			
Age	younger adults ($n = 71$)	59.94	1.00	2.00	−4.38	<0.001*	0.36
	older adults ($n = 80$)	90.25	3.00	2.00			

Me – median; *IQR* – interquartile range; *Z* – test value; *r* – effect size; M – male; F – female; * statistically significant.

Table 4. Comparison of the ante-mortem tooth loss (AMTL) stage between both sexes across the examined age categories

Category		AMTL stage			*Z*	*p*-value	*r*
		mean rank	*Me*	*IQR*			
Younger adults ($n = 71$)	M ($n = 32$)	34.13	1.00	1.75	−0.73	0.464	0.09
	F ($n = 39$)	37.54	2.00	2.00			
Older adults ($n = 80$)	M ($n = 60$)	41.36	3.00	2.00	−0.59	0.555	0.07
	F ($n = 20$)	37.93	3.00	1.00			

In 4 out of the 50 cases (8%), the lesions exhibited features consistent with periapical cyst formation, involving the uncontrolled proliferation of epithelial cells. In specimen No. 244 (Fig. 2), the process appears to have originated from an infection of the pulp of the maxillary canine. As the lesion enlarged, it extended into the body of the maxilla and eventually penetrated the maxillary sinus.



Fig. 2. Anterior view of skull No. 244 (male, *adultus*) (A), showing an extensive defect in the anterior wall of the alveolar process of the right maxilla, resulting from the growth of a periapical cyst. Palatal views of the skull (B, C), showing an oval defect in the alveolar process of the right maxilla. Radiograph of specimen No. 244 (C), showing the regular shape of the lesion and limited evidence of bone remodeling

Discussion

In the population from Gródek on the Bug River, individuals in the older age group with AMTL classified as stages III–V predominated (n = 45; 56%), whereas among younger adults, the majority were classified within stages 0–II (n = 56; 73%) (Table 2). As in other historical populations, the severity of AMTL increased with age, as evidenced by the more extensive tooth loss observed in older individuals. Tooth loss is an age-related process, making this finding unsurprising, as repeatedly reported in previous studies.[25–28]

Conversely, sex was not found to be a significant factor influencing the severity of AMTL, a finding also reported in some previous studies.[29] However, the results of other studies are inconclusive and warrant further discussion. Trombley et al. found that males from a medieval site in Italy had significantly greater tooth loss than females.[26] However, this difference was not observed when only young adults (18–29 years) were analyzed, as relatively little AMTL was recorded in this age group.[26] Similarly, when analyzing the percentage of AMTL in populations from medieval and modern-period Spanish sites, Lopez et al. found no sex-related differences among medieval individuals.[25] However, in the modern-period population, males had fewer remaining teeth than females, indicating a higher percentage of AMTL.[25]

The present study did not identify sex-related differences in AMTL among individuals from Gródek on the Bug River, in contrast to the findings of some researchers investigating other historical populations. This discrepancy may partly reflect differences in the methodological approaches employed, as the present study evaluated the stage of tooth loss rather than its percentage, as reported in some other studies. The stages of AMTL do not necessarily increase proportionally with the number of teeth lost; rather, they were designed to reflect the increasing functional impact on the SS when the adjacent teeth are lost. Thus, the assessment in the present study focused not simply on the quantity of AMTL, but primarily on the severity of its potential consequences.

The substantial tooth loss observed in the population from Gródek on the Bug River was associated with an increased risk of serious functional consequences. Even the loss of a single tooth can have consequences in the form of the Popov–Godon phenomenon, which occurs when the remaining teeth shift toward an edentulous space following tooth loss, potentially accompanied by the overeruption of the opposing teeth. Such changes in tooth alignment can result in various dental problems, including impaired mastication, increased tooth wear, and potential periodontal complications.[30] With further tooth loss, these problems may accumulate and, in the absence of effective prosthetic rehabilitation, lead to permanent changes in the oral cavity.

Various types of prostheses have been used throughout history to replace natural teeth; however, early solutions were generally limited in their functional effectiveness. Dentures with effective retention were first developed in the early 17th century and became more widely used in the 19th and 20th centuries, considerably later than the period represented by the Gródek skeletal series.[31] Consequently, this population was exposed to the direct consequences of tooth loss, including changes in facial morphology, TMJ disorders, and digestive problems resulting from impaired initial food processing in the oral cavity.

Tooth loss can also lead to changes in oral hygiene practices, dietary habits, and the overall condition of the remaining dentition, potentially increasing the risk of further dental problems. Individuals with missing teeth may shift toward softer, more cariogenic diets, which could further promote dental caries.[32] Tooth loss is also frequently associated with advanced periodontal disease, including stage IV periodontitis, which substantially increases the risk of further tooth loss due to persistent inflammation and the loss of periodontal attachment.[33] Other adverse consequences of tooth loss may include nutritional deficiencies, which can impair immune function and tissue healing, potentially exacerbating periodontal disease.[34] Thus, the loss of even a single tooth may initiate a cycle of progressive deterioration in oral and general health, ultimately reducing quality of life (QoL).

The classification proposed in the present study takes into account the functional progression of AMTL. In stages I and II, tooth loss is scattered, and the SS retains some adaptive capacity to compensate for the loss of individual teeth (e.g., through the previously mentioned Popov–Godon phenomenon). Stages III and IV, characterized by the clustered tooth loss affecting functional occlusal units, result in substantial functional impairment, whereas stage V represents an almost complete

loss of basic stomatognathic functions. Thus, this novel functional approach to AMTL classification can be applied to different populations and chronological periods, extending beyond traditional tooth-by-tooth assessments. It is also worth noting that the assessment of the prevalence of dental diseases, such as dental caries, is often complicated by post-mortem tooth loss (PMTL), whereas the evaluation of the alveolar processes in well-preserved skulls does not present the same difficulties.[35]

Diseases of the oral cavity, particularly dental caries, were likely the leading cause of tooth loss in the historical population of Gródek on the Bug River. This is supported by cases in which carious lesions are observed alongside the obliterated alveolar sockets (e.g., Fig. 3). In some individuals, the periapical inflammatory changes associated with carious lesions are also evident. Most of the observed periapical lesions were classified as granulomas, whereas only a small number were identified as inflammatory radicular cysts.



Fig. 3. Mandible of individual No. 260 (female, *maturus*), showing an extensive carious lesion affecting the left second molar, associated with the formation of a caries-induced periapical cyst

In the case of individual No. 10 (Fig. 1), the traumatic origin of the tooth loss affecting the left part of the maxillary alveolar process should be considered, given the extensive bone loss and pronounced signs of remodeling. It may be hypothesized that the injury occurred during combat with a right-handed opponent, resulting in the loss of the premolars following a blow. Various anatomical abnormalities of the SS may also have contributed to premature tooth loss.

In individual No. 344 (Fig. 4), an impacted tooth was observed, accompanied by extensive inflammation in the region of the left alveolar process, at the level of the premolar roots. In individual No. 252 (Fig. 5), an impacted lateral incisor was identified in the left maxilla. Individual No. 455 exhibited a mandibular torus (Fig. 6), a benign bony protuberance that may have made oral hygiene more difficult, potentially contributing to the faster development of carious lesions and, consequently, tooth loss.



Fig. 4. Radiograph of specimen No. 344 (male, *maturus*) (A), showing an impacted left maxillary canine. Anterior view of skull No. 344 (B), showing the impacted canine. Note the extensive ante-mortem tooth loss (AMTL) in the left maxillary alveolar process and evidence of ongoing inflammatory changes within the alveolar bone (C)

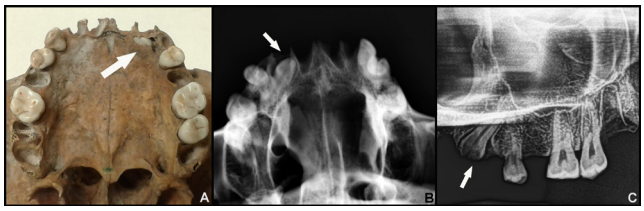

Fig. 5. Skull No. 252 (male, *maturus*), showing an impacted left maxillary lateral incisor. Note the ante-mortem loss of the left canine, possibly associated with a developmental anomaly



Fig. 6. Mandible of individual No. 455 (female, *adultus*), showing bilateral mandibular tori (torus mandibularis). Note the bilateral ante-mortem loss of the first molars adjacent to the areas of bony overgrowth

Tooth loss also has significant long-term health consequences that extend beyond the oral cavity, affecting overall health and QoL. Tooth loss, particularly when it occurs early in adulthood, can lead to long-term complications, and is associated with an increased risk of systemic diseases and mortality. In contemporary populations, it has been linked to an increased risk of cardiovascular diseases and stroke.[36] Tooth loss also affects the diversity and quality of dietary intake, often leading individuals to favor softer foods that require less chewing. Consequently, they may consume more processed foods and fewer raw vegetables.[37,38] In the Middle Ages, when prosthetic rehabilitation

options were limited, and modern processed foods and dietary supplements were unavailable, tooth loss, particularly complete edentulism, could have substantially affected dietary habits, potentially resulting in nutritional deficiencies and further deterioration of general health.[37] Thus, AMTL can be regarded as an indicator not only of oral health, but also of broader health conditions and general well-being.[39]

Oral care has been shown to be inversely associated with mortality among individuals experiencing tooth loss.[40] For instance, Adolph et al. demonstrated a strong association between poor oral health, including the loss of at least 10 teeth or a masticatory unit count of fewer than 5, and increased all-cause mortality.[41] Particular attention has been directed toward periodontal diseases as a major cause of AMTL. Untreated periodontal diseases tend to become chronic and may lead to persistent low-grade systemic inflammation, potentially contributing to the exacerbation or progression of various systemic disorders, including cardiovascular diseases.[39,42,43] Chronic inflammation originating in the oral cavity has also been associated with an increased risk of diabetes and stroke.[44] Tooth loss is considered an indicator of poor oral health, particularly when an individual has fewer than 20 natural teeth.[39]

The dental health of the inhabitants of historical Gródek on the Bug River was poor, as evidenced by the extent of tooth loss: 62% of all individuals had experienced substantial AMTL, corresponding to stages II–V of the classification system. This was particularly evident among individuals belonging to the older age categories. Although the population of Gródek on the Bug River appears to have been socially stratified, this differentiation was not significantly reflected in the oral hygiene and dental health of the examined individuals. The widespread occurrence of oral pathologies may have contributed to a substantial chronic inflammatory burden and potentially increased the risk of systemic diseases.

As demonstrated by contemporary research, oral health is increasingly recognized as an important indicator of general health, with numerous studies highlighting the relationships between oral conditions and systemic diseases. Assessments of oral health can provide valuable insights into an individual's overall health status, as oral pathologies may also reflect the underlying systemic conditions. Assiri et al. demonstrated that individuals with poor oral health, as indicated by factors such as periapical lesions and tooth loss, frequently had a history of systemic diseases, including diabetes, hypertension and anemia.[45] Wasterlain et al. demonstrated how dental pathologies reflected living conditions in a skeletal sample from the late 19th and early 20th centuries.[46] Similarly, DeWitte and Bekvalac, examining the prevalence of caries and periodontitis in the skeletal remains excavated from the medieval English cemetery of St. Mary Graces, demonstrated associations between oral health status, reduced immune function, and an increased mortality risk in this historical population.[47]

Thus, the assessment of oral pathologies and their potential impact on QoL can provide valuable insights into an individual's overall health status and help identify health-related changes over time. In the case of the historical population from Gródek on the Bug River, the extensive AMTL observed may be regarded as a potential indicator of compromised general health and an increased overall health burden. However, further comparative studies involving other historical skeletal populations and incorporating a broader range of paleopathological indicators are necessary to establish more general patterns of health and disease in past populations.

Conclusions

Ante-mortem tooth loss is a common consequence of poor oral hygiene, inadequate diet and advancing age in historical populations. However, AMTL is a more complex phenomenon, as its consequences can have a substantial and long-term negative impact on general health. The present study revealed a high proportion of individuals from Gródek on the Bug River (11th–15th centuries) with moderate to extensive (62%; stages II–IV) and complete (2%; stage V) tooth loss. The oral health status of historical populations can also provide insights into disease patterns that cannot be directly identified through the examination of skeletal remains. The observed patterns of AMTL may reflect difficulties in maintaining oral health, and may be associated with broader health and dietary conditions, although the direct assessment of systemic health status was not possible in the present study.

Ethics approval and consent to participate

Not applicable.

Data availability

The datasets supporting the findings of the current study are available from the corresponding author on reasonable request.

Consent for publication

Not applicable.

Use of AI and AI-assisted technologies

Not applicable.

ORCID iDs

Agata Izabela Cieślik https://orcid.org/0000-0003-3180-6974
Wioletta Nowaczewska https://orcid.org/0000-0003-1907-554X
Paweł Dąbrowski https://orcid.org/0000-0001-6016-9201
Tomasz Dzieńkowski https://orcid.org/0000-0002-3899-3170
Joanna Wysocka https://orcid.org/0000-0003-1436-6700

References

1. Majewski SW. Gnatofizjologia stomatologiczna. *Normy okluzji i funkcje układu stomatognatycznego.* Warsaw, Poland: Wydawnictwo Lekarskie PZWL; 2007.
2. Herber RP, Fong J, Lucas SA, Ho SP. Imaging an adapted dentoalveolar complex. *Anat Res Int*. 2012;2012:782571. doi:10.1155/2012/782571
3. Manziuc MM, Savu MM, Almăşan O, et al. Insights into occlusal analysis: Articulating paper versus digital devices. *J Clin Med*. 2024;13(15):4506. doi:10.3390/jcm13154506
4. Lukacs JR. Dental trauma and antemortem tooth loss in prehistoric Canary Islanders: Prevalence and contributing factors. *Int J Osteoarchaeol*. 2007;17(2):157–173. doi:10.1002/oa.864
5. Lukacs JR. Dental paleopathology and agricultural intensification in South Asia: New evidence from Bronze Age Harappa. *Am J Phys Anthropol*. 1992;87(2):133–150. doi:10.1002/ajpa.1330870202
6. Tomczyk J, Olczak-Kowalczyk D, Turska-Szybka A, Studnicki M. Oral health behaviors and tooth decay at the age of 12 and 15–18 years in Poland. *Dent Med Probl*. 2025;62(1):13–22. doi:10.17219/dmp/184054
7. Smith MO, Betsinger TK. Patterns of antemortem tooth loss in late prehistoric west-central Tennessee. *Dent Anthropol*. 2021;34(2):3–20. doi:10.26575/daj.v34i2.320
8. Cieślik AI, Dąbrowski P, Przysiężna-Pizarska MA. The face of conflict: Significant sharp force trauma to the mid-facial skeleton in an individual of probable 16th–17th century date excavated from Byczyna, Poland. *Int J Paleopathol*. 2017;17:75–78. doi:10.1016/j.ijpp.2017.02.003
9. Pietrusewsky M, Douglas MT. Tooth ablation in old Hawai'i. *J Polyn Soc*. 1993;102(3):255–272. https://www.jstor.org/stable/20706517. Accessed May 27, 2025.
10. Briggs LC. *The Stone Age Races of Northwest Africa*. Cambridge, MA: Peabody Museum Press;1955.
11. Kusaka S, Ikarashi T, Hyodo F, Yumoto T, Katayama K. Variability in stable isotope ratios in two Late-Final Jomon communities in the Tokai coastal region and its relationship with sex and ritual tooth ablation. *Anthropol Sci*. 2008;116(2):171–181. doi:10.1537/ase.070703
12. Clarke J. Toothaches and death. *J Hist Dent*. 1999;47(1):11–13. PMID:10686905.
13. Nicklisch N, Nasse D, Ganslmeier R, Alt KW. Oral infections and the risk of mortality in the Iron Age. *Bull Int Assoc Paleodont*. 2008;2(2):6–13. https://hrcak.srce.hr/file/51723. Accessed May 27, 2025.
14. Bartecki B, Borowska B, Dzieńkowski T, Hajdas I, Hyrchała A, Wołoszyn M. Early Medieval inhumation cemeteries in Gródek-Volyn'. Research status and future prospects. In: Jonaitis R, Kaplūnaitė I, eds. *From Paganism to Christianity: Burial Rites During the Transition Period*. Vilnius, Lithuania: Lithuanian Institute of History; 2024:145–171. https://www.istorija.lt/data/public/uploads/2025/02/9-2024-from-paganism-bartomiej-bartecki.pdf. Accessed May 27, 2025.
15. Belniak T, Krupiński T, Magnuszewicz M, Rauhut J, Szczotkowa Z. Cmentarzysko w Gródku nad Bugiem (XIII-XVII w.). *Mater Pr Antropol*. 1961;50:1–110.
16. Cieślik A. The number and state of preservation of the skeletons from Gródek upon the Bug River, site 1A (excavations in the years 1952–1955) housed at the L. Hirszfeld Institute of Immunology and Experimental Therapy, PAS in Wroclaw. In: Wołoszyn M, ed. *The Early Medieval Settlement Complex at Gródek Upon the Bug River in the Light of Results from Past Research (1952–1955): Material Evidence*. Krakow – Leipzig – Rzeszow – Warsaw: Leipziger Universitätsverlag; 2018:943–964.
17. Kuśnierz J. Gródek upon the Bug River, site 1A. The results of the excavations in the years 1952–1955. Cemetery at the ward of the stronghold. In: Wołoszyn M, ed. *The Early Medieval Settlement Complex at Gródek Upon the Bug River in the Light of Results from Past Research (1952–1955): Material Evidence*. Krakow – Leipzig – Rzeszow – Warsaw: Leipziger Universitätsverlag; 2018:699–734.
18. Cybulska M, Marciniak M, Sielski J. The early medieval textile finds from Gródek upon the Bug River. An analysis of materials, manufacturing techniques and origin. In: Wołoszyn M, ed. *The Early Medieval Settlement Complex at Gródek Upon the Bug River in the Light of Results from Past Research (1952–1955): Material Evidence*. Krakow – Leipzig – Rzeszow – Warsaw: Leipziger Universitätsverlag; 2018:735–800.
19. Brothwell DR. *Digging Up Bones: The Excavation, Treatment, and Study of Human Skeletal Remains*. 3rd ed. Oxford, UK: Oxford University Press; 1981.
20. Meindl RS, Lovejoy CO. Ectocranial suture closure: A revised method for the determination of skeletal age at death based on the lateral-anterior sutures. *Am J Phys Anthropol*. 1985;68(1):57–66. doi:10.1002/ajpa.1330680106
21. Ferembach D, Schwidetzky I, Stoukal M. Recommendations for age and sex diagnoses of skeletons. *J Hum Evol*. 1980;9:517–549. doi:10.1016/0047-2484(80)90061-5
22. Martin R, Saller K. *Lehrbuch der Anthropologie I–II*. Jena, Germany: Gustav Fischer; 1957.
23. Kennedy E. *Partial Denture Construction: A Text Book Describing the Technics of Impression Taking and the Construction of that Type of Removable Partial Dentures Which Are Supported and Retained by External Attachments*. 2nd ed. New York, NY: Dental Items of Interest Publishing Co.; 1942.
24. Dias GJ, Prasad K, Santos AL. Pathogenesis of apical periodontal cysts: Guidelines for diagnosis in palaeopathology. *Int J Osteoarchaeol*. 2007;17(6):619–626. doi:10.1002/oa.902
25. Lopez B, Pardiñas AF, Garcia-Vazquez E, Dopico E. Socio-cultural factors in dental diseases in the Medieval and early Modern Age of northern Spain. *Homo*. 2012;63(1):21-42. doi:10.1016/j.jchb.2011.12.001
26. Trombley TM, Agarwal SC, Beauchesne PD, et al. Making sense of medieval mouths: Investigating sex differences of dental pathological lesions in a late medieval Italian community. *Am J Phys Anthropol*. 2019;169(2):253–269. doi:10.1002/ajpa.23821
27. Trombley TM, Goodson CJ, Agarwal SC. Medieval mouths in context: Biocultural and multi-scalar considerations of the mouth and the case of late-medieval Villamagna, Italy. *Mediev Archaeol*. 2023;67(1):187–220. doi:10.1080/00766097.2023.2204729
28. Dąbrowski W, Jagiełło K, Mossakowska M, et al. Evaluating changes in dental status among Polish older adults over a decade: A comparative analysis of PolSenior (2009) and PolSenior2 (2019) surveys. *Dent Med Probl*. 2025;62(1):23–30. doi:10.17219/dmp/196535
29. Novak M. Dental health and diet in early medieval Ireland. *Arch Oral Biol*. 2015;60(9):1299–1309. doi:10.1016/j.archoralbio.2015.06.004
30. Mamikon DK. Correction of the tooth alignment in case of the Popov–Godon phenomenon using a dental implant with immediate loading (clinical case). *J Glob Pharma Technol*. 2018;10(4):869.
31. Powers N. Archaeological evidence for dental innovation: An eighteenth century porcelain dental prosthesis belonging to Archbishop Arthur Richard Dillon. *Br Dent J*. 2006;201(7):459–463. doi:10.1038/sj.bdj.4814117
32. Cunha de Medeiros TC, Souza AA, Prates RC, Chapple I, Steffens JP. Association between tooth loss, chronic conditions, and common risk factors: Results from the 2019 Brazilian Health Survey. *J Periodontol*. 2022;93(8):1141–1149. doi:10.1002/JPER.21-0433
33. Siow DS, Goh EXJ, Ong MMA, Preshaw PM. Risk factors for tooth loss and progression of periodontitis in patients undergoing periodontal maintenance therapy. *J Clin Periodontol*. 2023;50(1):61–70. doi:10.1111/jcpe.13721
34. Darwish HA, Alkhalaf HE, Alraddadi AS et al. Association between teeth loss and nutritional deficiencies: A literature review. *EC Dent Sci*. 2020;19(2):1–7. https://ecronicon.net/assets/ecde/pdf/association-between-teeth-loss-and-nutritional-deficiencies-a-literature-review.pdf. Accessed May 27, 2025.
35. Dąbrowski P, Nowaczewska W, Domagała D, et al. Searching for a relationship between the elemental composition of archaeological bones and the occurrence of caries. *Dent Med Probl*. 2024;61(6):875–884. doi:10.17219/dmp/186623
36. Cheng F, Zhang M, Wang Q, et al. Tooth loss and risk of cardiovascular disease and stroke: A dose–response meta analysis of prospective cohort studies. *PLoS One*. 2018;13(3):e0194563. doi:10.1371/journal.pone.0194563
37. Joshipura KJ, Willett WC, Douglass CW. The impact of edentulousness on food and nutrient intake. *J Am Dent Assoc*. 1996;127(4):459–467. doi:10.14219/jada.archive.1996.0237
38. Tada A, Miura H. Association of mastication and factors affecting masticatory function with obesity in adults: A systematic review. *BMC Oral Health*. 2018;18(1):76. doi:10.1186/s12903-018-0525-3
39. Kramarczyk K, Skowron K, Skowron P, Kaczmarzyk T. The multifaceted impact of missing teeth on general health: A narrative review. *Folia Med Cracov*. 2024;64(1):25–37. doi:10.24425/fmc.2024.150139

40. Hayasaka K, Tomata Y, Aida J, Watanabe T, Kakizaki M, Tsuji I. Tooth loss and mortality in elderly Japanese adults: Effect of oral care. *J Am Geriatr Soc*. 2013;61(5):815–820. doi:10.1111/jgs.12225
41. Adolph M, Darnaud C, Thomas F, et al. Oral health in relation to all-cause mortality: The IPC cohort study. *Sci Rep*. 2017;7:44604. doi:10.1038/srep44604
42. DeStefano F, Anda RF, Kahn HS, Williamson DF, Russell CM. Dental disease and risk of coronary heart disease and mortality. *BMJ*. 1993;306(6879):688–691. doi:10.1136/bmj.306.6879.688
43. Seymour GJ, Ford PJ, Cullinan MP, Leishman S, Yamazaki K. Relationship between periodontal infections and systemic disease. *Clin Microbiol Infect*. 2007;13(Suppl 4):3–10. doi:10.1111/j.1469-0691.2007.01798.x
44. Shahi S, Farhoudi M, Dizaj SM, et al. The link between stroke risk and orodental status – a comprehensive review. *J Clin Med*. 2022;11(19):5854. doi:10.3390/jcm11195854
45. Assiri KI, Sandeepa NC, Asiri RS, Mulawi SA, Najmi SM, Srivastava KC. Assessment of oral–systemic disease association amongst dental patients: A retrospective panoramic radiographic study. *J Contemp Dent Pract*. 2020;21(7):748–755. PMID:33020357.
46. Wasterlain SN, Cunha E, Hillson S. Periodontal disease in a Portuguese identified skeletal sample from the late nineteenth and early twentieth centuries. *Am J Phys Anthropol*. 2011;145(1):30–42. doi:10.1002/ajpa.21464
47. DeWitte SN, Bekvalac J. Oral health and frailty in the medieval English cemetery of St Mary Graces. *Am J Phys Anthropol*. 2010;142(3):341–354. doi:10.1002/ajpa.21228

Original paper

Risk of malignant transformation in oral lichen planus and oral lichen planus with dysplasia: A retrospective clinical study of 435 histologically verified cases

Jan Liska[1,A–D], Veronika Liskova[1,B,E,F], Nikoleta Molnarova[1,B], Ondrej Topolcan[2,E,F], Jan Netolicky[1,B], Pavel Andrle[1,B], Lucie Nechutna[1,B], Lukas Hauer[1,B], Denisa Kacerovska[3,4,E,F]

[1] Department of Stomatology, University Hospital Pilsen, Faculty of Medicine in Pilsen, Charles University, Pilsen, Czech Republic
[2] Department of Immnunochemistry Diagnostics, University Hospital Pilsen, Faculty of Medicine in Pilsen, Charles University, Pilsen, Czech Republic
[3] Sikl Department of Pathology, Faculty of Medicine in Pilsen, Charles University, Pilsen, Czech Republic
[4] Bioptical Laboratory, Pilsen, Czech Republic

A – research concept and design; B – collection and/or assembly of data; C – data analysis and interpretation;
D – writing the article; E – critical revision of the article; F – final approval of the article

Dental and Medical Problems, ISSN 1644-387X (print), ISSN 2300-9020 (online) *Dent Med Probl*. 2026;63(5):1147–1154

Address for correspondence
Veronika Liskova
E-mail: liskovav@fnplzen.cz

Funding sources
None declared

Conflict of interest
None declared

Acknowledgements
None declared

Received on July 21, 2025
Reviewed on August 5, 2025
Accepted on August 27, 2025

Published online on September 30, 2026

Abstract

Background. Chronic activity of the subepithelial lymphocytic infiltrate may induce epithelial changes associated with malignant transformation (MT) in oral lichen planus (OLP) cases.

Objectives. This study compared the risk of developing oral squamous cell carcinoma (OSCC) in a large cohort of patients with OLP and OLP with epithelial dysplasia (OLD). Special attention was paid to carcinoma location and clinical factors, such as desquamative gingivitis and reticular, erosive or ulcerative status.

Material and methods. This retrospective study included 435 histologically verified OLP/OLD cases treated between 2004 and 2024. To assess risk factors, medical history data on medication, smoking and comorbidities was collected. Clinical and pathological aspects were correlated. Statistical analyses were performed using SigmaXL software.

Results. Of the cases included in the study, 59.8% were classified as OLP (260/435) and 40.2% as OLD (175/435). A case was considered a true MT only if it followed the OLP/OLD biopsy results. According to this criterion, 30 OSCCs were diagnosed in 21 patients. Oral squamous cell carcinoma developed in 2.3% of OLP cases (6/260) and 8.6% of OLD cases (15/175), with a statistically significant difference between the groups ($p = 0.0027$). The most common site for OSCC was the gingiva/alveolar mucosa, accounting for 33.3% (10/30) of tumors, followed by the tongue (20.0%, 6/30). Two alveolar carcinomas were located at sites of peri-implantitis associated with desquamative gingivitis. In 2 patients, synchronous OSCCs were diagnosed in the maxilla and mandible.

Conclusions. In this study, 8.6% of patients with OLD developed OSCC. Although OLP without dysplasia still carries a risk of OSCC, this risk was approx. 4 times lower, at 2.3%. Cases with desquamative gingivitis require close monitoring due to their higher risk of carcinoma development. We recommend careful observation of desquamative gingivitis around dental implants or in areas of ongoing dental inflammation. Surgical revision with biopsy should be considered if a resorptive process around an implant is suspected.

Keywords: oral lichen planus, oral squamous cell carcinoma, oral potentially malignant disorder, desquamative gingivitis, oral epithelial dysplasia

Cite as
Liska J, Liskova V, Molnarova N, et al. Risk of malignant transformation in oral lichen planus and oral lichen planus with dysplasia: A retrospective clinical study of 435 histologically verified cases. *Dent Med Probl.* 2026;63(5):1147–1154. doi:10.17219/dmp/209982

DOI
10.17219/dmp/209982

Copyright
Copyright by Author(s)
This is an article distributed under the terms of the Creative Commons Attribution 3.0 Unported (CC BY 3.0) (https://creativecommons.org/licenses/by/3.0/)

Highlights

- Oral lichen planus (OLP) is associated with the development of oral epithelial dysplasia in 40% of cases.
- The presence of dysplasia in OLP increases the risk of malignant transformation almost fourfold.
- This study identifies demographic and clinical risk factors associated with malignant transformation in OLP.

Introduction

Oral lichen planus (OLP) is one of the most common non-infectious inflammatory diseases of the oral mucosa, affecting approx. 0.5–2.5% of the population.[1–3] The condition was first described by Sir Erasmus Wilson in 1869.[3] Oral lichen planus predominantly affects individuals over the age of 40, with a higher prevalence among women.[4]

Clinically, OLP is characterized by white hyperkeratotic reticular (lacy) or linear patches, as well as atrophic and erosive lesions.[1–3] The clinical presentation of OLP is illustrated in Fig. 1. A specific manifestation commonly observed in OLP is desquamative gingivitis, whereas plaque-like lesions may also be seen on the dorsal surface of the tongue.[4–6] While the etiology of OLP remains largely idiopathic, OLP-like lesions may sometimes be associated with adverse effects of medications or local irritation caused by dental materials.[2,4,7–12] The clinical course of OLP is typically characterized by periods of remission and relapse.[1] Furthermore, OLP is frequently associated with comorbidities, particularly immune-mediated liver and thyroid disorders.[13–15]



Fig. 1. Clinical presentation of erosive oral lichen planus (OLP) with desquamative gingivitis in a 59-year-old woman

The histopathological criteria for OLP include parakeratosis, acanthosis and a well-defined subepithelial lymphocytic infiltrate.[2,6,16–18] This infiltrate consists primarily of $CD8^+$ cytotoxic T lymphocytes, which may contribute to impaired epithelial regeneration by targeting basal cells.[4,19] Oral lichen planus is associated with systemic immune responses.[20] Specific antibodies against OLP have not been identified, but patients may have elevated antinuclear antibody titers.[4] Salivary immunoglobulin A may contribute to the local immune response.[20–22] The diagnosis of OLP is established through clinical evaluation and histopathological correlation, and augmented by direct immunofluorescence that typically demonstrates shaggy fibrinogen deposition along the basement membrane zone (Fig. 2).[23–25]

The reticular-erythematous-ulcerative (REU) index and the visual analog scale (VAS) are established tools used to comprehensively assess the progression of lesions and subjective complaints during the monitoring process.[26,27] The REU index was introduced by Piboonniyom in 2005.[26] Numerous studies have indicated a correlation between hyperkeratotic lesions and an asymptomatic disease course, whereas erythematous and ulcerative lesions are often associated with pain and burning sensation.[1–3]

Biopsy of an OLP lesion is a critical procedure not only for establishing an accurate initial diagnosis but also for identifying the presence of oral epithelial dysplasia (OED).[2,23,28,29] When OED coexists with OLP, the condition is termed OLP with dysplasia (OLD).[2] Immunohistochemistry serves as a vital tool in enhancing the interpretation of histological findings. The most frequently used markers include p53 and Ki-67 proteins.[28,30,31] The p53 protein plays a significant role in cell cycle regulation,[31] whereas Ki-67 positivity is associated with increased cellular proliferation.[32] Notably, many dysplastic epithelial nuclei may exhibit a mutated form of p53.[1,33,34] In cases of OLD, a differentiated type of oral intraepithelial neoplasia (dOIN) is often observed. This pathology was defined in 2010 as a high-risk lesion with a considerable likelihood of malignant transformation (MT) into oral squamous cell carcinoma (OSCC) within 5 years.[35]

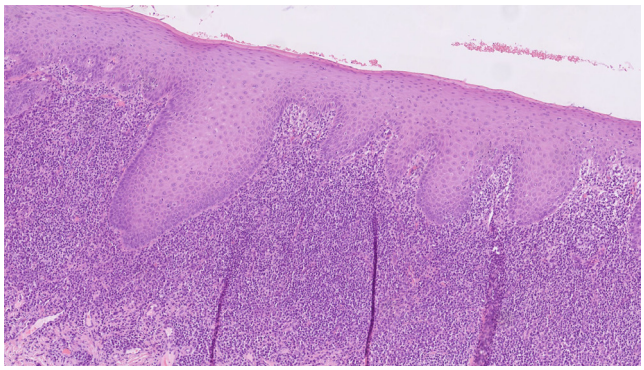

Fig. 2. Histopathological features of oral lichen planus (OLP) in a 62-year-old woman (hematoxylin and eosin staining, ×100 magnification; image courtesy of Prof. Kacerovska)

The first case of an MT of OLP to OSCC was recorded over a century ago. Since 1978, OLP has been recognized as a precancerous condition. It was included among oral potentially malignant disorders (OPMDs) in the 3rd and 4th editions of the World Health Organization (WHO) classification.[1,28] According to the definition of an OPMD provided in the 5th edition of the WHO classification, published in 2022, it is important to accurately correlate the clinical behavior of chronic lesions with the criteria for OED and to assess human papillomavirus (HPV) status in biopsy samples.[28] Malignant transformation associated with OLP is characterized by increased proliferation of atypical epithelial cells alongside the accumulation of changes induced by carcinogens or chronic inflammatory processes.[36,37] Research that fails to differentiate between OLP, OLD and other related lesions may overestimate the risk of carcinoma attributable specifically to OLP. Systematic reviews have indicated that the rate of MT in OLP ranges from 0% to 3.5%.[38] However, when cases lacking a minimum 6-month interval between the diagnosis of OLP and OSCC are excluded, this rate decreases significantly to approx. 0.44%.[36] Furthermore, erosive forms of OLP are considered to carry a greater risk. Other significant contributing factors include the infection with *Candida albicans* and the presence of OED in biopsy specimens.[28]

Accurate differentiation between these disorders is essential, particularly when distinguishing OLP and OLD from the more serious condition of proliferative verrucous leukoplakia (PVL).[28] These conditions share several characteristics, including multifocal hyperkeratotic lesions, a lymphocytic subepithelial infiltrate and frequent involvement of the gingiva.[28] However, PVL is distinctly characterized by the presence of verrucous lesions, aggressive proliferation and a high propensity for early recurrence following excision, as specified in the diagnostic criteria for this condition.[39] Notably, the rates of MT associated with PVL range from 50% to 100%.[38]

Topical treatment of OLP primarily involves corticosteroids such as dexamethasone acetate or clobetasol propionate.[40,41] In cases where a lesion is associated with severe clinical symptoms, surgical removal is performed, and the tissue is submitted for histopathological examination. Comprehensive treatment also addresses subjective complaints and includes the management of secondary oral candidiasis that may arise following corticosteroid use. Supportive management may include a combination of dexpanthenol, lidocaine hydrochloride, laser therapy, and antifungal medications.[6,42–46]

The issue of MT in OLP remains controversial. The available data is often limited to malignancy rates without consideration of the clinical aspects of OLP. This study aims to conduct a comprehensive comparison of factors associated with MT in differentiated OLP and OLD case cohorts. Additionally, we aim to examine the correlation between risk factors and clinical or demographic characteristics, such as the REU index, mycological culture results and smoking status.

Material and methods

This retrospective study examined 435 histologically verified cases of OLP and OLD that were diagnosed and treated between 2004 and 2024 at the Department of Stomatology-Oral Medicine (University Hospital Pilsen, Czech Republic). The mean duration of clinical follow-up was 5.4 years.

Inclusion criteria

Only OLP and OLD cases verified both clinically and histopathologically were included in the study. For the calculation of MT, only OSCCs that developed within clinically documented OLP or OLD lesions were included.

Exclusion criteria

Clinical cases of OLP without histopathological verification were excluded, as were cases meeting the Cerero-Lapiedra criteria for PVL.[39] Five patients previously treated for OLD were excluded due to a diagnosis of PVL. Oral squamous cell carcinoma cases with no proven association with previously verified OLP or OLD sites were also excluded.

Histopathological, clinical and microbiological assessment

The histopathological diagnosis of all cases of OLP and OLD was based on routine biopsy specimens stained with hematoxylin and eosin. All histological examinations were performed at a single institution, the tertiary care hospital. Oral epithelial dysplasia was graded using a three-tier system (OED I–III) according to the proportion of the epithelial thickness exhibiting dysplastic features. To clarify findings concerning epithelial atypia and dysplasia, immunohistochemical assessment of mutated p53 protein expression was conducted and classified as negative, positive in single nuclei, or positive in short or long lines of nuclei. The positivity of mutant p53 protein in a long line of nuclei was considered a risk-associated sign. The final outcome was the occurrence of MT of OLP/OLD lesions into OSCC.

Medical histories were obtained to collect data on comorbidities, particularly lichen ruber planus and lichen atrophicus, as well as medication use and allergies. The clinical manifestations of OLP and OLD were assessed using the REU index (range: 1–115, divided into 10 reticular, 45 erythematous and 60 erosive OLP areas), with cases categorized as either erosive or non-erosive and gingival involvement recorded. Mucosal swabs for fungal culture were obtained from all patients to diagnose primary oral candidiasis at the beginning of treatment or secondary corticosteroid-related fungal infection. The results were assessed by the microbiology laboratory using the colony-forming unit (CFU) system for both *C. albicans* and non-*albicans Candida* species (range: 0–150).

A VAS was used to measure subjective complaints such as pain and burning sensation in all cases (range: 0–10). The VAS was assessed regularly throughout follow-up. The collected data was analyzed using SigmaXL software (v. 10; SigmaXL Inc., Kitchener, Canada).

Results

This retrospective study comprised 435 OLP/OLD cases, including 300 females and 135 males. The female-to-male ratio was 2.2:1 (69% female and 31% male). The average age of the participants at the time of first contact was 56.5 years. The mean duration of treatment was 5.4 years. Within the study cohort, 19.7% (86/435) of patients reported smoking habits. Additionally, thyroid disease was observed in 19.3% (84/435) of cases, with one-third of these diagnoses made following clinical referral.

Surgical interventions included either diagnostic or therapeutic excision of the most clinically significant lesion in each case. Furthermore, topical antifungal agents, including nystatin suspension and miconazole gel, were used in 20.7% (90/435) of cases with elevated *Candida* culture results.

The cohort was categorized according to the presence of OED in biopsy specimens, resulting in 2 distinct groups: OLP and OLD. Patients with OLP represented 59.8% of the cohort, comprising 260 cases out of 435, while OLD accounted for 40.2%, with 175 cases. The OED criteria were present in one-third of the epithelium in 80.0% (140/175) of OLD cases, in two-thirds in 14.3% (25/175), and in the entire epithelial thickness in 5.7% (10/175). Regarding direct immunofluorescence testing, positive results were identified in 64.3% of OLP cases (144/224) and in 37.4% of OLD cases (52/139). The demographic and clinical characteristics, including sex distribution, age at onset, smoking status, subjective complaints, and REU index, were comparable between the 2 groups. Furthermore, dysplastic cases were more frequently associated with erosive lesions and exhibited p53 positivity in long lines of basal cell nuclei. The correlation between OLD and the presence of p53-positive nuclei arranged in long lines within the basal cell layer was statistically significant ($p < 0.0001$; two-sample *t*-test; SigmaXL). Table 1 presents a comparison of demographic and clinicopathological characteristics between OLP and OLD.

An OSCC was classified as an MT only when it was diagnosed more than 6 months after a biopsy-confirmed diagnosis of OLP or OLD. According to these criteria, 30 OSCCs were diagnosed in 21 patients. Four additional cases of OLD were excluded from the MT calculations because OPMD and OSCC were diagnosed on concurrent biopsies or because OLD was identified after a previous diagnosis of malignancy.

In the cohort of patients with OLP, the rate of MT into OSCC was 2.3% (6/260). In contrast, the rate of MT in OLD was significantly higher, at 8.6% (15/175), with the difference being statistically significant ($p = 0.0027$; two-sample *t*-test). If the minimum 6-month interval were not applied, the rate of MT in OLD would increase to 10.9% (19/175) and potentially to 13.3% (24/180) if PVL-positive cases were included.

Table 1. Demographic and clinicopathological characteristics of patients with oral lichen planus (OLP) and OLP with epithelial dysplasia (OLD) ($N = 435$)

Variable	OLP	OLD
Cases, *n* (%)	260 (59.8)	175 (40.2)
Age at first contact [years] *M*	56.4	56.9
Female sex, *n* (%)	182 (70.0)	119 (68.0)
Erosive lesions, *n* (%)	95 (36.5)	76 (43.4)
Desquamative gingivitis, *n* (%)	112 (43.1)	69 (39.4)
Maximum REU score (range: 1–115) *M*	10.0	10.4
VAS pain score (range: 0–10) *M*	1.27	1.37
VAS burning score (range: 0–10) *M*	2.46	2.17
Smokers, *n* (%)	52 (20.0)	34 (19.4)
Smoking exposure [pack-years] *M*	26.0	28.1
Candida albicans CFU count (range: 0–150) *M*	14.7	11.2
Non-*albicans Candida* CFU count (range: 0–150) *M*	1.6	1.4
p53 protein positivity in long lines of nuclei, *n* (%)	19/63 (30.2)	98/151 (64.9)

REU – reticular-erythematous-ulcerative; VAS – visual analog scale; *M* – mean; CFU – colony forming units.

The gingiva/alveolar mucosa was the most frequently affected site of OSCC, accounting for 33.3% (10/30) of cases. A case of OLP with MT in the alveolar region is shown in Fig. 3.

The tongue and labial mucosa were the next most frequently affected sites, accounting for 20.0% each (6/30), followed by the buccal mucosa at 16.7% (5/30 cases). Additionally, 2 cases of alveolar carcinoma were identified in patients with peri-implantitis accompanied by desquamative gingivitis. Furthermore, 2 individuals presented with synchronous OSCCs involving both the maxilla and mandible. Seven patients developed 2 carcinomas, while 1 patient developed 3 carcinomas. A case of OLP exhibiting synchronous MT in the maxillary and mandibular regions is presented in Fig. 4.

Table 2 presents a comparison of the 6 OLP and 15 OLD cases that underwent MT into OSCC. The sex ratio among patients with MT was comparable to that of the overall cohort, with 66.7% of patients with MT being female. Notably, the mean REU score was 15, compared with 10 for the entire cohort. Furthermore, risk factors appeared to be more prevalent among OLD cases with an erosive form, which accounted for 73.3% (11/15), and among OLD cases with desquamative gingivitis, which accounted for 53.3% (8/15).

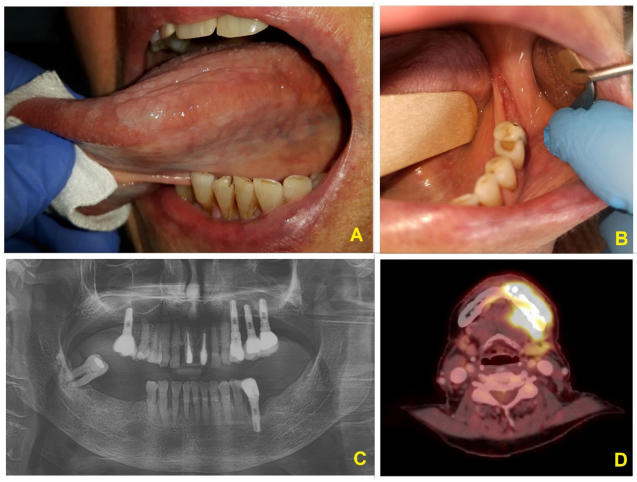

Fig. 3. Malignant transformation (MT) of oral lichen planus (OLP) associated with desquamative gingivitis and peri-implantitis in an 83-year-old woman (case 11/21 in Table 2)

The interval between the OLP and oral squamous cell carcinoma (OSCC) biopsies was 2 years. A. Plaque-type OLP of the tongue without subsequent MT; B. OSCC of the mandibular alveolar ridge associated with desquamative gingivitis; C. Radiograph showing peri-implantitis at site 35; D. Positron emission tomography (PET)/magnetic resonance (MR) image showing recurrent OSCC progression before radiotherapy (total dose: 70 Gy).

Table 2. Cases of oral lichen planus (OLP)/OLP with epithelial dysplasia (OLD) with malignant transformation (MT)

No.	Sex	Age at onset [years]	Smoking exposure [pack-years]	Clinical form	OED grade (0–III)	REU score	Time to MT [years]	Follow-up [years]	OSCC site
1	M	66	0	NE-OLP	0	3	4	9.0	BM, Alv, Pal*
2	F	55	0	DG, E-OLP	0	9	8	12.4	Alv, Alv*
3	M	55	55	E-OLP	0	8	6	26.4	BM, BM*
4	M	57	0	DG, E-OLP	0	59	16	16.4	Alv, Alv*
5	F	48	0	NE-OLP	0	15	11	14.3	Lab, Lab*
6	F	84	0	NE-OLP	0	10	3	5.3	Lab
7	F	64	0	DG, NE-OLD	II	3	15	22.7	Lab, Alv*
8	F	59	0	E-OLD	I	9	6	12.7	Ton
9	M	73	0	DG, E-OLD	II	19	1	3.8	Alv
10	F	56	0	DG, E-OLD	I	42	3	9.8	Ton, Lab*
11	F	64	0	DG, E-OLD	I	11	2	19.8	Alv
12	F	36	22	DG, E-OLD	I	19.5	1	4.0	BM
13	F	41	20	DG, E-OLD	III	27	13	17.2	BM
14	F	75	0	E-OLD	II	7	3	6.8	FM
15	F	68	55	NE-OLD	I	2	4	5.7	FM
16	M	57	50	NE-OLD	III	2	8	10.0	Ton
17	F	59	0	DG, E-OLD	I	31	1	19.9	Lab, Alv*
18	F	67	0	E-OLD	I	18	10	22.2	Ton
19	M	40	0	NE-OLD	I	6	2	7.5	Ton
20	M	37	0	DG, E-OLD	II	5	7	8.4	Alv
21	F	55	0	E-OLD	I	10.5	11	20.0	Ton

M – male; F – female; MT – malignant transformation; OSCC – oral squamous cell carcinoma; NE – non-erosive; E – erosive; BM – buccal mucosa; FM – floor of the mouth; Ton – tongue; Alv – alveolar; Pal – palatal; DG – desquamative gingivitis; Lab – labial. Bold case numbers indicate the cases illustrated in Fig. 3 and Fig. 4. An asterisk (*) in the OSCC site column indicates patients with multiple OSCCs.

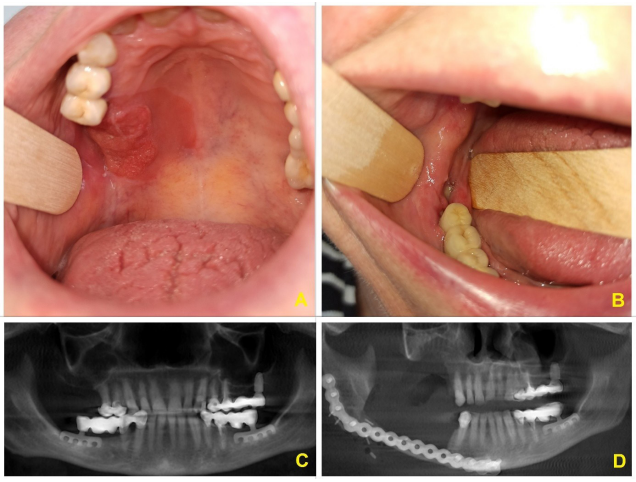

Fig. 4. Synchronous malignant transformation (MT) of oral lichen planus (OLP) at 2 alveolar sites in a 64-year-old woman (case 2/21 in Table 2)

The interval between the OLP and OSCC biopsies was 8 years. A. OSCC of the maxillary alveolar ridge associated with desquamative gingivitis; B. Synchronous OSCC of the mandibular alveolar ridge; C. Radiograph showing peri-implantitis at site 47; D. Postoperative radiograph showing resection of the mandibular alveolar ridge distal to tooth 43 and reconstruction with an individually contoured Synthes MatrixRECON 2.5 plate; adjuvant radiotherapy was administered at a total dose of 60 Gy.

Discussion

The etiology of OLP remains largely unclear despite its prevalence exceeding 2% in the general population.[1–3] Current understanding suggests that an inappropriate immune response to an unidentified antigen may impair epithelial regeneration, a process mediated in part by cytotoxic $CD8^+$ T lymphocytes.[2,4,19]

Typically, individuals with OLP are older than 40 years, with a slight female predominance, reported at a ratio of 1.4:1.[4] Our study showed a more pronounced female predominance, with female-to-male ratios of 2.33:1 for OLP cases and 2.13:1 for OLD cases.

Oral lichen planus is associated with thyroidopathy in approx. 8% of cases.[14,15] In our study, this comorbidity was present in nearly one-fifth (19.3%) of patients. Notably, many cases of thyroidopathy were identified following our recommendation for further evaluation after the diagnosis of OLP or OLD,[14,15] highlighting the importance of comprehensive patient assessment in these instances.

Corticosteroids are frequently used for the topical treatment of OLP; however, they may contribute to secondary *Candida* growth in certain cases.[40–42] In our study, topical antifungal treatment was necessary in 20.7% of the cases analyzed.

Malignant transformation should be understood as a gradual process characterized by an increase in epithelial cell atypia rather than as a single event. Therefore, it is crucial to perform histological verification of OLP to detect the presence of OED. This verification enables appropriate adjustments to monitoring protocols and informs decisions regarding potential re-excision, both of which are key aspects of effective patient management. According to a systematic review published in 2019, the MT rate for OLP ranges from 0.0% to 3.5% over a period of 5–7 years.[38] This range is consistent with our MT rate for non-dysplastic OLP cases, which was 2.3%. Conversely, OLD cases showed a significantly higher MT rate of 8.6%. These calculations were performed after excluding cases with synchronous or preceding OSCC diagnoses and cases associated with PVL.

Several factors have been identified as potential predictors of MT in OLP, including the erosive form of the condition, tongue localization, smoking, and the presence of *Candida*.[18,28] In our study, 50.0% of MT cases involving OLP and 73.3% of OLD cases with MT presented with erosive manifestations. Additionally, MT cases exhibited a higher mean REU index than the general cohort (15 vs. 10), although there was considerable variation, with the values ranging from 2 to 59. Notably, smoking did not appear to be a direct risk factor, as the prevalence of smokers among patients with MT (23.0%) was comparable to that in the general study population (19.8%).

In our study cohort, one-third of OSCCs (10/30) occurred in the alveolar mucosa or gingiva. Within this subset, 2 cases presented with synchronous tumors involving both the maxilla and mandible, as illustrated in Fig. 3 and Fig. 4. These specific cases were identified in regions affected by peri-implantitis. Other gingival cases were associated with heightened inflammation at periodontal sites. Chronic inflammation has the potential to disrupt healing pathways, which may contribute to the emergence of epithelial atypia. Furthermore, aggressive periodontal pathogens have been associated with several local or distant malignancies.[47–51] This pathogenetic cofactor is likely responsible for the higher number of cases with MT observed at alveolar sites in the OLP cohort. Management of OLP affecting the gingiva should therefore include comprehensive periodontal care. In instances where there is suspicion of a progressive inflammatory process around dental roots or implants, particularly in conjunction with desquamative gingivitis, surgical revision with biopsy should be considered to establish an accurate diagnosis. Consequently, it is advisable to monitor the alveolar manifestations of OLP or OLD using orthopantomography or cone-beam computed tomography.

It is important to note that a persistent source of bias in research of this nature is the potential for inaccurate data. To minimize this issue, we included only histopathologically confirmed cases with comprehensive medical history and clinical documentation. There is a pressing need for more targeted studies to clarify the interactions between the oral microbiome, genetic alterations and the development of OED. In the near future, the use of neural networks could improve the detection of high-risk cases.[52] The issue of MT in alveolar OLP, particularly at dental implant sites, warrants investigation in large multicenter studies, similar to other projects in the field of cancer prevention and the management of malignant disease-related complications.[53,54]

Conclusions

The current criteria for OPMDs, published in the 5th edition of the WHO classification, are proving to be effective. Our study found that 8.6% of patients with OLD developed OSCC. Oral lichen planus without dysplasia was associated with a lower risk of MT, at 2.3%. Hence, our findings align with the WHO's assessments of these pathologies.

It is essential to manage cases of desquamative gingivitis carefully, as they demonstrate the highest risk for carcinoma development. Therefore, we recommend close clinical monitoring of desquamative gingivitis, especially in the vicinity of dental implants or in conjunction with ongoing dental inflammation. If a progressive resorptive process around an implant is suspected, surgical revision with biopsy should be considered.

Ethics approval and consent to participate

The scientific project was approved by the Institutional Review Board and Ethics Committee of the University Hospital Pilsen (Faculty of Medicine in Pilsen, Charles University, Pilsen, Czech Republic) (reference No. 231/24; August 1, 2024). The study was conducted in accordance with the Declaration of Helsinki. Written informed consent was obtained from all participants before their inclusion in the study.

Data availability

Not applicable.

Consent for publication

Not applicable.

Use of AI and AI-assisted technologies

Not applicable.

ORCID iDs

Jan Liska https://orcid.org/0000-0002-7315-1681
Veronika Liskova https://orcid.org/0000-0002-0078-0487
Nikoleta Molnarova https://orcid.org/0009-0007-2538-4185
Ondrej Topolcan https://orcid.org/0000-0001-6622-390X
Jan Netolicky https://orcid.org/0009-0008-1041-0579
Pavel Andrle https://orcid.org/0000-0003-1532-2486
Lucie Nechutna https://orcid.org/0009-0006-0982-1501
Lukas Hauer https://orcid.org/0000-0001-6639-2690
Denisa Kacerovska https://orcid.org/0000-0003-1893-535X

References

1. Warnakulasuriya S. Oral potentially malignant disorders: A comprehensive review on clinical aspects and management. *Oral Oncol*. 2020;102:104550. doi:10.1016/j.oraloncology.2019.104550
2. Warnakulasuriya S, Kujan O, Aguirre-Urizar JM, et al. Oral potentially malignant disorders: A consensus report from an international seminar on nomenclature and classification, convened by the WHO Collaborating Centre for Oral Cancer. *Oral Dis*. 2021;27(8):1862–1880. doi:10.1111/odi.13704
3. Solimani F, Forchhammer S, Schloegl A, Ghoreschi K, Meier K. Lichen planus – a clinical guide. *J Dtsch Dermatol Ges*. 2021;19(6):864–882. doi:10.1111/ddg.14565
4. Sugerman PB, Savage NW. Oral lichen planus: Causes, diagnosis and management. *Aust Dent J*. 2002;47(4):290–297. doi:10.1111/j.1834-7819.2002.tb00540.x
5. Warnakulasuriya S, Johnson NW, van der Waal I. Nomenclature and classification of potentially malignant disorders of the oral mucosa. *J Oral Pathol Med*. 2007;36(10):575–580. doi:10.1111/j.1600-0714.2007.00582.x
6. Al-Hashimi I, Schifter M, Lockhart PB, et al. Oral lichen planus and oral lichenoid lesions: Diagnostic and therapeutic considerations. *Oral Surg Oral Med Oral Pathol Oral Radiol Endod*. 2007;103 Suppl:S25.e1-12. doi:10.1016/j.tripleo.2006.11.001
7. Müller S. Oral lichenoid lesions: Distinguishing the benign from the deadly. *Mod Pathol*. 2017;30(s1):S54–S67. doi:10.1038/modpathol.2016.121
8. Scully C, Bagan JV. Adverse drug reactions in the orofacial region. *Crit Rev Oral Biol Med*. 2004;15(4):221–239. doi:10.1177/154411130401500405
9. Fricain JC, Sibaud V, Hafian H, Deminière C, Taiëb A, Boiron JM. Oral manifestations of chronic graft-versus-host disease [in French]. *Ann Dermatol Venereol*. 2005;132(12 Pt 1):1017–1025. doi:10.1016/S0151-9638(05)79574-0
10. Fortuna G, Aria M, Schiavo JH. Drug-induced oral lichenoid reactions: A real clinical entity? A systematic review. *Eur J Clin Pharmacol*. 2017;73(12):1523–1537. doi:10.1007/s00228-017-2325-0
11. McCartan BE, McCreary CE. Oral lichenoid drug eruptions. *Oral Dis*. 1997;3(2):58–63. doi:10.1111/j.1601-0825.1997.tb00013.x
12. Yuan A, Woo SB. Adverse drug events in the oral cavity. *Dermatol Clin*. 2020;38(4):523–533. doi:10.1016/j.det.2020.05.012
13. Kumar SA, Krishnam Raju PV, Gopal KVT, Rao TN. Comorbidities in lichen planus: A case–control study in Indian patients. *Indian Dermatol Online J*. 2019;10(1):34–37. doi:10.4103/idoj.IDOJ_48_18
14. Siponen M, Huuskonen L, Läärä E, Salo T. Association of oral lichen planus with thyroid disease in a Finnish population: A retrospective case–control study. *Oral Surg Oral Med Oral Pathol Oral Radiol Endod*. 2010;110(3):319–324. doi:10.1016/j.tripleo.2010.04.001
15. Li D, Li J, Li C, Chen Q, Hua H. The association of thyroid disease and oral lichen planus: A literature review and meta-analysis. *Front Endocrinol (Lausanne)*. 2017;8:310. doi:10.3389/fendo.2017.00310
16. Aguirre-Urizar JM, Alberdi-Navarro J, Lafuente-Ibáñez de Mendoza I, et al. Clinicopathological and prognostic characterization of oral lichenoid disease and its main subtypes: A series of 384 cases. *Med Oral Patol Oral Cir Bucal*. 2020;25(4):e554–e562. doi:10.4317/medoral.23576
17. Cheng YSL, Gould A, Kurago Z, Fantasia J, Muller S. Diagnosis of oral lichen planus: A position paper of the American Academy of Oral and Maxillofacial Pathology. *Oral Surg Oral Med Oral Pathol Oral Radiol*. 2016;122(3):332–354. doi:10.1016/j.oooo.2016.05.004
18. van der Meij EH, van der Waal I. Lack of clinicopathologic correlation in the diagnosis of oral lichen planus based on the presently available diagnostic criteria and suggestions for modifications. *J Oral Pathol Med*. 2003;32(9):507–512. doi:10.1034/j.1600-0714.2003.00125.x
19. Irani S. Pre-cancerous lesions in the oral and maxillofacial region: A literature review with special focus on etiopathogenesis. *Iran J Pathol*. 2016;11(4):303–322. PMID:28855922.
20. Sistig S, Vucićević-Boras V, Lukac J, Kusić Z. Salivary IgA and IgG subclasses in oral mucosal diseases. *Oral Dis*. 2002;8(6):282–286. doi:10.1034/j.1601-0825.2002.20844.x
21. Ajila V, Shetty V, Babu S, Hegde S, Rao S. Imunoglobulin A in oral pontentially malignant disorders and oral squamous cell carcinoma. *J Med Sci*. 2017;37(5):195–200. doi:10.4103/jmedsci.jmedsci_29_17
22. Mozaffari HR, Zavattaro E, Abdolahnejad A, et al. Serum and salivary IgA, IgG, and IgM levels in oral lichen planus: A systematic review and meta-analysis of case–control studies. *Medicina*. 2018;54(6):99. doi:10.3390/medicina54060099
23. Warnakulasuriya S. Clinical features and presentation of oral potentially malignant disorders. *Oral Surg Oral Med Oral Pathol Oral Radiol*. 2018;125(6):582–590. doi:10.1016/j.oooo.2018.03.011
24. Carey B, Setterfield J. Mucous membrane pemphigoid and oral blistering diseases. *Clin Exp Dermatol*. 2019;44(7):732–739. doi:10.1111/ced.13996

25. Tikkhanarak K, Wangboo D, Sookviboonpol N, Thongprasom K. Correlation of clinicopathological characteristics and direct immunofluorescence studies in oral lichenoid lesion in Thai patients. *J Investig Clin Dent*. 2019;10(4):e12433. doi:10.1111/jicd.12433
26. Park HK, Hurwitz S, Woo SB. Oral lichen planus: REU scoring system correlates with pain. *Oral Surg Oral Med Oral Pathol Oral Radiol*. 2012;114(1):75–82. doi:10.1016/j.oooo.2012.02.013
27. Gobbo M, Rupel K, Zoi V, et al. Scoring systems for oral lichen planus used by differently experienced raters. *Med Oral Patol Oral Cir Bucal*. 2017;22(5):e562–e571. doi:10.4317/medoral.21833
28. Bates TJ, Richards A, Pring M. Oral potentially malignant disorders: A practical review for the diagnostic pathologist. *Diagn Histopathol*. 2023;29(4):208–224. doi:10.1016/j.mpdhp.2023.01.004
29. Speight PM, Khurram SA, Kujan O. Oral potentially malignant disorders: Risk of progression to malignancy. *Oral Surg Oral Med Oral Pathol Oral Radiol*. 2018;125(6):612–627. doi:10.1016/j.oooo.2017.12.011
30. Mello FW, Melo G, da Silva Guerra EN, Warnakulasuriya S, Garnis C, Rivero ERC. Prognostic biomarkers for malignant transformation of oral potentially malignant disorders: A scoping review protocol. *JBI Evid Synth*. 2020;18(6):1349–1357. doi:10.11124/JBISRIR-D-19-00259
31. Warnakulasuriya S, Soussi T, Maher R, Johnson N, Tavassoli M. Expression of p53 in oral squamous cell carcinoma is associated with the presence of IgG and IgA p53 autoantibodies in sera and saliva of the patients. *J Pathol*. 2000;192(1):52–57. doi:10.1002/1096-9896(2000)9999:9999<::AID-PATH669>3.0.CO;2-C
32. Warnakulasuriya S, Kovacevic T, Madden P, et al. Factors predicting malignant transformation in oral potentially malignant disorders among patients accrued over a 10-year period in South East England. *J Oral Pathol Med*. 2011;40(9):677–683. doi:10.1111/j.1600-0714.2011.01054.x
33. Sanketh DS, Kumari K, Rao RS, et al. Expression of Ki-67, p53, α-SMA and COX-2 in lichen planus and related lesions: A pilot study. *J Oral Biol Craniofac Res*. 2019;9(2):230–235. doi:10.1016/j.jobcr.2018.02.003
34. Villa A, Celentano A, Glurich I, et al. World Workshop on Oral Medicine VII: Prognostic biomarkers in oral leukoplakia: A systematic review of longitudinal studies. *Oral Dis*. 2019;25 Suppl 1(Suppl 1):64–78. doi:10.1111/odi.13087
35. Izumo T. Oral premalignant lesions: From the pathological viewpoint. *Int J Clin Oncol*. 2011;16(1):15–26. doi:10.1007/s10147-010-0169-z
36. Idrees M, Kujan O, Shearston K, Farah CS. Oral lichen planus has a very low malignant transformation rate: A systematic review and meta-analysis using strict diagnostic and inclusion criteria. *J Oral Pathol Med*. 2021;50(3):287–298. doi:10.1111/jop.12996
37. Zotti F, Nocini R, Capocasale G, et al. Oral lichen planus: Risk factors of malignant transformation and follow up. Ten years retrospective study. *J Clin Exp Dent*. 2021;13(7):e630–e636. doi:10.4317/jced.57688
38. González-Moles MÁ, Ruiz-Ávila I, González-Ruiz L, Ayén Á, Gil-Montoya JA, Ramos-García P. Malignant transformation risk of oral lichen planus: A systematic review and comprehensive meta-analysis. *Oral Oncol*. 2019;96:121–130. doi:10.1016/j.oraloncology.2019.07.012
39. Cerero-Lapiedra R, Baladé-Martínez D, Moreno-López LA, Esparza-Gómez G, Bagán JV. Proliferative verrucous leukoplakia: A proposal for diagnostic criteria. *Med Oral Patol Oral Cir Bucal*. 2010;15(6):e839–e845. doi:10.4317/medoral.15.e839
40. Marable DR, Bowers LM, Stout TL, et al. Oral candidiasis following steroid therapy for oral lichen planus. *Oral Dis*. 2016;22(2):140–147. doi:10.1111/odi.12399
41. Pereira TSF, Silva Alves JFC, Gomes CC, Rocha do Nascimento A, Stoianoff MAR, Gomez RS. Kinetics of oral colonization by *Candida* spp. during topical corticotherapy for oral lichen planus. *J Oral Pathol Med*. 2014;43(8):570–575. doi:10.1111/jop.12174
42. Bombeccari GP, Giannì AB, Spadari F. Oral *Candida* colonization and oral lichen planus. *Oral Dis*. 2017;23(7):1009–1010. doi:10.1111/odi.12681
43. Thongprasom K, Prapinjumrune C, Carrozzo M. Novel therapies for oral lichen planus. *J Oral Pathol Med*. 2013;42(10):721–727. doi:10.1111/jop.12083
44. Didona D, Caposiena Caro RD, Sequeira Santos AM, Solimani F, Hertl M. Therapeutic strategies for oral lichen planus: State of the art and new insights. *Front Med (Lausanne)*. 2022;9:997190. doi:10.3389/fmed.2022.997190
45. Akram Z, Abduljabbar T, Vohra F, Javed F. Efficacy of low-level laser therapy compared to steroid therapy in the treatment of oral lichen planus: A systematic review. *J Oral Pathol Med*. 2018;47(1):11–17. doi:10.1111/jop.12619
46. Mutafchieva MZ, Draganova-Filipova MN, Zagorchev PI, Tomov GT. Effects of low level laser therapy on erosive-atrophic oral lichen planus. *Folia Med (Plovdiv)*. 2018;60(3):417–424. doi:10.2478/folmed-2018-0008
47. Gholizadeh P, Eslami H, Yousefi M, Asgharzadeh M, Aghazadeh M, Kafil HS. Role of oral microbiome on oral cancers, a review. *Biomed Pharmacother*. 2016;84:552–558. doi:10.1016/j.biopha.2016.09.082
48. McIlvanna E, Linden GJ, Craig SG, Lundy FT, James JA. *Fusobacterium nucleatum* and oral cancer: A critical review. *BMC Cancer*. 2021;21(1):1212. doi:10.1186/s12885-021-08903-4
49. Irfan M, Delgado RZR, Frias-Lopez J. The oral microbiome and cancer. *Front Immunol*. 2020;11:591088. doi:10.3389/fimmu.2020.591088
50. Banthia R, Jain P, Jain AK, Belludi SA, Agarwal N, Patidar M. Evaluation of the association between periodontal disease and total cancer risk: A cross-sectional study. *Dent Med Probl*. 2024;61(6):843–850. doi:10.17219/dmp/175001
51. Minervini G, Shivakumar S, Ronsivalle V, Franco R, Cicciù M, Marrapodi MM. Microbiological aspects of cancer progression: A systematic review conducted according to the PRISMA 2020 guidelines and the Cochrane Handbook for Systematic Reviews of Interventions. *Dent Med Probl*. 2024;61(5):739–746. doi:10.17219/dmp/183712
52. Beristain-Colorado MDP, Castro-Gutiérrez MEM, Torres-Rosas R, et al. Application of neural networks for the detection of oral cancer: A systematic review. *Dent Med Probl*. 2024;61(1):121–128. doi:10.17219/dmp/159871
53. Duś-Ilnicka I. Neglected area of oral cancer: A word about the International Agency for Research on Cancer (IARC) "Handbook of Oral Cancer Prevention". *Dent Med Probl*. 2024;61(4):479–480. doi:10.17219/dmp/190468
54. Guo H, Yang Y. Assessing the efficacy of psychological interventions in enhancing the quality of life of patients diagnosed with cancer and psychiatric disorders: An umbrella analysis. *Adv Clin Exp Med*. 2025;34(6):871–884. doi:10.17219/acem/190503

Original paper

Oral microbiota diversity and composition in patients with oral lichen planus: An observational molecular analysis study

Elham Saberian[1,C,D,F*], Adriána Petrášová[1,B–D*], Andrej Jenča Jr.[1,C–E*], Janka Jenčová[1,B,D–F], Kimia Shirali[2,B,D,E], Andrej Jenča[1,B,C,F], Mieszko Adam Więckiewicz[3,B,D–F], Hadi Zare-Zardini[4,A,B,D,F], Meysam Ebrahimi Far[5,C–E]

[1] Clinic of Stomatology and Maxillofacial Surgery, Academy of Košice, Pavol Jozef Šafárik University, Košice, Slovakia
[2] Department of Dentistry, Faculty of Medicine, Pavol Jozef Šafárik University, Košice, Slovakia
[3] Department of Experimental Dentistry, Wroclaw Medical University, Poland
[4] Department of Biomedical Engineering, Meybod University, Iran
[5] Faculty of Pharmacy, Islamic Azad University – Shahreza Branch, Iran
* These authors contributed equally to this work.

A – research concept and design; B – collection and/or assembly of data; C – data analysis and interpretation; D – writing the article; E – critical revision of the article; F – final approval of the article

Dental and Medical Problems, ISSN 1644-387X (print), ISSN 2300-9020 (online) *Dent Med Probl*. 2026;63(5):1155–1166

Address for correspondence
Hadi Zare-Zardini
E-mail: hadizarezardini@gmail.com

Funding sources
None declared

Conflict of interest
None declared

Acknowledgements
The authors express their gratitude to all volunteers who participated in the study.

Received on July 16, 2025
Reviewed on August 28, 2025
Accepted on August 30, 2025

Published online on May 27, 2026

Cite as
Saberian E, Petrášová A, Jenča Jr. A, et al. Oral microbiota diversity and composition in patients with oral lichen planus: An observational molecular analysis study. *Dent Med Probl.* 2026;63(5):1155–1166. doi:10.17219/dmp/210087

DOI
10.17219/dmp/210087

Copyright
Copyright by Author(s)
This is an article distributed under the terms of the Creative Commons Attribution 3.0 Unported License (CC BY 3.0) (https://creativecommons.org/licenses/by/3.0/).

Abstract

Background. Oral lichen planus (OLP) is a chronic inflammatory condition affecting the oral mucosa. The oral microbiome has been identified as a potential contributing factor to OLP.

Objectives. The aim of the study was to evaluate the prevalence and diversity of the oral microbiota in patients with OLP.

Material and methods. This observational study included 78 patients with clinically and histopathologically confirmed OLP, recruited in accordance with the Strengthening the Reporting of Observational Studies in Epidemiology (STROBE) guidelines. Buccal mucosa samples were collected using standardized protocols. DNA was extracted from 12 high-quality samples and subjected to *16S rRNA* gene amplification and sequencing. Alpha and beta diversity indices were calculated using the Quantitative Insights Into Microbial Ecology (QIIME) platform. Statistical analyses were performed using the IBM SPSS Statistics for Windows software, v. 26.0 (IBM Corp., Armonk, USA) ($p < 0.05$).

Results. Intratissue bacterial communities exhibited decreased alpha diversity and increased beta diversity compared with those present on the mucosal surface. *Streptococcus*, a genus within the Firmicutes phylum, was found to be the most abundant, with 5 Streptococcus strains identified in the OLP samples. Following Streptococci, Bacilli and Clostridia displayed considerable diversity. Other frequently detected species included *Klebsiella pneumoniae*, *Escherichia coli*, *Pseudomonas aeruginosa*, *Eikenella corrodens*, *Actinobacillus*, as well as members of the Proteobacteria phylum, which are commonly found in high quantities in the oral cavity. *Prevotella* and *Capnocytophaga*, belonging to the Bacteroidetes phylum, were also frequently observed. Alpha diversity analysis revealed significant differences in the colony numbers of the investigated species across studied samples.

Conclusions. The findings indicate an association between the composition of the oral microbiota and OLP. The microbial populations obtained from affected individuals exhibited distinct bacterial compositions. Modulation of the oral microbiome may represent a potential strategy for improving the management of OLP.

Keywords: oral lichen planus, diversity, microbial population, oral microbiota

Highlights

- The prevalence and diversity of oral microorganisms were evaluated in patients with oral lichen planus (OLP).
- *Streptococcus* species were identified as the most abundant bacterial strains in OLP samples.
- High levels of *Klebsiella pneumoniae*, *Escherichia coli*, *Pseudomonas aeruginosa*, *Eikenella corrodens*, *Actinobacillus*, and members of the Proteobacteria phylum were detected in the oral cavity.
- Distinct bacterial compositions in the oral microbiome were observed in individuals with OLP, suggesting an association between microbial profiles and the disease.

Introduction

Lichen planus (LP) is an autoimmune condition in which the immune system targets the skin, mucosa, hair, or nails. In some cases, this process may be triggered by external factors such as medication or microbial agents.[1] Recent epidemiological data suggests that oral lichen planus (OLP) affects approx. 0.5–2.0% of the global population. The condition typically presents between the ages of 30 and 60, and is more prevalent in women. The development of OLP in children is infrequent.[1,2]

Available evidence indicates that immunological mechanisms play a role in the etiology of OLP. Genetic predisposition has also been identified as a potential risk factor, aligning with the STrengthening the REporting of Genetic Association studies (STREGA) guidelines for reporting genetic associations in autoimmune diseases. The disease is more prevalent in women and middle-aged individuals, with an estimated prevalence of 0.1–2.2%. However, the reported prevalence rates and other epidemiological indicators vary considerably across studies.[1–3] In addition to genetic predisposition, several factors such as stress, immunological reactions and trauma contribute to the development of oral lesions associated with OLP.[4]

Increasing attention has been given to the potential role of the oral microbiome in the development of OLP. Examples of microbes that inhabit the oral cavity include *Streptococcus* and *Corynebacterium* species. Together, these microorganisms form an ecosystem that functions in a manner analogous to the human gut microbiota.[5,6] Each region of the oral cavity possesses distinct surface characteristics, giving rise to the presence of different microbial communities. The tongue contains diverse microbial samples when compared to the gums or teeth since their surfaces provide suitable habitats for a variety of microbes.

The oral microbiome comprises over 700 bacterial species, including both aerobic and anaerobic bacteria. Important anaerobic genera include *Fusobacterium*, *Prevotella*, *Porphyromonas*, *Treponema*, and *Tannerella*, which play crucial roles in maintaining oral homeostasis but may also contribute to pathological conditions when dysbiosis occurs. Dental plaque and the tongue surface are densely populated with microbes and are considered the most microbially dense habitats.[7,8]

The clinical presentation of OLP varies considerably, with multiple subtypes and anatomical distributions observed in affected patients (Fig. 1). The buccal mucosa is the most affected site (63%), followed by the tongue (30%) and gingiva (10%). Lesions typically occur bilaterally and symmetrically. Among the clinical variants, reticular OLP is the most prevalent (45%), characterized by white lacy striae (Wickham's striae), while erosive (25%) and atrophic (20%) forms represent the symptomatic variants that often require therapeutic intervention (Fig. 1).[1,2,7,8]

Given the important role of the oral microbiome in the occurrence of oral diseases, its regulation is of utmost importance. Studies suggest that the disruption of the homeostatic balance of the oral microbiome leads to the activation of the defense pathways involved in oral inflammation associated with OLP.[9–11]

To date, contradictory reports have been published regarding the influence of the oral microbial composition and saliva structure on OLP. Some studies have reported elevated levels of *Porphyromonas* and *Solobacterium* in OLP,[12] whereas a 2017 report have identified increased abundance of *Fusobacterium*, *Leptotrichia* and *Lautropia* in the buccal mucosa.[13] Furthermore, the infiltration of T cells into the oral tissue due to the presence of bacteria in the layers of LP tissue has been reported.[14,15]

Studies demonstrate that an individual's immune status and the level of inflammation influence the diversity and composition of tissue and salivary microbial communities. The structure of an individual's microbial community may affect the development and progression of OLP.[14,16–18] Therefore, further research in the fields of immunology and microbiology is necessary to better understand the exact etiology of this disease.

The main objective of the present study is to investigate the bacteria present in the oral cavity of patients with OLP and to explore their potential role in the pathogenesis and development of the disease, which may provide a biological approach to prevent OLP. Specifically, this study aims to: (1) characterize bacterial diversity in OLP lesions using *16S rRNA* gene sequencing; (2) identify predominant bacterial taxa associated with OLP; and (3) assess differences in microbial composition between samples.

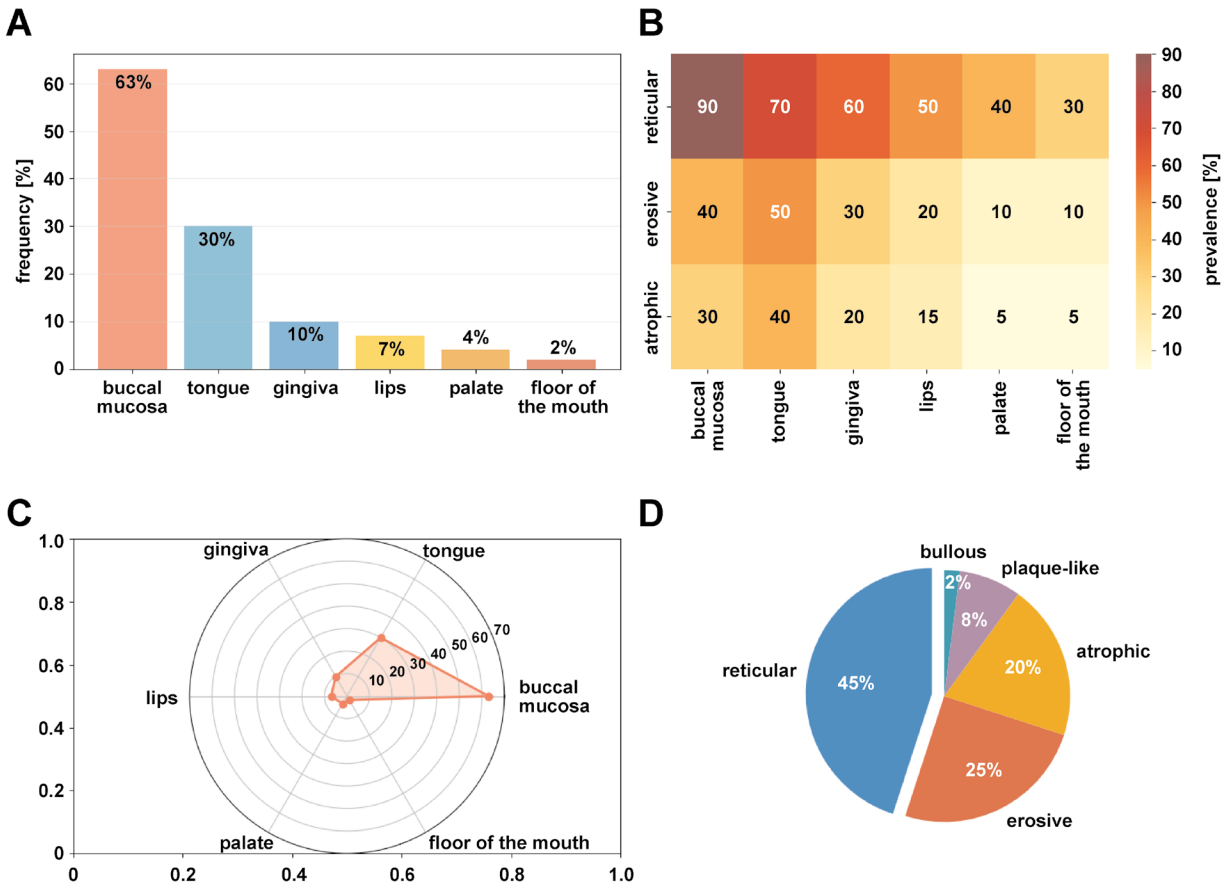

Fig. 1. Clinical presentation and anatomical distribution of oral lichen planus (OLP) lesions[1,2,7,8]

A. Distribution of lesions by anatomical site; B. Heatmap illustrating the distribution of OLP types; C. Radar chart showing the proportional distribution of OLP subtypes; D. Distribution of clinical types of OLP.

Material and methods

Study design and setting

This observational study was conducted in accordance with the Strengthening the Reporting of Observational Studies in Epidemiology (STROBE) guidelines and the STREGA extension for genetic epidemiology studies.

Study population

Consecutive patients presenting with oral mucosal lesions clinically suggestive of OLP were screened for eligibility at the Department of Oral Medicine (Tehran University of Medical Sciences, Iran). The sample size was calculated based on previous microbiome studies in oral diseases, indicating that a minimum of 10 samples is required for *16S rRNA* gene sequencing to achieve 80% power at $\alpha = 0.05$.[19]

Sample collection and clinical assessment

The study was approved by the Institutional Review Boards of the Dental Hospital of Tehran University of Medical Sciences, Iran, and the Faculty of Dentistry, Seoul National University, South Korea (approval No. S-D20180026), as well as by the Ethics Committee of the Clinic of Košice, Slovakia (approval No. REK01/2023). Written informed consent was obtained from all participants. All patients underwent standardized clinical examination performed by 2 calibrated examiners (inter-examiner $\kappa = 0.85$). The study workflow is presented in Fig. 2. Reticular lesions, without ulceration and with or without erythema, located on the buccal mucosa, were included. Bacteria present on the mucosal surface of the lesion were collected by placing a sterile 20-mm polyvinylidene difluoride (PVDF) membrane on the buccal mucosa for 30 s.

Subsequently, two 4-mm punch biopsy specimens were obtained: one was used to create a tissue block for pathological diagnosis, while the other was utlilized to extract DNA for microbiota analysis.

Inclusion and exclusion criteria

The inclusion criteria were as follows: clinically and histopathologically confirmed diagnosis of OLP; willingness to participate in the study; no history of antibiotic or steroid treatment in the past month; and absence of infectious diseases.

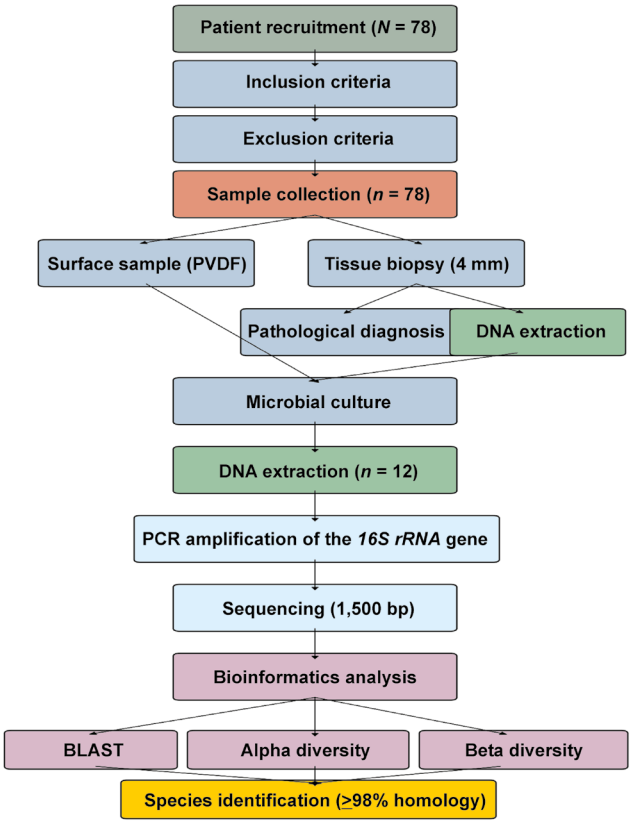

Fig. 2. Schematic representation of the study workflow

PVDF – polyvinylidene difluoride; PCR – polymerase chain reaction; BLAST – Basic Local Alignment Search Tool.

The exclusion criteria included the withdrawal of consent, low unstimulated whole salivary flow rate (≤0.1 mL/min), and smoking. Unstimulated whole saliva was collected at baseline over a 5-min period to determine salivary flow rate. All included subjects exhibited salivary flow rates that exceeded the exclusion threshold (range: 0.21–0.49 mL/min).

Screening and quantification of microorganisms in samples

Serial dilutions (1^{-10} to 10^{-10}) were prepared to assess the number of microorganisms present in the OLP samples. Under standard and sterile conditions, 0.5 g of each sample was transferred to the tube with sterile distilled water. The contents of the first tubes were mixed until the dilution was completely uniform. Then, 1 mL of the suspension was transferred into subsequent tubes under sterile conditions. One milliliter of each dilution was transferred to the agar culture medium under standard and sterile conditions and spread uniformly using a sterile pipette. Two plates were considered for each dilution. The plates were incubated at 25°C for 7 days. The average number of countable colonies was obtained, and the number of culturable bacteria per gram of sample was calculated based on dilution factors. Single colonies formed on the culture media were linearly cultivated to ensure the purity of oral bacteria.

DNA extraction

A total of 12 samples were selected for DNA extraction based on the predefined quality criteria: absence of blood contamination; sufficient tissue yield (>40 mg); and intact morphology. A DNA extraction kit (MACHEREY-NAGEL GmbH & Co. KG, Düren, Germany) was used to extract DNA from the buccal mucosa and tissue samples following the manufacturer's protocol, with modifications for oral tissue samples.

The following steps were performed during the DNA extraction process. The cells were collected from a culture medium by centrifugation in a microtube. A sample of 40 mg wet weight of the microbial cell culture medium plate was used. Finally, 100 µL of BE buffer solution was added, and a cell suspension was prepared. To homogenize and lyse the samples, the cell suspension was transferred to the NucleoSpin Bead Tube Type B (MACHEREY-NAGEL GmbH & Co. KG). The glass beads were subjected to a process of regeneration to ensure the removal of any remaining cell debris at the end of the tube. After centrifugation, 500–600 µL of the NucleoSpin Bead Tube column supernatant was transferred to a 2-mL tube. Subsequently, 500 µL of buffer B was added and centrifuged for 30 s at 11,000 g, and the column solution was collected in tubes. Then, 500 µL of B5 buffer was added to the column, centrifuged for 30 s at 11,000 g, and the column was collected in tubes. To dry the membrane, the column was centrifuged for 30 s at 11,000 g, removing any remaining washing buffer. The Nucleospin Bead Tube column was transferred to a 1.5-mL tube, and 100 µL of BE buffer was added to the column that was then incubated for 1 min at room temperature. Subsequently, the sample was centrifuged at 11,000 g for 30 s. The presence and quantity of DNA were evaluated by electrophoresis on 1% agarose gel. Additionally, the concentration of extracted DNA was measured using a spectrophotometer (NanoDrop Spectrophotometer; Thermo Fisher Scientific, Waltham, USA).

Polymerase chain reaction

Polymerase chain reaction (PCR) is a widely used technique in molecular biology and genetic disease research for the identification of new genes. The activity of genes can be measured through the implementation of PCR on their RNA. The conditions for performing PCR were as follows: a 2X PCR Master Mix kit was obtained from SinaClon BioScience Co. (Tehran, Iran). Selective primers for the amplification of the *16S rRNA* gene, designated as forward 9 and reverse 1541, were procured from Elgo Fanavaran Pars DNA Co. (Tehran, Iran), and their complete specifications are listed in Table 1.

Table 1. Primer sequences used for *16S rRNA* gene amplification

Primer number	Sequence (5′–3′)	Purification method	Concentration [nmol]
9F	GAGTTTGATYMTGGCTCAG	desalting	28.4
1541R	AAGGAGGTGWTCCARCC	desalting	34.2

After conducting PCR in accordance with standard protocols, the integrity of the amplicons was assessed, revealing a consistent band size of 1,500 base pairs. Following electrophoresis, purification was executed by TopazGene (Kamal Shahr, Iran) and Microsens (Lausanne, Switzerland), bypassing the cloning stage. Subsequently, sequencing was undertaken, and the resulting sequences were analyzed using the Basic Local Alignment Search Tool (BLAST). For agarose gel preparation, the volume of the cassette was instrumental in determining the required quantities of agarose gel powder and TBE buffer, ensuring a suitable matrix for electrophoretic separation.

Statistical analysis

During the statistical analysis, sequence identifications were aligned against the National Center for Biotechnology Information (NCBI) gene database. Strains exhibiting ≥98% sequence homology were grouped collectively. Alpha diversity metrics, including Chao1, abundance-based coverage estimator (ACE), and Shannon and Simpson indices, quantified species complexity, which was analyzed using the Quantitative Insights Into Microbial Ecology (QIIME) v. 2.1.0 platform (https://qiime2.org). Beta diversity assessments were conducted using QIIME v. 1.7.0. Statistical analyses were performed using the IBM SPSS Statistics for Windows software, v. 26.0 (IBM Corp., Armonk, USA). Differences between groups were evaluated using one-way analysis of variance (ANOVA) for normally distributed data or the Kruskal–Wallis test for non-normally distributed data. Normality was assessed using the Shapiro–Wilk test. A p-value <0.05 was considered statistically significant.

Bias control

To minimize selection bias, consecutive sampling was employed. Laboratory personnel performing molecular analyses were blinded to clinical data. Technical replicates were conducted for 20% of samples to assess reproducibility.

Results

Seventy-eight individuals with clinically and histopathologically confirmed OLP were included in the study. All participants completed the study protocol. The mean age of the patients was 49.70 ±15.54 years (range: 12–71 years), with 61% of the patients being male and 39% being female. Histopathological examination of all cases confirmed the diagnosis of OLP. Among the 78 collected samples, 53 (67.9%) yielded DNA of sufficient quality for initial screening. Of these, 12 samples (15.4%) met all predefined quality criteria for *16S rRNA* gene sequencing: DNA concentration >50 ng/μL; A260/A280 ratio of 1.8–2.0; and the absence of PCR inhibitors. Among the buccal mucosa and tissue samples, 53 specimens were cultured, as they were of good quality. Twelve samples from the target cultures were subjected to microbiological analysis (Table 2).

Table 2. Characteristics of the analyzed samples

Sample number	Sample name	Age [years]	REU score	
1	OLP1	51	R5E3	8.5
2	OLP2	74	R2E4	7
3	OLP3	39	R7E5	9.5
4	OLP4	58	R2E5	8
5	OLP5	61	R6E6U1	14
6	OLP6	59	R6E5	11.5
7	OLP7	67	R5E5	11
8	OLP8	46	R3E4U1	10.5
9	OLP9	53	R7E4	16
10	OLP10	61	R2E4	9
11	OLP11	63	R2E3U1	8.5
12	OLP12	70	R6E2	15

REU – reticulation/erythema/ulceration.

Detection of bacterial DNA in tissue samples

Agarose gel electrophoresis confirmed the detection of bacterial DNA within the samples. Specifically, the validation of the DNA extraction process, yielding bands representative of bacterial genomic material sourced from the buccal mucosa and tissue specimens, is visually presented in Fig. 3, attesting to the successful procurement and separation of nucleic acid fragments characteristic of the oral microbiome.

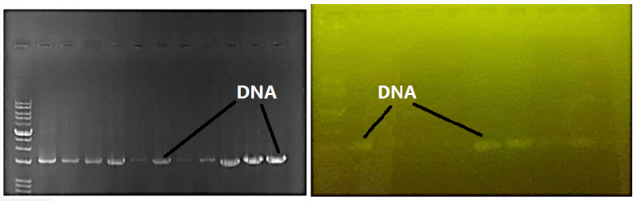

Fig. 3. Results of agarose gel electrophoresis of polymerase chain reaction (PCR) gene products

GraPhlAn display analysis

A classification tree was generated for all samples using the GraPhlAn software (Fig. 4). The analysis demonstrated that the Firmicutes phylum exhibited a predominant share in the microbial community, with a notable richness in species diversity, and was surpassed only by the Proteobacteria phylum. Within Firmicutes, the genus *Streptococcus* was the most abundant. The spectrum of the identified species included, but was not limited to, *Klebsiella pneumoniae*, *Escherichia coli*, *Pseudomonas aeruginosa*, *Eikenella corrodens*, *Actinobacillus*, and other members of the Proteobacteria phylum, which are well-documented as abundant inhabitants of the oral cavity. Additionally, the Bacteroidetes phylum was represented by genera *Prevotella* and *Capnocytophaga*, further enriching the oral microbiota profile.

Gene tree of tissue samples

An evolutionary phylogenetic tree was constructed to represent the species most frequently detected in the sampled cohort, leveraging next-generation sequencing data and the analytical prowess of the R&D software suite

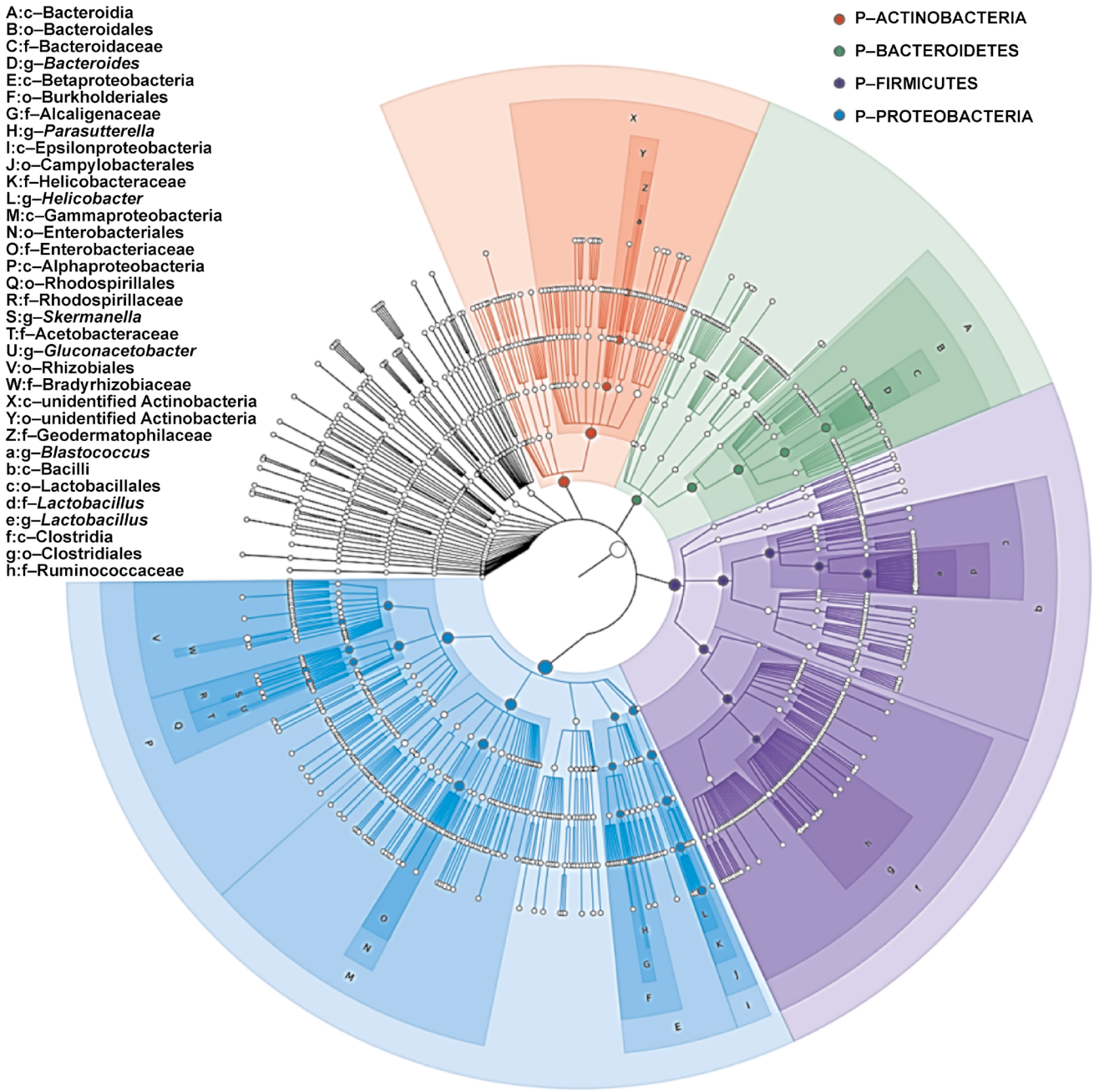

Fig. 4. Taxonomic classification tree of operational taxonomic units (OTUs) generated using the GraPhlAn software

Circle size corresponds to the abundance of taxa. Different colors represent distinct taxonomic groups, while uncolored circles indicate taxa included among the top 40 most abundant species.

of BLAST. As illustrated in Fig. 5, the pre-eminence of the Firmicutes phylum was pronounced, with *Streptococcus* identified as the most prevalent genus. Within this genus, species such as *Streptococcus mutans*, *Streptococcus sanguinis*, *Streptococcus salivarius*, and *Streptococcus sobrinus* were detected. Following *Streptococcus*, members of the classes Bacilli and Clostridia exhibited notable phylogenetic breadth. Beyond Firmicutes, Proteobacteria emerged as a significant phylum, comprising species such as *E. coli*, *P. aeruginosa* and *E. corrodens*, as well as *Actinobacillus*. Collectively, these taxa represent pivotal members within the Proteobacteria phylum, as determined by the study findings.

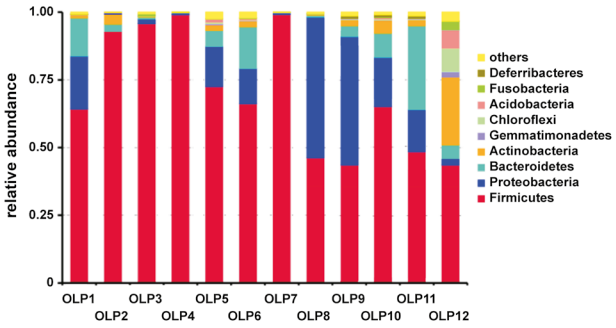

Fig. 6. Relative abundance of dominant bacterial taxa across samples
The top 9 phyla in different taxonomic categories were selected to form the histogram of relative abundance distribution.

Distribution of bacterial taxa

The analysis of bacterial distribution revealed marked disparities in bacterial populations among distinct buccal mucosa and tissue specimens. The genus abundance plot illustrated in Fig. 6 demonstrates that Firmicutes constitute the dominant phylum. Notably, samples OLP8, OLP9 and OLP10 exhibited a considerable representation of Proteobacteria. Conversely, samples OLP2, OLP3, OLP4, and OLP12 were dominated by Firmicutes, with comparatively lower proportions of Proteobacteria. Sample OLP12 displayed the highest compositional diversity, characterized by the coexistence of Firmicutes and Actinobacteria.

Sequencing-assisted alpha diversity analysis

Alpha diversity analysis, as initially characterized by Whittaker in 1972, fundamentally quantifies species richness, addressing species variety within a given sample. Empirically, this is achieved by enumerating observable species or operational taxonomic units (OTUs) per sample. The assessment of alpha diversity revealed substantial disparities in the number of colonies corresponding to the investigated species across samples. Indices such as phylogenetic diversity, ACE and Chao1 collectively indicated that samples OLP3 and OLP12 had the highest microbial diversity, whereas OLP2, OLP4, OLP7, and OLP8 exhibited the lowest diversity.

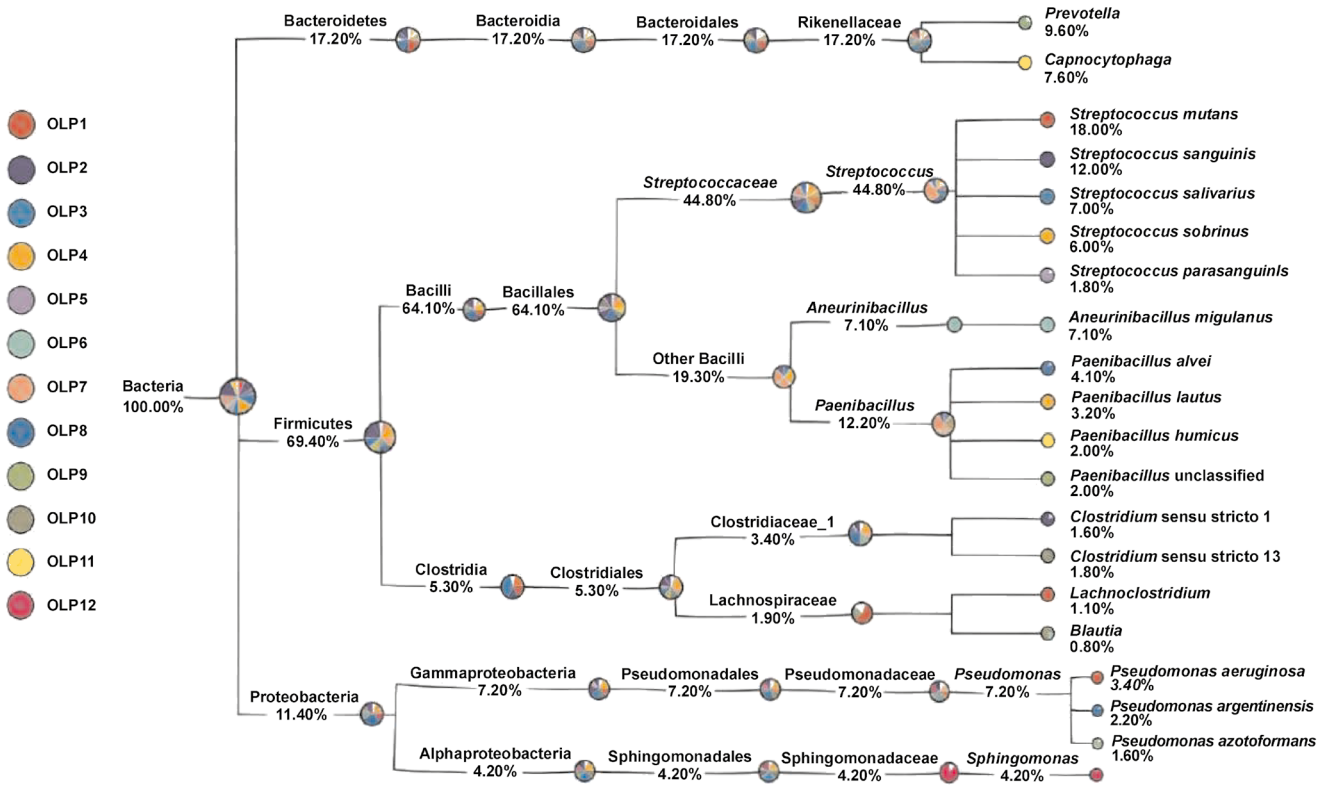

Fig. 5. Phylogenetic tree of the oral microbiota in patients with oral lichen planus (OLP) across taxonomic levels
Relative abundance is presented for each taxonomic level as the mean percentage of all samples.

The Shannon index, a measure encompassing both species richness and evenness, demonstrated that OLP3, OLP6, OLP10, and OLP12 had more diverse and evenly distributed microbial communities compared to the remaining samples, whereas OLP7 showed the lowest diversity. The Simpson index, which emphasizes the dominance of certain species, indicated higher diversity in samples OLP3, OLP6, OLP11, and OLP12, with OLP7 again demonstrating the lowest diversity and reflecting a less complex community structure (Table 3). These findings collectively underscore the heterogeneity in the microbial composition among the samples studied.

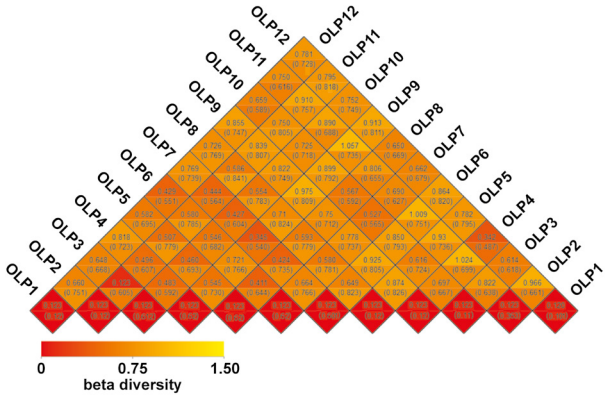

Fig. 7. Heatmap of beta diversity based on weighted and unweighted UniFrac distances

Values represent pairwise distance coefficients, with higher values indicating greater dissimilarity. Each cell contains 2 values corresponding to weighted and unweighted UniFrac distances, respectively.

Beta diversity analysis

Beta diversity analysis is a quantitative measure that explicates the distinction in microbial community structures by comparing their compositions. The heatmap analysis indicated that samples OLP12, OLP1, OLP4, OLP8, and OLP3 exhibited the greatest degree of dissimilarity in their microbial compositions. Notably, sample OLP1 demonstrated the highest level of dissimilarity, suggesting a unique microbial profile within the dataset (Fig. 7).

Discussion

The present study aimed to identify bacterial species associated with OLP by analyzing intratissue microbiota within OLP lesions. Intratissue bacterial communities were characterized by decreased alpha diversity and increased beta diversity compared with those present on the mucosal surface. The GraPhlAn display analysis revealed that the Firmicutes phylum was the dominant component of the microbial community, followed by the Proteobacteria phylum. Bacteria within the large genus *Streptococcus*, categorized under the Firmicutes phylum, were the most abundant. Five *Streptococcus* strains from the OLP samples were confirmed by means of whole genome sequencing. Following Streptococci, Bacilli and Clostridia demonstrated increased diversity. Other identified species included *K. pneumoniae*, *E. coli*, *P. aeruginosa*, *E. corrodens*, *Actinobacillus*, and other members

Table 3. Alpha diversity indices of the oral microbiota in oral lichen planus (OLP) samples

Sample	Observed species, *n*	Community diversity indices		Community richness indices		Sequencing depth index (Good's coverage)	Phylogenetic diversity whole tree index
		Shannon index	Simpson index	Chao1	ACE		
OLP1	574	5.13	0.86	622.92	641.29	0.993	60.27
OLP2	172	2.91	0.77	230.57	275.82	0.997	23.15
OLP3	1,131	8.32	0.99	1,234.13	1,221.49	0.981	83.41
OLP4	269	2.98	0.79	354.35	392.76	0.996	29.83
OLP5	561	4.80	0.74	585.80	583.41	0.998	68.90
OLP6	841	7.14	0.94	841.29	874.61	0.996	77.40
OLP7	147	0.78	0.18	232.40	323.81	0.996	21.92
OLP8	365	3.44	0.81	407.71	432.67	0.996	92.49
OLP9	731	6.02	0.91	971.11	1,260.10	0.991	74.87
OLP10	860	6.38	0.96	1,524.14	1,037.02	0.989	91.61
OLP11	609	6.71	0.97	700.33	717.67	0.994	67.26
OLP12	1,331	8.16	0.98	1,517.34	1,505.84	0.987	106.11

The Shannon index is a diversity index that takes into account the number of individuals and the number of species. The Simpson index is a diversity index that is focused on the dominant species in a given sample. Chao1 is a frequency-based estimator that is related to the frequency of species belonging to a certain class in a sample. The abundance-based coverage estimator (ACE) determines species richness based on the concept of sample cover. Higher sequencing depth values indicate a greater number of operational taxonomic units (OTUs). The phylogenetic diversity criterion of the entire genetic tree is defined as the total length of the branch covered by the tree, which includes all the species in the examined sample.

of the Proteobacteria phylum. According to previous studies, these species are found in significant quantities within the oral cavity. *Prevotella* and *Capnocytophaga*, belonging to the Bacteroidetes phylum, were identified as other prevalent bacteria in the samples. Studies have shown that the composition of saliva and buccal mucosa differs in healthy individuals, with genera such as *Neisseria* and *Prevotella* comprising nearly half of the bacterial composition of saliva. The bacterial community observed in OLP patients appears to be altered, with marked differences in diversity. Several reports have identified *Neisseria* and *Prevotella* among the predominant genera in OLP.[11,19] Colonization occurs at birth or shortly thereafter, with *S. salivarius* being one of the pioneer species. During the initial year of colonization, the oral cavity is also subject to invasion by other microorganisms, including *Streptococcus*, *Lactobacillus*, *Actinomyces*, *Neisseria*, and *Veillonella*.[20] Despite the presence of various microorganisms in the oral cavity, there is a symbiotic relationship between them, with non-pathogenic species generally preventing pathogenic species from adhering to the mucosa. In order to become pathogenic, bacteria must cross the commensal barrier, thus inducing infection and disease.[21,22]

The gene tree analysis of the studied samples showed that the members of the Firmicutes phylum, particularly Bacilli, were the most common bacterial species present, followed by *Clostridia*, *S. mutans*, *S. sanguinis*, *S. salivarius*, and *S. sobrinus*.

The evaluation of species distribution across samples revealed that in most of the infected patients, the dominant bacterial species belonged to the Firmicutes phylum. However, in samples OLP8, OLP9 and OLP10, members of the Proteobacteria phylum constituted a significant percentage of the bacterial population. In contrast, samples OLP2, OLP3, OLP4, and OLP12 were predominantly composed of Firmicutes, with Proteobacteria present in lower abundance. Sample OLP12 exhibited the highest microbial diversity, including representatives of both Firmicutes and Actinobacteria, whereas OLP8 showed a relatively high abundance of Proteobacteria.

Microbiological studies have reported the presence of various microbes in the oral cavity, including *Streptococcus* and *Corynebacterium* species, which collectively form an ecosystem that functions similarly to the human gut microbiota.[5,6] Various factors, including different treatments, can affect the population of oral bacteria.[23,24] The microbial population is influenced by the type and severity of the disease. The structure of oral biofilm is associated with the development of various oral diseases.[25–27] Systemic conditions, such as cardiovascular, digestive or endocrine disorders, may alter the oral microbiota. Body weight may also have an influence, with obese patients having a different salivary microbiome compared to those with normal weight. Additionally, liver diseases significantly alter the salivary microbiota and may invade the gut.[28–30] Sugar consumption, which changes the acidity of the oral environment, leads to modifications in the oral microbiota, with an increase in acidogenic bacteria.[31] Diet is a crucial factor in shaping the oral microbiome. For example, breastfed infants tend to have higher proportions of *Streptococcus*, while formula-fed infants exhibit increased levels of *Actinomyces* and *Prevotella*. Moreover, breastfed and formula-fed infants develop oral candidiasis less frequently than solid-fed infants.[32–34] Smoking has been shown to alter the oral flora by reducing Proteobacteria and increasing Firmicutes and Actinobacteria.[35,36]

Notably, in the present study, alpha diversity analysis revealed substantial inter-individual variability. Sample OLP7 exhibited the lowest microbial diversity (Shannon index: 0.78, Simpson index: 0.18), whereas OLP12 demonstrated the highest diversity (Shannon index: 8.16, Simpson index: 0.98). Clinically, OLP7 presented with higher erythema (R5E5) and a moderate reticulation/erythema/ulceration (REU) score, while OLP12 demonstrated lower erythema (R6E2) but a higher REU score. Histopathological examination confirmed the diagnosis of OLP in both cases without secondary infection or atypical dysplasia. As no clear differences in comorbidities, systemic diseases or medication use were identified between these 2 subjects, the observed variation in microbial diversity may reflect individual host–microbiome interactions or localized microenvironmental factors. This observation highlights the potential significance of patient-specific microbial diversity profiles in the pathogenesis of OLP.

Numerous studies have investigated various aspects of the etiology and treatment of OLP. Changes in saliva and its components may lead to a wide range of oral disorders and diseases.[37] Two types of peroxidase enzymes, which function as crucial defense factors, are secreted by salivary glands and polymorphonuclear leukocytes. The latter is discharged in the gingival crevice fluid. Peroxidase enzymes, in the presence of thiocyanate and hydrogen peroxide ions, cause the destruction of *Lactobacillus acidophilus*. They play a crucial role in fighting microbes and preventing the accumulation of harmful amounts of hydrogen peroxide.[38] In OLP, disturbances in redox homeostasis have been reported, including reduced antioxidant capacity and increased oxidative stress. Elevated levels of lactoferrin, lysozyme and salivary peroxidase have been observed in bacterial or viral infections. Increased levels of peroxidase enzymes in patients may contribute to oxidative imbalance, which could potentially influence autoimmune responses.[37,38]

The role of oxidative stress in oral inflammatory diseases has been extensively studied. Recent investigations have shown significant alterations in both enzymatic and non-enzymatic antioxidant systems in periodontitis. Toczewska et al. demonstrated reduced activity of antioxidant enzymes and decreased levels of non-enzymatic antioxidants in saliva and gingival crevicular fluid of patients with periodontitis.[39,40] These findings parallel our observations in OLP, suggesting shared oxidative stress

pathways in chronic oral inflammation. Moreover, the complexity of diagnosing and managing oral mucosal inflammatory conditions, as highlighted in the review of peri-implant mucositis by Lo Bianco et al.,[41] emphasizes the need for standardized diagnostic criteria and therapeutic protocols.

In the present study, the findings of alpha diversity analysis showed that the number of colonies associated with the investigated species exhibited significant differences and diversity among samples. The phylogenetic diversity index, as well as the ACE and Chao1 indices, revealed that OLP3 and OLP12 had higher microbial diversity, while the lowest diversity was observed in OLP2, OLP4, OLP7, and OLP8 samples. The Shannon index indicated that OLP3, OLP6, OLP10, and OLP12 demonstrated a greater number of microbial species than other samples. The Simpson index showed that the dominant species in OLP3, OLP6, OLP11, and OLP12 exhibited more microbial species than the other samples. These findings align with previous reports suggesting that increased disease severity may be associated with reduced microbial diversity.[13,42,43]

The findings of our study also demonstrate that *E. coli*, an indicator of oral contamination, was identified in abundance in patients with OLP. After *Streptococcus*, *Escherichia coli* has been identified as an effective pathogen in OLP. A recent study isolated 4 *Streptococcus* strains from additional OLP samples, and detected *E. coli* in most of the OLP tissues, suggesting its potential role in the pathogenesis of OLP.[44]

Contradictory reports have been published regarding the effect of the oral microbial community structure and saliva on OLP. Some reports indicate the presence of high levels of *Porphyromonas* and *Solobacterium* in OLP, while a 2017 report found that *Fusobacterium*, *Leptotrichia* and *Lautropia* exhibited high abundance in the buccal mucosa.[13] Additionally, the infiltration of T cells into oral tissues due to the presence of bacteria in OLP has been reported.[14,15]

Studies have shown that when the homeostatic balance of the oral microbiome is disrupted, the defense pathways involved in oral inflammation associated with OLP are activated. In other words, the occurrence of OLP is associated with the disruption of the oral microbiota due to microbial dysbiosis of the buccal mucosa.[9–11]

Study strengths and limitations

This study has several strengths, including the use of standardized clinical criteria, histopathological confirmation of all cases, and high-throughput *16S rRNA* gene sequencing for comprehensive microbial profiling. The application of both alpha and beta diversity measures enabled a thorough assessment of microbial community structure.

However, several limitations should be acknowledged. First, the observational design precluded causal inference regarding the relationship between microbial dysbiosis and the development of OLP. Second, the absence of a matched control group limited direct comparisons. However, the findings were compared with published data on healthy oral microbiota. Third, the final sample size for sequencing (n = 12) was relatively small due to stringent quality criteria, potentially limiting statistical power for subgroup analyses. Fourth, functional aspects of the microbiome or host–microbe interactions were not assessed. Finally, potential confounding factors such as diet, oral hygiene practices and subclinical systemic conditions were not systematically evaluated. Future longitudinal studies with larger sample sizes, matched controls and functional microbiome analyses are warranted to confirm these findings and elucidate the mechanistic role of the oral microbiome in OLP pathogenesis.

Conclusions

The present study demonstrated an association between the oral microbiome and OLP. The microbes obtained from samples of OLP patients exhibited a distinct bacterial population. Overall, the predominant bacterial genera were *Streptococcus*, followed by *Bacillus*. The difference in bacterial population may serve as an influential factor in the development of OLP. It is recommended that the bacteria identified in this study be compared with healthy oral microbiota and further evaluated in order to enhance understanding of the pathogenesis of OLP. While the present study identified facultative anaerobes, such as *Streptococcus* species, the potential role of obligate anaerobic bacteria in the pathogenesis of OLP warrants further investigation, particularly given their abundance in oral biofilms and their capacity to modulate local immune responses.

Ethics approval and consent to participate

The study was approved by the Institutional Review Boards of the Dental Hospital of Tehran University of Medical Sciences, Iran, and the Faculty of Dentistry, Seoul National University, South Korea (approval No. S-D20180026), as well as by the Ethics Committee of the Clinic of Košice, Slovakia (approval No. REK01/2023). Written informed consent was obtained from all participants.

Data availability

All data generated or analyzed during this study are included in the published article.

Consent for publication

Not applicable.

Use of AI and AI-assisted technologies

Not applicable.

ORCID iDs

Elham Saberian https://orcid.org/0000-0002-0590-9489
Adriána Petrášová https://orcid.org/0000-0002-4289-7691
Andrej Jenča Jr. https://orcid.org/0000-0003-4501-7407
Janka Jenčová https://orcid.org/0009-0007-4431-3227
Kimia Shirali https://orcid.org/0000-0002-2006-2343
Andrej Jenča https://orcid.org/0000-0002-9297-9134
Mieszko Adam Więckiewicz https://orcid.org/0000-0003-4953-7143
Hadi Zare-Zardini https://orcid.org/0000-0002-1501-2560
Meysam Ebrahimi Far https://orcid.org/0009-0006-2940-1045

References

1. Boorghani M, Gholizadeh N, Taghavi Zenouz A, Vatankhah M, Mehdipour M. Oral lichen planus: Clinical features, etiology, treatment and management; a review of literature. *J Dent Res Dent Clin Dent Prospects*. 2010;4(1):3–9. doi:10.5681/joddd.2010.002
2. Gorouhi F, Davari P, Fazel N. Cutaneous and mucosal lichen planus: A comprehensive review of clinical subtypes, risk factors, diagnosis, and prognosis. *ScientificWorldJournal*. 2014;2014:742826. doi:10.1155/2014/742826
3. Omal P, Jacob V, Prathap A, Thomas NG. Prevalence of oral, skin, and oral and skin lesions of lichen planus in patients visiting a dental school in southern India. *Indian J Dermatol*. 2012;57(2):107–109. doi:10.4103/0019-5154.94276
4. Pan Z, Zhang X, Xie W, et al. Revisited and innovative perspectives of oral ulcer: From biological specificity to local treatment. *Front Bioeng Biotechnol*. 2024;12:1335377. doi:10.3389/fbioe.2024.1335377
5. Eisenberg E. Oral lichen planus. A benign lesion. *J Oral Maxillofac Surg*. 2000;58(11):1278–1285. doi:10.1053/joms.2000.16629
6. Silverman S Jr. Oral lichen planus: A potentially premelignant lesion. *J Oral Maxillofac Surg*. 2000;59(11):1286–1288. doi:10.1053/joms.2000.16630
7. Silverman S, Gorsky M, Lozada-Nur F. A prospective follow-up study of 570 patients with oral lichen planus: Persistence, remission, and malignant association. *Oral Surg Oral Med Oral Pathol*. 1985;60(1):30–34. doi:10.1016/0030-4220(85)90210-5
8. Bagán-Sebastián JV, Milián-Masanet MA, Peñarrocha-Diago M, Jiménez Y. A clinical study of 205 patients with oral lichen planus. *J Oral Maxillofac Surg*. 1992;50(2):116–118. doi:10.1016/0278-2391(92)90354-3
9. Jung W, Jang S. Oral microbiome research on oral lichen planus: Current findings and perspectives. *Biology (Basel)*. 2022;11(5):723. doi:10.3390/biology11050723
10. Yu FY, Wang QQ, Li M, et al. Dysbiosis of saliva microbiome in patients with oral lichen planus. *BMC Microbiol*. 2020;20(1):75. doi:10.1186/S12866-020-01733-7
11. Wang X, Zhao Z, Tang N, et al. Microbial community analysis of saliva and biopsies in patients with oral lichen planus. *Front Microbiol*. 2020;11:629. doi:10.3389/fmicb.2020.00629
12. Wang K, Lu W, Tu Q, et al. Preliminary analysis of salivary microbiome and their potential roles in oral lichen planus. *Sci Rep*. 2016;6:22943. doi:10.1038/srep22943
13. He Y, Gong D, Shi C, Shao F, Shi J, Fei J. Dysbiosis of oral buccal mucosa microbiota in patients with oral lichen planus. *Oral Dis*. 2017;23(5):674–682. doi:10.1111/odi.12657
14. Choi YS, Kim Y, Yoon HJ, et al. The presence of bacteria within tissue provides insights into the pathogenesis of oral lichen planus. *Sci Rep*. 2016;6:29186. doi:10.1038/srep29186
15. Gao L, Xu T, Huang G, Jiang S, Gu Y, Chen F. Oral microbiomes: More and more importance in oral cavity and whole body. *Protein Cell*. 2018;9(5):488–500. doi:10.1007/s13238-018-0548-1
16. Prudent E, Raoult D. Fluorescence in situ hybridization, a complementary molecular tool for the clinical diagnosis of infectious diseases by intracellular and fastidious bacteria. *FEMS Microbiol Rev*. 2019;43(1):88–107. doi:10.1093/femsre/fuy040
17. Liu Y, Wong KKW, Ko EYL, et al. Systematic comparison of bacterial colonization of endometrial tissue and fluid samples in recurrent miscarriage patients: Implications for future endometrial microbiome studies. *Clin Chem*. 2018;64(12):1743–1752. doi:10.1373/clinchem.2018.289306
18. Frickmann H, Zautner AE, Moter A, et al. Fluorescence in situ hybridization (FISH) in the microbiological diagnostic routine laboratory: A review. *Crit Rev Microbiol*. 2017;43(3):263–293. doi:10.3109/1040841x.2016.1169990
19. Caselli E, Fabbri C, D'Accolti M, et al. Defining the oral microbiome by whole-genome sequencing and resistome analysis: The complexity of the healthy picture. *BMC Microbiol*. 2020;20(1):120. doi:10.1186/s12866-020-01801-y
20. Patil S, Rao RS, Amrutha N, Sanketh DS. Oral microbial flora in health. *World J Dent*. 2013;4(4):262–266. doi:10.5005/jp-journals-10015-1242
21. Avila M, Ojcius DM, Yilmaz O. The oral microbiota: Living with a permanent guest. *DNA Cell Biol*. 2009;28(8):405–411. doi:10.1089/dna.2009.0874
22. Marsh PD. Role of the oral microflora in health. *Microb Ecol Health Dis*. 2000;12:130–137. doi:10.1080/089106000750051800
23. Yu ZK, Xie RL, You R, et al. The role of the bacterial microbiome in the treatment of cancer. *BMC Cancer*. 2021;21(1):934. doi:10.1186/s12885-021-08664-0
24. Lynch SV, Pedersen O. The human intestinal microbiome in health and disease. *N Engl J Med*. 2016;375(24):2369–2379. doi:10.1056/NEJMra1600266
25. Heller D, Helmerhorst EJ, Oppenheim FG. Saliva and serum protein exchange at the tooth enamel surface. *J Dent Res*. 2017;96(4):437–443. doi:10.1177/0022034516680771
26. Bowen WH, Burne RA, Wu H, Koo H. Oral biofilms: Pathogens, matrix, and polymicrobial interactions in microenvironments. *Trends Microbiol*. 2018;26(3):229–242. doi:10.1016/j.tim.2017.09.008
27. Rath S, Bal SCB, Dubey D. Oral biofilm: Development mechanism, multidrug resistance, and their effective management with novel techniques. *Rambam Maimonides Med J*. 2021;12(1):e0004. doi:10.5041/rmmj.10428
28. Lapidot Y, Amir A, Ben-Simon S, et al. Alterations of the salivary and fecal microbiome in patients with primary sclerosing cholangitis. *Hepatol Int*. 2021;15(1):191–201. doi:10.1007/s12072-020-10089-z
29. Graves DT, Corrêa JD, Silva TA. The oral microbiota is modified by systemic diseases. *J Dent Res*. 2019;98(2):148–156. doi:10.1177/0022034518805739
30. Džunková M, Lipták R, Vlková B, et al. Salivary microbiome composition changes after bariatric surgery. *Sci Rep*. 2020;10(1):20086. doi:10.1038/s41598-020-76991-6
31. Esberg A, Haworth S, Hasslöf P, Lif Holgerson P, Johansson I. Oral microbiota profile associates with sugar intake and taste preference genes. *Nutrients*. 2020;12(3):681. doi:10.3390/nu12030681
32. Anderson AC, Rothballer M, Altenburger MJ, et al. Long-term fluctuation of oral biofilm microbiota following different dietary phases. *App Environ Microbiol*. 2020;86(20):e01421-20. doi:10.1128/aem.01421-20
33. Chumponsuk T, Gruneck L, Gentekaki E, et al. The salivary microbiota of Thai adults with metabolic disorders and association with diet. *Arch Oral Biol*. 2021;122:105036. doi:10.1016/j.archoralbio.2020.105036
34. Štšepetova J, Truu J, Runnel R, et al. Impact of polyols on oral microbiome of Estonian schoolchildren. *BMC Oral Health*. 2019;19(1):60. doi:10.1186/s12903-019-0747-z
35. Jia YJ, Liao Y, He YQ, et al. Association between oral microbiota and cigarette smoking in the Chinese population. *Front Cell Infect Microbiol*. 2021;11:658203. doi:10.3389/fcimb.2021.658203
36. Yang Y, Zheng W, Cai QY, et al. Cigarette smoking and oral microbiota in low-income and African-American populations. *J Epidemiol Community Health*. 2019;73(12):1108–1115. doi:10.1136/jech-2019-212474
37. Magacz M, Kędziora K, Sapa J, Krzyściak W. The significance of lactoperoxidase system in oral health: Application and efficacy in oral hygiene products. *Int J Mol Sci*. 2019;20(6):1443. doi:10.3390/ijms20061443

38. Rudney JD, Smith QT. Relationships between levels of lysozyme, lactoferrin, salivary peroxidase, and secretory immunoglobulin A in stimulated parotid saliva. *Infect Immun*. 1985;49(3):469–475. doi:10.1128/iai.49.3.469-475.1985
39. Toczewska J, Baczyńska D, Zalewska A, Maciejczyk M, Konopka T. The mRNA expression of genes encoding selected antioxidant enzymes and thioredoxin, and the concentrations of their protein products in gingival crevicular fluid and saliva during periodontitis. *Dent Med Probl*. 2023;60(2):255–265. doi:10.17219/dmp/150888
40. Toczewska J, Maciejczyk M, Zalewska A, Konopka T. Gingival fluid and saliva concentrations of selected non-enzymatic antioxidants in periodontitis. *Dent Med Probl*. 2022;59(4):555–564. doi:10.17219/dmp/148051
41. Lo Bianco L, Montevecchi M, Ostanello M, Checchi V. Recognition and treatment of peri-implant mucositis: Do we have the right perception? A structured review. *Dent Med Probl*. 2021;58(4):545–554. doi:10.17219/dmp/136359
42. Hijazi K, Morrison RW, Mukhopadhya I, et al. Oral bacterial diversity is inversely correlated with mucosal inflammation. *Oral Dis*. 2020;26(7):1566–1575. doi:10.1111/odi.13420
43. Baek K, Choi Y. The microbiology of oral lichen planus: Is microbial infection the cause of oral lichen planus? *Mol Oral Microbiol*. 2018;33(1):22–28. doi:10.1111/omi.12197
44. Baek K, Lee J, Lee A, et al. Characterization of intratissue bacterial communities and isolation of *Escherichia coli* from oral lichen planus lesions. *Sci Rep*. 2020;10(1):3495. doi:10.1038/s41598-020-60449-w

Original paper

Color atlas of resin-infiltrated white spot lesions: Data on aesthetic stability following resin infiltration, bleaching and re-bleaching

Christoph Matthias Schoppmeier[1,A–F], Malin Janson[2,B–E], Michael Jochen Wicht[1,A,C,E,F], Max von Kohout[3,C,E], Anna Greta Barbe[1,A,C–E]

[1] Polyclinic for Operative Dentistry and Periodontology, Faculty of Medicine and University Hospital Cologne, University of Cologne, Germany
[2] Department of Prosthetic Dentistry, Faculty of Medicine and University Hospital Cologne, University of Cologne, Germany
[3] Institute of Medical Statistics and Computational Biology, Faculty of Medicine and University Hospital Cologne, University of Cologne, Germany

A – research concept and design; B – collection and/or assembly of data; C – data analysis and interpretation;
D – writing the article; E – critical revision of the article; F – final approval of the article

Dental and Medical Problems, ISSN 1644-387X (print), ISSN 2300-9020 (online) *Dent Med Probl*. 2026;63(5):1167–1177

Address for correspondence
Christoph Matthias Schoppmeier
E-mail: christoph.schoppmeier@uk-koeln.de

Funding sources
None declared

Conflict of interest
Michael Jochen Wicht reports a relationship with DMG Chemisch-Pharmazeutische Fabrik GmbH (Hamburg, Germany) that includes speaking and lecture fees. All other authors declare that they have no known competing financial interests or personal relationships that could have appeared to influence the work reported in this paper.

Acknowledgements
The authors would like to thank Mr. Himanshu Rai from Chandigarh University (Mohali, India) for his valuable contributions to the development of the software code used in this study.

Received on July 21, 2025
Reviewed on August 21, 2025
Accepted on September 12, 2025

Published online on October 30, 2026

Cite as
Schoppmeier CM, Janson M, Wicht MJ, von Kohout M, Barbe AG. Color atlas of resin-infiltrated white spot lesions: Data on aesthetic stability following resin infiltration, bleaching and re-bleaching. *Dent Med Probl.* 2026;63(5):1167–1177. doi:10.17219/dmp/210668

DOI
10.17219/dmp/210668

Copyright
Copyright by Author(s)
This is an article distributed under the terms of the Creative Commons Attribution 3.0 Unported (CC BY 3.0) (https://creativecommons.org/licenses/by/3.0/)

Abstract

Background. Minimally invasive treatment of white spot lesions (WSLs) requires predictable and stable aesthetic outcomes.

Objectives. This in vitro study aimed to systematically analyze the color dynamics of resin-infiltrated WSLs across all relevant treatment phases and to develop a color atlas as a clinical and scientific reference.

Material and methods. Sixty extracted, caries-free third molars were randomly assigned to 4 groups: untreated control (URG); lesion + infiltration (LIG); lesion + infiltration + in-office bleaching (ICW); and lesion + infiltration + at-home bleaching (IAW). Standardized colorimetric measurements (L*, a*, b*) and ΔE values were collected at 10 defined stages (T0–T9): baseline (T0); post-WSL creation (T1); post-infiltration (T2); post-bleaching (T3); post-bleaching storage in distilled water for 14 days (T4); post-aging (thermocycling; T5); post-staining (coffee, day 6 and day 12; T6 and T7); post-re-bleaching (T8); and final water storage for 14 days (T9). Bleaching protocols included either four 15-min in-office bleaching applications or 5 days of at-home bleaching with 10% carbamide peroxide. Color changes were assessed using calibrated digital image analysis. A browser-based LAB Color Tool was developed to evaluate L*, a* and b* values against study-derived 95% and 99% confidence intervals (*CI*s), providing real-time traffic light feedback.

Results. Chromatic coordinates a* and b* showed a strong linear correlation with ΔE values, whereas lightness (L*) exhibited a non-linear distribution with high variability, especially after bleaching. At-home bleaching (IAW) resulted in the highest ΔE values after staining (group mean: 25.1 at T7), followed by the ICW (23.6), LIG (21.1) and URG groups (12.9). As ΔE values above 3.7 are generally considered perceptible at conversational distance, most post-staining changes in the bleaching groups, and all values above 10, represent clinically visible discoloration. Re-bleaching markedly reduced staining-induced discoloration in all groups and shifted a* and b* back to or below their post-infiltration levels. However, final mean ΔE values relative to baseline remained above the 3.7 threshold because residual differences persisted across all 3 CIELAB coordinates.

Conclusions. Chromatic parameters (a*, b*) are more predictive of perceptible color differences in resin-infiltrated WSLs than lightness (L*) alone. These findings support the use of a* and b* as primary metrics in aesthetic diagnostics. The developed color atlas and browser-based LAB Color Tool offer a standardized reference for clinical decision-making and future research.

Keywords: white spot lesion, resin infiltration, color mapping, colorimetry, CIELAB color system

Highlights

- The study develops a standardized color atlas to track dynamic L*, a*, b* parameters and ΔE changes in resin-infiltrated white spot lesions across treatment stages.
- The chromatic components a* and b* correlate more strongly with perceptible color changes than lightness (L*) alone.
- The study introduces a novel LAB color assessment tool that provides real-time feedback and reference-based evaluation using a traffic light system.
- Re-bleaching largely reverses staining-induced discoloration in resin-infiltrated enamel, although color values do not fully return to baseline.

Introduction

In recent years, aesthetic dentistry has become a central pillar of modern dental practice, reflecting growing patient demand for improvements in tooth appearance and color.[1] As patients increasingly value the appearance of their teeth, clinicians are more frequently confronted with concerns regarding discoloration of the anterior dentition, especially white opacities such as white spot lesions (WSLs) and dental fluorosis, as well as trauma-induced changes and yellowish-brown stains associated with molar–incisor hypomineralization (MIH).[2] These enamel defects, particularly WSLs, often exhibit a heterogeneous microstructure characterized by water and air inclusions that alter the refractive index of enamel and cause variations in appearance depending on the depth of the lesion.[3] In particular, orthodontically induced WSLs represent a frequent and clinically relevant challenge, and various adjunctive strategies have been investigated to effectively manage or prevent these lesions.[4,5] Patients frequently perceive these opacities as unaesthetic, leading to a growing demand for minimally invasive treatment options that can provide both immediate and long-term aesthetic improvement.[3] The primary therapeutic goal is the restoration of a visually homogeneous tooth color and the maintenance of color stability over time.[6]

The resin infiltration technique (RI) involves selective etching of the lesion body with 15% hydrochloric acid (HCl), followed by capillary-driven infiltration of a low-viscosity, triethylene glycol dimethacrylate (TEGDMA)-based resin into the porous enamel structure. This method has shown promising results in optically masking lesions and enhancing their mechanical stability.[7] However, despite its initially high aesthetic efficacy, the long-term color stability of infiltrated lesions remains uncertain due to various extrinsic factors.[8] For instance, studies have demonstrated that composite and resin-infiltrated materials show increased susceptibility to staining and bleaching-induced surface degradation, which can influence both color and surface texture over time.[9–11] In patients with fixed orthodontic appliances, tooth bleaching poses additional challenges due to limited agent diffusion and uneven whitening outcomes, necessitating careful consideration of timing and technique.[12] Furthermore, concerns regarding the cytotoxicity of bleaching agents, particularly in combination with restorative materials, have gained increasing attention.[9]

To date, most studies have assessed color changes only at isolated time points, without capturing the continuous, dynamic progression of color alterations throughout the entire treatment and aging cycle. This lack of longitudinal color mapping across multiple clinically relevant stages, such as bleaching, staining and re-bleaching, limits the ability to predict and standardize long-term outcomes.

The CIELAB color system, widely used in dentistry, enables precise quantification of color differences through its 3 coordinates: L* (lightness, ranging from 0 = black to 100 = white); a* (green–red axis, ranging from –128 = green to 127 = red); and b* (blue–yellow axis, ranging from –128 = blue to 127 = yellow).[13] Since its introduction in 1976, the CIELAB color space has been the standard in dental colorimetric analysis.[14] Although the ΔEab formula has been criticized for its reliance on uniform Euclidean distances,[15] the more recent CIEDE2000 (ΔE_{00}) formula has improved accuracy by successfully capturing subtle color differences.[16] However, recent detailed colorimetric studies have demonstrated that the ΔEab formula, contrary to earlier assumptions, aligns more closely with visually assessed color differences than the ΔE_{00} formula, reaffirming its clinical value in dentistry.[16] Thus, the CIELAB system remains the gold standard due to its universal compatibility, ease of use and essential role in precise and reproducible color measurements in aesthetic dentistry.[13]

The ΔE value, which quantifies color differences, serves as a key parameter in evaluating color stability over time and enables both pre- and post-treatment assessments and comparisons between different teeth. Among the various proposed thresholds, a ΔE value of 3.7 has been established as a threshold for visual perceptibility at a natural conversational distance and is therefore considered the most clinically relevant benchmark from the patient's perspective.[17] At or above this value, color differences become noticeable to the average observer without the aid of magnification or special lighting. In addition, ΔE values ≤1.0 are often interpreted as imperceptible, and those between 2.0 and 3.3 as clinically acceptable. Nonetheless, these alternative criteria are applied inconsistently, whereas the ΔE threshold of 3.7 has emerged as a more reliable and pragmatic

predictor of patient satisfaction.[18] Such benchmarks are essential for the standardized evaluation of long-term treatment efficacy, though variations in clinical context may necessitate adjustments to perceptibility limits.

Resin-infiltrated WSLs exhibit increased surface roughness due to their altered microstructure, which promotes the adhesion of pigments from the oral environment and facilitates extrinsic staining from food and beverages.[19] In addition, the infiltrant contains TEGDMA in combination with camphorquinone as a photoinitiator, which has a naturally yellowish hue. This color may partially persist after polymerization, prompting some patients to request additional tooth whitening shortly after treatment.[20] Over time, infiltrated teeth are subjected to thermocyclic aging, which induces microstructural changes and further increases their susceptibility to discoloration, possibly necessitating repeated bleaching interventions.[21] These factors underscore the multifactorial nature of long-term color stability in resin-infiltrated WSLs.

To date, studies investigating the color stability of infiltrated teeth have typically focused on isolated treatment phases, without accounting for the continuous color changes that occur throughout the full course of treatment.[22] The existing gap in the literature emphasizes the need for a systematic and standardized approach to tracking color changes throughout all treatment phases, thereby enabling a deeper understanding of the dynamics of color stability. Comprehensive mapping of CIELAB values at each treatment stage may contribute to the development of evidence-based reference standards. Accordingly, the primary aim of the present secondary analysis was to systematically quantify L*, a*, b*, and corresponding ΔE values across all clinically relevant treatment stages of resin-infiltrated WSLs, including lesion creation, resin infiltration, bleaching, aging, staining, and re-bleaching, and to compile this data into a standardized, evidence-based color atlas for clinical and research use. As a secondary objective, a prototype of a digital LAB Color Tool was developed to operationalize the atlas data and provide clinicians and researchers with an interactive platform for comparing individual measurements against reference ranges. Additionally, Cohen's *d* was calculated to determine the effect size of color changes, providing a quantitative basis for interpretation and planning of future controlled studies.

Material and methods

This study represents a secondary analysis of data derived from a previously conducted in vitro investigation involving 60 extracted, caries-free human third molars.[23] The teeth were obtained following clinical extractions performed for reasons unrelated to the research. Written informed consent was obtained from all donors, and the study was approved by the Ethics Committee of the Faculty of Medicine, University of Cologne, Germany (reference No. 23-1472; March 28, 2024). The present manuscript was prepared in accordance with the CRIS (Checklist for Reporting In-vitro Studies) guidelines to ensure transparent and standardized reporting of the study design, methodology and results.[24]

To minimize interspecimen variability, only caries-free human third molars of comparable size, morphology and shade (A2–A3 on the VITA Classical Shade Guide) were included. All specimens were stored in distilled water at 4°C until use and were randomly allocated to experimental groups to ensure comparability of baseline characteristics.

The specimens were assigned to the following experimental groups:

- URG – initially untreated reference group; sound enamel without WSL creation, resin infiltration or initial bleaching, serving as the reference for natural color stability. Like all groups, URG specimens subsequently underwent thermocycling, coffee staining and re-bleaching;
- LIG – lesion + infiltration group; artificial WSL creation using a 21-day pH-cycling protocol (16 h of demineralization at pH 4.3 and 8 h of remineralization per day), followed by 56 h of storage in artificial saliva, a single 2-min application of 15% HCl gel, ethanol drying, and resin infiltration (3 min, repeated for 1 min, each light-cured for 40 s) with a low-viscosity, TEGDMA-based infiltrant (Icon; DMG Dental, Hamburg, Germany); no initial bleaching was applied;
- ICW – lesion + infiltration + in-office bleaching group; the same WSL creation and resin infiltration protocol as in the LIG group, followed by in-office bleaching using the Zoom! Protocol (Discus Dental Europe, Rotterdam, the Netherlands): four 15-minute applications of 25% hydrogen peroxide gel, simulating a professional chairside whitening procedure;
- IAW – lesion + infiltration + at-home bleaching group; the same WSL creation and resin infiltration protocol as in the LIG group, followed by at-home bleaching with 10% carbamide peroxide gel (Opalescence 10% PF; Ultradent Products, South Jordan, USA) applied for 8 h per day on 5 consecutive days at 37°C, simulating a patient-administered whitening protocol.

Specimen handling, storage and processing were standardized across groups, with treatment protocols applied according to group assignment. After staining, all specimens were re-bleached: URG, LIG and ICW with the in-office protocol; and IAW with the at-home protocol described above. Given that this was a secondary analysis of an existing dataset, no additional stratification was introduced. Instead, randomization and uniform baseline selection in the original study helped minimize interspecimen heterogeneity. All treatment steps are summarized in the flowchart presented in Fig. 1. The materials used are listed in Table 1.

Color measurements were obtained at 10 defined stages: T0 – baseline; T1 – after WSL creation; T2 – after resin infiltration; T3 – after bleaching (ICW and IAW only); T4 – after 14 days of storage in distilled water; T5 – after

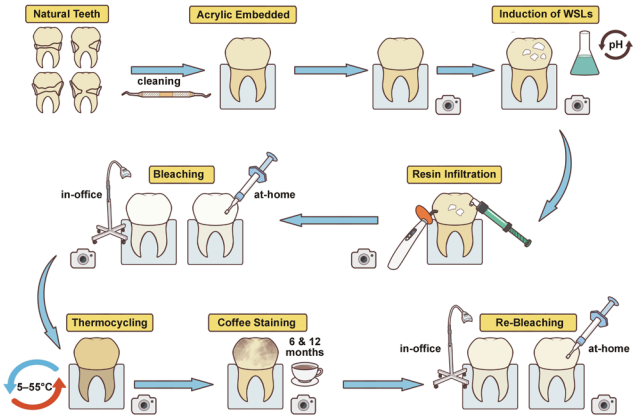

Fig. 1. Schematic flowchart illustrating all treatment steps and assessment time points in the in vitro study

Extracted caries-free human third molars were cleaned, embedded in acrylic resin and polished. White spot lesions (WSLs) were artificially induced in selected groups using a standardized 21-day pH cycling protocol. Following 56 h of storage in artificial saliva, resin infiltration was performed using a low-viscosity, triethylene glycol dimethacrylate (TEGDMA)-based infiltrant after enamel etching with 15% hydrochloric acid (HCl) and ethanol drying. Bleaching was performed via an in-office protocol (Zoom!, 4 × 15 min) or at-home protocol (Opalescence 10% PF, 8 h/day for 5 days at 37°C). All specimens underwent thermocycling (5,000 cycles between 5°C and 55°C) and subsequent coffee staining for 12 days (37°C; Nespresso Volluto; Nestlé Nespresso S.A., Vevey, Switzerland) to simulate 1 year of exposure. A final re-bleaching step was performed (in-office protocol for URG, LIG and ICW; at-home protocol for IAW). Standardized digital photographs were taken after each treatment phase to enable CIELAB colorimetric analysis.

thermocycling (5,000 cycles, 5–55°C); T6 – after 6 days of coffee staining; T7 – after 12 days of coffee staining; T8 – after re-bleaching (all groups); and T9 – after a final 14-day storage in distilled water. The ΔE values were calculated relative to the individual baseline values (T0).

Color analysis

Color analysis was performed using standardized digital photographs taken at each of the 10 treatment stages. For each specimen at each treatment stage, measurements were performed in triplicate (using 3 independent standardized photographs obtained under identical conditions), and the mean CIELAB values from these triplicate images were used for analysis. All camera settings and flash configurations followed the imaging protocol established by Schoppmeier et al.,[6] ensuring uniform imaging conditions throughout the study.

A controlled photographic environment was used, incorporating a PULUZ lightbox (40 cm, 24 W, 5,500 K white light; PULUZ, Shenzhen, China) and a tripod to stabilize the camera. The surface contour was delineated on the first image to ensure consistent region-of-interest alignment, and the same outline was applied to subsequent images, maintaining consistent size, orientation and position. Calibration was performed for each image using a ColorChecker Passport Photo neutral gray reference

Table 1. Materials, manufacturers, compositions, and application protocols used during different treatment phases of resin-infiltrated white spot lesions (WSLs)

Treatment	Material	Lot No.	Manufacturer	Composition	Application
WSL induction	–	–	in-house hospital pharmacy	demineralization solution: 2.0 mmol/L calcium, 2.0 mmol/L phosphate and 75 mmol/L acetate, at pH 4.3 remineralization solution: 1.5 mmol/L calcium, 0.9 mmol/L phosphate, 150 mmol/L potassium chloride, and 20 mmol/L cacodylate buffer, at pH 7.0 artificial saliva: 22.1 mmol/L hydrogen carbonate, 16.1 mmol/L potassium, 14.1 mmol/L sodium hydrogen, 2.6 mmol/L phosphate, 0.8 mmol/L boric acid, 0.7 mmol/L calcium, 0.4 mmol/L thiocyanate, and 0.2 mmol/L magnesium, at pH 7.4–7.8	16 h of demineralization followed by 8 h of remineralization, repeated daily for 21 days with freshly prepared solutions; stored in artificial saliva at 37°C for 56 h
Resin infiltration	Icon Etch	261396	DMG Dental, Hamburg, Germany	15% hydrochloric acid	2 min
	Icon Dry	261396	DMG Dental, Hamburg, Germany	99% ethanol	30 s
	Icon Infiltrant	261396	DMG Dental, Hamburg, Germany	TEGDMA, initiators, additives	3 min + 1 min
At-home bleaching	Opalescence PF 10%	BXJ83	Ultradent Products, Inc., South Jordan, USA	5.8% hydrogen peroxide equivalent, glycerin, water, urea peroxide, xylitol, carbomer, PEG-6, sodium hydroxide, EDTA, potassium nitrate, 0.11% fluoride ions	8 h/day for 5 days
In-office bleaching	Zoom!	23279010	Discus Dental Europe, Rotterdam, the Netherlands	25% hydrogen peroxide, potassium hydroxide, eugenol, 2,6-di-tert-butyl-4-methylphenol	4 × 15 min
Staining	Nespresso Volluto coffee capsule	3147098306	Nestlé Nespresso S.A., Vevey, Switzerland	100% Arabica coffee; origin: South America; roast: light; intensity: 4/13; quantity: 5 g per capsule	immersion at 37°C for 12 days (measurements after 6 and 12 days); coffee freshly brewed with a 19-bar capsule machine and replaced daily

WSL – white spot lesion; TEGDMA – triethylene glycol dimethacrylate; PEG – polyethylene glycol; EDTA – ethylenediaminetetraacetic acid. Each application step was standardized to enable the assessment of CIELAB color changes and aesthetic outcomes.

card (X-Rite, Inc., Grand Rapids, USA) placed adjacent to the specimen. This allowed for the correction of white balance and brightness standardization directly within Adobe Photoshop Lightroom 9.4 (Adobe Inc., San Jose, USA). Using the gray reference card, brightness deviations (L*) were corrected, and RGB (red, green, blue) values were extracted under standardized lighting conditions. The extracted RGB values were then converted to the CIELAB color space. Color distributions across all study phases were assessed according to the standards defined by the International Commission on Illumination (CIE).

Color differences (ΔE values) were calculated using the following formula:

$$\Delta E = \sqrt{(L_2 - L_1)^2 + (a_2 - a_1)^2 + (b_2 - b_1)^2}$$

A value of ΔE ≥ 3.7 was used to identify color differences equal to or exceeding the predefined threshold of clinical relevance.[17]

Statistical analysis

The data analyzed in this secondary analysis originated from a previously conducted, single-center in vitro study.[23] Although the colorimetric measurements were based on the prior dataset, the statistical analysis, including the estimation of bootstrap-based confidence intervals (*CIs*) and effect sizes, and the development of the LAB Color Tool and reference atlas were newly designed and implemented for the present manuscript. Colorimetric data (L*, a*, b* and ΔE) was analyzed descriptively and visually to assess temporal changes across all treatment phases. Scatterplots with locally estimated scatterplot smoothing (LOESS), a non-parametric regression technique that fits multiple low-degree polynomials to localized subsets of the data, were used to illustrate dynamic trends and key transition points in color alteration. Color differences (ΔE) were calculated using the CIELAB formula relative to the individual baseline measurement (T0) for each specimen. To account for the limited sample size and potential deviations from normality, bootstrap resampling (5,000 iterations, with replacement; n = 15 per group) was applied to estimate means, medians, standard deviations, and Cohen's d effect sizes. Between-group effect sizes were calculated as the first-named minus the second-named group (negative d = higher value in the second-named group); within-group effect sizes were calculated as the earlier minus the later time point (negative d = increase over time). Corresponding 95% and 99% *CIs* were computed to enhance robustness and facilitate comparisons across groups and time points. All statistical analyses were performed using R, v. 4.3.1 (R Foundation for Statistical Computing, Vienna, Austria), employing the boot and ggplot2 packages. This non-parametric approach enabled inference without requiring an assumption of normality.

LAB Color Tool

Based on the data generated in this study, a software-based analysis tool was developed (https://color-atlas-wsl.netlify.app) to evaluate CIELAB color values across various treatment phases of resin-infiltrated WSLs (Fig. 2A). A comprehensive reference database was created, containing mean values as well as 95% and 99% *CIs* for L*, a* and b* coordinates across all relevant treatment stages.

The LAB Color Tool allows users to enter individual LAB values (L*, a*, b*) along with optional statistical parameters

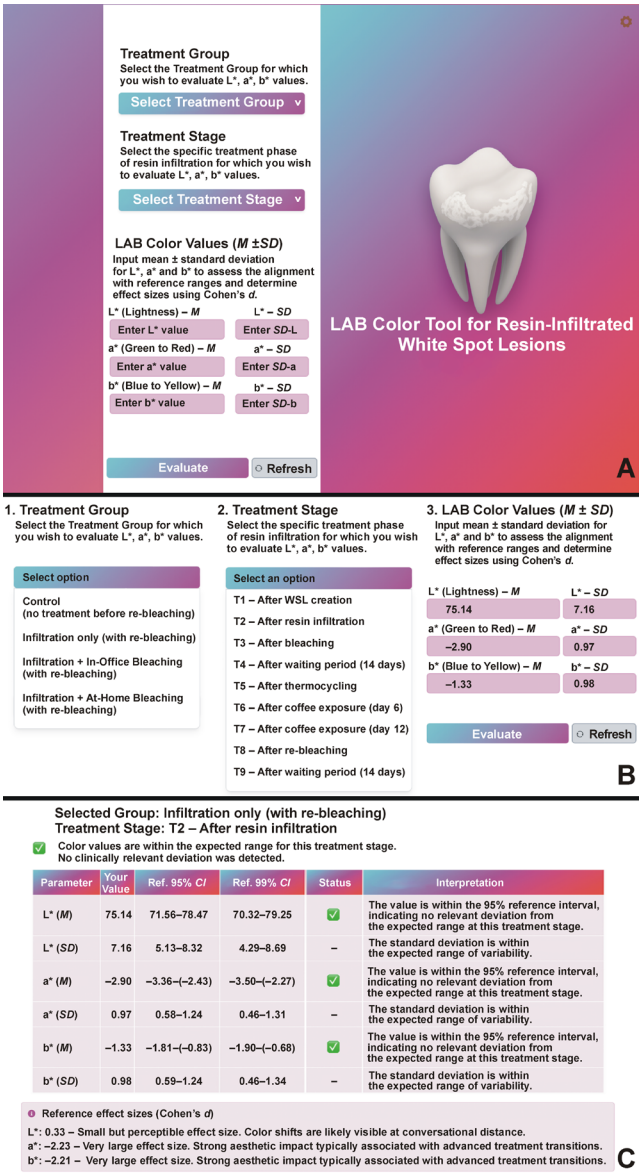

Fig. 2. Elements of the LAB Color Tool for the assessment of resin-infiltrated white spot lesions (WSLs)

A. Graphical user interface. The tool enables users to receive automated, real-time feedback through a three-tier traffic light system based on predefined 95% and 99% confidence intervals (*CIs*); B. Workflow; C. Evaluation output. An example of an assessment for the LIG group at T2 (after resin infiltration) is presented. Status indicators and detailed interpretations are provided based on the comparison with reference ranges. A reference box displays calculated Cohen's d values to facilitate the interpretation of the magnitude of colorimetric differences.

such as the mean and standard deviation. Users can specify the corresponding treatment stage, e.g., "natural tooth", "white spot lesion" or "post-infiltration" (Fig. 2B).

An internally developed algorithm automatically compares the entered values with the reference ranges and provides real-time feedback via a three-tier traffic light system (Fig. 2C):

- green – values within the 95% *CI*; the measurement is considered consistent with the reference mean;
- orange – values between the 95% and 99% *CIs*; minor methodological adjustments are recommended to optimize alignment with reference data;
- red – values outside the 99% *CI*; the system advises checking the experimental setup or measurement conditions due to a significant deviation from expected norms.

In addition to qualitative color assessment, the tool calculates Cohen's *d* as a measure of effect size, allowing for the quantification of the practical significance of deviations from reference values. This facilitates interpretation within an experimental context and supports accurate sample size estimation for future studies.

The tool was implemented as a browser-based web application (HTML/JavaScript) with the reference database embedded; all calculations are performed locally in the browser. The primary aim of the tool is to assist users in standardizing the evaluation of color changes, detecting methodological inconsistencies early, and enhancing the interpretive quality of aesthetic assessments in dental research and clinical practice.

Results

Analysis of CIELAB color parameters in relation to ΔE values

Effect sizes were interpreted according to Cohen's conventional thresholds, with $d = 0.2–0.49$ indicating a small effect, $d = 0.5–0.79$ – a medium effect, and $d \geq 0.8$ – a large effect. Additionally, values ≥1.2 were categorized as very large effects. Unlike the chromatic components (a* and b*), the lightness parameter (L*) in the CIELAB color space showed no linear correlation with the calculated ΔE values (Fig. 3). The L* value reflects the brightness of a color on a scale from 0 (black) to 100 (white), with higher values indicating lighter tooth shades. While both a* and b* values demonstrated an approximately linear relationship with ΔE, the L* component exhibited a non-linear distribution. Particularly in the medium-to-high brightness range (L* > 60), a greater dispersion of ΔE values was observed, without a consistent increase in ΔE as lightness increased.

In the control group (URG), the L* values remained stable at approx. 71 up to T5, with ΔE values far below the threshold of 3.7 (≤0.5). Only coffee staining produced large deviations (ΔE: 8.7–12.9 at T6–T7), which re-bleaching reduced but did not eliminate (ΔE: 7.2 at T9) (Fig. 3A). The LIG group

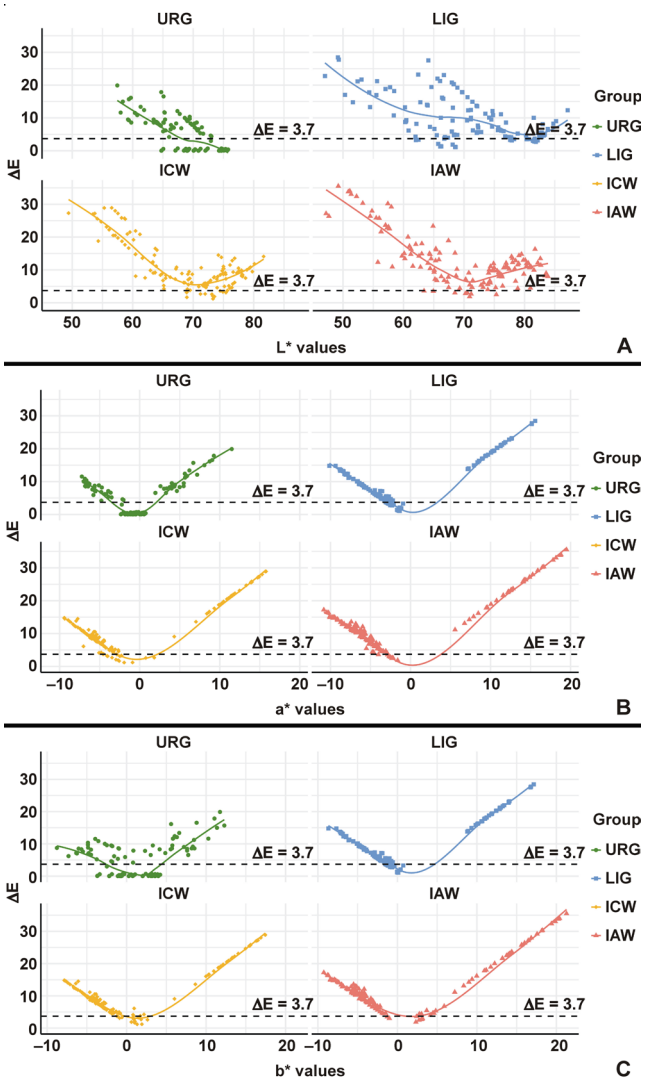

Fig. 3. Relationship between lightness (L*), a* and b* values and ΔE across the 4 treatment groups

A. L* values vs. ΔE; B. a* values vs. ΔE; C. b* values vs. ΔE. The horizontal dashed line indicates the predefined threshold for clinically relevant color differences (ΔE = 3.7).

URG – untreated control; LIG – lesion + infiltration; ICW – infiltration + in-office bleaching; IAW – infiltration + at-home bleaching.

showed a comparable pattern at a slightly higher lightness level (URG vs. LIG at T9: $d = -0.25$, 95% *CI*: –1.07, 0.47 for L*; $d = -0.87$, 95% *CI*: –1.81, –0.20 for ΔE). In contrast, both bleaching groups showed higher L* values and greater variability after bleaching (URG vs. ICW at T3: $d = -1.57$, 95% *CI*: –2.54, –0.98; URG vs. IAW at T3: $d = -1.80$, 95% *CI*: –3.14, –0.97). High ΔE values (>10) were observed both at high L* levels (>75; LIG vs. ICW at T3: $d = -3.02$, 95% *CI*: –4.39, –2.34) and in the mid-range after staining. The overall distribution of L* and ΔE data points was non-linear, with marked variability, especially in the bleaching groups.

The a* parameter (green–red axis) showed a largely linear relationship with ΔE across all groups (Fig. 3B). The a* values ranged from negative (greenish) to strongly positive (reddish), depending on group and stage. Low ΔE values (<3.7) were predominantly observed near a* ≈ 0. With

increasing a* values, ΔE also increased, most notably in the bleaching groups during staining (URG vs. IAW at T6: *d* = –2.80, 95% *CI*: –4.47, –2.05; at T7: *d* = –2.25, 95% *CI*: –3.51, –1.56). In the control group, a* and ΔE remained within narrow limits up to T5 (URG, T1 vs. T5: *d* = –0.35, 95% *CI*: –1.12, 0.34).

A similar positive correlation was found between the b* values (blue–yellow axis) and ΔE (Fig. 3C). Higher b* values (increased yellowness) were associated with greater color deviation. In the IAW group, the b* values exceeding 15 were associated with ΔE > 10 (URG vs. IAW at T7: *d* = –2.15, 95% *CI*: –3.29, –1.47). The bleaching groups also showed negative b* values immediately after bleaching, likewise accompanied by high ΔE values (URG vs. ICW at T3: *d* = 2.97, 95% *CI*: 2.22, 4.43). The control group demonstrated a narrower range of b* values and low ΔE values up to T5.

Temporal progression of CIELAB components across 9 treatment time points (T1–T9)

The progression of the L* values revealed group-specific patterns (Fig. 4A). In the control group, L* remained constant at approx. 71 from T1 to T5. Coffee staining caused a marked decline to approx. 64 at T7 (URG, T5 vs. T7: *d* = 2.00, 95% *CI*: 1.37, 2.99), followed by a partial recovery to approx. 67 after re-bleaching (T7 vs. T9: *d* = –0.79, 95% *CI*: –1.62, –0.09).

In the LIG group, lesion creation raised L* to approx. 78 (T1), and resin infiltration reduced it to approx. 75 (LIG, T1 vs. T2: *d* = 0.33, 95% *CI*: –0.38, 1.08; URG vs. LIG at T2: *d* = –0.70, 95% *CI*: –1.65, –0.02). Values remained at this level up to T5, dropped to approx. 61 during staining (T5 vs. T7: *d* = 1.85, 95% *CI*: 1.21, 2.74) and recovered to approx. 68 at T9 (T7 vs. T9: *d* = –1.02, 95% *CI*: –1.85, –0.37).

The bleaching groups exhibited more dynamic L* profiles. In the ICW group, L* increased from approx. 70 after infiltration to 76 after in-office bleaching (ICW, T2 vs. T3: *d* = –2.11, 95% *CI*: –3.18, –1.50; URG vs. ICW at T3: *d* = –1.57, 95% *CI*: –2.54, –0.98) and remained at approx. 75 at T4 (URG vs. ICW at T4: *d* = –1.49, 95% *CI*: –2.40, –0.86). The IAW group reached approx. 78 after at-home bleaching (URG vs. IAW at T3: *d* = –1.80, 95% *CI*: –3.14, –0.97). During staining (T6–T7), both bleaching groups showed the most pronounced decrease, reaching a minimum of approx. 57 at T7 (URG vs. ICW: *d* = 1.84, 95% *CI*: 1.22, 2.90; URG vs. IAW: *d* = 1.44, 95% *CI*: 0.75, 2.47). After re-bleaching, L* rose again to approx. 66 at T9 in both groups (ICW, T7 vs. T9: *d* = –3.28, 95% *CI*: –4.44, –2.70; IAW, T7 vs. T9: *d* = –1.96, 95% *CI*: –3.07, –1.29), no longer differing from the control group (URG vs. ICW at T9: *d* = 0.19, 95% *CI*: –0.54, 1.04; URG vs. IAW at T9: *d* = 0.29, 95% *CI*: –0.38, 1.13).

The a* values also followed distinct group-specific trajectories (Fig. 4B). In the control group, they remained close to the neutral axis (a* ≈ –1) through T5. From T6

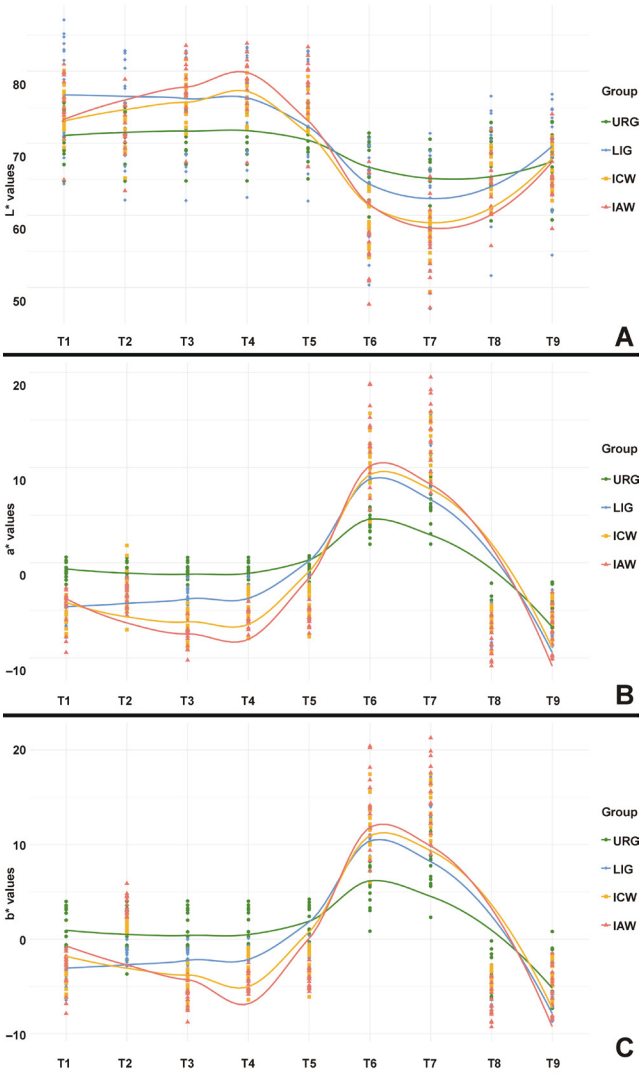

Fig. 4. Temporal progression of CIELAB coordinates across 9 treatment time points in the 4 experimental groups

A. L* values. Locally estimated scatterplot smoothing (LOESS)-smoothed lines with individual data points illustrate the evolution of lightness (L*) from T1 (after WSL creation) to T9 (14 days after re-bleaching); B. a* values; C. b* values.

T1 – after WSL creation; T2 – after resin infiltration; T3 – after bleaching (ICW and IAW only); T4 – after 14 days of storage in distilled water; T5 – after thermocycling; T6 – after 6 days of coffee staining; T7 – after 12 days of coffee staining; T8 – after re-bleaching; and T9 – after a final 14-day storage in distilled water.

onward, a noticeable increase in redness was observed, peaking at approx. 7 at T7 (URG, T5 vs. T7: *d* = –3.84, 95% *CI*: –6.02, –2.94). After re-bleaching of the control specimens with the in-office protocol (T8), the a* values fell to approx. –5 and remained there at T9 (T7 vs. T9: *d* = 5.51, 95% *CI*: 4.50, 8.21).

In the LIG group, the a* values were negative after lesion creation (approx. –5 at T1) and shifted toward neutral after resin infiltration (approx. –3 at T2; LIG, T1 vs. T2: *d* = –2.23, 95% *CI*: –3.19, –1.65; URG vs. LIG at T2: *d* = 2.36, 95% *CI*: 1.57, 3.82). They remained at this level up to T5, rose to approx. 10–11 during staining (T5 vs. T7: *d* = –7.40, 95% *CI*: –10.92, –6.11) and dropped to approx. –7 after re-bleaching (T7 vs. T8: *d* = 8.67, 95% *CI*: 7.35, 11.82).

In the bleaching groups, the a* values decreased further into the negative range (<–5) following whitening (URG vs. ICW at T3: *d* = 5.03, 95% *CI*: 4.15, 6.92), with a more pronounced decrease in the IAW group (URG vs. IAW at T3: *d* = 6.51, 95% *CI*: 5.26, 9.33). After stabilizing during T4–T5, the values increased substantially during staining (URG vs. IAW at T6: *d* = –2.80, 95% *CI*: –4.47, –2.05). The IAW group exhibited the highest a* values recorded in the study at T7 (approx. 14; URG vs. IAW: *d* = –2.25, 95% *CI*: –3.51, –1.56). After re-bleaching (T8), the a* values declined again across the groups, remaining below –5 at T9 (URG vs. IAW: *d* = 1.02, 95% *CI*: 0.38, 1.95).

The b* values also displayed characteristic patterns (Fig. 4C). In the control group, values remained stable around b* ≈ 1 until T5. From T6 onward, yellowness increased, reaching a maximum of approx. 8 at T7 (URG, T5 vs. T7: *d* = 2.76, 95% *CI*: –4.08, –2.06). After re-bleaching, values decreased and became negative (approx. –3 at T9; URG, T7 vs. T9: *d* = 4.54, 95% *CI*: 3.60, 6.34).

In the LIG group, the b* values were approx. –4 after lesion creation and approx. –1 from T2 to T5 (URG vs. LIG at T5: *d* = 1.13, 95% *CI*: 0.45, 2.18). Staining caused an increase to approx. 13 at T7 (T5 vs. T7: *d* = –7.29, 95% *CI*: –10.78, –5.96), and re-bleaching reduced them to approx. –5 (T7 vs. T8: *d* = 8.65, 95% *CI*: 7.32, 11.92).

In the bleaching groups, a marked decline in b* was observed after bleaching (T3), with minima of approx. –5 (ICW) and –6 (IAW) (URG vs. ICW: *d* = 2.97, 95% *CI*: 2.22, 4.43; URG vs. IAW: *d* = 3.65, 95% *CI*: 2.83, 5.23); values remained below –2 at T4 (URG vs. ICW: *d* = 1.93, 95% *CI*: 1.24, 3.02). During the subsequent aging and staining phases (T5–T7), the b* values increased sharply. The ICW group reached approx. 14 (URG vs. ICW at T7: *d* = –2.38, 95% *CI*: –3.61, –1.75), while the IAW group exhibited the highest values recorded throughout the study (b* > 15 at T7; URG vs. IAW: *d* = –2.15, 95% *CI*: –3.29, –1.47). After re-bleaching (T8), values decreased again, returning to the negative range at T9 (b* < –4; IAW, T7 vs. T9: *d* = 6.73, 95% *CI*: 5.63, 9.38; URG vs. IAW at T9: *d* = 0.88, 95% *CI*: 0.20, 1.79).

Discussion

This study provides a detailed visual and quantitative depiction of the aesthetic appearance of resin-infiltrated WSLs and changes in their color across the entire course of a multiphase treatment protocol. By simulating a clinically relevant discoloration cycle, we generated a comprehensive color atlas that may serve as a practical reference for both clinicians and researchers. While color atlases for dental hard tissues have been proposed in previous semi-quantitative ΔE studies, the novelty of our atlas lies in the combination of raw phase-specific CIELAB data, effect size statistics and visual mapping. The innovative merit of this approach lies not only in the dynamic, stage-by-stage monitoring of colorimetric changes, but also in enabling targeted comparisons between specific treatment points. This dual applicability allows for both longitudinal evaluation and assessments at individual time points, offering a versatile framework for aesthetic diagnostics and treatment planning – an aspect largely underrepresented in the existing literature. The CIELAB parameters and the derived ΔE values formed the basis of the atlas, enabling a nuanced and evidence-based assessment of color dynamics in infiltrated lesions.[17,25] Given the acknowledged differences between measurements obtained using digital image analysis and spectrophotometry, especially in complex enamel morphologies, we implemented a standardized photographic protocol (calibrated light source, neutral background, color calibration chart, 3 photographs per specimen) and used the mean of the 3 measurements for each specimen to minimize random error. Although direct spectrophotometric validation was outside the scope of the present study, the literature suggests that calibrated digital imaging can achieve acceptable agreement with spectrophotometry in determining ΔE values when strict acquisition protocols are followed.[6]

While previous studies primarily reported aggregated ΔE or ΔLAB values,[26] this investigation captured and analyzed individual CIELAB values at each treatment stage, providing a distinct advantage for objective aesthetic evaluation. A ΔE of ≥3.7 was defined as the threshold for clinically relevant color differences (the conservative upper limit), based on the CIE and dental visual perception literature, to ensure a consistent reference. A key finding was the non-linear relationship between lightness (L*) and ΔE. Although the a* and b* values showed a largely linear correlation with color difference, the L* values, especially in the medium-to-high lightness range (L* > 70), exhibited pronounced scatter. This indicates that lightness alone is not a reliable predictor of perceived color change. Notably, ΔE values >10 were observed in the bleaching groups despite comparable L* values, underscoring the dominant role of chromatic components in subjective color perception.

The trajectories of the a* and b* values provided meaningful insights into the dynamics of aesthetic changes throughout treatment. In teeth subjected to bleaching, the a* values, already negative after lesion creation and infiltration, decreased further after bleaching (T3), indicating a reduction in red hues and a shift toward greener tones. In some cases, particularly following at-home protocols, the a* values dropped below –5, reflecting a pronounced chromatic shift. Subsequent exposure to staining agents led to a marked increase in the a* values, underscoring the general susceptibility of bleached enamel to extrinsic pigment uptake. The b* values exhibited characteristic shifts throughout the treatment sequence. Immediately after bleaching (T3), they dropped below 0, indicating a reduction in the yellow component. Following coffee exposure (T7), specimens previously subjected to at-home bleaching

showed the most pronounced increase in b* (>15), while those subjected to in-office bleaching reached values of approx. 14. Even untreated control samples exhibited an increase to values exceeding 7. Re-bleaching (T8) led to a marked decrease in both a* and b* values across all experimental groups. At the final assessment (T9), values were below –5 for a* and below –3 for b* in all groups, underscoring the pronounced responsiveness of these colorimetric parameters to both staining and whitening stimuli and supporting their utility for aesthetic monitoring. Before staining, the L* values were approx. 71 in untreated and approx. 75 in resin-infiltrated specimens, within or at the upper margin of the reference range for healthy enamel reported by Karamouzos et al. (L* = 70–75, a* = 3.1–5.0, b* = 15–20).[27,28] Minor deviations in the a* values may be attributed to differences in measurement methodology, particularly between spectrophotometry and digital image[23] analysis, highlighting the importance of standardized calibration procedures, especially when assessing teeth with complex surface morphologies, such as premolars or molars.

Consistent with previous studies, the artificial creation of WSLs resulted in an increase in L* and a concomitant decrease in the a* and b* values.[29] Comparable studies have reported ΔE values of approx. 7.88 after lesion creation,[29] in line with our findings (ΔE: 7.3–7.9 at T1). Resin infiltration partially reversed these effects. The TEGDMA-based infiltrant contributed to the optical blending of the lesion with the surrounding enamel, as reflected in a moderate reduction in the L* values and a partial normalization of the a* and b* values. Knösel et al. reported ΔE values of 5.65, which were slightly above the perceptibility threshold of 3.7.[26,30] In contrast, Schoppmeier et al. found ΔE values below 3.7 in fluorotic lesions treated with triple etching and a 10-minute infiltration protocol.[6] Our findings fall between these 2 results, with ΔE values of approx. 3.0–4.1 after infiltration (mean approx. value: 3.6).

Color changes following bleaching closely matched those reported by Sinanovic et al.[31] for at-home bleaching and by Jacob et al.[32] for in-office bleaching. In the present study, bleaching resulted in an increase in lightness (L*) of approx. 6 units, along with reductions in a* of 3–4 units and in b* of 6–10 units. At-home bleaching induced numerically greater color changes (ΔE: 11.7 vs. 9.8 relative to baseline; ICW vs. IAW at T3: d = –0.80, 95% *CI*: –1.67, –0.12), although the original study found no significant difference in bleaching effectiveness between the 2 protocols.[23]

The staining susceptibility of resin-infiltrated enamel is well documented.[6,23,33] Owing to increased water sorption and a higher affinity for extrinsic pigments, RI-treated surfaces are more prone to staining.[34] The extent of coffee-induced discoloration observed in this study is consistent with previous findings,[35] showing a marked decline in L* and linear increases in a* and b*, especially in the IAW group (b* > 15; ΔE > 10), underscoring the susceptibility of this group to staining.

For the first time, this analysis documented CIELAB coordinate changes after re-bleaching of previously stained resin-infiltrated lesions. Re-bleaching reversed most of the staining-induced changes: ΔE relative to baseline decreased from 21.1, 23.6 and 25.1 at T7 to 9.5, 8.3 and 10.7 at T9 in the LIG, ICW and IAW groups, respectively (within-group T7 vs. T9 effect sizes for a* and b*: d = 5.5–9.5). However, a complete return to baseline or post-infiltration values was not achieved. The a* and b* values fell below their pre-staining levels (approx. –5 to –7 and –4 to –5, respectively), and L* remained approx. 6–9 units lower than before staining, so that final mean ΔE values exceeded 3.7 in all groups, including the re-bleached control (ΔE = 7.2). At T9, the L* values in the bleaching groups did not differ significantly from those of the control group (URG vs. ICW: d = 0.19, 95% *CI*: –0.54, 1.04; URG vs. IAW: d = 0.29, 95% *CI*: –0.38, 1.13), and the ICW group did not differ from the control in ΔE either (d = –0.49, 95% *CI*: –1.23, 0.23). The IAW group, however, retained a higher ΔE (10.7 vs. 7.2; URG vs. IAW: d = –1.22, 95% *CI*: –2.22, –0.54) and more negative a* and b* values than the control (d = 1.02, 95% *CI*: 0.38, 1.95; and d = 0.88, 95% *CI*: 0.20, 1.79, respectively). Thus, in-office bleaching did not worsen the final outcome compared with untreated enamel subjected to the same staining and re-bleaching protocols, whereas at-home bleaching left a small residual color difference. The convergence of the groups after re-bleaching supports the relative color stability of resin-infiltrated enamel under staining and re-bleaching, whereas the residual deviation from baseline shows that the simulated 12 months of coffee exposure left a persistent change in all groups.

Potential clinical relevance

The color atlas developed in this study may, following validation, provide clinicians with a tool to assist in treatment outcome prediction, planning and patient communication.

A major advantage of the atlas is its standardization of colorimetric evaluation criteria: clinicians can refer to defined reference ranges to objectively determine the effectiveness of each treatment step. This enables the differentiation between acceptable outcomes and those requiring additional interventions, such as re-infiltration or bleaching. By documenting color dynamics over time, the atlas also helps establish realistic expectations regarding potential relapses or long-term changes. Moreover, by capturing the dynamic progression of color changes across multiple treatment phases, the atlas allows clinicians to anticipate potential relapses or long-term aesthetic alterations. Building on this, the dataset may also serve as a foundation for the development of artificial intelligence (AI)-based predictive models. Such models could be trained to estimate post-treatment CIELAB values based on a tooth's baseline characteristics and the selected therapeutic pathway. In future applications, these predicted color values might be translated into visual representations

of the expected outcome, offering clinicians and patients an individualized, data-driven preview of treatment effects. This would not only support shared decision-making but also open new avenues for real-time clinical decision support. Further research is warranted to explore the feasibility, accuracy and clinical applicability of such AI-driven prediction systems within the CIELAB framework. As new data is continuously integrated and the underlying database expands, the precision of the color atlas will improve further. A broader dataset could enhance the differentiation between physiological and treatment-induced color changes and support the development of predictive models for the long-term color stability of resin-infiltrated lesions. In this sense, the atlas need not remain a static reference but could evolve with the growing body of evidence, offering an increasingly precise foundation for clinical and scientific decision-making.

Limitations

Despite providing a robust foundation for understanding color changes in resin-infiltrated WSLs, certain limitations must be acknowledged. The sample was restricted to extracted third molars. Although the simulation protocols expanded the dataset, larger and more diverse samples, particularly including anterior teeth, are needed to ensure broader clinical applicability. It remains unclear whether the observed color change patterns also apply to teeth of greater aesthetic relevance. In this in vitro model, the operator was not blinded to treatment allocation during the procedures such as bleaching or resin application; however, all measurements and data analyses were performed by an examiner blinded to group allocation. Clinical studies with larger, more heterogeneous patient populations are required to validate the long-term aesthetic outcomes of RI treatment. Longitudinal investigations may provide insights into the durability of treatment outcomes and allow for the systematic analysis of patient-dependent factors such as diet and oral care. In addition, the traffic light classification of the LAB Color Tool compares a measurement with the *CI* of the reference group mean rather than with a prediction interval for individual teeth; it should therefore be regarded as an exploratory aid, not as a diagnostic reference range. Further development of the LAB Color Tool is desirable, with a focus on improving precision and customization in the evaluation of color changes. Such research will help optimize the clinical application of resin infiltration in aesthetic dentistry and improve its predictive value in daily practice.

Conclusions

This study presents a systematically structured, phase-specific documentation of colorimetric changes in resin-infiltrated WSLs, encompassing all clinically relevant stages, from lesion creation to infiltration, bleaching, staining, and re-bleaching. While prior investigations have reported isolated ΔE values at selected time points, the present analysis offers a continuous, multiphase mapping of L*, a*, b*, and ΔE data, thereby enabling a nuanced understanding of dynamic color shifts in minimally invasive enamel therapy.

The results revealed that the chromatic components a* and b* correlated more strongly with measured color differences than the lightness parameter (L*), particularly in the context of bleaching-induced alterations. This underscores the clinical utility of chromatic monitoring in the aesthetic evaluation of infiltrated lesions. The accompanying LAB evaluation tool, while presently a prototype, provides standardized color metrics and a reference-based interpretive framework. By enabling objective phase-specific assessments and facilitating clinician–patient communication, it may support more reproducible decision-making in aesthetic dentistry. Future validation against spectrophotometric gold standards and interface enhancements (e.g., calibration routines, colorblind accessibility) are planned. Finally, re-bleaching largely reversed extrinsic discoloration in infiltrated enamel, although final color values did not fully return to baseline. At the final assessment, lightness did not differ between the bleaching groups and the untreated control, and only the at-home bleaching group retained a small residual color difference. These findings support the potential for aesthetic stability of resin infiltration under simulated aging and staining conditions, provided that discoloration is addressed by re-bleaching.

Ethics approval and consent to participate

The study was approved by the Ethics Committee of the Faculty of Medicine, University of Cologne, Germany (approval No. 23-1472; March 28, 2024).

Data availability

The datasets generated and/or analyzed during the current study are available from the corresponding author on reasonable request.

Consent for publication

Not applicable.

Use of AI and AI-assisted technologies

Claude (Anthropic, San Francisco, USA) was used as a coding assistant for the browser-based implementation of the LAB Color Tool presented in this manuscript. The authors reviewed and validated the generated code and the embedded reference data and take full responsibility for the content of the manuscript.

ORCID iDs

Christoph Matthias Schoppmeier https://orcid.org/0000-0002-3269-8920
Malin Janson https://orcid.org/0009-0006-6486-6825
Michael Jochen Wicht https://orcid.org/0000-0003-4693-7184
Max von Kohout https://orcid.org/0009-0006-7390-1557
Anna Greta Barbe https://orcid.org/0000-0003-0169-2582

References

1. Freire Y, Gómez Sánchez M, Sánchez Ituarte J, Frías Senande M, Díaz-Flores García V, Suárez A. Social media impact on students' decision-making regarding aesthetic dental treatments based on cross-sectional survey data. *Sci Rep*. 2024;14(1):21626. doi:10.1038/s41598-024-72442-8
2. Abbasi MS, Lal A, Das G, et al. Impact of social media on aesthetic dentistry: General practitioners' perspectives. *Healthcare (Basel)*. 2022;10(10):2055. doi:10.3390/healthcare10102055
3. Bourouni S, Dritsas K, Kloukos D, Wierichs RJ. Efficacy of resin infiltration to mask post-orthodontic or non-post-orthodontic white spot lesions or fluorosis – a systematic review and meta-analysis. *Clin Oral Investig*. 2021;25(8):4711–4719. doi:10.1007/s00784-021-03931-7
4. Yazarloo S, Arab S, Mirhashemi AH, Gholamrezayi E. Systematic review of preventive and treatment measures regarding orthodontically induced white spot lesions. *Dent Med Probl*. 2023;60(3):527–535. doi:10.17219/dmp/140964
5. Bakdach WMM, Hadad R. Effectiveness of different adjunctive interventions in the management of orthodontically induced white spot lesions: A systematic review of systematic reviews and meta-analyses. *Dent Med Probl*. 2020;57(3):305–325. doi:10.17219/dmp/118330
6. Schoppmeier CM, Derman SHM, Noack MJ, Wicht MJ. Power bleaching enhances resin infiltration masking effect of dental fluorosis. A randomized clinical trial. *J Dent*. 2018;79:77–84. doi:10.1016/j.jdent.2018.10.005
7. Borges AB, Caneppele TM, Masterson D, Maia LC. Is resin infiltration an effective esthetic treatment for enamel development defects and white spot lesions? A systematic review. *J Dent*. 2017;56:11–18. doi:10.1016/j.jdent.2016.10.010
8. Limvisitsakul A, Komalsingsakul A, Thamsrithip P, et al. The color stability of artificial white spot lesions treated with resin infiltration after exposure to staining beverages. *BMC Oral Health*. 2024;24(1):940. doi:10.1186/s12903-024-04693-w
9. Ozverel CS, Kurtulmus-Yilmaz S. Effect of the application of a hydrogen peroxide home bleaching agent on the cytotoxicity of different CAD–CAM restorative materials. *Dent Med Probl*. 2023;60(2):311–320. doi:10.17219/dmp/142761
10. Schoppmeier CM, Liebermann A, Janson M. In vitro evaluation of discoloration and surface alteration in self-adhesive resin cements using CIELAB and 3D profilometry. *Dent Med Probl*. 2026;63(2):385–396. doi:10.17219/dmp/205161
11. Janson M, Bassier V, Liebermann A, Schoppmeier CM, Gregorio-Schininà MD. Composite repair on zirconia: Influence of different sandblasting pretreatments and various universal adhesives on shear bond strength. *J Adhes Dent*. 2025;27:53–64. doi:10.3290/j.jad.c_1988
12. Lizarelli GTC, Manente R, Souza-Gabriel A, Corona SAM. Effect of tooth bleaching in patients with fixed orthodontic appliances: A systematic review. *Dent Med Probl*. 2025;62(2):343–350. doi:10.17219/dmp/171606
13. Joiner A, Luo W. Tooth colour and whiteness: A review. *J Dent*. 2017;67S:S3–S10. doi:10.1016/j.jdent.2017.09.006
14. Tejada-Casado M, Pérez MM, Della Bona A, Lübbe H, Ghinea R, Herrera LJ. Chroma-dependence of CIEDE2000 acceptability thresholds for dentistry. *J Esthet Restor Dent*. 2024;36(3):469–476. doi:10.1111/jerd.13153
15. Gómez-Polo C, Portillo Muñoz M, Lorenzo Luengo MC, Vicente P, Galindo P, Martín Casado AM. Comparison of two color-difference formulas using the Bland–Altman approach based on natural tooth color space. *J Prosthet Dent*. 2016;115(4):482–488. doi:10.1016/j.prosdent.2015.07.013
16. Hein S, Saleh O, Li C, Nold J, Westland S. Bridging instrumental and visual perception with improved color difference equations: A multicenter study. *Dent Mater*. 2024;40(10):1497–1506. doi:10.1016/j.dental.2024.07.003
17. Johnston WM, Kao EC. Assessment of appearance match by visual observation and clinical colorimetry. *J Dent Res*. 1989;68(5):819–822. doi:10.1177/00220345890680051301
18. Paravina RD, Ghinea R, Herrera LJ, et al. Color difference thresholds in dentistry. *J Esthet Restor Dent*. 2015;27 Suppl 1:S1–S9. doi:10.1111/jerd.12149
19. Sabti MY, Alfarhan IY, Akbar AA, Qudeimat MA. Evaluating color stability and enamel surface roughness following resin infiltration treatment. *Clin Exp Dent Res*. 2024;10(1):e2834. doi:10.1002/cre2.834
20. de Oliveira DCRS, Rocha MG, Correa IC, Correr AB, Ferracane JL, Sinhoreti MAC. The effect of combining photoinitiator systems on the color and curing profile of resin-based composites. *Dent Mater*. 2016;32(10):1209–1217. doi:10.1016/j.dental.2016.06.010
21. Leland A, Akyalcin S, English JD, Tufekci E, Paravina R. Evaluation of staining and color changes of a resin infiltration system. *Angle Orthod*. 2016;86(6):900–904. doi:10.2319/111615-777.1
22. Ibrahim DFA, Venkiteswaran A, Hasmun NN. Esthetic effects and color stability of resin infiltration on demineralized enamel lesions: A systematic review. *J Int Soc Prev Community Dent*. 2023;13(4):273–286. doi:10.4103/jispcd.JISPCD_29_23
23. Schoppmeier CM, von Kohout M, Sun L, et al. Influence of home or in-office tooth bleaching on the color stability of white-spot lesions after resin infiltration: An in vitro comparison. *J Am Dent Assoc*. 2025;156(7):517–529.e3. doi:10.1016/j.adaj.2025.04.009
24. Krithikadatta J, Gopikrishna V, Datta M. CRIS guidelines (Checklist for Reporting In-vitro Studies): A concept note on the need for standardized guidelines for improving quality and transparency in reporting in-vitro studies in experimental dental research. *J Conserv Dent*. 2014;17(4):301–304. doi:10.4103/0972-0707.136338
25. Wittich FK, Cebula M, Effenberger S, et al. Masking efficacy of bleaching and/ or resin infiltration of fluorotic spots on anterior teeth – a systematic review and meta-analysis. *J Dent*. 2024;149:105276. doi:10.1016/j.jdent.2024.105276
26. Knösel M, Eckstein A, Helms HJ. Long-term follow-up of camouflage effects following resin infiltration of post orthodontic white-spot lesions in vivo. *Angle Orthod*. 2019;89(1):33–39. doi:10.2319/052118-383.1
27. Karamouzos A, Papadopoulos MA, Kolokithas G, Athanasiou AE. Precision of in vivo spectrophotometric colour evaluation of natural teeth. *J Oral Rehabil*. 2007;34(8):613–621. doi:10.1111/j.1365-2842.2007.01744.x
28. Karamouzos A, Zafeiriadis AA, Kolokithas G, Papadopoulos MA, Athanasiou AE. In vivo evaluation of tooth colour alterations during orthodontic retention: A split-mouth cohort study. *Orthod Craniofac Res*. 2019;22(2):124–130. doi:10.1111/ocr.12298
29. Hammad SM, El Banna M, El Zayat I, Mohsen MA. Effect of resin infiltration on white spot lesions after debonding orthodontic brackets. *Am J Dent*. 2012;25(1):3–8. PMID:22558683.
30. Knösel M, Eckstein A, Helms HJ. Durability of esthetic improvement following icon resin infiltration of multibracket-induced white spot lesions compared with no therapy over 6 months: A single-center, split-mouth, randomized clinical trial. *Am J Orthod Dentofacial Orthop*. 2013;144(1):86–96. doi:10.1016/j.ajodo.2013.02.029
31. Sinanovic AL, Messer-Hannemann P, Samadi M, Schwendicke F, Effenberger S. Effect of bleaching on resin-infiltration-masked artificial white spots in vitro. *J Funct Biomater*. 2024;15(5):125. doi:10.3390/jfb15050125
32. Jacob SE, Varghese JO, Singh S, Natarajan S, Thomas MS. Effect of bleaching on color and surface topography of teeth with enamel caries treated with resin infiltration (ICON®) and remineralization (casein phosphopeptide–amorphous calcium phosphate). *J Conserv Dent Endod*. 2023;26(4):377–382. doi:10.4103/jcd.jcd_129_23
33. Borges A, Caneppele T, Luz M, Pucci C, Torres C. Color stability of resin used for caries infiltration after exposure to different staining solutions. *Oper Dent*. 2014;39(4):433–440. doi:10.2341/13-150-L
34. Meyer-Lueckel H, Paris S, Kielbassa AM. Surface layer erosion of natural caries lesions with phosphoric and hydrochloric acid gels in preparation for resin infiltration. *Caries Res*. 2007;41(3):223–230. doi:10.1159/000099323
35. Yeslam HE, AlZahrani SJ. Time-dependent effect of intense capsule-coffee and bleaching on the color of resin-infiltrated enamel white spot lesions: An in vitro study. *PeerJ*. 2022;10:e14135. doi:10.7717/peerj.14135

Original paper

Endoplasmic reticulum stress in women with polycystic ovary syndrome and gingivitis: A case–control study of metabolic–periodontal interplay

María Pelechá-Salvador*[1,C–F], Sandra López-Domènech*[1,A,C,E,F], Cecilia Fabiana Márquez-Arrico[2,B,F], Meylin Fernández-Reyes[1,B,C,F], Laura Perea-Galera[1,B,F], Jonathan Hermenejildo[1,B,F], Carlos Morillas[1,A,F], Pablo Fernández-Collazo[1,B,F], Javier Silvestre-Rangil[2,B], Víctor Manuel Víctor[3,4,A,F], Francisco Javier Silvestre[2,5,A,F], Milagros Rocha[1,4,A,C–F]

* first authors

[1] Department of Endocrinology and Nutrition, University Hospital Dr. Peset, Foundation for the Promotion of Health and Biomedical Research of the Valencian Community (Fisabio), Valencia, Spain

[2] Department of Stomatology, University of Valencia, Spain

[3] Department of Physiology, Biomedical Research Institute (INCLIVA), University of Valencia, Spain

[4] Biomedical Research Networking Center in Hepatic and Digestive Diseases (CIBERehd), Valencia, Spain

[5] Department of Stomatology, University Hospital Dr. Peset, Foundation for the Promotion of Health and Biomedical Research of the Valencian Community (Fisabio), Valencia, Spain

A – research concept and design; B – collection and/or assembly of data; C – data analysis and interpretation;
D – writing the article; E – critical revision of the article; F – final approval of the article

Dental and Medical Problems, ISSN 1644-387X (print), ISSN 2300-9020 (online) *Dent Med Probl*. 2026;63(5):1179–1188

Address for correspondence
Milagros Rocha
E-mail: milagros.rocha@fisabio.es

Funding sources
This research was supported by grants PI22/01009 (MR), PI22/00424 (VMV), CD23/0006 (SLD), FI23/00141 (LPG), and CM24/00261 (PFC) from the Carlos III Health Institute (Madrid, Spain), as well as by the Biomedical Research Networking Center in Hepatic and Digestive Diseases (CIBERehd; CB06/04/0071), co-funded by the European Regional Development Fund (ERDF; "A way to build Europe"). Additionally, the study was funded by grants CIPROM/2022/32 (VMV, MR), INVEST/2023/163 (MPS) and CIGRIS/2021/112 (JH) from the Regional Ministry of Innovation, Universities, Science and Digital Society, Generalitat Valenciana, and by the Horizon Europe EU programme (project No. 101136516 (MR, MFR)).

Conflict of interest
None declared

Acknowledgements
The authors would like to thank Rosa Falcon, Lydia Pelufo (Fisabio, Valencia, Spain) and Begoña Zaragoza (University Hospital Dr. Peset, Valencia, Spain) for their technical support, as well as Brian Normanly (University of Valencia, Spain; CIBERehd, Valencia, Spain) for his editing assistance.

Received on July 1, 2025
Reviewed on August 20, 2025
Accepted on September 27, 2025

Published online on February 9, 2026

Cite as
Pelechá-Salvador M, López-Domènech S, Márquez-Arrico CF, et al. Endoplasmic reticulum stress in women with polycystic ovary syndrome and gingivitis: A case–control study of metabolic–periodontal interplay. 2026;63(5):1179–1188. *Dent Med Probl.* doi:10.17219/dmp/211428

DOI
10.17219/dmp/211428

Copyright
Copyright by Author(s)
This is an article distributed under the terms of the
Creative Commons Attribution 3.0 Unported License (CC BY 3.0)
(https://creativecommons.org/licenses/by/3.0/).

Abstract

Background. Gingival inflammation has been increasingly linked to metabolic and endocrine disorders, such as polycystic ovary syndrome (PCOS). This connection may involve immune system activation and cellular stress mechanisms, particularly the unfolded protein response (UPR), which regulates endoplasmic reticulum (ER) stress.

Objectives. The aim of the study was to investigate whether gingivitis modulates UPR activation in peripheral blood mononuclear cells (PBMCs) of women with PCOS.

Material and methods. In this case–control study, female subjects were divided into 2 groups: a control group ($n = 48$); and a PCOS group ($n = 68$), which included 24 individuals with gingivitis (PCOS+). Anthropometric, biochemical and periodontal parameters were determined, namely probing pocket depth (PPD), clinical attachment level (CAL), bleeding on probing (BOP), and plaque index. Markers of oxidative stress, including total superoxide and glutathione peroxidase 1 (GPx1), and UPR mediators, such as glucose-regulated protein 78 (GRP78), activating transcription factor 6 (ATF6), phosphorylated eukaryotic initiation factor 2 alpha subunit (p-eIF2α), and C/EBP homologous protein (CHOP), were evaluated in PBMCs.

Results. Polycystic ovary syndrome was associated with an increased plaque index and significantly higher BOP in PCOS+. Increased superoxide and reduced GPx1 levels were observed in women with PCOS, with no significant differences between subgroups. Gingivitis in PCOS was correlated with the activation of specific UPR pathways; higher levels of p-eIF2α and CHOP and lower GRP78 levels were detected in PCOS+, while ATF6 was increased in the overall PCOS group. Moreover, BOP demonstrated a direct correlation with p-eIF2α and the plaque index.

Conclusions. The association of leukocyte ER stress responses in PCOS with gingival inflammation underscores the impact of periodontal disease on modulating systemic cellular stress in the context of multifactorial metabolic disorders.

Keywords: endoplasmic reticulum stress, gingivitis, polycystic ovary syndrome, unfolded protein response, oxidative stress

Highlights

- Gingival inflammation influences systemic immune responses and may exacerbate metabolic disturbances in women with polycystic ovary syndrome (PCOS).
- Periodontal disease is associated with increased oxidative stress in individuals with endocrine–metabolic dysfunction.
- Gingivitis modulates cellular stress pathways related to endoplasmic reticulum function in patients with PCOS.
- Bleeding on probing may serve as a clinical indicator of systemic inflammatory stress in affected patients.
- Integrating periodontal assessment into routine care may enhance prevention and management strategies for women with metabolic and reproductive disorders.

Introduction

Polycystic ovary syndrome (PCOS) is a hormonal and metabolic disorder that manifests in reproductive-age women and is characterized by hyperandrogenemia, anovulation and multiple ovarian cysts, often causing infertility, irregular menstrual cycles, acne, and hirsutism.[1] The condition is also linked to insulin resistance (IR), inflammation and oxidative stress.[2–4] Recent evidence suggests that women with PCOS are more prone to periodontal disease (PD), such as gingivitis and periodontitis,[5,6] probably due to the link between IR and periodontal inflammation.[7] Periodontal disease has also been associated with adverse reproductive outcomes, including preterm birth and low birth weight, further highlighting its relevance to women's reproductive health.[8]

Gingivitis may arise from a bacterial imbalance within dental plaque (dysbiosis).[9] When left untreated, gingivitis can progress to periodontitis, a condition characterized by persistent inflammation of the connective tissues supporting the teeth.[10,11] This ongoing dysbiosis facilitates bacterial spread into the periodontal pockets, leading to leukocyte recruitment and increased local oxidative stress. In advanced stages, periodontitis culminates in irreversible tissue damage and potential tooth loss.[11] Beyond oral consequences, both gingivitis and periodontitis have been closely associated with increased cardiovascular risk, which underscores their broader systemic health implications.[12]

While oxidative stress, IR and inflammation are common to both PCOS and PD, emerging research highlights endoplasmic reticulum (ER) stress as another shared component.[13,14] Endoplasmic reticulum stress occurs when misfolded proteins accumulate, activating the adaptive unfolded protein response (UPR).[15] Initially, the chaperone protein GRP78 (glucose-regulated protein 78) associates with unfolded proteins, thereby promoting the activation of 3 ER-localized transmembrane sensors: PKR-like endoplasmic reticulum kinase (PERK); inositol-requiring enzyme 1 (IRE1); and activating transcription factor 6 (ATF6). The unfolded protein response aims to restore ER homeostasis. However, prolonged ER stress can ultimately result in apoptosis through the overexpression of the transcription factor C/EBP homologous protein (CHOP).[16]

Extensive evidence supports a bidirectional relationship between oxidative stress and ER stress.[17] We have previously described increased markers of ER and oxidative stress in leukocytes of women with PCOS, particularly those with metabolic syndrome.[14] Endoplasmic reticulum stress has also been observed in granulosa cells in PCOS[18–20] and in periodontal tissues, including human periodontal ligament fibroblasts[21] and gingival samples.[22]

Taken together, these findings indicate a potential link between PCOS, PD and ER stress, although the underlying molecular mechanisms are poorly understood. Therefore, the aim of the present study was to determine whether gingivitis can modulate ER stress in leukocytes from women with PCOS, as these cells are key indicators of systemic metabolic and inflammatory features.[23]

Material and methods

Study design

This case–control study was conducted at University Hospital Dr. Peset (Valencia, Spain) between October 2019 and May 2022. The study population included women aged 18–45 years. Specifically, 48 healthy individuals (controls) and 68 patients with PCOS were enrolled. Of these patients, 44 subjects did not have PD (PCOS–), while 24 had gingivitis (PCOS+). The eligibility criteria encompassed female participants aged ≥18 years, recruited either as healthy controls or as patients with PCOS, according to the criteria detailed below. The participants included in the control group were clinically healthy women without a diagnosis of PCOS or other systemic conditions. They were recruited during routine check-ups in the Departments of Endocrinology, Nutrition, and Gynecology of University Hospital Dr. Peset. Patients with PCOS were identified according to the Rotterdam criteria[24] and were enrolled during routine appointments in the abovementioned departments. Gingivitis was diagnosed when bleeding on probing (BOP) was ≥10%, according to current periodontal guidelines.[25] Participants in the control group were matched with their PCOS counterparts based on the body mass index (BMI)

and age, as these parameters have been demonstrated to contribute to both PCOS-related metabolic alterations and periodontal inflammation. In this way, we have taken measure to account for potentially confounding effects.

The exclusion criteria for all participants included the presence of systemic diseases or conditions that could affect periodontal health, such as diabetes or autoimmune disorders, the use of medications known to influence periodontal or hormonal status, pregnancy or lactation, and a history of periodontal treatment within the previous 6 months. All participants provided written informed consent. The study was conducted in accordance with the ethical principles for medical research involving human subjects, as outlined in the Declaration of Helsinki. It was approved by the Ethics Committee of University Hospital Dr. Peset (study protocol ref. No. 95/19). All participants who met the eligibility criteria completed the study, resulting in no recorded dropouts.

Clinical examination

The patients completed a health questionnaire, including items adapted from the World Health Organization (WHO) Oral Health Questionnaire for Adults.[26] Information regarding medication use, medical conditions, alcohol and tobacco habits, and oral hygiene practices (teeth brushing frequency, use of interdental hygiene aids, and time since the last dental visit) was recorded. In addition, blood pressure and anthropometric data were noted. A peripheral venous blood sample was collected after 12 h of fasting, during the follicular phase of the menstrual cycle or bleeding deprivation. The biochemical parameters and reproductive hormone profiles were determined during the hospital's clinical analysis according to the standardized protocols.

A single clinician (CFMA) performed a full periodontal exam in accordance with the consensus criteria.[25] Using a periodontal chart, all teeth were probed at 6 sites per tooth (right permanent maxillary first molar, right permanent central incisor, left permanent first premolar, left permanent mandibular first molar, right permanent mandibular central incisor, and right permanent mandibular first premolar) with a Williams-type millimeter probe. Bleeding on probing, clinical attachment level (CAL), probing pocket depth (PPD), and plaque index (using the Silness and Löe index) were assessed.[27] The plaque index was determined by measuring the Ramfjord index teeth.[28]

Flow cytometry

After erythrocyte lysis using a red blood cell lysis buffer (Miltenyi Biotech, Bergisch Gladbach, Germany), a 200-µL blood sample was incubated with 5 µL of APC-CD45 antibody (BD Biosciences, San Jose, USA). Total superoxide production was assessed using 1-mM dihydroethidium (dHE) (Thermo Fisher Scientific, Waltham, USA). Fluorescence signals were measured using a flow cytometer (BD Accuri™ C6 Plus Flow Cytometer; BD Biosciences), and 10,000 events were recorded and analyzed for each experiment.

Isolation of PBMCs and protein expression analysis

Peripheral blood mononuclear cells (PBMCs) were isolated using the MACSprep™ leukocyte isolation kit (Milteny Biotech) according to the manufacturer's instructions. The cells were lysed in a radio-immunoprecipitation assay (RIPA) buffer supplemented with protease and phosphatase inhibitors. Protein concentration was determined using a bicinchoninic acid (BCA) assay (all products were obtained from Thermo Fisher Scientific). Equal amounts of protein (25 µg) were separated by sodium dodecyl sulfate–polyacrylamide gel electrophoresis (SDS-PAGE) and transferred onto nitrocellulose membranes. The target proteins were detected by incubating the membranes with primary antibodies against ATF6, GRP78, phosphorylated eukaryotic initiation factor 2 alpha subunit (p-eIF2α), CHOP, IRE1α, glutathione peroxidase 1 (GPx1), and actin. This was followed by incubation with the corresponding secondary antibodies (Supplementary File 2 (available on request from the corresponding author)). The detection of chemiluminescent signals was accomplished through the use of ECL Plus™ reagent (GE Healthcare, Chicago, USA). Signal visualization and densitometric analysis were performed using the Fusion FX5 Acquisition System and Bio1D software, v. 15.03a (Vilbert Lourmat, Marne-la-Vallée, France).

Statistical analysis

The present study was designed to achieve a power of 80% and an α risk of 0.05 to detect 30-unit differences in protein expression by western blot, assuming a standard deviation of 30 units. A minimum of 16 subjects per group were considered (control vs. PCOS and PCOS– vs. PCOS+). The assessment of normality was conducted through the use of the Kolmogorov–Smirnov test or the Shapiro–Wilk test. Parametric and non-parametric data was analyzed using the two-sample Student's *t*-test or the Mann–Whitney *U* test, respectively. Oral hygiene variables were evaluated as categorical data using the Kruskal–Wallis test or the Pearson's χ^2 test. To identify factors associated with gingivitis, multivariable linear regression analyses were performed for continuous dependent variables and binary logistic regression analyses for binary outcomes. The evaluation of correlations was conducted by employing Pearson's or Spearman's coefficients. The differences were considered significant at $p < 0.05$, with a 95% confidence interval (95% *CI*). The data analysis was conducted using GraphPad Prism software, v. 9.0.2 (GraphPad Software Inc., San Diego, USA) and the IBM SPSS Statistics for Windows software, v. 22.0 (IBM Corp., Armonk, USA).

Table 1. Comparison of anthropometric characteristics, biochemical parameters and pharmacological treatment in the study sample

Variable		Control ($n = 48$)	PCOS ($n = 68$)	p-value
Age [years]		28.9 ±6.3	27.9 ±5.8	0.375
BMI [kg/m^2]		24.9 ±3.8	25.4 ±5.1	0.272
Waist [cm]		71.5 (67.1, 77.8)	78.2 (70.0, 83.0)	0.006*
SBP [mm Hg]		111 ±14	111 ±12	0.984
DBP [mm Hg]		76 ±8	79 ±10	0.121
Glucose [mg/dL]		88 ±8	88 ±8	0.747
Insulin [µUI/mL]		6.71 ±2.39	9.68 ±6.81	0.002*
HOMA-IR		1.46 ±0.57	2.04 ±1.42	0.004*
TC [mg/dL]		179 ±27	192 ±36	0.039*
HDLc [mg/dL]		65 ±13	61 ±16	0.185
LDLc [mg/dL]		101 ±23	113 ±32	0.044*
Triglycerides [mg/dL]		63 (43, 70)	89 (53.5, 120)	0.001*
hsCRP [mg/L]		0.81 (0.34, 3.10)	3.16 (0.66, 5.32)	0.021*
C3c [mg/dL]		105 ±17	121 ±21	<0.001*
RBP4 [mg/dL]		1.76 ±0.42	2.19 ±0.55	<0.001*
Estradiol [pg/mL]		86 ±73	52 ±53	0.017*
Testosterone [ng/dL]		0.381 ±0.238	0.416 ±0.161	0.367
Androstenedione [ng/mL]		2.99 ±1.33	3.14 ±1.28	0.563
DHEAS [µg/dL]		231 ±101	277 ±121	0.056
17-OHP [ng/dL]		1.96 ±1.92	1.22 ±1.46	0.035*
SHBG [µg/dL]		85 ±70	147 ±145	0.003*
FAI [%]		1.98 ±1.18	2.50 ±3.40	0.257
Prolactin [ng/dL]		22.8 ±11.8	19.9 ±11.3	0.234
Medication, n (%)	oral contraceptives	5 (4.1)	33 (28.9)	<0.001*
	metformin	0 (0.0)	13 (11.4)	<0.001*

Data is presented as mean ±standard deviation (M ±SD), median and interquartile range (Me (IQR)), or frequency (percentage) (n (%)). Between-group comparisons were performed using the two-sample Student's t-test or the Mann–Whitney U test, as appropriate (* statistically significant, $p < 0.05$).
17-OHP –17-hydroxyprogesterone; BMI – body mass index; C3c – complement component c3; DBP – diastolic blood pressure; DHEAS – dehydroepiandrosterone sulfate; FAI – free androgen index; HDLc – high-density lipoprotein cholesterol; HOMA-IR – homeostasis model assessment of insulin resistance; hsCRP – high sensitive C-reactive protein; LDLc – low-density lipoprotein cholesterol; PCOS – polycystic ovary syndrome; RBP4 – retinol binding protein 4; SBP – systolic blood pressure; SHBG – sex hormone-binding globulin; TC – total cholesterol.

Results

A total of 48 healthy control females and 68 women with PCOS were recruited for the study, including 44 subjects without PD (PCOS–) and 24 individuals with gingivitis (PCOS+). No significant differences were observed in anthropometric or biochemical parameters between the PCOS– and PCOS+ groups, as reported by Márquez-Arrico et al.[29] Compared to controls, women with PCOS showed higher waist circumference, as well as increased levels of insulin, homeostasis model assessment of insulin resistance (HOMA-IR), total cholesterol, low-density lipoprotein cholesterol (LDLc), and triglycerides, while glucose and high-density lipoprotein cholesterol (HDLc) levels remained similar (Table 1). Elevated levels of inflammatory indicators, such as high sensitive C-reactive protein (hsCRP), complement component c3 (C3c) and retinol binding protein 4 (RBP4), as well as alterations in reproductive hormones were consistent with the pathophysiology of PCOS. Oral contraceptives and metformin had been prescribed to many of the PCOS patients as part of their routine treatment.

The study population had generally good oral hygiene habits (Table 2), with over 80% of participants in both the control and PCOS groups reporting brushing their teeth at least twice per day, with no statistically significant differences observed between the groups. Similarly, there were no significant differences in the use of interdental hygiene products, such as dental floss and interdental brushes, or mouthwash. The data on the frequency of dental visits and previous periodontal treatment was also collected, showing no differences between the groups.

Regarding periodontal parameters, no significant differences in PPD or CAL were detected between the control and PCOS groups (Fig. 1A–D). Bleeding on probing was significantly higher in the whole PCOS group compared to controls (Fig. 1E). However, no significant differences in BOP were observed between the control group and

Table 2. Oral hygiene practices of the study sample

Variable		Control	PCOS–	PCOS+	p-value
Frequency of toothbrushing	less than once/day	2 (5.6)	0 (0.0)	3 (12.5)	0.313
	once/day	1 (2.8)	6 (13.6)	1 (4.2)	
	≥2 times/day	33 (91.7)	38 (86.4)	20 (83.3)	
Use of interdental hygiene products	yes	17 (47.2)	17 (38.6)	13 (54.2)	0.604
	no	19 (52.8)	27 (61.4)	11 (45.8)	
Time since the last dental visit	<1 year	20 (55.6)	28 (63.6)	15 (62.5)	0.826
	1–5 years	13 (36.1)	13 (29.5)	6 (25.0)	
	>5 years	3 (8.3)	3 (6.8)	3 (12.5)	

Data is presented as n (%). Group differences were assessed using the Kruskal–Wallis test for ordinal variables and Pearson's χ^2 test for the categorical variables.
PCOS– – polycystic ovary syndrome without gingivitis; PCOS+ – polycystic ovary syndrome with gingivitis.

the PCOS– subgroup (1.935 ±2.336 vs. 3.211 ±2.644, respectively; $p > 0.05$), suggesting that the increased BOP in the overall PCOS group was driven primarily by the presence of gingivitis (PCOS+, Fig. 1F). All participants exhibited very low levels of plaque, with average plaque index scores under 1, below the threshold commonly associated with clinical gingivitis in the general population. However, the plaque index was significantly higher in the PCOS group (Fig. 1G), even though oral hygiene practices were similar to those of controls (Table 2). Moreover, within the PCOS group, the plaque index did not differ according to gingivitis status (Fig. 1H), suggesting that the increased plaque accumulation was a result of the PCOS pathology itself rather than oral hygiene practices.

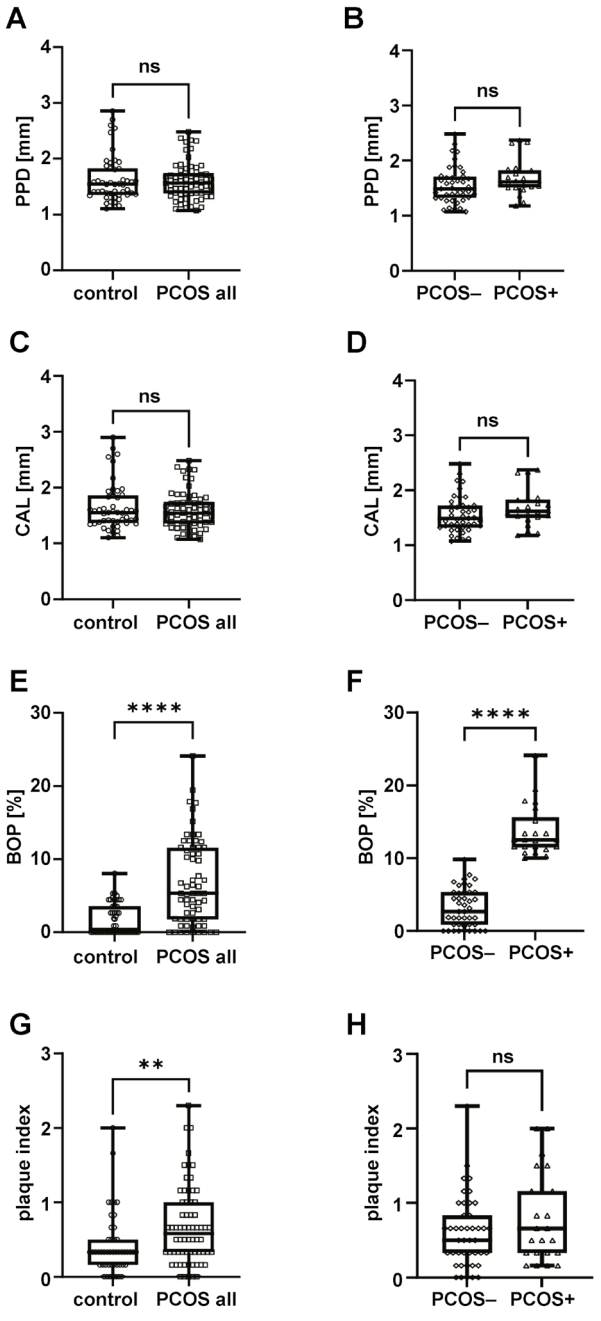

Fig. 1. Periodontal parameters in the study population according to the polycystic ovary syndrome (PCOS) status and the presence or absence of gingivitis

Probing pocket depth (PPD) (A, B), clinical attachment level (CAL) (C, D), bleeding on probing (BOP) (E, F), and plaque index (G, H).
Data is presented as box-and-whisker plots. Between-group comparisons were performed using the two-sample Student's *t*-test or the Mann–Whitney *U* test, as appropriate.
PCOS– – patients with polycystic ovary syndrome without gingivitis; PCOS+ – patients with polycystic ovary syndrome with gingivitis; PCOS all – all patients with polycystic ovary syndrome; ns – not significant; ** $p < 0.01$; **** $p < 0.0001$.

In order to determine the factors independently associated with gingivitis, 2 binary logistic regression models were constructed using the enter method (Table 3). Model 1 demonstrated that both PCOS status and poor oral hygiene were independently associated with the presence of gingivitis. Specifically, participants diagnosed with PCOS had a significantly higher risk of gingivitis in comparison to the control group ($p < 0.001$). Moreover, the practice of brushing once per day or less was associated with an increased risk ($p = 0.008$). In model 2, which assessed the influence of pharmacological treatments, only PCOS status was significantly associated with gingivitis ($p = 0.001$). Neither metformin use nor the use of oral contraceptives showed a significant association with gingival inflammation ($p > 0.05$). These findings support the role of PCOS as an independent risk factor for gingival inflammation, even after taking into account oral hygiene habits and medication use.

Considering the biological correlation between ER stress, oxidative stress, and both PCOS and PD, we proceeded to analyze relevant molecular markers. The results revealed elevated levels of superoxide (Fig. 2A) and reduced GPx1 expression (Fig. 2C) in women diagnosed with PCOS, with no observed differences between the PCOS– and PCOS+ groups (Fig. 2B,D).

The UPR-related proteins exhibited elevated levels of ATF6 and p-eIF2α in PCOS (Fig. 3C,G), with no

Table 3. Logistic regression analysis models evaluating polycystic ovary syndrome (PCOS) status, oral hygiene and medication use as independent determinants of gingivitis

Model No.	Dependent variable	Independent variable	*OR*	95% *CI*	*p*-value
1	BOP	oral hygiene (≤1/day)	11.50	1.91–69.60	0.008*
		oral hygiene (≥2/day)	0.92	0.25–3.44	0.904
		PCOS	5.78	2.27–14.70	0.000*
2	BOP	PCOS	4.89	1.87–12.70	0.001*
		use of metformin	0.66	0.28–1.54	0.336
		use of oral contraceptives	1.67	0.47–6.00	0.430

Two separate binary logistic regression models were constructed using the enter method. In both models, the dependent variable was the presence of gingivitis, defined as bleeding on probing (BOP) ≥10%. PCOS status and medication use were included as binary variables and coded as yes (1) or no (2). Brushing frequency was categorized as follows: 1 = ≤1 brushing per day (poor hygiene); 2 = ≥2 brushings per day (adequate hygiene).
CI – confidence interval; *OR* – odds ratio; * statistically significant ($p < 0.05$).

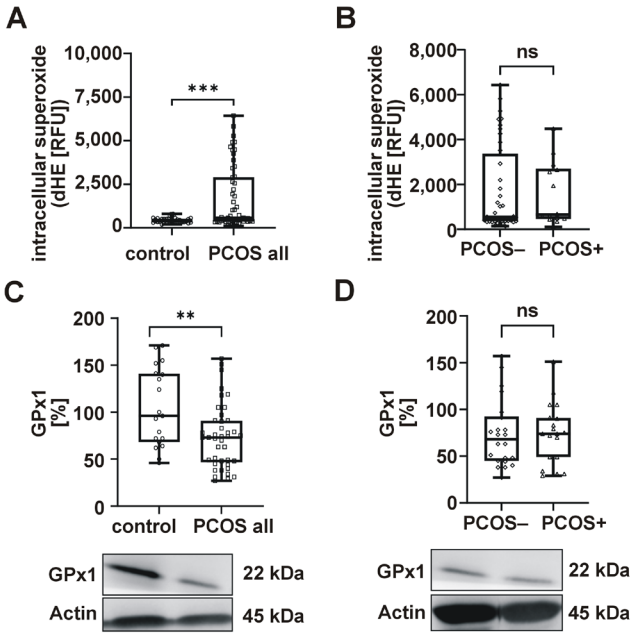

Fig. 2. Oxidative stress parameters in peripheral blood mononuclear cells (PBMCs) from women with polycystic ovary syndrome (PCOS) with and without gingivitis and from control subjects

Median intensity of dihydroethidium (dHE) fluorescence (A, B) and glutathione peroxidase 1 (GPx1) protein expression (C, D), analyzed for controls vs. all patients with PCOS (A, C) and for PCOS– vs. PCOS+ subgroups (B, D), with representative western blot images.
Data is presented as box-and-whisker plots. Between-group comparisons were performed using the two-sample Student's *t*-test or the Mann–Whitney *U* test, as appropriate.
RFU – relative fluorescence units; ** $p < 0.01$; *** $p < 0.001$.

changes observed in GRP78 or IRE1α (Fig. 3A,E), indicating selective activation of the UPR pathways. To assess the activation of UPR downstream proapoptotic pathways, CHOP levels were measured, which were reduced overall in women with PCOS (Fig. 3I). However, when the periodontal status was considered, levels of p-eIF2α and CHOP were higher (Fig. 3H,J), and GRP78 decreased (Fig. 3B) in women with both PCOS and gingivitis, suggesting proapoptotic PERK pathway activation. A subanalysis, with adjustments made for medication (metformin, oral contraceptives), revealed no significant impact on ER stress markers when comparing the control group with the PCOS group, or the PCOS– group with the PCOS+ group.

The correlation analysis revealed that BOP was positively correlated with triglycerides ($r = 0.215$, $p < 0.05$), HOMA-IR ($r = 0.314$, $p < 0.001$) and plaque index ($r = 0.393$, $p < 0.0001$), and negatively with HDLc ($r = -0.261$, $p < 0.01$) (Fig. 4). Additionally, BOP was correlated with p-eIF2α ($r = 0.389$, $p < 0.01$), and plaque index was associated with ATF6 ($r = 0.293$, $p < 0.05$), suggesting a link between PD and ER stress in PCOS. The multivariable analysis identified p-eIF2α (β = 0.335), triglycerides (β = 0.260) and plaque index (β = 0.254) as independent predictors of BOP, explaining 25.7% of its variance (Table 4).

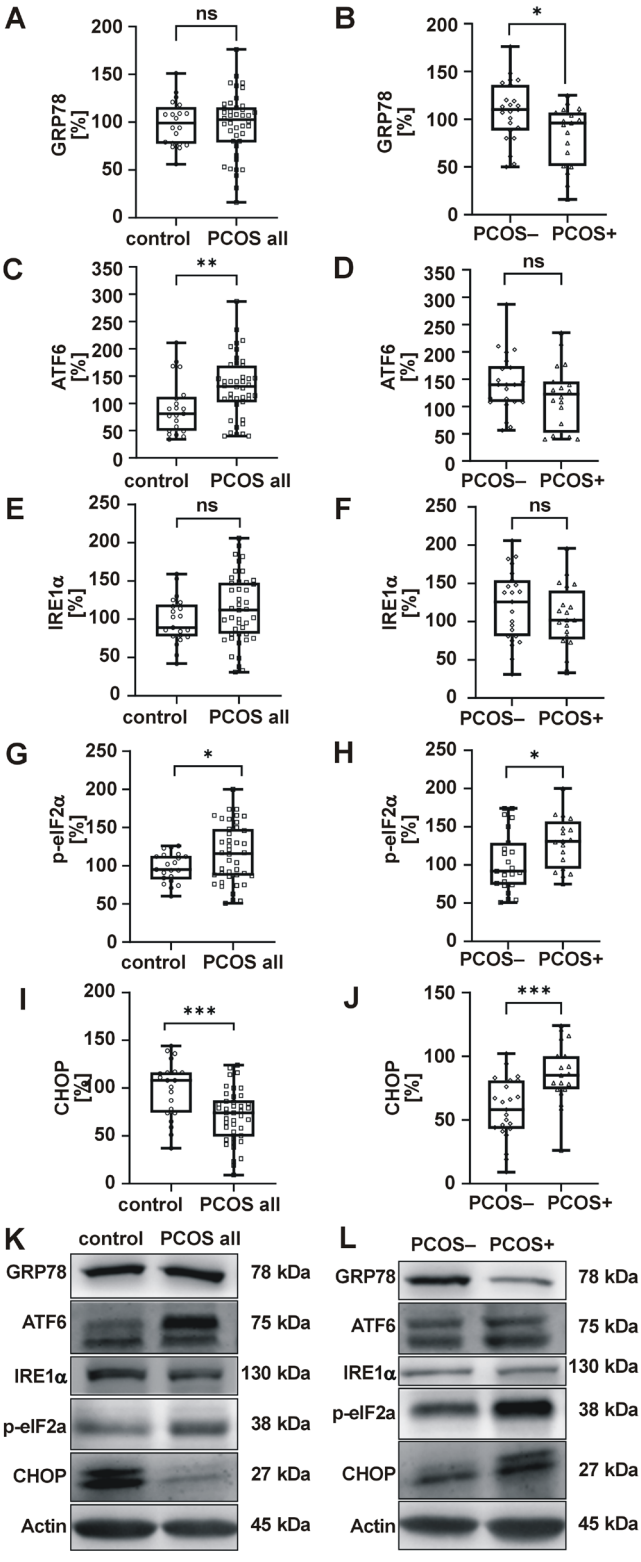

Fig. 3. Unfolded protein response (UPR) markers in peripheral blood mononuclear cells (PBMCs) from women with polycystic ovary syndrome (PCOS) with and without gingivitis and from control subjects

Relative protein expression of glucose-regulated protein 78 (GRP78) (A, B), activating transcription factor 6 (ATF6) (C, D), inositol-requiring enzyme 1α (IRE1α) (E, F), phosphorylated eukaryotic initiation factor 2 alpha subunit (p-eIF2α) (G, H), and C/EBP homologous protein (CHOP) (I, J), with representative western blot images (K, L).
Data is presented as box-and-whisker plots. Between-group comparisons were performed using the two-sample Student's *t*-test or the Mann–Whitney *U* test, as appropriate.
* $p < 0.05$; ** $p < 0.01$; *** $p < 0.001$.

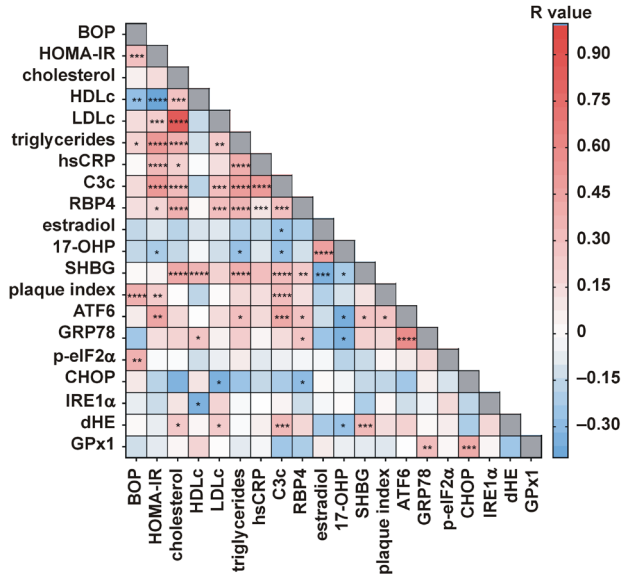

Fig. 4. Heatmap of Spearman's correlation coefficients depicting relationships between biochemical parameters, periodontal parameters, unfolded protein response (UPR)-related protein expression, and oxidative stress markers

Negative correlations are shown in blue and positive correlations in red, with color intensity reflecting correlation strength. 17-OHP – 17-hydroxyprogesterone; C3c – complement component c3; HDLc – high-density lipoprotein cholesterol; HOMA-IR – homeostatic model assessment for insulin resistance index; hsCRP – high-sensitive C-reactive protein; LDLc – low-density lipoprotein cholesterol; RBP4 – retinol binding protein 4; SHBG – sex hormone-binding globulin; * $p < 0.05$; ** $p < 0.01$; *** $p < 0.001$; **** $p < 0.0001$.

Table 4. Univariate linear regression analyses of biochemical parameters, markers of oxidative stress and unfolded protein response (UPR)-related proteins

Dependent variable	Independent variable	B	Standard error	Beta coefficient	Adjusted R^2	*p*-value
BOP	–	–	–	–	0.257	<0.001*
	p-eIF2α	0.056	0.020	0.335	–	0.007*
	triglycerides	0.036	0.017	0.260	–	0.039*
	plaque index	2.665	1.275	0.254	–	0.042*

p-eIF2α – phosphorylated eukaryotic initiation factor 2 alpha subunit; * statistically significant ($p < 0.05$).

Discussion

The present findings confirm the presence of oxidative stress and UPR activation via the ATF6 branch in circulating leukocytes of women with PCOS, and offer novel insights into the interplay between PD and metabolic conditions. Gingivitis modulates the UPR by promoting the activation of CHOP and eIF2α, fostering a pro-apoptotic environment that is independently associated with BOP. In contrast, the absence of gingivitis favors a cytoprotective response that is mediated by elevated chaperone GRP78 levels.

Polycystic ovary syndrome is characterized by metabolic disturbances, including altered glucose/lipid metabolism, hormonal imbalance, oxidative stress, and inflammation.[2–4] In this study, we report elevated insulin, HOMA-IR, LDLc, triglycerides, and altered sex hormone-binding globulin (SHBG), estradiol and 17-hydroxyprogesterone (17-OHP) levels, all consistent with the pathophysiology of PCOS.

Oral health is increasingly recognized as an essential component of women's general health, with implications for various reproductive stages.[30] In this sense, emerging evidence links PCOS to a higher prevalence of PD.[6,31] Although dental plaque is the main etiological factor for gingivitis, the results of this study support the interpretation that PCOS is an independent risk factor for periodontal inflammation. In the multivariable analyses, PCOS status was consistently associated with a higher risk of gingival inflammation, even after adjusting for oral hygiene habits and medication. Despite plaque levels being similar across the groups, women with PCOS exhibited greater gingival inflammation, indicating a heightened inflammatory response that cannot be attributed to local factors or medication effects. This interpretation aligns with previous evidence suggesting that PCOS can exacerbate periodontal inflammation independently of plaque levels, likely through systemic mechanisms involving oxidative stress and immune dysregulation.[29]

In order to further explore potential shared mechanisms underlying PCOS and PD, an assessment of markers of oxidative stress and ER stress was conducted. Oxidative stress has been identified as a key factor in the systemic impact of PD and comorbidities such as cardiovascular disease, metabolic syndrome and diabetes.[32,33] Indeed, the interplay between oxidative stress and inflammation is a central pathogenic mechanism across a broad spectrum of diseases ranging from diabetic nephropathy[34] to skin cancer.[35] Thus, it can be hypothesized that any interaction between PD and PCOS is influenced by oxidative stress. Only 3 studies have analyzed systemic oxidative stress in women diagnosed with both PCOS and PD. Saglam et al. reported impaired redox status in serum and saliva, as indicated by elevated levels of 8-hydroxy-2'-deoxyguanosine and malondialdehyde, and reduced total antioxidant capacity in subjects with PCOS and periodontitis.[36] Dursun et al. observed elevated myeloperoxidase and nitric oxide levels in gingival crevicular fluid.[5] Our group reported high myeloperoxidase levels and reduced glutathione levels in women with PCOS, with no gingivitis-related differences.[29]

In the present study, we have evaluated intracellular oxidative stress in PBMCs, which serve as systemic sensors of metabolic disease,[37] and have found increased intracellular superoxide production and reduced GPx1 levels in women with PCOS, both of which are consistent with serum markers of oxidative stress. However, no differences emerged when gingivitis was considered, possibly due to its early, reversible nature. In fact, prior research has demonstrated that severe periodontitis is

associated with increased intracellular superoxide levels, though no differences were observed in mild or moderate cases.[38]

Oxidative stress and ER stress are closely interconnected; the accumulation of reactive oxygen species (ROS) intensifies protein misfolding in the ER, further exacerbating oxidative damage and triggering inflammatory responses.[39] Our findings demonstrated elevated levels of ATF6 and p-eIF2α in PBMCs of women with PCOS. Moreover, the correlation between superoxide and hyperlipidemia, as well as elevated C3c and SHBG levels, was identified. Concurrently, the association between diminished GPx1 and GRP78 and CHOP downregulation was determined. These findings suggest that redox imbalance in PCOS may induce UPR activation. Our data align with reports of ER stress activation in granulosa and cumulus cells of women with PCOS.[18,40,41]

Endoplasmic reticulum stress has also been observed in PD models.[21,22,42] For instance, periodontal ligament stem cells from patients with periodontitis exhibited elevated UPR markers.[43] Moreover, increased UPR gene expression was noted in periodontal ligament fibroblasts exposed to lipopolysaccharide.[21] However, no previous study has evaluated ER stress in leukocytes of women with both PCOS and gingivitis. In the current study, we observed the activation of pro-apoptotic mechanisms triggered by ER stress through PERK pathway activation, as increased p-eIF2α levels induce ATF4 translation, thereby promoting CHOP expression.[16,44] Previous studies have reported the upregulation of apoptosis via the PERK/eIF2α/ATF4/CHOP signal pathway in human periodontal ligament cells derived from patients with periodontitis.[45] Accordingly, our findings suggest that the upregulation of CHOP and p-eIF2α may contribute to a pro-apoptotic profile in the PBMCs of women with PCOS and gingivitis. Conversely, an augmented GRP78 pro-survival signal in the absence of gingivitis may indicate a compensatory mechanism.[46] Interestingly, both clinical indicators of gingivitis, namely BOP and plaque index, were positively associated with p-eIF2α and ATF6, respectively. In contrast, GRP78, ATF6 and CHOP were correlated with systemic clinical parameters. These findings suggest that UPR activation in women with PCOS is primarily driven by underlying metabolic dysfunction and hormonal imbalance, and further exacerbated by the presence of PD.

To the best of our knowledge, this is the first study to examine systemic UPR activation in the context of gingivitis, a condition that remains largely understudied. Given the limited literature on the topic, we referenced studies on more advanced stages of PD to guide the interpretation of the results. Nonetheless, our conclusions are strengthened by the high methodological rigor of the study, including comprehensive periodontal assessments by an experienced dentist, the use of validated oral health questionnaires, and robust statistical analyses accounting for key confounders.

Limitations

This study has several limitations. First, the number of patients with gingivitis was relatively small, despite a prior sample size calculation, and the cross-sectional design precludes causal inference. Second, the hospital-based setting may introduce some selection bias; however, all diagnoses were made in a tertiary care following rigorous clinical and diagnostic standards to ensure consistency and reliability. Additionally, although PCOS phenotypes may differ in their metabolic and inflammatory profiles, we did not stratify participants by phenotype because of limited access to standardized clinical assessments and reliance on routine androgen assays. The sample size further restricted statistical power for subgroup analyses. Collectively, these limitations highlight the need for future studies with larger cohorts and detailed phenotyping.

Conclusions

Overall, our findings elucidate the role of gingivitis in aggravating metabolic dysfunction in women with PCOS and highlight shared ER/oxidative stress pathways. These insights underscore the importance of early periodontal care in the management of metabolic disorders and encourage future interdisciplinary research to further clarify the underlying biological mechanisms.

Trial registration

This observational study was registered at ClinicalTrials.gov (registration No. NCT06184412; https://clinicaltrials.gov/study/NCT06184412).

Ethics approval and consent to participate

All participants provided written informed consent. The study was conducted in accordance with the ethical principles for medical research involving human subjects as outlined in the Declaration of Helsinki and was approved by the Ethics Committee of University Hospital Dr. Peset, Valencia, Spain (study protocol ref. No. 95/19).

Data availability

The datasets generated and/or analyzed during the current study are available from the corresponding author on reasonable request.

Consent for publication

Not applicable.

Use of AI and AI-assisted technologies

ChatGPT (OpenAI, San Francisco, USA) has been employed to enhance the language and modify the text's length.

ORCID iDs

María Pelechá-Salvador https://orcid.org/0000-0002-2141-6422
Sandra López-Domènech https://orcid.org/0000-0003-2067-9308
Cecilia Fabiana Márquez-Arrico https://orcid.org/0000-0002-0185-6180
Meylin Fernández-Reyes https://orcid.org/0000-0001-6311-8864
Laura Perea-Galera https://orcid.org/0009-0001-3719-3614
Jonathan Hermenejildo https://orcid.org/0000-0001-8954-6621
Carlos Morillas https://orcid.org/0000-0002-3745-4423
Pablo Fernández-Collazo https://orcid.org/0009-0001-7192-2905
Javier Silvestre-Rangil https://orcid.org/0000-0003-4356-5063
Víctor Manuel Víctor https://orcid.org/0000-0002-3027-3945
Francisco Javier Silvestre https://orcid.org/0000-0001-7858-7735
Milagros Rocha https://orcid.org/0000-0003-2923-6546

References

1. Escobar-Morreale HF. Polycystic ovary syndrome: Definition, aetiology, diagnosis and treatment. *Nat Rev Endocrinol*. 2018;14(5):270–284. doi:10.1038/nrendo.2018.24
2. Dunaif A. Insulin resistance and the polycystic ovary syndrome: Mechanism and implications for pathogenesis. *Endocr Rev*. 1997;18(6):774–800. doi:10.1210/edrv.18.6.0318
3. Zuo T, Zhu M, Xu W. Roles of oxidative stress in polycystic ovary syndrome and cancers. *Oxid Med Cell Longev*. 2016;2016:8589318. doi:10.1155/2016/8589318
4. Rostamtabar M, Esmaeilzadeh S, Tourani M, et al. Pathophysiological roles of chronic low-grade inflammation mediators in polycystic ovary syndrome. *J Cell Physiol*. 2021;236(2):824–838. doi:10.1002/jcp.29912
5. Dursun E, Akalın FA, Güncü GN, et al. Periodontal disease in polycystic ovary syndrome. *Fertil Steril*. 2011;95(1):320–323. doi:10.1016/j.fertnstert.2010.07.1052
6. Márquez-Arrico CF, Silvestre-Rangil J, Gutiérrez-Castillo L, Martinez-Herrera M, Silvestre FJ, Rocha M. Association between periodontal diseases and polycystic ovary syndrome: A systematic review. *J Clin Med*. 2020;9(5):1586. doi:10.3390/jcm9051586
7. Demmer RT, Squillaro A, Papapanou PN, et al. Periodontal infection, systemic inflammation, and insulin resistance: Results from the continuous National Health and Nutrition Examination Survey (NHANES) 1999–2004. *Diabetes Care*. 2012;35(11):2235–2242. doi:10.2337/dc12-0072
8. Bhavsar NV, Trivedi S, Vachhani KS, et al. Association between preterm birth and low birth weight and maternal chronic periodontitis: A hospital-based case–control study. *Dent Med Probl*. 2023;60(2):207–217. doi:10.17219/dmp/152234
9. Pihlstrom BL, Michalowicz BS, Johnson NW. Periodontal diseases. *Lancet*. 2005;366(9499):1809–1820. doi:10.1016/S0140-6736(05)67728-8
10. Meyle J, Chapple I. Molecular aspects of the pathogenesis of periodontitis. *Periodontol 2000*. 2015;69(1):7–17. doi:10.1111/prd.12104
11. Papapanou PN, Sanz M, Buduneli N, et al. Periodontitis: Consensus report of workgroup 2 of the 2017 World Workshop on the Classification of Periodontal and Peri-Implant Diseases and Conditions. *J Periodontol*. 2018;89 Suppl 1:S173–S182. doi:10.1002/JPER.17-0721
12. Dewan M, Pandit AK, Goyal L. Association of periodontitis and gingivitis with stroke: A systematic review and meta-analysis. *Dent Med Probl*. 2024;61(3):407–415. doi:10.17219/dmp/158793
13. Koike H, Harada M, Kusamoto A, et al. Roles of endoplasmic reticulum stress in the pathophysiology of polycystic ovary syndrome. *Front Endocrinol (Lausanne)*. 2023;14:1124405. doi:10.3389/fendo.2023.1124405
14. Bañuls C, Rovira-Llopis S, Martinez de Marañon A, et al. Metabolic syndrome enhances endoplasmic reticulum, oxidative stress and leukocyte-endothelium interactions in PCOS. *Metabolism*. 2017;71:153–162. doi:10.1016/j.metabol.2017.02.012
15. Almanza A, Carlesso A, Chintha C, et al. Endoplasmic reticulum stress signalling – from basic mechanisms to clinical applications. *FEBS J*. 2019;286(2):241–278. doi:10.1111/febs.14608
16. Gorman AM, Healy SJM, Jäger R, Samali A. Stress management at the ER: Regulators of ER stress-induced apoptosis. *Pharmacol Ther*. 2012;134(3):306–316. doi:10.1016/j.pharmthera.2012.02.003
17. Cao SS, Kaufman RJ. Endoplasmic reticulum stress and oxidative stress in cell fate decision and human disease. *Antioxid Redox Signal*. 2014;21(3):396–413. doi:10.1089/ars.2014.5851
18. Takahashi N, Harada M, Hirota Y, et al. Activation of endoplasmic reticulum stress in granulosa cells from patients with polycystic ovary syndrome contributes to ovarian fibrosis. *Sci Rep*. 2017;7(1):10824. doi:10.1038/s41598-017-11252-7
19. Harada M, Takahashi N, Azhary JM, Kunitomi C, Fujii T, Osuga Y. Endoplasmic reticulum stress: A key regulator of the follicular microenvironment in the ovary. *Mol Hum Reprod*. 2021;27(1):gaaa088. doi:10.1093/molehr/gaaa088
20. Wang C, Zhang Y. Endoplasmic reticulum stress: A new research direction for polycystic ovary syndrome? *DNA Cell Biol*. 2022;41(4):356–367. doi:10.1089/dna.2021.1050
21. Wang Y, Gong J, Zeng H, et al. Lipopolysaccharide activates the unfolded protein response in human periodontal ligament fibroblasts. *J Periodontol*. 2016;87(5):e75–e81. doi:10.1902/jop.2015.150413
22. Yamada H, Nakajima T, Domon H, Honda T, Yamazaki K. Endoplasmic reticulum stress response and bone loss in experimental periodontitis in mice. *J Periodontal Res*. 2015;50(4):500–508. doi:10.1111/jre.12232
23. Sen P, Kemppainen E, Orešič M. Perspectives on systems modeling of human peripheral blood mononuclear cells. *Front Mol Biosci*. 2018;4:96. doi:10.3389/fmolb.2017.00096
24. Rotterdam ESHRE/ASRM-Sponsored PCOS consensus workshop group. Revised 2003 consensus on diagnostic criteria and long-term health risks related to polycystic ovary syndrome (PCOS). *Hum Reprod*. 2004;19(1):41–47. doi:10.1093/humrep/deh098
25. Chapple ILC, Mealey BL, Van Dyke TE, et al. Periodontal health and gingival diseases and conditions on an intact and a reduced periodontium: Consensus report of workgroup 1 of the 2017 World Workshop on the Classification of Periodontal and Peri-Implant Diseases and Conditions. *J Periodontol*. 2018;89 Suppl 1:S74–S84. doi:10.1002/JPER.17-0719
26. Petersen PE, Baez RJ; World Health Organization. *Oral Health Surveys: Basic Methods*. 5th ed. Geneva, Switzerland: World Health Organization; 2013. https://iris.who.int/server/api/core/bitstreams/b00e659f-ab38-4e61-b786-0152d91b5f1b/content. Accessed July 30, 2025.
27. Silness J, Loe H. Periodontal disease in pregnancy. II. Correlation between oral hygiene and periodontal condition. *Acta Odontol Scand*. 1964;22:121–135. doi:10.3109/00016356408993968
28. Ramfjord SP. The periodontal disease index (PDI). *J Periodontol*. 1967;38(6):602–610. doi:10.1902/jop.1967.38.6.602
29. Márquez-Arrico CF, Silvestre FJ, Fernández-Reyes M, et al. Gingival inflammation and leukocyte–endothelium cell interactions in women with polycystic ovary syndrome. *J Periodontol*. 2025;96(5):478–489. doi:10.1002/JPER.24-0148
30. Radwan-Oczko M, Hirnle L, Szczepaniak M, Duś-Ilnicka I. How much do pregnant women know about the importance of oral health in pregnancy? Questionnaire-based survey. *BMC Pregnancy Childbirth*. 2023;23(1):348. doi:10.1186/s12884-023-05677-4
31. Işık Y, Telatar GY, Neşelioğlu S, Biçer C, Gürlek B. Evaluation of periodontal status in different phenotypes of polycystic ovary syndrome in untreated patients of early reproductive age: A case–control study. *J Obstet Gynaecol Res*. 2020;46(3):459–465. doi:10.1111/jog.14179
32. Bullon P, Morillo JM, Ramirez-Tortosa MC, Quiles JL, Newman HN, Battino M. Metabolic syndrome and periodontitis: Is oxidative stress a common link? *J Dent Res*. 2009;88(6):503–518. doi:10.1177/0022034509337479
33. Lamster IB, Pagan M. Periodontal disease and the metabolic syndrome. *Int Dent J*. 2017;67(2):67–77. doi:10.1111/idj.12264
34. Yu H, Guo M. Renal protection by acacetin in streptozotocin-induced diabetic nephropathy via TLR4/NF-κB pathway modulation in rats. *Adv Clin Exp Med*. 2025;34(8):1353–1363. doi:10.17219/acem/192225

35. Sun Y, Ma Y, Wang H. Chemopreventive role of β-caryophyllene in DMBA-induced skin cancer: Modulation of apoptotic pathways and PI3K/Akt signaling in Swiss albino mice. *Adv Clin Exp Med*. 2025;34(9):1541–1552. doi:10.17219/acem/194482
36. Saglam E, Canakci CF, Sebin SO, et al. Evaluation of oxidative status in patients with chronic periodontitis and polycystic ovary syndrome: A cross-sectional study. *J Periodontol*. 2018;89(1):76–84. doi:10.1902/jop.2017.170129
37. Kramer PA, Ravi S, Chacko B, Johnson MS, Darley-Usmar VM. A review of the mitochondrial and glycolytic metabolism in human platelets and leukocytes: Implications for their use as bioenergetic biomarkers. *Redox Biol*. 2014;2:206–210. doi:10.1016/j.redox.2013.12.026
38. Martinez-Herrera M, López-Domènech S, Silvestre FJ, et al. Chronic periodontitis impairs polymorphonuclear leucocyte–endothelium cell interactions and oxidative stress in humans. *J Clin Periodontol*. 2018;45(12):1429–1439. doi:10.1111/jcpe.13027
39. Xue X, Piao JH, Nakajima A, et al. Tumor necrosis factor alpha (TNFα) induces the unfolded protein response (UPR) in a reactive oxygen species (ROS)-dependent fashion, and the UPR counteracts ROS accumulation by TNFα. *J Biol Chem*. 2005;280(40):33917–33925. doi:10.1074/jbc.M505818200
40. Zhao Y, Wu X, Meng F, et al. ER stress-induced LINC00173 promotes the apoptosis of ovarian granulosa cells by regulating the HRK/PI3K/AKT pathway in polycystic ovary syndrome. *Sci Rep*. 2024;14(1):24636. doi:10.1038/s41598-024-75178-7
41. Jin J, Ma Y, Tong X, et al. Metformin inhibits testosterone-induced endoplasmic reticulum stress in ovarian granulosa cells via inactivation of p38 MAPK. *Hum Reprod*. 2020;35(5):1145–1158. doi:10.1093/humrep/deaa077
42. Feng Y, Zhang R, Wang YR, et al. Inhibition of endoplasmic reticulum stress by 4-phenyl butyric acid presents therapeutic effects on periodontitis: Experimental studies in vitro and in rats. *Stem Cells Int*. 2021;2021:6618943. doi:10.1155/2021/6618943
43. Xue P, Li B, An Y, et al. Decreased MORF leads to prolonged endoplasmic reticulum stress in periodontitis-associated chronic inflammation. *Cell Death Differ*. 2016;23(11):1862–1872. doi:10.1038/cdd.2016.74
44. Cnop M, Toivonen S, Igoillo-Esteve M, Salpea P. Endoplasmic reticulum stress and eIF2α phosphorylation: The Achilles heel of pancreatic β cells. *Mol Metab*. 2017;6(9):1024–1039. doi:10.1016/j.molmet.2017.06.001
45. Liu Q, Guo S, Huang Y, et al. Inhibition of TRPA1 ameliorates periodontitis by reducing periodontal ligament cell oxidative stress and apoptosis via PERK/eIF2α/ATF-4/CHOP signal pathway. *Oxid Med Cell Longev*. 2022;2022:4107915. doi:10.1155/2022/4107915
46. Lee AS. The ER chaperone and signaling regulator GRP78/BiP as a monitor of endoplasmic reticulum stress. *Methods*. 2005;35(4):373–381. doi:10.1016/j.ymeth.2004.10.010

Original paper

Does the prevalence of temporomandibular disorders increase as a result of tooth loss or prosthodontic rehabilitation? A national representative cross-sectional study

Emőke Márta Takács[A,C,D,F*], Ibolya Süveges[B,D,F*], Szilvia Ambrus[C–F*], Péter Schmidt[B,E,F], Bálint Jász[B,E,F], Péter Hermann[E,F], Szandra Körmendi[A,E,F], Máté Jász[A,B,E,F]

Department of Prosthodontics, Semmelweis University, Budapest, Hungary
*These authors contributed equally to this work.

A – research concept and design; B – collection and/or assembly of data; C – data analysis and interpretation; D – writing the article; E – critical revision of the article; F – final approval of the article

Dental and Medical Problems, ISSN 1644-387X (print), ISSN 2300-9020 (online) *Dent Med Probl*. 2026;63(5):1189–1197

Address for correspondence
Emőke Márta Takács
E-mail: takacs.emoke@semmelweis.hu

Funding sources
None declared

Conflict of interest
None declared

Acknowledgements
The authors would like to thank the main organizer of the screening study, late Prof. Pál Fejérdy, and the data collectors for their conscientious and thorough work, without which the preparation of this article would not have been possible.

Received on May 8, 2025
Reviewed on August 6, 2025
Accepted on September 27, 2025

Published online October 30, 2026

Abstract

Background. Temporomandibular disorders (TMDs) are a group of musculoskeletal pathologies that are characterized by pain that occurs or worsens during function, temporomandibular joint (TMJ) noises, and limited jaw movements. The relationship between occlusion and TMDs has been the subject of extensive research, yet the findings have been contradictory.

Objectives. The aim of the present study was to examine the relationship between partial edentulism, prosthodontic rehabilitation, and a selection of TMD symptoms. Therefore, we re-examined data from a national screening examination from a novel perspective.

Material and methods. A retrospective analysis was conducted on data from a representative national epidemiological pathfinder survey for oral symptoms. In our analysis, we investigated the registered major TMD symptoms in 3 groups: patients with extensive tooth loss; patients with prosthodontic rehabilitation; and patients with normal dentition as control.

Results. The present study utilized data from a total of 3,342 patients. A significantly higher prevalence of TMD symptoms was observed in the group with extensive tooth loss (28.21%) as compared to the control group (21.56%) ($p = 0.017$; *OR*: 1.429). Similarly, a higher prevalence of TMD symptoms was observed in the group with prosthodontic rehabilitation (25.32%) ($p = 0.057$; *OR*: 1.233) as compared to the control group. The difference was even more pronounced for pain-related TMDs. The logistic regression analysis revealed that female gender was a significant predictor of pain, limited mouth opening and TMJ clicking.

Conclusions. Our findings suggest that tooth loss or prosthodontic rehabilitation may contribute to the development of TMD symptoms. They also show that the replacement of missing teeth alone does not appear to eliminate the elevated risk of TMDs. Consistent with the existing literature, being female elevates the risk of developing TMDs.

Keywords: temporomandibular disorders, dental occlusion, cross-sectional survey, prosthetic rehabilitation, tooth loss

Cite as
Takács EM, Süveges I, Ambrus S, et al. Does the prevalence of temporomandibular disorders increase as a result of tooth loss or prosthodontic rehabilitation? A national representative cross-sectional study. *Dent Med Probl.* 2026;63(5):1189–1197. doi:10.17219/dmp/211427

DOI
10.17219/dmp/211427

Copyright
Copyright by Author(s)
This is an article distributed under the terms of the Creative Commons Attribution 3.0 Unported (CC BY 3.0) (https://creativecommons.org/licenses/by/3.0/)

Highlights

- Temporomandibular disorders (TMDs) are a common health problem, but their relationship with occlusal factors remains unclear.
- A significantly higher prevalence of TMD symptoms was observed in the groups with tooth loss and prosthodontic rehabilitation compared with the control group.
- These findings suggest that tooth loss may contribute to the development of TMD symptoms, while prosthodontic rehabilitation alone does not appear to eliminate this association.

Introduction

Temporomandibular disorders (TMDs) are a group of musculoskeletal pathologies that are characterized by 3 major symptoms in the orofacial region. These symptoms include pain that occurs or worsens during function, temporomandibular joint (TMJ) noises, and limited jaw movements, according to the Diagnostic Criteria for Temporomandibular Disorders (DC/TMD).[1]

Current estimates suggest that the prevalence of TMDs in the general population is substantially higher than previously thought, at approx. 34%.[2] A wide range of psychosocial, behavioral, and physiological features have been described as etiological factors in TMDs. Depression and anxiety are well-documented psychological comorbidities,[3] while behavioral factors,[4] such as awake[5,6] and sleep bruxism,[7–9] as well as sleep quality,[10] have been identified as significant contributors. The relationship between bruxism and TMDs remains somewhat controversial. However, recent studies have reported a co-occurrence rate of 18%.[2] In addition, individual biological characteristics, ranging from genetic factors to dentition-related features, have been shown to contribute to the development and persistence of TMDs.[11]

Further research is essential to advance the diagnosis of TMDs, patient pathways, and interprofessional collaboration. In view of the findings of recent research, it is worthwhile to examine the medications used to treat chronic conditions that coexist with TMDs.[12] Information about changes in the tissues and the volume of the surrounding structures, such as the neck muscles, may also be important.[13] New questionnaires may be of significant help in assessing the emotional state of patients.[14] Furthermore, it may be worthwhile to consider evaluating therapeutic alternatives for bruxism,[15] which is common among patients with TMDs.

The potential links between occlusal factors and TMDs have been the subject of investigation for decades, yet neither definitive proof nor comprehensive refutation has emerged.[16] A number of studies have identified a correlation between occlusal factors and TMDs,[17–20] while others have not.[21–23] Okeson provides a useful framework for interpreting the disparate results of previous studies: "One might conclude that if occlusion were the major etiologic factor in TMD, the profession would have confirmed this many years ago. On the other hand, if occlusion has nothing to do with TMD, the profession would have likewise already confirmed this conclusion."[24] Current knowledge suggests that TMDs may result from multiple etiological factors, thus indicating a biopsychosocial origin.[25]

In the field of TMD treatment, conservative therapy has been identified as the most effective approach in the majority of the existing literature.[16] This approach encompasses counselling, self-management techniques, physical therapy, pharmacotherapy, and splint therapy, which are considered the preferred treatment modalities in most cases. Irreversible therapies include the provision of dental prostheses; however, the classification of dentures as a therapeutic intervention for TMDs remains debatable.

A review of the literature reveals numerous examples of studies investigating the relationship between tooth loss and TMDs. For instance, in 2023, Rawat et al. conducted a systematic review of 13 selected publications, which indicated that tooth loss affects TMJ function.[26] The negative effect appears to increase with the number of missing teeth, and the absence of posterior teeth is associated with greater TMJ damage. However, due to the complexity of TMD development, it cannot be definitively concluded that tooth loss causes TMDs.[26]

In 2023, Manfredini et al. initiated an investigation to address 2 key questions – "Can prosthodontic rehabilitation be used as treatment for TMDs?" and "Can prosthodontic rehabilitation cause TMDs?"[27] However, they were unable to include any articles in the planned systematic review due to the lack of high-quality clinical trials or randomized clinical trials (RCTs) on this topic.[27] This suggests that very little evidence is available in the existing literature regarding the effects of prosthodontic rehabilitation on TMJ.

The aim of the present study was to examine the relationship between partial edentulism, the presence of prosthodontic restorations, and selected TMD symptoms. Therefore, we re-examined data from a national screening examination from a novel perspective. The null hypothesis was that tooth loss or prosthodontic rehabilitation would not be associated with an increased prevalence of TMDs.

Material and methods

A retrospective analysis was conducted using data from a representative national oral epidemiological pathfinder survey. The survey was carried out by calibrated physicians and assistants from the Department of Prosthodontics at Semmelweis University, Budapest, Hungary, and was based on the World Health Organization (WHO) criteria for screening surveys.[28] Data were collected over a 2-year period, from 2003 to 2004. Ethical approval was obtained from the Regional and Institutional Committee for Scientific and Research Ethics of Semmelweis University (SE TUKEB 206/2003).

To determine the appropriate sample size for the study, the number of subjects required to detect small clinical effects was assessed. A sample size of more than 2,180 participants was considered sufficient to detect small clinical effects with 90% statistical power.[29]

Dental screening was conducted in conjunction with chest X-ray examinations. In Hungary, the chest X-ray screening program has a long history, having originally been introduced to detect tuberculosis. All Hungarian adults aged 18 years and older receive postal invitations every 5 years. Although this examination is no longer mandatory, high participation rates are observed among the population. A total of 304 locations were randomly selected from the comprehensive list of chest X-ray stations in Hungary, thereby ensuring the representation of all types of settlements. To determine the appropriate sample composition, data on gender and age groups at each location were used in accordance with data from the Hungarian Central Statistical Office. Socioeconomic characteristics were not directly taken into account during sample selection; however, as these characteristics correlate with a geographical region in Hungary, regional differences were also considered. All individuals who volunteered to participate and provided written informed consent underwent screening.

The inclusion criteria were as follows: participants had to be at least 18 years of age and provide written informed consent to participate in the study. The gender distribution and age of participants at each study site were determined as outlined above to ensure the representativeness of the survey. The exclusion criterion was refusal to participate in the study.

The survey team comprised 7 calibrated examiners and 5 data recorders, all affiliated with the Department of Prosthodontics at Semmelweis University. All team members had previously undergone theoretical and practical training and calibration. Inter-examiner reliability during examiner calibration demonstrated almost perfect agreement, with a Cohen's kappa value of 0.85.

Dental screening examinations were conducted using a portable dental X-ray chair with a headrest, appropriate artificial lighting, and a range of diagnostic instruments, including a dental probe, a dental mirror, a dental forceps, and a WHO periodontal probe.

A questionnaire was used to collect the following information about the participants: gender; age; type of settlement; educational level; general health status; oral hygiene habits; frequency of dental visits; and smoking status.

The clinical data obtained during the dental examinations were analyzed. The condition of each tooth was recorded according to the following categories: intact; decayed; filled; prepared for fixed prostheses; or missing. Where applicable, the type of partial tooth loss and the existing prosthodontic appliances were recorded. Partially edentulous cases were classified according to the Fábián and Fejérdy classification of partial edentulism.

Additionally, selected TMD symptoms were assessed during the clinical examination. All pain triggered or aggravated by jaw movements was documented, irrespective of its origin, whether in the muscles involved in jaw movements or in TMJ. The degree of mouth opening was measured using a ruler, and any limitation was recorded. The presence of TMJ clicking was also documented.

Data collection was conducted before the development of validated diagnostic criteria; therefore, no such criteria were used.

Although the most widely recognized classification system for tooth loss is the Kennedy classification,[30] a logical and straightforward classification system for partial edentulism was developed in Hungary at Semmelweis University: the Fábián and Fejérdy classification.[31–34] This classification is based on an analysis of the forces acting on the planned prosthodontic appliance. Each class is determined by the position of the remaining teeth, which may provide support against the chewing forces acting on the dental prosthesis. Consequently, the classification also provides recommendations regarding the most appropriate type of prosthodontic appliance. In the national representative screening survey, tooth loss was classified according to this system.

The Fábián and Fejérdy classification differentiates between 3 principal classes (Classes 1–3), 2 or 3 subclasses (1A, 1B, 2A, 2B, and 2A/1), and 2 categories: the completely edentulous situation (T); and the dentate situation without tooth loss (Class 0).

In Class 1, a fixed prosthetic appliance can be constructed, since no torque forces are present (Class 1A) (Fig. 1), or because the torque forces can be compensated for by extending the bridge (Class 1B) (Fig. 2). In Class 1A, a sufficient number of occlusal units are present in

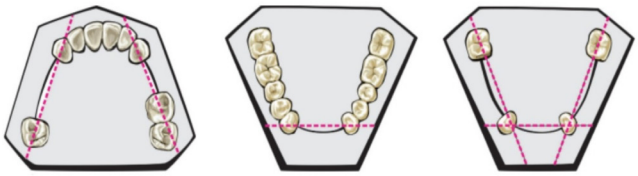

Fig. 1. Examples of Class 1A of the Fábián and Fejérdy classification

The dashed lines indicate the potential axes of rotation. In this class, a fixed prosthesis may be fabricated. Courtesy of Dr. Ildikó Berze.

each quadrant, thereby maintaining stable occlusion. This class is analogous to Kennedy Class III, in which the teeth on either side of the edentulous area can be used as abutments.

In Classes 2 (Fig. 3 and 4) and 3 (Fig. 5), the extent of tooth loss necessitates the fabrication of either a removable partial denture or a complex prosthesis, constructed in accordance with the established prosthodontic principles. In these classes, the absence of stable occlusion is attributed to the extensive edentulous areas located posterior to the remaining teeth. Class 2 is analogous to Kennedy Classes I and II, whereas Class 2A/1 (Fig. 6) encompasses subtotal edentulism with only 1 or 2 remaining teeth.

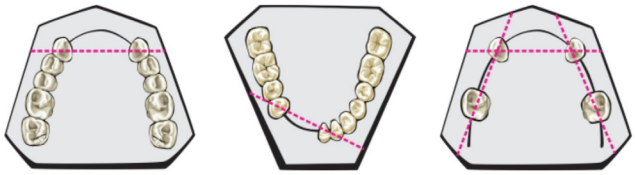

Fig. 2. Examples of Class 1B of the Fábián and Fejérdy classification

The dashed lines indicate the potential axes of rotation. In this class, additional abutments are required to compensate for the generated torque forces, thereby enabling the fabrication of a fixed prosthesis. Courtesy of Dr. Ildikó Berze.

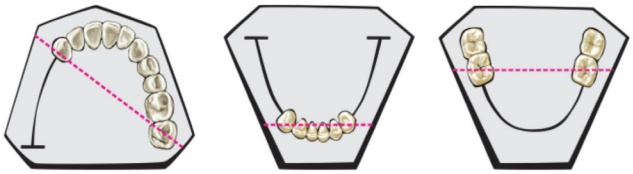

Fig. 3. Examples of Class 2A of the Fábián and Fejérdy classification

The dashed lines indicate the potential axis of rotation.

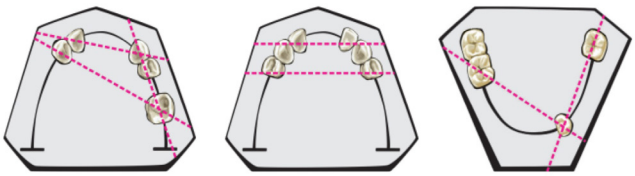

Fig. 4. Examples of Class 2B of the Fábián and Fejérdy classification

The dashed lines indicate the potential axes of rotation. The extensive tooth loss in this class necessitates the provision of complex prostheses or removable partial dentures. Courtesy of Dr. Ildikó Berze.

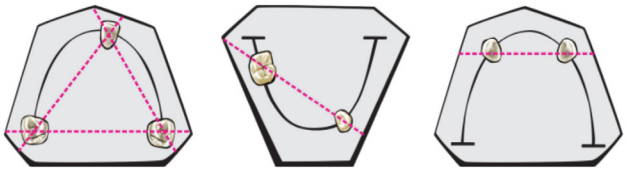

Fig. 5. Examples of Class 3 of the Fábián and Fejérdy classification

The dashed lines indicate the potential axes of rotation. The considerable tooth loss in this class necessitates the provision of overdentures or removable partial dentures. Courtesy of Dr. Ildikó Berze.

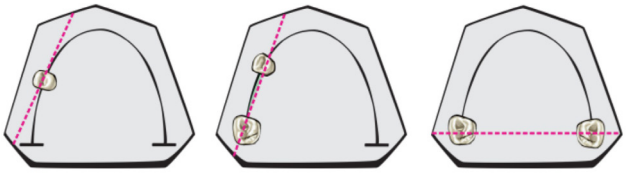

Fig. 6. Examples of Class 2A/1 of the Fábián and Fejérdy classification

The dashed lines indicate the potential axis of rotation. Due to the extensive tooth loss associated with this class, an overdenture is the treatment of choice. Courtesy of Dr. Ildikó Berze.

In our analysis, the recorded TMD symptoms were investigated in 3 distinct groups. Patients classified as prosthodontic Classes 1B or 2 according to the Fábián and Fejérdy classification were assigned to the tooth loss (L) group. These patients had several missing teeth, so occlusion was not stable in all quadrants. Patients with any type of prosthodontic restoration, either fixed or removable, regardless of whether the restorations were appropriately designed or occlusally sound, were assigned to the prosthodontic (P) group. Patients without extensive tooth loss, with stable occlusion in all quadrants (Classes 0 and 1A according to the Fábián and Fejérdy classification), and without prosthodontic appliances were assigned to the control (C) group. If the two dental arches belonged to different classes, the more extensive tooth loss was taken into account for group assignment. If a prosthodontic restoration was present in only one dental arch, even if it consisted of a single crown, the patient was assigned to the P group.

Statistical analysis

The data were processed using Microsoft Excel spreadsheets, and statistical analysis was performed using the GraphPad Prism software (v. 8.0.1). The χ^2 test was used as an omnibus test, followed by Fisher's exact test for post hoc pairwise comparisons. Multivariable logistic regression analysis was also performed, with effect sizes calculated where applicable.

Although the following values are commonly used to define effect sizes according to Cohen's *d* – small: 0.2, medium: 0.5, and large: 0.8 – Zieliński and Gawda proposed lower effect size thresholds for TMD research, categorizing them as follows: 0.1 for small; 0.2 for medium; and 0.7 for large effects.[29] As categorical variables were used in our study, the proposed thresholds were converted into odds ratios (*OR*s). The following values were adopted: *OR* = 1.2 for small effects; *OR* = 1.7 for medium effects; and *OR* = 3.6 for large effects.

Results

A total of 6,397 individuals were invited to participate in the screening process at the designated sites. Of these, 28% (1,791 individuals) did not respond. The majority of non-respondents cited a lack of time as the reason for their

non-participation. Of the 4,606 individuals who underwent screening, those classified as Class 2A/1, Class 3 or Class T according to the Fábián and Fejérdy classification, indicating complete edentulism or the presence of no more than 3 remaining teeth, were excluded from the present study (n = 1,264; 27.4%). This exclusion was based on the study objective, which was to examine the relationship between tooth loss, the use of partial dentures, and TMDs.

The present study included data from 3,342 participants. The study population consisted of 1,341 males (40.1%) and 2,001 females (59.9%). The mean age of the participants was 43.9 ±15.0 years. The group with extensive tooth loss (L) comprised 429 individuals (12.8%), with a mean age of 50.4 ±13.0 years. The gender distribution in this group was 217 males (50.6%) and 212 females (49.4%). The group with prosthodontic rehabilitation (P) consisted of 1,568 individuals (46.9%), with a mean age of 51.1 ±12.6 years. Of these, 490 (31.3%) were male and 1,078 (68.8%) were female. A total of 1,345 participants (40.2%) were included in the control group (C), in which occlusion was stable in all quadrants. Their mean age was 33.5 ±11.9 years, and 634 (47.1%) were male and 711 (52.9%) were female (Table 1). The mean age of the control group appeared to be lower than that of the L and P groups. However, multivariable logistic regression analysis revealed no statistically significant association between age and group membership (*OR*: 0.99; 95% confidence interval (*CI*): 0.99–1.00).

A total of 808 participants (24.18%) exhibited symptoms consistent with TMDs. The most prevalent symptom was TMJ clicking, which was present in 786 individuals (23.52%). Pain triggered or aggravated by jaw movements was reported by 48 participants (1.44%), while limited jaw movement was observed in 12 participants (0.36%). In 36 participants (1.08%), 2 major TMD symptoms occurred simultaneously, while all 3 major symptoms were present in one participant (0.03%) (Table 1).

The gender distribution showed a notable difference, with males accounting for 31% of participants presenting with TMD symptoms and females accounting for the majority (69%). Among the 1,341 male participants examined, 248 (18.49%) exhibited TMD symptoms, whereas among the 2,001 female participants, 560 (27.99%) presented with TMD symptoms ($p < 0.01$). Multivariable logistic regression analysis further demonstrated that women had higher odds of presenting with TMD symptoms than men (*OR*: 1.71; 95% *CI*: 1.44–2.03). A greater proportion of female participants also reported limited mouth opening (*OR*: 3.79; 95% *CI*: 0.99–24.87), pain in TMJ or the orofacial region (*OR*: 4.85; 95% *CI*: 2.21–12.81), and joint clicking (*OR*: 1.66; 95% *CI*: 1.40–1.97) (Table 2). The distribution of individual symptoms was similar in both sexes, with joint clicking being overwhelmingly the most prevalent symptom. Among male participants presenting with TMD symptoms, joint clicking was reported in 98.79%, compared with 96.61% of female participants presenting with TMD symptoms.

Table 1. General characteristics of the study population

Characteristics		N = 3,342
Age [years]		43.9 ±15.0
Gender	M	1,341 (40.1)
	F	2,001 (59.9)
Group design	tooth loss (L)	429 (12.8)
	prosthodontic rehabilitation (P)	1,568 (46.9)
	control (C)	1,345 (40.2)
TMD signs and symptoms[a]	overall	808 (24.18)
	pain[†]	48 (1.44)
	clicking	786 (23.52)
	limited mouth opening	12 (0.36)
	2 symptoms	36 (1.08)
	3 symptoms	1 (0.03)

Data presented as mean ± standard deviation (*M* ±*SD*), or as number (percentage) (*n* (%)).
TMD – temporomandibular disorder; M – male; F – female; [a] in proportion to the whole examined population; [†] any pain triggered or aggravated by jaw movements.

Table 2. Multivariable logistic regression analysis

Covariate (gender: F)		*p*-value	*OR*	95% *CI*
Any TMD symptoms		≤0.0001*	1.71	1.44–2.03
Type of symptoms	pain[†]	0.0003*	4.85	2.21–12.81
	clicking	≤0.0001*	1.66	1.40–1.97
	limited mouth opening	0.0875*	3.79	0.99–24.87

OR – odds ratio; *CI* – confidence interval; [†] any pain triggered or aggravated by jaw movements; * statistically significant.

Upon examining the occurrence of TMD symptoms across the 3 groups, differences in their prevalence were observed. A significantly higher prevalence of TMD symptoms was observed in the group with extensive tooth loss compared with the control group (p = 0.017; *OR*: 1.429; 95% *CI*: 1.116–1.830). Similarly, a higher prevalence of TMD symptoms was observed in the group with prosthodontic rehabilitation compared with the control group (p = 0.057; *OR*: 1.233; 95% *CI*: 1.038–1.466). Multivariable logistic regression analysis further demonstrated that the group with tooth loss had higher odds of presenting with TMD symptoms (*OR*: 1.55; 95% *CI*: 1.18–2.04). No significant difference was observed in the prevalence of TMD symptoms between the groups with tooth loss and prosthodontic rehabilitation. With regard to individual symptoms, a similar pattern was observed for joint clicking. The occurrence of this symptom was higher in both the L group (p = 0.016; *OR*: 1.437; 95% *CI*: 1.120–1.844) and the P group (p = 0.051; *OR*: 1.241; 95% *CI*: 1.042–1.477) compared with the control group (Table 3).

In the multivariable logistic regression analysis of pain triggered or aggravated by jaw movements, a significant association with a large effect size was found for tooth loss (*OR*: 3.60; 95% *CI*: 1.42–8.88), whereas prosthodontic rehabilitation was associated with a medium effect size (*OR*: 2.03; 95% *CI*: 0.93–4.60) (Table 4).

Table 3. Manifestation of temporomandibular disorder (TMD) symptoms among different cohorts

TMD symptoms		Control (C) n = 1,345	Tooth loss (L) n = 429	p- value†	OR†	95% CI†	Prosthodontic rehabilitation (P) n = 1,568	p-value††	OR††	95% CI††	Total N = 3,342
Any TMD symptoms		290 (21.56)	121 (28.21)	0.017*	1.429	1.116–1.830	397 (25.32)	0.057	1.233	1.038–1.466	808 (24.18)
Type of symptoms[b]	pain†††	13 (4.48)	10 (8.26)	–	–	–	25 (6.30)	–	–	–	48 (5.94)
	clicking	281 (96.90)	118 (97.52)	0.016*	1.437	1.120–1.844	387 (97.48)	0.051	1.241	1.042–1.477	786 (97.28)
	limited mouth opening	6 (2.07)	2 (1.65)	–	–	–	4 (1.01)	–	–	–	12 (1.49)
	2 symptoms	10 (3.45)	9 (7.44)	–	–	–	17 (4.28)	–	–	–	36 (4.46)
	3 symptoms	0	0	–	–	–	1 (0.25)	–	–	–	1 (0.12)

Data presented as *n* (%).
[b] in proportion to the number of symptomatic patients in a particular group; † group C vs. group L (Fisher's exact test); †† group C vs. group P (Fisher's exact test); ††† any pain triggered or aggravated by jaw movements; * statistically significant.

Table 4. Pain triggered or aggravated by jaw movements (multivariable logistic regression analysis)

Covariate	OR	95% CI
Tooth loss	3.60	1.42–8.88
Prosthodontic rehabilitation	2.03	0.93–4.60

Discussion

The aim of this study was to examine the relationship between partial edentulism, the presence of prosthodontic appliances, and selected TMD symptoms. The null hypothesis was that tooth loss or prosthodontic rehabilitation would not increase the prevalence of TMD symptoms. The findings of the present study revealed statistically significant differences in the prevalence of TMD symptoms, particularly pain triggered or aggravated by jaw movements, between the control group and the groups with tooth loss (L) and prosthodontic rehabilitation (P). Therefore, the null hypothesis was rejected.

The results of the nationwide comprehensive oral epidemiological pathfinder survey conducted in Hungary have previously been evaluated from several different perspectives. These include general epidemiology,[35] dental caries,[36] periodontology,[37] and prosthodontics.[38–40] Previous studies have also addressed several other topics, including oral mucosal lesions,[41] nutritional and oral hygiene habits,[42] and the association between TMDs and certain orthodontic abnormalities.[43]

The association between occlusion and TMDs has also been investigated through the analysis of national surveys conducted in other countries. A study comparable to the present research was conducted in Finland as part of the nationally representative Health 2000 Survey, with data collection taking place between 2000 and 2001.[19] In 2013, Sipilä et al. published their findings on the impact of tooth loss and the use of prosthodontic appliances on the clinical manifestations of TMDs. The authors concluded that complete edentulism, the use of complete dentures, and the wearing of poorly maintained removable dentures were associated with pain-related TMD symptoms in women. Furthermore, they found that these associations were influenced by psychosocial factors.[19]

In a study published in 2023, Liu et al. investigated the relationship between congenital tooth agenesis and the occurrence of TMDs.[44] The study included 583 patients with congenital edentulism and 586 controls. The results indicated a significant association between congenital edentulism and both intra-articular (p = 0.017) and pain-related TMDs (p = 0.009). Additionally, the number of quadrants with missing teeth was found to be associated with the occurrence of TMDs.[44]

A comparable finding was reported by Jaber et al. in a radiological study examining TMJs in patients with TMDs.[45] The study indicated that unilateral tooth loss was associated with a higher occurrence of TMDs.[45]

Tallents et al. investigated the potential association between the absence of posterior teeth and TMDs.[46] They compared findings from magnetic resonance imaging (MRI) of the TMJs in patients with asymptomatic and pain-related TMDs with the number of missing premolars and molars. The results showed that TMD-related pain and MRI-confirmed disc displacement were significantly positively associated with the number of missing premolars and molars ($p < 0.05$).[46]

In their retrospective cross-sectional study, Chatzopoulos et al. examined the relationship between TMDs, parafunctional habits and missing teeth using patient questionnaires and radiographs.[47] The results demonstrated statistically significant associations between the number of missing teeth, gender, age, and the occurrence of TMD symptoms (difficulty opening and closing the mouth, joint clicking, TMJ pain, and difficulty chewing). TMD symptoms were more prevalent among women and younger individuals. However, only chewing difficulty was found to be positively associated with the number of missing teeth, and this complaint is not necessarily directly related to TMDs.[47]

In a study examining the relationship between missing posterior teeth and TMDs, Wang et al. identified slight

associations between the occurrence of TMDs and patients' gender, age, and the number of missing teeth using multivariable logistic regression analysis.[48] Furthermore, the study investigated the distribution of missing teeth according to the number of affected dental quadrants. This distribution was also found to be associated with the occurrence of TMDs. The findings suggest that the odds of presenting with TMDs are higher among individuals with missing posterior teeth in a greater number of quadrants ($p < 0.01$), particularly among young women.[48]

De Sousa et al. investigated potential associations between malocclusion, the presence of 5 or more missing teeth, and TMDs.[49] Their findings suggest that these factors contribute only minimally to the development of TMDs.[49]

In a study published in 2016, Malheiros et al. found that TMD severity was higher among completely edentulous patients.[50] However, they were unable to demonstrate any statistically significant differences between partially edentulous and dentate patients.[50]

A systematic literature review published in 2024 included 21 publications and aimed to examine the relationships between malocclusion and TMJ morphology, as well as the effects of tooth loss and bruxism on TMDs.[51] Eight studies addressing the relationship between TMDs and tooth loss were selected for analysis. Of these, 3 examined morphometric features using radiographs, 2 identified TMD symptoms through self-reported questionnaires, and the remaining 3 performed and reported clinical examinations. These 3 studies concluded that pain and joint noises were associated with the number of missing teeth. These findings are consistent with those of our study, which demonstrated a higher prevalence of TMD symptoms in the group with extensive tooth loss compared with the control group. As outlined in the systematic review, the findings suggest that malocclusion is associated with alterations in TMJ morphology, tooth loss is associated with an increased prevalence and altered characteristics of TMDs, and bruxism is associated with TMD symptoms, including myofascial pain, disc displacement, joint pain, and muscle disorders.[51]

The results of the aforementioned studies are consistent with those obtained in our investigation. The present study revealed differences in the prevalence of selected TMD symptoms among the 3 examined groups: individuals with extensive tooth loss (L); those with prosthodontic rehabilitation (P); and the control group (C). A comparison between the control group and the group with extensive tooth loss revealed a significantly higher prevalence of TMD symptoms in the latter (Fisher's exact test; $p = 0.017$). The corresponding effect size was *OR*: 1.429, which is slightly below the threshold for a medium effect. Logistic regression analysis further revealed that the odds of presenting with TMD symptoms were 1.55 times higher in the presence of tooth loss. The association between the control and prosthodontic rehabilitation groups was less pronounced, with a small effect size (*OR*: 1.233).

A further analysis focusing on pain triggered or aggravated by jaw movements revealed larger effect sizes in both the tooth loss and prosthodontic rehabilitation groups (*OR*: 3.60 and 2.03, respectively). These findings are consistent with the existing literature, which suggests that occlusal factors may play a modest role in the development of TMDs, particularly in cases involving pain that occurs or worsens with jaw movements.

The results of our study revealed a notably high prevalence of TMD symptoms, with nearly ¼ of the individuals examined exhibiting at least one of the major symptoms. Women accounted for approx. twice as many cases as men among participants presenting with TMD symptoms. A significantly higher proportion of women than men exhibited at least one of the major TMD symptoms. Furthermore, although the most prevalent finding in both sexes was joint clicking, pain triggered or aggravated by jaw movements and limited mouth opening were also observed more frequently among women. In the multivariable logistic regression analysis, female gender was identified as a significant predictor of pain triggered or aggravated by jaw movements and limited mouth opening, with large effect sizes (*OR*: 4.85 and 3.79, respectively). Female gender was also associated with a higher likelihood of joint clicking and the occurrence of any of the examined TMD symptoms. The effect sizes in these cases were medium (*OR*: 1.66 for joint clicking and *OR*: 1.71 for the occurrence of major TMD symptoms).

There are several potential explanations for the higher prevalence of TMD symptoms among women, and accumulating evidence suggests that pain sensitivity differs between males and females.[52,53] In addition, pain amplification resulting from the co-occurrence of multiple pain conditions has been identified as a contributing factor to the higher prevalence of TMDs in women. For instance, a study conducted by Marciniak et al. reported a significantly higher prevalence of TMDs (77.3%) among women diagnosed with endometriosis compared with the general population.[54]

Limitations

It is important to acknowledge the limitations of the present study. The data were collected between 2003 and 2004, which should be taken into consideration when interpreting the findings. Epidemiological data collected 2 decades ago may not be directly comparable with the current findings. Nevertheless, the results remain relevant, as they provide insights into the potential impact of tooth loss and prosthodontic rehabilitation on TMJ function and TMD symptoms.

Another limitation is that, at the time of data collection, the diagnostic criteria for TMDs were not as clearly established as they are today. The Diagnostic Criteria for Temporomandibular Disorders (DC/TMD) protocol was not published until 2014,[1] and no Hungarian translation of the Research Diagnostic Criteria for Temporomandibular Disorders (RDC/TMD), originally published in 1992, was available.[55] Consequently, the identification of TMD symptoms relied on the clinical

expertise of the data collectors rather than on the standardized diagnostic criteria. Furthermore, no information was available regarding comorbidities, potential mental health conditions or previous TMD treatment.

Although our study, which was based on the results of a cross-sectional screening examination, would not meet the inclusion criteria established by Manfredini et al., it provides some insight into the 2 questions they posed – "Can prosthodontic rehabilitation be used as treatment for TMDs?" and "Can prosthodontic rehabilitation cause TMDs?"[27] In other words, if prosthodontic rehabilitation were an effective therapeutic approach for TMDs, one might expect the group with the restored dentition to exhibit a lower prevalence of TMD symptoms. Conversely, if prosthodontic rehabilitation contributed to the development of TMDs, a higher prevalence of TMD symptoms might be expected in this group.

Conclusions

The relationship between TMDs and tooth loss has been the focus of extensive research. Despite mounting evidence suggesting that occlusal factors play only a limited role in the development of TMD symptoms, the findings of the present study suggest that tooth loss may be associated with a higher prevalence of TMD symptoms, particularly pain triggered or aggravated by jaw movements. Moreover, prosthodontic rehabilitation alone does not appear to eliminate this association. Female gender was also identified as a significant predictor of the occurrence of all the TMD symptoms examined.

Ethics approval and consent to participate

The study was conducted in accordance with the Declaration of Helsinki, and approved by the Regional and Institutional Committee for Scientific and Research Ethics of Semmelweis University, Budapest, Hungary (SE TUKEB 206/2003). Written informed consent was obtained from all subjects involved in the study.

Data availability

The datasets supporting the findings of the current study are available from the corresponding author on reasonable request.

Consent for publication

Not applicable.

Use of AI and AI-assisted technologies

Artificial intelligence technology was solely utilized to verify the linguistic accuracy of the text.

ORCID iDs

Emőke Márta Takács https://orcid.org/0009-0001-1851-6676
Ibolya Süveges https://orcid.org/0009-0003-7537-8382
Szilvia Ambrus https://orcid.org/0009-0005-5405-4324
Péter Schmidt https://orcid.org/0000-0002-4543-1707
Bálint Jász https://orcid.org/0000-0002-5556-137X
Péter Hermann https://orcid.org/0000-0002-9148-0139
Szandra Körmendi https://orcid.org/0000-0003-4694-1343
Máté Jász https://orcid.org/0000-0002-6717-5126

References

1. Schiffman E, Ohrbach R, Truelove E, et al. Diagnostic Criteria for Temporomandibular Disorders (DC/TMD) for clinical and research applications: Recommendations of the International RDC/TMD Consortium Network and Orofacial Pain Special Interest Group. *J Oral Facial Pain Headache*. 2014;28(1):6–27. doi:10.11607/jop.1151
2. Zieliński G, et al. Global co-occurrence of bruxism and temporomandibular disorders: A meta-regression analysis. *Dent Med Probl*. 2025;62(2):309–321. doi:10.17219/dmp/201376
3. Wieckiewicz M, Jenca Jr. A, Seweryn P, et al. Determination of pain intensity, pain-related disability, anxiety, depression, and perceived stress in Polish adults with temporomandibular disorders: A prospective cohort study. *Front Integr Neurosci*. 2022;16:1026781. doi:10.3389/fnint.2022.1026781
4. Mitrowska-Guźmińska M, Gębska M, Jonko K, et al. Effect of personality type on the occurrence of temporomandibular disorders – a cross-sectional study. *Int J Environ Res Public Health*. 2022;20(1):352. doi:10.3390/ijerph20010352
5. Colonna A, Lobbezoo F, Bracci A, Ferrari M, Val M, Manfredini D. Long-term study on the fluctuation of self-reported awake bruxism in a cohort of healthy young adults. *J Oral Rehabil*. 2025;52(1):37–42. doi:10.1111/joor.13872
6. Šimunović L, Varga ML, Vranić DN, Čuković-Bagić I, Bergman L, Meštrović S. The role of malocclusion and oral parafunctions in predicting signs and symptoms of temporomandibular disorders – a cross-sectional study. *Dent J (Basel)*. 2024;12(7):213. doi:10.3390/dj12070213
7. Bartolucci ML, Parenti SI, Bortolotti F, et al. Sleep bruxism and orofacial pain in patients with sleep disorders: A controlled cohort study. *J Clin Med*. 2023;12(8):2997. doi:10.3390/jcm12082997
8. Walczyńska-Dragon K, Kurek-Górecka A, Niemczyk W, et al. Cannabidiol intervention for muscular tension, pain, and sleep bruxism intensity – a randomized, double-blind clinical trial. *J Clin Med*. 2024;13(5):1417. doi:10.3390/jcm13051417
9. Cigdem Karacay B, SahbazT. Investigation of the relationship between probable sleep bruxism, awake bruxism and temporomandibular disorders using the Diagnostic Criteria for Temporomandibular Disorders (DC/TMD). *Dent Med Probl*. 2023;60(4):601–608. doi:10.17219/dmp/158926
10. Seweryn P, Orzeszek SM, Waliszewska-Prosół M, et al. Relationship between pain severity, satisfaction with life and the quality of sleep in Polish adults with temporomandibular disorders. *Dent Med Probl*. 2023;60(4):609–617. doi:10.17219/dmp/171894
11. Maixner W, Diatchenko L, Dubner R, et al. Orofacial pain prospective evaluation and risk assessment study – the OPPERA study. *J Pain*. 2011;12(Suppl 11):T4–T11.e1-2. doi:10.1016/j.jpain.2011.08.002
12. Grad K, Kazibudzka Z, Pihut M, Wieczorek A. Influence of the pharmacotherapy of general diseases on the severity of symptoms of temporomandibular disorders. *Dent Med Probl*. 2025;62(2):247–253. doi:10.17219/dmp/175417
13. Kaynak BA, Taş S, Tüfek MT, Dağ F, Dikici R. Fatty infiltration and morphology of cervical muscles in patients with temporomandibular disorders: A case–control study. *Dent Med Probl*. 2024;61(4):525–532. doi:10.17219/dmp/166266
14. Pihut ME, Kostrzewa-Janicka J, Orczykowska M, Biegańska-Banaś J, Gibas-Stanek M, Gala A. Initial assessment of the psycho-emotional state of patients with temporomandibular disorders: A pilot study. *Dent Med Probl*. 2024;61(1):153–159. doi:10.17219/dmp/178325
15. Chattrattrai T, Thymi M, Su N, Lobbezoo F. Changes in self-reported sleep and awake bruxism in relation to the management of temporomandibular disorders ("care as usual") in a specialty clinic population. *Dent Med Probl*. 2024;61(5):697–704. doi:10.17219/dmp/193125

16. de Kanter RJ, Battistuzzi PG, Truin GJ. Temporomandibular disorders: "Occlusion" matters! *Pain Res Manag*. 2018;2018:8746858. doi:10.1155/2018/8746858
17. Lai YC, Yap AU, Türp JC. Prevalence of temporomandibular disorders in patients seeking orthodontic treatment: A systematic review. *J Oral Rehabil*. 2020;47(2):270–280. doi:10.1111/joor.12899
18. Al-Khatieeb MM, Nissan LM, Al-Labban YR, Abid M. Occlusal features and temporomandibular joint disorder: A cross-sectional study. *Int J Dent*. 2024;2024:8715166. doi:10.1155/2024/8715166
19. Sipilä K, Näpänkangas R, Könönen M, Alanen P, Suominen AL. The role of dental loss and denture status on clinical signs of temporomandibular disorders. *J Oral Rehabil*. 2013;40(1):15–23. doi:10.1111/j.1365-2842.2012.02345.x
20. Shi Q, Wang Y. Investigation of the prevalence of temporomandibular disorders in 352 aged edentulous individuals [in Chinese]. *Zhonghua Kou Qiang Yi Xue Za Zhi*. 2012;47(1):19–21. doi:10.3760/cma.j.issn.1002-0098.2012.01.007.
21. Manfredini D, Lombardo L, Siciliani G. Temporomandibular disorders and dental occlusion. A systematic review of association studies: End of an era? *J Oral Rehabil*. 2017;44(11):908 –923. doi:10.1111/joor.12531
22. Manfredini D, Perinetti G, Stellini E, Di Leonardo B, Guarda-Nardini L. Prevalence of static and dynamic dental malocclusion features in subgroups of temporomandibular disorder patients: Implications for the epidemiology of the TMD-occlusion association. *Quintessence Int*. 2015;46(4):341–349. doi:10.3290/j.qi.a32986
23. Thomas DC, Singer SR, Markman S. Temporomandibular disorders and dental occlusion: What do we know so far? *Dent Clin North Am*. 2023;67(2):299–308. doi:10.1016/j.cden.2022.11.002
24. Okeson JP. *Management of Temporomandibular Disorders and Occlusion*. 8th ed. St. Louis, MO: Elsevier/Mosby; 2019.
25. Manfredini D, Häggman-Henrikson B, Al Jaghsi A, et al.; International Network for Orofacial Pain and Related Disorders Methodology. Temporomandibular disorders: INfORM/IADR key points for good clinical practice based on standard of care. *Cranio*. 2025;43(1):1–5. doi:10.1080/08869634.2024.2405298
26. Rawat P, Saxena D, Srivastava PA, Sharma A, Swarnakar A, Sharma A. Prevalence and severity of temporomandibular joint disorder in partially versus completely edentulous patients: A systematic review. *J Indian Prosthodont Soc*. 2023;23(3):218–225. doi:10.4103/jips.jips_136_23
27. Manfredini D, Saracutu OI, Cagidiaco EF, Ferrari M. EPA Consensus Project Paper: The relationship between prosthodontic rehabilitations and temporomandibular disorders. *Eur J Prosthodont Restor Dent*. 2023. doi:10.1922/EJPRD_2484Manfredini05
28. European Observatory Policy Brief Series. *European Observatory on Health Systems and Policies*. https://www.ncbi.nlm.nih.gov/books/NBK464588.
29. Zieliński G, Gawda P. Defining effect size standards in temporomandibular joint and masticatory muscle research. *Med Sci Monit*. 2025;31:e948365. doi:10.12659/MSM.948365
30. Kennedy E. Partial Denture Construction: *A Text Book Describing the Technics of Impression Taking and the Construction of That Type of Removable Partial Dentures Which Are Supported and Retained by External Attachments*. Charleston, SC: Tradd Street Press; 2026.
31. Berze I, et al. Prosthetic classification of missing teeth providing possible treatment options. Presented at: ICP & EPA Joint Meeting; September 4–7, 2019, Amsterdam, the Netherlands.
32. Fábián T, Fejérdy P. Prosthetic classification of partially edentulous jaws [in Hungarian]. *Fogorv Sz*. 1979;72(10):310–315. PMID:387455.
33. Fábián T, Fejérdy P. Prosthetic classification of partial edentulousness [in Hungarian]. *Protet Stomatol*. 1981;31(1):35–41
34. Fábián TK, Fejérdy P, Hermann P, eds. *Dentures: Types, Benefits and Potential Complications*. Hauppauge, NY: Nova Science Publishers; 2012.
35. Borbély J, Gera I, Fejérdy P, Soós B, Madléna M, Hermann P. Oral health assessment of Hungarian adult population based on epidemiologic examination [in Hungarian]. *Fogorv Sz*. 2011;104(1):3–8. PMID:21789930.
36. Madléna M, Hermann P, Jáhn M, Fejérdy P. Caries prevalence and tooth loss in Hungarian adult population: Results of a national survey. *BMC Public Health*. 2008;8:364. doi:10.1186/1471-2458-8-364
37. Hermann P, Gera I, Borbély J, Fejérdy P, Madléna M. Periodontal health of an adult population in Hungary: Findings of a national survey. *J Clin Periodontol*. 2009;36(6):449–457. doi:10.1111/j.1600-051X.2009.01395.x
38. Fejérdy P, Borbély J, Schmidt J, Jánh M, Hermann P. Removable partial denture design and its effect on remaining teeth, based on Hungarian national survey [in Hungarian]. *Fogorv Sz*. 2008;101(1):3–11. PMID:18488739.
39. Fejérdy P, Tollas OL, Fejérdy L, Borbély J, Hermann P. Monitoring trends in fixed partial denture design based on national surveys [in Hungarian]. *Fogorv Sz*. 2007;100(6):279–288. PMID:18361200.
40. Tollas OL, Somogyi E, Madléna M, Fejérdy P. Some characteristics of distal cantilever bridges on the basis of two representative studies (in Hungary) [in Hungarian]. *Fogorv Sz*. 2008;101(1):29–32. PMID:18488742.
41. Jáhn M, Schmidt J, Fejérdy L, Tollas OL, Fejérdy P, Madléna M. The prevalence of oral mucosal lesions in Hungary [in Hungarian]. *Fogorv Sz*. 2007;100(2):59–63. PMID:17546896.
42. Madléna M, Hermann P, Tollas O, Gerle J, Fejérdy P. Oral hygienic, nutritional habits and dental surgeon attendance of Hungarian adult population [in Hungarian]. *Fogorv Sz*. 2007;100(3):91–97. PMID:17695044.
43. Madléna M, Fejérdy P, Kaán M, Hermann P. Frequency of signs and symptoms of temporomandibular joint disorders, vertical orthodontic anomalies and their relationships based on screening of a large population [in Hungarian]. *Fogorv Sz*. 2015;108(1):25–31. PMID:26117956.
44. Liu Y, Yin T, He M, Fang C, Peng S. Association of congenitally missing teeth with adult temporomandibular disorders in the urban health checkup population. *BMC Oral Health*. 2023;23(1):188. doi:10.1186/s12903-023-02855-w
45. Jaber M, Khalid A, Gamal A, Faisal R, Mathew A, Ingafou M. A comparative study of condylar bone pathology in patients with and without temporomandibular joint disorders using orthopantomography. *J Clin Med*. 2023;12(18):5802. doi:10.3390/jcm12185802
46. Tallents RH, Macher DJ, Kyrkanides S, Katzberg RW, Moss ME. Prevalence of missing posterior teeth and intraarticular temporomandibular disorders. *J Prosthet Dent*. 2002;87(1):45–50. doi:10.1067/mpr.2002.121487
47. Chatzopoulos GS, Sanchez M, Cisneros A, Wolff LF. Prevalence of temporomandibular symptoms and parafunctional habits in a university dental clinic and association with gender, age, and missing teeth. *Cranio*. 2019;37(3):159–167. doi:10.1080/08869634.2017.1399649
48. Wang MQ, Xue F, He JJ, Chen JH, Chen CS, Raustia A. Missing posterior teeth and risk of temporomandibular disorders. *J Dent Res*. 2009;88(10):942–945. doi:10.1177/0022034509344387
49. de Sousa ST, Cardoso de Mello VV, Magalhães BG, et al. The role of occlusal factors on the occurrence of temporomandibular disorders. *Cranio*. 2015;33(3):211–216. doi:10.1179/2151090314Y.0000000015
50. Malheiros AS, Carvalhal ST, Pereira TL, et al. Association between tooth loss and degree of temporomandibular disorders: A comparative study. *J Contemp Dent Pract*. 2016;17(3):235–239. doi:10.5005/jp-journals-10024-1833
51. Lekaviciute R, Kriauciunas A. Relationship between occlusal factors and temporomandibular disorders: A systematic literature review. *Cureus*. 2024;16(2):e54130. doi:10.7759/cureus.54130
52. Ostrom C, Bair E, Maixner W, et al. Demographic predictors of pain sensitivity: Results from the OPPERA study. *J Pain*. 2017;18(3):295–307. doi:10.1016/j.jpain.2016.10.018
53. Seweryn P, Waliszewska-Prosół M, Straburzyński M, et al. Prevalence of central sensitization and somatization in adults with temporomandibular disorders – a prospective observational study. *J Oral Facial Pain Headache*. 2024;38(4):33–44. doi:10.22514/jofph.2024.037
54. Marciniak T, Walewska N, Skoworodko A, Bobowik P, Kruk-Majtyka W. Prevalence of temporomandibular disorders in adult women with endometriosis. *J Clin Med*. 2024;13(24):7615. doi:10.3390/jcm13247615
55. Dworkin SF, LeResche L. Research Diagnostic Criteria for Temporomandibular Disorders: Review, criteria, examinations and specifications, critique. *J Craniomandib Disord*. 1992;6(4):301–355. PMID:1298767.

Original paper

Predicting osteoradionecrosis in nasopharyngeal carcinoma: The role of the GLUCAR index

Efsun Somay[1,A–F], Erkan Topkan[2,A–F], Sibel Bascil[3,A–F], Sukran Senyurek[4,A–F], Duriye Ozturk[5,A–F], Nilufer Kılıc Durankuş[4,A–F], Ugur Selek[4,A–F]

[1] Department of Oral and Maxillofacial Surgery, Faculty of Dentistry, Baskent University, Ankara, Turkey
[2] Department of Radiation Oncology, Faculty of Medicine, Baskent University, Adana, Turkey
[3] Department of Periodontology, Faculty of Dentistry, Baskent University, Ankara, Turkey
[4] Department of Radiation Oncology, School of Medicine, Koc University, Istanbul, Turkey
[5] Department of Radiation Oncology, Faculty of Medicine, Afyonkarahisar Health Sciences University, Turkey

A – research concept and design; B – collection and/or assembly of data; C – data analysis and interpretation;
D – writing the article; E – critical revision of the article; F – final approval of the article

Dental and Medical Problems, ISSN 1644-387X (print), ISSN 2300-9020 (online) *Dent Med Probl*. 2026;63(5):1199–1208

Address for correspondence
Efsun Somay
E-mail: efsuner@gmail.com

Funding sources
None declared

Conflict of interest
None declared

Acknowledgements
None declared

Received on August 11, 2025
Reviewed on September 9, 2025
Accepted on September 27, 2025

Published online on October 30, 2026

Abstract

Background. Osteoradionecrosis (ORN) is a debilitating complication of concurrent chemoradiotherapy (CCRT) in patients with locally advanced nasopharyngeal carcinoma (LANPC). The early identification of patients at risk is crucial.

Objectives. The aim of the present study was to evaluate the predictive value of the GLUCAR index, which integrates fasting glucose and the C-reactive protein (CRP)-to-albumin ratio (CAR), for assessing the risk of ORN in patients with LANPC undergoing CCRT.

Material and methods. A retrospective analysis was conducted in a consecutive cohort of 220 patients with LANPC who underwent definitive CCRT. The patients were stratified into high- and low-GLUCAR groups according to their pre-treatment GLUCAR index levels, using the optimal cut-off value determined by the receiver operating characteristic (ROC) curve analysis. Osteoradionecrosis was defined as the event of interest. Multivariate Cox proportional hazards regression analysis was performed to identify independent predictors of ORN development.

Results. The overall incidence of ORN was 10.9%. The optimal cut-off value of the GLUCAR index for predicting ORN was 35.7 (area under the curve (AUC): 0.773; sensitivity: 75.0%, and specificity: 76.5%). Patients with a GLUCAR index ≥35.7 had a significantly higher incidence of ORN than those with a GLUCAR index <35.7 (27.3% vs. 3.9%; $p < 0.001$). The multivariate analysis identified a GLUCAR index ≥35.7 as an independent predictor of ORN development (odds ratio (*OR*): 9.09; 95% confidence interval (*CI*): 2.48–25.02; $p < 0.001$). Other independent predictors included smoking, pre-CCRT tooth extractions, a higher number of chemotherapy cycles, and a higher mandibular radiation dose ($p < 0.05$ for all).

Conclusions. The results of this study suggest that a pre-treatment GLUCAR index ≥35.7 is independently associated with an increased risk of ORN in patients with LANPC undergoing definitive CCRT.

Keywords: nasopharyngeal carcinoma, osteoradionecrosis, predictive biomarker, GLUCAR index, chemoradiotherapy

Cite as
Somay E, Topkan E, Bascil S, et al. Predicting osteoradionecrosis in nasopharyngeal carcinoma: The role of the GLUCAR index. *Dent Med Probl*. 2026;63(5):1199–1208. doi:10.17219/dmp/211426

DOI
10.17219/dmp/211426

Copyright
Copyright by Author(s)
This is an article distributed under the terms of the Creative Commons Attribution 3.0 Unported (CC BY 3.0) (https://creativecommons.org/licenses/by/3.0/)

Highlights

- An elevated pre-treatment GLUCAR index (≥35.7) independently predicts osteoradionecrosis (ORN) in patients with with locally advanced nasopharyngeal carcinoma (LANPC) undergoing concurrent chemoradiotherapy (CCRT).
- The GLUCAR index outperformed other significant clinical factors in predicting ORN, with an area under the curve (AUC) of 82.2%.
- The GLUCAR index may help identify high-risk patients, implement appropriate preventive strategies, optimize supportive care and individualize radiation treatment planning.

Introduction

Nasopharyngeal carcinoma (NPC) is a distinct malignancy within the spectrum of head and neck cancers, characterized by unique epidemiological features and marked sensitivity to both radiotherapy and chemotherapy. In patients with locally advanced nasopharyngeal carcinoma (LANPC), concurrent chemoradiotherapy (CCRT) remains the cornerstone of curative treatment, administered either as definitive therapy or following induction chemotherapy, and is associated with high rates of locoregional control and improved survival.[1,2] However, with the increasing intensity of treatment protocols, the risk of serious late radiation-induced complications, particularly osteoradionecrosis (ORN) of the jaw, has become an important clinical concern.

Although the primary tumor site in NPC is anatomically distant from the mandible, cumulative radiation exposure, particularly in patients with advanced primary tumors or extensive nodal disease requiring larger radiation fields, may still compromise mandibular structures and lead to ORN. Although the incidence of ORN in NPC is generally lower than that reported in oral cavity or oropharyngeal cancers, the reported rates in LANPC populations remain substantial, reaching 7–10%.[3–6] Given the debilitating nature of ORN and its profound impact on patients' quality of life (QoL), the early identification of individuals at high risk remains an important unmet clinical need.

Osteoradionecrosis (ORN) is defined as exposed irradiated bone that fails to heal within 3 months, in the absence of tumor recurrence or metastatic involvement of the mandible.[7] Its development involves a multifactorial pathogenesis characterized by radiation-induced endarteritis, tissue hypoxia, hypocellularity, and progressive fibrosis, which collectively impair the regenerative capacity of bone.[8] While traditional risk assessment has primarily focused on local factors, such as the radiation dose, dental status and oral hygiene, increasing attention is being paid to systemic factors that may influence tissue healing and host susceptibility to ORN.[9]

The GLUCAR index, an emerging composite biomarker integrating the fasting blood glucose levels with the C-reactive protein (CRP)-to-albumin ratio (CAR), has been proposed as a potential indicator of systemic metabolic stress and inflammation.[10] Both components of the GLUCAR index are associated with biological mechanisms that can compromise wound healing. Hyperglycemia disrupts angiogenesis and impairs immune function, whereas an elevated CAR reflects systemic inflammation, immune dysregulation and malnutrition, all of which may synergistically impair tissue recovery following radiation therapy.[11–13] Elevated glucose levels promote the accumulation of advanced glycation end-products (AGEs), induce endothelial dysfunction and interfere with bone remodeling.[14] Similarly, an elevated CAR reflects a catabolic state characterized by depleted protein reserves, potentially limiting the availability of essential substrates for cellular repair and collagen synthesis.[13]

Clinically, the first pivotal study by Somay et al. investigated the prognostic value of the GLUCAR index for tooth loss following CCRT in patients with LANPC.[8] The authors demonstrated that patients with a pre-treatment GLUCAR index ≥31.8 had a significantly higher risk of tooth loss than those with lower values (84.4% vs. 47.4%; $p < 0.001$).[8] These findings suggest that hyperglycemia, systemic inflammation and hypoalbuminemia may collectively reflect an inflammatory-catabolic state that predisposes patients to radiation-induced bone complications.

Beyond NPC, the GLUCAR index has also demonstrated prognostic significance in other malignancies characterized by systemic inflammation and metabolic dysregulation. For instance, a recent analysis showed that a GLUCAR index ≥42.8 independently predicted poorer survival in patients with locally advanced pancreatic cancer.[15] Despite its potential biological relevance, no previous studies have investigated the predictive value of the GLUCAR index for ORN in patients with LANPC undergoing definitive CCRT.

Given the established associations between metabolic-inflammatory dysregulation and impaired tissue healing following radiation therapy, we hypothesized that an elevated pre-treatment GLUCAR index could serve as a systemic marker of ORN risk.[16] Accordingly, this study aimed to investigate the association between pre-treatment GLUCAR index levels and the subsequent ORN development, with the ultimate goal of refining the current risk stratification models and informing individualized pre-radiation management strategies.

Patients and methods

Ethical considerations

This retrospective study was conducted in collaboration with the Department of Radiation Oncology and the Dentistry Clinics at Baskent University Faculty of Medicine, Adana, Turkey. Before data collection, the study protocol received formal approval from the Institutional Review Board of Baskent University Faculty of Medicine (project no. DKA:19/39), ensuring compliance with applicable ethical standards. Eligible participants were selected according to the predefined inclusion criteria, and provided written informed consent before undergoing comprehensive oral and dental assessments and CCRT. The consent covered the collection and subsequent analysis of relevant clinical data, including blood samples, sociodemographic characteristics, medical history, and dental radiographs, as well as the use of anonymized data for academic presentations and publications. The present study was reported in accordance with the Strengthening the Reporting of Observational Studies in Epidemiology (STROBE) guidelines.[17]

Patient selection

The Dentistry Clinics at Baskent University Adana Research and Treatment Center reviewed the medical records of patients with LANPC who underwent CCRT, including pre- and post-CCRT oral and dental examinations performed between February 2010 and January 2025. Patients were eligible for inclusion if they met the following criteria: age ≥18 years; histopathologically confirmed squamous cell carcinoma (SCC); locally advanced disease according to the 8th edition of the American Joint Committee on Cancer (AJCC) staging system; and no history of previous malignancy, systemic chemotherapy, or head and neck radiotherapy. Additionally, patients were required to have available complete blood count (CBC) and biochemical test results obtained before CCRT initiation, as well as documented pre- and post-CCRT dental examination findings and panoramic radiographs.

Patients with mandibular invasion by the primary tumor or metastatic lymph nodes, a previous diagnosis of jaw ORN, a history of jaw surgery, the current use of corticosteroids or other immunomodulatory agents, or a history of blood transfusion within 30 days before CCRT initiation were excluded from the study. Additionally, patients with active systemic inflammatory or immunological conditions, including rheumatological, renal and respiratory diseases, viral hepatitis, immunosuppressive conditions, collagen vascular diseases, chronic inflammatory disorders, and glycogen storage diseases, were considered ineligible.

These restrictions were applied to minimize potential confounding related to pre-existing systemic, metabolic, inflammatory, and immunological conditions, as well as medication use. To further reduce potential bias, patients with periodontitis, cardiovascular or other vascular diseases, a history of stroke, metabolic syndrome, or diabetes mellitus were also excluded, as these conditions may independently increase the risk of tooth loss.

Baseline oral examination

All patients underwent a comprehensive dental assessment performed by an experienced oral and maxillofacial surgeon (E.S.) before initiating CCRT. The assessment followed the established protocols of the American Dental Association (ADA) and the relevant regulations of the US Food and Drug Administration (FDA).[18] Panoramic radiographic examinations were performed using the J. Morita Veraviewepocs 2D system (Kyoto, Japan) to facilitate a thorough evaluation of each patient's dental status. These examinations formed part of the routine dental assessment protocol for all patients diagnosed with head and neck cancer.

Each tooth was carefully examined for dental caries in accordance with the World Health Organization (WHO) criteria.[19] Clinical examinations were performed using illuminated dental mirrors and explorers to detect even subtle signs of caries. Teeth with inadequate periodontal support, extensive structural deterioration rendering them non-restorable, or apical lesions considered unsuitable for successful endodontic treatment were scheduled for extraction. Superficial carious lesions were treated with appropriate dental restorations to prevent further progression.

To optimize oral health before and during oncological treatment, all patients received individualized instructions on appropriate oral hygiene practices. Professional dental scaling was also performed to remove plaque and calculus, thereby improving oral hygiene and helping maintain dental health throughout the treatment period.

GLUCAR index calculation and measurement

The GLUCAR index, previously developed by our research group as a novel prognostic biomarker, was calculated using the following formula: GLUCAR index = (fasting glucose [mg/dL] × CRP [mg/dL]) / albumin [g/dL].[8] This index integrates pre-treatment systemic glucose metabolism, inflammation, immune status, and nutritional status using routinely available clinical parameters. Fasting glucose, CRP and serum albumin levels were measured in the blood samples collected on the first day of CCRT. All biochemical analyses were performed using the Abbott ARCHITECT c8000 biochemistry autoanalyzer (Chicago, USA), in accordance with the manufacturer's instructions and standard quality assurance protocols.[20]

Chemoradiotherapy protocol

All patients received simultaneous integrated boost intensity-modulated radiotherapy (SIB-IMRT), as previously described.[21] Target volumes were delineated using co-registered imaging modalities, including computed tomography (CT), 18-F-fluorodeoxyglucose positron emission tomography/CT (18-F-FDG PET/CT) and magnetic resonance imaging (MRI). The prescribed radiation doses were 70 Gy, 59.4 Gy, and 54 Gy for the high-, intermediate-, and low-risk planning target volumes (PTVs), respectively, delivered in 33 daily fractions, with no treatment sessions scheduled on weekends.[22] Concurrent cisplatin chemotherapy was administered every 21 days for 3 cycles during radiotherapy. Following CCRT, all patients were advised to receive 2 additional cycles of adjuvant chemotherapy consisting of cisplatin and 5-fluorouracil. Antiemetic medication, hydration and nutritional support were provided as clinically indicated.

Follow-up examination

The protocol described in the "Baseline oral examination" section was consistently applied to ensure a comprehensive assessment of each patient's oral health. Additional oral and dental evaluations were performed according to a predefined follow-up schedule, including routine examinations at 1, 3, 6, 9, and 12 months after CCRT, followed by assessments every 6 months thereafter or more frequently, as clinically indicated. At each follow-up visit, clinical findings and radiographic data were systematically recorded to monitor changes in oral health and facilitate the early detection of potential complications. Using the same assessment criteria described in the "Baseline oral examination" section, each patient's ongoing dental care needs were evaluated, taking into consideration oral hygiene status, periodontal health, and any signs of treatment-related adverse effects. All findings were thoroughly documented to provide a comprehensive record for guiding subsequent dental management and therapeutic interventions.

Diagnosis of osteoradionecrosis of the jaw

The diagnosis of ORN was established based on clinical and radiological findings, including radiographic evidence of ORN in the presence of intact overlying mucosa.[23] Clinically, ORN was defined as necrotic irradiated bone that remained unhealed for at least 3 months, in the absence of evidence of tumor recurrence or metastatic disease. To facilitate early detection, all patients underwent systematic clinical and radiological assessments at 1, 3, 6, 9, 12, 18, and 24 months after the completion of CCRT. Thereafter, the same follow-up protocol was continued at 6-month intervals or more frequently if ORN was detected. The severity of ORN was classified according to the Notani classification system, which takes into account the anatomical extent of the lesions and the associated osseous changes.[24]

Statistical analysis

The primary objective of this study was to evaluate the association between pre-treatment GLUCAR index values and the subsequent incidence of ORN during the follow-up period. Continuous variables were summarized using medians (*Me*) and interquartile ranges (*IQR*), while categorical variables were presented as frequencies and percentages. Between-group comparisons were performed using appropriate statistical methods, including Student's t test for continuous variables and the χ^2 test for categorical variables. The receiver operating characteristic (ROC) curve analysis was performed to determine the optimal cut-off value of the pre-treatment GLUCAR index for discriminating between patients with and without ORN. The optimal cut-off was identified using the maximum Youden index (J), which represents the difference between the true-positive rate (sensitivity) and the false-positive rate (1 – specificity), thereby optimizing the balance between sensitivity and specificity. Furthermore, logistic regression analysis was performed to identify independent predictors of ORN development following treatment. All statistical analyses were conducted using IBM SPSS Statistics for Windows, v. 26.0 (IBM Corp., Armonk, USA). All statistical tests were two-sided, and a p-value of less than 0.05 was considered statistically significant.

Results

This analysis involved 220 patients who met the inclusion criteria. The optimal cut-off value of the GLUCAR index for predicting the risk of ORN was determined using the ROC curve analysis, which identified an optimal threshold of 35.7 (area under the curve (AUC): 77.3%; sensitivity: 75.0%; specificity: 76.5%; Youden's J index: 0.515). Based on this threshold, 154 patients (70.0%) were classified as having a GLUCAR index <35.7, while 66 patients (30.0%) had a GLUCAR index ≥35.7 (Fig. 1).

Baseline characteristics

Baseline characteristics according to GLUCAR index group are summarized in Table 1. The median age of the overall cohort was 55.5 years (range: 18–78 years). Patients with a GLUCAR index ≥35.7 were significantly younger than those with a GLUCAR index <35.7, with median ages of 53.5 and 57.0 years, respectively (p = 0.015). The cohort comprised 145 males (65.9%) and 75 females (34.1%), with no significant differences in gender distribution between the GLUCAR index groups (p = 0.350). Smoking prevalence was higher in the GLUCAR index <35.7

Table 1. Baseline and treatment characteristics of the entire study cohort according to the 2 GLUCAR index groups (Student's *t* test or the χ^2 test)

Characteristics		All patients (*N* = 220)	GLUCAR index <35.7 (*n* = 154)	GLUCAR index ≥35.7 (*n* = 66)	*p*-value
Age [years]		55.5 (18–78)	57.0 (18–77)	53.5 (18–78)	0.015*
Gender	M	145 (65.9)	98 (63.6)	47 (71.2)	0.350
	F	75 (34.1)	56 (36.4)	19 (28.8)	
Smoking status	yes	68 (30.9)	54 (35.1)	14 (21.2)	0.042*
	no	152 (69.1)	100 (64.9)	52 (78.8)	
Alcohol consumption	yes	124 (56.4)	89 (57.8)	35 (53.0)	0.550
	no	96 (43.6)	65 (42.2)	31 (47.0)	
Diabetes mellitus	present	172 (78.2)	133 (86.4)	39 (59.1)	0.001*
	absent	48 (21.8)	21 (13.6)	27 (40.9)	
Pre-CCRT tooth extraction	yes	142 (64.5)	82 (53.2)	60 (90.9)	<0.001*
	no	78 (35.5)	72 (46.8)	6 (9.1)	
T-stage group	1–2	90 (40.9)	61 (39.6)	29 (43.9)	0.480
	3–4	130 (59.1)	93 (60.4)	37 (56.1)	
N-stage group	0–1	152 (69.1)	109 (70.8)	43 (65.2)	0.032*
	2–3	68 (30.9)	45 (29.2)	23 (34.8)	
Fasting glucose [mg/dL]		98 (73–189)	96 (73–158)	107 (82–189)	0.032*
CAR		2.9 (2.3–6.9)	2.4 (2.3–3.4)	3.9 (2.7–6.9)	0.004*

Data presented as median (interquartile range) (*Me* (*IQR*)), or as number (percentage) (*n* (%)).
CCRT – concurrent chemoradiotherapy; T – tumor; N – node; CAR – C-reactive protein (CRP)-to-albumin ratio; M – male; F – female; * statistically significant.

group (35.1%) than in the GLUCAR index ≥35.7 group (21.2%) (p = 0.042). Additionally, a significantly larger proportion of patients in the GLUCAR index ≥35.7 group had diabetes mellitus (40.9%) than in the GLUCAR index <35.7 group (13.6%) (p = 0.001). The frequency of pre-CCRT tooth extractions was also significantly higher in the GLUCAR index ≥35.7 group (90.9%) than in the GLUCAR index <35.7 group (53.2%) (p < 0.001). No significant differences were observed between the groups regarding alcohol consumption, T-stage or N-stage. The median follow-up duration for the entire cohort was 36.0 months (range: 12–78 months).

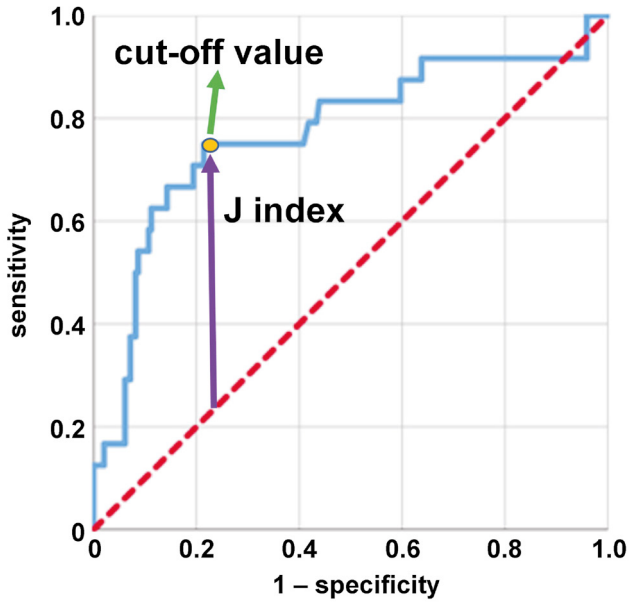

Fig. 1. Receiver operating characteristic (ROC) curve of the GLUCAR index for predicting the risk of osteoradionecrosis (ORN)

The optimal cut-off value of 35.7 yields an area under the curve (AUC) value of 0.773, sensitivity of 75.0% and specificity of 76.5%.

Post-CCRT characteristics

The characteristics observed following CCRT are summarized in Table 2. The prevalence of tooth extractions after CCRT was significantly higher in the GLUCAR index ≥35.7 group (90.9%) than in the GLUCAR index <35.7 group (53.2%) (p < 0.001). Additionally, the incidence of ORN was significantly higher in the GLUCAR index ≥35.7 group (27.3%) than in the GLUCAR index <35.7 group (3.9%) (p < 0.001). No significant differences were found between the groups regarding the number of concurrent or adjuvant chemoradiotherapy cycles, the maximum mandibular dose (MMD), or the MMD group.

The overall incidence of ORN in the study cohort was 10.9%, with 24 of the 220 patients affected. Among these 24 patients, the distribution of the Notani stages was as follows: stage 0 in 1 patient (4.2%); stage 1 in 14 patients (58.3%); and stage 2 in 9 patients (37.5%). In the subgroup analysis, ORN was observed in 27.3% of patients with a GLUCAR index ≥35.7, compared with 3.9% of those with a GLUCAR index <35.7 (p < 0.001). No significant differences in Notani stage distribution were observed between the 2 GLUCAR index groups (p = 0.790)

Table 2. Post-CCRT (concurrent chemoradiotherapy) characteristics of the entire cohort according to the 2 GLUCAR index groups (Student's *t* test or the χ^2 test)

Characteristics		All patients (*N* = 220)	GLUCAR index <35.7 (*n* = 154)	GLUCAR index ≥35.7 (*n* = 66)	*p*-value
CCRT cycles	1	43 (19.5)	26 (16.9)	17 (25.8)	0.170
	2–3	177 (80.5)	128 (83.1)	49 (74.2)	
Adjuvant chemoradiotherapy cycles	0	62 (28.2)	37 (24.0)	25 (37.9)	0.120
	1–2	158 (71.8)	117 (76.0)	41 (62.1)	
Post-CCRT tooth extractions	present	142 (64.5)	82 (53.2)	60 (90.9)	<0.001*
	absent	78 (35.5)	72 (46.8)	6 (9.1)	
MMD [Gy]		37.0 (11.3–52.3)	36.8 (11.3–52.3)	37.6 (12.2–51.1)	0.780
MMD group	<37.0 Gy	109 (49.5)	75 (48.7)	34 (51.5)	0.670
	≥37.0 Gy	111 (50.5)	79 (51.3)	32 (48.5)	
ORN	present	24 (10.9)	6 (3.9)	18 (27.3)	<0.001*
	absent	196 (89.1)	148 (96.1)	48 (72.7)	
Notani ORN stage[a]	0	1 (4.2)	0 (0.0)	1 (5.6)	0.790
	1	14 (58.3)	4 (66.7)	10 (55.6)	
	2	9 (37.5)	2 (33.3)	7 (38.9)	

Data presented as *Me* (*IQR*), or as *n* (%).
MMD – maximum mandibular dose; ORN – osteoradionecrosis; [a] for 24 patients with ORN (*n* = 6 for the GLUCAR index <35.7 group, and *n* = 18 for the GLUCAR index ≥35.7 group); * statistically significant.

Osteoradionecrosis predictors: Univariate and multivariate analysis

In the univariate analysis (Table 3), the following factors were significantly associated with the occurrence of ORN: smoking status (p = 0.011); pre-CCRT tooth extractions (p = 0.003); the number of CCRT cycles (p = 0.030); the MMD group (p < 0.001); and the GLUCAR index group (p < 0.001).

In the multivariate logistic regression analysis, the following factors were identified as independent predictors of ORN: smoking status (odds ratio (*OR*): 3.70; 95% confidence interval (*CI*): 1.85–8.33; p = 0.024); pre-CCRT tooth extractions (*OR*: 5.88; 95% *CI*: 2.70–7.14; p = 0.007); the number of CCRT cycles (*OR*: 1.69; 95% *CI*: 1.19–2.44; p = 0.042); the MMD group (*OR*: 4.76; 95% *CI*: 1.54–8.17; p < 0.001); and the GLUCAR index group (*OR*: 9.09; 95% *CI*: 2.44–25.67; p < 0.001). Patients with a GLUCAR index ≥35.7 had a substantially higher risk of developing ORN than those with a GLUCAR index <35.7 (27.3% vs. 3.9%; p < 0.001), independent of other clinical factors (Table 3, Fig. 2).

The ROC curve analysis evaluating the predictive performance of the 5 significant factors for ORN demonstrated that GLUCAR index grouping was the strongest predictor, with the highest AUC (82.2%), followed by pre-CCRT tooth extraction status (76.0%), the MMD group (66.9%), smoking status (65.2%), and the number of CCRT cycles (62.7%) (Fig. 3).

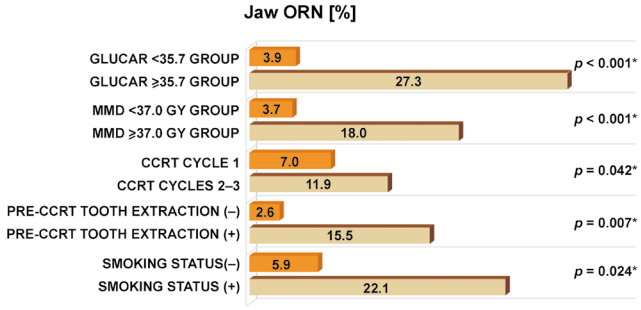

Fig. 2. Bar chart showing the rates of osteoradionecrosis (ORN) according to each factor identified as an independent predictor in the multivariate analysis

*statistically significant.

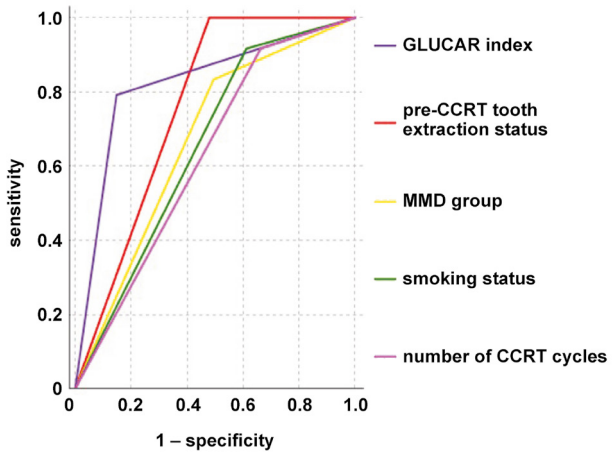

Fig. 3. Receiver operating characteristic (ROC) curves illustrating the predictive performance of factors identified as independently associated with osteoradionecrosis (ORN) in the multivariate analysis

The respective AUCs were as follows: GLUCAR index grouping, 82.2%; pre-CCRT tooth extraction status, 76.0%; the MMD group, 66.9%; smoking status, 65.2%; and the number of CCRT cycles, 62.7%.

Table 3. Univariate and multivariate analyses of the risk factors for osteoradionecrosis (ORN) (the univariate analysis was performed using the log-rank test, and the multivariate analysis was conducted using logistic regression)

Factors		All patients *N* = 220	Patients with ORN *n* = 24	Univariate analysis *p*-value	Multivariate analysis *p*-value	*OR* (95% *CI*)
Gender	M	145 (65.9)	16 (11.3)	0.930	–	–
	F	75 (34.1)	8 (10.7)			
Smoking status	yes	68 (30.9)	15 (22.1)	0.011*	0.024*	3.70 (1.85–8.33)
	no	152 (69.1)	9 (5.9)			
Alcohol consumption	yes	124 (56.4)	13 (10.5)	0.830	–	–
	no	96 (43.6)	11 (11.5)			
Diabetes mellitus	present	172 (78.2)	20 (11.6)	0.320	–	–
	absent	48 (21.8)	4 (8.3)			
Pre-CCRT tooth extractions	yes	142 (64.5)	22 (15.5)	0.003*	0.007*	5.88 (2.70–7.14)
	no	78 (35.5)	2 (2.6)			
T-stage group	1–2	90 (40.9)	8 (8.9)	0.270	–	–
	3–4	130 (59.1)	16 (12.3)			
N-stage group	0–1	68 (30.9)	6 (8.8)	0.410	–	–
	2–3	152 (69.1)	18 (11.8)			
CCRT cycles	1	43 (19.5)	3 (7.0)	0.030*	0.042*	1.69 (1.19–2.44)
	2–3	177 (80.5)	21 (11.9)			
Adjuvant chemoradiotherapy cycles	0	62 (28.0)	6 (9.7)	0.580	–	–
	1–2	158 (72.0)	18 (11.4)			
MMD group	<37.0 Gy	109 (49.5)	4 (3.7)	<0.001*	<0.001*	4.76 (1.54–8.17)
	≥37.0 Gy	111 (50.5)	20 (18.0)			
GLUCAR index group	<35.7	154 (70.0)	6 (3.9)	<0.001*	<0.001*	9.09 (2.44–25.67)
	≥35.7	66 (30.0)	18 (27.3)			

Data presented as *n* (%).
OR – odds ratio; *CI* – confidence interval; * statistically significant.

Discussion

In this retrospective study of 220 patients with LANPC treated with CCRT, we found that an elevated pre-treatment GLUCAR index (≥35.7), a novel composite biomarker reflecting metabolic, immune, inflammatory, and nutritional status, was independently associated with a significantly increased risk of developing jaw ORN. To the best of our knowledge, this is the first study to investigate the predictive value of the GLUCAR index for radiation-induced bone complications in patients with NPC.

In addition to the GLUCAR index, our multivariate analysis identified several independent risk factors associated with an increased risk of ORN, including smoking, pre-CCRT tooth extractions and the number of CCRT cycles. Smoking is a well-established risk factor for impaired tissue health, as it promotes hypoxia, impairs angiogenesis and alters immune responses, all of which compromise soft tissue and bone healing following radiotherapy.[25,26] Moreover, the vasoconstrictive and pro-inflammatory effects of tobacco constituents may exacerbate radiotherapy-induced endothelial damage, further increasing the risk of ORN.[27] Although pre-CCRT dental extractions are often necessary to eliminate potential sources of infection, these procedures may predispose patients to ORN, particularly when radiotherapy begins before adequate healing of the oral mucosa and the underlying bone has occurred.[28] Our results also indicate that patients receiving more intensive CCRT regimens, as reflected by a higher number of CCRT cycles, may face an increased risk of ORN. This association may reflect cumulative systemic toxicity, which can impair bone remodeling, increase oxidative stress, deplete the essential nutrients required for tissue repair, and exacerbate radiation-induced endothelial dysfunction and hypoxia.[29] Taken together, these factors may create an unfavorable environment for mandibular bone healing, particularly when compounded by high radiation doses.

The incidence of ORN in our cohort was 10.9%, which is consistent with previously reported rates of 7–10% in high-risk LANPC populations treated with modern intensity-modulated radiation therapy (IMRT) techniques.[29,30] The pathogenesis of ORN is multifactorial and involves radiation-induced vascular injury, chronic hypoxia, hypocellularity, and impaired bone remodeling.[7,29,31] High-dose radiation damages endothelial cells in small blood vessels, leading to progressive obliterative endarteritis, reduced tissue perfusion and persistent hypoxia. This chronic ischemic state compromises osteoblast function

and suppresses bone remodeling, both of which are essential for maintaining skeletal integrity and facilitating tissue repair.[32] Moreover, radiation induces fibroatrophic changes in the periosteum and bone marrow, further diminishing the regenerative capacity of these tissues.[33] Importantly, patients undergoing CCRT may be at an increased risk of ORN compared with those receiving radiotherapy alone, as chemotherapy may potentiate radiation-induced damage to bone and the surrounding soft tissues.[34]

In addition to the detrimental effects of radiation on bone healing, systemic pro-inflammatory and catabolic states, including hyperglycemia, increased systemic inflammation, immunosuppression, and malnutrition, as reflected by an elevated CAR, may further impair tissue repair mechanisms by promoting oxidative stress, dysregulated cytokine signaling and impaired cellular metabolism. In this context, the novel GLUCAR index, which integrates fasting glucose and CAR, may serve as a surrogate marker of host vulnerability to ORN. Hyperglycemia disrupts endothelial nitric oxide signaling, promotes the formation of AGEs and induces oxidative stress, all of which contribute to endothelial dysfunction, impaired angiogenesis and reduced collagen synthesis.[8,10] Furthermore, hyperglycemia adversely affects osteoblast differentiation and promotes osteoclast-mediated bone resorption, thereby compounding the detrimental effects of radiation on bone metabolism. Therefore, an elevated GLUCAR index may reflect an unfavorable systemic metabolic and inflammatory environment that facilitates the initiation and progression of ORN following CCRT.

Nonetheless, despite the compelling biological rationale supporting this hypothesis, it requires validation through well-designed basic and clinical research. Future studies should aim to elucidate the underlying biological mechanisms and provide a more comprehensive understanding of the predictive capacity of the GLUCAR index for ORN. Such investigations will help establish more robust evidence regarding the clinical utility of the GLUCAR index as a predictive tool.

From a translational perspective, the current findings highlight the potential of the GLUCAR index as a pretreatment biomarker for stratifying the risk of ORN in patients with LANPC undergoing definitive CCRT. If validated in prospective multicenter studies, the routine assessment of the GLUCAR index could facilitate the early identification of patients at increased risk of radiation-induced mandibular injury. In these high-risk individuals, appropriate preventive strategies could be implemented proactively. These may include stricter glycemic control, individualized nutritional interventions aimed at optimizing protein and micronutrient intake, and intensified dental management protocols designed to minimize the need for tooth extractions during or after treatment.

Beyond systemic interventions, the GLUCAR index may also have implications for radiation treatment planning. In patients with elevated GLUCAR index values, clinicians could consider more aggressive mandibular-sparing approaches, including advanced IMRT techniques with stricter mandibular dose constraints or, where available, intensity-modulated proton therapy (IMPT), to further reduce radiation exposure to the mandible. Such individualized approaches may help reduce the incidence of ORN, preserve long-term oral function, and ultimately improve QoL in this vulnerable population.[25,26,30,35]

Limitations

Several limitations of this study should be acknowledged. First, the retrospective design may have introduced inherent biases, including selection bias and unmeasured confounding. Although we attempted to address these issues through multivariate analysis incorporating key clinical factors, the inherent limitations of retrospective studies may still affect the robustness of our findings. Second, this study was conducted at a single institution, which may limit the generalizability of the results. Validation in large, independent, multicenter cohorts encompassing diverse clinical settings, patient demographics and radiotherapy techniques is therefore necessary to establish the broader applicability of our findings. Third, although the overall incidence of ORN in our cohort (10.9%) was consistent with previously reported rates, the absolute number of ORN cases (n = 24) was relatively small. This limitation may have reduced the statistical power of subgroup analyses, particularly those evaluating the relationship between the GLUCAR index and Notani stage distribution, which reflects ORN severity. Fourth, although the GLUCAR index incorporates important metabolic, immune, inflammatory, and nutritional markers, it does not account for other systemic factors that may significantly influence bone healing. These include vitamin D deficiency, sarcopenia, and alterations in the oral and gut microbiomes. Therefore, future prospective studies should consider incorporating these additional variables and evaluating changes in the GLUCAR index throughout treatment. Such approaches may provide a more comprehensive understanding of the pathophysiology of ORN and facilitate the development of more accurate predictive models for identifying patients at risk.

Conclusions

The findings of this study suggest that an elevated GLUCAR index, reflecting systemic disturbances in metabolic, immune, inflammatory, and nutritional status, is a significant independent predictor of ORN in patients with LANPC undergoing CCRT. If validated in future studies, incorporating GLUCAR index assessment into routine pre-CCRT evaluations could help clinicians identify patients at increased risk and implement appropriate preventive strategies, optimize supportive care and individualize radiation treatment planning. Such approaches may ultimately reduce the incidence of ORN and improve patient outcomes.

Ethics approval and consent to participate

The study was conducted in accordance with the Declaration of Helsinki. The study protocol received formal approval from the Institutional Review Board of Baskent University Faculty of Medicine, Andana, Turkey (project no. DKA:19/39), ensuring compliance with applicable ethical standards. Written informed consent was obtained from all the participants. The consent covered the collection and subsequent analysis of relevant clinical data, as well as the use of anonymized data for academic presentations and publications.

Data availability

Data are available from Baskent University Institutional Data Access Committee for researchers meeting criteria for confidential data access.

Consent for publication

Not applicable.

Use of AI and AI-assisted technologies

Not applicable.

ORCID iDs

Efsun Somay https://orcid.org/0000-0001-8251-6913
Erkan Topkan https://orcid.org/0000-0001-8120-7123
Sibel Bascil https://orcid.org/0000-0002-0225-2477
Sukran Senyurek https://orcid.org/0000-0003-3010-6132
Duriye Ozturk https://orcid.org/0000-0002-3265-2797
Nilufer Kılıc Durankuş https://orcid.org/0000-0001-9255-8340
Ugur Selek https://orcid.org/0000-0001-8087-3140

References

1. Chen YP, Chan ATC, Le QT, Blanchard P, Sun Y, Ma J. Nasopharyngeal carcinoma. *Lancet*. 2019;394(10192):64–80. doi:10.1016/S0140-6736(19)30956-0
2. Lee AWM, Ng WT, Chan LL, et al. Evolution of treatment for nasopharyngeal cancer – success and setback in the intensity-modulated radiotherapy era. *Radiother Oncol*. 2014;110(3):377–384. doi:10.1016/j.radonc.2014.02.003
3. Lee J, Hueniken K, Cuddy K, et al. Dental extractions before radiation therapy and the risk of osteoradionecrosis in patients with head and neck cancer. *JAMA Otolaryngol Head Neck Surg*. 2023;149(12):1130–1139. doi:10.1001/jamaoto.2023.3429
4. De Maesschalck T, Dulguerov N, Caparrotti F, et al. Comparison of the incidence of osteoradionecrosis with conventional radiotherapy and intensity-modulated radiotherapy. *Head Neck*. 2016;38(11):1695–1702. doi:10.1002/hed.24505
5. Aarup-Kristensen S, Hansen CR, Forner L, Brink C, Eriksen JG, Johansen J. Osteoradionecrosis of the mandible after radiotherapy for head and neck cancer: Risk factors and dose–volume correlations. *Acta Oncol*. 2019;58(10):1373–1377. doi:10.1080/0284186X.2019.1643037
6. Kojima Y, Otsuru M, Hasegawa T, et al. Risk factors for osteoradionecrosis of the jaw in patients with oral or oropharyngeal cancer: Verification of the effect of tooth extraction before radiotherapy using propensity score matching analysis. *J Dent Sci*. 2022;17(2):1024–1029. doi:10.1016/j.jds.2021.10.019
7. Moreno AC, Watson EE, Humbert-Vidan L, et al. International expert-based consensus definition, classification criteria, and minimum data elements for osteoradionecrosis of the jaw: an interdisciplinary modified Delphi study. *Int J Radiat Oncol Biol Phys*. 2025;122(2):341–354. doi:10.1016/j.ijrobp.2024.12.017
8. Somay E, Topkan E, Yilmaz B, Besen AA, Mertsoylu H, Selek U. Predicting teeth extraction after concurrent chemoradiotherapy in locally advanced nasopharyngeal cancer patients using the novel GLUCAR index. *Diagnostics (Basel)*. 2023;13(23):3594. doi:10.3390/diagnostics13233594
9. Banthia R, Jain P, Jain AK, Belludi SA, Agarwal N, Patidar M. Evaluation of the association between periodontal disease and total cancer risk: A cross-sectional study. *Dent Med Probl*. 2024;61(6):843–850. doi:10.17219/dmp/175001
10. Giacco F, Brownlee M. Oxidative stress and diabetic complications. *Circ Res*. 2010;107(9):1058–1070. doi:10.1161/CIRCRESAHA.110.223545
11. Wang X, Wang H, Zhang T, Cai L, Dai E, He J. Diabetes and its potential impact on head and neck oncogenesis. *J Cancer*. 2020;11(3):583–591. doi:10.7150/jca.35607
12. Luan CW, Yang HY, Tsai YT, Hsieh MC, Chou HH, Chen KS. Prognostic value of C-reactive protein-to-albumin ratio in head and neck cancer: A meta-analysis. *Diagnostics (Basel)*. 2021;11(3):403. doi:10.3390/diagnostics11030403
13. Danan D, Shonka Jr. DC, Selman Y, Chow Z, Smolkin ME, Jameson MJ. Prognostic value of albumin in patients with head and neck cancer. *Laryngoscope*. 2016;126(7):1567–1571. doi:10.1002/lary.25877
14. Singh VP, Bali A, Singh N, Jaggi AS. Advanced glycation end products and diabetic complications. *Korean J Physiol Pharmacol*. 2014;18(1):1–14. doi:10.4196/kjpp.2014.18.1.1
15. Topkan E, Senyurek S, Kılic Durankus N, Ozturk D, Selek U. Novel Somay's GLUCAR index efficiently predicts survival outcomes in locally advanced pancreas cancer patients receiving definitive chemoradiotherapy: A propensity-score-matched cohort analysis. *J Pers Med*. 2024;14(7):746. doi:10.3390/jpm14070746
16. Minervini G, Shivakumar S, Ronsivalle V, Franco R, Cicciù M, Marrapodi MM. Microbiological aspects of cancer progression: A systematic review conducted according to the PRISMA 2020 guidelines and the Cochrane Handbook for Systematic Reviews of Interventions. *Dent Med Probl*. 2024;61(5):739–746. doi:10.17219/dmp/183712
17. von Elm E, Altman DG, Egger M, Pocock SJ, Gøtzsche PC, Vandenbroucke JP; STROBE Initiative. The Strengthening the Reporting of Observational Studies in Epidemiology (STROBE) statement: Guidelines for reporting observational studies. *Lancet*. 2007;370(9596):1453–1457. doi:10.1016/S0140-6736(07)61602-X
18. White SC, Pharoah MJ. *Oral Radiology: Principles and Interpretation*. 8th ed. St. Louis, MO: Elsevier/Mosby; 2018:808–832.
19. World Health Organization (WHO). Oral Health Surveys: Basic Methods. 4th ed. Geneva, Switzerland: WHO; 1997:66. https://iris.who.int/handle/10665/41905.
20. Pauli D, Seyfarth M, Dibbelt L. The Abbott Architect c8000: Analytical performance and productivity characteristics of a new analyzer applied to general chemistry testing. *Clin Lab*. 2005;51(1–2):31–41. PMID:15719702.
21. Yilmaz B, Somay E, Topkan E, Pehlivan B, Selek U. Pre-chemoradiotherapy low hemoglobin levels indicate increased osteoradionecrosis risk in locally advanced nasopharyngeal cancer patients. *Eur Arch Otorhinolaryngol*. 2023;280:2575–2584. doi:10.1007/s00405-023-07864-7
22. Yilmaz B, Somay E, Selek U, Topkan E. Pretreatment systemic immune-inflammation index predicts needs for teeth extractions for locally advanced head and neck cancer patients undergoing concurrent chemoradiotherapy. *Ther Clin Risk Manag*. 2021;17:1113–1121. doi:10.2147/TCRM.S334556
23. Lyons A, Ghazali N. Osteoradionecrosis of the jaws: Current understanding of its pathophysiology and treatment. *Br J Oral Maxillofac Surg*. 2008;46(8):653–660. doi:10.1016/j.bjoms.2008.04.006
24. Notani KI, Yamazaki Y, Kitada H, et al. Management of mandibular osteoradionecrosis corresponding to the severity of osteoradionecrosis and the method of radiotherapy. *Head Neck*. 2003;25(3):181–186. doi:10.1002/hed.10237

25. Chang CJ, Jou IM, Wu TT, Su FC, Tai TW. Cigarette smoke inhalation impairs angiogenesis in early bone healing processes and delays fracture union. *Bone Joint Res*. 2020;9(3):99–107. doi:10.1302/2046-3758.93.BJR-2019-0089.R1
26. Topkan E, Somay E, Bascil S, Selek U. Comment on prospective comparison of acute severe toxicities between smokers and non-smokers during radiotherapy for head and neck cancers. *Oral Oncol*. 2024;155:106898. doi:10.1016/j.oraloncology.2024.106898
27. Hahad O, Kuntic M, Kuntic I, Daiber A, Münzel T. Tobacco smoking and vascular biology and function: Evidence from human studies. *Pflugers Arch*. 2023;475(7):797–805. doi:10.1007/s00424-023-02805-z
28. Chang DT, Sandow PR, Morris CG, et al. Do pre-irradiation dental extractions reduce the risk of osteoradionecrosis of the mandible? *Head Neck*. 2007;29(6):528–536. doi:10.1002/hed.20538
29. Robbins ME, Zhao W. Chronic oxidative stress and radiation-induced late normal tissue injury: A review. *Int J Radiat Biol*. 2004;80(4):251–259. doi:10.1080/09553000410001692726
30. Somay E, Yılmaz B, Topkan E, Kucuk A, Pehlivan B, Selek U. Assessment of the impact of osteoradionecrosis on quality-of-life measures in patients with head and neck cancer. In: Somay E, Yılmaz B, Topkan E, et al., eds. *Advancements in Cancer Research* [Internet]. Brisbane, Australia: Exon Publications; 2023. Chapter 3. doi:10.36255/osteoradionecrosis-quality-of-life
31. Delanian S, Lefaix JL. The radiation-induced fibroatrophic process: Therapeutic perspective via the antioxidant pathway. *Radiother Oncol*. 2004;73(2):119–131. doi:10.1016/j.radonc.2004.08.021
32. Rowe P, Koller A, Sharma S. Physiology, bone remodeling. In: StatPearls [Internet]. Treasure Island, FL: StatPearls Publishing; 2023. https://www.ncbi.nlm.nih.gov/books/NBK499863.
33. Green DE, Rubin CT. Consequences of irradiation on bone and marrow phenotypes, and its relation to disruption of hematopoietic precursors. *Bone*. 2014;63:87–94. doi:10.1016/j.bone.2014.02.018
34. Yoo JS, Rosenthal DI, Mitchell K, Ginsberg LE. Osteoradionecrosis of the hyoid bone: Imaging findings. *AJNR Am J Neuroradiol*. 2010;31(4):761–766. doi:10.3174/ajnr.A1892
35. Nabil S, Samman N. Incidence and prevention of osteoradionecrosis after dental extraction in irradiated patients: A systematic review. *Int J Oral Maxillofac Surg*. 2011;40(3):229–243. doi:10.1016/j.ijom.2010.10.005

Original paper

Immunohistochemical expression of GRP78 in temporomandibular joint dysfunction

Luis Eduardo Almeida[1,A,B], Matthew Beck[1,E,F], Olivia Kraft[1,B,C], Samuel Zammuto[1,E], Flavio de Alcantara Camejo[2,B,C], Maria Maddalena Marrapodi[3,4,B,C], Gabriele Cervino[5,D,E], Andrea Doetzer[6,A,B], Giuseppe Minervini[7,E,F]

[1] Oral and Maxillofacial Surgery, Department of Diagnostic and Surgical Sciences, Marquette University School of Dentistry, Milwaukee, USA
[2] Department of Oral and Maxillofacial Surgery and Hospital Dentistry, Indiana University Scholl of Dentistry, Indianapolis, USA
[3] Saveetha Dental College and Hospitals, Saveetha Institute of Medical and Technical Sciences (SIMATS), Chennai, India
[4] Department of Woman, Child and General and Specialist Surgery, University of Campania "Luigi Vanvitelli", Naples, Italy
[5] Department of Biomedical and Dental Sciences, Morphological and Functional Images, University of Messina, "G. Martino" Polyclinic, Italy
[6] Oral and Maxillofacial Surgery, School of Dentistry, Pontifical Catholic University of Paraná (PUCPR), Curitiba, Brazil
[7] Multidisciplinary Department of Medical-Surgical and Odontostomatological Specialties, University of Campania "Luigi Vanvitelli", Naples, Italy

A – research concept and design; B – collection and/or assembly of data; C – data analysis and interpretation;
D – writing the article; E – critical revision of the article; F – final approval of the article

Dental and Medical Problems, ISSN 1644-387X (print), ISSN 2300-9020 (online) *Dent Med Probl*. 2026;63(5):1209–1214

Address for correspondence
Giuseppe Minervini
E-mail: giuseppe.minervini@unicampania.it

Funding sources
None declared

Conflict of interest
None declared

Acknowledgements
None declared

Received on July 15, 2025
Reviewed on September 4, 2025
Accepted on September 30, 2025

Published online on October 30, 2026

Cite as
Almeida LE, Beck M, Kraft O, et al. Immunohistochemical expression of GRP78 in temporomandibular joint dysfunction. *Dent Med Probl.* 2026;63(5):1209–1214. doi:10.17219/dmp/211576

DOI
10.17219/dmp/211576

Copyright
Copyright by Author(s)
This is an article distributed under the terms of the Creative Commons Attribution 3.0 Unported (CC BY 3.0) (https://creativecommons.org/licenses/by/3.0/)

Abstract

Background. Glucose-regulated protein 78 (GRP78), also known as binding immunoglobulin protein (BiP), is an endoplasmic reticulum (ER) chaperone involved in protein folding and processing, particularly during the unfolded protein response (UPR). It has become an important subject of research in cancer biology and cell proliferation.

Objectives. The aim of the present study was to investigate the relationship between GRP78 expression and temporomandibular disorders (TMDs). Given that alterations in the structure and morphology of the articular disc have been implicated in the pathogenesis of temporomandibular joint (TMJ) symptoms, investigating the role of GRP78 in chondrocyte proliferation may provide further insight into the underlying mechanisms of TMDs.

Material and methods. A total of 22 human TMJ disc samples underwent immunohistochemical staining for GRP78, followed by an assessment of staining intensity. The sample comprised 6 specimens from patients with anterior disc displacement with reduction (ADDwR), 12 from patients with anterior disc displacement without reduction (ADDwoR), and 4 control specimens.

Results. A statistically significant difference in GRP78 staining intensity was observed between the control and experimental groups. GRP78 expression was significantly higher in both experimental groups than in the control group ($p < 0.0001$). These findings suggest that GRP78 may play an important role in the pathogenesis of TMDs.

Conclusions. GRP78 expression may be involved in the pathogenesis of TMDs, as its expression differed significantly between TMJ discs affected by TMDs and those from unaffected controls.

Keywords: inflammation, temporomandibular joint, protein expression, immunohistochemical analysis, GRP-78

Highlights

- GRP78 expression was significantly elevated in temporomandibular joint (TMJ) discs from patients with temporomandibular disorders (TMDs).
- Immunohistochemical analysis demonstrated an association between GRP78 expression and disc displacement disorders (anterior disc displacement with reduction (ADDwR) and anterior disc displacement without reduction (ADDwoR)).
- Findings suggest a potential role for GRP78 in TMJ chondrocyte proliferation and cartilage remodeling.
- GRP78 may represent a potential biomarker of TMJ disc pathology and warrants further investigation.
- These results provide a foundation for future research into the molecular mechanisms underlying TMJ degeneration.

Introduction

The temporomandibular joint (TMJ), which articulates the mandibular condyle with the glenoid fossa of the temporal bone, is considered one of the most complex joints in the human body. Classified as a ginglymoarthrodial joint, TMJ allows both hinge and gliding movements.[1] Due to its anatomical and functional complexity, temporomandibular disorders (TMDs) are relatively common in the general population, with affected individuals frequently reporting jaw pain and restricted mouth opening.[2] Limited knowledge of the underlying pathophysiology of TMDs makes it challenging for clinicians to develop effective treatment strategies and restore normal joint function and mobility. Consequently, current management approaches remain largely symptomatic rather than targeting the underlying causes of the disorders.

Recent studies have highlighted molecular mechanisms involved in TMJ pathology, including the association between mandibular condylar hyperplasia and vascular endothelial growth factor (VEGF), emphasizing the potential role of molecular markers in joint remodeling.[3] Furthermore, the influence of health literacy on conditions such as bruxism illustrates how biological mechanisms and patient-related factors intersect in clinical management.[4]

Temporomandibular disorders are frequently associated with the anterior disc displacement (ADD) of the temporomandibular joint disc. Anterior disc displacement is characterized by an abnormal disc position relative to the mandibular condyle during jaw movement and the protrusion of the mandible, and is classified as either with reduction (ADDwR), when the disc returns to its normal position during mouth opening or closing, or without reduction (ADDwoR), when the displaced disc fails to return to its normal physiological position during mandibular movement. Since TMD management in the USA is largely palliative, patients may remain dissatisfied with treatment outcomes, and TMD-related symptoms continue to be a common reason for seeking dental care.[5]

The aim of the present study is to investigate the relationship between TMDs and binding immunoglobulin protein (BiP), also known as glucose-regulated protein 78 (GRP78). BiP/GRP78 is an endoplasmic reticulum (ER) chaperone that plays a central role in protein folding and quality control, particularly during the unfolded protein response (UPR).[6,7] Specifically, GRP78 facilitates the proper folding and refolding of unfolded or misfolded proteins to maintain cellular homeostasis. When these processes are insufficient to restore protein homeostasis, misfolded proteins may be targeted for ER-associated degradation (ERAD), a quality control pathway responsible for removing aberrant proteins.[7] According to Walter and Ron, impaired ERAD can result in the accumulation of misfolded proteins within the ER lumen and membrane, contributing to ER stress,[11] a phenomenon implicated in several diseases.[6–11] Under normal physiological conditions, GRP78 binds to the ER stress sensors – activating transcription factor 6 (ATF6), protein kinase R-like endoplasmic reticulum kinase (PERK) and inositol-requiring enzyme 1 (IRE1), maintaining them in an inactive state. In response to ER stress, GRP78 dissociates from these sensors, allowing UPR signaling pathways to become activated.[11]

GRP78 was selected as the primary marker in this study because of its central role in the ER stress response and its potential relevance to cartilage biology. Its expression may therefore provide valuable insight into the cellular stress mechanisms associated with TMJ disc pathology. Compared with other UPR-related markers, such as C/EBP homologous protein (CHOP) and spliced X-box binding protein 1 (XBP1s), GRP78 offers an opportunity to investigate an upstream component of the ER stress response.

Various pathological conditions can induce ER stress, and consequently activate UPR, including viral infections, mutations affecting secretory proteins, and nutrient or electrolyte imbalances.[12] When the UPR mechanisms fail to adequately resolve ER stress and restore cellular homeostasis, apoptotic pathways may be activated, ultimately leading to cell death.[13] Given that many pathological conditions involve dysregulated cell proliferation and/or apoptosis, GRP78 has attracted increasing research interest because of growing evidence

of its involvement in a wide range of diseases.[6] Its broad involvement in cellular stress responses raises the question of whether GRP78 also contributes to the pathogenesis of TMDs. Although its role in chondrogenesis remains poorly understood, GRP78 is believed to participate in cartilage formation, remodeling, cellular proliferation, and apoptosis.[13] This perspective is consistent with emerging research highlighting the contribution of genetic factors and cellular stress-response pathways to disease pathogenesis.[14,15]

It is important to note that GRP78 is expressed in the growth plates of chondrocytes, and its overexpression has been shown to promote chondrocyte proliferation by accelerating cell-cycle progression through the G1 phase.[13] Given that alterations in the structure and morphology of the TMJ articular disc have been implicated in the pathogenesis of TMDs, investigating the role of GRP78 in chondrocyte proliferation may provide further insight into the underlying mechanisms of these disorders.

This study investigates the association between GRP78 expression and disc displacement in TMDs, acknowledging that the findings reflect a correlation rather than an etiological relationship.

Material and methods

A total of 22 articular disc samples were collected from patients treated at Hospital Universitário Evangélico de Curitiba (Mackenzie Evangelical University Hospital in Curitiba), Brazil, between 2002 and 2009. Of these, 4 samples consisted of unaffected human articular discs and served as the control group. The mean age of the patients was 31 years (range: 19–45 years). Control samples were obtained from patients undergoing surgery for condylar fractures who had no history of TMDs.

All participants completed a medical history questionnaire and provided written informed consent. The exclusion criteria for the control group comprised a history of orthodontic treatment, systemic diseases (e.g., diabetes, hepatitis, or human immunodeficiency virus (HIV) infection), immunosuppressive therapy, pregnancy, immune dysfunction, severe jaw trauma, dentofacial deformities, previous TMJ surgery, or other TMD-related interventions.

All patients who met the preliminary eligibility criteria were asked to complete a pain questionnaire and underwent clinical examinations performed by an experienced oral and maxillofacial (OMF) surgeon. The examination included the palpation of the TMJ region, auscultation for joint sounds, including crepitus, and a functional assessment. Any signs of pain during mandibular movements were recorded. Following the initial evaluation, patients whose pain was attributed exclusively to muscular spasms were excluded from the experimental group.

After inclusion in the study, all participants underwent magnetic resonance imaging (MRI) and panoramic radiography. Based on the MRI findings, patients were classified into 2 experimental subgroups according to their disc displacement status: anterior disc displacement with reduction (ADDwR; $n = 6$) and anterior disc displacement without reduction (ADDwoR; $n = 12$). The control group consisted of 4 articular disc samples obtained from patients undergoing surgery for condylar fractures who had no history of TMDs.

The staining protocol was adapted from the Thermo Fisher Scientific Ultra-Sensitive ABC Peroxidase Standard Staining Kit, with all steps modified as appropriate. The articular disc samples were deparaffinized in xylene, and subsequently rehydrated using graded ethanol solutions. This process involved 9 sequential solvent baths in Coplin jars, comprising 3 xylene baths, 2 baths of 100% ethanol, 2 baths of 95% ethanol and 5% deionized water, and a final two-step rinse with 100% deionized water.

Antigen retrieval was then performed to unmask potential antigenic sites. The samples were immersed in 10 mM sodium citrate buffer and heated to boiling for 14 min, followed by a 20-minute cooling period. Subsequently, the samples were treated with a peroxidase suppressor to inhibit endogenous peroxidase activity and incubated with a 5% bovine serum albumin (BSA) blocking solution in phosphate-buffered saline (PBS) for 15 min.

All samples were incubated with the GRP78 primary antibody (1:200 dilution; Thermo Fisher Scientific, Rockford, USA) for 30 min at 16°C. Subsequently, the samples were incubated with a biotinylated secondary antibody (1:400 dilution) for an additional 30 min at the same temperature. All antibodies were diluted in PBS.

The avidin–biotin complex (ABC) was applied to the samples to amplify the immunohistochemical signal. The samples were incubated with the ABC reagent for 30 min, followed by a 5-minute application of 3,3'-diaminobenzidine (DAB) chromogen, prepared at a 1:9 dilution from the 10× concentrate. The slides were subsequently dehydrated using deionized water, ethanol and xylene. The same sequence of solvent baths used for deparaffinization was followed in reverse order, with each bath lasting 18 s. Following dehydration, the articular disc sections were systematically examined under a light microscope, and staining intensity and the number of stained fibroblasts were recorded.

Evaluation protocol

Staining intensity was evaluated using a 5-point scale ranging from 0 to 4, where 0 indicated no staining, 1 – light staining, 2 – moderate staining, 3 – strong staining, and 4 – very strong staining.

This study was reported in accordance with the Strengthening the Reporting of Observational Studies in Epidemiology (STROBE) .

Statistical analysis

Statistical analysis was performed using the SPSS software, v. 12.0 (SPSS Inc., Chicago, USA). For the analysis of staining area and density, the average of the measurements obtained from all available samples for each patient was calculated. Group means were compared using the one-way analysis of variance (ANOVA), followed by the Bonferroni post hoc test for multiple comparisons. A p-value of less than 0.05 was considered statistically significant.

Results

Following immunohistochemical staining, GRP78 expression was found to be higher in both experimental groups than in the control group. Five areas of each sample were subjectively evaluated for staining intensity using the 0–4 scale. The resulting scores were analyzed using ANOVA. A marked increase in GRP78 immunoreactivity was observed in both the ADDwR and ADDwoR groups (Fig. 1) compared with the control group (Fig. 2). This difference was statistically significant ($p < 0.0001$). However, no statistically significant difference was observed between the ADDwR and ADDwoR groups ($p = 0.198$). The mean staining intensity scores are presented in Table 1: 3.58 ±0.31 for ADDwR, 3.27 ±0.35 for ADDwoR, and 0.28 ± 0.22 for the control group.

Discussion

The human skeleton is in a constant state of remodeling, and a healthy TMJ is no exception.[16–25] Optimal function and mobility are maintained throughout life through extensive adaptation, healing and inherent regenerative potential.[20] When an inflammatory process develops and the joint no longer functions at an optimal level, the disc often undergoes a well-documented displacement from its normal functional position.[18,21] Symptoms often begin with clicking or popping during mandibular opening, and may progress to muscle tenderness, limited maximum mouth opening, headaches, and other symptoms.[20,21]

The results of this study clearly demonstrate an increased prevalence of GRP78 in pathological joints. It has been shown that GRP78 overexpression enhances cell proliferation during chondrocyte development.[13,17,18] Increased expression of GRP78 within the joint space may alter the remodeling processes that occur in TMJ. Increased cartilage deposition could affect proper disc positioning and contribute to the development of TMD symptoms, which may originate at the microscopic level.[17–21]

In line with our findings, recent reports have expanded the biomarker-based approach to oral and maxillofacial research. For instance, machine-learning models, such as Light Gradient Boosting Machine (LightGBM), have been employed to predict quality of life (QoL) among oral cancer survivors.[22] Similarly, imaging-based reviews have

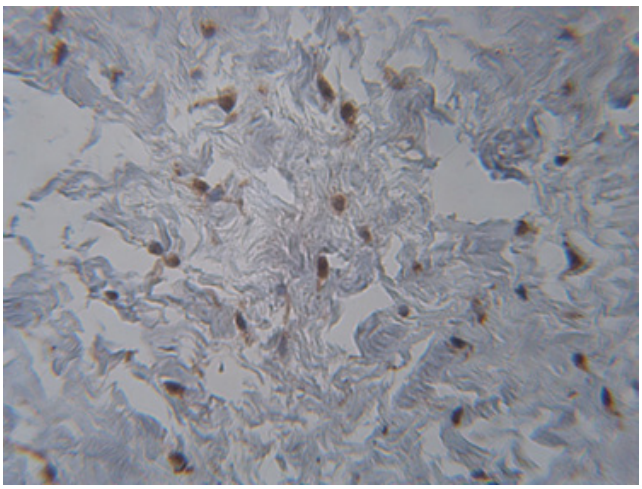

Fig. 1. GRP78 immunoreactivity in a selected experimental sample

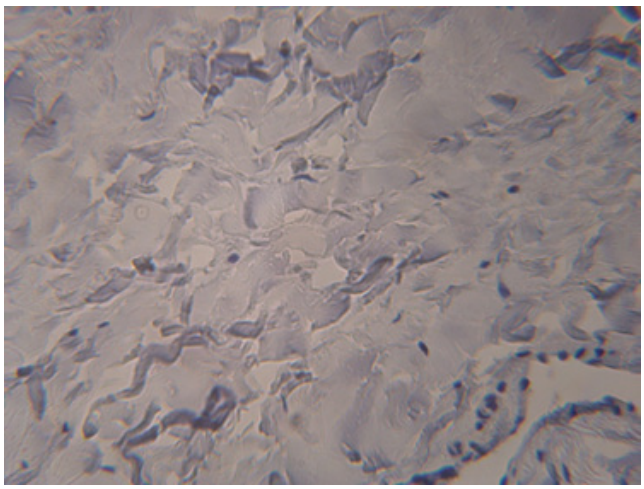

Fig. 2. GRP78 immunoreactivity in a selected control group sample

Table 1. Intensity of GRP78 expression in the study groups

Group	*n*	*M* ±*SD*	*SE*	95% *CI*		min	max
				lower bound	upper bound		
ADDwR	12	3.5833 ±0.3125	0.1276	3.2554	3.9113	3.10	4.00
ADDwoR	6	3.2667 ±0.3525	0.1018	3.0427	3.4906	2.50	3.70
Control	4	0.2750 ±0.2217	0.1109	–0.0778	0.6278	0.00	0.50
Total	22	2.8091 ±1.2686	0.2705	2.2466	3.3716	0.00	4.00

ADDwR – anterior disc displacement with reduction; ADDwoR – anterior disc displacement without reduction; *M* – mean; *SD* – standard deviation; *SE* – standard error; *CI* – confidence interval; min – minimum; max – maximum.

evaluated the comparative effectiveness of different palatal expansion techniques using cone-beam computed tomography (CBCT).[23] These complementary efforts highlight the growing convergence of molecular biology, computational analysis and advanced imaging in shaping contemporary oral health research.

Digital workflows are increasingly shaping orthodontic and prosthetic practice, offering more efficient and precise approaches to treatment.[24,25] Preliminary implant studies and systematic reviews further highlight the potential of translational research approaches to improve our understanding of TMJ pathology and inform rehabilitation strategies.[26,27]

Following the same line of thinking, recent studies have further expanded our understanding of TMDs and related conditions from both clinical and molecular perspectives. Conservative approaches, such as Kinesio Taping, have demonstrated measurable improvement in mandibular mobility and pain reduction in patients with TMDs, supporting the role of non-invasive therapies in symptom management.[28] At the same time, experimental studies investigating agents such as penehyclidine hydrochloride have demonstrated protective effects against inflammation and oxidative stress through the activation of the ROS/Nrf2/HO-1 pathway, highlighting the important role of cellular stress responses in musculoskeletal disorders.[29] Research on stress-related disorders further suggests that biological, mechanical and psychosocial factors interact in the development and progression of TMDs.[30] These findings reinforce the rationale for investigating molecular markers such as GRP78 to better understand the contribution of cellular stress pathways to the pathogenesis of TMDs.

Our findings demonstrate elevated GRP78 expression in pathological discs; however, this observation remains correlative in nature. Therefore, no causal relationship can be inferred, and GRP78 should currently be regarded as a potential biomarker rather than an established therapeutic target.

Conclusions

In this preliminary study, GRP78 expression was significantly elevated in discs from patients with TMDs compared with those from control subjects. These findings suggest that GRP78 may have potential as a biomarker of disc displacement. Further studies are needed to validate this association and establish the clinical relevance of GRP78 expression in TMDs.

Ethics approval and consent to participate

This study was conducted in accordance with the Declaration of Helsinki. The study was approved by the Research Ethics Committee at the Pontifical Catholic University of Paraná (PUCPR), Curitiba, Brazil (CAAE: 55535716.8.0000.0100; approval No. 1.533.139). The subsequent analysis of the de-identified specimens at Marquette University, Milwaukee, USA, was reviewed by the Marquette University Institutional Review Board (protocol No. HR-2859), which determined that it did not constitute human subjects research; therefore, further IRB approval was not required. All participants provided written informed consent prior to participation in the study.

Data availability

The datasets supporting the findings of the current study are available from the corresponding author on reasonable request.

Consent for publication

Not applicable.

Use of AI and AI-assisted technologies

During the preparation of this manuscript, the authors used DeepL Translate for language checking and grammar correction. Following its use, the authors thoroughly reviewed, verified and revised all content to ensure accuracy and originality.

ORCID iDs

Luis Eduardo Almeida https://orcid.org/0000-0001-8781-6050
Matthew Beck https://orcid.org/0000-0001-8726-2107
Olivia Kraft https://orcid.org/0009-0002-8059-746X
Samuel Zammuto https://orcid.org/0009-0008-9788-2375
Flavio de Alcantara Camejo https://orcid.org/0000-0003-1193-2375
Maria Maddalena Marrapodi https://orcid.org/0000-0002-9494-6942
Gabriele Cervino https://orcid.org/0000-0003-4619-4691
Andrea Doetzer https://orcid.org/0000-0003-3361-241X
Giuseppe Minervini https://orcid.org/0000-0002-8309-1272

References

1. Almeida LE, Hresko K, Sorenson A, et al. Immunohistochemical expression of TLR-4 in temporomandibular joint dysfunction. *Cranio*. 2019;37(5):323–328. doi:10.1080/08869634.2018.1446770
2. Okeson J. *Management of Temporomandibular Disorders and Occlusion*. 8th ed. St. Louis, MO: Elsevier/Mosby; 2019.
3. Almeida LE, Cicciù M, Doetzer A, Beck ML, Cervino G, Minervini G. Mandibular condylar hyperplasia and its correlation with vascular endothelial growth factor. *J Oral Rehabil*. 2023;50(9):845–851. doi:10.1111/joor.13487
4. Minervini G, Marrapodi MM, Cicciù M. Online bruxism-related information: Can people understand what they read? A cross-sectional study. *J Oral Rehabil*. 2023;50(11):1211–1216. doi:10.1111/joor.13519
5. Simmons HC 3rd. Rehabilitative vs palliative care for the temporomandibular joint disc displacement patient. *Cranio*. 2018;36(3):141–142. doi:10.1080/08869634.2018.1456187
6. Wang M, Wey S, Zhang Y, Ye R, Lee AS. Role of the unfolded protein response regulator GRP78/BiP in development, cancer, and neurological disorders. *Antioxid Redox Signal*. 2009;11(9):2307–2316. doi:10.1089/ars.2009.2485
7. Ibrahim IM, Abdelmalek DH, Elfiky AA. GRP78: A cell's response to stress. *Life Sci*. 2019;226:156–163. doi:10.1016/j.lfs.2019.04.022

8. Verhoeff MC, Wetselaar P, Lobbezoo F. Assessing the prevalence and risk of tooth wear in Parkinson's disease: A narrative review. *Dent Med Probl*. 2024;61(5):759–764. doi:10.17219/dmp/183842
9. Orzeszek S, Martynowicz H, Smardz J, et al. Assessment of sleep quality in patients with orofacial pain and headache complaints: A polysomnographic study. *Dent Med Probl*. 2024;61(4):549–562. doi:10.17219/dmp/177008
10. Sorrenti NG, Manfredini D, Sornig F, Ferrari M, Colonna A, Val M. Correlation between bilateral TMJ MRI findings: A systematic review of the literature. *Dent Med Probl*. 2024;61(3):401–406. doi:10.17219/dmp/184325
11. Walter P, Ron D. The unfolded protein response: From stress pathway to homeostatic regulation. *Science*. 2011;334(6059):1081–1086. doi:10.1126/science.1209038
12. Osiewicz M, Ciapała B. Is malocclusion a predictor of pain in patients suffering from TMD pain? *Dent Med Probl*. 2024;61(6):851–854. doi:10.17219/dmp/176032
13. Xiong Z, Jiang R, Li X, Liu Y, Guo F. Different roles of GRP78 on cell proliferation and apoptosis in cartilage development. *Int J Mol Sci*. 2015;16(9):21153–21176. doi:10.3390/ijms160921153
14. Mariani P, Zhurakivska K, Santoro R, Laino G, Russo D, Laino L. Hereditary gingival fibromatosis associated with the missense mutation of the *KCNK4* gene. *Oral Surg Oral Med Oral Pathol Oral Radiol*. 2021;131(6):e175–e182. doi:10.1016/j.oooo.2020.08.006
15. Inchingolo AD, Inchingolo AM, Bordea IR, et al. SARS-CoV-2 disease through viral genomic and receptor implications: An overview of diagnostic and immunology breakthroughs. *Microorganisms*. 2021;9(4):793. doi:10.3390/microorganisms9040793
16. Thymi M, Farzan A, Ahlberg J, Manfredini D, Lobbezoo F. Qualitative suggestions for the further development of the Standardized Tool for the Assessment of Bruxism (STAB). *Dent Med Probl*. 2024;61(3):323–333. doi:10.17219/dmp/183692
17. Martynowicz H, Wichniak A, Więckiewicz M. Sleep disorders and cardiovascular risk: Focusing on sleep fragmentation. *Dent Med Probl*. 2024;61(4):475–477. doi:10.17219/dmp/185395
18. Arias CF, Herrero MA, Echeverri LF, Oleaga GE, López JM. Bone remodeling: A tissue-level process emerging from cell-level molecular algorithms. *PLoS One*. 2018;13(9):e0204171. doi:10.1371/journal.pone.0204171
19. Murphy MK, MacBarb RF, Wong ME, Athanasiou KA. Temporomandibular disorders: A review of etiology, clinical management, and tissue engineering strategies. *Int J Oral Maxillofac Implants*. 2013;28(6):e393–e414. doi:10.11607/jomi.te20
20. Shaffer SM, Brismée JM, Sizer PS, Courtney CA. Temporomandibular disorders. Part 1: Anatomy and examination/diagnosis. *J Man Manip Ther*. 2014;22(1):2–12. doi:10.1179/2042618613Y.0000000060
21. Gauer RL, Semidey MJ. Diagnosis and treatment of temporomandibular disorders. *Am Fam Physician*. 2015;91(6):378–386. PMID:25822556.
22. Ramalingam K, Yadalam PK, Ramani P, et al. Light gradient boosting-based prediction of quality of life among oral cancer-treated patients. *BMC Oral Health*. 2024;24(1):349. doi:10.1186/s12903-024-04050-x
23. Coloccia G, Inchingolo AD, Inchingolo AM, et al. Effectiveness of dental and maxillary transverse changes in tooth-borne, bone-borne, and hybrid palatal expansion through cone-beam tomography: A systematic review of the literature. *Medicina (Kaunas)*. 2021;57(3):288. doi:10.3390/medicina57030288
24. Vaid NR, Adel SM. Contemporary orthodontic workflows: A panacea for efficiency? *Semin Orthod*. 2023;29(1):1–3. doi:10.1053/j.sodo.2023.02.002
25. Pellegrino G, Anselmo G, Barausse C, et al. Impression reference technique for the open flap digital workflow in the immediate loading rehabilitation of the upper and lower jaws. *Prosthesis*. 2024;6(6):1479–1490. doi:10.3390/prosthesis6060107
26. Galletti F, D'Angelo T, Fiorillo L, et al. Micro-CT structure analysis on dental implants: Preliminary in vitro trial. *Prosthesis*. 2024;6(6):1437–1447. doi:10.3390/prosthesis6060104
27. Nery JC, Manarte-Monteiro P, Aragão L, Perreira da Silva L, Pinto Brandão GS, Lemos BF. Clinical effects of interproximal contact loss between teeth and implant-supported prostheses: Systematic review and meta-analysis. *Prosthesis*. 2024;6(4):825–840. doi:10.3390/prosthesis6040059
28. Gębska M, Dalewski B, Pałka Ł, Kiczmer P, Kołodziej Ł. Kinesio Taping as an alternative therapy for limited mandibular mobility with pain in female patients with temporomandibular disorders: A randomized controlled trial. *Dent Med Probl*. 2024;61(5):659–670. doi:10.17219/dmp/173126
29. Guo Q, Zhang C, Gao J, Shi W, Liu X. Penehyclidine hydrochloride alleviates LPS-induced inflammatory responses and oxidative stress via ROS/Nrf2/HO-1 activation in RAW264.7 cells. *Adv Clin Exp Med*. 2025;34(1):101–111. doi:10.17219/acem/183883
30. Moradikor N. Non-pharmacological approaches for stress-related neuropsychiatric disorders: Focus on physical activity and natural compounds. *Adv Clin Exp Med*. 2025;34(3):309–313. doi:10.17219/acem/202674

Original paper

Incidental detection of carotid artery calcification on CBCT: A retrospective analysis of 890 scans (108 cases)

Walla Samara[1,A,D,E], Omid Moztarzadeh[1,2,A,E,F], Mohammad Najeh Samara[3,A,C], Lukas Hauer[1,E,F], Jan Pernicky[2,4,B,C]

[1] Department of Stomatology, University Hospital Pilsen, Faculty of Medicine in Pilsen, Charles University, Pilsen, Czech Republic
[2] Department of Anatomy, Faculty of Medicine in Pilsen, Charles University, Pilsen, Czech Republic
[3] Department of Systems Science and Industrial Engineering, State University of New York at Binghamton, USA
[4] Department of Imaging Methods, University Hospital Pilsen, Faculty of Medicine in Pilsen, Charles University, Pilsen, Czech Republic

A – research concept and design; B – collection and/or assembly of data; C – data analysis and interpretation;
D – writing the article; E – critical revision of the article; F – final approval of the article

Dental and Medical Problems, ISSN 1644-387X (print), ISSN 2300-9020 (online) *Dent Med Probl*. 2026;63(5):1215–1224

Address for correspondence
Omid Moztarzadeh
E-mail: omid.moztarzadeh@lfp.cuni.cz

Funding sources
None declared

Conflict of interest
None declared

Acknowledgements
None declared

Received on August 17, 2025
Reviewed on September 9, 2025
Accepted on October 10, 2025

Published online on October 6, 2026

Abstract

Background. Carotid artery calcifications (CACs) are markers of atherosclerosis and an increased risk of stroke. Therefore, their incidental detection on dental cone beam computed tomography (CBCT) scans can be clinically relevant. Early detection allows timely intervention, potentially reducing the risk of serious cerebral and cardiovascular complications.

Objectives. The aim of the study was to retrospectively analyze the prevalence and severity of CACs on CBCT images and their association with patient characteristics and various risk factors.

Material and methods. This retrospective study evaluated 890 CBCT examinations. Of these, 108 patients exhibiting sclerotic changes in the internal carotid artery (ICA) were included and classified as mild, moderate or severe based on the severity of calcification. The study excluded individuals younger than 50 years, as well as cases in which similar radiopacities could not be clearly differentiated. The associations between various clinical variables, including lipid profile parameters, smoking status, a history of chronic diseases, and the severity of calcifications were statistically analyzed.

Results. A total of 108 patients were categorized based on the severity of calcification as mild ($n = 53$), moderate ($n = 41$) or severe ($n = 14$). The findings indicated significant associations between CAC severity and age ($p < 0.001$), low-density lipoprotein (LDL) levels ($p < 0.001$), triglyceride levels (TAG) ($p = 0.002$), and hypertension ($p = 0.027$). Low-density lipoprotein levels demonstrated the strongest correlation with the severity of stenosis ($p = 0.102$).

Conclusions. Cone beam computed tomography may incidentally reveal CACs, highlighting the potential need for further medical evaluation. Larger studies are required to confirm the clinical significance of these findings.

Keywords: cone-beam computed tomography, carotid artery atherosclerosis, vascular incidental findings, calcifications

Cite as
Samara W, Moztarzadeh O, Samara MN, Hauer L, Pernicky J. Incidental detection of carotid artery calcification on CBCT: A retrospective analysis of 890 scans (108 cases). *Dent Med Probl*. 2026;63(5):1215–1224. doi:10.17219/dmp/211938

DOI
10.17219/dmp/211938

Copyright
Copyright by Author(s)
This is an article distributed under the terms of the Creative Commons Attribution 3.0 Unported (CC BY 3.0) (https://creativecommons.org/licenses/by/3.0/)

Highlights

- Cone beam computed tomography (CBCT) can incidentally detect carotid artery calcifications (CACs) during routine dental imaging, providing an opportunity for early detection of vascular disease.
- Recognizing incidental CACs may allow dentists to guide patients for timely medical evaluation and stroke prevention.
- This retrospective analysis demonstrates a measurable prevalence of CACs across different risk groups.
- Carotid artery calcifications were detected in 108 patients over 50 years of age, including 14 individuals with severe calcifications.
- Chronic cardiovascular risk factors were associated with CACs, with the strongest correlation observed between CACs and elevated low-density lipoprotein levels.

Introduction

Atherosclerosis is a chronic disease characterized by the buildup of lipid-rich plaques in the arterial walls, leading to intimal fibrosis, necrosis, vessel narrowing, and potential stenosis. It can result in vessel stiffening, hemodynamic disturbances, and acute occlusion due to plaque rupture, which may cause serious secondary conditions such as heart attacks and strokes.[1] Atherosclerosis is the primary contributor to cardiovascular and cerebrovascular diseases, which remain the leading causes of mortality and morbidity worldwide, affecting large and medium-sized arteries. It tends to develop at arterial bends or bifurcations, where there is decreased endothelial shear stress or disrupted blood flow. The impact of atherosclerosis varies depending on its location, such as the coronary arteries, where it may lead to coronary artery syndrome, or the carotid and intracranial arteries, where it may result in stroke or transient ischemic attack (TIA).[2]

Vascular calcifications are present in 80–90% of atheromas and are recognized as both a sign of aging and an active, self-regulating process involving complex cellular and enzymatic mechanisms. Calcification can occur in the medial and intimal layers of blood vessels, including the intracranial and cervical carotid arteries, and contribute to the formation of atheromatous plaques. These plaques can narrow or block blood vessels, potentially resulting in serious health issues such as carotid artery stenosis (CAS), ischemic stroke, vision loss, and an overall increase in morbidity and mortality.[3] Carotid artery calcifications (CACs), seen as radiopacities in the cervical region, are known as extracranial carotid calcifications, while those along the internal carotid artery (ICA) within the cranium are referred to as intracranial carotid calcifications. Various methods, such as computed tomography (CT), magnetic resonance imaging (MRI) and angiography, are used to detect and assess these calcifications. The occurrence and frequency of CACs differ according to sex, age, genetic predisposition, and lifestyle-related risk factors and comorbidities.[4]

Carotid artery stenosis is a frequently encountered condition in routine medical practice. It is a significant cause of acute ischemic stroke, accounting for around 20% of cases. Carotid artery stenosis can be categorized as either symptomatic or asymptomatic, with this distinction greatly influencing the treatment approach. Symptomatic disease may present as acute neurological ischemia or amaurosis fugax, requiring immediate vascular or emergency evaluation. Conversely, asymptomatic disease may be identified after detecting a carotid bruit or incidentally during imaging.[5] Panoramic radiographs commonly used in dental practice can incidentally reveal CACs as irregular, nodular opacities near the mandibular angle at the C3–C4 vertebral levels.[6] Due to the widespread use of panoramic radiography in routine dental care, dental professionals are well-positioned to detect signs of CAC. This situates them as potential frontline contributors to cardiovascular risk screening, enabling timely identification and appropriate referral for further medical assessment.[7,8] Radiographic examination plays an important role in dentistry, and the detection of carotid artery atheromas on panoramic radiographs may facilitate the prevention of cerebrovascular events, although general practitioners may have limited diagnostic expertise in this area. Advances in cone beam computed tomography (CBCT) allow for detailed three-dimensional (3D) imaging, improving diagnostic accuracy and dental treatment planning. Cone beam computed tomography, with its wide cone-shaped X-ray beam, enables evaluation of the carotid artery bifurcation at the epiglottis level, in relation to the C3 and C4 vertebrae and the upper thyroid cartilage.[9]

Cone beam computed tomography is becoming increasingly significant due to its accurate multiplanar imaging, which is crucial for thorough structural assessments. The technique enables adjustment of the field of view (FOV) according to the specific requirements of the examination. Smaller FOVs concentrate on the maxillofacial complex, while larger volumes can capture the sinuses and other craniofacial structures. Progress in CBCT technology, improved image quality, heightened awareness of medicolegal issues, and increasing expertise among practitioners have resulted in more incidental findings during 3D evaluations. However, standardized protocols for managing these unexpected outcomes remain limited.[10] Unlike traditional two-dimensional (2D) radiography, CBCT provides volumetric data, allowing visualization of anatomical structures in all

dimensions. As a result, clinicians can identify pathologies that fall outside the primary region of interest, including those affecting anatomically significant areas.[11] Beyond its role in diagnostic imaging, CBCT is increasingly applied to clinical decision-making, such as for the evaluation of sagittal root position for immediate implant placement in the anterior maxilla. The versatility of CBCT is also evident in emerging diagnostic applications, such as the use of pulp chamber volume to estimate chronological age in teeth with open apices.[12,13]

An incidental radiographic finding refers to any discovery made by diagnostic imaging techniques such as CT or CBCT that is unrelated to the original reason for conducting the assessment. When examining CBCT scans, it is crucial for medical professionals to analyze the entire image volume instead of focusing solely on the area of interest. Thorough and methodical assessment enables the identification of incidental findings of potential clinical significance.[14] In recent years, artificial intelligence (AI) has gained attention as a tool for detecting CACs in dental imaging. A systematic review by Arzani et al. highlighted the growing potential of AI-based methods for identifying CACs on dental radiographs.[15] Yoo et al. developed CACSNet, a deep learning model capable of automatically classifying and segmenting CACs on panoramic radiographs.[16] While these advances are promising, most focus on 2D imaging, and volumetric CBCT-based assessment with vascular correlation remains limited.[15,16]

Missed lesions are the leading cause of malpractice in radiology, raising concerns for clinicians due to the frequent occurrence of incidental findings in CBCT scans. These findings may involve either skeletal structures or soft tissues; however, soft tissues may not be clearly visible due to CBCT's limited contrast resolution. Therefore, clinicians who use CBCT must have a comprehensive understanding of head and neck anatomy, along with an awareness of the occurrence of pathological abnormalities and false-positive results in CBCT examinations.[17] The aim of the present study was to retrospectively evaluate the role of CBCT in the early detection of CACs as incidental findings.

Material and methods

Study sample selection

The protocol of the study was approved by the Ethics Committee of the University Hospital and the Faculty of Medicine in Pilsen, Charles University (reference No. 93/25).

Cone beam computed tomography examinations of 890 patients performed between January 2023 and December 2024 at the Stomatology Department of the University Hospital Pilsen (Czech Republic) were retrospectively reviewed. Of these, 108 CBCT scans obtained from patients aged over 50 years with identified CACs were included in the study. All scans were acquired using the maxillofacial protocol mode, either with a full-volume or large FOV setting, to ensure comprehensive imaging of the anatomical area of interest.

Exclusion criteria included patients under 50 years of age, scans with significant motion artifacts or metallic fixation that could obscure the area being evaluated, and cases with other potential sources of calcification. For each included case, the patient's age and sex were recorded. When available, data on lipid profile parameters (low-density lipoprotein (LDL), high-density lipoprotein (HDL) and triglycerides (TAG)) was also retrieved from routine clinical records obtained within 6 months before or 3 months after the CBCT scan. Laboratory values were linked to imaging findings and compiled into a de-identified dataset for analysis. Smoking status, history of cardiovascular disease, coagulation disorders, hypertension, diabetes, and the use of anticoagulant therapy were also recorded.

An experienced radiologist evaluated the CBCT scans and categorized the patients into 3 groups based on the severity of atherosclerotic changes: mild; moderate; and severe. The associations between various demographic and clinical variables and the severity of calcification were statistically analyzed. Furthermore, we investigated the relationship between patient characteristics and the degree of CAS in patients with severe calcifications, as assessed by CT angiography.

Imaging procedure

The examinations were performed using the KaVo OP 3D Vision device (KaVo Dental, Biberach, Germany). The FOV of the scans ranged from 150 mm × 150 mm to 160 mm × 100 mm. Of the 108 patients, 68 underwent CBCT with an FOV of 150 mm × 150 mm, 5 with an FOV of 160 mm × 130 mm, and 35 with an FOV of 160 mm × 100 mm. The voxel size ranged from 0.6 mm to 0.3 mm, with a scan time of 10–18 s depending on the selected resolution. The radiation dose was determined based on the slice thickness – for 0.6 mm, the reported dose was 80–100 mGy/cm^2, whereas for 0.3 mm, it was approx. 300 Gy/cm^2. Radiation dose values were obtained from the metrics reported by the device. Effective dose and dose–area product (DAP) values were not available for retrospective extraction and thus could not be consistently reported.

The most commonly used slice thickness was 0.3 mm. Both CBCT and CT examinations were radiologically analyzed using syngo.via for CT software (Siemens Healthineers, Erlangen, Germany). A total of 108 CBCT images from patients referred for various dental indications, primarily implant planning or third molar assessment, were analyzed. Although the primary indication for imaging was purely dental, the scan volume incidentally included the cervical spine (C3–C4) and extracranial ICA region, allowing the detection of CACs. The scans were evaluated by an experienced radiologist with 9 years of professional experience.

Assessment of findings

A total of 108 CBCT examinations in which CACs were identified in the extracranial segment of the ICA region were selected for analysis. Calcifications were confirmed as carotid in origin only if they were visible in at least 3 consecutive axial slices and aligned with the known anatomical course of the ICA (lateral to the pharyngeal wall, adjacent to the C3–C4 vertebral level, and medial to the styloid process). Calcifications in the tonsillar region and other sources of radiopacity (e.g., tonsilloliths, calcified triticeous cartilage, stylohyoid ligament ossification, and lymph node calcifications) were excluded based on their distinct morphology and anatomical position on multiplanar CBCT reconstructions. Further evaluation was conducted by an experienced radiologist using syngo.via for CT software.

The classification was based on a predefined visual scale introduced by Fisher et al. to estimate the severity of atherosclerosis.[18] The grading was performed on axial reconstructions at the level of the extracranial segment of the ICA (segment C1), using bony and cartilaginous landmarks for localization. The severity categories were defined as follows:

– mild: sclerotic changes are slight, thin or discontinuous, without evidence of plaque thickening;
– moderate: sclerotic changes are wider and may be continuous, following the course of the ICA;
– severe: sclerotic changes are thick, irregular and continuous, consistent with a densely calcified atheromatous plaque.

Statistical analysis

All statistical analyses were performed using Python programming language with appropriate statistical packages, including SciPy, NumPy and Pandas. This study employed a two-tier analytical approach reflecting the hierarchical nature of the data collection: a primary analysis of all patients with CBCT-detected calcifications (n = 108); and a secondary analysis of the subset with severe calcifications confirmed by CT angiography (n = 14).

Primary analysis: CAC severity

This analysis included 108 patients, identified among 890 CBCT examinations, who had detectable CACs and were categorized as having mild, moderate or severe calcifications. Parametric and non-parametric tests were applied for the analysis of associations between patient characteristics and CAC severity, according to the distribution of data:

– continuous variables (age, LDL cholesterol, HDL cholesterol, and TAG): one-way analysis of variance (ANOVA) was used to compare mean values across the 3 calcification severity groups (mild, moderate and severe) for normally distributed continuous variables. Post hoc analyses were performed where appropriate to identify specific between-group differences;
– categorical variables (sex, smoking status, diabetes, hypertension, coagulation disorders, and cardiovascular disease): χ^2 test of independence was employed for categorical variables with adequate expected cell frequencies. Fisher's exact test was used when expected cell frequencies were insufficient, ensuring robust analysis despite small cell counts in some categories.

Secondary analysis: CT angiography stenosis subset

This analysis focused exclusively on the 14 patients with severe calcifications who underwent confirmatory CT angiography. Given the limited sample size, which provided approx. 30% power to detect large effect sizes, non-parametric tests were employed to avoid distributional assumptions. These findings should be interpreted as exploratory and hypothesis-generating rather than confirmatory, as the small sample size limits the ability to detect statistically significant associations even when meaningful trends may exist. Given the small sample size, the following non-parametric tests were applied for the analysis of associations between patient characteristics and the percentage of CAS measured by CT angiography, regardless of data distribution:

– continuous variables (age, LDL cholesterol, HDL cholesterol, and TAG): Spearman's rank correlation coefficient (rho). This non-parametric correlation method was chosen because it does not assume linearity or normality of data distribution;
– categorical variables (sex, smoking status, diabetes status, hypertension, antihypertensive therapy, cardiovascular disease, coagulation disorders, anticoagulant use, and antidiabetic medication use): Mann–Whitney U test was used to compare percentages of stenosis between two-group categorical variables;
– comparative analysis: Spearman's correlation was used to examine the relationship between CT angiography and ultrasound measurements. Pearson's correlation coefficient (r) was additionally reported for comparison.

Interpretation of statistical findings

For the primary analysis (n = 108), we conducted 10 statistical comparisons: age; sex; smoking status; diabetes; hypertension; coagulation disorders; cardiovascular disease; LDL cholesterol; HDL cholesterol; and TAG. To control for type I error inflation due to multiple testing, a Bonferroni correction was applied (adjusted α = 0.05/10 = 0.005). Variables with p-values <0.005 were considered statistically significant after correction. We report both unadjusted and Bonferroni-adjusted significance levels in the results. For the secondary analysis (n = 14), results are presented as exploratory findings with unadjusted p-values,

acknowledging the limited statistical power. For the secondary analysis, a *p*-value <0.05 (unadjusted) was considered statistically significant. Results are presented as mean ± standard deviation (*M* ±*SD*) for continuous variables and as frequencies with percentages for categorical variables. All findings from the CT angiography subset should be interpreted as hypothesis-generating rather than confirmatory due to the limited sample size.

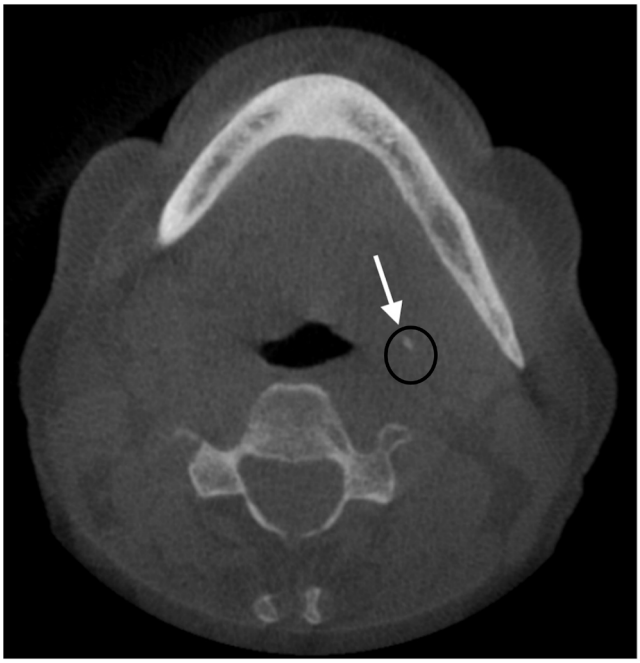

Fig. 1. Axial cone beam computed tomography (CBCT) image showing a midly calcified lesion (white arrow)

The lesion is thin, hairline-like and discontinuous.

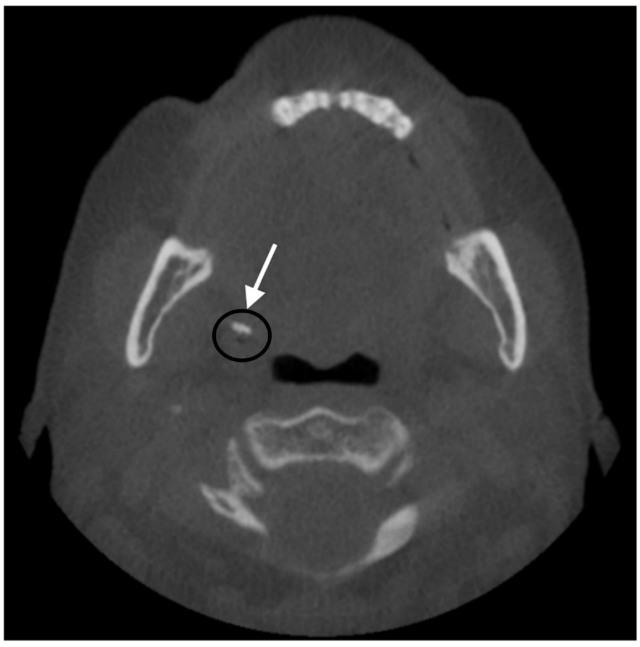

Fig. 2. Axial cone beam computed tomography (CBCT) image showing a moderately calcified lesion (white arrow)

The lesion is wider and slightly coarser and may be continuous.

Results

Of the 890 CBCT examinations performed between January 2023 and December 2024, CACs were identified in 108 patients (12.1%). These calcifications were classified as mild (*n* = 53, 49.1%), moderate (*n* = 41, 38.0%) or severe (*n* = 14, 13.0%) (Fig. 1–3). All 14 patients with severe CACs underwent confirmatory vascular imaging: 3 initially underwent Doppler ultrasonography (Fig. 4) followed by CT angiography (Fig. 5), while 11 proceeded directly to CT angiography. The study population (*N* = 108) included 53.7% of women and 46.3% of men, all of whom were over 50 years of age.

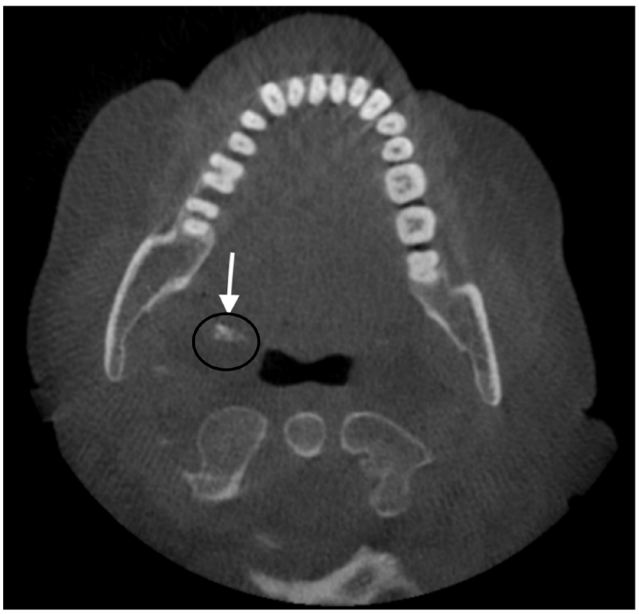

Fig. 3. Axial cone beam computed tomography (CBCT) image showing a severely calcified lesion (white arrow)

The lesion is continuous, wide, thick, and irregular.

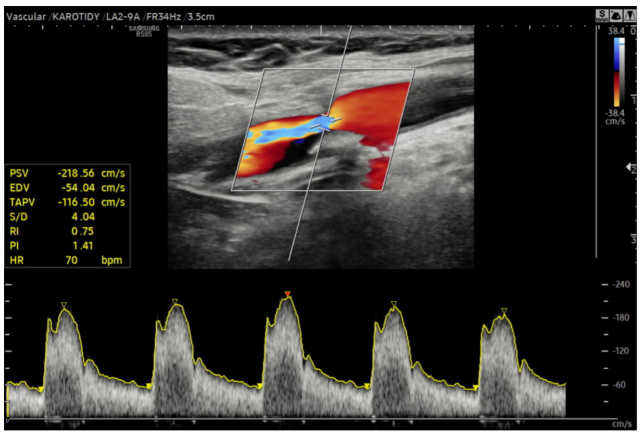

Fig. 4. Doppler ultrasonography of one of the examined patients

The image shows a longitudinal view of the internal carotid artery (ICA) with a rough atherosclerotic plaque and a maximum systolic velocity of 218 cm/s, corresponding to approx. 60–70% stenosis. The degree of stenosis was further confirmed by computed tomography (CT) angiography.
PSV – peak systolic velocity; EDV – end-diastolic velocity; TAPV – time-averaged peak velocity; S/D – systolic/diastolic ratio; RI – resistive index; PI – pulsatility index; HR – heart rate.

Analysis of CAC severity in relation to patient characteristics

Analysis of the 108 patients revealed significant associations between calcification severity and several cardiovascular risk factors (Table 1). Age showed the strongest association ($p < 0.001$), with mean age increasing progressively across the mild (60.8 ±7.4 years), moderate (65.2 ±7.5 years) and severe (73.9 ±5.1 years) groups. Lipid abnormalities were also strongly correlated with severity. High LDL cholesterol was significantly associated with more severe disease ($p < 0.001$), with 87.0% of patients with high LDL levels presenting with moderate or severe calcifications compared with 24.2% of patients with low LDL levels. Elevated TAG similarly showed a significant association ($p < 0.001$ for TAG category; $p = 0.002$ for TAG as a continuous variable), with severe calcifications observed in 26.1% of patients with high TAG vs. 3.2% of those with normal levels. Hypertension was associated with disease severity ($p = 0.027$), and severe condition was observed in 22.2% of hypertensive patients and 6.5% of normotensive patients.

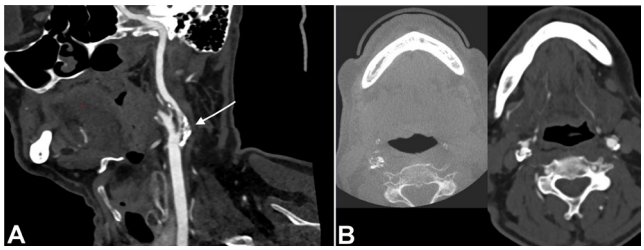

Fig. 5. Computed tomography (CT) angiography and cone beam computed tomography (CBCT) findings

A. CT angiography of the neck and brain arteries showing a longitudinal view of the common carotid artery (CCA) and internal carotid artery (ICA). The arrow indicates an extensive atherosclerotic lesion causing significant narrowing of the ICA; B. Comparison of CBCT and CT angiography findings at the corresponding axial level in the same patient.

After Bonferroni correction for multiple testing (adjusted $\alpha = 0.005$), age, LDL cholesterol and TAG remained statistically significant. Hypertension no longer reached statistical significance after correction, suggesting that this correlation should be interpreted with caution. No significant associations were found with sex, smoking, diabetes, coagulation disorders, or a history of cardiovascular disease. High-density lipoprotein cholesterol approached significance at $p = 0.051$.

Table 1. Association between patient characteristics and the severity of carotid artery calcification (CAC)

Variable		Mild ($n = 53$)	Moderate ($n = 41$)	Severe ($n = 14$)	Total ($N = 108$)	p-value
Sex, *n* (%)	male	25 (50.0)	21 (42.0)	4 (8.0)	50 (46.3)	0.335
	female	28 (48.3)	20 (34.5)	10 (17.2)	58 (53.7)	
Age [years] *M* ±*SD*		60.8 ±7.4	65.2 ±7.5	73.9 ±5.1	64.2 ±8.3	<0.001†
Smoking, *n* (%)	no	38 (52.8)	26 (36.1)	8 (11.1)	72 (66.7)	0.504
	yes	15 (42.9)	15 (42.9)	5 (14.3)	35 (32.4)	
Diabetes, *n* (%)	no	46 (51.7)	33 (37.1)	10 (11.2)	89 (82.4)	0.373
	yes	7 (36.8)	8 (42.1)	4 (21.1)	19 (17.6)	
Hypertension, *n* (%)	yes	17 (37.8)	18 (40.0)	10 (22.2)	45 (41.7)	0.027*
	no	36 (58.1)	22 (35.5)	4 (6.5)	62 (57.4)	
Coagulation disorder, *n* (%)	no	50 (50.5)	37 (37.4)	12 (12.1)	99 (91.7)	0.534
	yes	3 (33.3)	4 (44.4)	2 (22.2)	9 (8.3)	
LDL [mmol/L] *M* ±*SD*		3.08 ±0.56	3.64 ±0.63	4.29 ±0.48	3.45 ±0.71	<0.001†
LDL category, *n* (%)	high	6 (13.0)	27 (58.7)	13 (28.3)	46 (42.6)	<0.001†
	low	47 (75.8)	14 (22.6)	1 (1.6)	62 (57.4)	
HDL [mmol/L] *M* ±*SD*		1.19 ±0.22	1.20 ±0.31	1.01 ±0.26	1.17 ±0.27	0.051
HDL category, *n* (%)	high	21 (46.7)	19 (42.2)	5 (11.1)	45 (41.7)	0.718
	low	32 (50.8)	22 (34.9)	9 (14.3)	63 (58.3)	
TAG [mmol/L] *M* ±*SD*		1.72 ±0.44	1.81 ±0.44	2.21 ±0.43	1.82 ±0.46	0.002†
TAG category, *n* (%)	low	39 (62.9)	21 (33.9)	2 (3.2)	62 (57.4)	<0.001†
	high	14 (30.4)	20 (43.5)	12 (26.1)	46 (42.6)	
Cardiovascular disease, *n* (%)	yes	10 (45.5)	8 (36.4)	4 (18.2)	22 (20.4)	0.714
	no	43 (50.0)	33 (38.4)	10 (11.6)	86 (79.6)	

Continuous variables were compared using one-way analysis of variance (ANOVA); categorical variables were compared using the χ^2 test of independence or Fisher's exact test where expected cell frequencies were insufficient. Hypertension status was unavailable for 1 patient.
* statistically significant ($p < 0.05$ (unadjusted)); † statistically significant ($p < 0.005$, after Bonferroni correction); LDL – low-density lipoprotein; HDL – high-density lipoprotein; TAG – triglycerides; *M* – mean; *SD* – standard deviation.

Association between patient characteristics and the degree of carotid artery stenosis on CT angiography

This exploratory analysis examined the 14 patients with severe calcifications who underwent confirmatory CT angiography. Given the limited sample size, these findings should be interpreted cautiously as hypothesis-generating rather than definitive. We investigated the relationship between patient characteristics and the degree of stenosis as measured by CT angiography. This subset had a mean age of 73.9 years and was predominantly female (n = 10, 71.4%) (Table 2,3).

Categorical variables vs. stenosis

As shown in Table 2, none of the examined categorical variables demonstrated statistically significant associations with the percentage of stenosis measured on CT angiography. The relationship between coagulation disorder status and the percentage of stenosis approached but did not reach statistical significance (U = 23.00, p = 0.052). Patients without coagulation disorders exhibited higher mean stenosis values (73.75%) compared to those with coagulation disorders (57.50%); however, this difference was not statistically significant and should be interpreted with caution given the small sample size. Among the other categorical variables, smokers had higher mean percentages of stenosis (75.00%) than non-smokers (72.08%), and patients with diabetes showed higher stenosis values (75.00%) compared to non-diabetic individuals (70.00%). However, these differences did not reach statistical significance (p = 0.226 and p = 0.430, respectively).

Continuous variables vs. stenosis

Table 3 presents the correlations between continuous variables and the percentage of stenosis. Low-density lipoprotein levels showed the strongest correlation with

Table 2. Association between categorical patient characteristics and the percentage of carotid artery stenosis (CAS) on computed tomography (CT) angiography

Characteristic			Patients, *n*	Carotid artery stenosis [%] *M* ±*SD*	Mann–Whitney *U*	*p*-value
Demographic factors	sex	male	4	71.25 ±5.06	17.00	0.720
		female	10	71.50 ±9.54		
Cardiovascular risk factors	smoking	no	6	72.08 ±7.91	2.98	0.226
		yes	5	75.00 ±7.53		
	hypertension	yes	10	71.50 ±9.93	23.00	0.720
		no	4	71.25 ±2.50		
	antihypertensive therapy	no	5	72.00 ±3.54	21.00	0.892
		yes	9	71.11 ±10.24		
	cardiovascular disease	no	10	71.00 ±9.31	21.00	0.943
		yes	4	72.50 ±5.00		
Coagulation parameters	coagulation disorder	no	12	73.75 ±5.63	23.00	0.052
		yes	2	57.50 ±10.61		
	anticoagulant use	no	13	71.92 ±8.00	11.00	0.314
		yes	1	65.00 (*SD* not applicable)		
Metabolic factors	diabetes	no	10	70.00 ±8.50	14.00	0.430
		yes	4	75.00 ±7.07		
	antidiabetic medication use	no	11	70.91 ±8.61	16.00	1.000
		yes	3	73.33 ±7.64		

Smoking status was unavailable for 3 patients.

Table 3. Correlation between continuous variables and the percentage of carotid artery stenosis (CAS) on computed tomography (CT) angiography

Variable	Patients, *n*	Spearman's rho	*p*-value	Correlation strength	Pearson's *r*	*p*-value
Age	14	–0.1904	0.514	weak negative	–0.3416	0.232
LDL	14	0.4549	0.102	moderate positive	0.4294	0.126
HDL	14	–0.0871	0.767	weak negative	–0.1584	0.589
TAG	14	0.1962	0.501	weak positive	0.2483	0.392
CT angiography vs. Doppler USG	3	0.5000	0.667	moderate positive	0.4339	0.714

Correlation strength refers to Spearman's rho. No correlation reached statistical significance (p < 0.05).
USG – ultrasonography.

stenosis severity (rho = 0.4549, p = 0.102), indicating a moderate positive association, although this did not reach statistical significance. Higher LDL levels were associated with greater percentages of stenosis, which aligns with established pathophysiology of atherosclerosis. Age showed a weak negative correlation (rho = −0.1904, p = 0.514), while HDL cholesterol demonstrated a very weak negative correlation (rho = −0.0871, p = 0.767). Triglyceride levels exhibited a weak positive correlation with the percentage of stenosis (rho = 0.1962, p = 0.501). We also examined the association between CT angiography and ultrasound measurements, finding a moderate positive correlation (rho = 0.5000, p = 0.667) that did not reach statistical significance, likely due to the limited sample size.

None of the examined continuous variables demonstrated statistically significant correlations with the percentage of stenosis. Given the small sample size (n = 14) and lack of statistical significance, these numerical associations should not be interpreted as clinically meaningful trends but rather as preliminary observations requiring validation in adequately powered studies. In summary, the analysis of the CT angiography subset (n = 14) did not identify any statistically significant associations between patient characteristics and the severity of stenosis. The limited sample size precludes definitive conclusions, and all observations from this subset should be considered exploratory and hypothesis-generating only.

Discussion

The carotid arteries deliver oxygen-rich blood to the head, neck and brain, bifurcating into the external and internal carotid arteries typically at the C3–C4 vertebral level. Carotid atherosclerosis accounts for approx. 20% of all ischemic strokes and TIAs. According to most studies, prevalence of CACs in dental images ranges from 2.00% to 31.57%. Thus, early detection of carotid calcifications may help identify previously undiagnosed coronary artery disease and facilitate referral for further evaluation.[19] Atherosclerosis is influenced by various factors, such as diabetes mellitus, obesity, hypertension, smoking, alcohol intake, and chronic renal disorders. Atherosclerosis can lead to strokes when the carotid arteries, which supply blood to the brain, are compromised. It can also cause myocardial infarctions when the coronary arteries, which supply blood to the heart, are affected. These conditions contribute substantially to global mortality.[20]

Sialolithiasis, tonsilloliths and calcification of lymph nodes and blood vessels may manifest in the cervical area. The need to distinguish these calcifications not only from each other but also from different anatomical structures and structures capable of calcification, such as the stylohyoid ligament, triticeous cartilage and thyroid cartilage, makes the diagnosis of atheromas more complex. While the oral surgeon may find it challenging to differentiate atheromatous calcifications on CBCT from other anatomical and pathological structures, the ability to detect carotid atheromas using CBCT presents an opportunity for early treatment, thereby potentially reducing morbidity and mortality.[9] Cone beam computed tomography scans have been increasingly used in recent years for various applications in the dental field. Their value lies in the practitioner's ability to discover clinically significant incidental findings beyond the area of interest for which CBCT was indicated.[14]

The objective of this study was to retrospectively assess the prevalence and severity of CACs identified incidentally on CBCT. A study comparing carotid ultrasonography and CBCT revealed that CBCT may identify and quantify minimal calcification volumes, as little as 1 mm^3, indicating its high sensitivity in selected cases. Nevertheless, CT remains the preferred imaging modality for a more thorough assessment of CACs, especially in regions outside the typical coverage of CBCT.[21] Several imaging modalities have been used to evaluate CACs, including modified posteroanterior radiographs of the neck, where calcifications manifest lateral to the spine, along with CT, which exhibits high sensitivity for identifying intracranial calcifications. Additional techniques include panoramic radiographs, magnetic resonance (MR) angiography, Doppler ultrasonography, and CBCT. In contrast to Doppler ultrasonography and MR angiography, CBCT provides high-resolution 3D imaging of calcifications while potentially reducing costs and radiation exposure compared with conventional CT in selected dental indications.[22]

The present study highlights the critical role of CBCT in the early detection of CACs as incidental findings during routine dental imaging. A total of 890 patients were evaluated, and CACs of mild, moderate or severe grade were identified in 108 patients along the course of the ICA. Among these patients, severe calcifications were detected in 14 individuals, underscoring the potential of CBCT as a valuable diagnostic tool beyond its primary dental applications. Our findings revealed significant associations between severe CACs and established cardiovascular risk factors, including advanced age, elevated LDL levels, increased TAG levels, and hypertension. These results are consistent with existing literature, indicating that dyslipidemia and blood pressure abnormalities significantly contribute to atherosclerotic lesions in the carotid arteries. Moreover, patients with severe CACs underwent further vascular assessment with CT angiography, which allowed for the evaluation of the presence and degree of CAS. However, due to the small sample size and the fact that CT angiography was performed only in patients with severe CACs, the present study cannot establish a direct correlation between the extent of calcification on CBCT and the degree of CAS.

Such findings emphasize the need to refer patients with suspected CACs for further comprehensive medical assessment, as they may be at elevated risk for cerebrovascular events such as stroke. The results of this study are notable

for combining a detailed evaluation of CACs with an assessment of a broad range of associated risk factors. The identification of significant associations between severe calcification and risk factors such as elevated LDL, TAG, hypertension, and advanced age highlights the multifactorial nature of carotid artery disease. By considering these varied parameters together, our study provides broader insight into the possible systemic implications of incidental calcifications identified on CBCT scans.

Our study aligns with previous research showing a clear association between abnormal lipid profiles and CACs. A study by Taengsakul et al. found that high levels of LDL and TAG were closely linked to the development of carotid artery narrowing in patients receiving radiotherapy.[23] Likewise, Smith et al. reported that lipid disorders significantly contributed to plaque buildup and vascular stenosis in this population.[24] These findings reinforce our conclusion that lipid imbalances play an important role in the progression of carotid calcification. Monitoring lipid levels in patients with CBCT-detected calcifications may therefore enable earlier identification of cardiovascular risk and prompt clinical management.[23,24] Brar et al. provided additional evidence supporting the clinical relevance of CACs seen on dental imaging.[6] Their findings demonstrated a strong correlation between calcifications detected on panoramic radiographs and the presence of conditions such as hypertension, hyperlipidemia, diabetes mellitus, stroke, and heart disease.[6]

Cone beam computed tomography provides 3D information, allowing precise localization of calcifications and volumetric assessment. In addition, by applying a structured severity-based classification and correlating selected cases with vascular imaging, this study highlights aspects that have not been systematically addressed in earlier dental imaging research. These features support the novelty of our approach and underline the role of CBCT as a useful adjunct for the incidental detection of potentially significant findings. Damaskos et al. examined 391 CBCT scans and reported both extracranial and intracranial carotid calcifications, showing associations with systemic risk factors.[25] Their findings support the clinical relevance of CBCT in vascular assessment and are in line with the correlations observed in our study.[25]

Similarly, the CBCT-based staging approach for external carotid calcifications proposed by Kadyan et al. illustrates the value of structured classifications.[19] Our work differs by applying a severity-based assessment to internal CACs, with additional correlation with vascular imaging, thereby extending the potential diagnostic contribution of CBCT.[19] Furthermore, our retrospective design is consistent with other CBCT-based studies that have examined anatomical and pathological associations, such as the link between Schneiderian membrane thickness and the severity of periodontitis.[26]

The incidental finding of CACs on CBCT scans provides a distinctive opportunity for the early identification of individuals who may be at increased risk for cardiovascular disease, particularly among asymptomatic patients who might otherwise remain undiagnosed. This highlights a valuable role for dental professionals and radiologists, who should recognize these findings and refer patients for further medical evaluation when necessary. While CBCT is not a substitute for dedicated vascular imaging, its widespread use in dental clinics makes it a practical, non-invasive tool for identifying patients who may benefit from further assessment. As CBCT becomes more common in clinical practice, the implementation of appropriate training and protocols for the recognition of incidental CACs may contribute to earlier diagnosis and the improvement of prevention strategies.

Limitations

This study provides important observations; however, several methodological limitations should be acknowledged. The study is limited by its retrospective design and the relatively small CT angiography subset, which may affect generalizability. However, the use of standardized assessment criteria and a large initial CBCT sample provides meaningful insights. Further prospective studies are needed to confirm these findings.

Conclusions

Cone beam computed tomography has become a valuable tool not only for dental diagnosis but also for the incidental detection of clinically relevant findings such as CACs. This study demonstrates that CACs may be identified incidentally on CBCT examinations and that their presence may warrant further medical evaluation. Given the retrospective design and the limited sample, these findings should be interpreted cautiously and confirmed in larger studies.

Cone beam computed tomography provides 3D visualization, which may facilitate more accurate detection of CACs than conventional dental radiographs. Early recognition of such findings may prompt appropriate medical referral and potentially prevent serious complications.

Ethics approval and consent to participate

The protocol of the study was approved by the Ethics Committee of the University Hospital and the Faculty of Medicine in Pilsen, Charles University (reference No. 93/25).

Data availability

The datasets generated and/or analyzed during the current study are available from the corresponding author on reasonable request.

Consent for publication

Not applicable.

Use of AI and AI-assisted technologies

AI-assisted tool (ChatGPT; OpenAI, San Francisco, USA) was used to refine the language. All scientific content and references were written, reviewed and verified by the authors.

ORCID iDs

Walla Samara https://orcid.org/0009-0001-6556-0872
Omid Moztarzadeh https://orcid.org/0000-0002-4768-2382
Mohammad Najeh Samara https://orcid.org/0009-0004-9890-4936
Lukas Hauer https://orcid.org/0000-0001-6639-2690
Jan Pernicky https://orcid.org/0000-0002-7789-9021

References

1. Möst T, Winter L, Ballheimer YE, et al. Prevalence of carotid artery calcification detected by different dental imaging techniques and their relationship with cardiovascular risk factors, age and gender. *BMC Oral Health*. 2023;23(1):949. doi:10.1186/s12903-023-03564-0
2. Cheng YW, Chen CH, Yeh SJ, et al. Association between modifiable vascular risk factors and rapid progression of postradiation carotid artery stenosis. *J Chin Med Assoc*. 2023;86(7):627–632. doi:10.1097/JCMA.0000000000000936
3. Ahmed M, McPherson R, Abruzzo A, Thomas SE, Gorantla VR. Carotid artery calcification: What we know so far. *Cureus*. 2021;13(10):e18938. doi:10.7759/cureus.18938
4. Mutalik S, Tadinada A. Assessment of relationship between extracranial and intracranial carotid calcifications – a retrospective cone beam computed tomography study. *Dentomaxillofac Radiol*. 2019;48(8):20190013. doi:10.1259/dmfr.20190013
5. Arasu R, Arasu A, Muller J. Carotid artery stenosis: An approach to its diagnosis and management. *Aust J Gen Pract*. 2021;50(11):821–825. doi:10.31128/AJGP-10-20-5664
6. Brar A, DeColibus K, Rasner DS, et al. Carotid artery calcification detected on panoramic radiography is significantly related to cerebrovascular accident, coronary artery disease, and poor oral health: A retrospective cross-sectional study. *Dent J (Basel)*. 2024;12(4):99. doi:10.3390/dj12040099
7. Amitay M, Barnett-Itzhaki Z, Sudri S, et al. Deep convolution neural network for screening carotid calcification in dental panoramic radiographs. *PLOS Digit Health*. 2023;2(4):e0000081. doi:10.1371/journal.pdig.0000081
8. Janiszewska-Olszowska J, Jakubowska A, Gieruszczak E, Jakubowski K, Wawrzyniak P, Grocholewicz K. Carotid artery calcifications on panoramic radiographs. *Int J Environ Res Public Health*. 2022;19(21):14056. doi:10.3390/ijerph192114056
9. Soares ADS, Wanzeler AMV, Renda MDO, Marinho CG, Tuji FM. Cone-beam computed tomography findings in the early diagnosis of calcified atheromas. *J Oral Maxillofac Surg*. 2017;75(1):143–148. doi:10.1016/j.joms.2016.06.179
10. Kadkhodayan S, Almeida FT, Lai H, Pacheco-Pereira C. Uncovering the hidden: A study on incidental findings on CBCT scans leading to external referrals. *Int Dent J*. 2024;74(4):808–815. doi:10.1016/j.identj.2023.11.013
11. Damaskos S, Tsiklakis K, Syriopoulos K, van der Stelt P. Extra- and intracranial arterial calcifications in adults depicted as incidental findings on cone beam CT images. *Acta Odontol Scand*. 2015;73(3):202–209. doi:10.3109/00016357.2014.979867
12. Habib S, Motiwala MA, Khan FR. Does the sagittal root position of maxillary anterior teeth affect the decision making on immediate implants in the anterior maxilla? A CBCT-based study. *Dent Med Probl*. 2024;61(1):65–70. doi:10.17219/dmp/133072
13. Kolcakoglu K, Amuk M, Kizilci E, Sirin Sarıbal G, Askaroglu Ö, Korkut Dİ. Chronological age estimation by measuring pulp chamber volume in teeth with open apices: A CBCT analysis. *Dent Med Probl*. 2025;62(5):889–906. doi:10.17219/dmp/153419
14. Zain-Alabdeen EH, El Khateeb SM. Incidental cone beam computed tomographic findings among Taibah University patients, KSA: A retrospective study. *J Taibah Univ Med Sci*. 2016;12(2):131–138. doi:10.1016/j.jtumed.2016.10.014
15. Arzani S, Soltani P, Karimi A, et al. Detection of carotid artery calcifications using artificial intelligence in dental radiographs: A systematic review and meta-analysis. *BMC Med Imaging*. 2025;25(1):174. doi:10.1186/s12880-025-01719-9
16. Yoo SW, Yang S, Kim JE, et al. CACSNet for automatic robust classification and segmentation of carotid artery calcification on panoramic radiographs using a cascaded deep learning network. *Sci Rep*. 2024;14(1):13894. doi:10.1038/s41598-024-64265-4
17. Newaz ZA, Barghan S, Katkar RA, Bennett JA, Nair MK. Incidental findings of skull-base abnormalities in cone-beam computed tomography scans with consultation by maxillofacial radiologists. *Am J Orthod Dentofacial Orthop*. 2015;147(1):127–131. doi:10.1016/j.ajodo.2014.09.019
18. Fisher CM, Gore I, Okabe N, White PD. Calcification of the carotid siphon. *Circulation*. 1965;32(4):538–548. doi:10.1161/01.cir.32.4.538
19. Kadyan V, Vaddi A, Nagpal A, Molina MR, Lurie AG, Tadinada A. Evaluation of cone-beam computed tomography scans to develop a staging method of external carotid artery calcification. *J Clin Med*. 2024;13(11):3189. doi:10.3390/jcm13113189
20. Samara W, Moztarzadeh O, Pernicky J, et al. Carotid artery stenosis on panoramic radiographs and CT scans in patients with malignancies after radiotherapy. *Anticancer Res*. 2023;43(12):5657–5662. doi:10.21873/anticanres.16770
21. Jashari F, Ibrahimi P, Johansson E, et al. Atherosclerotic calcification detection: A comparative study of carotid ultrasound and cone beam CT. *Int J Mol Sci*. 2015;16(8):19978–19988. doi:10.3390/ijms160819978
22. Paknahad M, Shahidi S, Abbasi R, Paknahad M. Evaluation of the prevalence of atherosclerosis within the course of internal carotid artery in cone beam computed tomography images. *Indian J Otolaryngol Head Neck Surg*. 2022;74(Suppl 3):5242–5251. doi:10.1007/s12070-020-01958-y
23. Taengsakul N, Nivatpumin P, Chotchutipan T, Tungfung S. Carotid artery stenosis and ischemic cerebrovascular events after radiotherapy in patients with head and neck cancer. *PLOS One*. 2025;20(1):e0314861. doi:10.1371/journal.pone.0314861
24. Smith J, Margalit D, Golledge J, Nastasi D, Nohria A, McDowell L. Carotid artery stenosis and ischemic stroke in patients with head and neck cancer treated with radiation therapy: A critical review. *Int J Radiat Oncol Biol Phys*. 2024;119(6):1437–1454. doi:10.1016/j.ijrobp.2024.03.044
25. Damaskos S, Zoukos A, Vlachopoulos C, Angelopoulos C. Vascular-related cone-beam computed tomographic findings in healthy and medically compromised patients: A study based on self-reported medical history data. *Imaging Sci Dent*. 2025;55(2):197–205. doi:10.5624/isd.20250029
26. Veluri S, Gottumukkala SNVS, Penmetsa G, et al. Retrospective analysis of the relationship between Schneiderian membrane thickness and periodontitis severity using cone beam computed tomography (CBCT). *Dent Med Probl*. 2025;62(1):65–72. doi:10.17219/dmp/147105

Original paper

Correlation of dental status and denture use with functional disability (VES-13) and frailty syndrome (Fried phenotype) in Polish older adults: A cross-sectional study

Dorota Pylińska-Dąbrowska[1,A–D,F*], Hanna Kujawska-Danecka[2,A,C,E,F*], Kacper Jagiełło[3,B,C,F], Małgorzata Mossakowska[3,4,A,C,E,F], Tomasz Roman Zdrojewski[3,A,B,E,F]

[1] Department of Dental Prosthetics, Institute of Dentistry, Faculty of Medicine, Medical University of Gdańsk, Poland
[2] Departament of Rheumatology, Clinical Immunology, Geriatrics and Internal Medicine, Faculty of Medicine, Medical University of Gdańsk, Poland
[3] Division of Preventive Medicine and Education, Medical University of Gdańsk, Poland
[4] Aging and Longevity Strategic Project, International Institute of Molecular and Cell Biology, Warsaw, Poland
* These authors contributed equally to this work.

A – research concept and design; B – collection and/or assembly of data; C – data analysis and interpretation;
D – writing the article; E – critical revision of the article; F – final approval of the article

Dental and Medical Problems, ISSN 1644-387X (print), ISSN 2300-9020 (online) *Dent Med Probl*. 2026;63(5):1225–1231

Address for correspondence
Dorota Pylińska-Dąbrowska
E-mail: d.pylinska@gmail.com

Funding sources
None declared

Conflict of interest
None declared

Acknowledgements
Manuscript preparation was supported through Harvard Medical School's Polish Clinical Scholars Research Training (P-CSRT) Program, organized by the Medical Research Agency (Agencja Badań Medycznych, ABM), Warsaw, Poland.

Received on August 28, 2025
Reviewed on September 14, 2025
Accepted on October 16, 2025

Published online on October 7, 2026

Cite as
Pylińska-Dąbrowska D, Kujawska-Danecka H, Jagiełło K, Mossakowska M, Zdrojewski TR. Correlation of dental status and denture use with functional disability (VES-13) and frailty syndrome (Fried phenotype) in Polish older adults: A cross-sectional study. *Dent Med Probl.* 2026;63(5):1225–1231. doi:10.17219/dmp/213281

DOI
10.17219/dmp/213281

Copyright
Copyright by Author(s)
This is an article distributed under the terms of the Creative Commons Attribution 3.0 Unported (CC BY 3.0) (https://creativecommons.org/licenses/by/3.0/)

Abstract

Background. Tooth loss is highly prevalent among older adults and may contribute to frailty and functional decline, yet population-based data from Central and Eastern Europe remains limited.

Objectives. The aim of the study was to investigate the association of dental status and denture use with 2 indicators of vulnerability – frailty and functional impairment – in a nationally representative sample of older adults in Poland.

Material and methods. Cross-sectional data from 5,457 participants aged ≥60 years who were enrolled in the PolSenior2 study (2018–2019) was analyzed. Dental status was categorized as functional dentition (≥20 teeth), partial dentition (1–19 teeth) or edentulism (0 teeth), with or without denture use. Outcomes included frailty (Fried phenotype ≥3) and functional vulnerability (Vulnerable Elders Survey-13 (VES-13) score ≥3). Descriptive analyses were performed and weighted multivariable logistic regression models were applied, with adjustment for age, sex, body mass index (BMI), education level, place of residence, and smoking status.

Results. Edentulism was independently associated with increased odds of frailty (odds ratio (*OR*) = 1.47, 95% confidence interval (95% *CI*): 1.08–2.01) and functional vulnerability (*OR* = 1.38, 95% *CI*: 1.10–1.74). Denture use was correlated with lower odds of these outcomes. Partial dentition showed a weaker association, which was statistically significant only for functional vulnerability (VES-13). Male sex was associated with lower odds of both outcomes. A clear gradient was observed across dental categories, from functional dentition to untreated edentulism.

Conclusions. Tooth loss, particularly when uncorrected by dentures, is a strong, independent marker of frailty and functional vulnerability in older adults. Denture use is associated with lower odds of these conditions but does not fully restore the benefits of natural dentition. Oral health assessment and access to prosthetic rehabilitation should be integrated into geriatric care and public health strategies to support healthy aging.

Keywords: frailty, dental status, edentulism, VES-13, elderly

Highlights

- The study investigated the association of dental status and denture use with frailty and functional vulnerability in older adults.
- Edentulism was strongly associated with frailty and functional disability.
- Denture use partially mitigated the negative impact of edentulism on health outcomes.
- Smoking and lower education level were associated with poorer dental and functional status.

Introduction

Population aging poses a growing public health challenge. Globally, individuals aged ≥65 years accounted for 9.3% of the population in 2020, with this proportion projected to reach 16.0% by 2050.[1] In Europe, the share of older adults has more than doubled since 1960, reflecting a rapid demographic transition.[2] Oral diseases are increasingly important in this context. In 2021, more than 353 million people worldwide were edentulous, and this number is expected to exceed 660 million by 2050, making edentulism a major contributor to years lived with disability (YLDs).[3] Compared with the global average (22.7%), the prevalence of edentulism in the World Health Organization (WHO) European Region is higher (31.3%), and it reaches 36.1% in Poland, placing the country among the most affected in Europe.[1,4,5] These differences highlight both international and regional inequalities in oral health and underline the urgent need for research on the determinants and consequences of tooth loss in aging populations.

Tooth loss is primarily caused by caries and periodontal disease, with smoking recognized as a major modifiable risk factor.[6–9] However, socioeconomic status, education level and access to dental care strongly influence its prevalence, with a higher risk consistently observed among women, individuals with lower levels of education, and residents of rural areas.[10] Socioeconomic and health-related factors have also been shown to significantly influence oral health, with lower economic status and smoking associated with a greater number of untreated decayed teeth and poorer oral hygiene.[11]

Edentulism is not only a medical but also a social condition. When left untreated, it impairs chewing, restricts dietary variety, and contributes to malnutrition and chronic disease.[12–14] Beyond nutritional limitations, tooth loss has far-reaching psychosocial consequences, including reduced self-esteem, difficulties with speech and communication, social withdrawal, and an increased risk of depression and anxiety.[15–17] These outcomes may contribute to functional decline in older adults.

Frailty, characterized by reduced physiological reserve and increased vulnerability to stressors, is closely linked to tooth loss. It is associated with falls, disability, hospitalization, and mortality.[18] Standardized tools such as the Fried frailty phenotype and the Vulnerable Elders Survey-13 (VES-13) are widely used for the assessment of frailty and vulnerability. Each instrument, however, has its limitations: the Fried frailty phenotype captures objective deficits but may underrepresent psychosocial aspects, while the VES-13 emphasizes self-reported functioning and may be influenced by subjective perceptions of health. Their combined use allows for a more comprehensive assessment of vulnerability in older populations, yet their specific role in oral health research remains underexplored.[19,20]

Despite growing international evidence, data from Central and Eastern Europe remain scarce. To address this gap, we used nationally representative data from the PolSenior2 study to examine the associations of dental status and denture use with frailty and functional vulnerability among older adults in Poland.

Material and methods

Study design and population

This cross-sectional study used data from the PolSenior2 project, a nationally representative survey conducted between September 2018 and December 2019. A three-stage stratified random sampling strategy was applied to select community-dwelling individuals aged ≥60 years across Poland. Participants were drawn from the personal identification number (PESEL) registry, maintained by the Polish Ministry of the Interior and Administration. Medical data, including dental examination data, was collected by trained healthcare professionals as part of the PolSenior2 protocol and not by the authors of this paper.[5,21] The study was approved by the Independent Bioethics Committee of the Medical University of Gdańsk, Poland (approval No. NKBBN/257/2017). Written informed consent was obtained from all participants.

Key measures

Frailty was measured using the Fried frailty phenotype, which includes 5 components: (1) unintentional weight loss; (2) self-reported exhaustion; (3) weakness (grip strength); (4) slowness (gait speed); and (5) low physical activity. Participants were classified as non-frail (0), pre-frail (1–2) or frail (≥3) based on validated cut-off points.[18,19]

Functional vulnerability was assessed using the VES-13, a validated tool for the evaluation of the risk of health

deterioration and disability. A total score ≥3 was considered indicative of vulnerability. The tool covers self-reported age, health status, functional limitations, and disability in activities of daily living.[20]

Oral examinations were conducted by trained professionals, and participants were categorized into the following groups based on the dentition status (the number of natural teeth):

- functional dentition (≥20 teeth);
- partial dentition (1–19 teeth);
- edentulism (0 teeth).

Additionally, denture use was recorded and classified as "no denture use" or "partial/complete denture use". All oral examinations were conducted by trained professionals according to a standardized protocol.[21]

Based on the theoretical rationale and the existing literature, the following covariates were included in the analysis: age (per 5-year increase); sex (male/female); place of residence (rural, urban with <50,000 residents, urban with 50,000–200,000 residents, or urban with >200,000 residents); education level (primary/incomplete, vocational, secondary/post-secondary or higher); body mass index (BMI) (<18.5, 18.5–24.99 or ≥25.00); and self-reported smoking status (current smoker, former smoker or non-smoker).

Statistical analysis

Descriptive statistics were calculated for baseline characteristics using unweighted data. Group comparisons were performed using weighted χ^2 tests for categorical variables. Both unadjusted and multivariable-adjusted logistic regression models were fitted. Sampling weights from the PolSenior2 dataset were applied to ensure national representativeness.

Univariate logistic regression was used to assess crude associations between dental status and the 2 primary outcomes: (1) frailty, defined as a Fried score ≥3; and (2) functional vulnerability, defined as a VES-13 score ≥3. Variables that were statistically significant ($p < 0.05$) in univariate analyses were included in the multivariable regression models. Results were reported as odds ratios (*OR*s) with 95% confidence intervals (95% *CI*s). A *p*-value <0.05 was considered statistically significant. For categorical variables, effect sizes were reported as Cramér's *V*, with thresholds of 0.1 (small), 0.3 (medium) and 0.5 (large). For continuous variables compared using analysis of variance (ANOVA), effect sizes were reported as eta squared (η^2), with thresholds of 0.01 (small), 0.06 (medium) and 0.14 (large). All analyses were performed using R v. 3.6.3 statistical software (R Foundation for Statistical Computing, Vienna, Austria; https://cran.mi2.ai) and SAS®9.4 TS1M5 (SAS Institute, Inc., Cary, USA).

Results

Table 1 presents the relationship between dental status and frailty/functional vulnerability. A clear gradient was observed across dentition categories. The prevalence of frailty increased from 5.8% among individuals with ≥20 teeth to 27.0% among edentulous individuals. Similarly, the mean VES-13 score increased from 1.5 to 4.2 across these groups, indicating worsening functional status with increasing tooth loss. The association with frailty was of moderate strength, and a similar moderate effect was observed for functional vulnerability as measured by the VES-13.

Participants with functional dentition (≥20 teeth) were generally younger, more educated, and more likely to live in large urban areas than those with partial dentition or edentulism. For example, among individuals aged 60–64 years, 34.7% had ≥20 teeth, compared with only 15.9% among edentulous individuals in the same age group. In contrast, edentulism was most prevalent among those aged 85 years and older (62.9–70.2%).

Higher education was strongly associated with better dental status: 43.4% of participants with ≥20 teeth had higher education, compared with only 14.0% in the edentulous group. Edentulous individuals were also more likely to reside in rural areas and had a mean BMI of 29.1 kg/m^2 compared with 28.8 kg/m^2 among participants with ≥20 teeth. The partial dentition group represented the largest proportion across all smoking categories (47.8% of current smokers, 50.6% of former smokers and 49.9% of non-smokers).

Table 1. Distribution of frailty status and Vulnerable Elders Survey-13 (VES-13) scores according to dental status in the study sample

Variable		Functional dentition (≥20 teeth)	Partial dentition (1–19 teeth)	Edentulism (0 teeth)
Fried frailty phenotype	non-frail (0)	45.8 (40.5–51.2)	29.0 (26.1–31.9)	15.7 (12.7–18.7)
	pre-frail (1–2)	48.4 (43.0–53.9)	57.0 (54.0–60.0)	57.3 (54.0–60.6)
	frail (≥3)	5.8 (3.8–7.8)	14.0 (12.4–15.6)	27.0 (24.5–29.5)
VES-13 score		1.5 (1.4–1.7)	2.5 (2.4–2.6)	4.2 (4.0–4.4)
Test/effect size		frailty status: χ^2, $p < 0.001$ Cramér's $V = 0.20$ (moderate)	VES-13: ANOVA, $p < 0.001$ $\eta^2 = 0.11$ (moderate)	–

Data presented as percentage (95% confidence interval) (% (95% *CI*)) for frailty results, and mean (95% confidence interval) (*M* (95% *CI*)) for the VES-13. Effect size thresholds: small ($\eta^2 = 0.01$; Cramér's $V = 0.1$); moderate ($\eta^2 = 0.06$; Cramér's $V = 0.3$); large ($\eta^2 = 0.14$; Cramér's $V = 0.5$).
ANOVA – analysis of variance.

Table 2 presents the associations between dental status, denture use, and 2 indicators of vulnerability – frailty syndrome according to the Fried frailty phenotype and functional vulnerability measured using the VES-13. Marked differences in frailty status and functional vulnerability were observed across dentition and denture use categories. Among participants with ≥20 natural teeth, only 5.8% met the criteria for frailty, and the mean VES-13 score was the lowest (1.5, 95% *CI*: 1.4–1.7). In contrast, edentulous individuals who were not using dentures had the highest prevalence of frailty (46.0%, 95% *CI*: 36.6–55.4) and the highest average VES-13 score of 6.1 (5.5–6.7). Denture use was associated with better outcomes across all categories. For example, among edentulous individuals, those using dentures had a substantially lower prevalence of frailty (24.9% vs. 46.0%) and better functional status, as reflected by a lower mean VES-13 score (4.0 vs. 6.1). Similarly, among those with 1–19 teeth, denture wearers presented a lower prevalence of frailty (12.9% vs. 17.7%) and poorer functional status. Effect size analyses indicated that the association with frailty was of moderate strength, whereas the association with functional vulnerability was large.

Univariate logistic regression analyses revealed a strong associations of dental status with frailty and functional vulnerability, as determined by the VES-13 (Table 3). Compared with participants with functional dentition, individuals with 1–19 teeth had approx. 2.5-fold higher *OR*s, and edentulous patients almost 7-fold higher *OR*s regarding frailty and functional vulnerability. Among the other covariates analyzed, age, sex, BMI, education level, and smoking status were associated with both frailty and functional vulnerability. Regarding place of residence, a statistically significant association was observed for frailty among participants living in urban areas with <50,000 residents compared with those living in cities with >200,000 residents. No significant associations with VES-13-defined functional vulnerability were observed.

In multivariable logistic regression models that included covariates significant in the univariate analyses, edentulism was independently associated with significantly higher odds of both frailty (*OR* = 1.47) and functional vulnerability (*OR* = 1.38). Partial dentition (1–19 teeth) did not show a significant association with either outcome. Increasing age was a strong predictor of both frailty (*OR* = 1.12) and vulnerability (*OR* = 1.18) ($p < 0.001$). Male sex was associated with lower odds of frailty (*OR* = 0.60) and VES-13-defined vulnerability (*OR* = 0.63). Lower education levels were consistently associated with higher odds; individuals with primary education had more than twice the odds of both frailty and vulnerability compared to those with higher education. Residence in rural areas was associated with a reduced risk of frailty (*OR* = 0.65), but was not significantly associated with VES-13-defined vulnerability. Finally, smoking was not significantly linked to frailty but was associated with higher odds of functional vulnerability (*OR* = 1.31).

Discussion

This nationally representative study of older adults in Poland demonstrates a robust association between edentulism and increased odds of both physical frailty and functional vulnerability, independent of sociodemographic and clinical covariates. Participants with functional dentition had the most favorable health profiles, whereas edentulous individuals, especially those without dentures, showed the highest prevalence of functional deterioration and vulnerability. Effect size analyses indicated that these associations were not only statistically significant but also clinically meaningful. The relationship between dental status and frailty showed a moderate effect (Cramér's $V = 0.20$), as did the relationship between dental status and functional vulnerability ($\eta^2 = 0.11$), while the association between dentition/denture use and functional vulnerability, as measured by the VES-13, was large ($\eta^2 = 0.14$).

Our findings are consistent with international studies conducted in the UK, China and Brazil, which have reported higher frailty rates among older adults with few teeth and no dentures than among those retaining functional dentition.[22–26] By confirming these associations in a Central European population, our study adds important regional evidence to the existing literature.

Tobacco smoking is a well-established risk factor for periodontal disease and tooth loss, contributing to poor oral health outcomes and compounding the effects

Table 2. Distribution of frailty status and Vulnerable Elders Survey-13 (VES-13) scores according to dentition and denture use in the study sample

Dentition/denture use	Non-frail	Pre-frail	Frail	VES-13 score
≥20 teeth/not applicable	46.0 (40.6–51.4)	48.2 (42.8–53.7)	5.8 (3.8–7.8)	1.5 (1.4–1.7)
1–19 teeth/no denture use	21.9 (17.1–26.8)	60.3 (54.3–66.3)	17.7 (13.7–21.8)	2.3 (2.2–2.5)
1–19 teeth/denture use	31.1 (27.9–34.3)	56.0 (52.6–59.4)	12.9 (11.1–14.8)	3.2 (2.9–3.5)
Edentulous/no denture use	7.6 (3.2–12.0)	46.4 (36.3–56.5)	46.0 (36.6–55.4)	6.1 (5.5–6.7)
Edentulous/denture use	16.6 (13.3–19.8)	58.5 (55.1–61.9)	24.9 (22.3–27.6)	4.0 (3.8–4.3)
Test/effect size		frailty status: χ^2, $p < 0.001$ Cramér's $V = 0.21$ (moderate)		VES-13: ANOVA, $p < 0.001$ $\eta^2 = 0.14$ (large)

Data presented as % (95% *CI*) for frailty results, and *M* (95% *CI*) for the VES-13. Effect size thresholds: small ($\eta^2 = 0.01$; Cramér's $V = 0.1$); moderate ($\eta^2 = 0.06$; Cramér's $V = 0.3$); large ($\eta^2 = 0.14$; Cramér's $V = 0.5$).

Table 3. Logistic regression analyses of the associations of dental status and sociodemographic and health-related factors with frailty and functional vulnerability in older adults (PolSenior2)

Variable		Frailty *OR* (95% *CI*)	*p*-value	Frailty *AOR* (95% *CI*)	*p*-value	VES-13 score ≥3 *OR* (95% *CI*)	*p*-value	VES-13 score ≥3 *AOR* (95% *CI*)	*p*-value
Dentition	≥20 teeth (ref.)	–	–	–	–	–	–	–	–
	1–19 teeth	2.34 (1.79–3.06)	<0.001*	1.32 (0.99–1.76)	0.059	2.42 (2.04–2.87)	<0.001*	1.05 (0.85–1.29)	0.639
	edentulism	5.22 (4.00–6.81)	<0.001*	1.47 (1.08–2.01)	0.015*	6.09 (5.08–7.30)	<0.001*	1.38 (1.10–1.74)	0.006*
Age (per 5-year increase)		1.13 (1.12–1.14)	<0.001*	1.12 (1.11–1.13)	<0.001*	1.18 (1.17–1.20)	<0.001*	1.18 (1.17–1.19)	<0.001*
Sex (male)		0.98 (0.87–1.12)	0.810	0.60 (0.50–0.72)	<0.001*	0.80 (0.72–0.88)	<0.001*	0.63 (0.54–0.73)	<0.001*
Place of residence	urban, >200,000 residents (ref.)	–	–	–	–	–	–	–	–
	urban, 50,000–200,000 residents	0.89 (0.73–1.08)	0.240	0.81 (0.63–1.03)	0.088	1.02 (0.87–1.20)	0.829	–	–
	urban, <50,000 residents	0.82 (0.68–0.99)	0.038*	0.76 (0.60–0.96)	0.020*	0.91 (0.78–1.06)	0.226	–	–
	rural	0.90 (0.76–1.07)	0.245	0.65 (0.52–0.80)	<0.001*	1.11 (0.97–1.28)	0.141	–	–
Education	higher (ref.)	–	–	–	–	–	–	–	–
	secondary	1.10 (0.87–1.38)	0.426	1.43 (1.08–1.89)	0.013*	1.14 (0.97–1.35)	0.121	1.45 (1.15–1.82)	0.001*
	vocational	1.10 (0.87–1.40)	0.429	1.75 (1.30–2.36)	<0.001*	1.07 (0.90–1.28)	0.447	1.85 (1.45–2.35)	<0.001*
	primary	2.92 (2.34–3.64)	<0.001*	2.08 (1.57–2.77)	<0.001*	4.12 (3.44–4.94)	<0.001*	2.49 (1.95–3.17)	<0.001*
BMI [kg/m^2]	18.5–24.99 (ref.)	–	–	–	–	–	–	–	–
	<18.5	2.19 (1.30–3.69)	0.003*	1.54 (0.83–2.86)	0.173	2.19 (1.29–3.72)	0.004*	1.55 (0.76–3.16)	0.224
	≥25.0	0.83 (0.71–0.96)	0.014*	1.07 (0.89–1.28)	0.486	0.88 (0.78–1.00)	0.042*	1.14 (0.96–1.35)	0.137
Smoking status	non-smoker (ref.)	–	–	–	–	–	–	–	–
	former smoker	0.75 (0.65–0.86)	<0.001*	0.96 (0.81–1.13)	0.634	0.69 (0.62–0.77)	<0.001*	1.02 (0.87–1.19)	0.852
	current smoker	0.50 (0.40–0.63)	<0.001*	1.10 (0.83–1.47)	0.503	0.47 (0.40–0.56)	<0.001*	1.31 (1.04–1.65)	0.023*

Values are presented as odds ratios (*OR*s) and adjusted odds ratios (*AOR*s) with 95% *CI*s from univariable and multivariable logistic regression models for physical frailty (Fried score ≥3) and functional vulnerability (VES-13 score ≥3); * statistically significant ($p < 0.05$); BMI – body mass index; ref. – reference category.

of edentulism on overall health and frailty.[27,28] Tooth loss compromises mastication and limits dietary variety, reducing the intake of fruits, vegetables and protein-rich foods – factors linked to malnutrition, sarcopenia and impaired immune function, all of which are relevant to frailty.[29–31] Inflammatory processes associated with oral disease may further contribute to systemic aging, and recent evidence indicates that periodontal parameters such as the gingival index (GI) and clinical attachment level (CAL) are significantly associated with mild cognitive impairment in adults aged ≥55 years, independent of education level or sex.[32,33] Chronic diseases may further exacerbate oral health deterioration in older adults. For example, patients with Parkinson's disease are at increased risk of tooth wear, which is associated with impaired quality of life, bruxism and temporomandibular disorders.[34] Moreover, salivary biomarkers have been investigated as potential predictors of systemic aging and frailty, linking oral and general health through biological pathways.[35] The psychosocial impact of edentulism, including impaired speech, social withdrawal and reduced self-esteem, may also contribute to functional decline.[36–38] Chronic pain, which disproportionately affects older adults, may interact with oral disease, further reducing quality of life and accelerating functional decline.[39]

Denture use appeared to attenuate the observed risks of both physical frailty and functional vulnerability. Among edentulous participants, individuals who did not use dentures had the highest prevalence of frailty and a higher VES-13 score (6.1) than denture users (4.0). The apparent

discrepancy between the prevalence of frailty and VES-13-defined vulnerability likely reflects differences between the tools. The Fried frailty phenotype captures objective deficits, while the VES-13 emphasizes subjective health and independence. Similar findings from Asia support the beneficial role of prosthetic rehabilitation.[40] Nonetheless, denture users had less favorable outcomes than those with natural dentition, underscoring the importance of tooth retention as a primary goal for healthy aging.[41]

Male sex was inversely associated with frailty and functional vulnerability. This may reflect a combination of biological resilience and behavioral differences, such as men's tendency to underreport limitations, which can influence self-reported measures like the VES-13.[42]

Finally, frailty and functional vulnerability were, as expected, related to sociodemographic factors such as age, BMI and education, supporting the contribution of both biological and social determinants to age-related vulnerability.[43] Lower education was strongly associated with both frailty and functional vulnerability, underlining the importance of social determinants and health literacy in late-life trajectories. Rural and small-town residence appeared to be associated with lower odds of frailty, which may reflect greater physical activity or traditional dietary patterns, although further research is required. The BMI showed a complex pattern, consistent with the so-called "obesity paradox", in which underweight was linked to higher vulnerability, whereas overweight did not increase the odds after adjustment.[44]

Strengths and limitations

This study is among the first in Central Europe to investigate the relationship between dental status and frailty/functional vulnerability using a large, nationally representative dataset of older adults. The combined application of the Fried frailty phenotype and the VES-13 provided a multidimensional perspective, capturing both objective deficits and self-reported vulnerability.

Nevertheless, several limitations should be noted. First, the cross-sectional design precludes causal inference, and longitudinal studies are needed to clarify the temporal sequence of the observed associations. Second, comorbidities were not included in the analyses, and these may have confounded the observed associations. Third, important clinical variables such as denture fit, prosthesis type and masticatory performance were not captured, limiting the ability to assess the protective role of prosthetic rehabilitation. Fourth, dietary intake and physical activity were not directly assessed, although they represent key pathways linking oral health to frailty and disability. Fifth, some variables were based on self-reported data, which may have introduced recall or reporting bias. Although regression models were adjusted for sex, education and place of residence, unequal group sizes may have introduced residual confounding.

Conclusions

This study demonstrates that edentulism is a strong and independent predictor of both physical frailty and functional vulnerability in older adults. The associations persisted after adjustment for key demographic and clinical factors, highlighting the role of oral health as a critical, yet often overlooked, determinant of aging outcomes. Denture use appears to be correlated with more favorable outcomes but does not fully compensate for the loss of natural dentition. Given the high prevalence of tooth loss in aging populations, oral health assessments should be integrated into geriatric screening protocols, and efforts to promote lifelong oral care and access to prosthetic rehabilitation should be prioritized in public health strategies.

Ethics approval and consent to participate

The study was approved by the Independent Bioethics Committee of the Medical University of Gdańsk, Poland (approval No. NKBBN/257/2017). Written informed consent was obtained from all participants.

Data availability

The datasets generated and/or analyzed during the current study are available from the corresponding author on reasonable request.

Consent for publication

Not applicable.

Use of AI and AI-assisted technologies

ChatGPT (OpenAI, San Francisco, USA) was used for language support and linguistic editing.

ORCID iDs

Dorota Pylińska-Dąbrowska https://orcid.org/0000-0002-3617-2213
Hanna Kujawska-Danecka https://orcid.org/0000-0002-1416-620X
Kacper Jagiełło https://orcid.org/0000-0001-7138-5049
Małgorzata Mossakowska https://orcid.org/0000-0002-9340-3188
Tomasz Roman Zdrojewski https://orcid.org/0000-0001-6015-8561

References

1. World Health Organization. *Oral Health in Ageing Societies: Integration of Oral Health and General Health*. Geneva, Switzerland: World Health Organization; 2006. https://iris.who.int/bitstream/handle/10665/43531/9789241594501_eng.pdf;jsessionid=57DD73C039CDB6A1E3AA4AF5441F804C?sequence=1. Accessed June 20, 2024.
2. Peres MA, Macpherson LMD, Weyant RJ, et al. Oral diseases: A global public health challenge. *Lancet*. 2019;394(10194):249–260. doi:10.1016/S0140-6736(19)31146-8
3. Nascimento GG, Alves-Costa S, Romandini M. Burden of severe periodontitis and edentulism in 2021, with projections up to 2050: The Global Burden of Disease 2021 study. *J Periodontal Res*. 2024;59(5):823–867. doi:10.1111/jre.13337

4. Müller F, Naharro M, Carlsson GE. What are the prevalence and incidence of tooth loss in the adult and elderly population in Europe? *Clin Oral Implants Res*. 2007;18 Suppl 3:2–14. doi:10.1111/j.1600-0501.2007.01459.x
5. Dąbrowski W, Jagiełło K, Mossakowska M, et al. Evaluating changes in dental status among Polish older adults over a decade: A comparative analysis of PolSenior (2009) and PolSenior2 (2019) surveys. *Dent Med Probl*. 2025;62(1):23–30. doi:10.17219/dmp/196535
6. Thomson WM. Epidemiology of oral health conditions in older people. *Gerodontology*. 2014;31 Suppl 1:9–16. doi:10.1111/ger.12085
7. Holm G. Smoking as an additional risk for tooth loss. *J Periodontol*. 1994;65(11):996–1001. doi:10.1902/jop.1994.65.11.996
8. Souto MLS, Rovai ES, Villar CC, Braga MM, Pannuti CM. Effect of smoking cessation on tooth loss: A systematic review with meta-analysis. *BMC Oral Health*. 2019;19(1):245. doi:10.1186/s12903-019-0930-2
9. LaMonte MJ, Genco RJ, Hovey KM, et al. History of periodontitis diagnosis and edentulism as predictors of cardiovascular disease, stroke, and mortality in postmenopausal women. *J Am Heart Assoc*. 2017;6(4):e004518. doi:10.1161/JAHA.116.004518
10. Zhang Y, Leveille SG, Shi L. Multiple chronic diseases associated with tooth loss among the US adult population. *Front Big Data*. 2022;5:932618. doi:10.3389/fdata.2022.932618
11. Peršić Bukmir R, Paljević E, Pezelj-Ribarić S, Brekalo Pršo I. Association of the self-reported socioeconomic and health status with untreated dental caries and the oral hygiene level in adult patients. *Dent Med Probl*. 2022;59(4):539–545. doi:10.17219/dmp/138908
12. Wang F, Li T, Han Q, et al. Associations of tooth loss with risk of all-cause and cause-specific mortality among US adults with diabetes mellitus. *J Dent*. 2024;149:105304. doi:10.1016/j.jdent.2024.105304
13. Emami E, de Souza RF, Kabawat M, Feine JS. The impact of edentulism on oral and general health. *Int J Dent*. 2013;2013:498305. doi:10.1155/2013/498305
14. Yu J, Ye A, Fei Y, Wang D, Zhang Y, Li X. The association between oral frailty and HbA1c among older adults with T2DM: The chain mediating effect of nutritional status and physical frailty. *Eur Geriatr Med*. 2024;15(6):1891–1898. doi:10.1007/s41999-024-01081-z
15. Kunrath I, Silva AER. Oral health and depressive symptoms among older adults: Longitudinal study. *Aging Ment Health*. 2021;25(12):2265–2271. doi:10.1080/13607863.2020.1855104
16. Skośkiewicz-Malinowska K, Malicka B, Ziętek M, Kaczmarek U. Oral health condition and occurrence of depression in the elderly. *Medicine (Baltimore)*. 2018;97(41):e12490. doi:10.1097/MD.0000000000012490
17. Zhang W, Wu YY, Wu B. Does oral health predict functional status in late life? Findings from a national sample. *J Aging Health*. 2018;30(6):924–944. doi:10.1177/0898264317698552
18. Fried LP, Tangen CM, Walston J, et al.; Cardiovascular Health Study Collaborative Research Group. Frailty in older adults: Evidence for a phenotype. *J Gerontol A Biol Sci Med Sci*. 2001;56(3):M146–M157. doi:10.1093/gerona/56.3.M146
19. Pitter JG, Zemplényi A, Babarczy B, Németh B, Kaló Z, Vokó Z. Frailty prevalence in 42 European countries by age and gender: Development of the SHARE Frailty Atlas for Europe. *GeroScience*. 2024;46(2):1807–1824. doi:10.1007/s11357-023-00975-3
20. Saliba D, Elliott M, Rubenstein LZ, et al. The Vulnerable Elders Survey: A tool for identifying vulnerable older people in the community. *J Am Geriatr Soc*. 2001;49(12):1691–1699. doi:10.1046/j.1532-5415.2001.49281.x
21. Wierucki Ł, Kujawska-Danecka H, Mossakowska M, et al. Health status and its socio-economic covariates in the older population in Poland – the assumptions and methods of the nationwide, cross-sectional PolSenior2 survey. *Arch Med Sci*. 2022;18(1):92–102. doi:10.5114/aoms.2020.100898
22. Zhang XM, Cao S, Teng L, Xie X, Wu X. The association between the number of teeth and frailty among older adults: A systematic review and meta-analysis. *Aging Clin Exp Res*. 2025;37(1):156. doi:10.1007/s40520-025-03053-0
23. Ramsay SE, Papachristou E, Watt RG, et al. Influence of poor oral health on physical frailty: A population-based cohort study of older British men. *J Am Geriatr Soc*. 2018;66(3):473–479. doi:10.1111/jgs.15175
24. Zhang J, Xu G, Xu L. Number of teeth and denture use are associated with frailty among Chinese older adults: A cohort study based on the CLHLS from 2008 to 2018. *J Nutr Health Aging*. 2023;27(11):972–979. doi:10.1007/s12603-023-2014-x
25. de Andrade FB, Lebrão ML, Santos JLF, Duarte YAO. Relationship between oral health and frailty in community-dwelling elderly individuals in Brazil. *J Am Geriatr Soc*. 2013;61(5):809–814. doi:10.1111/jgs.12221
26. Bassim C, Mayhew AJ, Ma J, et al. Oral health, diet, and frailty at baseline of the Canadian longitudinal study on aging. *J Am Geriatr Soc*. 2020;68(5):959–966. doi:10.1111/jgs.16377
27. Hughes JR. Comorbidity and smoking. *Nicotine Tob Res*. 1999;1 Suppl 2:S149–S166. doi:10.1080/14622299050011981
28. Couch C, Alawieh AM, Toutonji A, Atkinson C, Tomlinson S. Evaluating the comorbidities of age and cigarette smoking on stroke outcomes in the context of anti-complement mitigation strategies. *Front Immunol*. 2023;14:1161051. doi:10.3389/fimmu.2023.1161051
29. Roberts S, Collins P, Rattray M. Identifying and managing malnutrition, frailty and sarcopenia in the community: A narrative review. *Nutrients*. 2021;13(7):2316. doi:10.3390/nu13072316
30. Ligthart-Melis GC, Luiking YC, Kakourou A, Cederholm T, Maier AB, van der Schueren MAE. Frailty, sarcopenia, and malnutrition frequently (co-)occur in hospitalized older adults: A systematic review and meta-analysis. *J Am Med Dir Assoc*. 2020;21(9):1216–1228. doi:10.1016/j.jamda.2020.03.006
31. Krzymińska-Siemaszko R, Deskur-Śmielecka E, Kaluźniak-Szymanowska A, et al. Socioeconomic risk factors of poor nutritional status in polish elderly population: The results of PolSenior2 study. *Nutrients*. 2021;13(12):4388. doi:10.3390/nu13124388
32. Iwasaki M, Kimura Y, Ogawa H, et al. Periodontitis, periodontal inflammation, and mild cognitive impairment: A 5-year cohort study. *J Periodontal Res*. 2019;54(3):233–240. doi:10.1111/jre.12623
33. Aranda Romo S, Garrocho-Rangel A, Marín González A, et al. Cognitive status and periodontitis: Is there a correlation? A cross-sectional study. *Dent Med Probl*. 2025;62(4):591–600. doi:10.17219/dmp/177412
34. Verhoeff MC, Wetselaar P, Lobbezoo F. Assessing the prevalence and risk of tooth wear in Parkinson's disease: A narrative review. *Dent Med Probl*. 2024;61(5):759–764. doi:10.17219/dmp/183842
35. Tabor E, Hüpsch H, Rokicka J, et al. Limited utility of salivary mineral content in prediction of fragility fractures among postmenopausal women. *Adv Clin Exp Med*. 2024;33(12):1343–1348. doi:10.17219/acem/181178
36. Cademartori MG, Gastal MT, Nascimento GG, Demarco FF, Corrêa MB. Is depression associated with oral health outcomes in adults and elders? A systematic review and meta-analysis. *Clin Oral Invest*. 2018;22(8):2685–2702. doi:10.1007/s00784-018-2611-y
37. Dai M, Song Q, Lin T, et al. Tooth loss, denture use, and all-cause and cause-specific mortality in older adults: A community cohort study [published correction appears in *Front Public Health*. 2024;11:1360927. doi:10.3389/fpubh.2023.1360927]. *Front Public Health*. 2023;11:1194054. doi:10.3389/fpubh.2023.1194054
38. Lim N, Lee D, Shin SY, Won CW, Kim M. Association between number of functional teeth and physical function among community-dwelling older adults: Korean frailty and aging cohort study. *BMC Geriatr*. 2024;24(1):1024. doi:10.1186/s12877-024-05585-y
39. Sobieszczańska MI. Chronic pain in the elderly: A constant challenge. *Adv Clin Exp Med*. 2025;34(2):149–151. doi:10.17219/acem/200647
40. Zitzmann NU, Hagmann E, Weiger R. What is the prevalence of various types of prosthetic dental restorations in Europe? [published correction appears in *Clin Oral Implants Res*. 2008;19(3):326–328]. *Clin Oral Implants Res*. 2007;18 Suppl 3:20–33. doi:10.1111/j.1600-0501.2007.01435.x
41. Alqahtani MK, Alammari MR, Fageeha YT. Awareness, knowledge, and acceptance of dental implants among the geriatric population of Jeddah, Saudi Arabia. *J Pharm Bioallied Sci*. 2022;14(Suppl 1):S464–S469. doi:10.4103/jpbs.jpbs_674_21
42. Oksuzyan A, Juel K, Vaupel JW, Christensen K. Men: Good health and high mortality. Sex differences in health and aging. *Aging Clin Exp Res*. 2008;20(2):91–102. doi:10.1007/BF03324754
43. Srivastava S, Muhammad T. Socioeconomic vulnerability and frailty among community-dwelling older adults: Cross-sectional findings from longitudinal aging study in India, 2017–18. *BMC Geriatr*. 2022;22(1):201. doi:10.1186/s12877-022-02891-1
44. Heymsfield SB, Cefalu WT. Does body mass index adequately convey a patient's mortality risk? *JAMA*. 2013;309(1):87–88. doi:10.1001/jama.2012.185445

Original paper

Frontal sinus morphology and surgical implications in forehead feminization: A radiographic and 3D anthropometric study

Rafał Pokrowiecki[1,2,A–D,F], Caner Bakici[3,B–D], Anna Lipowicz[4,C,E], Barbora Sufliarsky[5,C–E], Krzysztof Dowgierd[6,E,F]

[1] Prive Esthetic and Facial Feminization Surgery Center, Warsaw, Poland
[2] Department of Cranio-Maxillofacial Surgery, Oral Surgery and Implantology, Medical University of Warsaw, Poland
[3] Department of Anatomy, Faculty of Veterinary Medicine, Ankara University, Turkey
[4] Department of Anthropology, Institute of Environmental Biology, Wroclaw University of Environmental and Life Sciences, Poland
[5] Department of Oral and Maxillofacial Surgery, Faculty of Medicine, Comenius University in Bratislava and University Hospital, Slovakia
[6] Head and Neck Surgery Clinic for Children and Young Adults, Department of Clinical Pediatrics, University of Warmia and Mazury, Olsztyn, Poland

A – research concept and design; B – collection and/or assembly of data; C – data analysis and interpretation;
D – writing the article; E – critical revision of the article; F – final approval of the article

Dental and Medical Problems, ISSN 1644-387X (print), ISSN 2300-9020 (online) *Dent Med Probl*. 2026;63(5):1233–1241

Address for correspondence
Rafał Pokrowiecki
E-mail: dr.pokrowiecki@gmail.com

Funding sources
None declared

Conflict of interest
None declared

Acknowledgements
None declared

Received on July 8, 2025
Reviewed on August 27, 2025
Accepted on November 2, 2025

Published online on October 30, 2026

Cite as
Pokrowiecki R, Bakici C, Lipowicz A, Sufliarsky B, Dowgierd K. Frontal sinus morphology and surgical implications in forehead feminization: A radiographic and 3D anthropometric study. *Dent Med Probl.* 2026;63(5):1233–1241. doi:10.17219/dmp/213853

DOI
10.17219/dmp/213853

Copyright
Copyright by Author(s)
This is an article distributed under the terms of the Creative Commons Attribution 3.0 Unported (CC BY 3.0) (https://creativecommons.org/licenses/by/3.0/)

Abstract

Background. More than 90% of transgender patients undergoing gender-affirming procedures are individuals transitioning from male to female. Forehead feminization is one of the most commonly performed procedures in this patient population. Frontal sinus and fronto-orbital anatomy are crucial considerations in determining the surgical approach and technique.

Objectives. The present study aimed to analyze the anatomy of the frontal sinus and fronto-orbital region in transgender women undergoing forehead feminization surgery.

Material and methods. A retrospective analysis of computed tomography (CT) scans of 32 patients of European ethnicity, obtained between June 2022 and June 2024, was performed. Cross-sectional facial CT images were acquired using the Carestream CS 9600 system with the following scanning parameters: 120 kV; 5 mAs; and a voxel size of 300 × 300 × 300 µm. The modeling and superimposition of the frontal sinuses were performed. The data were analyzed using IBM SPSS Statistics for Windows, v. 22.0.

Results. The mean frontal sinus dimensions were as follows: height – 37.90 mm; width – 63.30 mm; and depth – 31.03 mm. Bilaterally developed frontal sinuses with a central septum were observed in 88% of patients. Additional septations were identified on the right side in 25% of cases and on the left side in 22%. The anatomy of the supraorbital foramina varied considerably. The separate foramen variant was observed in 34% of cases on the right and 56% on the left, whereas the notch variant was observed in 66% and 44% of cases, respectively. Frontal bone osteotomy and setback were required in 28 cases (87.5%), while osteoplasty alone was performed in 4 cases (12.5%). The mean setback/reduction of the frontal prominence was 4.86 ±1.56 mm, corresponding to 6.14 ±1.9% of its initial size, to reduce masculine forehead characteristics.

Conclusions. The anatomy of the frontal sinus, bone thickness, the size of the frontal prominence, the location of a central septum and/or additional septations, and the exit points of the supraorbital nerves may significantly influence the surgical technique used in forehead feminization.

Keywords: surgery, computed tomography, craniofacial, facial feminization

Highlights

- The study demonstrates considerable frontal sinus anatomical variability in transgender women undergoing forehead feminization.
- Frontal sinus anatomy, anterior wall thickness, frontal prominence, septal morphology, and supraorbital nerve exit points may significantly influence surgical planning and technique selection.
- Three-dimensional (3D) virtual surgical planning facilitates individualized preoperative assessment and may contribute to safer surgery, more predictable outcomes and reduced complication risks, and eventually to greater patient satisfaction.
- Frontal bone reconstruction (Type III surgery) was required in 87.5% of patients, highlighting the importance of frontal bone thickness and prominence in determining the appropriate surgical technique.

Introduction

More than 90% of transgender patients seeking gender-affirming care are individuals transitioning from male to female.[1] Forehead reduction is one of the most frequently performed procedures in transgender women, as the upper third of the face accounts for approximately 35% of facial height, and its anatomical features play an important role in the perception and psychological categorization of an individual's appearance.[2]

Some anatomical differences between male and female faces are subtle, whereas others are more distinctive. Sexual dimorphism in cranial morphology, in addition to differences in the overall body size and proportions, is an important factor contributing to differences in appearance between the sexes. The overall size and shape of male and female faces differ, particularly in the upper third of the face and the mandibular region.[3] Female faces are generally smaller, with a more prominent forehead, more pronounced frontal eminences, and higher, more arched eyebrows. Females also tend to have relatively larger eyes with a slightly more oblique orientation.[4,5] Male skulls are generally characterized by more pronounced cranial contours. The male forehead is relatively lower, the eyebrows are positioned lower, and the eyeballs are more deeply set. The glabellar region and the supraorbital ridges are also more strongly pronounced compared with female skulls.[5] Physicians performing surgery in this region must be aware of the anthropological diversity and anatomical variations of the craniofacial region.[6,7]

Typically masculine features, such as prominent brow ridges and frontal bossing, are reduced and reshaped during forehead feminization surgery. The surgical approaches to forehead reduction were first described by Sir D. Ousterhout in his work on facial feminization surgery (FFS).[8,9] Type I surgery involves the reduction of the frontal cortical bone through burring. This is the most basic technique and is generally appropriate when the frontal sinus is underdeveloped and/or the anterior table of the frontal sinus is sufficiently thick to achieve the desired esthetic outcome while maintaining bone wall integrity. It is also considered the safest approach, since the frontal sinus is not entered during the procedure.[9,10] Type II surgery is performed when no frontal bone setback is required, but the augmentation of the forehead is necessary to achieve a more feminine forehead slope and nasofrontal angle (the angle formed between the facial line and the vertical line of the nasal dorsum, which is generally greater in females than in males). Type III surgery, however, is a considerably more advanced technique and involves the complete reconstruction of the forehead through frontal bone osteotomy, followed by the remodeling and setback of the frontal bone segment, usually stabilized with plates and screws or wires.[1,9] Nowadays, Type III surgery is performed in more than 90% of transgender patients requiring forehead feminization.[11–14]

The surgical procedure must be performed in a manner that avoids the disruption of the nasofrontal drainage pathway, injury to vital structures such as the supraorbital and olfactory nerves, and cerebrospinal fluid leakage. The extent of reduction should be determined according to the individual patient's facial anatomy and esthetic expectations. Limiting the extent of reduction solely out of concern about entering the frontal sinus is a common surgical mistake. This may result in patient dissatisfaction with the esthetic outcome and the need for revision surgery, which is frequently associated with complications related to re-entry, such as ischemia, hair loss, scarring, and an increased risk of injury to nerves and blood vessels.[2] The undercorrection of frontal bossing is, therefore, one of the most common reasons for revision surgery, highlighting the importance of meticulous preoperative assessment.[7,15]

The anatomy of a central septum and additional septations may influence the surgical technique used for the osteotomy, removal and stabilization of the frontal bone segment. Therefore, the precise localization of the septa is important when planning osteotomy and bone resection, which may be performed as a single-piece or two-piece procedure. Bone thickness along the borders of the repositioned anterior wall determines the appropriate length of the screws and the type of plate system required for bone fixation. Inadequate stabilization may lead to non-union, inflammation, sinusitis, and mucocele formation.[11,14]

From this perspective, it is particularly important to consider modern approaches, such as digital surgical planning. Wide-field cone-beam computed tomography (CBCT) can be used to plan bone resections and anticipate the final surgical outcome, as described by Perrotti et al.[16] Recent advances in three-dimensional (3D) surgical planning also provide detailed insight into frontal sinus anatomy and have been shown to be beneficial in facial feminization procedures.[17,18]

The aim of this study was to evaluate the anatomical landmarks of the frontal sinus in transgender women (individuals transitioning from male to female) to identify features that may be helpful in surgical planning and decision-making.[19–21] Through this work, we aspired to contribute to broader scientific discourse on craniofacial anatomy and its application in surgical interventions tailored to individual facial anthropometry. To the best of the authors' knowledge, this is the first study to propose an approach to surgical feminization of the upper face based on frontal sinus anatomy using 3D modeling, and to compare frontal sinus anatomy between cisgender and transgender women.

Material and methods

The study was approved by the Bioethics Committee of the Medical University of Warsaw, Poland (approval No. AKBE/21/2025).

A retrospective case–control analysis of computed tomography (CT) scans from 32 patients of European ethnicity who underwent forehead feminization surgery between June 2022 and June 2024 was performed (case group). The facial CT images were acquired using the Carestream CS 9600 system with the following scanning parameters: 120 kV; 5 mAs; and a voxel size of 300 × 300 × 300 µm.

The inclusion criteria were as follows: patients undergoing gender-affirming facial surgery involving the orbitofrontal region; at least 6 months of hormone replacement therapy (HRT); and ongoing care under the supervision of a psychologist and sexologist. The exclusion criteria comprised incomplete medical records, facial surgery not involving the upper third of the face, and age below 18 years.

For comparison, the CT scans of the skulls of 32 adult cisgender women were retrieved and analyzed as the control group.

3D modeling and superimposition of the frontal sinuses

The modeling and superimposition of the frontal sinuses of transgender women (n = 32) and cisgender women (n = 32) were performed. For each participant, a 3D model of the frontal sinus was generated by the segmentation of the corresponding Digital Imaging and Communications in Medicine (DICOM) data.

The raw imaging data were stored in the DICOM format and imported into 3D Slicer software (v. 4.1.20; GitHub). Before segmentation, all image data were analyzed using identical parameters (window level: 485 HU; window width: 2,730 HU). The coronal slices of the outer compact layer of the frontal bone were obtained perpendicular to the hard palate, extending posteriorly to the posterior wall of the sphenoid bone. In contrast, axial slices were restricted to the soft tissue region.

The Segment Editor module was used to isolate the frontal sinus from the surrounding tissues. Three-dimensional models were generated using a semi-automatic segmentation procedure, which involved automatic segmentation followed by manual inspection and the correction of segment boundaries and cross-sectional contours. The intensity threshold for the segmentation of the frontal sinus in the 3D reconstructed models ranged from –1,023 to –350 HU. The axial views of the cross-sectional CT images were primarily used for 3D modeling, while coronal and sagittal views were used to identify and correct unwanted or incorrectly segmented areas, using the Segment Editor tool (3D Slicer, v. 4.1.20, stable release). The final 3D models were subsequently generated and exported according to the software's model-exporting procedure.

Subsequently, the reconstructed frontal sinus models were superimposed to evaluate anatomical similarities and differences between the groups. The CT-derived 3D models were aligned and registered using the ImageJ software (v. 1.42; National Institutes of Health (NIH), Bethesda, USA). All images were registered and stacked using identical spatial resolution and inter-slice distances with the Z Project function (ImageJ, v 1.42). The degree of overlap between the models was then evaluated using root mean square (RMS) values. This process generated a color-coded map illustrating the accuracy of superimposition.

The resulting color scale ranged from blue to red, with red indicating areas of substantial overlap between the models and therefore a high degree of congruence, while blue represented regions with minimal or no overlap, indicating anatomical discrepancies. Green represented an intermediate degree of alignment. This color-coded representation enabled the visualization and comparison of anatomical variations and alignment between the groups, providing insight into the structural variability of the frontal sinuses in transgender and cisgender women.

Anatomical measurements and clinical parameters

Using the 3D reconstructed models, the following anatomical parameters were assessed and measured in cisgender and transgender women: frontal sinus morphology (unilateral or bilateral development); the location and number of septa; and sinus width, height and depth (Fig. 1). Based on these measurements, the volume of each frontal sinus was calculated. To assess intra-rater reliability, all

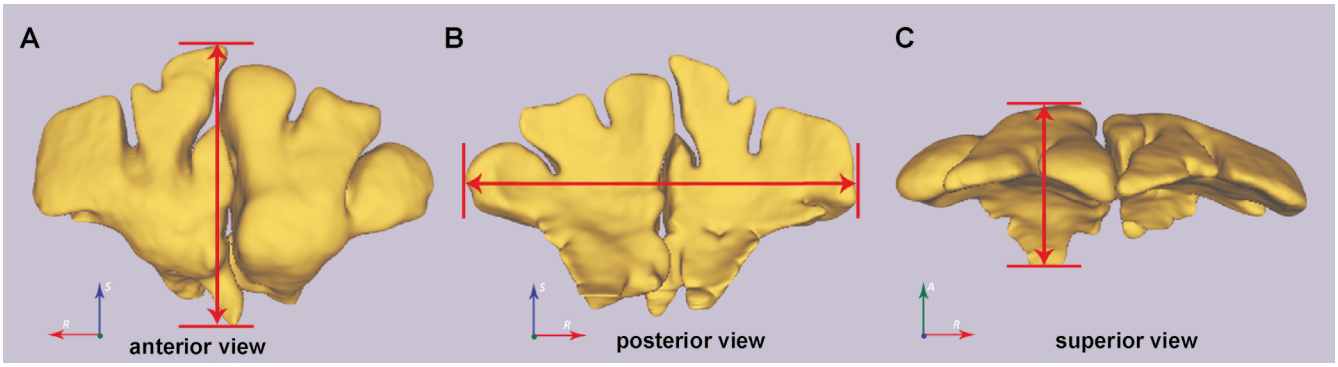

Fig. 1. Three-dimensionally (3D) reconstructed model of frontal sinus anatomy in transgender patients

A – anterior view of the 3D frontal sinus model (red arrow – maximum height of the frontal sinus); B – posterior view of the 3D frontal sinus model (red arrow – maximum width of the frontal sinus); C – superior view of the 3D frontal sinus model (red arrow – maximum depth of the frontal sinus).

measurements were repeated after a 15-day interval, and the mean values of the two measurements were used for subsequent analysis.

Frontal bone thickness was measured at the midpoint between the coronal suture and the nasion, and was referred to as anterior wall thickness. The distance from the outer table of the frontal sinus to the midsellar point was also measured and defined as the frontal prominence-to-midsella distance (hereafter referred to as frontal prominence). These parameters were assessed both before and after surgery in transgender women. Additionally, the type of surgery required for forehead feminization and the extent of anterior wall reduction/setback were evaluated.

Statistical analysis

Before conducting the analyses, sample size calculations were performed to ensure sufficient statistical power. Cohen's effect size (d) was estimated at 1.98. Assuming a significance level of $\alpha = 0.01$ and a statistical power of 0.95, the required sample size was 22 individuals (11 in each of the 2 study groups). With a total sample size of 64 individuals, the achieved statistical power was estimated to exceed 99.99%.

Descriptive statistics, including the mean (M), standard deviation (SD), and minimum–maximum (min–max)values, were calculated for all frontal sinus measurements. Differences in frontal sinus measurements between cisgender and transgender women were assessed using the Mann–Whitney U test. Changes in frontal prominence before and after surgery were evaluated using the Wilcoxon signed-rank test. Differences in frontal prominence between preoperative and postoperative measurements in transgender women and measurements in cisgender women were assessed using Tukey's post hoc test.

Additionally, the frequencies of individuals with or without a central septum and with additional septations on the right and/or left sides were calculated. The frequencies and percentages of supraorbital foramina and notches, as well as their distribution between the right and left sides, were also determined. The χ^2 test was used to assess the statistical significance of differences in categorical variables. Pearson's correlation coefficient was used to evaluate the relationship between preoperative frontal prominence and the extent of the required setback/reduction.

All statistical analyses were performed using IBM SPSS Statistics for Windows, v. 22.0 (IBM Corp., Armonk, USA), and Statistica, v. 13.3 (StatSoft. Krakow, Poland). A p-value of less than 0.05 was considered statistically significant (supplementary material: Statistical analysis, available on request from the corresponding author)

Results

A total of 32 adult transgender women who underwent FFS involving the upper third of the face were included in the study. Patients ranged in age from 18 to 51 years, with a mean age of 30.91 ±9.45 years. The mean height of the frontal sinuses was 37.90 mm, while the mean width and depth were 63.30 mm and 31.03 mm, respectively. The mean frontal prominence was 79.09 ±3.30 mm, and the mean anterior wall thickness was 2.63 ±1.73 mm. In the control cohort, consisting of adult cisgender women within the same age range, the mean frontal sinus dimensions were as follows: height – 29.30 mm; width – 51.10 mm; and depth – 23.9 mm (Table 1). One individual in the cisgender cohort had an absent frontal sinus. Three-dimensional superimposition enabled the generation of a model-based visualization of frontal sinus anatomy in transgender women before feminization surgery, compared with the anatomy of cisgender women (Fig. 2, supplementary material: Video 1).

Transgender women exhibited bilaterally developed frontal sinuses. A central septum was observed in 88% of cases, whereas it was absent in the remaining 12%. Additional septations were identified on the right side in 25% of cases and on the left side in 22%, with no statistically significant difference in their occurrence between sides (Fig. 3A). The anatomy of the supraorbital foramina also varied. The notch variant was observed in 66% of cases on the right and 44% on the left, whereas the separate

Table 1. Comparison of the upper face and frontal sinus measurements in cis- and transgender women

Measurements	Cisgender women		Transgender women		Δ trans–cis	*Z* / *p*-value (Mann–Whitney *U* test)
	M ±*SD*	min–max	*M* ±*SD*	min–max		
Frontal prominence [mm]	72.15 ±4.04	61.5–79.8	79.09 ±3.30	72.3-86.7	6.94	–5.65 / <0.0001*
Anterior wall thickness [mm]	3.22 ±1.49	1.2–6.8	2.63 ±1.73	0.9–8.8	–0.59	2.22 / 0.0263*
Frontal sinus height [mm]	29.30 ±7.00	13.7–45.0	37.90 ±6.40	28.0–54.3	8.60	4.22 / <0.0001*
Frontal sinus width [mm]	51.10 ±12.60	25.8–78.9	63.30 ±12.80	33.0–91.0	12.20	3.43 / 0.0006*
Frontal sinus depth [mm]	23.90 ±4.80	14.3–35.2	31.03 ±6.03	21.9–49.0	7.13	4.39 / <0.0001*
Volume [mm3]	5,859.5 ±3,454.4	1,458–17,643	1,284.7 ±5,524.5	3,143–31,315	–4,574.8	4.86 / <0.0001*

M – mean; *SD* – standard deviation; min – minimum; max– maximum; * statistically significant.

foramen variant was observed in 34% on the right and 56% on the left (Fig. 3B). A statistically significant difference in supraorbital anatomy between the right and left sides was observed in the transgender cohort ($p = 0.035$).

Type III surgery was required in 28 cases (87.5%), whereas osteoplasty (Type I) was performed in 4 cases (12.5%) (Fig. 4 and 5). No indications for Type II or Type IV surgery were identified in this study.

The mean required setback of the frontal bone was 4.86 ±1.56 mm, while the mean desired frontal prominence after surgery was 74.22 ±3.08 mm (Table 2).

Patients with thinner anterior frontal sinus walls more frequently required bone reconstruction (Type III surgery) rather than bone burring (Type I surgery) ($p = 0.002$). An anterior wall thickness of 5.1 mm or greater was associated with a 95% probability of achieving satisfactory results using Type I surgery (Fig. 6A).

A statistically significant correlation was also observed between preoperative frontal prominence and the extent of forehead reduction required, with greater frontal prominence being associated with an increased likelihood of requiring Type III surgery ($p = 0.005$) (Fig. 6B). Each 1-mm increase in preoperative frontal prominence was associated with a 0.25-mm increase in the required setback/reduction.

In patients undergoing Type III surgery in whom a thick central septum was identified preoperatively on CT scans, a two-piece segmental frontal bone ostectomy was performed, followed by the reduction of the septum using a surgical burr.

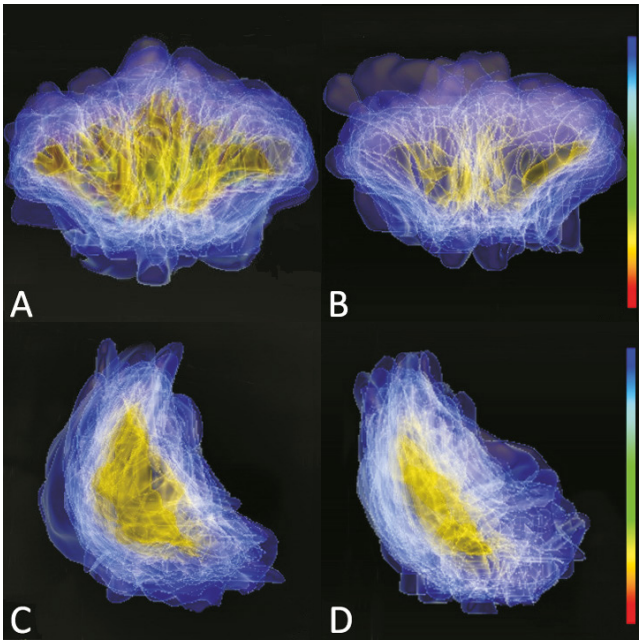

Fig. 2. Superimposition of all frontal sinus models reconstructed from computed tomography (CT) scans

A – transgender women, frontal view; B – cisgender women, frontal view; C – transgender women, lateral view; and D – cisgender women, lateral view. Following the registration of all models, the software generated an average color-coded representation based on root mean square (RMS) values. The color scale ranged from blue to red, with red indicating a high degree of superimposition between models and blue indicating minimal overlap; green and yellow represented intermediate degrees of alignment. The comparison demonstrates substantial differences in the volume and dimensions of the frontal sinuses between transgender and cisgender women, highlighting the anatomical challenges that must be considered when planning forehead feminization surgery involving the upper third of the face.

Table 2. Frontal prominence measurements before and after surgery in transgender women

Measurement	Transgender women								*Z* / *p*-value (Wilcoxon test)
	before surgery		after surgery		reduction				
	M ±*SD*	min–max	*M* ±*SD*	min–max	*M* ±*SD*	min–max	% *M* ±*SD*	% min–max	
Frontal prominence [mm]	79.09 ±3.30	72.3–86.7	74.22 ±3.08	68.0–81.0	4.86 ±1.56	2.2–8.7	6.14 ±1.90	2.7–10.4	4.94 / <0.0001*

* statistically significant.

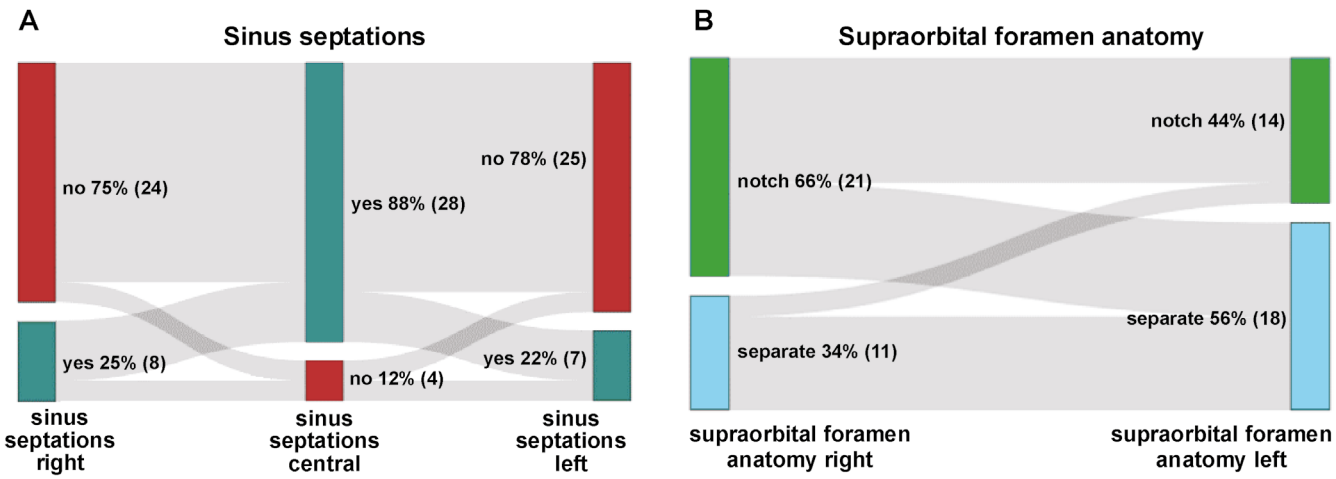

Fig. 3. Distribution and percentage of sinus septations (A) and the anatomical variants of the supraorbital/supratrochlear nerves (B) in the analyzed transgender women

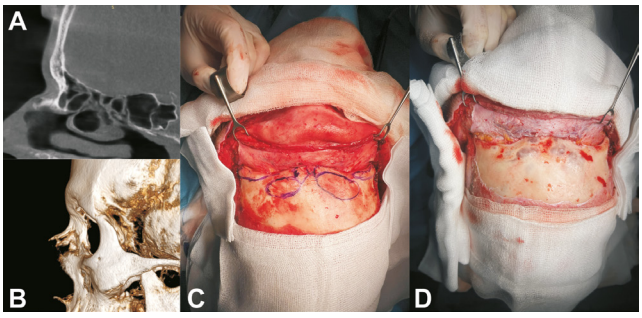

Fig. 4. Sagittal computed tomography (CT) cross-section (A) and 3D reconstruction (B) showing an underdeveloped frontal sinus and typical male frontal bossing. Intraoperative photograph showing the areas marked for bone reduction by burring/ostectomy (Type I surgery). Intraoperative photograph showing the reduced frontal bossing and frontal eminences, with the areas around the orbital apertures marked for osteoplasty (C). Postoperative view (D)

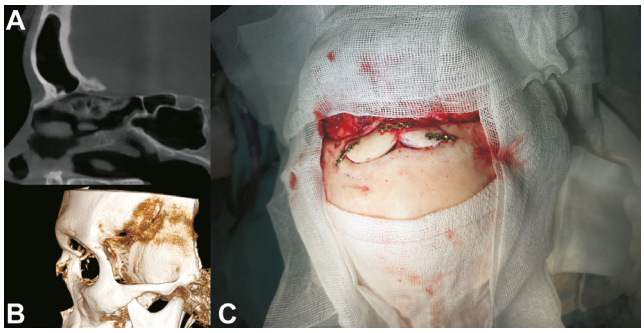

Fig. 5. Sagittal computed tomography (CT) cross-section (A) and 3D reconstruction (B) showing a pneumatized frontal sinus and frontal bossing. Intraoperative view of the frontal sinus following the completion of the anterior wall osteotomy, repositioning and setback, with fixation using titanium microplates and screws (Type III surgery) (C) (ChM, Lewickie, Poland)

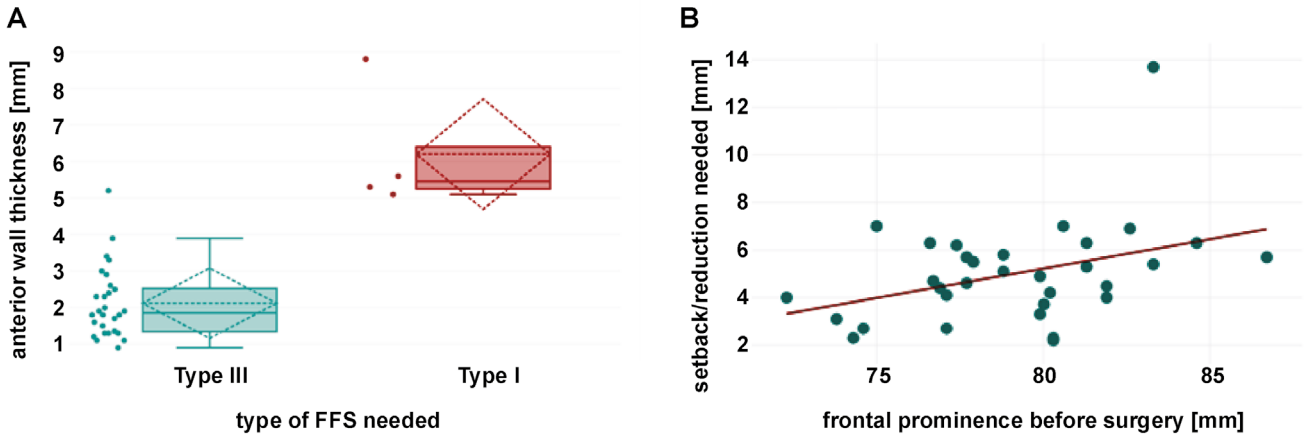

Fig. 6. A – Comparison of anterior wall thickness [mm] between patients requiring Type III and Type I surgery (Mann–Whitney *U* test). A statistically significant difference in anterior wall thickness was observed between the 2 groups ($p = 0.002$); B – Pearson's correlation analysis demonstrating a moderate positive correlation ($r = 0.37$) between preoperative frontal prominence and the extent of the required setback/reduction ($p = 0.037$)

FFS – facial feminization surgery..

Discussion

Recently, a growing body of literature has focused on quantitative assessments in reconstructive oral and maxillofacial surgery, particularly regarding facial characteristics and the roles of both hard and soft tissues.[22–24] Volumetric assessments of the frontal sinuses and maxillofacial region are increasingly performed using 3D reconstruction techniques based on high-resolution imaging technologies, such as CT.[25–28]

Studies by Hamed et al.[29] and Mrożek et al.[30] demonstrated that the measurements of frontal sinus dimensions, particularly the anteroposterior length, are valuable in investigating sexual dimorphism between biological males and females. Similarly, our study revealed significant differences in anteroposterior sinus length, height and width between transgender and cisgender women. Additionally, sex-related differences were observed in other dimensions of the fronto-orbital region: cisgender women had significantly smaller frontal prominences, greater anterior wall thicknesses, and, consequently, smaller frontal sinus volumes. The magnitude and statistical significance of these differences highlight the importance of detailed anatomical assessment for surgeons performing facial feminization surgery in transgender women.

Forehead feminization is one of the most commonly performed procedures in transgender women. Therefore, a precise and individualized surgical plan is essential to avoid undercorrection, patient dissatisfaction, and eventually the need for revision surgery. In a recent study by Rochlin et al., undercorrection and patient dissatisfaction were identified as the main reasons for revision surgery, which was required in 25% of cases.[7] Similar observations were reported in our previous study.[2] These outcomes may result from inadequate preoperative diagnostics and surgical planning, a conservative surgical approach, insufficient experience or equipment, fear of entering the frontal sinus, or other contributing factors. Computed tomography and 3D surgical planning should include an assessment of frontal prominence (defined as the distance from the anterior table of the frontal sinus to the midsellar point), the degree of frontal sinus pneumatization, and frontal bone thickness.[18] By evaluating these anatomical parameters, the surgical technique can be safely tailored to each individual case.

In our study, forehead feminization involved a mean anterior wall setback of 4.86 ±1.56 mm to achieve the desired esthetic outcome, corresponding to 6.14 ±1.9% of preoperative frontal prominence. The mean postoperative frontal prominence was 74.22 mm, which is comparable to the results reported by other authors.[12] Importantly, the range of postoperative frontal prominence values in transgender women was not significantly different from the range observed in cisgender women. Frontal sinus aplasia has been reported in approx. 3–4% of individuals. In our transgender cohort, no cases of frontal sinus aplasia were observed. However, one individual in the cisgender cohort lacked a frontal sinus (3.1%), which is consistent with previously published literature.

In our study, no patients required Type II surgery, which is relatively uncommon and reportedly accounts for less than 10% of forehead feminization procedures in transgender women. Particular care should be taken when determining the indications for Type II surgery, as some patients may actually require Type III reconstruction. Surgical access to the orbital region requires the elevation of a subperiosteal flap through a coronal incision or its modifications, depending on the shape and position of the hairline.[2,31] During dissection, the surgeon must avoid injury to the supraorbital nerves, which provide sensory innervation to the forehead. Therefore, the position and morphology of the supraorbital foramina should be carefully evaluated preoperatively. The extracranial passage of these nerves may occur through a notch continuous with the supraorbital margin or through a distinct foramen separated from the margin. When a supraorbital notch is present, the supraorbital neurovascular bundles are released and protected intraoperatively. When a distinct foramen is present, osteotomy may be required to release and protect the neurovascular bundle.[18,32]

Regarding flap preparation and nerve preservation, the supraorbital notch variant may provide a more predictable anatomical landmark during flap elevation than multiple foramina. This is particularly relevant, as orbital feminization requires wide exposure of the orbital aperture and the reduction of its upper and lateral borders. The extent of frontal bone reduction and setback may also be influenced by the presence and morphology of a central septum. In cases involving a thick central septum, the frontal bone may need to be resected in 2 separate segments. Forceful removal of the bone segment should be avoided, as this may result in the fractures of the frontal bone or the septum, and potentially damage the adjacent structures, including the ethmoidal cribriform plate, crista galli, the nasal cavity, and the orbital roof or its superomedial portion. Such complications may require additional surgical management similar to that used in the treatment of frontal bone fractures. To the best of the authors' knowledge, this is also the first study to discuss the relevance of frontal sinus septations in planning upper-face feminization surgery.

Limitations

We acknowledge several limitations of this study. First, the study design did not account for differences in body measurements between the 2 groups (transgender and cisgender women). Body size exhibits biological sexual dimorphism, with significant differences between biological sexes not only in the overall body height ,but also in skull length, width and height. These differences may have influenced frontal sinus dimensions and anterior wall thickness before surgery, as well as the dimensions of the frontal sinus and the frontal region after surgery. Nevertheless, the postoperative frontal prominence values in transgender women were comparable to those observed in the cisgender control group, which was one of the primary goals of the surgical interventions. Second, no patients in the surgical cohort met the criteria for Type II or Type IV surgery, which limited the possibility of evaluating the applicability of these surgical techniques in our study population.

Conclusions

Within the limitations of this retrospective study, the frontal sinus was present in almost all transgender women undergoing the feminization surgery of the upper third of the face. The frontal sinuses were significantly more pneumatized than those in the cisgender control group, although considerable anatomical variability was observed among individual patients. The application of 3D virtual surgical planning is therefore crucial for ensuring safe and individualized surgical treatment, as the considerable variability in frontal sinus anatomy requires meticulous preoperative evaluation. Precise preoperative imaging enables the surgical plan to be tailored to each patient's individual anatomy, potentially resulting in more predictable outcomes, shorter operative times, and a reduced risk of complications, while helping to achieve satisfactory esthetic effects and improve patient satisfaction.

Ethics approval and consent to participate

The study was approved by the Bioethics Committee of the Medical University of Warsaw, Poland (approval no. AKBE/21/2025), and was conducted in accordance with the Declaration of Helsinki. Written informed consent was obtained from all study participants.

Data availability

The datasets supporting the findings of the current study, including all the supplementary materials, are available from the corresponding author on reasonable request.

Consent for publication

Written informed consent was obtained from individuals whose photographs are presented in this article.

Use of AI and AI-assisted technologies

Not applicable.

ORCID iDs

Rafał Pokrowiecki https://orcid.org/0000-0001-8604-1468
Caner Bakici https://orcid.org/0000-0003-2413-3142
Anna Lipowicz https://orcid.org/0000-0002-9182-6953
Barbora Sufliarsky https://orcid.org/0000-0002-1394-4719
Krzysztof Dowgierd https://orcid.org/0000-0002-7605-2080

References

1. Ousterhout DK. Facial feminization surgery: The forehead. Surgical techniques and analysis of results. *Plast Reconstr Surg*. 2015;136(4):560e–561e. doi:10.1097/PRS.0000000000001425
2. Pokrowiecki R, Šufliarsky B, Jagielak M. Feminization surgery of the upper face as the crucial factor in gender confirmation – pearls and pitfalls. *Medicina (Kaunas)*. 2024;60(1):120. doi:10.3390/medicina60010120
3. Matthews HS, Mahdi S, Penington AJ, et al. Using data-driven phenotyping to investigate the impact of sex on 3D human facial surface morphology. *J Anat*. 2023;243(2):274–283. doi:10.1111/joa.13866
4. Tomaszewska A, Kwiatkowska B, Jankauskas R. Is the area of the orbital opening in humans related to climate? *Am J Hum Biol*. 2015;27(6):845–850. doi:10.1002/ajhb.22735
5. Tanikawa C, Zere E, Takada K. Sexual dimorphism in the facial morphology of adult humans: A three-dimensional analysis. *Homo*. 2016;67(1):23–49. doi:10.1016/j.jchb.2015.10.001
6. Altman K. Facial feminization surgery. In: Bouman WP, Arcelus J, eds. *The Transgender Handbook: A Guide for Transgender People, Their Families and Professionals*. New Yor, NY: Nova Science Publishers, Inc.; 2017:301–318.
7. Rochlin DH, Chaya BF, Colon RR, Onuh O, Rojas A, Rodriguez ED. Secondary surgery in facial feminization: Reasons and recommendations. *Ann Plast Surg*. 2022;89(6):652–655. doi:10.1097/SAP.0000000000003308
8. Dassi CS, Demarco FR, Mangussi-Gomes J, Weber R, Balsalobre L, Stamm AC. The frontal sinus and frontal recess: Anatomical, radiological and surgical concepts. *Int Arch Otorhinolaryngol*. 2020;24(3):e364–e365. doi:10.1055/s-0040-1713923
9. Ousterhout DK, Deschamps-Braly JC. Special edition on transgender facial surgery. *J Craniofac Surg*. 2019;30(5):1326–1327. doi:10.1097/SCS.0000000000005387
10. Ousterhout DK, Vargervik K. Surgical treatment of the jaw deformities in hemifacial microsomia. *Aust N Z J Surg*. 1987;57(2):77-87. doi:10.1111/j.1445-2197.1987.tb01310.x
11. Telang PS. Facial feminization surgery: A review of 220 consecutive patients. *Indian J Plast Surg*. 2020;53(2):244–253. doi:10.1055/s-0040-1716440
12. Capitán L, Simon D, Kaye K, Tenorio T. Facial feminization surgery: The forehead. Surgical techniques and analysis of results. *Plast Reconstr Surg*. 2014;134(4):609–619. doi:10.1097/PRS.0000000000000545
13. Sathyanarayanan R, Raghu K, Deepika S, Sarath K. Management of frontal sinus injuries. *Ann Maxillofac Surg*. 2018;8(2):276–280. doi:10.4103/ams.ams_187_18
14. Sawatari Y, Caceres J. Management of frontal sinus fractures. In: Bagheri SC, Bell RB, Khan HA. *Current Therapy in Oral and Maxillofacial Surgery*. Philadelphia, PA: Elsevier/Saunders; 2011:346–353. doi:10.1016/B978-1-4160-2527-6.00043-8
15. Dang BN, Hu AC, Bertrand AA, et al. Evaluation and treatment of facial feminization surgery: Part I. Forehead, orbits, eyebrows, eyes, and nose. *Arch Plast Surg*. 2021;48(5):503–510. doi:10.5999/aps.2021.00199
16. Perrotti G, Reda R, Rossi O, D'Apolito I, Testori T, Testarelli L. A radiation free alternative to CBCT volumetric rendering for soft tissue evaluation. *Braz Dent Sci*. 2023;26(1). doi:10.4322/bds.2023.e3726
17. Gray R, Nguyen K, Lee JC, et al. Osseous transformation with facial feminization surgery: Improved anatomical accuracy with virtual planning. *Plast Reconstr Surg*. 2019;144(5):1159–1168. doi:10.1097/PRS.0000000000006166
18. Callen AL, Badiee RK, Phelps A, et al. Facial feminization surgery: Key CT findings for preoperative planning and postoperative evaluation. *AJR Am J Roentgenol*. 2021;217(3):709–717. doi:10.2214/AJR.20.25228
19. Hacl A, Costa A, Oliveira JM, Tucunduva MJ, Girondi JR, Nahás-Scocate AC. Three-dimensional volumetric analysis of frontal sinus using medical software. *J Forensic Radiol Imaging*. 2017;11:1–5. doi:10.1016/J.JOFRI.2017.08.004
20. Viana Wanzeler AM, Alves-Júnior SM, Ayres L, da Costa Prestes MC, Gomes JT, Tuji FM. Sex estimation using paranasal sinus discriminant analysis: A new approach via cone beam computerized tomography volume analysis. *Int J Legal Med*. 2019;133(6):1977–1984. doi:10.1007/s00414-019-02100-6
21. Issa J, Kulczyk T, Rychlik M, Czajka-Jakubowska A, Olszewski R, Dyszkiewicz-Konwińska M. Artificial intelligence versus semi-automatic segmentation of the inferior alveolar canal on cone-beam computed tomography scans: A pilot study. *Dent Med Probl*. 2024;61(6):893–899. doi:10.17219/dmp/175968
22. Park JA, Lee YJ, Yeo IS, Koh KS, Song WC. Three-dimensional linear and volumetric computed tomography analysis of the frontal sinus. *Anat Cell Biol*. 2022;55(2):142–147. doi:10.5115/acb.22.037
23. Terletskyi R, Dowgierd K, Chepurnyi Y, Kopchak A, Neff A. Influence of preoperative anatomy and functional status on outcomes after total temporomandibular joint replacement with patient-specific endoprostheses: A retrospective cohort study. *Dent Med Probl*. 2025;62(1):57–64. doi:10.17219/dmp/174598

24. Asgharlou MA, Esfehani M, Tofangchiha M, et al. Comparison of facial soft tissue thickness in subjects with different malocclusions according to the lateral cephalograms of an Iranian adult population. *Dent Med Probl*. 2025;62(2):255–263. doi:10.17219/dmp/171501
25. Kim DI, Lee UY, Park SO, Kwak DS, Han SH. Identification using frontal sinus by three-dimensional reconstruction from computed tomography. *J Forensic Sci*. 2013;58(1):5–12. doi:10.1111/j.1556-4029.2012.02185.x
26. Sahlstrand-Johnson P, Jannert M, Strömbeck A, Abul-Kasim K. Computed tomography measurements of different dimensions of maxillary and frontal sinuses. *BMC Med Imaging*. 2011;11:8. doi:10.1186/1471-2342-11-8
27. Dastan F, Ghaffari H, Shishvan HH, Zareiyan M, Akhlaghian M, Shahab S. Correlation between the upper airway volume and the hyoid bone position, palatal depth, nasal septum deviation, and concha bullosa in different types of malocclusion: A retrospective cone-beam computed tomography study. *Dent Med Probl*. 2021;58(4):509–514. doi:10.17219/dmp/130099
28. Tayebi A, Pournaghdi M, Aslanbeigi F, Tofangchiha M, Javadi A. Investigating the relationship between the type of occlusion and mandibular radiomorphometric indices in patients with normal facial height. *Dent Med Probl*. 2024;61(6):829–835. doi:10.17219/dmp/130100
29. Hamed SS, El-Badrawy AM, Fattah SA. Gender identification from frontal sinus using multi-detector computed tomography. *J Forensic Radiol Imaging*. 2014;2(3):117–120. doi:10.1016/j.jofri.2014.03.006
30. Mrożek K, Marchewka J, Borowska B, et al. Morphology and morphometry of frontal sinuses as a tool in sex determination based on 17th–18th century skulls from Poland. *Anthropol Rev*. 2024;87(2):63–84. doi:10.18778/1898-6773.87.2.03
31. Louis M, Travieso R, Oles N, Coon D. Narrative review of facial gender surgery: Approaches and techniques for the frontal sinus and upper third of the face. *Ann Transl Med*. 2021;9(7):606–606. doi:10.21037/atm-20-6432
32. Haładaj R, Polguj M, Topol M. Anatomical variations of the supraorbital and supratrochlear nerves: Their intraorbital course and relation to the supraorbital margin. *Med Sci Monit*. 2019;25:5201–5210. doi:10.12659/MSM.915447

Original paper

HAp–ZrO_2–AgNP-reinforced polystyrene dental nanocomposites: Antibacterial, antiplaque and self-cleaning properties

Hadi Zare-Zardini[1,A,B,D–F*], Elham Saberian[2,B–D*], Andrej Jenča Jr.[2,B,D*], Adriána Petrášová[2,B–D], Janka Jenčová[2,B–D], Andrej Jenča[2,C–E], Eliška Kubíková[3,B–D], Tetyana Pyndus[2,B–D], Mieszko Adam Więckiewicz[4,B–D]

[1] Department of Biomedical Engineering, Meybod University, Iran
[2] Clinic of Dentistry and Maxillofacial Surgery, Academy of Košice, Pavol Jozef Šafárik University, Košice, Slovakia
[3] Department of Anatomy, Faculty of Medicine, Comenius University Bratislava, Slovakia
[4] Department of Experimental Dentistry, Wroclaw Medical University, Poland
* These authors contributed equally to this work.

A – research concept and design; B – collection and/or assembly of data; C – data analysis and interpretation; D – writing the article; E – critical revision of the article; F – final approval of the article

Dental and Medical Problems, ISSN 1644-387X (print), ISSN 2300-9020 (online) *Dent Med Probl*. 2026;63(5):1243–1258

Address for correspondence
Hadi Zare-Zardini
E-mail: hadizarezardini@gmail.com

Funding sources
None declared

Conflict of interest
None declared

Acknowledgements
None declared

Received on September 15, 2025
Reviewed on October 28, 2025
Accepted on November 2, 2025

Published online on June 17, 2026

Cite as
Zare-Zardini H, Saberian E, Jenča Jr. A, et al. HAp–ZrO_2–AgNP-reinforced polystyrene dental nanocomposites: Antibacterial, antiplaque and self-cleaning properties. *Dent Med Probl.* 2026;63(5):1243–1258. doi:10.17219/dmp/213852

DOI
10.17219/dmp/213852

Copyright
Copyright by Author(s)
This is an article distributed under the terms of the Creative Commons Attribution 3.0 Unported License (CC BY 3.0) (https://creativecommons.org/licenses/by/3.0/).

Abstract

Background. Dental biofilms, primarily driven by *Streptococcus mutans*, are the main etiological agents of caries and restorative failure.

Objectives. The aim of the study was to design and synthesize a novel polystyrene (PS)-based nanocomposite reinforced with hydroxyapatite (HAp), zirconia (ZrO_2) and silver nanoparticles (AgNPs).

Material and methods. Hydroxyapatite, ZrO_2 and AgNPs were synthesized via wet precipitation, sol–gel and citrate reduction methods, respectively. The nanoparticles (5 wt% total loading) were uniformly dispersed in a toluene-based PS matrix using ultrasonic-assisted solution casting. The resulting films were characterized in terms of morphology (scanning electron microscopy (SEM), transmission electron microscopy (TEM), atomic force microscopy (AFM)), composition (energy-dispersive X-ray spectroscopy (EDX)), thermal stability (thermogravimetric analysis (TGA)), mechanical properties (tensile strength, Young's modulus, Vickers hardness), surface wettability (water contact angle (WCA)), antibacterial efficacy (zone of inhibition (ZOI), minimum inhibitory concentration/minimum bactericidal concentration (MIC/MBC), colony-forming unit (CFU) assay), and antibiofilm activity (crystal violet staining, confocal laser scanning microscopy (CLSM)). Statistical analysis was performed using one-way analysis of variance (ANOVA) and Tukey's honestly significant difference (HSD) test ($p < 0.05$).

Results. The nanocomposite exhibited a 30% increase in tensile strength (32.5 MPa vs. 25 MPa for pure PS) and a 25% rise in elastic modulus (1.5 GPa vs. 1.2 GPa). The water contact angle increased from 85° ±2° (pure PS) to 115° ±3° (nanocomposite), confirming significantly enhanced hydrophobicity. The composite demonstrated strong antibacterial activity, with a ZOI of 15.3 mm, MIC of 6.25 mg/mL, MBC of 12.5 mg/mL, and 99.8% bacterial reduction within 24 h. Antibiofilm performance was also notable, showing a 91.2% reduction in biofilm biomass after 72 h and 74.8% decrease in biofilm thickness (from 32.5 µm to 8.2 µm). Confocal laser scanning microscopy revealed a marked shift in the live/dead cell ratio (from 4.7:1 to 0.6:1), confirming bactericidal rather than bacteriostatic action. All nanoparticles were homogeneously distributed without agglomeration, as confirmed by SEM/EDX and TEM.

Conclusions. The HAp–ZrO_2–AgNP-reinforced PS nanocomposite integrates enhanced mechanical properties, self-cleaning surface characteristics, and potent, long-lasting antibiofilm activity against *S. mutans*. While further biocompatibility and clinical translation studies are warranted, this material represents a significant leap toward durable, infection-resistant dental applications.

Keywords: antibacterial, zirconia, hydroxyapatite, silver nanoparticles, dental biofilms

Highlights

- A novel HAp–ZrO_2–AgNP-reinforced polystyrene nanocomposite was developed.
- Increased hydrophobicity was achieved through synergistic surface roughness induced by ZrO_2 and AgNPs.
- The nanocomposite demonstrated significantly enhanced mechanical properties and strong bactericidal activity against *Streptococcus mutans*.
- Biofilm formation was markedly inhibited, with structural disruption of mature biofilms.
- Tri-component nanoparticles (HAp, ZrO_2, AgNPs) were successfully incorporated into the polystyrene matrix without agglomeration.

Introduction

Dental caries and periodontal diseases remain among the most prevalent chronic conditions worldwide, affecting nearly 3.5 billion people according to the World Health Organization (WHO).[1–3] The etiology of dental caries is primarily attributed to dental plaque, a complex biofilm formed by microbial communities adhering to tooth surfaces. The pathogenesis of caries involves acid-producing bacteria (e.g., *Streptococcus mutans*, *Lactobacillus* spp.), which metabolize dietary sugars and induce demineralization of tooth enamel (Fig. 1).[4–8] Periodontal diseases, on the other hand, are mainly associated with gram-negative anaerobes (e.g., *Porphyromonas gingivalis*, *Fusobacterium nucleatum*), which trigger inflammatory responses and tissue destruction.[9,10]

Conventional preventive strategies, such as mechanical plaque removal (toothbrushing and flossing) and the use of antimicrobial agents (fluoride, chlorhexidine), present several limitations. Mechanical methods often fail to reach inaccessible areas, while prolonged use of antimicrobial agents may disrupt the balance of the oral microbiota and promote resistance.[6,7] Additionally, dental restorative materials (e.g., composites, resins) lack inherent antibacterial properties, making them susceptible to secondary caries and biofilm accumulation.[11–15]

Recent studies have explored various approaches to enhance the antibacterial properties of dental materials. For instance, modification of glass ionomer cements (GICs) with polyamidoamine (PAMAM) and bioactive glass (BAG) has been shown to significantly reduce *S. mutans* colonization and promote ion release, indicating improved antibacterial efficacy.[16] Similarly, natural compounds, such as *Zataria multiflora* extract, have demonstrated inhibitory effects against oral microorganisms and plaque formation, suggesting potential alternatives to traditional antimicrobials.[17] Nanochitosan-modified GICs have also been investigated for their antibacterial and preventive effects on initial enamel caries lesions, showing promising results in terms of microshear bond strength and antibacterial activity.[18] Furthermore, natural agents such as propolis and hesperidin have been compared with synthetic agents (e.g., silver diamine fluoride) in deep carious dentin, with propolis showing significant remineralizing and antimicrobial effects.[19] Lastly, herb-mediated nanocomposite mouthwashes, such as those using amla seed extract to synthesize graphene oxide–silver nanocomposites, have demonstrated antibacterial and anti-inflammatory effects in the management of plaque-induced gingivitis, offering a novel approach to oral hygiene.[20]

To address these challenges, nanotechnology-based dental materials have emerged as a promising solution. Incorporating hydroxyapatite (HAp), zirconia (ZrO_2) and silver nanoparticles (AgNPs) into polymer matrices can enhance mechanical strength, impart antibacterial effects and reduce biofilm adhesion. Hydroxyapatite, the primary mineral component of enamel, promotes remineralization and biocompatibility.[21,22] Zirconia improves mechanical durability, while AgNPs provide broad-spectrum antibacterial activity through membrane disruption and reactive oxygen species (ROS) generation.[22] This study introduces a novel polystyrene (PS)-based nanocomposite reinforced with HAp, ZrO_2 and AgNPs, designed to combine self-cleaning, antibacterial and antiplaque properties. The material has been developed to inhibit bacterial adhesion, disrupt biofilm formation and enhance mechanical performance, offering a multifunctional platform for dental restoration and oral health maintenance.

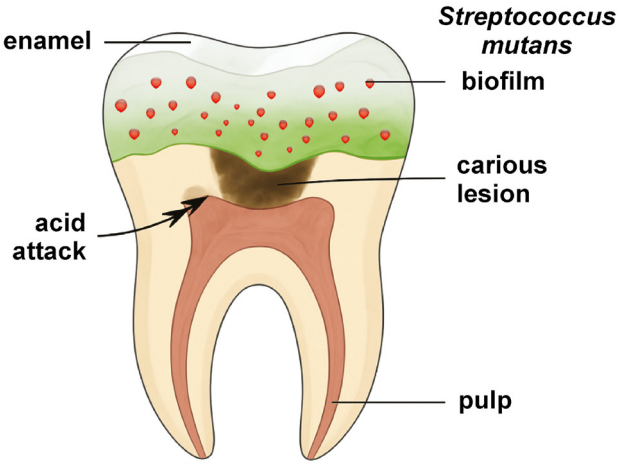

Fig. 1. Schematic representation of dental plaque formation and caries progression

Material and methods

Chemicals and reagents

All chemicals used in this study were of analytical grade and were employed without further purification, unless otherwise stated. The following materials were employed:

- silver nitrate ($AgNO_3$, ≥99.9%; Sigma-Aldrich, St. Louis, USA);
- trisodium citrate dihydrate ($C_6H_5Na_3O_7 \cdot 2H_2O$, ≥99%; Merck, Darmstadt, Germany);
- zirconium(IV) oxynitrate hydrate ($ZrO(NO_3)_2 \cdot xH_2O$, 99%; Alfa Aesar, Ward Hill, USA);
- citric acid ($C_6H_8O_7$, ≥99.5%; Sigma-Aldrich);
- calcium nitrate tetrahydrate ($Ca(NO_3)_2 \cdot 4H_2O$, ≥99%; Sigma-Aldrich);
- diammonium hydrogen phosphate ($(NH_4)_2HPO_4$, ≥99%; Merck);
- ammonium hydroxide (NH_4OH, 25% w/w in water; Sigma-Aldrich);
- PS pellets (molecular weight ~280,000 g/mol; Sigma-Aldrich);
- toluene (C_7H_8, ≥99.5%, anhydrous; Sigma-Aldrich);
- Mueller–Hinton agar (MHA; Oxoid, Basingstoke, UK);
- brain heart infusion (BHI) broth (Oxoid);
- crystal violet ($C_{16}H_{18}ClN_3$, ≥90%; Sigma-Aldrich);
- LIVE/DEAD™ BacLight™ Bacterial Viability Kit (Invitrogen, Carlsbad, USA).

Equipment and instrumentation

The following instruments were used for material characterization:

- X-ray diffractometer (D8 Advance; Bruker, Bremen, Germany) – Cu–Kα radiation (λ = 1.5406 Å); 2θ range: 10°–80°; step size: 0.02°; scan speed: 1°/min;
- transmission electron microscope (JEM-2100; JEOL Ltd., Tokyo, Japan) – accelerating voltage: 200 kV; magnification: ×50,000–200,000;
- dynamic light scattering (DLS) and zeta potential analyzer (Zetasizer Nano ZS; Malvern Panalytical, Malvern, UK) – laser wavelength: 633 nm; scattering angle: 173°; temperature: 25°C;
- scanning electron microscope (FEI Quanta 250; FEI Company, Hillsboro, USA) – accelerating voltage: 15 kV; working distance: 10 mm; secondary electron detector;
- atomic force microscope (Dimension Icon; Bruker, Billerica, USA) – tapping mode; scan area: 5 μm × 5 μm; scan rate: 0.5 Hz;
- universal testing machine (Instron 5969; Instron, Norwood, USA) – load cell: 1 kN; crosshead speed: 1 mm/min for flexural tests;
- Vickers hardness tester (MicroMet 5100; Buehler, Lake Bluff, USA) – load: 100 g; dwell time: 15 s;
- contact angle goniometer (ramé-hart 500 Series; ramé-hart instrument co., Succasunna, USA) – sessile drop method; droplet volume: 5 μL; measurement time: 10 s;
- microplate reader (SpectraMax i3x; Molecular Devices, San Jose, USA) – absorbance measurement at 595 nm;
- confocal laser scanning microscope (LEICA TCS SP8; Leica Microsystems, Wetzlar, Germany) – excitation/emission: 488 nm/500–530 nm for SYTO 9 and 561 nm/575–620 nm for propidium iodide.

Synthesis of nanoparticles

Silver nanoparticles

Silver nanoparticles were synthesized using a chemical reduction method based on the citrate reduction of silver nitrate ($AgNO_3$). Briefly, an aqueous solution of $AgNO_3$ was heated to boiling under vigorous stirring. A trisodium citrate solution was then quickly added to the boiling $AgNO_3$ solution. The color of the solution changed from colorless to pale yellow and then to a characteristic ruby red, indicating the formation of AgNPs. The reaction mixture was maintained at boiling for 30 min until the color stabilized, then allowed to cool to room temperature under continuous stirring. The synthesized AgNPs were characterized using X-ray diffraction (XRD) (D8 Advance), transmission electron microscopy (TEM) (JEM-2100) and DLS (Zetasizer Nano ZS).

Zirconia nanoparticles

Zirconia nanoparticles were synthesized via a sol–gel method using zirconium(IV) oxynitrate hydrate as a precursor and citric acid as a chelating agent. In summary, zirconium oxynitrate was dissolved in deionized water, followed by the addition of citric acid under constant stirring at 60°C to obtain a homogeneous solution. The mixture was then heated to 80°C and stirred until a viscous gel was formed. The gel was dried overnight at 120°C and subsequently calcined at 600°C for 3 h to obtain crystalline ZrO_2 nanoparticles. The resulting nanoparticles were analyzed using XRD (D8 Advance) and TEM (JEM-2100).

Hydroxyapatite nanoparticles

Hydroxyapatite nanoparticles were synthesized using a wet chemical precipitation technique. Calcium and phosphate precursors, namely calcium nitrate tetrahydrate and diammonium hydrogen phosphate, were separately dissolved in deionized water. The phosphate solution was then slowly added to the calcium solution under continuous stirring. The pH was maintained at 10–11 by the addition of ammonium hydroxide. The resulting precipitate was aged for 24 h, washed with deionized water and ethanol, and dried at 80°C overnight. The HAp nanoparticles were characterized using XRD (D8 Advance) and TEM (JEM-2100).

Incorporation of nanoparticles into the polystyrene matrix

The incorporation of HAp, ZrO_2 and AgNPs into the PS matrix was achieved by solution mixing and a casting process. First, PS pellets were dissolved in toluene (10% w/v) under magnetic stirring at 60°C for 2 h to obtain a homogeneous solution. Separately, the synthesized HAp, ZrO_2 and Ag nanoparticles were dispersed in toluene (1 mg/mL) using ultrasonication (40 kHz, 30 min) to ensure uniform dispersion. The nanoparticle suspensions were then added dropwise to the PS solution under constant stirring (500 rpm) at room temperature. The mixture was further stirred for 4 h to ensure thorough mixing and prevent the agglomeration of the nanoparticles. The resulting composite solution was poured into Teflon molds and dried at room temperature in a fume hood for 24 h to allow solvent evaporation. The dried films were subsequently vacuum-dried at 60°C for 12 h to remove residual solvent. The obtained PS–HAp–ZrO_2–Ag nanocomposite films were characterized using SEM (FEI Quanta 250) and energy-dispersive X-ray spectroscopy (EDX).

Evaluation of mechanical properties

The mechanical properties of the nanocomposite materials were evaluated in terms of tensile strength, Young's modulus and elongation at break using a universal testing machine (Instron 5969), in accordance with ASTM D638,[23] on dog bone-shaped specimens (gauge length: 25 mm, width: 4 mm, thickness: 2 mm). The hardness of the samples was measured using a Vickers hardness tester (MicroMet 5100), following ISO 6507-1.[24] Prior to testing, the samples were polished to a mirror finish, and at least 5 indents were made per sample, with a minimum spacing of 3 diagonal divisions to avoid interaction effects. These tests were conducted to assess the influence of nanoparticle incorporation (HAp, ZrO_2, Ag) on the mechanical performance of the PS matrix, which is crucial to assess the suitability and durability of the material in dental applications.

Evaluation of self-cleaning properties

The self-cleaning properties of the nanocomposite surfaces were evaluated by measuring the water contact angle (WCA) using a contact angle goniometer (ramé-hart 500 Series) at room temperature. For each measurement, a 5-µL droplet of deionized water was placed on the surface of the nanocomposite material, and the static contact angle was recorded within 10 s using the sessile drop method. Prior to measurements, the nanocomposite films were cleaned with ethanol and dried under nitrogen flow. At least 5 measurements were taken at different locations on each sample. The average contact angle values were reported together with the standard deviation (*SD*), which served as a measure of surface wettability and self-cleaning potential.

Evaluation of antibacterial and antiplaque properties

Zone of inhibition assay

Antibacterial activity was primarily tested using the zone of inhibition (ZOI) assay against *S. mutans* on MHA plates. Sterile paper disks (6-mm diameter, Whatman filter paper) were impregnated with 50 µL of nanocomposite solution (10 mg/mL in tetrahydrofuran (THF)) or small pieces of nanocomposite film (5-mm diameter) for solid samples. The disks were placed on agar plates inoculated with *S. mutans* at a concentration of 1.5×10^8 CFU/mL (McFarland standard 0.5) and incubated at 37°C for 24 h under aerobic conditions. After incubation, the diameter of the clear zone around the plates (ZOI), which is indicative of antibacterial activity, was measured in millimeters using a digital caliper.

Minimum inhibitory concentration and minimum bactericidal concentration

The minimum inhibitory concentration (MIC) and minimum bactericidal concentration (MBC) were determined using the broth microdilution method in 96-well microplates. Nanocomposite extracts were prepared by immersing nanocomposite films (10 mg/mL) in sterile BHI broth for 24 h at 37°C with shaking. These extracts, along with serial twofold dilutions of AgNP solutions (ranging from 0.78 ppm to 100 ppm), were serially diluted in BHI broth in the microplates. A bacterial suspension of *S. mutans* adjusted to 5×10^5 CFU/mL was added to each well (100 µL bacterial suspension + 100 µL diluted extract/AgNPs). The plates were incubated at 37°C for 24 h. The MBC was determined visually as the lowest concentration of nanocomposite extract or AgNPs that inhibited visible bacterial growth, as indicated by the absence of turbidity in the wells.

Colony-forming unit assay

Quantitative antibacterial efficacy of the nanocomposite was evaluated using a colony-forming unit (CFU) assay. The nanocomposite films (1 cm × 1 cm) were sterilized under ultraviolet (UV) light for 30 min before testing. The films were then immersed in 1 mL of *S. mutans* bacterial suspension at a concentration of 1×10^6 CFU/mL in BHI broth for different time intervals (1, 3, 6, and 24 h) at 37°C. At each time point, 100 µL of the bacterial suspension was serially diluted in sterile phosphate-buffered saline (PBS), and 100 µL of each dilution was plated in triplicate on BHI agar plates. After incubation at 37°C for 24 h, colonies were counted manually, and the percentage of bacterial reduction compared to the control group (bacteria incubated without nanocomposite films) was calculated.

Antiplaque biofilm assay

The formation of *S. mutans* biofilms on nanocomposite films was evaluated using the crystal violet assay. Sterile nanocomposite films (1 cm × 1 cm) were placed in 24-well plates and inoculated with 1 mL of *S. mutans* suspension (1×10^6 CFU/mL) in BHI broth supplemented with 1% sucrose (Sigma-Aldrich) to promote biofilm formation for 24, 48 and 72 h at 37°C under static conditions. After incubation, the planktonic bacteria were carefully aspirated, and the biofilms were gently washed twice with 1 mL of PBS (pH 7.4). The biofilms were then fixed with 500 µL of absolute methanol per well for 20 min. After fixation, methanol was removed and the biofilms were stained with 500 µL of crystal violet solution (0.1% w/v in water) per well for 30 min. The excess stain was removed by washing the wells 3 times with 1 mL of PBS. The dye bound to the biofilm was then dissolved by adding 500 µL of 33% acetic acid per well and incubating at room temperature for 30 min. Finally, 200 µL of the dissolved dye solution from each well was transferred to a 96-well microplate, and the absorbance was measured at 595 nm using a microplate reader (SpectraMax i3x). Biofilm biomass was quantified based on the absorbance values, with higher absorbance indicating greater biofilm formation.

Confocal laser scanning microscopy

A confocal laser scanning microscope (LEICA TCS SP8) was used for detailed visualization of the biofilms. The *S. mutans* biofilms were grown on nanocomposite films for 48 h, as described above. After incubation, the biofilms were carefully washed with PBS and stained using the LIVE/DEAD™ BacLight™ Bacterial Viability Kit according to the manufacturer's protocol. SYTO 9 (green fluorescence) stains viable cells, whereas propidium iodide (red fluorescence) labels dead bacteria. The imaging of the biofilms was conducted using confocal laser scanning microscopy (CLSM) with excitation/emission wavelengths of 488 nm/500–530 nm for SYTO 9 and 561 nm/575–620 nm for propidium iodide. Z-stack images were taken at 1-µm intervals. The thickness and structure of the biofilm, including the distribution of live and dead bacteria, were analyzed using the ImageJ software (https://imagej.net/ij/download.html).

Statistical analysis

The quantitative data was expressed as mean ±*SD* from at least 3 independent experiments. Statistical analysis was performed using one-way analysis of variance (ANOVA) for comparisons involving more than 2 groups, or Student's *t*-test for comparisons between 2 groups. When ANOVA indicated significant differences, Tukey's honestly significant difference (HSD) post hoc test was applied to perform pairwise comparisons and determine which groups were significantly different from each other. The analyses were conducted using the GraphPad Prism v. 9.0 software (GraphPad Software, San Diego, USA). A p-value <0.05 was considered statistically significant.

Results

Synthesis of silver nanoparticles

Silver nanoparticles were successfully synthesized via a chemical reduction method using trisodium citrate as a reducing and stabilizing agent. Within 5 min of citrate addition, the initially colorless $AgNO_3$ solution turned pale yellow, indicating the nucleation of AgNPs. After 15 min of boiling, the solution exhibited a characteristic ruby-red color, confirming the formation of spherical AgNPs due to surface plasmon resonance (SPR). The deep red color remained stable after 30 min of boiling, indicating complete reduction and stabilization of the nanoparticles. The synthesized AgNPs showed a strong SPR peak at 460 nm, characteristic of spherical AgNPs with a diameter of 20–30 nm (Fig. 2A). The narrow peak width indicated a monodisperse size distribution. The hydrodynamic diameter of the AgNPs was 25 ±3 nm with a polydispersity index (PDI) of 0.12, confirming uniformity (Fig. 2B). The zeta potential was −30 ±2 mV, indicating high colloidal stability due to electrostatic repulsion imparted by the citrate cap. The nanoparticles were well dispersed, with minimal aggregation observed. The XRD analysis exhibited 4 distinct peaks at 2θ values of 38.1°, 44.3°, 64.4°, and 77.4°, corresponding to the (111), (200), (220), and (311) crystallographic planes of face-centered cubic (FCC) silver (JCPDS No. 04-0783) (Fig. 2C). The crystallite size, calculated using the Scherrer equation, was 18 nm, which is consistent with TEM observations. Transmission electron micrographs confirmed the formation of spherical AgNPs with an average diameter of 22 ±4 nm (Fig. 2D).

Synthesis of zirconia nanoparticles

Zirconia nanoparticles were successfully synthesized via a sol–gel method using zirconium(IV) oxynitrate hydrate as a precursor and citric acid as a chelating agent. The process involved controlled gelation, drying and calcination to produce crystalline ZrO_2 nanoparticles. The addition of citric acid to the zirconium oxynitrate solution resulted in a clear, homogeneous mixture after 30 min of stirring at 60°C. When heated to 80°C, the solution gradually transformed into a viscous, translucent gel within 4 h, indicating the formation of a zirconium citrate complex. The gel was dried overnight at 120°C, resulting in a brittle, yellowish xerogel. Calcination at 600°C for 3 h yielded a white crystalline powder, confirming the removal of organic residues and the formation of ZrO_2. The XRD analysis revealed sharp diffraction peaks

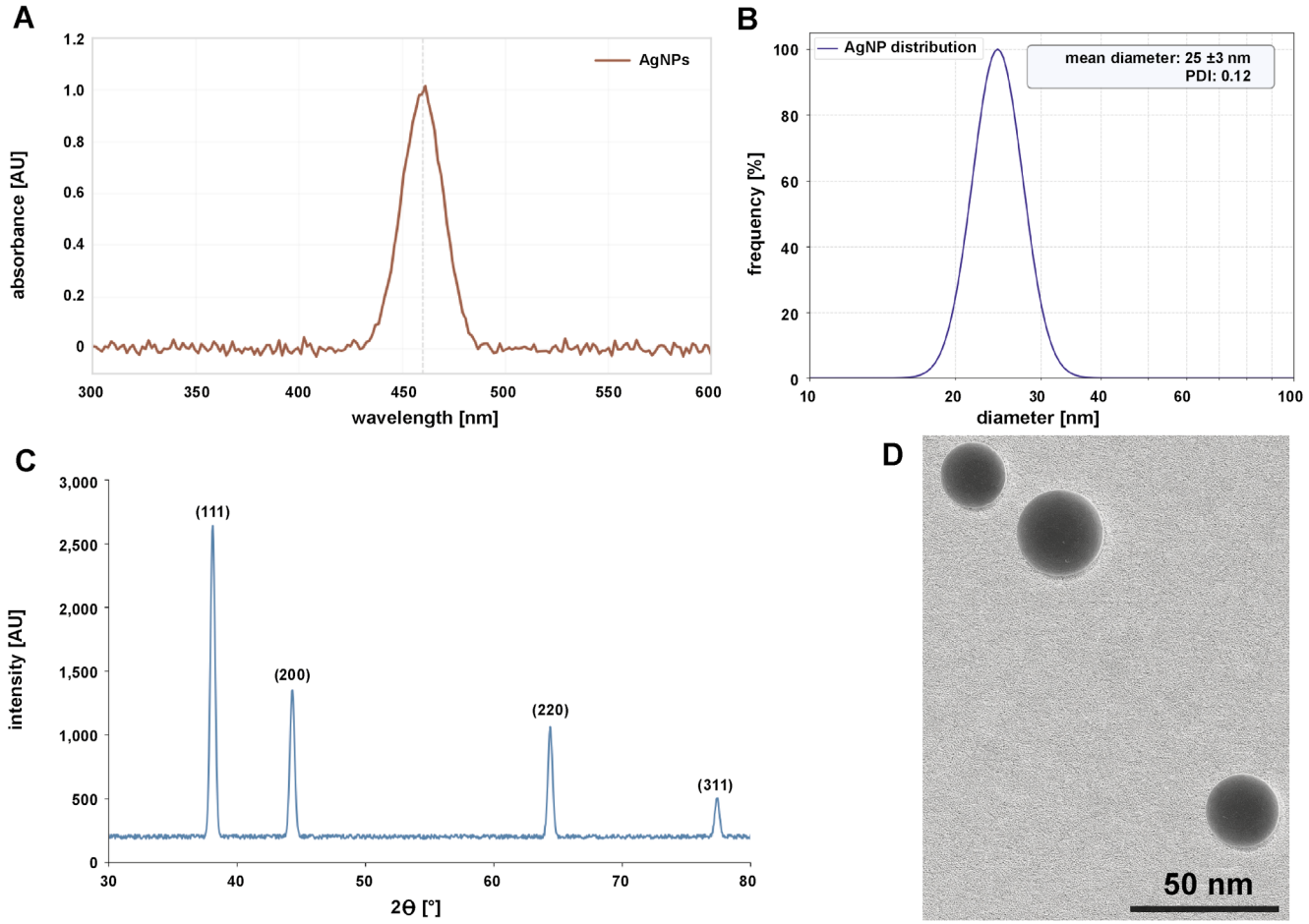

Fig. 2. Characterization of silver nanoparticles (AgNs)

A. Ultraviolet (UV)-visible absorption spectrum; B. Dynamic light scattering (DLS) size distribution; C. X-ray diffraction (XRD) pattern; D. Transmission electron microscopy (TEM) image.
PDI – polydispersity index.

at 2θ values of 30.2°, 35.2°, 50.4°, and 60.1°, corresponding to the (011), (110), (112), and (121) planes of tetragonal zirconia (JCPDS No. 17-0923) (Fig. 3A). The absence of impurity peaks confirmed the high purity of the synthesized ZrO_2. The crystallite size, calculated according to the Scherrer equation, was 15 nm. The nanoparticles exhibited low agglomeration, with clear lattice fringes (d-spacing = 0.29 nm) corresponding to the (011) plane of tetragonal ZrO_2. The hydrodynamic diameter of ZrO_2 nanoparticles in aqueous suspension was 22 ±4 nm with a PDI of 0.18, indicating a narrow size distribution. The zeta potential was −25 ±1 mV, denoting moderate colloidal stability due to residual citrate ions on the surface (Fig. 3B). Transmission electron micrographs showed spherical to quasi-spherical morphology with an average particle size of 18 ±3 nm (Fig. 3C).

Synthesis of hydroxyapatite nanoparticles

Hydroxyapatite nanoparticles were successfully synthesized using a wet chemical precipitation method with calcium nitrate tetrahydrate and diammonium hydrogen phosphate as calcium and phosphate precursors, respectively. The reaction was carried out at a controlled pH of 10–11 to ensure the formation of stoichiometric HAp. After adding the phosphate solution dropwise to the calcium solution, a milky white precipitate formed immediately, indicating nucleation. The reaction mixture was stored at room temperature for 24 h to promote crystallinity and particle growth. The precipitate was washed 3 times with deionized water and ethanol via centrifugation (5,000 rpm, 10 min) to remove residual ammonium and nitrate ions. After drying overnight at 80°C, a fine white powder was obtained. The XRD analysis confirmed the formation of phase-pure HAp, with characteristic peaks at 2θ values of 25.9°, 31.8°, 32.9°, 34.1°, and 39.8°, corresponding to the (002), (211), (112), (202), and (310) planes of hexagonal HAp, respectively (JCPDS No. 09-432) (Fig. 4A). The sharp, well-defined peaks indicate high crystallinity, with a crystallite size of 30 nm, as calculated using the Scherrer equation. The hydrodynamic diameter of the HAp nanoparticles in aqueous suspension was 85 ±12 nm with a PDI of 0.25, indicating slight agglomeration in the solution (Fig. 4B). The zeta potential

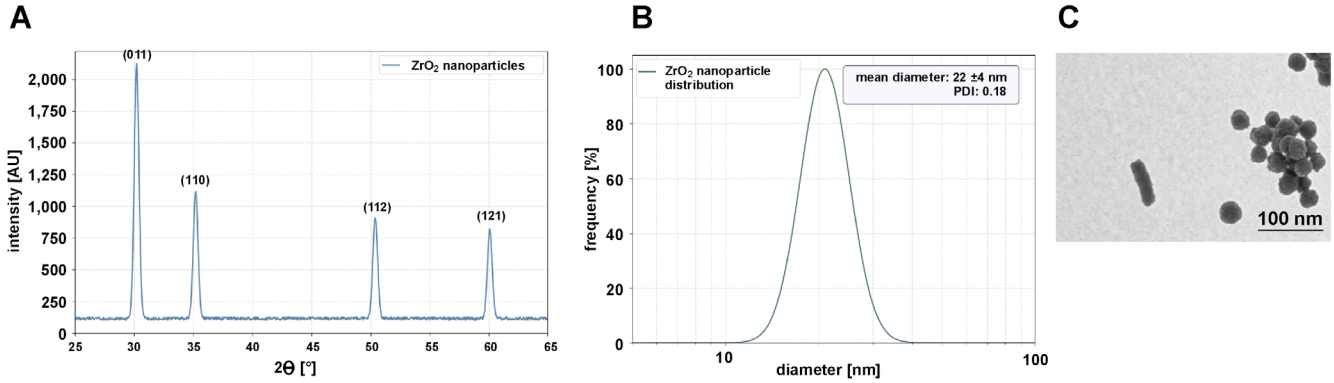

Fig. 3. Characterization of zirconia nanoparticles (ZrO_2)
A. XRD pattern; B: DLS size distribution; C. TEM image.

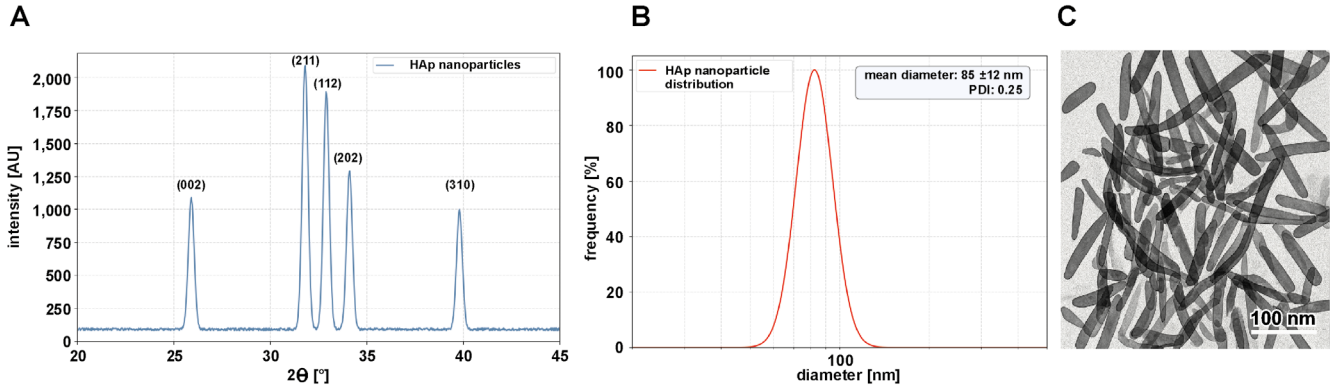

Fig. 4. Characterization of hydroxyapatite (HAp) nanoparticles
A. XRD pattern; B: DLS size distribution; C. TEM image.

was –20 ±2 mV, suggesting moderate colloidal stability due to the presence of hydroxyl groups on the surface. Transmission electron micrographs revealed rod-shaped HAp nanoparticles with an average length of 60 ±10 nm and a diameter of 20 ±5 nm. The nanoparticles exhibited uniform morphology with minimal aggregation, consistent with the controlled pH and aging process (Fig. 4C).

Characterization of the PS–HAp–ZrO_2–Ag nanocomposite

The PS–HAp–ZrO_2–Ag nanocomposite was successfully prepared by mixing and pouring a solution, which ensured uniform dispersion of HAp, ZrO_2 and AgNPs within the PS matrix. The PS solution in toluene (10% w/v) remained clear and homogeneous after 2 h of stirring at 60°C. The suspensions of nanoparticles (HAp, ZrO_2, Ag) in toluene showed no visible sedimentation after ultrasonication, indicating effective dispersion. After dropwise addition of the nanoparticle suspensions to the PS solution, the mixture retained a uniform, slightly opaque appearance, suggesting good compatibility between the nanoparticles and the polymer matrix. The composite solution was cast into Teflon molds, yielding flexible, free-standing films after 24 h of solvent evaporation. Subsequent vacuum drying at 60°C for 12 h resulted in smooth, crack-free films with a thickness of 200 ±10 µm. Scanning electron microscopy images revealed a homogeneous surface morphology without visible nanoparticle agglomeration. At higher magnification, well-dispersed nanoparticles embedded in the PS matrix were observed, with HAp rods and spherical ZrO_2 and AgNPs. The EDX mapping confirmed the uniform distribution of Ca (HAp), Zr (ZrO_2) and Ag (AgNPs) across the composite surface (Fig. 5).

Thermogravimetric analysis (TGA) of pure PS and the PS–HAp–ZrO_2–Ag nanocomposite is presented in Fig. 6. The TGA curve for pure PS shows a single degradation step, with onset at around 350°C and significant weight loss between 400°C and 450°C, which corresponds to the decomposition temperature of PS. The nanocomposite displayed a similar decomposition step within the same temperature range (400–450°C), indicating that the incorporation of nanoparticles did not significantly change the thermal decomposition characteristics of the PS matrix. However, the residual mass of the nanocomposite at 600°C is 5.2%, closely matching the theoretical nanoparticle loading (5 wt%). This result confirms the successful incorporation of HAp, ZrO_2 and Ag nanoparticles into the PS matrix. A slight variation in the onset

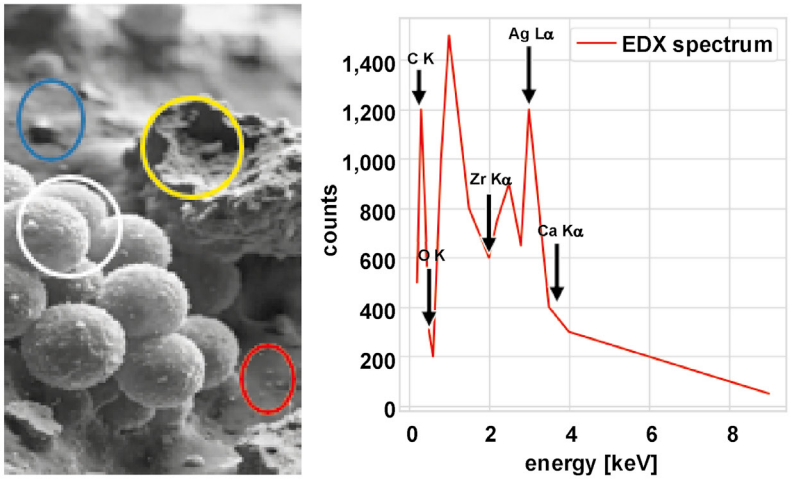

Element	Weight [%]	Atomic [%]
C (PS)	55.0	62.0
O (HAp–ZrO_2–PS)	20.0	18.0
Ca (HAp)	10.0	5.0
Zr (ZrO_2)	12.0	6.0
Ag (NPs)	3.0	1.0

Fig. 5. Scanning electron microscopy (SEM) and energy-dispersive X-ray spectroscopy (EDX) analysis of the PS–HAp–ZrO_2–Ag nanocomposite

In the SEM image, silver (Ag) nanoparticles are marked with a red circle, zirconia (ZrO_2) nanoparticles with a blue circle, hydroxyapatite (HAp) nanoparticles with a yellow circle, and the polystyrene (PS) matrix with a white circle. The EDX analysis confirms the presence of Ag, Zr, calcium (Ca), and carbon (C) in the sample, corresponding to the Ag, ZrO_2, HAp, and PS components, respectively. Additionally, the presence of oxygen (O) has been confirmed, corresponding to the HAp and ZrO_2 components of the nanocomposite.

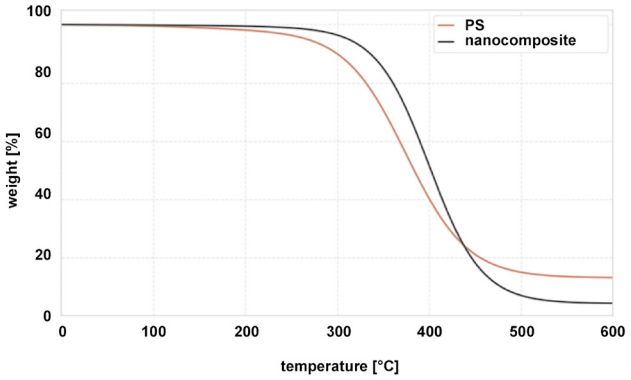

Fig. 6. Thermogravimetric analysis (TGA) curves of pure polystyrene (PS) and the PS–HAp–ZrO_2–Ag nanocomposite

of degradation between the pure PS and the nanocomposite could be attributed to the presence of the nanoparticles, which may slightly affect the thermal stability of the polymer matrix. Nevertheless, the overall thermal decomposition profile remained largely unchanged, indicating that the nanoparticles were well dispersed and did not significantly interfere with the thermal degradation process of PS. The consistency between the experimental residual mass and the theoretical loading confirms the synthesis and composition of the nanocomposite.

The mechanical properties of pure PS and the PS–HAp–ZrO_2–Ag nanocomposite were evaluated using tensile testing and Vickers hardness measurements. Tensile testing revealed a significant improvement in the mechanical strength of the nanocomposite. The tensile strength increased by 30% (from 25.0 ±2.1 MPa for pure PS to 32.5 ±1.8 MPa for the nanocomposite; $p < 0.01$), indicating a reinforcing effect due to the incorporation of nanoparticles. Similarly, the Young's modulus increased by 25% (from 1.2 ±0.15 GPa to 1.5 ±0.12 GPa), although the difference was not statistically significant. However, the elongation at break decreased slightly by 15.5% (from 4.5 ±0.3% to 3.8 ±0.25%; $p = 0.07$), consistent with the expected trade-off between stiffness and ductility due to the addition of rigid nanoparticles. Vickers hardness measurements further confirmed mechanical reinforcement. The nanocomposite exhibited a significant increase in hardness compared to pure PS. The Vickers hardness number (HV) for the nanocomposite was 15.6 ±1.2, whereas pure PS had a hardness of 12.3 ±0.8 ($p < 0.05$), corresponding to an approximate 27% increase. This improvement is attributed to the high hardness of the ceramic nanoparticles (HAp and ZrO_2), which enhanced the overall resistance of the nanocomposite to indentation (Fig. 7).

The self-cleaning properties of the PS–HAp–ZrO_2–Ag nanocomposite were evaluated by measuring the WCA using the sessile drop method. Pure PS exhibited a WCA of 85° ±2°, indicating moderate hydrophobicity due to its non-polar nature. In contrast, the nanocomposite showed a significantly higher WCA of 115° ±3°, reflecting a marked improvement in hydrophobicity compared to pure PS ($p < 0.001$) (Fig. 8). This increase in water repellency can be attributed to the combined effects of low surface energy (from ZrO_2 and AgNPs) and surface micro/nanoroughness, which may promote air trapping and reduce the contact area between water droplets and the solid surface. While the surface exhibited low water adhesion and a beading effect, it did not meet the criterion for superhydrophobicity (WCA > 150°). Nevertheless, the increased hydrophobicity contributes to reduced bacterial adhesion and improved self-cleaning potential, as water droplets roll off more easily, carrying away contaminants such as bacteria and organic debris.

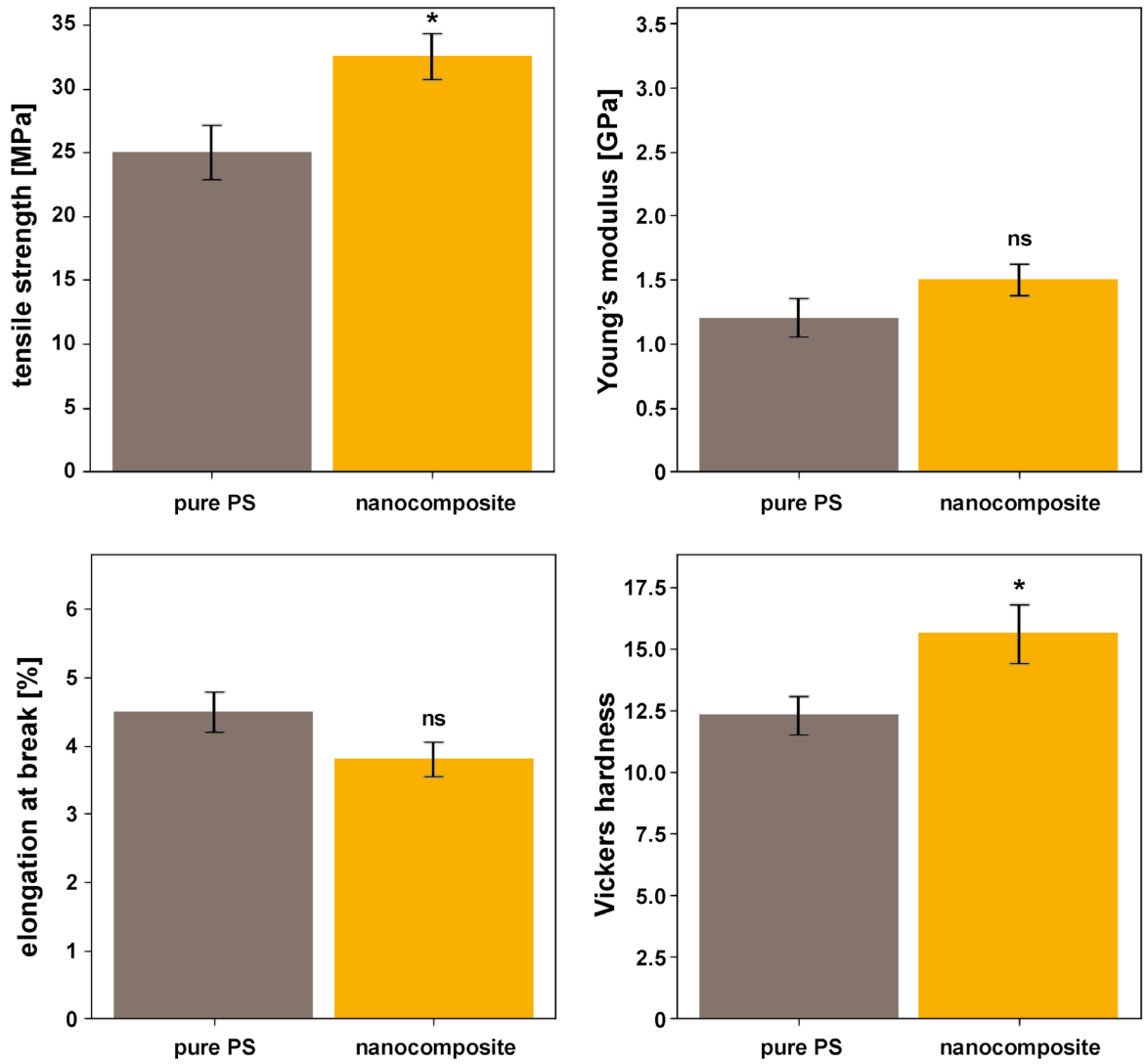

Fig. 7. Comparison of mechanical properties of pure polystyrene (PS) and the PS–HAp–ZrO_2–Ag nanocomposite

* statistically significant ($p < 0.05$, Student's *t*-test); ns – not significant.

Results of antibacterial activity assessment

The ZOI assay demonstrated significant antibacterial activity of the PS–Hap–ZrO_2–Ag nanocomposite against *S. mutans* (Fig. 9). For the nanocomposite solution (10 mg/mL in THF), the impregnated disks produced a mean inhibition zone of 15.3 ±1.2 mm (n = 3), whereas solid nanocomposite films (5-mm diameter) produced a smaller zone of 9.7 ±0.8 mm (n = 3). These results confirm the release of bioactive agents likely due to the presence of AgNPs, which effectively inhibited bacterial growth around the test samples.

Both ZOI values exceeded the threshold for clinically relevant antibacterial activity (>6 mm), highlighting the potential of the nanocomposites to interfere with *S. mutans* proliferation. The larger inhibition zones observed for solution-based samples compared to solid films suggest improved diffusion of antibacterial components

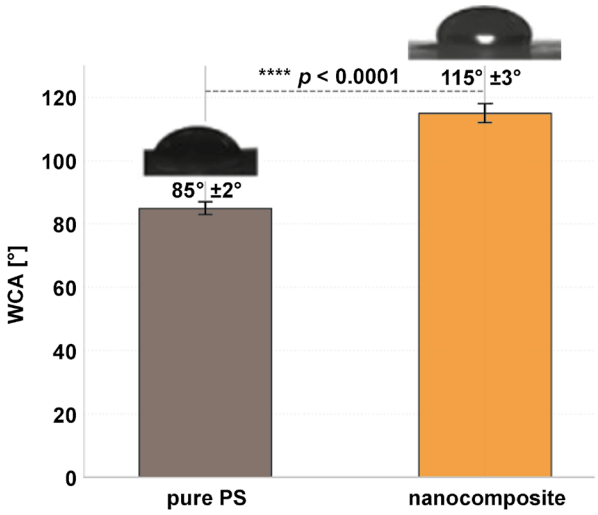

Fig. 8. Comparison of water contact angle (WCA) between pure polystyrene (PS) and the PS–HAp–ZrO_2–Ag nanocomposite

Error bars represent standard deviation (n = 5).

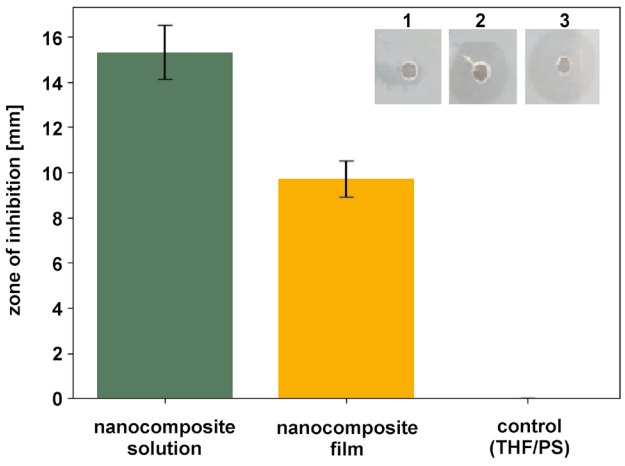

Fig. 9. Zone of inhibition (ZOI) of *Streptococcus mutans* for the PS–HAp–ZrO_2–Ag nanocomposite

All images were taken under identical conditions (24 h, 37°C). Error bars represent standard deviation (n = 3).
THF – tetrahydrofuran.

in the liquid phase. Control samples (THF-impregnated disks or pristine PS films) showed no inhibition (0 mm), confirming that the antibacterial effect is intrinsic to the nanocomposite formulation.

These results confirm the successful incorporation of AgNPs into the HAp–ZrO_2–PS matrix and emphasize their crucial role in conferring antibacterial properties relevant for dental applications.

Minimum inhibitory concentration and minimum bactericidal concentration

Both the nanocomposite extract and AgNPs exhibited strong antibacterial activity against *S. mutans* (Table 1). The MIC was 6.25 mg/mL for the nanocomposite extract and 3.12 ppm for the AgNPs, indicating a strong inhibitory effect. The MBC values were twice as high as the MIC values (12.5 mg/mL for the nanocomposite and 6.25 ppm for the AgNPs), confirming the bactericidal effect. No visible bacterial growth was observed at these concentrations, and bacterial viability was reduced by ≥99.9%.

Colony-forming unit assay

The nanocomposite films exhibited time-dependent antibacterial activity (Table 2). A reduction in bacterial count was observed after 1 h (25.4%) and increased progressively. After 24 h, a 99.8% reduction in CFU/mL was observed compared to the control. Complete inhibition (>99.9%) was achieved at AgNP concentrations ≥6.25 ppm.

Time–kill kinetics of the nanocomposite films against *S. mutans* was also investigated using the CFU assay (Fig. 10). A rapid and exponential reduction in bacterial viability was observed over 24 h. While the control samples maintained a stable bacterial count

Table 1. Minimum inhibitory concentration (MIC) and minimum bactericidal concentration (MBC) of the nanocomposite extract and silver nanoparticles (AgNPs) against *Streptococcus mutans*

Sample	MIC	MBC
Nanocomposite extract [mg/mL]	6.25 ±0.5	12.5 ±1.1
AgNPs [ppm]	3.12 ±0.3	6.25 ±0.6

Data presented as mean ± standard deviation ($M \pm SD$) (n = 3).

Table 2. Time-dependent reduction in bacterial counts following exposure to nanocomposite films

Time	Control [CFU/mL (×10^6)]	Nanocomposite [CFU/mL (×10^6)]	Reduction [%]
1 h	1.05 ±0.12	0.78 ±0.09	25.4 ±2.1
3 h	1.12 ±0.15	0.41 ±0.05	63.2 ±3.8
6 h	1.08 ±0.11	0.12 ±0.02	88.9 ±2.5
24 h	1.10 ±0.13	0.002 ±0.001	99.8 ±0.1

Data presented as $M \pm SD$ (n = 3); CFU – colony-forming units.

(1.05 ±0.12 × 10^6 CFU/mL to 1.10 ±0.13 × 10^6 CFU/mL), the nanocomposite-treated samples showed a time-dependent bactericidal effect. The semi-logarithmic plot illustrates the ability of the nanocomposite to achieve >3-log reduction (99.9% elimination) within 24 h ($p < 0.001$, one-way ANOVA) (Fig. 10).

Antibiofilm assay

Biofilm formation

The nanocomposite films significantly inhibited the biofilm formation of *S. mutans* in a time-dependent manner (Table 3). Crystal violet staining showed a 75.6% reduction in biofilm biomass after 24 h compared to the PS control ($p < 0.001$). After 72 h, biofilm inhibition increased to 91.2% ($p < 0.001$), with absorbance values decreasing from 1.25 ±0.15 (control) to 0.11 ±0.02 (nanocomposite).

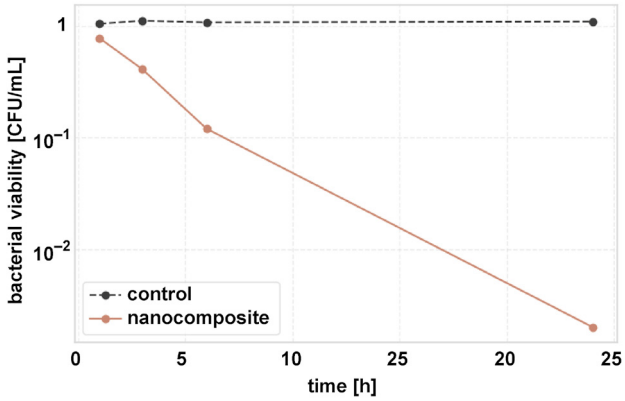

Fig. 10. Time-dependent antibacterial activity of the PS–HAp–ZrO_2–Ag nanocomposite against *Streptococcus mutans*

CFU – colony-forming units.

Confocal laser scanning microscopy

Confocal laser scanning microscopy showed significant disruption of *S. mutans* biofilm architecture on nanocomposite surfaces. Quantitative analysis showed a 74.8% reduction in biofilm thickness, decreasing from 32.5 ±3.1 µm (control) to 8.2 ±1.5 µm after 48 h of incubation. The live/dead cell ratio shifted markedly from 4.7:1 (predominantly viable cells in control biofilms) to 0.6:1 (predominantly dead cells on nanocomposite surfaces), confirming strong bactericidal activity rather than mere growth inhibition. Structurally, control samples exhibited dense, multilayered biofilms with nearly complete surface coverage, whereas nanocomposite-treated surfaces showed fragmented microcolonies and sparse colonization covering less than 20% of the surface. The control biofilms demonstrated high green fluorescence due to the dominance of live *S. mutans* cells, with minimal red fluorescence from dead cells. This reflects the natural progression of biofilm maturation, where viable cells dominate the structure (Fig. 11A–C). These results emphasize the dual antiplaque mechanism of the nanocomposite: direct killing of bacteria and physical disruption

Table 3. Quantitative analysis of biofilm biomass based on absorbance at 595 nm

Time	Control	Nanocomposite	Reduction [%]	*p*-value
24 h	0.52 ±0.06	0.15 ±0.02	75.6 ±3.2	<0.001*
48 h	0.98 ±0.11	0.28 ±0.04	83.1 ±2.8	<0.001*
72 h	1.25 ±0.15	0.11 ±0.02	91.2 ±1.9	<0.001*

Data presented as *M* ±*SD* (*n* = 6); * statistically significant ($p < 0.05$, Student's *t*-test).

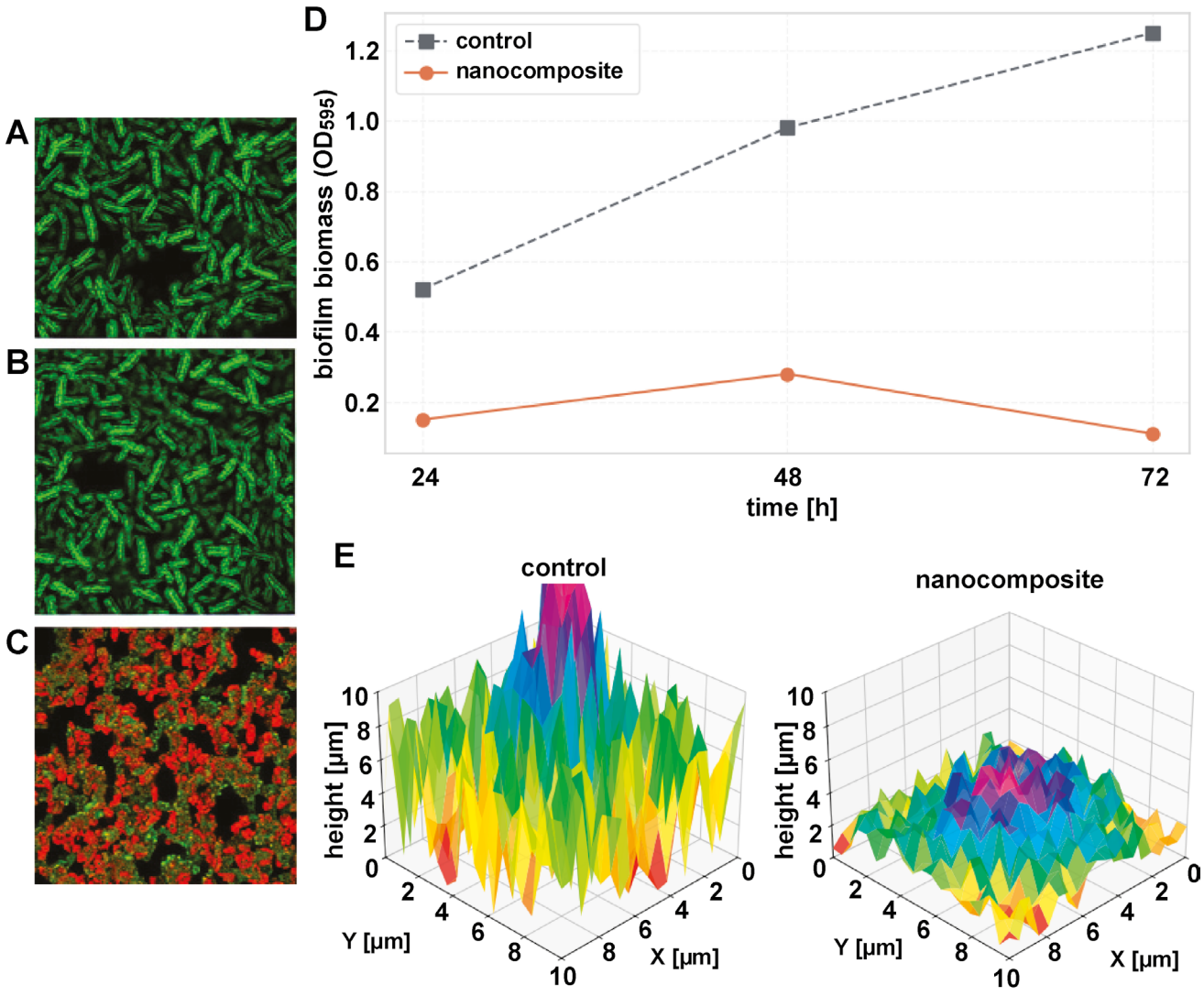

Fig. 11. Comparison of *Streptococcus mutans* biofilms on control and nanocomposite surfaces

A. Control biofilm; B: Pure polystyrene (PS); C. PS–HAp–ZrO_2–Ag nanocomposite. Green fluorescence indicates live cells, and red fluorescence denotes dead cells; D. Time-dependent biofilm inhibition by the PS–HAp–ZrO_2–Ag nanocomposite. The control group (black squares) exhibited progressive biofilm accumulation, whereas the nanocomposite-treated group (red circles) demonstrated significant inhibition ($p < 0.001$, two-way ANOVA). E. Three-dimensional (3D) reconstruction of biofilm architecture on control and nanocomposite surfaces.
OD – optical density.

of biofilm maturation. The time-dependent antibiofilm efficacy of the HAp–ZrO_2–PS nanocomposite was quantitatively evaluated using crystal violet staining (Fig. 11D). Across all evaluated time points, the biofilm biomass values of the nanocomposite-treated group remained significantly lower than those of the PS control group, with absorbance values decreasing by 75.6% ($p < 0.001$) at 24 h and by 91.2% ($p < 0.001$) at 72 h compared to the PS control. The nanocomposite group showed minimal biofilm formation (optical density $(OD)_{595}$ = 0.11 ±0.02), while the control samples showed progressive biofilm accumulation after 72 h (OD_{595} = 1.25 ±0.15). To better visualize the biofilm architecture, three-dimensional (3D) reconstructions were generated from CLSM Z-stack images. Figure 11E shows the 3D representation of *S. mutans* biofilms on control and PS–HAp–ZrO_2–Ag nanocomposite surfaces. The control samples exhibited a dense, multilayered biofilm structure with high vertical variation, indicating thick and mature biofilm formation. In contrast, the nanocomposite surfaces showed significantly thinner, discontinuous structures with reduced vertical height and sparse bacterial clusters, reflecting the material's ability to inhibit biofilm maturation and promote bacterial cell death. These results demonstrate the ability of the nanocomposite to suppress both the initial bacterial adhesion and the long-term maturation of the biofilm.

Discussion

This study demonstrates a novel approach to the development of multifunctional dental nanocomposites based on a PS matrix enriched with HAp, ZrO_2 and AgNPs. The main objective was to design a material exhibiting self-cleaning, antibacterial and antiplaque properties that utilizes the synergistic effects of these nanoscale components. The results confirm the successful synthesis of individual nanoparticles, their effective incorporation into the PS matrix and the achievement of the desired functionalities.

The successful synthesis of well-defined nanoparticles is of fundamental importance for the performance of the final nanocomposite. The chemical reduction method yielded spherical AgNPs with an average size of approx. 22 nm (TEM) and a hydrodynamic diameter of 25 nm (DLS), exhibiting a characteristic SPR peak at 460 nm and high colloidal stability (–30 mV zeta potential).[25–27] These results are consistent with previous reports on citrate-stablized AgNPs, which typically produce spherical nanoparticles in the 10–50 nm range with strong SPR absorption (420–460 nm) and good stability due to citrate capping.[28–31] The narrow size distribution (PDI = 0.12) and confirmed FCC structure (XRD) further validate the synthesis protocol. The small particle size and high surface area are crucial for maximizing the antibacterial efficacy of AgNPs.[32]

Similarly, the sol–gel synthesis produced relatively monodisperse tetragonal ZrO_2 nanoparticles (TEM: ~18 nm; DLS: 22 nm; PDI = 0.18). The tetragonal phase, confirmed by XRD, is known for its superior mechanical properties compared to the monoclinic phase, making it desirable for reinforcement applications.[33,34] The particle size is consistent with sol–gel methods where calcination occurs at moderate temperatures (e.g., 600°C).[35] The moderate zeta potential (–25 mV) indicates adequate dispersion stability, which is supported by residual citrate from the synthesis process.

The wet precipitation method yielded phase-pure, crystalline, rod-shaped HAp nanoparticles (approx. 60 nm × 20 nm), corresponding to the targeted hexagonal structure (JCPDS No. 09-432). This morphology is commonly observed in HAp synthesized under controlled pH and aging conditions.[36] While well-defined rods were noted in TEM, the larger hydrodynamic diameter (85 nm) and higher PDI (0.25) in DLS indicate some degree of agglomeration in aqueous suspension, a known challenge for HAp nanoparticles.[37] Nevertheless, the successful synthesis of nanoscale HAp, a biocompatible and osteoconductive material structurally similar to dental enamel, is essential for potential dental applications. Moreover, it contributes to the biointegration and mechanical strength of the composite.[38]

Solution mixing followed by solvent casting proved effective for the fabrication of homogeneous PS–HAp–ZrO_2–Ag nanocomposites. Scanning electron microscopy imaging in conjunction with EDX mapping confirmed uniform distribution of all nanoparticle components within the PS matrix, which is crucial for achieving uniform properties of the material.[39] The absence of large agglomerates minimizes stress concentration and ensures optimal load transfer and surface properties.[40]

The TGA results showed that the incorporation of 5 wt% nanoparticles did not significantly alter the onset of thermal degradation of the PS matrix, indicating good interfacial compatibility and no catalytic degradation by the nanoparticles at these temperatures. The measured residual mass corresponded to the theoretical loading, confirming the successful incorporation of the inorganic components.[41] The preserved thermal stability is sufficient for many dental processing techniques and intraoral conditions.

Mechanical testing demonstrated a significant improvement in material performance. The tensile strength increased by 30%, while the modulus of elasticity showed a 25% increase compared to pure PS. This enhancement is attributed to the high stiffness of the ceramic HAp and ZrO_2 nanoparticles and effective stress transfer from the polymer matrix to the well-dispersed fillers.[42,43] The rod-like morphology of HAp may further contribute to reinforcement.[44] The slight decrease in elongation at break reflects a typical trade-off, where rigid fillers are incorporated into a polymer matrix, indicating increased stiffness

and reduced extensibility. These improved mechanical properties are advantageous for dental materials that require durability and wear resistance.[45]

An important innovation of this study is the improvement in self-cleaning properties. The surface of the nanocomposite showed a significantly increased hydrophobicity (WCA = 115°) compared to moderately hydrophobic pure PS (WCA = 85°). Although this value does not meet the criterion for superhydrophobicity (>150°), it indicates a clear shift toward a low-energy, water-repellent surface. This behavior is likely due to the combined influence of the low surface energy ZrO_2 nanoparticles and the AgNPs forming a hierarchical micro/nanostructure on the surface.[46,47] The induced roughness can trap air pockets (Cassie–Baxter state) and minimize the contact area between water droplets and the solid surface.[48] Although HAp is generally hydrophilic, its nanoscale dispersion and potential partial coverage by the hydrophobic matrix or other nanoparticles seem to prevent it from dominating the surface wettability. Increased hydrophobicity is closely related to reduced bacterial adhesion and easier removal of impurities, which is beneficial for limiting plaque accumulation.[49,50] Similar increases in hydrophobicity have been reported for polymer composites containing ZrO_2 or other nanoparticles designed for reduced fouling.[51,52]

The incorporation of AgNPs conferred significant antibacterial activity to the nanocomposite, as shown in several tests with *S. mutans*, a major causative agent of dental caries.[53] The ZOI assay confirmed the release of active compounds from both the dissolved and solid forms of the nanocomposite, with inhibition zones exceeding clinically relevant thresholds.[54] The larger zones observed for solution-based samples indicate easier diffusion of Ag^+ ions or nanoparticles.[55]

The MIC and MBC results quantified this potency and showed strong inhibitory (MIC = 6.25 mg/mL for extract, MIC = 3.12 ppm for AgNPs) and bactericidal (MBC = 12.5 mg/mL for extract, MBC = 6.25 ppm for AgNPs) effects. These values are comparable to or better than those reported for other AgNP-based dental materials.[56,57] The twofold difference between MIC and MBC values supports a bactericidal mechanism rather than just bacteriostatic activity. The CFU assay further corroborated these results, showing a time-dependent reduction in bacterial viability, achieving >3-log reduction (>99.9%) within 24 h. This rapid bactericidal effect is attributed to the release of Ag^+ ions, which destroy bacterial cell membranes, impair metabolic enzymes and trigger oxidative stress via ROS formation.[22,58,59]

In addition to killing planktonic bacteria, the nanocomposite exhibited significant efficacy in preventing and disrupting *S. mutans* biofilms, which are the predominant form of bacterial growth in the oral cavity and are notoriously difficult to eradicate. Crystal violet assays showed significant, time-dependent reductions in biofilm biomass, reaching 91.2% inhibition after 72 h. This suggests that the nanocomposite interferes with the critical stages of biofilm development, including initial attachment, microcolony formation and maturation.[60]

The CLSM analysis provided convincing visual and quantitative evidence for the antibiofilm mechanism. Compared to dense, thick (32.5 μm) and predominantly living biofilms on control PS surfaces, biofilms on the nanocomposite were significantly thinner (8.2 μm), sparsely distributed (<20% surface coverage), structurally compromised, and contained a high proportion of dead cells (the ratio of living to dead cells shifted from 4.7:1 to 0.6:1). This dual effect, namely the inhibition of adhesion/growth and killing of embedded bacteria, is highly desirable for an antiplaque material.[61,62] The combination of surface hydrophobicity (reduction of initial adhesion) and sustained AgNP activity (killing of adherent and proliferating bacteria) is presumably the basis for this strong antibiofilm performance.[63–65] The observed efficacy of the material compares favorably with that of other advanced antibiofilm dental materials containing active ingredients such as quaternary ammonium compounds or other nanoparticles.[66,67]

The bactericidal mechanism of the PS–HAp–ZrO_2–Ag nanocomposite is primarily attributed to the presence of AgNPs, which release Ag^+ ions and generate ROS, damaging bacterial cellular components and preventing replication. The hierarchical structure provided by HAp and ZrO_2 nanoparticles may also contribute to the overall antimicrobial efficacy by inhibiting bacterial adhesion.

While the developed PS–HAp–ZrO_2–Ag nanocomposite demonstrates significant improvements in mechanical strength, antibacterial activity and self-cleaning properties, its practical performance in dental applications must be considered. Key factors include wear resistance, color stability and adhesion to dental tissues. Wear resistance is crucial for restorative materials, as they are subjected to masticatory forces and abrasive food particles.[68–70] The incorporation of ZrO_2 nanoparticles is expected to enhance wear resistance due to their high hardness and toughness.[71] Color stability is also essential for aesthetic restorations, as discoloration can compromise the material's appearance.[72] The presence of AgNPs may potentially affect color stability due to potential oxidation and subsequent darkening.[73] Adhesion to dental tissues is another critical factor, as it directly impacts the material's ability to bond with tooth structures and withstand clinical stresses.[74] The incorporation of HAp nanoparticles may promote biointegration and enhance adhesion to dental tissues due to their structural similarity to natural tooth enamel.[68]

In this study, HAp, ZrO_2 and AgNPs were successfully integrated into a PS matrix, creating a multifunctional nanocomposite with improved mechanical properties, increased hydrophobicity, strong antibacterial activity, and significant antibiofilm efficacy against *S. mutans*. The novelty of this work lies in the specific combination

of these nanoparticles within a polymer matrix to achieve several desired functionalities for potential dental applications such as coatings, temporary restorations or orthodontic components.

Limitations and further directions

Despite the promising results, this study has several limitations that must be acknowledged. Firstly, PS was used as a model polymer matrix due to its low cost, ease of processing and compatibility with nanoparticles. However, PS is not clinically relevant for dental applications, which typically rely on dental-specific polymers such as polymethyl methacrylate (PMMA) or bisphenol-A glycidyl methacrylate (Bis-GMA)-based resins. Therefore, translating this concept to clinically relevant materials would require significant adjustments in nanoparticle dispersion methods, resin compatibility and curing protocols to ensure homogeneous integration and optimal mechanical performance. Secondly, the antibacterial and antiplaque assessments were conducted in vitro using a single bacterial species, *S. mutans*. While *S. mutans* is a well-established model for early caries development, natural dental plaque is a complex multispecies biofilm comprising hundreds of bacterial species, including gram-negative anaerobes (e.g., *P. gingivalis*, *F. nucleatum*), that play key roles in plaque maturation, immune modulation and periodontal disease progression. Thus, future studies should evaluate the performance of the nanocomposite against multispecies biofilms to better reflect clinical conditions and assess selective antibacterial activity and microbiome balance. Thirdly, the long-term stability, biocompatibility and safety of the nanocomposite require thorough investigation. Although HAp and ZrO_2 are generally considered biocompatible, the release kinetics of AgNPs and Ag^+ ions remain a concern. Chronic exposure to Ag^+ ions may lead to cytotoxicity, microbial resistance or disruption of the oral microbiome. Therefore, comprehensive biocompatibility assessments in accordance with ISO 10993 standards are essential, including in vitro cytotoxicity, genotoxicity and in vivo toxicity studies. Additionally, the optimization of AgNP concentration is crucial to balance antibacterial efficacy with safety. Fourthly, several critical dental properties were not evaluated in this study, including abrasion resistance, color stability and adhesion to dental tissues. These factors are vital for the clinical success of any dental restorative material. For example, color stability ensures aesthetic durability, while strong adhesion to enamel and dentin is essential for marginal integrity and long-term retention.

To address these limitations, future research should focus on the following:

- material translation: developing methods to integrate HAp, ZrO_2 and AgNPs into dental resins (e.g., PMMA, Bis-GMA) with improved dispersion and interfacial bonding;
- multispecies biofilm testing: evaluating the antiplaque and antibacterial efficacy against clinically relevant multispecies biofilms, including cariogenic and periodontopathogenic consortia;
- comprehensive biocompatibility assessment: conducting ISO 10993-compliant tests, including cytotoxicity, genotoxicity and in vivo studies to evaluate long-term safety;
- degradation and stability studies: assessing material degradation under simulated oral conditions (thermal cycling, pH cycling, wear) to ensure long-term durability;
- mechanical and functional properties: evaluating abrasion resistance, color stability and adhesion strength to enamel and dentin to ensure clinical feasibility;
- microbiome impact studies: investigating the effects of the nanocomposite on oral microbial ecology, including plaque composition, bacterial diversity and biofilm architecture;
- optimization of formulation: optimizing the nanoparticle loading ratios, dispersion techniques and material composition to enhance performance and minimize risks.

Addressing these aspects would facilitate the translation of the nanocomposite into a next-generation dental material that not only provides structural integrity but also actively promotes oral health through antibacterial, antiplaque and self-cleaning properties.

Conclusions

In summary, this study reports the successful development of a novel PS-based nanocomposite reinforced with HAp, ZrO_2 and Ag nanoparticles. The material exhibited significantly improved mechanical strength, increased surface hydrophobicity indicating self-cleaning potential, strong bactericidal activity against *S. mutans*, and remarkable efficacy in inhibiting biofilm formation. The uniform dispersion of the nanoparticles and their synergistic contributions to the overall performance of the composite were confirmed. Although further optimization as well as extensive biocompatibility and long-term testing are required, especially in clinically relevant polymer matrices, this work provides a strong proof of concept for the development of multifunctional dental materials. Such materials have the potential to actively combat bacterial colonization and plaque formation, thereby contributing improved oral health outcomes.

Ethics approval and consent to participate

Not applicable.

Data availability

The datasets generated and/or analyzed during the current study are available from the corresponding author on reasonable request.

Consent for publication

Not applicable.

Use of AI and AI-assisted technologies

Not applicable.

ORCID iDs

Hadi Zare-Zardini https://orcid.org/0000-0002-1501-2560
Elham Saberian https://orcid.org/0000-0002-0590-9489
Andrej Jenča Jr. https://orcid.org/0000-0002-9297-9134
Adriána Petrášová https://orcid.org/0000-0002-4289-7691
Janka Jenčová https://orcid.org/0009-0007-4431-3227
Andrej Jenča https://orcid.org/0000-0003-4501-7407
Eliška Kubíková https://orcid.org/0000-0002-8370-9618
Tetyana Pyndus https://orcid.org/0000-0002-9570-9287
Mieszko Adam Więckiewicz https://orcid.org/0000-0003-4953-7143

References

1. Saleh MHA, Dias DR, Kumar P. The economic and societal impact of periodontal and peri-implant diseases. *Periodontol 2000*. 2025;98(1):100–118. doi:10.1111/prd.12568
2. World Health Organization. *Global Oral Health Status Report: Towards Universal Health Coverage for Oral Health by 2030*. Geneva, Switzerland: World Health Organization; 2022.
3. Beikler T, Flemmig TF. Oral biofilm-associated diseases: Trends and implications for quality of life, systemic health and expenditures. *Periodontol 2000*. 2011;55(1):87–103. doi:10.1111/j.1600-0757.2010.00360.x
4. Zhao W, Zhang Y, Chen J, Hu D. Revolutionizing oral care: Reactive oxygen species (ROS)–Regulating biomaterials for combating infection and inflammation. *Redox Biol*. 2025;79:103451. doi:10.1016/j.redox.2024.103451
5. Jakubovics NS, Goodman SD, Mashburn-Warren L, Stafford GP, Cieplik F. The dental plaque biofilm matrix. *Periodontol 2000*. 2021;86(1):32–56. doi:10.1111/prd.12361
6. Takenaka S, Ohsumi T, Noiri Y. Evidence-based strategy for dental biofilms: Current evidence of mouthwashes on dental biofilm and gingivitis. *Jpn Dent Sci Rev*. 2019;55(1):33–40. doi:10.1016/j.jdsr.2018.07.001
7. Min K, Bosma ML, John G, et al. Quantitative analysis of the effects of brushing, flossing, and mouthrinsing on supragingival and subgingival plaque microbiota: 12-week clinical trial. *BMC Oral Health*. 2024;24(1):575. doi:10.1186/s12903-024-04362-y
8. Cho K, Rajan G, Farrar P, Prentice L, Prusty BG. Dental resin composites: A review on materials to product realizations. *Compos B Eng*. 2022;230:109495. doi:10.1016/j.compositesb.2021.109495
9. T SK, Chandrasekaran R. Harnessing the functional role of polymeric nanocomposite in dental caries disease: A comprehensive review. *Hybrid Adv*. 2025;10:100433. doi:10.1016/j.hybadv.2025.100433
10. Pfeifer CS, Lucena FS, Tsuzuki FM. Preservation strategies for interfacial integrity in restorative dentistry: A non-comprehensive literature review. *J Funct Biomater*. 2025;16(2):42. doi:10.3390/jfb16020042
11. Nicolae CL, Pîrvulescu DC, Niculescu AG, Rădulescu M, Grumezescu AM, Croitoru GA. An overview of nanotechnology in dental medicine. *J Compos Sci*. 2024;8(9):352. doi:10.3390/jcs8090352
12. Alsuraifi A, Sulaiman ZM, Mohammed NAR, et al. Explore the most recent developments and upcoming outlooks in the field of dental nanomaterials. *Beni-Suef Univ J Basic Appl Sci*. 2024;13(1):82. doi:10.1186/s43088-024-00540-7
13. Gronwald B, Kozłowska L, Kijak K, et al. Nanoparticles in dentistry – current literature review. *Coatings*. 2023;13(1):102. doi:10.3390/coatings13010102
14. Islam MA, Hossain N, Hossain S, et al. Advances of hydroxyapatite nanoparticles in dental implant applications. *Int Dent J*. 2025;75(3):2272–2313. doi:10.1016/j.identj.2024.11.020
15. Patil NA, Kandasubramanian B. Biological and mechanical enhancement of zirconium dioxide for medical applications. *Ceram Int*. 2020;46(4):4041–4057. doi:10.1016/j.ceramint.2019.10.220
16. Elbahie DM, Badawy RES, Ibrahim SAM, Hassan M, Habib NA. Assessment of the antibacterial activity of glass ionomer cements modified by polyamidoamine and bioactive glass: An in vitro study. *Dent Med Probl*. 2026;63(1):199–207. doi:10.17219/dmp/166140
17. Mehdipour A, Pourreisi R, Amini-Khoei H, Shams S. Evaluating the antibacterial and antibiofilm activity of *Zataria multiflora* in comparison with chlorhexidine, using a tooth model: A preliminary study. *Dent Med Probl*. 2025;62(2):293–298. doi:10.17219/dmp/150652
18. Shalaby HA, Soliman NK, Al-Saudi KW. Antibacterial and preventive effects of newly developed modified nano-chitosan/glass-ionomer restoration on simulated initial enamel caries lesions: An in vitro study. *Dent Med Probl*. 2024;61(3):353–362. doi:10.17219/dmp/158835
19. Anani H, Elasser D, Niazy M, Jamil W, Elsharkawy D. Evaluation of the remineralization and antibacterial effect of natural versus synthetic materials on deep carious dentin: A randomized controlled trial. *Dent Med Probl*. 2023;60(1):87–97. doi:10.17219/dmp/147075
20. Soundarajan S, Rajasekar A. Antibacterial and anti-inflammatory effects of a novel herb-mediated nanocomposite mouthwash in plaque-induced gingivitis: A randomized controlled trial. *Dent Med Probl*. 2023;60(3):445–451. doi:10.17219/dmp/150728
21. Zhang X, Wu X, Shi J. Additive manufacturing of zirconia ceramics: A state-of-the-art review. *J Mater Res Technol*. 2020;9(4):9029–9048. doi:10.1016/j.jmrt.2020.05.131
22. More PR, Pandit S, De Filippis A, Franci G, Mijakovic I, Galdiero M. Silver nanoparticles: Bactericidal and mechanistic approach against drug resistant pathogens. *Microorganisms*. 2023;11(2):369. doi:10.3390/microorganisms11020369
23. ASTM International. *ASTM D638-14. Standard Test Method for Tensile Properties of Plastics*. West Conshohocken, PA: ASTM International; 2014. doi:10.1520/D0638-14
24. International Organization for Standardization. *ISO 6507-1:2018. Metallic materials—Vickers hardness test—Part 1: Test method*. Geneva, Switzerland: ISO; 2018.
25. Rodrigues AS, Batista JGS, Rodrigues MÁV, et al. Advances in silver nanoparticles: A comprehensive review on their potential as antimicrobial agents and their mechanisms of action elucidated by proteomics. *Front Microbiol*. 2024;15:1440065. doi:10.3389/fmicb.2024.1440065
26. Dhaka A, Chand Mali S, Sharma S, Trivedi R. A review on biological synthesis of silver nanoparticles and their potential applications. *Results Chem*. 2023;6:101108. doi:10.1016/j.rechem.2023.101108
27. Mallineni SK, Sakhamuri S, Kotha SL, et al. Silver nanoparticles in dental applications: A descriptive review. *Bioengineering*. 2023;10(3):327. doi:10.3390/bioengineering10030327
28. Moskalyuk OA, Belashov AV, Beltukov YM, et al. Polystyrene-based nanocomposites with different fillers: Fabrication and mechanical properties. *Polymers*. 2020;12(11):2457. doi:10.3390/polym12112457
29. Haider S, Kausar A, Muhammad B. Overview on polystyrene/nanoclay composite: Physical properties and application. *Polym Plast Technol Eng*. 2017;56(9):917–931. doi:10.1080/03602559.2016.1233563
30. Bastús NG, Merkoçi F, Piella J, Puntes V. Synthesis of highly monodisperse citrate-stabilized silver nanoparticles of up to 200 nm: Kinetic control and catalytic properties. *Chem Mater*. 2014;26(9):2836–2846. doi:10.1021/cm500316k
31. Sati A, Ranade TN, Mali SN, Ahmad Yasin HK, Pratap A. Silver nanoparticles (AgNPs): Comprehensive insights into bio/synthesis, key influencing factors, multifaceted applications, and toxicity – A 2024 update. *ACS Omega*. 2025;10(8):7549–7582. doi:10.1021/acsomega.4c11045
32. Mahmud KM, Hossain MM, Polash SA, et al. Investigation of antimicrobial activity and biocompatibility of biogenic silver nanoparticles synthesized using *Syzigyum cymosum* extract. *ACS Omega*. 2022;7(31):27216–27229. doi:10.1021/acsomega.2c01922
33. Shukla S, Seal S. Thermodynamic tetragonal phase stability in sol–gel derived nanodomains of pure zirconia. *J Phys Chem B*. 2004;108(11):3395–3399. doi:10.1021/jp037532x

34. Chevalier J, Loh J, Gremillard L, Meille S, Adolfson E. Low-temperature degradation in zirconia with a porous surface. *Acta Biomater.* 2011;7(7):2986–2993. doi:10.1016/j.actbio.2011.03.006
35. Dwivedi R, Maurya A, Verma A, Prasad R, Bartwal KS. Microwave assisted sol–gel synthesis of tetragonal zirconia nanoparticles. *J Alloys Compd*. 2011;509(24):6848–6851. doi:10.1016/j.jallcom.2011.03.138
36. Sadat-Shojai M, Khorasani MT, Jamshidi A, Irani S. Nano-hydroxyapatite reinforced polyhydroxybutyrate composites: A comprehensive study on the structural and in vitro biological properties. *Mater Sci Eng C Mater Biol Appl*. 2013;33(5):2776–2787. doi:10.1016/j.msec.2013.02.041
37. Ferraz MP, Monteiro FJ, Manuel CM. Hydroxyapatite nanoparticles: A review of preparation methodologies. *J Appl Biomater Biomech*. 2004;2(2):74–80. PMID:20803440.
38. Zhou H, Lee J. Nanoscale hydroxyapatite particles for bone tissue engineering. *Acta Biomater.* 2011;7(7):2769–2781. doi:10.1016/j.actbio.2011.03.019
39. Paul DR, Robeson LM. Polymer nanotechnology: Nanocomposites. *Polymer*. 2008;49(15):3187–3204. doi:10.1016/j.polymer.2008.04.017
40. Ulusoy U. A review of particle shape effects on material properties for various engineering applications: From macro to nanoscale. *Minerals*. 2023;13(1):91. doi:10.3390/min13010091
41. Kashiwagi T, Du F, Douglas JF, Winey KI, Harris Jr RH, Shields JR. Nanoparticle networks reduce the flammability of polymer nanocomposites. *Nat Mater.* 2005;4(12):928–933. doi:10.1038/nmat1502
42. Musharavati F, Jaber F, Nasor M, et al. Micromechanical properties of hydroxyapatite nanocomposites reinforced with CNTs and ZrO_2. *Ceram Int*. 2023;49(5):7466–7475. doi:10.1016/j.ceramint.2022.10.218
43. Kumar VA, Raju PRM, Bhargavi R, Madhusudan S, Rajesh S. Investigations on microstructure and mechanical properties of HAp nanocomposites reinforced with ZrO_2 and TiO_2. *J Phys Conf Ser.* 2024;2765:012009. doi:10.1088/1742-6596/2765/1/012009
44. Mohammadi A, Tamang S, Rethinasabapathy M, et al. Eco-friendly synthesis of rod-like hydroxyapatite on spherical carbon: A dual-function composite for selective cobalt removal and enhanced oxygen evolution reaction. *J Hazard Mater.* 2025;487:137164. doi:10.1016/j.jhazmat.2025.137164
45. Ferracane JL. Resin composite – state of the art. *Dent Mater.* 2011;27(1):29–38. doi:10.1016/j.dental.2010.10.020
46. Roach P, Shirtcliffe NJ, Newton MI. Progess in superhydrophobic surface development. *Soft Matter.* 2008;4(2):224–240. doi:10.1039/B712575P
47. Xu C, Yang D, Mei L, et al. Encapsulating gold nanoparticles or nanorods in graphene oxide shells as a novel gene vector. *ACS Appl Mater Interfaces*. 2013;5(7):2715–2724. doi:10.1021/am400212j
48. Sheng YJ, Jiang S, Tsao HK. Effects of geometrical characteristics of surface roughness on droplet wetting. *J Chem Phys*. 2007;127(23):234704. doi:10.1063/1.2804425
49. Murakami A, Arimoto T, Suzuki D, et al. Antimicrobial and osteogenic properties of a hydrophilic-modified nanoscale hydroxyapatite coating on titanium. *Nanomedicine*. 2012;8(3):374–382. doi:10.1016/j.nano.2011.07.001
50. Seyfi J, Goodarzi V, Wurm FR, et al. Developing antibacterial superhydrophobic coatings based on polydimethylsiloxane/silver phosphate nanocomposites: Assessment of surface morphology, roughness and chemistry. *Prog Org Coat*. 2020;149:105944. doi:10.1016/j.porgcoat.2020.105944
51. Tan YZ, Alias NH, Aziz MHA, Jaafar J, Othman FEC, Chew JW. Progress on improved fouling resistance-nanofibrous membrane for membrane distillation: A mini-review. *Membranes*. 2023;13(8):727. doi:10.3390/membranes13080727
52. Liu H, Webster TJ. Mechanical properties of dispersed ceramic nanoparticles in polymer composites for orthopedic applications. *Int J Nanomedicine*. 2010;5:299–313. doi:10.2147/ijn.s9882
53. Hamouda RA, Makharita RR, Qarabai FAK, et al. Antibacterial activities of Ag/cellulose nanocomposites derived from marine environment algae against bacterial tooth decay. *Microorganisms*. 2023;12(1):1. doi:10.3390/microorganisms12010001
54. Pérez-Díaz MA, Boegli L, James G, et al. Silver nanoparticles with antimicrobial activities against *Streptococcus mutans* and their cytotoxic effect. *Mater Sci Eng C Mater Biol Appl*. 2015;55:360–366. doi:10.1016/j.msec.2015.05.036
55. Ahmed O, Sibuyi NRS, Fadaka AO, et al. Plant extract-synthesized silver nanoparticles for application in dental therapy. *Pharmaceutics*. 2022;14(2):380. doi:10.3390/pharmaceutics14020380
56. Hernández-Sierra JF, Galicia-Cruz O, Salinas-Acosta A, Ruíz F, Pierdant-Pérez M, Pozos-Guillén AJ. In vitro cytotoxicity of silver nanoparticles on human periodontal fibroblasts. *J Clin Pediatr Dent*. 2011;36(1):37–42. doi:10.17796/jcpd.36.1.d677647166398886
57. Cheng L, Weir MD, Xu HHK, et al. Antibacterial and physical properties of calcium–phosphate and calcium–fluoride nanocomposites with chlorhexidine. *Dent Mater.* 2012;28(5):573–583. doi:10.1016/j.dental.2012.01.006
58. Ahmad SA, Sachi Das S, Khatoon A, et al. Bactericidal activity of silver nanoparticles: A mechanistic review. *Mater Sci Energy Technol*. 2020;3:756–769. doi:10.1016/j.mset.2020.09.002
59. Chatterjee N, Pal S, Dhar P. Green silver nanoparticles from bacteria-antioxidant, cytotoxic and antifungal activities. *Next Nanotechnol*. 2024;6:100089. doi:10.1016/j.nxnano.2024.100089
60. Beyth N, Yudovin-Farber I, Perez-Davidi M, Domb AJ, Weiss EI. Polyethyleneimine nanoparticles incorporated into resin composite cause cell death and trigger biofilm stress in vivo. *Proc Natl Acad Sci USA*. 2010;107(51):22038–22043. doi:10.1073/pnas.1010341107
61. Kalia VC, Patel SKS, Lee JK. Bacterial biofilm inhibitors: An overview. *Ecotoxicol Environ Saf*. 2023;264:115389. doi:10.1016/j.ecoenv.2023.115389
62. Mitwalli H, Alsahafi R, Balhaddad AA, Weir MD, Xu HHK, Melo MAS. Emerging contact-killing antibacterial strategies for developing anti-biofilm dental polymeric restorative materials. *Bioengineering (Basel)*. 2020;7(3):83. doi:10.3390/bioengineering7030083
63. Khan SA, Shakoor A. Recent strategies and future recommendations for the fabrication of antimicrobial, antibiofilm, and antibiofouling biomaterials. *Int J Nanomedicine*. 2023;18:3377–3405. doi:10.2147/IJN.S406078
64. Chen X, Zhou J, Qian Y, Zhao LZ. Antibacterial coatings on orthopedic implants. *Mater Today Bio*. 2023;19:100586. doi:10.1016/j.mtbio.2023.100586
65. Yazdani-Ahmadabadi H, Felix DF, Yu K, et al. Durable surfaces from film-forming silver assemblies for long-term zero bacterial adhesion without toxicity. *ACS Cent Sci*. 2022;8(5):546–561. doi:10.1021/acscentsci.1c01556
66. Cheng L, Zhang K, Melo MAS, Weir MD, Zhou X, Xu HHK. Anti-biofilm dentin primer with quaternary ammonium and silver nanoparticles. *J Dent Res*. 2012;91(6):598–604. doi:10.1177/0022034512444128
67. Atar-Froyman L, Sharon A, Weiss EI, et al. Anti-biofilm properties of wound dressing incorporating nonrelease polycationic antimicrobials. *Biomaterials*. 2015;46:141–148. doi:10.1016/j.biomaterials.2014.12.047
68. Paluch E, Sobierajska P, Okińczyc P, et al. Nanoapatites doped and co-doped with noble metal ions as modern antibiofilm materials for biomedical applications against drug-resistant clinical strains of *Enterococcus faecalis* VRE and *Staphylococcus aureus* MRSA. *Int J Mol Sci*. 2022;23(3):1533. doi:10.3390/ijms23031533
69. Paluch E, Rewak-Soroczyńska J, Jędrusik I, Mazurkiewicz E, Jermakow KJ. Prevention of biofilm formation by quorum quenching. *Appl Microbiol Biotechnol*. 2020;104(5):1871–1881. doi:10.1007/s00253-020-10349-w
70. Yadav S, Gangwar S. A critical evaluation of tribological interaction for restorative materials in dentistry. *Int J Polym Mater Polym Biomater.* 2019;68(17):1005–1019. doi:10.1080/00914037.2018.1525544
71. Ravikumar K, Sarkar D, Basu B. ZrO_2-toughened Al_2O_3 composites with better fracture and wear resistance properties. *J Biomater Appl*. 2018;32(9):1174–1186. doi:10.1177/0885328217750820
72. Alqahtani AAM, Al Mafraq SMA, Alshahrani MAM, et al. Discoloration of different aesthetic restorative materials: Effects of various finishing systems on surface roughness and staining susceptibility. *J Int Crisis Risk Commun Research*. 2024;7(S6):570–576. doi:10.63278/jicrcr.vi.1929
73. Qasim SSB, Ali D, Soliman MS, Zafiropoulos GG. The effect of chitosan derived silver nanoparticles on mechanical properties, color stability of glass ionomer luting cements. *Mater Res Express*. 2021;8(8):085401. doi:10.1088/2053-1591/ac1cd5
74. Zhao Z, Wang Q, Zhao J, Zhao B, Ma Z, Zhang C. Adhesion of teeth. *Front Mater.* 2021;7:615225. doi:10.3389/fmats.2020.615225

Original paper

Factors affecting the duration of hospitalization due to odontogenic abscesses in children

Liat Chaushu[1,A–F], Shiri Lapides[2,B–D,F], Gal Avishai[3,B,C,F], Aya Vituri[4,C,E], Sigalit Blumer[2,A–F]

[1] Department of Periodontology and Implant Dentistry, The Maurice and Gabriela Goldschleger School of Dental Medicine, Tel Aviv University, Israel
[2] Department of Pediatric Dentistry, The Maurice and Gabriela Goldschleger School of Dental Medicine, Tel Aviv University, Israel
[3] Department of Oral and Maxillofacial Surgery, Rabin Medical Centre, Bellinson Hospital, Petach Tikva, Israel
[4] Department of Biostatistics, Tel Aviv University, Israel

A – research concept and design; B – collection and/or assembly of data; C – data analysis and interpretation;
D – writing the article; E – critical revision of the article; F – final approval of the article

Dental and Medical Problems, ISSN 1644-387X (print), ISSN 2300-9020 (online) *Dent Med Probl*. 2026;63(5):1259–1265

Address for correspondence
Liat Chaushu
E-mail: liat.natanel@gmail.com

Funding sources
None declared

Conflict of interest
None declared

Acknowledgements
None declared

Received on January 6, 2025
Reviewed on February 19, 2025
Accepted on February 22, 2025

Published online on October 30, 2026

Abstract

Background. The spread of an odontogenic abscess can have serious consequences and may result in severe morbidity or death. There is no consensus regarding the factors that may predict the length of hospital stay (LOHS) in children hospitalized for odontogenic abscesses.

Objectives. The aim of the study was to examine the factors affecting LOHS among children and adolescents who were hospitalized for surgical treatment of odontogenic abscesses.

Material and methods. A retrospective cohort study included children and adolescents aged 1–17 years who were admitted to the pediatric emergency department of the Scheneider Children's Medical Center of Israel between 2018 and 2022 for a dentoalveolar or odontogenic abscess.

Results. In total, 127 patients (55.9% male) with a median age of 6 years were included. Dental caries was the most common odontogenic cause of abscess formation (72%). The median LOHS was 3 days (range: 2–8 days). The logistic regression analysis identified age, body temperature at admission, white blood cell (WBC) count at admission, and the year of admission as predictors of LOHS, explaining 44.9% of the model's variance. Sex, C-reactive protein (CRP) levels and neutrophil, monocyte and eosinophil counts were not significant predictors of LOHS in this patient population.

Conclusions. Age, body temperature at admission, WBC count at admission, and the year of admission were associated with LOHS in children and adolescents hospitalized for odontogenic abscesses.

Keywords: pediatric dentistry, hospitalization, dental abscess, blood counts

Cite as
Chaushu L, Lapides S, Avishai G, Vituri A, Blumer S. Factors affecting the duration of hospitalization due to odontogenic abscesses in children. *Dent Med Probl.* 2026;63(5):1259–1265. doi:10.17219/dmp/202208

DOI
10.17219/dmp/202208

Copyright
Copyright by Author(s)
This is an article distributed under the terms of the Creative Commons Attribution 3.0 Unported (CC BY 3.0) (https://creativecommons.org/licenses/by/3.0/)

Highlights

- Age, body temperature and white blood cell count at admission were associated with longer hospital stays among children and adolescents hospitalized for odontogenic abscesses.
- C-reactive protein levels were not significant predictors of length of hospital stay in this patient population.
- Avoiding unnecessary hospitalization may help reduce its short- and long-term consequences.

Introduction

Odontogenic abscesses are infectious processes whose severity depends on the virulence of the causative bacteria, regional anatomy and individual resistance factors. Until the end of the last century, odontogenic abscesses received relatively limited research attention. Since then, it has become clear that the spread of an odontogenic abscess can have serious consequences and may lead to severe morbidity and even death.[1] Management requires prompt intervention, such as root canal treatment, periodontal treatment or extraction, to eliminate the source of infection and prevent its further spread. In children with unerupted teeth, such interventions may also minimize the risk of damage to adjacent tooth germs and surrounding tissues.

Odontogenic and dentoalveolar abscesses are localized collections of purulent fluid in the alveolar bone at the tooth root apex. These abscesses are usually secondary to caries, trauma, deep restorations, or unsuccessful root canal treatment. Following disruption of pulp integrity and bacterial invasion of the pulp chamber, microorganisms may colonize the root canal system, form biofilms and cause acute inflammation, leading to abscess formation.[1–3] The symptoms of an acute odontogenic abscess include pain, swelling and erythema, which are usually localized to the area of the affected tooth. The nature of the infection and the extent of its spread also depend on the individual's immune response.[4] If an abscess is not adequately treated at an early stage, the infection may progress and spread rapidly to nearby anatomical structures, causing serious complications such as sepsis, cavernous sinus thrombosis (CST), brain abscess, septic shock, and even death.[1–3]

Children presenting with facial swelling or cellulitis of odontogenic origin require prompt clinical assessment and treatment aimed at eliminating the source of infection, including surgical drainage when indicated. If the tooth is not restorable, extraction is indicated. In otherwise healthy children with localized infections and no systemic involvement, antibiotic treatment is unnecessary following the surgical procedure. Analgesics may be administered as needed. Signs suggesting systemic involvement and sepsis include fever, weakness, facial asymmetry, facial swelling, lymphadenopathy, tachycardia, dysphagia, and respiratory distress. These findings require urgent clinical evaluation and treatment of the infection source, with intravenous antibiotics and hospitalization when clinically indicated. Laboratory evaluation includes a complete blood count (CBC), measurement of C-reactive protein (CRP) levels, and bacterial culture.[5,6]

The various components of the CBC may serve as sensitive indicators of a patient's physiological and pathological status. The white blood cell (WBC) count helps assess infectious and non-infectious diseases.[7] White blood cells contribute to immune defense by producing, transporting and distributing antibodies. White blood cell counts may increase in response to acute infection, trauma or inflammation. In some conditions, such as sepsis, the increase is so pronounced that it resembles that observed in leukemia.[8] C-reactive protein is involved in the innate immune system response. It is synthesized primarily in the liver and increases following the release of interleukin-1 by macrophages in areas of damaged tissue. C-reactive protein levels increase in response to systemic inflammation, infection, vascular inflammation, or autoimmune diseases. Increased CRP levels activate neutrophils, eliminate antigens and activate the complement system.[9] In healthy individuals, serum CRP concentrations vary from 0 mg/L to 3 mg/L, depending on the inflammatory processes occurring in the body. During an acute inflammatory response, serum CRP levels begin to rise within a few hours. The association between CRP concentrations and the severity and duration of the infection makes CRP a highly sensitive marker of inflammation. Because leukocyte lifespans are 5–6 days, CRP levels more accurately reflect the progression of infection, whereas WBC counts provide less reliable information about the timing of the onset of infection.[4,10,11]

Length of hospital stay (LOHS) is an important healthcare outcome. Prolonged LOHS is associated with an increased risk of complications, including surgical-site and other hospital-acquired infections.[12] In children, prolonged hospitalization may also impose a greater financial burden on families and the healthcare system, as well as cause emotional stress for children and their parents.[13] Therefore, analyzing factors associated with LOHS is critical to reducing the burden on children, families and healthcare services.

There is no consensus regarding the factors that may predict LOHS among children hospitalized for odontogenic abscesses. We retrospectively examined the factors associated with LOHS among children and adolescents hospitalized for surgical treatment of odontogenic abscesses. Specifically, we hypothesized that serum CRP levels and CBC parameters measured at hospital admission would correlate with disease severity and could predict LOHS.

Material and methods

Study design and setting

This retrospective cohort study was conducted in the Scheneider Children's Medical Center of Israel affiliated with Rabin Medical Center, Petah Tikva, Israel. The study was approved by the Helsinki Committee at Rabin Medical Center (approval No. RMC-0601-21). The requirement for informed consent was waived due to the study's retrospective design. The study was reported in accordance with the Strengthening the Reporting of Observational Studies in Epidemiology (STROBE) statement, using the checklist for cohort studies.

Participants

The electronic medical records of consecutive patients aged 1–17 years who presented to the pediatric emergency department of Scheneider Children's Medical Center of Israel with a dentoalveolar or odontogenic abscess and were hospitalized in the department of oral and maxillofacial surgery between 2018 and 2022 were reviewed.

Children were hospitalized if at least one of the following criteria was met: airway compromise; uncontrolled pain; eating difficulty; significant facial swelling; increase in facial swelling for more than 4 days despite appropriate oral antibiotic treatment; poor adherence to oral antibiotic treatment; or facial swelling accompanied by persistent fever of dental origin for more than 48 h.

The assessment of risk factors related to a child's physical status is essential before surgical intervention. The American Society of Anesthesiologists (ASA) Physical Status (ASA-PS) Classification System is a widely accepted tool for preoperative assessment.[14] Accordingly, ASA-PS class I or II was an additional inclusion criterion. Patients were excluded if they had an ASA-PS classification higher than II, diabetes, an autoimmune disease, or immunosuppression, if they had received immunosuppressive therapy, or if their medical records were incomplete.

Data collection

The primary outcome was LOHS. Data extracted from the electronic medical records included age, sex, year of hospitalization, diagnosis, teeth involved, body temperature at admission, treatment administered, serum CRP levels, and CBC parameters measured at admission as variables potentially associated with LOHS.

Statistical analysis

The statistical analysis was performed using the IBM SPSS Statistics for Windows software, v. 29.0 (IBM Corp., Armonk, USA), and R, v. 4.4.0 (The R Foundation for Statistical Computing, Vienna, Austria).

The median LOHS was 3 days. Accordingly, patients were divided into 2 groups: a short LOHS group (≤3 days); and a long LOHS group (>3 days). Student's *t*-test was used to compare the means of continuous variables between the short and long LOHS groups. An F test was conducted to assess differences in group variances, and Welch's *t*-test was applied when the variances differed significantly. The χ^2 test of independence was implemented to assess correlations between categorical variables and LOHS group. Fisher's exact test was used when expected cell counts were <5.

The binomial test was conducted to compare the proportions of infections involving upper molars vs. lower molars, those attributable to caries vs. other odontogenic causes, those involving primary vs. permanent teeth, upper teeth vs. lower teeth, those treated with both extraction and drainage vs. either procedure alone, and those treated with amoxicillin–clavulanate vs. other antibiotics. Odds ratios (*OR*s) and 95% confidence intervals (95% *CI*s) were calculated.

The logistic regression analysis was performed using variables that were statistically significant or approached statistical significance in the univariate analyses to identify factors associated with longer LOHS. *P*-values were adjusted for multiple comparisons using the Benjamini–Hochberg procedure.

Results

Of the 175 consecutive patient medical records reviewed, 127 patients (55.9% male) met the eligibility criteria and were included in the analysis. The distribution of patients by admission year was as follows: 2018 – 27 (21.3%); 2019 – 33 (26.0%); 2020 – 31 (24.4%); 2021 – 31 (24.4%); 2022 – 5 (3.9%). Excluding 2022, for which only 5 patients were included (data collection was only conducted until the end of 2022), a mean of 30.25 individuals were hospitalized annually between 2018 and 2021 (range: 27–33), demonstrating steady annual enrollment with little variation. Consequently, the data from these 4 years was grouped for further analysis.

The patients' median age was 7 years (range: 1–17 years), and the mean age was 7 ±3.2 years (Fig. 1). Table 1 summarizes the demographic and clinical characteristics of the study population. The median body temperature at admission was 37.2°C (range: 35.9–39.5°C), and the mean temperature was 37.4 ±0.8°C. The most common odontogenic cause of abscess formation was primary caries (72%; $p < 0.001$ compared with other causes) (Fig. 2). Most abscesses (77.2%) involved primary teeth, and more than half involved mandibular teeth (55.1%), with lower primary molars accounting for 52.8% of cases. The majority of patients (68.5%) underwent both extraction and drainage. The most common antibiotic administered was penicillin (90.6%). The median LOHS was 3 days

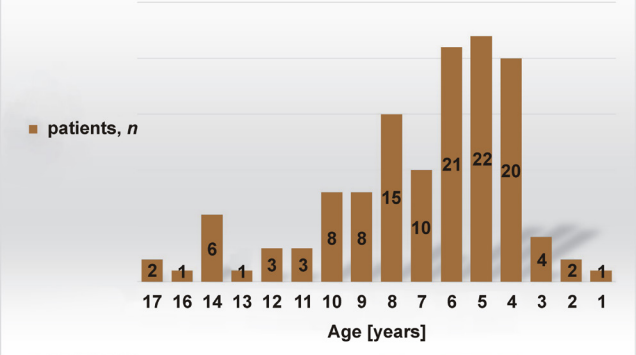

Fig. 1. Age distribution of the study population

Table 1. Baseline demographic and clinical characteristics of the study population

Variable		Total (*N* = 127)
Age [years]	*Me* (*IQR*)	6 (1–17)
	M ±*SD*	7 ±3.2
Sex, *n* (%)	male	71 (55.9)
	female	56 (44.1)
Dentition, *n* (%)	primary	98 (77.2)
	permanent	28 (22.0)
	unknown	1 (0.8)
Site, *n* (%)	mandible	70 (55.1)
	maxilla	56 (44.1)
	unknown	1 (0.8)
Teeth involved, *n* (%)	mandibular primary molars	67 (52.8)
	maxillary primary molars	40 (31.5)
	unknown	20 (15.7)
Body temperature at admission [°C]	*Me* (*IQR*)	37.2 (35.9–39.5)
	M ±*SD*	37.4 ±0.8
LOHS [days] *Me* (*IQR*)		3 (2–8)
Long LOHS during 2018–2019 [%]		71.0
Long LOHS during 2020–2021 [%]		31.7
LOHS during 2018–2019 [days] *M* ±*SD*		4.1 ±1.3
LOHS during 2020–2021 [days] *M* ±*SD*		3.3 ±1.1
Treatment modalities, *n* (%)	extraction	6 (4.7)
	extraction and drainage	87 (68.5)
	drainage	34 (26.8)
Antibiotics administered, *n* (%)	amoxicillin–clavulanate	115 (90.6)
	clindamycin	8 (6.3)
	amoxicillin–clavulanate and clindamycin	1 (0.8)
	other	2 (1.6)

Me – median; *M* – mean; *SD* – standard deviation; *IQR* – interquartile range; LOHS – length of hospital stay.

(range: 2–8 days). Infections involving primary teeth were significantly more frequent than those involving permanent teeth (77.2% vs. 22.1%, respectively; $p < 0.001$). Similarly, infections involving mandibular teeth were more prevalent than those involving maxillary teeth (55.1% vs. 44.1%, respectively; $p = 0.025$), and mandibular molar involvement was more frequent than maxillary molar involvement (52.8% vs. 31.5%, respectively; $p = 0.004$). Combined extraction and drainage were performed significantly more often than either procedure alone (68.5%; $p < 0.001$).

The univariate analysis showed that patients hospitalized during 2020–2021 had a significantly shorter LOHS than those hospitalized during 2018–2019 (*OR* = 0.190, 95% *CI*: 0.088, 0.410; $p < 0.001$). Female patients demonstrated a trend for a longer LOHS than male patients, although the association was not statistically significant (*OR* = 1.822, 95% *CI*: 0.897, 3.701; $p = 0.096$). Infections originating from mandibular molars showed a trend for a longer LOHS than those originating from maxillary molars (*OR* = 2.436, 95% *CI*: 0.941, 6.306; $p = 0.063$).

Longer LOHS was associated with higher mean body temperature at admission (37.58 ±0.83°C vs. 37.19 ±0.67°C; $p = 0.005$), higher mean WBC counts (14.32 ±4.76 vs. 11.72 ±3.36 × 10^3 cells/μL; $p = 0.001$), higher mean neutrophil counts (10.37 ±4.51 vs. 7.71 ±2.94 × 10^3 cells/μL; $p = 0.0001$) and lower mean eosinophil counts (0.20 ±0.20 vs. 0.27 ±0.23 × 10^3 cells/μL; $p = 0.049$) compared with the short LOHS group. Additionally, patients in the long LOHS group tended to be older (7.58 ±3.33 years vs. 6.48 ±3.00 years; $p = 0.052$) and had higher mean monocyte counts (0.76 ±0.29 vs. 0.67 ±0.26 × 10^3 cells/μL; $p = 0.066$). No statistically significant associations were observed between LOHS and the type of antibiotics administered, reason for hospitalization, teeth involved, type of treatment, CRP levels, red blood cell counts, hemoglobin levels, hematocrit, mean corpuscular volume, mean corpuscular hemoglobin concentration, platelet counts, or lymphocyte, basophil or leukocyte counts. Additionally, elevated CRP levels were not significantly associated with the dentition type (primary or permanent) affected by the abscess.

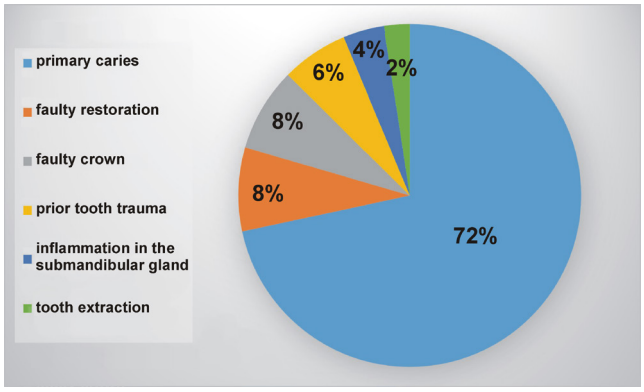

Fig. 2. Odontogenic causes of abscess formation in the study population

The logistic regression model was statistically significant ($\chi^2(9) = 45.577$; $p < 0.001$). The model explained 44.9% (Nagelkerke R^2) of the variance in LOHS. The odds of a longer LOHS increased significantly with age, body temperature at admission, WBC count at admission, and differed according to the period of admission. Specifically, the probability of a longer LOHS increased by a factor of 1.215 (95% *CI*: 1.035, 1.426; $p = 0.039$) for each additional year of age, by a factor of 2.339 (95% *CI*: 1.204, 4.545; $p = 0.036$) for each 1°C increase in body temperature, and by a factor of 1.580 (95% *CI*: 1.137, 2.197; $p = 0.029$) for each increase of 1×10^3 cells/μL in WBC count. Patients admitted during 2020–2021 had significantly lower odds of a longer LOHS than those admitted during 2018–2019 (*OR* = 0.094, 95% *CI*: 0.032, 0.278; $p < 0.001$). Sex, CRP levels, and neutrophil, monocyte and eosinophil counts were not significant predictors of longer LOHS in this patient population.

Discussion

The present study assessed parameters associated with LOHS among children and adolescents aged 1–17 years who were hospitalized for odontogenic abscesses between 2018 and 2022.

A slight male predominance was observed in the present cohort, consistent with previous studies on surgical treatment of odontogenic abscesses.[4,15–17] In contrast to other studies, which reported longer hospitalization among patients with acute odontogenic abscesses and elevated CRP levels,[4,18] we found that CRP levels at admission were not significant predictors of LOHS. Previous studies have also identified CRP as a marker of infection severity.[18,19] In our cohort, higher WBC counts, older age and elevated body temperature at admission were significantly associated with longer LOHS. The correlation between older age and longer LOHS is consistent with previous reports.[16] Other studies have also noted a positive association between WBC counts and LOHS in patients with odontogenic abscesses.[16–18] Higher WBC counts have been linked to an increased risk for re-operation.[20]

In the present cohort, the cause of abscess formation, sex, teeth involved, type of treatment, and type of antibiotics administered were not significantly associated with LOHS. Mandibular involvement was more likely to cause a severe infection than maxillary involvement, presumably due to anatomical differences, the greater vascularity of the maxilla, and higher bone density in the mandible.[4,21,22] However, mandibular infections tend to occur in older patients, whereas maxillary infections are more common in younger patients.[16,17]

Our model also showed that patients admitted to the hospital during 2020–2021 had significantly lower odds of a longer LOHS than those admitted during 2018–2019. This difference may be explained by the coronavirus disease 2019 (COVID-19) pandemic. As in other countries, guidance issued by the Israeli Ministry of Health during the first COVID-19 lockdown instructed citizens to remain at home, seek medical advice over telephone whenever feasible, and refrain from visiting hospitals and dental clinics unless urgent care was required. These guidelines aimed to reduce the severe acute respiratory syndrome coronavirus 2 (SARS-CoV-2) transmission while preserving hospital emergency capacity for patients with COVID-19. This might be the reason for the decline in LOHS during 2020–2021 compared to 2018–2019 in pediatric patients with odontogenic infections. Furthermore, concerns about SARS-CoV-2 exposure may have discouraged patients from seeking hospital-based care. Previous studies have similarly reported that despite the implementation of safety measures, patients experienced anxiety about attending dental appointments during the COVID-19 pandemic.[23–26] Instead, they may have sought treatment from community-based pediatric dentists. This substantial decline implies that a considerable portion of the cases that were routinely referred to the hospital in the pre-pandemic period might have been effectively managed by community-based pediatric dentists.

The median LOHS reported in studies involving adults is 6 days,[27] compared with 3 days in the present pediatric cohort, although considerable variation has been reported in the literature.[28] Several risk factors for prolonged hospitalization have been identified in adults.[27] Coexisting systemic conditions have been strongly associated with the severity of odontogenic infections and LOHS.[29] Among numerous comorbidities, diabetes stands out as a factor correlated with prolonged LOHS.[30] Advanced age is also associated with more severe odontogenic infections and longer LOHS.[31] Mandibular involvement is linked to longer LOHS due to poor vascularity.[21] Reports correlate increased LOHS with penicillin allergy.[32] The spread of infection through interconnected fascial spaces in the head and neck region may also increase LOHS.[33] Furthermore, a longer interval between initial incision and drainage and definitive removal of the infection source has been associated with the prolonged hospitalization.[27] When comparing the outcomes of odontogenic infections with those of post-traumatic enophthalmos, the morbidity was lower in the adult group.[23] Because the clinical presentation of orbital floor fractures differs between children and adults, the diagnosis and treatment of orbital fractures in children may be more challenging. For example, bone graft reconstruction has been reported to yield better outcomes in adults.[23]

The majority of studies evaluating the factors that affect LOHS in patients hospitalized for odontogenic abscesses have included both adults and children. In contrast, the present study evaluated only children and adolescents, with a median age of 7 years. Because the pediatric population differs from the adult population, this study may help identify factors specifically correlated with LOHS in children and adolescents.

Dental infections requiring hospitalization are associated with substantial morbidity and, occasionally, mortality. They may also impose a considerable financial burden on patients, their families and healthcare systems. Our study provides insights into the characteristics of hospitalized individuals with odontogenic abscesses and analyses patient demographics, clinical characteristics, diagnostic approaches, management strategies, and clinical outcomes.

Severe pain and acute facial swelling are common clinical manifestations of odontogenic infections that may prompt patients to seek emergency care. The median LOHS was 3 days for the short LOHS group. The reported absence of mortality and low frequency of complications suggest favorable clinical outcomes. Nevertheless, the social and financial impact of odontogenic infections remains a significant concern. Consequently, an important clinical question arises: Were all these hospital admissions necessary? A short hospital stay may indicate a rapid clinical resolution, even when surgical intervention is required. Identifying the characteristics of patients with a shorter LOHS may help clinicians determine which children could potentially be managed safely in outpatient settings. In selected cases, community-based treatment provided by a pediatric dentist my be sufficient and could reduce the burden on hospital services, as seen during the COVID-19 pandemic.

Limitations

The limitations of this study primarily arise from its retrospective design, which restricted the available variables and introduced potential sources of bias. The data was obtained from medical records based on existing clinical documentation. Retrospective studies are an important tool for studying diseases. However, they have several limitations owing to their design. Because they rely on medical records that were not originally collected for research purposes, some potentially relevant information may be missing. Differences in treatment approaches between patients and variations in clinical decision-making among healthcare professionals may also have introduced bias. Moreover, the study was conducted at a single medical center and included a relatively small sample, which may limit the generalizability of the findings and lead to bias. Single-arm trials lack randomization and blinding, which limits their capacity to establish treatment effects compared with randomized controlled trials.[34] This study included only children referred to a single medical center, and healthcare-seeking behavior during the COVID-19 pandemic may have influenced patient selection. Consequently, some children may have received treatment from community-based pediatric dentists without being referred to the medical center. Future studies using standardized data collection protocols may improve accuracy of the available information.

Conclusions

Age, body temperature at admission and WBC count at admission were independently associated with longer LOHS among children and adolescents hospitalized for odontogenic abscesses. Future studies should further characterize children with shorter hospital stays and determine whether these characteristics could help identify patients who may be safely treated without hospitalization. Clinicians should follow evidence-based protocols and established clinical criteria when defining the treatment plan. Avoiding unnecessary hospitalization may reduce its short- and long-term consequences. These include not only the physical suffering and distress that exert stress on the body but also factors that negatively affect the patient's psychological state. The practical implication of the present findings is the potential role of community-based dental care in reducing hospital admissions.[35,36]

Ethics approval and consent to participate

The study was approved by the Helsinki Committee at Rabin Medical Center, Petah Tikva, Israel (approval No. RMC-0601-21).

Data availability

The datasets generated and/or analyzed during the current study are available from the corresponding author on reasonable request.

Consent for publication

Not applicable.

Use of AI and AI-assisted technologies

Not applicable.

ORCID iDs

Liat Chaushu https://orcid.org/0000-0002-5755-7526
Shiri Lapides https://orcid.org/0009-0008-7175-9512
Gal Avishai https://orcid.org/0000-0001-5111-8496
Aya Vituri https://orcid.org/0000-0002-6281-6350
Sigalit Blumer https://orcid.org/0000-0002-4114-2852

References

1. Shweta, Prakash SK. Dental abscess: A microbiological review. *Dent Res J (Isfahan)*. 2013;10(5):585–591. PMID:24348613.
2. Nair PNR. Pathogenesis of apical periodontitis and the causes of endodontic failures. *Crit Rev Oral Biol Med*. 2004;15(6):348–381. doi:10.1177/154411130401500604
3. Shu M, Wong L, Miller JH, Sissons CH. Development of multi-species consortia biofilms of oral bacteria as an enamel and root caries model system. *Arch Oral Biol*. 2000;45(1):27–40. doi:10.1016/s0003-9969(99)00111-9
4. Heim N, Wiedemeyer V, Reich RH, Martini M. The role of C-reactive protein and white blood cell count in the prediction of length of stay in hospital and severity of odontogenic abscess. *J Craniomaxillofac Surg*. 2018;46(12):2220–2226. doi:10.1016/j.jcms.2018.10.013

5. Robertson DP, Keys W, Rautemaa-Richardson R, Burns R, Smith AJ. Management of severe acute dental infections. *BMJ*. 2015;350:h1300. doi:10.1136/bmj.h1300
6. American Academy of Pediatric Dentistry. Use of antibiotic therapy for pediatric dental patients. In: *The Reference Manual of Pediatric Dentistry*. Chicago, IL: American Academy of Pediatric Dentistry; 2023.
7. Travis RT, Steinle CJ. The effects of odontogenic infection on the complete blood count in children and adolescents. *Pediatr Dent*. 1984;6(4):214–219. PMID:6596568.
8. Aminzadeh Z, Parsa E. Relationship between age and peripheral white blood cell count in patients with sepsis. *Int J Prev Med*. 2011;2(4):238–242. PMID:22174963.
9. Sproston NR, Ashworth JJ. Role of C-reactive protein at sites of inflammation and infection. *Front Immunol*. 2018;9:754. doi:10.3389/fimmu.2018.00754
10. Bilavsky E, Yarden-Bilavsky H, Ashkenazi S, Amir J. C-reactive protein as a marker of serious bacterial infections in hospitalized febrile infants. *Acta Paediatr*. 2009;98(11):1776–1180. doi:10.1111/j.1651-2227.2009.01469.x
11. Isaacman DJ, Burke BL. Utility of the serum C-reactive protein for detection of occult bacterial infection in children. *Arch Pediatr Adolesc Med*. 2002;156(9):905–909. doi:10.1001/archpedi.156.9.905
12. Whitehouse JD, Friedman ND, Kirkland KB, Richardson WJ, Sexton DJ. The impact of surgical-site infections following orthopedic surgery at a community hospital and a university hospital: Adverse quality of life, excess length of stay, and extra cost. *Infect Control Hosp Epidemiol*. 2002:23(4):183–189. doi:10.1086/502033
13. Lesha E, Roach JT, Miller LE, et al. Length of stay following elective craniotomy for tumor resection in children and young adults: A retrospective case series. *J Neurooncol*. 2025;171(3):651–658. doi:10.1007/s11060-024-04887-w
14. Diller TA. Overview of preoperative risk analysis: American Society of Anesthesiology physical status classification and the surgical risk calculator. *AANA J*. 2022;90(6):469–475. PMID:36413193.
15. Zirk M, Buller J, Goeddertz P, et al. Empiric systemic antibiotics for hospitalized patients with severe odontogenic infections. *J Craniomaxillofac Surg*. 2016;44(8):1081–1088. doi:10.1016/j.jcms.2016.05.019
16. Joachim MV, Abdo M, Alkeesh K, Oettinger-Barak O, Abozaid S, El-Naaj IA. Factors associated with prolonged hospitalizations from odontogenic infections in children. *J Clin Pediatr Dent*. 2022;46(6):40–44. doi:10.22514/jocpd.2022.024
17. Kara A, Ozsurekci Y, Tekcicek M, et al. Length of hospital stay and management of facial cellulitis of odontogenic origin in children. *Pediatr Dent*. 2014;36(1):18e–22e. PMID:24717702.
18. Sharma A, Giraddi G, Krishnan G, Shahi AK. Efficacy of serum prealbumin and CRP levels as monitoring tools for patients with fascial space infections of odontogenic origin: A clinicobiochemical study. *J Maxillofac Oral Surg*. 2014;13(1):1–9. doi:10.1007/s12663-012-0376-4
19. Ylijoki S, Suuronen R, Jousimies-Somer H, Meurman JH, Lindqvist C. Differences between patients with or without the need for intensive care due to severe odontogenic infections. *J Oral Maxillofac Surg*. 2001;59(8):867–872. doi:10.1053/joms.2001.25017
20. Aditya NK, Lakshmi S, Bharani S. Prognostic determinants in severe odontogenic space infections: A single-center retrospective analysis. *Minerva Dent Oral Sci*. 2023;72(1):1–7. doi:10.23736/s2724-6329.22.04556-9
21. Pourdanesh F, Dehghani N, Azarsina M, Malekhosein Z. Pattern of odontogenic infections at a tertiary hospital in Tehran, Iran: A 10-year retrospective study of 310 patients. *J Dent (Tehran)*. 2013;10(4):319–328. PMID:24396351.
22. Hwang T, Antoun JS, Lee KH. Features of odontogenic infections in hospitalised and non-hospitalised settings. *Emerg Med J*. 2011;28(9):766–769. doi:10.1136/emj.2010.095562
23. Koryczan P, Zapała J, Gontarz M, Wyszyńska-Pawelec G. Comparison of the results of the treatment of enophthalmos in orbital blowout fracture in children/adolescents and adults. *Dent Med Probl*. 2021;58(2):179–186. doi:10.17219/dmp/130815
24. Łazarz-Półkoszek MJ, Orczykowska M, Gala A, Pihut M. Impact of the COVID-19 pandemic on patients' anxiety levels related to dental appointments in Poland. *Dent Med Probl*. 2023;60(3):367–373. doi:10.17219/dmp/163476
25. Paradowska-Stolarz AM. Oral manifestations of COVID-19: Brief review. *Dent Med Probl*. 2021;58(1):123–126. doi:10.17219/dmp/131989
26. Słotwińska-Pawlaczyk A, Orzechowska-Wylęgała B, Latusek K, Roszkowska AM. Analysis of clinical symptoms and biochemical parameters in odontogenic cellulitis of the head and neck region in children. *Children (Basel)*. 2023;10(1):172. doi:10.3390/children10010172
27. Tavakoli M, Bagheri A, Faraz M, Salehirad S, Roghaee S. Orbital cellulitis as a complication of mandibular odontogenic infection. *Ophthalmic Plast Reconstr Surg*. 2013;29(1):e5–e7. doi:10.1097/IOP.0b013e318254132a
28. Heim N, Berger M, Wiedemeyer V, Reich R, Martini M. A mathematical approach improves the predictability of length of hospitalization due to acute odontogenic infection: A retrospective investigation of 303 patients. *J Craniomaxillofac Surg*. 2019;47(2):334–340. doi:10.1016/j.jcms.2018.12.002
29. Boffano P, Roccia F, Pittoni D, Di Dio D, Forni P, Gallesio C. Management of 112 hospitalized patients with spreading odontogenic infections: Correlation with DMFT and oral health impact profile 14 indexes. *Oral Surg Oral Med Oral Pathol Oral Radiol*. 2012;113(2):207–213. doi:10.1016/j.tripleo.2011.02.006
30. Flynn TR, Shanti RM, Hayes C. Severe odontogenic infections, part 2: Prospective outcomes study. *J Oral Maxillofac Surg*. 2006;64(7):1104–1113. doi:10.1016/j.joms.2006.03.031
31. Rao DD, Desai A, Kulkarni RD, Gopalkrishnan K, Rao CB. Comparison of maxillofacial space infection in diabetic and nondiabetic patients. *Oral Surg Oral Med Oral Pathol Oral Radiol Endod*. 2010;110(4):e7–e12. doi:10.1016/j.tripleo.2010.04.016
32. Wang LF, Kuo WR, Tsai SM, Huang KJ. Characterizations of life-threatening deep cervical space infections: A review of one hundred ninety-six cases. *Am J Otolaryngol*. 2003;24(2):111–117. doi:10.1053/ajot.2003.31
33. Macy E, Contreras R. Health care use and serious infection prevalence associated with penicillin "allergy" in hospitalized patients: A cohort study. *J Allergy Clin Immunol*. 2014;133(3):790–796. doi:10.1016/j.jaci.2013.09.021
34. Rogers JG, Adams GG, Wright FAC, Roberts-Thomson K, Morgan MV. Reducing potentially preventable dental hospitalizations of young children: A community-level analysis. *JDR Clin Trans Res*. 2018;3(3):272–278. doi:10.1177/2380084418764312
35. Rattray JE, Johnston M, Wildsmith JAW. Predictors of emotional outcomes of intensive care. *Anaesthesia*. 2005;60(11):1085–1092. doi:10.1111/j.1365-2044.2005.04336.x
36. Koncak G, Tolunay O, Unal A, Celiloglu C, Celik U. Short-term side effects of pulse steroid treatment in children. *J Coll Physicians Surg Pak*. 2022;32(2):262–264. doi:10.29271/jcpsp.2022.02.262

Original paper

Interactions between sleep parameters and heart rate variability in temporomandibular disorders

Helena Martynowicz[1,A,C–F], Małgorzata Trocha[1,A,C–F], Karol Marschollek[2,C–F], Piotr Macek[3,B,D–F], Wiktor Trzepietowski[1,B,D–F], Jakub Przegrałek[4,B,D–F], Katarzyna Madziarska[1,C,E,F], Mieszko Więckiewicz[4,A,D–F]

[1] Clinical Department of Diabetology, Hypertension and Internal Diseases, Faculty of Medicine, Wroclaw Medical University, Poland
[2] Department of Neurology, Faculty of Medicine, Wroclaw Medical University, Poland
[3] Department of Environmental Health, Occupational Medicine and Epidemiology, Faculty of Health Sciences, Wroclaw Medical University, Poland
[4] Department of Experimental Dentistry, Faculty of Dentistry, Wroclaw Medical University, Poland

A – research concept and design; B – collection and/or assembly of data; C – data analysis and interpretation;
D – writing the article; E – critical revision of the article; F – final approval of the article

Dental and Medical Problems, ISSN 1644-387X (print), ISSN 2300-9020 (online) *Dent Med Probl*. 2026;63(5):1267–1275

Address for correspondence
Karol Marschollek
E-mail: karol.marschollek@gmail.com

Funding sources
None declared

Conflict of interest
None declared

Acknowledgements
None declared

Received on October 21, 2025
Reviewed on December 15, 2025
Accepted on January 18, 2026

Published online on October 28, 2026

Abstract

Background. Temporomandibular disorders (TMD) cause pain and dysfunction in the temporomandibular joints (TMJs) and masticatory muscles and significantly impact quality of life. Temporomandibular disorder-related pain is associated with sleep disorders and affects heart rate (HR) parameters; however, data from polysomnographic studies remains inconclusive.

Objectives. The aim of the study was to evaluate the impact of TMD on sleep parameters recorded using video-polysomnography (vPSG) and heart rate variability (HRV) monitored with the use of a 24-hour electrocardiogram (ECG).

Material and methods. A cross-sectional study included 93 patients with TMD diagnosed according to the Diagnostic Criteria for Temporomandibular Disorders (DC/TMD). Video-polysomnography and 24-hour ECG monitoring were conducted. Pain was assessed using the numeric rating scale (NRS) (0–10) and categorized as mild (≤5) or severe (>5).

Results. The study included 93 patients with TMD, divided into groups of low pain intensity ($n = 66$) and high pain intensity ($n = 27$). The group with high pain intensity demonstrated lower sleep efficiency (87.7% vs. 90.8%, $p = 0.022$) and lower oxygen saturation (94.7% vs. 95.2%, $p = 0.036$). Heart rate variability parameters were similar in both groups. Women reported a higher total pain score (20 vs. 10, $p = 0.007$) and had a higher percentage of normal-to-normal (NN) intervals differing by more than 50 ms (pNN50) (24 h: 22.5% vs. 14.2%, $p = 0.013$; daytime: 18.0% vs. 9.8%, $p = 0.002$), higher daytime root mean square of successive differences (RMSSD) (41.7 vs. 34.8, $p = 0.026$), and a higher nighttime HR (63.8 vs. 60.5, $p = 0.047$). Additionally, women demonstrated lower values for very low frequency (VLF) power (1,402.4 vs. 2,214.5, $p = 0.010$), low frequency (LF) power (1,415.5 vs. 2,494.5, $p = 0.028$), and the low frequency/high frequency (LF/HF) ratio (1.3 vs. 2.5, $p < 0.001$).

Conclusions. High TMD-related pain intensity is associated with reduced sleep efficiency and lower mean oxygen saturation during sleep. Women experience higher pain intensity but lower sympathetic activation than men.

Keywords: sleep, heart rate variability, temporomandibular disorders

Cite as
Martynowicz H, Trocha M, Marschollek K, et al. Interactions between sleep parameters and heart rate variability in temporomandibular disorders. *Dent Med Probl.* 2026;63(5):1267–1275. doi:10.17219/dmp/217119

DOI
10.17219/dmp/217119

Copyright
Copyright by Author(s)
This is an article distributed under the terms of the Creative Commons Attribution 3.0 Unported (CC BY 3.0) (https://creativecommons.org/licenses/by/3.0/)

Highlights

- Temporomandibular disorders comprise a broad range of painful conditions and dysfunctions affecting the masticatory muscles and temporomandibular joints.
- Severe pain associated with temporomandibular disorders is linked to reduced sleep efficiency and lower oxygen saturation but does not significantly affect heart rate variability.
- Women experience higher pain intensity but lower sympathetic activation than men.

Introduction

Temporomandibular disorders (TMD) encompass a broad category of painful conditions and dysfunctions that affect the masticatory muscles and temporomandibular joints (TMJs). Temporomandibular disorders represent the second most common pain-related condition in the orofacial region, with a complex etiology. Contributing factors include biomechanical, neuromuscular, biological, and biopsychosocial elements. According to the Diagnostic Criteria for Temporomandibular Disorders (DC/TMD), it is estimated that TMD affect approx. 34% of the global population,[1] although rates depend strongly on case definitions and population characteristics. The DC/TMD assessment is divided into Axis I (physical) and Axis II (psychosocial). Temporomandibular disorders commonly present as pain-related disorders (muscle or joint pain, headaches) or TMJ-related conditions (disc displacements, degenerative changes).[2] Key mechanisms sustaining pain involve sensitization of supraspinal neurons and second-order neurons in the dorsal horn of the spinal cord or the trigeminal nucleus, as well as an impaired balance of analgesic mechanisms.[3]

Numerous studies indicate a relationship between TMD and obstructive sleep apnea (OSA).[4] However, even in TMD patients without OSA, fragmented, non-restorative sleep and frequent nocturnal awakenings are observed. Conversely, chronic sleep disturbances exacerbate pain symptoms, partly by increasing the sympathetic nervous system (SNS) activity and activating inflammatory processes.[5,6] A statistically significant correlation has been found between TMD-related pain and poorer subjective sleep quality, as measured by the Pittsburgh sleep quality index (PSQI).[7,8] Furthermore, TMD-associated headache, along with factors such as older age, female sex and excessive daytime sleepiness, is a predictor of worsening sleep quality.[9] Findings from polysomnographic studies vary and often show small differences that correlate more strongly with mood than with pain intensity.[10]

Heart rate variability (HRV) is an indicator of fluctuations in the time intervals between consecutive heartbeats, primarily resulting from the dynamic regulation of the sinoatrial node by the autonomic nervous system (ANS).[11] High HRV reflects effective autonomic regulation and good adaptive capacity of the body. A relationship between HRV, cognitive performance and the functioning of the prefrontal cortex, which is relevant to both physical and mental health, has been demonstrated.[12] For HRV analysis, time-domain, frequency-domain and geometric parameters are utilized. Certain parameters are considered markers of the activity of different components of the ANS. Some studies have suggested the association between specific frequency bands and the ANS activity, linking low-frequency (LF) bands to the SNS activity and high-frequency (HF) bands and the root mean square of successive differences (RMSSD) to the parasympathetic nervous system (PNS) activity. The LF/HF ratio has been treated as an indicator of balance between these systems.[13] However, the recent data has shown that these parameters are not direct or quantitative measures of sympathovagal balance, as they can be influenced by other factors.[14] Higher LF power and a higher LF/HF ratio have been shown to correlate with an increased risk of cardiovasular disease.[15] Lower HRV, a higher heart rate (HR) and impaired baroreceptor sensitivity are associated with the presence of painful forms of TMD[16] and may indicate sympathetic dominance and impaired parasympathetic regulation.[17,18]

Given the high prevalence of TMD and its association with subjectively perceived poorer sleep quality, it seems justified to investigate the impact of these conditions on sleep quality and HRV parameters using objective recording methods. Therefore, our study aimed to analyze sleep architecture and quality, as well as HRV, in patients with TMD using 24-hour electrocardiographic (ECG) monitoring with the assessment of HRV and video-polysomnography (vPSG).

Material and methods

Study design

This single-center, cross-sectional observational study was conducted at the Department of Experimental Dentistry, Wroclaw Medical University, Poland. The assessment of the TMJs and masticatory muscles was performed in accordance with the Axis I of the DC/TMD.[2] Individuals presenting to the Outpatient Clinic for Temporomandibular Disorders with complaints of masticatory muscle pain and/or dysfunction, TMJ pain and/or dysfunction, or TMD-related headache between 2017 and 2024 were included in the study. Patients were recruited consecutively throughout the study period, and all individuals meeting the eligibility criteria were invited to participate. The examination was conducted by a dentist with

at least 5 years of experience in diagnosing and treating TMD. Patients with a confirmed TMD diagnosis were referred to the Sleep Laboratory of the Clinical Department of Diabetology, Hypertension and Internal Diseases (Wroclaw Medical University), where vPSG and 24-hour ECG monitoring with HRV assessment were performed. The study was conducted in accordance with the principles of the Declaration of Helsinki, and approval was obtained from the Ethics Committee of Wroclaw Medical University (approval No. KB-794/2019). All participants provided written informed consent to participate in the study. Information on clinical trial registration is available in the ClinicalTrials.gov database (identifier No. NCT04214561).

Inclusion and exclusion criteria

The study included 93 patients aged 18 years and older with a confirmed diagnosis of TMD in accordance with the DC/TMD. Exclusion criteria encompassed genetic disorders, inability to undergo polysomnography, neurological disorders or neuropathic pain (including primary headaches), coexisting respiratory failure or active inflammatory processes, active malignant neoplasms, severe psychiatric disorders, significant intellectual disability, pregnancy, the postpartum period, the use of or addiction to analgesics and/or medications affecting the nervous system, muscles or respiration, as well as lack of consent to participate in the study.

Assessment of masticatory muscle pain intensity

The intensity of pain in the temporomandibular region was assessed separately for the right and left temporalis muscles and the right and left masseter muscles. During palpation with a force of 1 kg for 2 s at 9 points on each muscle, participants rated their pain using the numeric rating scale (NRS), which ranged from 0 to 10, where 0 indicated no pain and 10 indicated unbearable pain or an equivalent description. Pain intensity was categorized into 2 groups: mild (NRS ≤ 5); and severe (NRS > 5).[19] The average NRS value for each muscle was calculated based on all examined points. The total pain score represented the sum of the mean pain ratings across 4 muscles.

Polysomnographic assessment

Video-polysomnography was conducted using the Nox A1 device (Nox Medical, Reykjavík, Iceland) from 10 pm to 6 am the following day. The examination included electroencephalography, ECG, electrooculography, and electromyography (EMG) of the submental muscles and bilateral masseter muscles, as well as recordings of thoracic and abdominal respiratory movements, assessment of position, and audio and video recordings. Oxygen saturation and pulse rate were measured using the NONIN WristOx$_2$ 3150 pulse oximeter (Nonin Medical, Inc., Plymouth, USA). All vPSG recordings were analyzed in 30-second epochs by a single qualified physician, blinded to pain group allocation, in accordance with the American Academy of Sleep Medicine (AASM) guidelines for the evaluation of sleep and associated events.[20]

24-hour ECG with HRV assessment

Each patient included in the study underwent 24-hour ECG monitoring using a Lifecard CF 12-channel recorder (serial No. LIFE-045348/2015), performed concurrently with vPSG at night and during daytime activities. Patients were instructed to refrain from intense physical activity, caffeine consumption for ≥8 h before bedtime, and alcohol for 24 h prior to monitoring. A standardized activity log was maintained; patients adhered to a structured activity schedule (daytime: 6 am–11 pm; nighttime: 11 pm–6 am). The analysis of HRV was conducted using the Sentinel and Pathfinder SL systems (v. 1.9.4.14474; Spacelabs Healthcare, Snoqualmie, USA). Prior to HRV analysis, ECG recordings were manually verified to remove artifacts and ectopic beats. Subsequently, time-domain, frequency-domain and geometric parameters were calculated. Frequency-domain analysis based on the fast Fourier transform (FFT) included the very low frequency (VLF) (0.003–0.04 Hz), LF (0.04–0.15 Hz), HF (0.15–0.4 Hz), and very high frequency (VHF) (0.4–0.5 Hz) bands, as well as the LF/HF ratio expressed in normalized units. Short-term HRV was assessed in two 20-minute segments (one during daytime and one during N3 sleep stage) to minimize the impact of respiratory events.

The 20-minute N3 segment was selected by the physician analyzing the polysomnograms. The inclusion criterion was stable, good-quality sleep. Exclusion criteria included the presence of arousals, awakenings, periodic limb movements, and sleep bruxism episodes. The physician had no access to the Holter ECG monitoring results.

Respiratory events were detected using a nasal pressure cannula. Apneic and hypopneic events were analyzed as follows: apneas were defined as a 90% reduction in airflow lasting ≥10 s; and hypopneas were identified as a ≥30% reduction in airflow lasting ≥10 s accompanied by a ≥3% decrease in blood oxygen saturation, as measured by pulse oximetry, or by an arousal. Saturation level (SpO_2%) and pulse rate were recorded using a pulse oximeter (Nonin Medical Inc.).

The artifact threshold was set according to the recommendation of the AASM and implemented in the Nox A1 device. Additionally, a physician certified in polysomnography by the Polish Sleep Research Society manually assessed the recordings for respiratory events and artifacts.

The analysis was performed by an experienced clinician in accordance with the guidelines of the European Society of Cardiology (ESC) and the Heart Rhythm Society (HRS) (formerly the North American Society of Pacing and Electrophysiology (NASPE)).[21]

Statistical analysis

Patients were divided into 2 groups based on TMD pain intensity: low TMD pain intensity (LOW) and high TMD pain intensity (HIGH), to investigate the relationship of TMD pain with HRV parameters and vPSG-derived sleep parameters. Additionally, differences in HRV and TMD pain parameters were analyzed according to sex, with separate subgroups for women and men. Analyses were performed using Statistica 13 (Dell Inc., Round Rock, USA). Categorical variables were presented as counts and percentages, and continuous variables as the mean (*M*) and standard deviation (*SD*) or the median (*Me*) and interquartile range (*IQR*). Normality and variance assumptions were evaluated before conducting between-group comparisons. Continuous variables were inspected visually using histograms and formally tested with the Shapiro–Wilk test. Homogeneity of variances was assessed using the Levene's test. The χ^2 test and Student's *t*-test were used for normally distributed data, and the Mann–Whitney *U* test was applied for non-normally distributed variables. A *p*-value <0.05 was considered statistically significant.

Results

Demographic data

The study population was divided into the LOW ($n = 66$) and HIGH ($n = 27$) groups. The mean age of the participants was 33.5 ±9.5 years in the LOW group and 36.4 ±9.0 years in the HIGH group ($p > 0.05$). Women accounted for 61.3% ($n = 57$) of the entire study population, with 57.6% ($n = 38$) in the LOW group and 70.4% ($n = 19$) in the HIGH group. The mean body mass index (BMI) was 24.0 ±3.7 kg/m^2 in the LOW group and 25.5 ±5.3 kg/m^2 in the HIGH group ($p > 0.05$).

Relationship between TMD pain intensity, HRV and vPSG

No statistically significant differences in HRV parameters were observed between the HIGH and LOW groups. Significantly lower sleep efficiency and lower mean oxygen saturation were observed in the HIGH group than in the LOW group (87.7% vs. 90.8%, $p = 0.022$; and 94.7% vs. 95.2%, $p = 0.036$, respectively) (Table 1).

Table 1. Video polysomnography (vPSG) sleep parameters and heart rate variability (HRV) parameters in patients with low and high temporomandibular disorder (TMD)-related pain intensity

Parameter		LOW ($n = 66$)	HIGH ($n = 27$)	*p*-value	*q*-value
vPSG parameters	TST [min]	445.9 (417.5–470.5)	442.8 (408.5–476.9)	0.588	0.93
	SE [%]	90.8 (86.0–93.4)	87.7 (82.5–90.2)	0.022*	0.92
	WASO [min]	22.9 (15.5–43.5)	37.5 (16.0–48.5)	0.220	0.92
	SL [min]	15.6 (8.0–24.7)	24.3 (9.5–35.3)	0.096	0.92
	N1 [% of TST]	3.0 (1.5–5.7)	3.5 (1.0–4.9)	0.773	0.93
	N2 [% of TST]	48.3 (41.9–52.3)	49.8 (44.5–55.7)	0.229	0.92
	N3 [% of TST]	24.8 (20.4–29.7)	21.3 (19.2–26.5)	0.133	0.92
	REM [% of TST]	23.5 (19.8–28.3)	24.0 (19.5–29.4)	0.803	0.93
	AHI [n/h]	2.5 (0.8–5.7)	2.0 (0.9–4.3)	0.477	0.93
	ODI [n/h]	2.8 (1.3–6.0)	2.4 (1.2–5.7)	0.816	0.93
	snoring [% of TST]	2.7 (0.1–16.1)	0.4 (0.1–9.9)	0.429	0.93
	apnea index [n/h]	0.3 (0.0–1.0)	0.6 (0.2–0.8)	0.299	0.93
	OA [n/h]	0.0 (0.0–0.4)	0.1 (0.0–0.5)	0.137	0.92
	MA [n/h]	0.0 (0.0–0.0)	0.0 (0.0–0.0)	0.673	0.93
	CA [n/h]	0.1 (0.0–0.4)	0.2 (0.0–0.5)	0.390	0.93
	HI [n/h]	1.9 (0.6–4.8)	1.2 (0.7–3.7)	0.330	0.93
	mean SpO_2 [%]	95.2 (94.4–95.8)	94.7 (93.5–95.3)	0.036*	0.92
	minimum SpO_2 [%]	91.0 (87.0–92.0)	89.0 (85.0–92.0)	0.143	0.92
	time with SpO_2 < 90% [% of TST]	0.0 (0.0–0.1)	0.0 (0.0–0.4)	0.143	0.92
	average desaturation drop [%]	3.2 (3.0–3.4)	3.2 (2.7–3.4)	0.619	0.93
	arousals [n/h]	3.5 (1.7–5.8)	2.8 (1.7–5.1)	0.571	0.93
	mean pulse rate [beats/min]	61.4 (56.9–66.9)	59.1 (54.1–66.5)	0.284	0.93
	maximum pulse rate [beats/min]	97.0 (92.0–103.0)	96.0 (88.0–103.0)	0.369	0.93
	minimum pulse rate [beats/min]	49.0 (46.0–54.0)	48.0 (43.0–56.0)	0.825	0.93

Parameter			LOW (n = 66)	HIGH (n = 27)	p-value	q-value
HRV parameters	T	SDNN [ms]	131.5 (116.6–150.2)	126.5 (107.2–171.6)	0.846	0.93
		RMSSD [ms]	43.7 (35.9–57.1)	36.1 (29.5–66.2)	0.454	0.93
		SDSD [ms]	30.4 (23.2–39.8)	25.4 (19.8–48.0)	0.571	0.93
		HRV index [ms]	38.0 (31.7–47.5)	36.6 (29.9–51.0)	0.651	0.93
		TINN [ms]	593.8 (476.6–734.4)	546.9 (460.9–804.7)	0.754	0.93
		pNN50 [%]	18.8 (10.1–29.5)	13.3 (7.1–33.1)	0.419	0.93
	D	SDNN [ms]	121.6 (104.8–137.5)	118.0 (102.1–146.1)	0.956	1.00
		RMSSD [ms]	39.4 (31.9–55.1)	34.8 (27.8–56.4)	0.542	0.93
		SDSD [ms]	27.6 (21.6–37.2)	24.2 (18.5–37.5)	0.520	0.93
		pNN50 [%]	15.1 (7.6–24.3)	10.8 (6.3–27.4)	0.512	0.93
	N	SDNN [ms]	100.9 (85.8–113.4)	95.7 (71.0–126.5)	0.729	0.93
		RMSSD [ms]	52.5 (37.8–63.4)	39.5 (32.2–78.0)	0.462	0.93
		SDSD [ms]	33.9 (25.8–43.6)	28.4 (20.9–53.0)	0.424	0.93
		pNN50 [%]	26.4 (14.8–38.0)	15.5 (8.9–46.8)	0.388	0.93
	T	VLF power [ms^2]	1,658.8 (1,089.0–3,250.2)	1,820.0 (952.6–3,782.0)	0.963	1.00
		LF power [ms^2]	1,664.1 (1,023.7–3,382.1)	1,683.8 (945.5–4,707.8)	0.997	1.00
		HF power [ms^2]	1,142.6 (634.8–2,650.0)	1,236.8 (324.6–2,193.9)	0.783	0.93
		VHF power [ms^2]	131.4 (62.7–220.8)	91.5 (48.8–477.9)	0.568	0.93
		total power [ms^2]	4,823.9 (3,086.5–9,454.0)	4,573.7 (2,357.0–13,682.8)	1.000	1.00
		LF/HF ratio	1.7 (1.1–2.5)	2.0 (1.0–2.7)	0.697	0.93
	D	VLF power [ms^2]	859.9 (638.6–1,507.6)	671.8 (438.9–1,830.1)	0.189	0.92
		LF power [ms^2]	1,126.0 (585.4–1,841.3)	1,456.4 (482.9–2,205.8)	0.742	0.93
		HF power [ms^2]	459.1 (210.4–901.2)	388.9 (282–1005.8)	0.910	0.98
		VHF power [ms^2]	59.4 (35.1–145.2)	56.6 (27.3–137.1)	0.675	0.93
		total power [ms^2]	2,922.6 (1,617.3–4,480.6)	2,819.5 (1523.9–4145.8)	0.776	0.93
		LF/HF ratio	2.6 (1.3–4.3)	2.6 (1.4–6.7)	0.623	0.93
	N	VLF power [ms^2]	709.9 (301.5–1,122.0)	476.9 (188.6–1055.6)	0.269	0.93
		LF power [ms^2]	779.0 (341.6–1,455.2)	538.5 (188.2–1183.4)	0.186	0.92
		HF power [ms^2]	787.6 (364.2–1,422.5)	429.5 (158.2–775.8)	0.096	0.92
		VHF power [ms^2]	51.4 (24.5–114.8)	31.6 (21.1–71.1)	0.208	0.92
		total power [ms^2]	2,476.7 (1,488.9–4,196.6)	1,907.6 (632.1–4066.9)	0.161	0.92
		LF/HF ratio	1.2 (0.6–2.1)	1.2 (0.6–2.7)	0.695	0.93

Values presented as median and interquartile range (*Me* (*IQR*)); * statistically significant ($p < 0.05$, Mann–Whitney *U* test); q-value – Benjamini–Hochberg false discovery rate (FDR)-adjusted p-value; TST – total sleep time; SE – sleep efficiency; WASO – wake after sleep onset; SL – sleep latency; N1 – sleep stage 1; N2 – sleep stage 2; N3 – sleep stage 3; AHI – apnea–hypopnea index; ODI – oxygen desaturation index; OA – obstructive apneas; MA – mixed apneas; CA – central apneas; HI – hypopnea index; SpO_2 – oxygen saturation; T – total; D – day; N – night; SDNN – standard deviation of normal-to-normal (NN) intervals; RMSSD – root mean square of successive differences; SDSD – standard deviation of successive differences; TINN – triangular interpolation of NN interval histogram; pNN50 – percentage of NN intervals that differ by more than 50 ms; VLF – very low frequency; LF – low frequency; HF – high frequency; VHF – very high frequency; REM – rapid eye movement.

Sex-based differences

In the female group, greater pain intensity was observed in individual muscles and in the total score across the 4 muscle sites compared with the male group. Regarding HRV parameters, women exhibited higher pNN50 values over the entire 24-hour period and during daytime activity, higher daytime RMSSD values, and a higher mean HR at night.

Frequency domain analysis revealed significant differences between women and men. Over the 24-hour period, women showed significantly lower VLF and LF power, as well as a lower LF/HF ratio. A lower LF/HF ratio in female participants was also observed in both the daytime and nighttime analyses, whereas lower VLF power was observed only at night (Table 2).

Table 2. Heart rate variability (HRV) parameters in patients with temporomandibular disorders (TMD) according to sex

	Parameter	Women (n = 57)	Men (n = 36)	p-value	q-value
T	SDNN [ms]	129.7 (112.9–149.2)	135.5 (105.7–160.5)	0.419	0.61
	RMSSD [ms]	46.6 (33.2–64.0)	39.9 (30.6–50.7)	0.097	0.20
	SDSD [ms]	32.2 (23.2–42.5)	28.7 (19.8–35.9)	0.234	0.36
	HRV index [ms]	37.0 (31.3–44.3)	42.8 (31.7–51.1)	0.121	0.20
	TINN [ms]	562.5 (468.8–679.7)	640.6 (476.6–800.8)	0.116	0.20
	pNN50 [%]	22.5 (11.0–35.6)	14.2 (8.5–22.1)	0.013*	0.05
D	SDNN [ms]	120.4 (106.2–141.3)	124.0 (99.6–140.4)	0.792	0.87
	RMSSD [ms]	41.7 (33.4–58.1)	34.8 (27.3–43.9)	0.026*	0.09
	SDSD [ms]	28.6 (21.7–39.0)	25.7 (17.7–33.5)	0.067	0.18
	pNN50 [%]	18.0 (10.2–31.5)	9.8 (6.1–17.4)	0.002*	0.02
N	SDNN [ms]	97.3 (80.1–113.8)	103.8 (84.6–119.5)	0.662	0.82
	RMSSD [ms]	54.0 (34.3–71.6)	46.0 (35.0–60.2)	0.461	0.64
	SDSD [ms]	33.6 (22.5–45.4)	31.7 (23.1–43.0)	0.934	0.96
	pNN50 [%]	27.9 (11.9–45.7)	20.9 (9.9–31.3)	0.132	0.21
T	VLF power [ms^2]	1,402.4 (944.7–2,667.2)	2,214.5 (1,517.3–5,253.7)	0.010*	0.05
	LF power [ms^2]	1,415.5 (907.7–2,480.6)	2,494.5 (1,387.1–4,756.7)	0.028*	0.09
	HF power [ms^2]	1,261.0 (624.3–2,126.0)	935.0 (459.5–2,886.4)	0.737	0.87
	VHF power [ms^2]	113.7 (63.2–209.4)	109.1 (55.5–409.3)	0.972	0.97
	total power [ms^2]	4,373.6 (2,734.7–8,339.2)	6,277.9 (3,670.4–12,336.6)	0.094	0.20
	LF/HF ratio	1.3 (0.9–2.1)	2.5 (1.8–3.1)	<0.001*	<0.001
D	VLF power [ms^2]	794.0 (574.2–1,830.1)	848.7 (593.3–1,201.6)	0.541	0.72
	LF power [ms^2]	1,151.4 (669.9–1,985.0)	1,054.4 (552.0–1,862.1)	0.575	0.74
	HF power [ms^2]	617.0 (349.5–1,438.7)	269.3 (140.3–486.4)	<0.001*	<0.001
	VHF power [ms^2]	68.9 (42.6–186.7)	41.1 (21.6–102.0)	0.012*	0.05
	total power [ms^2]	2,922.6 (1,738.5–5,329.7)	2,422.4 (1,410.4–3,676.5)	0.115	0.20
	LF/HF ratio	1.8 (1.1–2.9)	4.5 (2.9–7.1)	<0.001*	<0.001
N	VLF power [ms^2]	480.4 (236.8–935.8)	777.6 (487.1–1,514.8)	0.037*	0.10
	LF power [ms^2]	639.8 (287.9–1,111.4)	808.7 (373.9–1,924.3)	0.111	0.20
	HF power [ms^2]	739.5 (325.3–1,267.5)	427.7 (329.2–1,505.9)	0.821	0.88
	VHF power [ms^2]	47.6 (25.8–101.4)	45.6 (19.6–89.1)	0.768	0.87
	total power [ms^2]	2,190.4 (934.1–3,689.3)	3,181.2 (1,339.0–4,952.4)	0.090	0.20
	LF/HF ratio	1.0 (0.6–1.4)	1.8 (1.0–3.1)	0.010*	0.05

Values presented as *Me* (*IQR*); * statistically significant ($p < 0.05$, Mann–Whitney *U* test); q-value – Benjamini–Hochberg false discovery rate (FDR)-adjusted p-value.

Discussion

Pain associated with TMD is often linked to sleep disturbances. A significant proportion of patients with chronic pain conditions report poor sleep quality in studies using various scales and questionnaires.[22] The PSQI appears to be one of the most effective and commonly used tools, enabling the assessment of 4 sleep characteristics: sleep onset; sleep maintenance; sleep adequacy; and daytime sleepiness. Higher PSQI scores in patients with TMD-related pain indicate poorer sleep quality,[23] particularly in the mixed (myofascial and articular) and myalgia groups compared with the arthralgia group.[24] However, polysomnographic studies show only minor differences related to pain intensity, which appear to be more strongly associated with depressive symptoms than with pain itself, suggesting that subjective sleep complaints in TMD are not fully reflected in objective sleep measures.[10]

Therefore, considering these discrepancies, we decided to focus on objective sleep physiology assessed using vPSG. In our study, among multiple sleep quality and sleep architecture parameters, slightly lower sleep efficiency and reduced mean oxygen saturation were observed in patients with higher pain intensity. Sleep efficiency, defined as the ratio of total sleep time to total recording time, represents the percentage of time spent

asleep while in bed; values below 85% may indicate sleep-disrupting factors such as TMD-related pain.[20] These findings are consistent with those of Edwards et al., who demonstrated that lower sleep efficiency and shorter total sleep time are risk factors for reduced pain inhibitory modulation in TMD, which may contribute to the persistence of chronic symptoms.[25] Dysfunction of endogenous opioid systems has been proposed as a mechanism underlying impaired pain inhibition.[26]

The relationship between lower oxygen saturation and pain intensity in TMD is complex and may relate to hypoxemia, which has been shown to increase sympathetic activity and inflammation. This aligns with studies linking OSA and recurrent hypoxic episodes to greater TMD pain.[27]

The significant differences in sleep efficiency and mean saturation level between patients in our study are small in magnitude, and their clinical relevance remains to be established. Such alterations are not sufficient to justify incorporating routine screening for sleep-related disorders in TMD, but they may support greater attention to sleep quality in patients with TMD and more severe pain, as a supplement to existing standards of care.[28] This may include inquiring about sleep complaints during routine TMD evaluations or considering simple behavioral interventions such as sleep hygiene support, optimization of analgesic timing, the use of low-burden home pulse oximetry, and, when indicated, referral for formal sleep assessment.

The imbalance of the ANS in patients with TMD is associated with reduced HRV,[29] which is accompanied by elevated salivary cortisol levels and greater psychological distress.[30] Very low frequency power reflects long-term regulatory mechanisms, including ANS imbalances in response to stress, which may be associated with chronic pain.[31] In our study, HRV parameters were similar in both studied groups, suggesting no significant association between these parameters and TMD intensity.

Studies indicate that women with TMD experience 1.5–2.0 times greater pain intensity than men and account for 80% of patients treated for TMD.[32] The OPPERA study demonstrated that women have lower pain thresholds and greater central sensitization compared with men.[33] This may result from multiple factors. Greater pain sensitivity is associated, for example, with higher estrogen levels,[34] but also with psychological factors such as anxiety and depression, as demonstrated by Manfredini et al.[35] In our study, we observed significantly greater pain intensity in women than in men.

A novel aspect of our study was the analysis of HRV in the context of sex differences. We demonstrated greater parasympathetic activity in women, which aligns with the findings of other authors.[34] In the time domain, women showed higher pNN50 values over 24 h and during daytime activity, higher RMSSD values during the day, and a higher mean HR at night. Regarding frequency domain analysis, women exhibited significantly lower VLF and LF power and a lower LF/HF ratio over the 24-hour period, a lower LF/HF ratio both during the day and at night, and lower VLF power at night. These results may support the hypothesis that higher vagal activity in women could be related to the effects of acetylcholine on diastolic depolarization of cardiac pacemaker cells, producing lower HR oscillations in the presence of shorter RR intervals.[36]

In our cohort, the absence of significant HRV differences between higher- and lower-pain intensity groups, alongside the observed sex-related differences, suggests that pain intensity may not be a strong marker of autonomic alterations, while the influence of sex may be detectable even within a relatively small population. From a clinical perspective, these findings support a comprehensive approach that considers multiple contributing factors. The observed differences between men and women may contribute to individual variability in fatigue or treatment tolerance and could potentially influence sex-dependent rehabilitation strategies. However, given the exploratory nature of the present study, these implications should be viewed as preliminary and should not yet inform changes in routine counseling or rehabilitation without confirmation in larger, prospective studies.

Alternative explanations must also be considered. Differences in measurement conditions, including respiratory patterns, sampling duration and signal quality, may partly account for the observed HRV variations. It should be noted that HRV is also influenced by factors such as age, smoking and leisure-time physical activity, which are not always controllable and may reduce the reliability of the results.[37] It has been shown that aging may attenuate sex differences.[34] Similarly, the phase of the menstrual cycle can influence HRV parameters: vagal activity decreases from the follicular to the luteal phase, with estrogens exerting a beneficial effect that is attenuated under combined estrogen–progesterone therapy.[38] Therefore, further studies should be conducted across different age groups, taking into account the phase of the menstrual cycle in women and the use of hormone therapy.

It is worth noting that in TMD, the predominant pattern is characterized by low RMSSD, SDNN and HF values, along with an elevated LF/HF ratio.[29] Our findings suggest that, despite reporting higher pain intensity, women with TMD exhibit a weaker physiological response to pain, manifested as increased activity of the PNS.

The present study has several methodological strengths that enhance the reliability and validity of the findings. The use of 2 objective diagnostic methods, namely vPSG and Holter ECG monitoring, ensured precise data collection and analysis. The analysis of HRV with the use of a non-invasive, reliable and widely accepted tool, enabled the assessment of the ANS function in the context of TMD pathophysiology. Additionally, the study was conducted on a relatively large sample size, which increased its statistical power and the generalizability of the results. All procedures, including vPSG, clinical assessments and diagnostic

criteria, were carried out in accordance with standardized and validated protocols, ensuring consistency and methodological rigor.

Limitations

Nevertheless, the study has certain limitations. Polysomnography was performed without an adaptation night, which may have induced a first-night effect, potentially influencing the accuracy of measurements and sleep architecture. Lifestyle-related factors that may affect the ANS activity and HRV (e.g., stress, caffeine intake, noise) were not fully controlled. It should be noted that HRV parameters do not solely reflect the ANS function but are also influenced by other mechanisms such as baroreceptor sensitivity, the renin–angiotensin system and respiratory rate. Furthermore, patients with hypertension and those taking medications that could affect HRV were not excluded from the study. This study was exploratory in nature and included a broad set of HRV and vPSG metrics without adjustment for potential confounders, and no multivariable analysis was performed. An a priori power calculation was not conducted, as the study was designed without prespecified primary endpoints. The cross-sectional study design is an additional limitation because it only captures data at a single point in time. Consequently, temporal relationships and causality between variables could not be established, and the observed associations may have been influenced by unmeasured confounding factors. In addition, formal inter-rater reliability of pain assessment was not re-evaluated in the cohort, and detailed clinical phenotyping, such as pain duration and specific TMD subtypes, was not available, reflecting the exploratory nature of the study.

Conclusions

Based on the results of the present study, it can be concluded that patients with high TMD-related pain intensity exhibit reduced sleep efficiency and lower oxygen saturation, without significant differences in HRV parameters. Women report higher masticatory muscle pain intensity than men. Time- and frequency-domain HRV parameters indicate greater parasympathetic activity in women with TMD compared to men. Additionally, the dissociation between higher pain intensity and the observed pattern of autonomic activation in women suggests possible sex-related differences in pain processing, which warrant further investigation and may have implications for personalized treatment approaches.

Trial registration

Information on clinical trial registration is available at the ClinicalTrials.gov database (identifier No. NCT04214561).

Ethics approval and consent to participate

The study was conducted in accordance with the principles of the Declaration of Helsinki, and approval was obtained from the Ethics Committee of Wroclaw Medical University, Poland (approval No. KB-794/2019). All participants provided written informed consent to participate in the study.

Data availability

The datasets generated and/or analyzed during the current study are available from the corresponding author on reasonable request.

Consent for publication

Not applicable.

Use of AI and AI-assisted technologies

Not applicable.

ORCID iDs

Helena Martynowicz https://orcid.org/0000-0003-1283-8460
Małgorzata Trocha https://orcid.org/0000-0002-3951-205X
Karol Marschollek https://orcid.org/0000-0001-9093-180X
Piotr Macek https://orcid.org/0000-0003-3787-0344
Wiktor Trzepietowski https://orcid.org/0009-0001-3707-1772
Jakub Przegrałek https://orcid.org/0009-0005-7202-5420
Katarzyna Madziarska https://orcid.org/0000-0002-3624-3691
Mieszko Więckiewicz https://orcid.org/0000-0003-4953-7143

References

1. Zieliński G, Pająk-Zielińska B, Ginszt M. A meta-analysis of the global prevalence of temporomandibular disorders. *J Clin Med*. 2024;13(5):1365. doi:10.3390/jcm13051365
2. Schiffman E, Ohrbach R, Truelove E, et al.; International RDC/TMD Consortium Network, International association for Dental Research; Orofacial Pain Special Interest Group, International Association for the Study of Pain. Diagnostic Criteria for Temporomandibular Disorders (DC/TMD) for clinical and research applications: Recommendations of the International RDC/TMD Consortium Network* and Orofacial Pain Special Interest Group†. *J Oral Facial Pain Headache*. 2014;28(1):6–27. doi:10.11607/jop.1151
3. Seweryn P, Waliszewska-Prosol M, Petrasova A, et al. Central sensitisation, anxiety and depressive symptoms in patients with chronic masticatory muscle pain. *J Oral Rehabil*. 2025;52(11):2010–2020. doi:10.1111/joor.70007
4. Machado CAO, de Resende CMBM, Stuginski-Barbosa J, et al. Association between obstructive sleep apnea and temporomandibular disorders: A meta-analysis. *J Oral Rehabil*. 2024;51(10):2220–2233. doi:10.1111/joor.13794
5. Więckiewicz M, Lavigne G, Martynowicz H. Decrypting the putative interrelation between sleep bruxism, masticatory muscle pain and sleep breathing disorders: Nosology and the role of hypoxia. *Dent Med Probl*. 2024;61(2):165–167. doi:10.17219/dmp/175686
6. Finan PH, Goodin BR, Smith MT. The association of sleep and pain: An update and a path forward. *J Pain*. 2013;14(12):1539–1552. doi:10.1016/j.jpain.2013.08.007
7. Seweryn P, Orzeszek SM, Waliszewska-Prosół M, et al. Relationship between pain severity, satisfaction with life and the quality of sleep in Polish adults with temporomandibular disorders. *Dent Med Probl*. 2023;60(4):609–617. doi:10.17219/dmp/171894

8. Orzeszek S, Martynowicz H, Smardz J, et al. Assessment of sleep quality in patients with orofacial pain and headache complaints: A polysomnographic study. *Dent Med Probl*. 2024;61(4):549–562. doi:10.17219/dmp/177008
9. Lee YH, Chon S, Auh QS, Verhoeff MC, Lobbezoo F. Clinical, psychological, and hematological factors predicting sleep bruxism in patients with temporomandibular disorders. *Sci Rep*. 2025;15(1):19148. doi:10.1038/s41598-025-03339-3
10. Chan C, Dubrovsky B, Bouchard M, Tartter VC, Raphael KG. Sleep misperception in women with myofascial temporomandibular disorder. *J Clin Sleep Med*. 2025;21(1):55–64. doi:10.5664/jcsm.11330
11. Sztajzel J. Heart rate variability: A noninvasive electrocardiographic method to measure the autonomic nervous system. *Swiss Med Wkly*. 2004;134(35–36):514–522. doi:10.4414/smw.2004.10321
12. Thayer JF, Hansen AL, Saus-Rose E, Johnsen BH. Heart rate variability, prefrontal neural function, and cognitive performance: The neurovisceral integration perspective on self-regulation, adaptation, and health. *Ann Behav Med*. 2009;37(2):141–153. doi:10.1007/s12160-009-9101-z
13. Agorastos A, Mansueto AC, Hager T, Pappi E, Gardikioti A, Stiedl O. Heart rate variability as a translational dynamic biomarker of altered autonomic function in health and psychiatric disease. *Biomedicines*. 2023;11(6):1591. doi:10.3390/biomedicines11061591
14. Hayano J, Yuda E. Assessment of autonomic function by long-term heart rate variability: Beyond the classical framework of LF and HF measurements. *J Physiol Anthropol*. 2021;40(1):21. doi:10.1186/s40101-021-00272-y
15. Narkiewicz K, Montano N, Cogliati C, van de Borne PJ, Dyken ME, Somers VK. Altered cardiovascular variability in obstructive sleep apnea. *Circulation*. 1998;98(11):1071–1077. doi:10.1161/01.cir.98.11.1071
16. Maixner W, Greenspan JD, Dubner R, et al. Potential autonomic risk factors for chronic TMD: Descriptive data and empirically identified domains from the OPPERA case–control study. *J Pain*. 2011;12(11 Suppl):T75–T91. doi:10.1016/j.jpain.2011.09.002
17. Cutrim RC, Santos-de-Araújo AD, Pontes-Silva A, et al. Short-term heart rate variability at rest in individuals with temporomandibular disorder: A comparative analysis. *Clin Oral Investig*. 2023;27(11):6559–6566. doi:10.1007/s00784-023-05261-2
18. Troisi G, Di Giacomo P, Forte G, Langher V, Casagrande M, Di Paolo C. The "Wear and Tear" of the organism in temporomandibular disorders: A pilot study investigating the effects of allostatic load on heart rate variability and inhibitory control. *J Pers Med*. 2024;14(8):787. doi:10.3390/jpm14080787
19. Boonstra AM, Stewart RE, Köke AJA, et al. Cut-off points for mild, moderate, and severe pain on the numeric rating scale for pain in patients with chronic musculoskeletal pain: Variability and influence of sex and catastrophizing. *Front Psychol*. 2016;7:1466. doi:10.3389/fpsyg.2016.01466
20. Berry RB, Brooks R, Gamaldo C, et al. AASM Scoring Manual Updates for 2017 (version 2.4). *J Clin Sleep Med*. 2017;13(5):665–666. doi:10.5664/jcsm.6576
21. Heart rate variability. Standards of measurement, physiological interpretation, and clinical use. Task Force of the European Society of Cardiology and the North American Society of Pacing and Electrophysiology. *Eur Heart J*. 1996;17(3):354–381. PMID:8737210.
22. Cole JC, Dubois D, Kosinski M. Use of patient-reported sleep measures in clinical trials of pain treatment: A literature review and synthesis of current sleep measures and a conceptual model of sleep disturbance in pain. *Clin Ther*. 2007;29 Suppl:2580–2588. doi:10.1016/j.clinthera.2007.12.005
23. Yatani H, Studts J, Cordova M, Carlson CR, Okeson JP. Comparison of sleep quality and clinical and psychologic characteristics in patients with temporomandibular disorders. *J Orofac Pain*. 2002;16(3):221–228. PMID:12221738.
24. Thymi M, Verhoeff MC, Visscher CM, Lobbezoo F. Patient-based experiences with the use of an ambulatory electromyographic device for the assessment of masticatory muscle activity during sleep. *J Oral Rehabil*. 2020;47(5):557–566. doi:10.1111/joor.12945
25. Edwards RR, Grace E, Peterson S, Klick B, Haythornthwaite JA, Smith MT. Sleep continuity and architecture: Associations with pain-inhibitory processes in patients with temporomandibular joint disorder. *Eur J Pain*. 2009;13(10):1043–1047. doi:10.1016/j.ejpain.2008.12.007
26. Ram KC, Eisenberg E, Haddad M, Pud D. Oral opioid use alters DNIC but not cold pain perception in patients with chronic pain – new perspective of opioid-induced hyperalgesia. *Pain*. 2008;139(2):431–438. doi:10.1016/j.pain.2008.05.015
27. Smith MT, Wickwire EM, Grace EG, et al. Sleep disorders and their association with laboratory pain sensitivity in temporomandibular joint disorder. *Sleep*. 2009;32(6):779–790. doi:10.1093/sleep/32.6.779
28. Manfredini D, Häggman-Henrikson B, Al Jaghsi A, et al.; International Network for Orofacial Pain and Related Disorders Methodology. Temporomandibular disorders: INfORM/IADR key points for good clinical practice based on standard of care. *Cranio*. 2025;43(1):1–5. doi:10.1080/08869634.2024.2405298
29. Eze-Nliam CM, Quartana PJ, Quain AM, Smith MT. Nocturnal heart rate variability is lower in temporomandibular disorder patients than in healthy, pain-free individuals. *J Orofac Pain*. 2011;25(3):232–239. PMID:21837290.
30. Chinthakanan S, Laosuwan K, Boonyawong P, Kumfu S, Chattipakorn N, Chattipakorn SC. Reduced heart rate variability and increased saliva cortisol in patients with TMD. *Arch Oral Biol*. 2018;90:125–129. doi:10.1016/j.archoralbio.2018.03.011
31. Kim HG, Cheon EJ, Bai DS, Lee YH, Koo BH. Stress and heart rate variability: A meta-analysis and review of the literature. *Psychiatry Investig*. 2018;15(3):235–245. doi:10.30773/pi.2017.08.17
32. Warren MP, Fried JL. Temporomandibular disorders and hormones in women. *Cells Tissues Organs*. 2001;169(3):187–192. doi:10.1159/000047881
33. Greenspan JD, Slade GD, Bair E, et al. Pain sensitivity risk factors for chronic TMD: Descriptive data and empirically identified domains from the OPPERA case control study. *J Pain*. 2011;12(11 Suppl):T61–T74. doi:10.1016/j.jpain.2011.08.006
34. Koenig J, Thayer JF. Sex differences in healthy human heart rate variability: A meta-analysis. *Neurosci Biobehav Rev*. 2016;64:288–310. doi:10.1016/j.neubiorev.2016.03.007
35. Manfredini D, Landi N, Romagnoli M, Cantini E, Bosco M. Etiopathogenesis of parafunctional habits of the stomatognathic system. *Minerva Stomatol*. 2003;52(7–8):339–349. PMID:14608255.
36. Zaza A, Lombardi F. Autonomic indexes based on the analysis of heart rate variability: A view from the sinus node. *Cardiovasc Res*. 2001;50(3):434–442. doi:10.1016/s0008-6363(01)00240-1
37. Damoun N, Amekran Y, Taiek N, Hangouche AJE. Heart rate variability measurement and influencing factors: Towards the standardization of methodology. *Glob Cardiol Sci Pract*. 2024;2024(4):e202435. doi:10.21542/gcsp.2024.35
38. von Holzen JJ, Capaldo G, Wilhelm M, Stute P. Impact of endo- and exogenous estrogens on heart rate variability in women: A review. *Climacteric*. 2016;19(3):222–228. doi:10.3109/13697137.2016.1145206

Original paper

Antibacterial and antifungal properties of compomer materials modified with silver nanoparticles and copper oxide, with determination of their cytotoxicity

Adam Lubojański[1,A–D,F], Katarzyna Szyszka[2,A–C,E], Bartosz Mielan[3,A–C,E,F], Magdalena Pajączkowska[4,B,D], Joanna Nowicka[4,B,D], Magdalena Ziąbka[5,B,C,E], Adam Watras[2,B,C,E], Rafal Jakub Wiglusz[2,A,E,F], Maciej Dobrzyński[1,A,E,F]

[1] Department of Pediatric Dentistry and Preclinical Dentistry, Wroclaw Medical University, Poland
[2] Institute of Low Temperature and Structure Research, Polish Academy of Sciences, Wrocław, Poland
[3] Pre-Clinical Research Centre, Wroclaw Medical University, Poland
[4] Department of Microbiology, Faculty of Medicine, Wroclaw Medical University, Poland
[5] Department of Ceramics and Refractories, Faculty of Materials Science and Ceramics, AGH University of Krakow, Poland

A – research concept and design; B – collection and/or assembly of data; C – data analysis and interpretation;
D – writing the article; E – critical revision of the article; F – final approval of the article

Dental and Medical Problems, ISSN 1644-387X (print), ISSN 2300-9020 (online) *Dent Med Probl*. 2026;63(5):1277–1287

Address for correspondence
Adam Lubojański
E-mail: adam.lubojanski@student.umw.edu.pl

Funding sources
The study was funded by subsidies from Wroclaw Medical University, Poland (SUBK.B180.24.047, SUBZ.B180.26.012).

Conflict of interest
None declared

Acknowledgements
None declared

Received on April 28, 2026
Reviewed on June 6, 2026
Accepted on June 17, 2026

Published online on July 31, 2026

Cite as
Lubojański A, Szyszka K, Mielan B, et al. Antibacterial and antifungal properties of compomer materials modified with silver nanoparticles and copper oxide, with determination of their cytotoxicity. *Dent Med Probl.* 2026;63(5):1277–1287. doi:10.17219/dmp/224719

DOI
10.17219/dmp/224719

Copyright
Copyright by Author(s)
This is an article distributed under the terms of the Creative Commons Attribution 3.0 Unported (CC BY 3.0) (https://creativecommons.org/licenses/by/3.0/)

Abstract

Background. Tooth decay is a common problem, particularly among young patients. Compomer materials combine favorable aesthetic properties and durability with antibacterial activity resulting from fluoride release. The incorporation of silver (Ag^0) and copper oxide (CuO) particles may further enhance their antimicrobial properties, reducing the risk of complications such as secondary caries and pulpitis.

Objectives. The aim of the study was to evaluate the cytotoxic and antibacterial properties of compomer materials doped with 0.125 wt%, 0.25 wt% and 0.5 wt% CuO and Ag^0 particles using both static and dynamic methods in the Centers for Disease Control and Prevention (CDC) biofilm reactor.

Material and methods. Reference microbial strains were stored at –80°C in tryptic soy broth (TSB) supplemented with 15 wt% glycerol and cultured under strain-specific conditions before the experiments. *Streptococcus mutans*, *Lactobacillus rhamnosus*, *Candida albicans*, and *Staphylococcus epidermidis* were grown on appropriate media under aerobic, anaerobic or elevated CO_2 conditions. Microbiological analysis involved preparing standardized microbial suspensions (0.5 McFarland), incubating them with the tested biomaterials under appropriate conditions. After incubation, biofilms were detached using saponin, serially diluted and plated on selective media, after which colony-forming units (CFU/mL and CFU/cm^2) were calculated. The experiments were performed in 6 replicates using both static and dynamic (flow reactor) biofilm models. Cytotoxicity was evaluated according to the ISO 10993 standard using L929 fibroblasts and BALB/3T3 cells exposed for 24 h to extracts or disks containing Ag^0 and CuO at concentrations of 0.125 wt%, 0.25 wt% and 0.5 wt%.

Results. Both Ag^0 and CuO exhibited statistically significant dose-dependent antibacterial activity against *S. mutans* and *S. epidermidis*. Silver nanoparticles at concentrations of 0.25 wt% and 0.5 wt% demonstrated the highest cytotoxicity in both BALB/3T3 and L929 cell lines.

Conclusions. The incorporation of both CuO and Ag^0 particles into compomer materials enhanced their antimicrobial activity against *S. mutans* and *S. epidermidis*.

Keywords: copper oxide, biofilms, biocompatible materials, silver nanoparticles, dental materials

Highlights

- In the L929 cell line, all compomer materials modified with silver nanoparticles or copper oxide, except those containing 0.5 wt% silver nanoparticles, exhibited cytotoxicity comparable to or lower than that of the control material.
- Increasing silver nanoparticle and copper oxide concentrations enhanced the antimicrobial activity of the tested materials.
- Silver nanoparticles and copper oxide demonstrated significant antimicrobial activity against *Streptococcus mutans* and *Staphylococcus epidermidis*.
- No statistically significant effect on microbes was observed for *Candida albicans* and *Lactobacillus rhamnosus*.

Introduction

Compomers, also known as polyacid-modified composite resins, were introduced into dentistry in the early 1990s. They were designed to combine the favorable properties of composite and glass ionomer materials. The former provide good aesthetics and durability, while the latter release fluoride, which is widely utilized and valued in dentistry. Owing to these characteristics, compomers are widely used, particularly in pediatric dentistry, where treatment may be complicated by limited patient cooperation. However, compomers also exhibit certain drawbacks, including greater leakage and lower bonding strength.[1,2] The amount of fluoride released varies among different groups of materials. In a study by Sagmak et al., glass ionomer materials, resin-modified glass ionomer materials, and compomers were compared with respect to fluoride release.[3] After 7 days, the mean fluoride release was 24.36 mg/L for glass ionomer materials, 3.17–23.53 mg/L for compomers, and 34.53–67.98 mg/L for resin-modified glass ionomer materials. Compomers exhibited the weakest antimicrobial activity against *S. mutans*, which was considered insufficient to effectively inhibit advanced carious lesions.[3,4] Compomer materials are frequently used in pediatric dentistry due to poor patient compliance and difficulty maintaining appropriate surgical conditions. Increasing antibacterial and antifungal properties of the material may reduce the risk of complications, such as secondary caries or pulpitis. The incorporation of various particles, including silver (Ag), copper oxide (CuO), zinc oxide (ZnO), and titanium dioxide (TiO_2), can enhance antimicrobial properties. Nanoparticles range in size from 10 nm to 100 nm, while submicron particles are smaller than 1 μm.[5,6]

Copper oxide has been widely used in medicine due to its antibacterial and anticancer properties. In dentistry, CuO-containing coatings have been developed. However, scientists point to the potential cytotoxicity of CuO.[7–9] The exact antimicrobial mechanism of CuO nanoparticles is not fully understood. A commonly reported mechanism is the increased production of reactive oxygen species (ROS) in bacterial cells, especially in CuO–water suspensions. The antibacterial activity of CuO nanoparticles depends not only on bacterial characteristics, such as cell wall structure, but also on the ratio of surface area to particle size. In general, a larger surface area-to-volume ratio enhances antimicrobial activity. Copper oxide nanoparticles exhibit high toxicity in both in vitro and in vivo models. Their toxicity is mainly determined by copper bioavailability and is influenced by particle size, surface charge and dissolution behavior. Numerous studies involving algae, protozoa, invertebrates, vertebrates, and mammalian cells have shown that CuO nanoparticles induce oxidative stress, mitochondrial dysfunction, DNA damage, and reduced cell proliferation.[7,10] As with cytotoxicity, the higher the concentration of CuO, the greater its antimicrobial activity. However, CuO does not affect all microorganisms equally. A concentration associated with acceptable cytotoxicity does not always reduce the number of microbes.[11,12]

Due to their antiviral, antifungal and antibacterial properties, Ag nanoparticles are widely used in medicine, veterinary medicine and the food industry. Similar to other nanoparticles, their properties are influenced by particle size and shape. The generation of ROS, disruption of cell membrane structure, alterations in cell signaling pathways, and damage to DNA and proteins are among the proposed antimicrobial mechanisms. The cytotoxicity and antimicrobial activity of Ag nanoparticles are related to particle size and concentration. Therefore, it is important to identify a concentration that ensures antimicrobial activity while maintaining biocompatibility and minimizing cytotoxic effects on surrounding tissues. Maintaining antimicrobial activity at lower concentrations of Ag nanoparticles can be achieved by combining them with other particles that possess antimicrobial properties.[7,13,14] It should be noted that Ag nanoparticles are not equally effective against all microorganisms. Their effectiveness depends on their concentration, which influences their cytotoxicity. Another important factor is the method used to produce the particles. Chemically synthesized particles exhibit greater cytotoxicity than particles produced using green synthesis.[15]

The Centers for Disease Control and Prevention (CDC) biofilm reactor is a device that simulates conditions found in the oral cavity. The tested material, in the form of discs, is immersed in a medium containing selected microbes that flow through the container. A biofilm is a complex structure composed of various microorganisms. It is characterized by high resistance to antimicrobial agents and

the immune system. The formation of biofilm significantly increases the risk of developing caries and periodontitis.[16–18] Unlike the static method, the dynamic method continuously supplies nutrients while simultaneously removing toxins and metabolites, and the presence of shear stress makes these conditions more similar to those found in the oral cavity. It also allows greater control over the experimental process, including the addition of various agents. Due to these properties, the dynamic method provides a more accurate representation of oral conditions for both monospecies and multispecies biofilms.[19–21]

The aim of the study was to evaluate the cytotoxic, antibacterial and antifungal properties of compomer materials modified with different concentrations of Ag^0 nanoparticles and CuO particles using both a static in vitro model and a CDC biofilm reactor. The hypothesis of the study was that the incorporation of Ag^0 nanoparticles and CuO particles into the compomer material would enhance its antimicrobial properties while maintaining cytotoxicity similar to or lower than that of the unmodified compomer.

Material and methods

Preparation of nanoparticles

Silver nanoparticles were synthesized using a hydrothermal reduction method, with silver nitrate ($AgNO_3$; Chempur, Piekary Śląskie, Poland) as the silver precursor. Silver nitrate was first dissolved in distilled water, after which aqueous ammonia (Chempur) was added dropwise until a clear diamminesilver(I) complex was formed, $[Ag(NH_3)_2]^+$. Alpha-D-Glucose (Sigma-Aldrich, St. Louis, USA) and TWEEN 100 (POCH S.A., Gliwice, Poland) were added to the solution. The prepared reaction mixture was transferred to a hydrothermal reactor (Magnum II; ERTEC-Poland, Wrocław, Poland). The reactor was heated to 115–120°C and maintained at approx. 30 bar for 60 min. After the hydrothermal reaction, the autoclave was allowed to cool to room temperature. The synthesized Ag^0 particles were purified by repeated washing with a 1:1 mixture of 96% ethanol and distilled water. The suspension was centrifuged at 15,000 rpm for 10 min, and the washing–centrifugation cycle was performed 3 times to ensure complete removal of residual reagents and impurities.

Copper oxide was synthesized using copper(II) chloride ($CuCl_2$) and L-ascorbic acid as a reducing agent via a hydrothermal method followed by thermal treatment. In a typical procedure, an aqueous solution of $CuCl_2$ was prepared by dissolving $CuCl_2{\cdot}2H_2O$ in deionized water under constant stirring. Subsequently, a stoichiometric amount of L-ascorbic acid ($C_6H_8O_6$) was added to the solution. The prepared reaction mixture was transferred to a hydrothermal reactor. The reactor was heated to 115–120°C and maintained at approx. 30 bar for 60 min. After completion of the hydrothermal reaction, the reactor was allowed to cool naturally to room temperature. The synthesized CuO particles were purified by repeated washing in a 1:1 mixture of 96 wt% ethanol and distilled water. The suspension was centrifuged at 15,000 rpm for 10 min, and the washing–centrifugation cycle was performed 3 times to ensure complete removal of residual reagents and impurities. The obtained product was calcined in air at 500°C for 3 h and characterized using scanning electron microscopy (SEM).

Preparation of specimens

The synthesized Ag^0 and CuO particles were incorporated into a compomer matrix, and disc-shaped specimens were prepared using standardized molds. The fabricated discs were subsequently finished, and excess material was removed using a polishing rubber. Finally, the specimens were subjected to steam sterilization at 121°C under a pressure of 2 bar for 45 min. The study was conducted using reference strains obtained from the American Type Culture Collection (ATCC): *Candida albicans* (ATCC 90028); *Streptococcus mutans* (ATCC 25175); *Lactobacillus rhamnosus* (ATCC 9595); and *Staphylococcus epidermidis* (ATCC 35984). The last bacterial strain served as a positive control due to its strong adhesive properties.

The materials analyzed included an unmodified compomer (Dyract® flow A2; Dentsply Sirona, Charlotte, USA) and its modifications containing CuO and Ag^0 in the form of discs with a diameter of 12.7 mm and a thickness of 3.8 mm (Fig. 1).

Description of experimental groups

In both the microbiological and cytotoxicity studies, the compomer material (Dyract® flow A2) and its modifications containing Ag^0 and CuO particles were tested. Each modification contained 0.125 wt%, 0.25 wt% or 0.5 wt% of the respective particles.

In the microbiological study, both the dynamic method using the CDC biofilm reactor and the static method were applied to each of the 7 experimental groups. Their effect on the formation of a multispecies biofilm consisting of *S. mutans*, *L. rhamnosus* and *C. albicans* was examined,

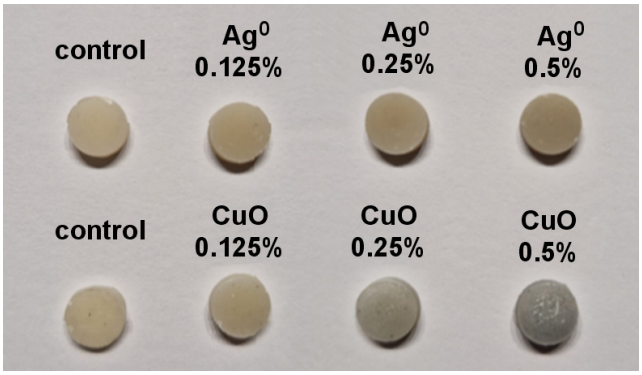

Fig. 1. Prepared compomer specimens

whereas the effect on the formation of a monospecies biofilm of *S. epidermidis* was assessed separately. In total, 7 groups of materials were tested against 2 different biofilm models using both the static and dynamic methods. Each group was tested in 6 replicates, resulting in a total of 294 samples, corresponding to 42 samples for each tested material.

For the cytotoxicity study using the L929 cell line, extracts from each of the 7 material groups were tested. Each group was analyzed in 4 replicates. For the BALB/3T3 cell line, 2 samples from each of the 7 groups were tested.

Preparation of microbiological experiments

The study was conducted using reference strains obtained from the American Type Culture Collection (ATCC): *C. albicans* (ATCC 90028); *S. mutans* (ATCC 25175); *L. rhamnosus* (ATCC 9595); and *S. epidermidis* (ATCC 35984).

The reference strains were stored at −80°C in tryptic soy broth (TSB) supplemented with 15 wt% glycerol. Each strain was stored in several replicates. Before each experimental cycle, the strains were cultured under conditions appropriate for each microorganism:

- *S. mutans* was cultured on Brain Heart Infusion (BHI) broth (BioMaxima S.A., Lublin, Poland) at 37°C for 48 h, under conditions of elevated CO_2 levels;
- *L. rhamnosus* was cultured on De Man–Rogosa–Sharpe (MRS) agar (BioMaxima S.A.) at 37°C for 48 h under anaerobic conditions;
- *S. epidermidis* was cultured on Tryptic Soy Agar (TSA) (BioMaxima S.A.) at 37°C for 48 h under aerobic conditions;
- *C. albicans* was cultured on Sabouraud Dextrose Agar (BioMaxima S.A.) at 37°C for 48 h under aerobic conditions.

Methodology of microbiological studies

Static method

A suspension with a density of 0.5 McFarland was prepared from fresh cultures of the analyzed strains in liquid BHI broth supplemented with 5% sucrose (BioMaxima S.A.) for *C. albicans*, *S. mutans* and *L. rhamnosus*. Subsequently, a mixed microbial suspension, consisting of 200 µL of *S. mutans*, 100 µL of *L. rhamnosus*, 200 µL of *C. albicans*, and 1,500 µL of BHI broth supplemented with sucrose, was prepared, resulting in a final volume of 2 mL. After the specimens had been placed in the microbial suspension, the entire mixture was incubated at 37°C under microaerophilic conditions for 24 h.

For *S. epidermidis*, 200 µL of a 0.5 McFarland suspension prepared in BHI broth supplemented with 5% sucrose was mixed with 1,800 µL of BHI broth containing sucrose and incubated with the specimens under aerobic conditions at 37°C for 24 h.[22,23] After the incubation period, the specimens were rinsed 3 times with 0.9% NaCl and shaken for 1 min in a 0.5% saponin solution (Sigma-Aldrich). The resulting suspension (100 µL) was diluted in geometric progression and seeded on solid BHI agar (3-species biofilm). For *S. epidermidis*, the diluted suspension was plated on TSA.

Dynamic method

The experiments were performed according to a standard protocol.[24] The coupons (test samples) were placed in the reactor. A 1-mL inoculum containing the 3 microorganisms (*S. mutans*, *C. albicans* and *L. rhamnosus*) or *S. epidermidis* alone was introduced into a reactor containing 340 mL of 40% BHI broth (14.8 g/L) supplemented with 5% sucrose. The reactor was maintained at 37°C during a 4-h stationary phase under continuous stirring at 120 rpm. Subsequently, 20% BHI broth supplemented with sucrose was supplied to the reactor for 24 h using a peristaltic pump (HV-77913-70 Masterflex®; Cole-Parmer Company, Montreal, Canada) at a constant flow rate of 11.67 mL/min. After the incubation period, the specimens were rinsed 3 times with 0.9% NaCl and shaken for 1 min in a 0.5% saponin solution (Sigma-Aldrich). The subsequent procedure was identical to that used for the static biofilm model. The experiment was performed in 6 independent replicates.

Following incubation at 37°C using both methods (24 h; elevated CO_2 conditions for the multispecies biofilm and aerobic conditions for the monospecies biofilm), the colonies were counted, and the colony forming units were calculated (CFU/mL) and expressed per coupon surface area. The experiments were performed in 6 independent replicates.[22–24]

Calculation of colony-forming units

Colony-forming units were calculated using the following formula:

CFU/mL = average number of colonies × reciprocal of dilution × dilution factor

To determine the number of bacteria per unit surface area, the following equation was used:

$$\log_{10}\left(\mathrm{CFU/cm^2}\right) = \log_{10}\left[\left(\frac{X}{B}\right)\left(\frac{V}{A}\right)D\right]$$

where:
X – average number of CFU;
B – plated volume (0.02 mL);
V – suspension volume after shaking (1 mL);
A – sample surface area (4.1 cm^2);
D – dilution factor (50; i.e., 1,000/20).

Imaging of samples using scanning electron microscopy

Scanning electron microscopy (Nova NanoSEM 200; FEI Company, Hillsboro, USA) was used to evaluate the structure of the biofilm formed under flow conditions on the coupons. After the incubation period, the samples were rinsed with NaCl, immersed in a 2.5 wt% glutaraldehyde solution (Chempur), and stored for 2 h at 4°C. The specimens were then dehydrated using ethyl alcohol solutions (25 wt%, 50 wt%, 70 wt%, 90 wt%, 95 wt%). Dehydration was performed for 10 min at each concentration at room temperature. Subsequently, the samples were sputter-coated and examined using SEM. Observations were performed using Everhart–Thornley detector (ETD) and in-lens (T1) detectors under high-vacuum conditions at an accelerating voltage of 5 kV. Representative SEM images are shown in Fig. 2.

Methodology of cytotoxicity studies

The BALB/3T3 cells were cultured in Dulbecco's Modified Eagle Medium (DMEM; Gibco, Waltham, USA) supplemented with 10 wt% fetal bovine serum (FBS; Sigma-Aldrich) and 1% antibiotic–antimycotic solution. The cells were maintained at 37°C in a humidified atmosphere containing 5% CO_2 and subcultured at 70–80% confluence using trypsin–ethylenediaminetetraacetic acid (EDTA). The cells were harvested, counted and seeded into 6-well plates at a density of 1.5×10^5 cells per well. They were allowed to adhere and stabilize for 24 h under standard culture conditions. The test samples consisted of disks containing Ag^0 and CuO at concentrations of 0.125 wt%, 0.25 wt% and 0.5 wt%. After 24 h, sterile disks were gently placed into each well to ensure direct contact with the cell layer. The cells were then incubated with the materials for an additional 24 h under previously described conditions.

L929 fibroblasts (NCTC clone 929; ATCC, Manassas, USA) were also used. The cells were seeded into 96-well plates at a density of 10^4 cells/well in 100 µL of DMEM (Gibco) supplemented with 10% FBS (Sigma-Aldrich) and 1% penicillin/streptomycin (P/S; Sigma-Aldrich). After 24 h, the medium was removed and replaced with 100 µL of the test extract.

The extracts were prepared according to the ISO 10993 standard. The samples were immersed in cell culture medium at a ratio of 0.1 g/10 mL and incubated at 37°C for 24 h. A high-density polyethylene extract (HDPE) served as the negative control. A sodium lauryl sulfate (SLS) solution in DMEM (0.2 mg/mL), prepared at dilutions of 1:1, 1:2 and 1:4, was used as the positive control. The cells were incubated with the extracts for 24 h, after which photographs were taken.

To assess fibroblast viability, a colorimetric MTT assay was performed in accordance with EN ISO 10993-5:2009, the standard for the biological evaluation of medical devices. The MTT solution was prepared by dissolving 50 mg of MTT salt (3[4,5-dimethyl-2-yl]-2,5-diphenyltetrazolium) in 50 mL of phosphate-buffered saline (PBS) to obtain a concentration of 1 mg/mL. The solution was then sterilized using a syringe filter. After removal of the culture medium, 100 µL of the MTT solution was added to each well. The cells were incubated for 2 h at 37°C in a 5% CO_2 environment. The MTT solution was then removed and replaced with 100 µL of isopropanol per well. The plate was shaken for 30 min to ensure complete dissolution of purple formazan crystals. Aliquots of 100 µL were transferred to a 96-well plate, and the absorbance was measured at 570 nm using a spectrophotometer (BioTek Epoch 2; Agilent Technologies, Santa Clara, USA). The absorbance values served as a direct indicator of metabolic activity, allowing for a comparative analysis of cell survival rates across the tested samples.

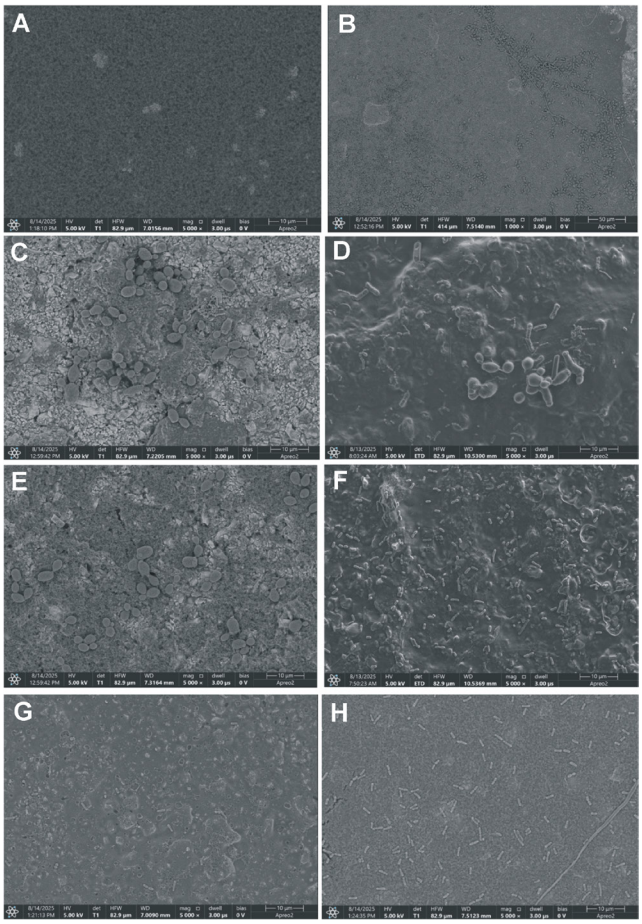

Fig. 2. Scanning electron microscopy (SEM) images of specimens

A. Control without biofilm; B. Control with biofilm; C. Copper oxide (CuO), 0.125 wt%; D. Silver (Ag^0), 0.125 wt%; E. CuO, 0.25 wt%; F. Ag^0, 0.25 wt%; G. CuO, 0.5 wt%; H. Ag^0, 0.5 wt%.
All samples except the control without biofilm were covered with a three-species biofilm consisting of *Candida albicans*, *Streptococcus mutans* and *Lactobacillus rhamnosus*.

Statistical analysis

Statistical analyses were performed using the R software (v. 4.2; R Foundation for Statistical Computing,

Vienna, Austria). For each experimental group, the normality of the analysis of variance (ANOVA) residuals was assessed using the Shapiro–Wilk test, and homogeneity of variance was evaluated using Levene's test. When both assumptions were satisfied, a one-way ANOVA followed by Tukey's honestly significant difference (HSD) post hoc test was performed. Where the normality assumption was violated, the Kruskal–Wallis test followed by Dunn's test with Bonferroni correction was used instead. The same procedure was applied to the cytotoxicity data (L929, MTT assay), for which the Kruskal–Wallis test followed by Dunn–Bonferroni post hoc analysis was selected because the normality assumption was not met. All pairwise comparisons were performed against the unmodified compomer control. Statistical significance was set at $\alpha = 0.05$.

Results

Figures 3–6 present the results of the static and dynamic microbiological tests.

As shown in Fig. 3, Tukey's HSD post hoc test did not reveal any significant differences between the individual experimental groups and the control group for *C. albicans* under static conditions. Neither CuO nor Ag^0 at any of the tested concentrations significantly affected the number of *C. albicans* compared with the unmodified compomer. Under flow conditions, the data was not normally distributed, and Dunn's post hoc test identified 2 significant comparisons relative to the control group. The 0.125 wt% Ag^0 group showed significantly lower values than the control, and the 0.5 wt% CuO group demonstrated slightly higher values than the control group.

The results for *L. rhamnosus* under static conditions were not statistically significant for any concentration of CuO and Ag^0. Under flow conditions, Tukey's HSD post hoc test identified a significant difference in the 0.25 wt% Ag^0 group, with values that were higher than those observed in the control group (Fig. 4).

The findings for *S. mutans* under static conditions revealed that all 3 CuO-modified groups had significantly lower values than the control group (Tukey's HSD post hoc test). None of the Ag^0-modified groups differed significantly from the control group. Under flow conditions, Dunn's post hoc test with Bonferroni correction showed that the 0.125 wt% CuO and 0.5 wt% CuO groups were significantly lower than the control group, whereas the 0.25 wt% Ag^0 and 0.5 wt% Ag^0 groups were significantly higher than the control group.

Figure 6 presents the results for *S. epidermidis*. Tukey's HSD post hoc analysis showed that only the 0.5 wt% Ag^0 group had significantly lower values than the control group. None of the CuO-modified groups differed significantly from the control group. Under flow conditions, Tukey's HSD post hoc test showed that only the 0.125 wt% CuO group differed significantly from the control group.

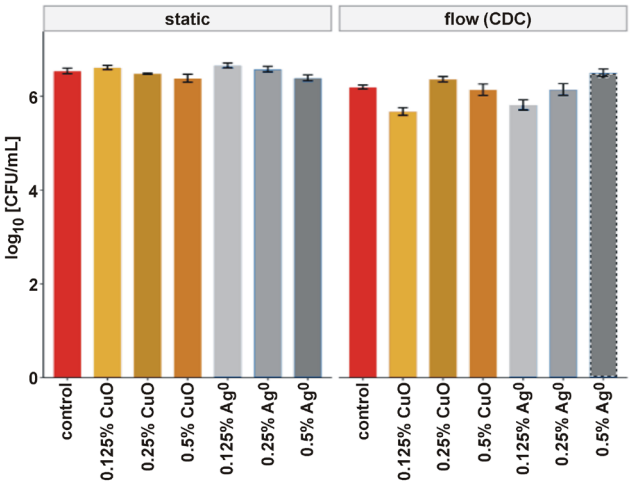

Microorganism	Method	Test	Overall result	Significant differences compared to the control group
C. albicans	static	ANOVA	F(6.35) = 3.41 $p = 0.009$	none
C. albicans	flow (CDC)	KW	H(6) = 25.58 $p < 0.001$	0.125% Ag^0↓** 0.5% CuO↑*

Fig. 3. Effect of silver (Ag^0) and copper oxide (CuO) particles on *Candida albicans*

↑ significantly higher than the control group (stimulatory effect);
↓ significantly lower than the control group (inhibitory effect);
* $p < 0.05$; ** $p < 0.01$; CDC – Centers for Disease Control biofilm reactor; ANOVA – analysis of variance; KW – Kruskal–Wallis test.

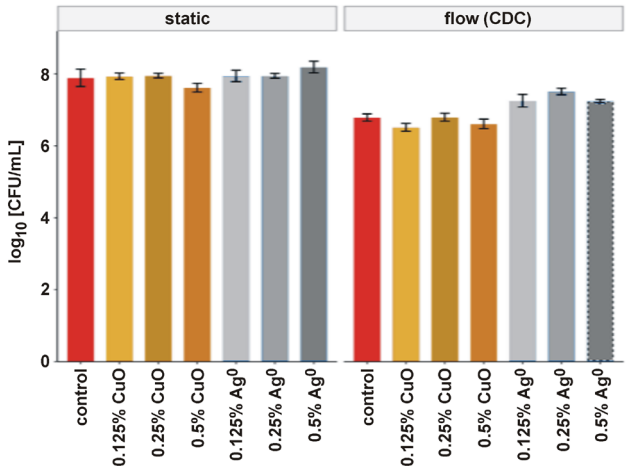

Microorganism	Method	Test	Overall result	Significant differences compared to the control group
L. rhamnosus	static	KW	H(6) = 8.39 $p = 0.211$	none
L. rhamnosus	flow (CDC)	ANOVA	F(6.35) = 10.64 $p < 0.001$	0.25% Ag^0↑**

Fig. 4. Effect of silver (Ag^0) and copper oxide (CuO) particles on *Lactobacillus rhamnosus*

↑ significantly higher than the control group (stimulatory effect); ** $p < 0.01$.

Figures 7 and 8 present the results of the L929 cytotoxicity assay. Dunn's post hoc test with Bonferroni correction identified a statistically significant differences relative to the unmodified compomer control. The 0.125 wt% Ag^0 group showed significantly higher cell viability, which reflected the very low baseline viability of the unmodified compomer rather than the cytotoxic effect of the additive itself.

All CuO-modified groups exhibited significantly higher cell viability than that of the control. In contrast, the 0.25 wt% Ag^0 and 0.5 wt% Ag^0 groups showed significantly reduced cell viability, comparable to that observed for the SLS positive control. In the Ag^0 groups, a marked dose-dependent decrease in cell viability was observed, whereas CuO exhibited moderate, concentration-independent cytotoxicity across the entire tested concentration range. Figure 9 presents the results of the cytotoxicity assay performed using the BALB/3T3 cells. Similar to the L929 assay, the highest cytotoxicity was observed for samples containing 0.25 wt% Ag^0 and 0.5 wt% Ag^0.

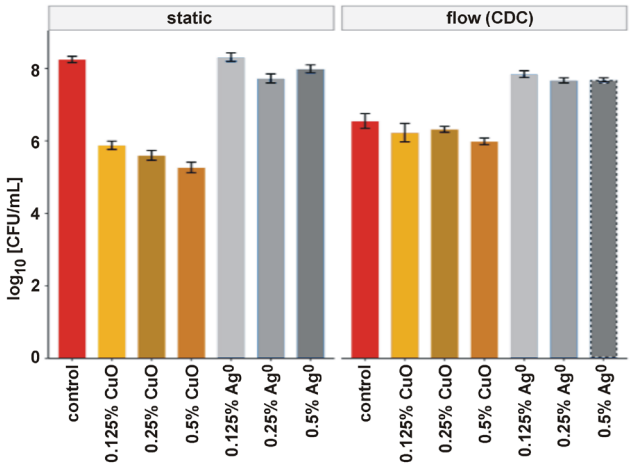

Microorganism	Method	Test	Overall result	Significant differences compared to the control group
S. mutans	static	ANOVA	F(6.35) = 125.41 $p < 0.001$	0.125% CuO↓*** 0.25% CuO↓*** 0.5% CuO↓***
S. mutans	flow (CDC)	KW	H(6) = 32.86 $p < 0.001$	0.125% CuO↓** 0.5% CuO↓** 0.25% Ag^0↑*** 0.5% Ag^0↑*

Fig. 5. Effect of silver (Ag^0) and copper oxide (CuO) particles on *Streptococcus mutans*

↑ significantly higher than the control group (stimulatory effect); ↓ significantly lower than the control group (inhibitory effect); * $p < 0.05$; ** $p < 0.01$; *** $p < 0.001$.

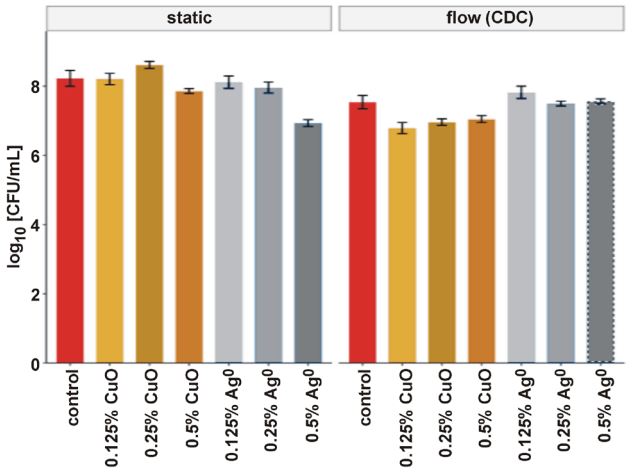

Microorganism	Method	Test	Overall result	Significant differences compared to the control group
S. epidermidis	static	ANOVA	F(6.35) = 11.91 $p < 0.001$	0.5% Ag^0↓***
S. epidermidis	flow (CDC)	ANOVA	F(6.35) = 8.22 $p < 0.001$	0.125% CuO↓**

Fig. 6. Effect of silver (Ag^0) and copper oxide (CuO) particles on *Staphylococcus epidermidis*

↓ significantly lower than the control group (inhibitory effect); ** $p < 0.01$; *** $p < 0.001$.

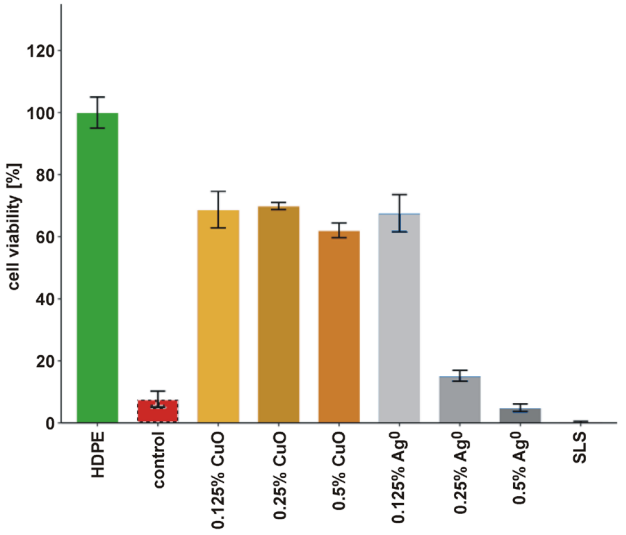

Test	Overall result	Significant differences compared to the control group
Dunn's post hoc test with Bonferroni correction	*df* = 6 $p < 0.001$	0.125% Ag^0**

Fig. 7. Statistical analysis of L929 cell cytotoxicity

HDPE – high-density polyethylene extract (negative control); SLS – sodium lauryl sulfate (positive control); *df* – degrees of freedom; ** $p < 0.01$.

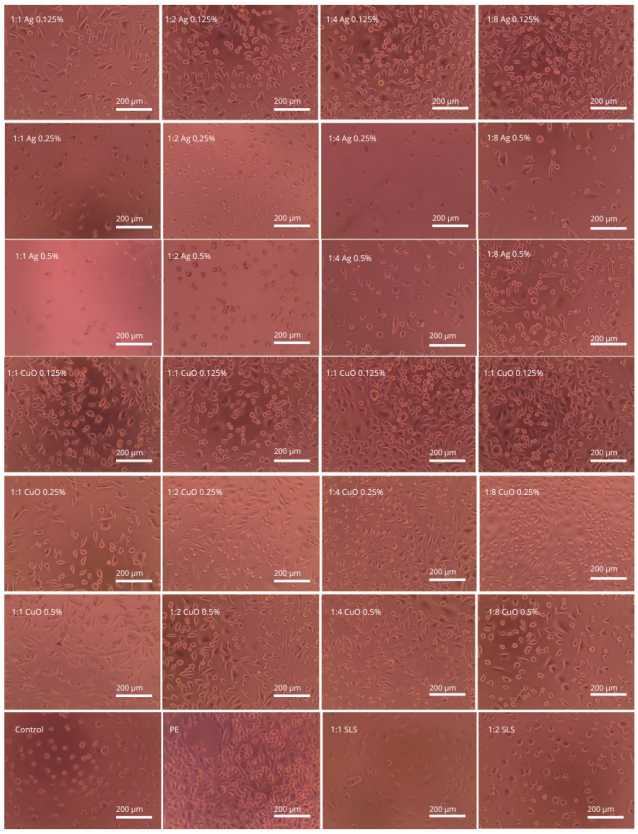

Fig. 8. Representative optical images of L929 cells after 24 h of incubation (×100 magnification)

Figure 10 presents representative SEM images of the synthesized particles. Figure 10A shows the copper(II) oxide sample, which consists of distinctly angular, faceted, polyhedral, and plate-like structures with flat surfaces and sharp edges. The sample is composed of large, block-like crystals measuring from 1 µm to over 2 µm along their longest axis. These larger structures are accompanied by numerous smaller, irregularly shaped particles distributed around and directly on the surfaces of the larger crystals. Figure 10B presents the Ag^0 nanoparticles that exhibit predominantly spherical and quasi-spherical morphologies. The primary particles are grouped into dense, three-dimensional clusters and larger aggregates. The individual particles visible within these structures vary considerably in size, ranging from less than 100 nm to approx. 300 nm in diameter.

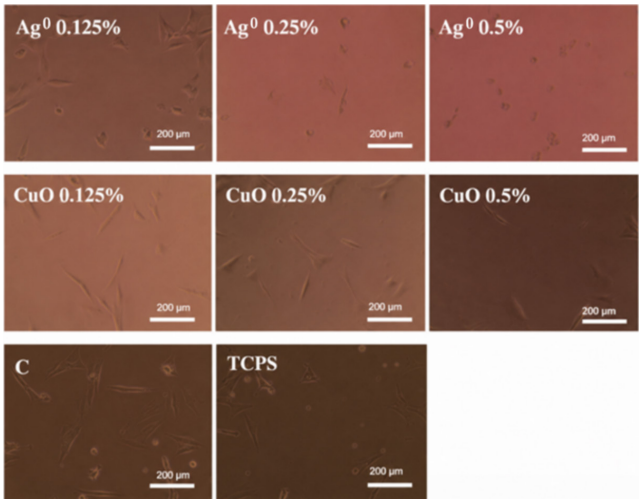

Fig. 9. Representative optical images of BALB/3T3 cells after 24 h of incubation (×100 magnification)

TCPS – tissue culture polystyrene; C – control group.

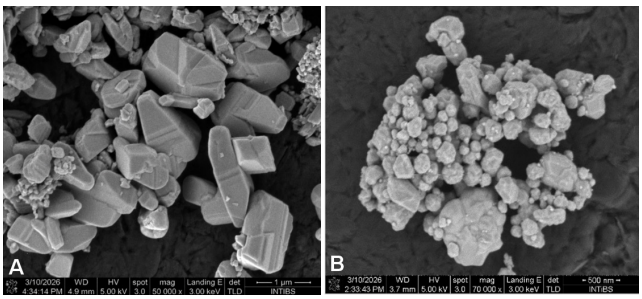

Fig. 10. Scanning electron microscopy (SEM) images of copper oxide (CuO) particles (A) and silver (Ag^0) nanoparticles (B)

Discussion

Many different types of restorative materials are used in dentistry, and newer, more advanced materials, including those modified with various particles, are constantly being developed. These materials are enhanced with additives that provide antibacterial and antifungal properties, thereby reducing the risk of biofilm formation and secondary caries.

Nanoparticle additives are commonly used in dental materials. However, their effectiveness depends on their concentration in the material. In general, higher concentrations produce stronger antibacterial and antifungal effects but are also associated with increased cytotoxicity. Owing to their small size, nanoparticles can easily penetrate human cells. Yang et al. pointed out the potential impact of nanoparticles on the central nervous system and emphasized the need for further research.[25]

There are relatively few studies on modifications of compomer materials. However, numerous studies have investigated the incorporation of nanoparticles into other dental materials, such as composites and glass ionomers. Guo et al. demonstrated, among other findings, that modifications with both Ag nanowires and Ag nanoparticles reduced bacterial biofilm formation, including that of *L. rhamnosus* and *S. mutans*.[26] Cytotoxicity testing in human gingival fibroblasts revealed no statistically significant differences between glass ionomer cements modified with 0.05%, 0.1%, 0.3%, or 0.5% Ag nanowires and those modified with 0.5% Ag nanoparticles.[26] In contrast, studies investigating the effects of Ag nanoparticles on human periodontal fibroblasts have shown that particles smaller than 20 nm exert significant negative effects on the cells. It should be noted that these studies evaluated relatively low concentrations ranging from 0 µM to 1,000 µM, whereas most studies have investigated concentrations between 0.1 wt% and 1 wt%.[27] In a comprehensive study evaluating the toxicity and antibacterial properties of Ag nanoparticles, Niska et al. demonstrated, using human gingival fibroblasts (HGF-1), that cytotoxicity was not statistically significant at concentrations up to 20 µg/mL (0.002 wt%). Within this concentration range, Ag nanoparticles were also effective against *S. epidermidis* and *S. mutans*. It should be noted that the tested Ag nanoparticles consisted of 10-nm particles suspended in solution, and only monospecies, 1-day-old biofilms were evaluated. The authors also reported that the cytotoxicity of Ag nanoparticles could be reduced using capping agents, such as polyethylene glycol, lipoic acid and tannic acid, while maintaining antimicrobial properties. However, uncapped Ag nanoparticles exhibited a broader antimicrobial spectrum.[28] Hernández-Sierra et al. demonstrated statistically significant cytotoxicity in human periodontal fibroblast monolayers at a concentration of 25 mg/mL (0.0025 wt%).[27] Similar conclusions regarding cytotoxicity in L929 cells were reported by Takamiya et al.[29] In a study by Eslami et al., the cytotoxic effects of various colloidal solutions, including Ag nanoparticles (0.4 wt%) and CuO nanoparticles (0.1 wt%), were compared.[30] A higher percentage of apoptosis was observed for CuO nanoparticles. It is worth noting that the level of apoptosis was only slightly lower than that observed for chlorhexidine, which served as the positive control.[30] Shaban et al. incorporated Ag^0 and CuO nanoparticles into an acrylic resin denture

base and investigated their effects on *C. albicans*.[31] Complete eradication was achieved at concentrations as low as 0.3 wt% (Ag^0) and 0.5 wt% (CuO).[31] Another study investigated the effects of Ag and CuO incorporated at concentrations of 0.5 wt% and 1 wt% into orthodontic composites against *S. mutans*.[32] Biofilm formation was assessed after 3, 15 and 30 days. Statistically significant differences were observed after 3 and 15 days, but not after 30 days. It should be noted that the nanoparticle concentrations used in that study were higher than those evaluated in most previous reports.[32] Prior publications have also confirmed the effectiveness of CuO nanoparticles against *S. mutans* and *C. albicans* in soft denture liners and suspensions.[33,34] Copper oxide nanoparticles derived from *Nilgirianthus ciliatus* leaf extract demonstrated low cytotoxicity toward L929 cells.[35] The cytotoxicity of Ag and CuO nanoparticles depends on both particle concentration and size. In general, smaller particles exhibit greater antibacterial activity, which is also associated with increased cytotoxicity. In the present study, Ag^0 nanoparticles ranged in size from 100 nm to 300 nm, whereas CuO particles measured approx. 1,000–2,000 nm. The relatively large size of the CuO particles may explain their lower cytotoxicity.[36–39] In the L929 assay, the CuO-modified materials exhibited significantly lower cytotoxicity than the Ag^0-modified materials, which may be related to the particle size.[36–39] In a study using the MDPC-23 cell line, the addition of 0.1 wt% and 0.2 wt% Ag^0 nanoparticles had no statistically significant effect on the cytotoxicity of glass ionomer cements. It should be noted, however, that Vitrebond exhibited cytotoxicity even in the absence of nanoparticle additives. Similarly, in a study investigating solutions containing Ag (4,000 ppm) and CuO nanoparticles (1,000 ppm), Ag nanoparticles showed lower cytotoxicity toward human gingival fibroblasts.[30,40] Karkehabadi et al. also demonstrated, using stem cells from the apical papilla (SCAPs), that CuO nanoparticle concentrations exceeding 10 μg/mL exhibit cytotoxic properties.[41]

The literature indicates that approx. 500 bacterial species inhabit the oral cavity. In the present study, 1 multispecies biofilm and 1 monospecies *S. epidermidis* biofilm, representing a species with strong adhesive properties, were investigated. Compared with studies evaluating monospecies biofilms or planktonic microorganisms, the antimicrobial effect observed in the present study was considerably weaker, particularly for *C. albicans*.[28,34] Numerous factors influence biofilm formation on dental materials, including ion release, the shape of the filling, and its interaction with dental tissues. Tooth anatomy is highly complex and varies among individuals, as does the quality of restoration placement. Maintaining good oral hygiene remains the foundation for preventing biofilm formation, and, consequently, secondary caries. For the samples used in the study, the authors will present the results of fluoride release in a separate publication. The CDC biofilm reactor enables simulation of oral conditions, and studies using dentin–composite models have confirmed the detrimental effects of biofilm on restorations. Therefore, inhibition of biofilm growth through the incorporation of metal compounds and their ions may increase restoration longevity.[42]

The results of the present study demonstrated differences between the static and dynamic methods. Copper oxide consistently inhibited *S. mutans* under static conditions (all concentrations) and under flow conditions (0.125 wt% and 0.5 wt%). It also inhibited *S. epidermidis* under flow conditions at 0.125 wt%. No inhibitory effect was observed against *C. albicans* and *L. rhamnosus*. Silver exhibited a significant inhibitory effect only against *S. epidermidis* under static conditions. In contrast, stimulatory rather than inhibitory effects were observed for *S. mutans* and *L. rhamnosus*. Therefore, neither CuO nor Ag^0 demonstrated a consistent or clinically meaningful antifungal effect against *L. rhamnosus*. Studies using both L929 and BALB/3T3 cells showed lower cytotoxicity than the control group for all modified materials except the sample containing 0.5 wt% Ag^0. However, the sample containing 0.25 wt% Ag^0 also exhibited high cytotoxicity, indicating a dose-dependent relationship between Ag^0 concentration and cytotoxicity. In contrast, the considerably larger CuO particles showed lower cytotoxicity.

Oral biofilm is a complex microbial community comprising numerous interacting species, making its inhibition substantially more challenging. In the present study, the biofilm consisted of 3 species. Although CuO and Ag^0 possess antimicrobial properties, most previous studies have evaluated either monospecies biofilms or nanoparticles suspended in a solution rather than particles incorporated into restorative materials, which may substantially influence their antimicrobial efficacy.[43,44] The present study did not demonstrate that CuO and Ag^0 particles are equally effective against all tested microorganisms. Once again, the importance of particle size should be emphasized. A study evaluating 10-nm Ag particles against planktonic *S. mutans* reported a minimum inhibitory concentration (MIC) of 4 ppm, whereas statistically significant cytotoxicity toward human dermal fibroblasts occurred at concentrations above 10 ppm.[45] The study also used a CDC biofilm reactor, in which bacterial reduction was observed only at a concentration of 100 ppm. These findings illustrate the significant impact of biofilm on the effectiveness of Ag nanoparticles.[45]

In the present study, the specimens were prepared for testing using steam sterilization. However, sterilization itself may affect the structure of the material. Farrugia et al. reported the presence of bubbles on the surface following steam sterilization of compomers.[46] In addition, the microhardness of the compomer increased after sterilization. Although the specimens in the present study were polished before sterilization, possible structural changes resulting in increased porosity may have influenced biofilm formation.[46]

Another limitation is illustrated in Fig. 2, which depicts the samples tested in the experiment. A visible color

change occurred with increasing particle content, particularly in the CuO-modified materials. An advantage of compomer materials is their favorable aesthetics, which were compromised by the addition of 0.25 wt% and 0.5 wt% CuO. Similar esthetic limitations have been reported for other restorative materials modified with antimicrobial additives. Therefore, the selection of an optimal particle concentration should consider not only cytotoxicity and antimicrobial activity but also esthetic properties, which are of considerable importance to patients.[47,48]

Further studies evaluating fluoride release and physicochemical properties are needed to determine the optimal concentration and particle size of Ag^0 and CuO without compromising the mechanical properties of the compomer. Modified compomer materials should meet the same performance standards as the original material to ensure long-term clinical durability with minimal risk of complications.

Conclusions

Compomer materials are frequently used in young patients who are at an increased risk of complications associated with microleakage and microbial growth. Enhancing their antimicrobial properties through the incorporation of selected particles may reduce biofilm formation and thereby decrease the risk of secondary complications. The present study demonstrated that the incorporation of CuO inhibited the growth of *S. mutans* at all tested concentrations under static conditions and at 0.125 wt% and 0.5 wt% under flow conditions. *Staphylococcus epidermidis* was inhibited only by 0.5 wt% Ag^0 under static conditions; however, this concentration exhibited unacceptable cytotoxicity. Additionally, the 0.125 wt% CuO group showed significant inhibition under flow conditions.

The clinical applicability of the modified materials also depends on their aesthetic properties, which were adversely affected by the addition of CuO at concentrations of 0.25 wt% and 0.5 wt%. The study demonstrated a dose-dependent increase in cytotoxicity, particularly for Ag^0-containing materials. Although both Ag^0 and CuO exhibited antimicrobial activity, their overall effectiveness was limited. Therefore, identifying an optimal particle concentration that provides antimicrobial efficacy while maintaining acceptable cytotoxicity remains essential.

Ethics approval and consent to participate

Not applicable.

Data availability

The datasets generated and/or analyzed during the current study are available from the corresponding author on reasonable request.

Consent for publication

Not applicable.

Use of AI and AI-assisted technologies

Not applicable.

ORCID iDs

Adam Lubojański https://orcid.org/0000-0002-9229-3300
Katarzyna Szyszka https://orcid.org/0000-0001-8603-7776
Bartosz Mielan https://orcid.org/0000-0002-1226-3540
Magdalena Pajączkowska https://orcid.org/0000-0002-9881-8294
Joanna Nowicka https://orcid.org/0000-0002-4001-4189
Magdalena Ziąbka https://orcid.org/0000-0003-0702-7137
Adam Watras https://orcid.org/0000-0003-4736-0356
Rafal Jakub Wiglusz https://orcid.org/0000-0001-8458-1532
Maciej Dobrzyński https://orcid.org/0000-0003-2368-1534

References

1. Saravanan SM, Srinivasan D, Senthil Eagappan A, Divya Priyal S. Comparative assessment of compomers and ormocers as pit and fissure sealants in permanent molars among children aged 7–9 years. *Int J Clin Pediatr Dent*. 2024;17(7):742–747. doi:10.5005/jp-journals-10005-2954
2. Kizilci E, Gorgen VA. Residual monomer release after the polymerization of different-colored flowable compomer. *Niger J Clin Pract*. 2024;27(1):1–7. doi:10.4103/njcp.njcp_1995_21
3. Sagmak S, Bahsi E, Ozcan N, Satici O. Comparative evaluation of antimicrobial efficacy and fluoride release of seven different glass-ionomer-based restorative materials. *Oral Health Prev Dent*. 2020;18(3):521–528. doi:10.3290/j.ohpd.a44140
4. Garoushi S, Vallittu PK, Lassila L. Characterization of fluoride releasing restorative dental materials. *Dent Mater J*. 2018;37(2):293–300. doi:10.4012/dmj.2017-161
5. Joseph TM, Kar Mahapatra D, Esmaeili A, et al. Nanoparticles: Taking a unique position in medicine. *Nanomaterials (Basel)*. 2023;13(3):574. doi:10.3390/nano13030574
6. Błaszczak B, Słaby K, Rogula-Kopiec P. The role of fine and submicron aerosol particles in urban air pollution in the context of meeting new air quality standards. *Sci Rep*. 2025;16(1):915. doi:10.1038/s41598-025-30407-5
7. Lubojanski A, Dobrzynski M, Nowak N, et al. Application of selected nanomaterials and ozone in modern clinical dentistry. *Nanomaterials (Basel)*. 2021;11(2):259. doi:10.3390/nano11020259
8. Kusior A, Mazurkow J, Jelen P, et al. Copper oxide electrochemical deposition to create antiviral and antibacterial nanocoatings. *Langmuir*. 2024;40(29):14838–14846. doi:10.1021/acs.langmuir.4c00642
9. Devaraji M, Thanikachalam PV, Elumalai K. The potential of copper oxide nanoparticles in nanomedicine: A comprehensive review. *Biotechnol Notes*. 2024;5:80–99. doi:10.1016/j.biotno.2024.06.001
10. Grigore ME, Biscu ER, Holban AM, Gestal MC, Grumezescu AM. Methods of synthesis, properties and biomedical applications of CuO nanoparticles. *Pharmaceuticals (Basel)*. 2016;9(4):75. doi:10.3390/ph9040075
11. Zubair M, Albalawi Y, Alatawy R. Antifungal, antibiofilm and anticytotoxic properties of biogenic CuO nanoparticles derived from *Moringa oleifera* leaves against vaginal candidiasis. *Int J Womens Health*. 2025;17:5045–5058. doi:10.2147/ijwh.s567527
12. Angelé-Martínez C, Ameer FS, Raval YS, et al. Polyphenol effects on CuO-nanoparticle-mediated DNA damage, reactive oxygen species generation, and fibroblast cell death. *Toxicol In Vitro*. 2022;78:105252. doi:10.1016/j.tiv.2021.105252
13. Hao Z, Wang M, Cheng L, Si M, Feng Z, Feng Z. Synergistic antibacterial mechanism of silver-copper bimetallic nanoparticles. *Front Bioeng Biotechnol*. 2024;11:1337543. doi:10.3389/fbioe.2023.1337543
14. Danai L, Rolband LA, Perdomo VA, Skelly E, Kim T, Afonin KA. Optical, structural and antibacterial properties of silver nanoparticles and DNA-templated silver nanoclusters. *Nanomedicine (Lond)*. 2023;18(9):769–781. doi:10.2217/nnm-2023-0082

15. Oetiker N, Salinas D, Lucero-Mora J, et al. Antimicrobial effect of copper nanoparticles on relevant supragingival oral bacteria. *Microorganisms*. 2024;12(3):624. doi:10.3390/microorganisms12030624
16. Khubchandani M, Thosar NR, Dangore-Khasbage S, Srivastava R. Applications of silver nanoparticles in pediatric dentistry: An overview. *Cureus*. 2022;14(7):e26956. doi:10.7759/cureus.26956
17. Kwon TH, Lamster IB, Levin L. Current concepts in the management of periodontitis. *Int Dent J*. 2021;71(6):462–476. doi:10.1111/idj.12630
18. Jakubovics NS, Goodman SD, Mashburn-Warren L, Stafford GP, Cieplik F. The dental plaque biofilm matrix. *Periodontol 2000*. 2021;86(1):32–56. doi:10.1111/prd.12361
19. Ramachandra SS, Wright P, Han P, Abdal-Hay A, Lee RSB, Ivanovski S. Evaluating models and assessment techniques for understanding oral biofilm complexity. *Microbiologyopen*. 2023;12(4):e1377. doi:10.1002/mbo3.1377
20. An SQ, Hull R, Metris A, Barrett P, Webb JS, Stoodley P. An in vitro biofilm model system to facilitate study of microbial communities of the human oral cavity. *Lett Appl Microbiol*. 2022;74(3):302–310. doi:10.1111/lam.13618
21. Ramachandra SS, Sime FB, Naicker S, et al. An in vitro dynamic bioreactor model for evaluating antimicrobial effectiveness on periodontal polymicrobial biofilms: A proof-of-concept study. *J Periodontol*. 2024;95(4):384–396. doi:10.1002/jper.23-0086
22. Wilson C, Lukowicz R, Merchant S, et al. Quantitative and qualitative assessment methods for biofilm growth: A mini-review. *Res Rev J Eng Technol*. 2017;6(4). PMID:30214915.
23. Chevalier M, Ranque S, Prêcheur I. Oral fungal-bacterial biofilm models in vitro: A review. *Med Mycol*. 2018;56(6):653–667. doi:10.1093/mmy/myx111
24. Biosurface Technologies Corporation. FC 310 Treatment Imaging Flow Cell Operator's Manual. 2022. https://biofilms.biz/wp-content/uploads/2025/07/FC-310-Operators-Manual-Dec2022.pdf. Accessed March 3, 2026.
25. Yang Z, Liu ZW, Allaker RP, et al. A review of nanoparticle functionality and toxicity on the central nervous system. *J R Soc Interface*. 2010;7 Suppl 4:S411–S422. doi:10.1098/rsif.2010.0158.focus
26. Guo T, Wang D, Gao SS. The antibiofilm effect and mechanism of silver nanowire-modified glass ionomer cement against multi-species oral biofilm. *BMC Oral Health*. 2025;25(1):160. doi:10.1186/s12903-025-05536-y
27. Hernández-Sierra JF, Galicia-Cruz O, Salinas-Acosta A, Ruiz F, Pierdant-Pérez M, Pozos-Guillén AJ. In vitro cytotoxicity of silver nanoparticles on human periodontal fibroblasts. *J Clin Pediatr Dent*. 2011;36(1):37–42. doi:10.17796/jcpd.36.1.d677647166398886
28. Niska K, Knap N, Kędzia A, Jaskiewicz M, Kamysz W, Inkielewicz-Stepniak I. Capping agent-dependent toxicity and antimicrobial activity of silver nanoparticles: An in vitro study. Concerns about potential application in dental practice. *Int J Med Sci*. 2016;13(10):772–782. doi:10.7150/ijms.16011
29. Takamiya AS, Monteiro DR, Bernabé DG, et al. In vitro and in vivo toxicity evaluation of colloidal silver nanoparticles used in endodontic treatments. *J Endod*. 2016;42(6):953–960. doi:10.1016/j.joen.2016.03.014
30. Eslami N, Fasihi F, Jamalinasab A, Ahrari F. Biocompatibility of several colloidal solutions containing nanoparticles on human gingival fibroblasts. *Dent Res J*. 2021;18:8. doi:10.4103/1735-3327.310037
31. Shaban AA, Sabry HA, Mahrous AI. Evaluation of anti-fungal effect of nanoparticles within different types of acrylic resin denture bases. *Egypt Dent J*. 2015;61(3):3443–3449.
32. Yassaei S, Nasr A, Zandi H, Motallaei MN. Comparison of antibacterial effects of orthodontic composites containing different nanoparticles on *Streptococcus mutans* at different times. *Dental Press J Orthod*. 2020;25(2):52–60. doi:10.1590/2177-6709.25.2.052-060.oar
33. Ansarifard E, Zareshahrabadi Z, Sarafraz N, Zomorodian K. Antimicrobial and antibiofilm activities of copper oxide nanoparticles within soft denture liners against oral pathogens. *Bioinorg Chem Appl*. 2021;2021:9939275. doi:10.1155/2021/9939275
34. Amiri M, Etemadifar Z, Daneshkazemi A, Nateghi M. Antimicrobial effect of copper oxide nanoparticles on oral bacteria and Candida species. *J Dent Biomater*. 2017;4(1):347–352. PMID:28959764.
35. Rajamma R, Nair SG, Khadar FA, Baskaran B. Antibacterial and anticancer activity of biosynthesised CuO nanoparticles. *IET Nanobiotechnol*. 2020;14(9):833–838. doi:10.1049/iet-nbt.2020.0088
36. Park MVDZ, Neigh AM, Vermeulen JP, et al. Effect of particle size on cytotoxicity and inflammation of silver nanoparticles. *Biomaterials*. 2011;32(36):9810–9817. doi:10.1016/j.biomaterials.2011.08.085
37. Shafaee H, Khosropanah H, Rahimi H, Darroudi M, Rangrazi A. Effects of adding cinnamon, ZnO, and CuO nanoparticles on the antibacterial properties of a glass ionomer cement as the luting agent for orthodontic bands and their cytotoxicity. *J Compos Sci*. 2022;6(11):336. doi:10.3390/jcs6110336
38. Mahmoudi Anzabi R, Divband B, Tukmachi MS, et al. Assessment of physicochemical properties, cytotoxicity, antimicrobial activity, and flexural strength of self-cured acrylic resin with silver nanoparticles on delaminated clay for removable appliances. *Int J Dent*. 2025;2025:7939455. doi:10.1155/ijod/7939455
39. Ali A, Ershad M, Vyas VK, et al. Studies on effect of CuO addition on mechanical properties and in vitro cytocompatibility in 1393 bioactive glass scaffold. *Mater Sci Eng C Biol Appl*. 2018;93:341–355. doi:10.1016/j.msec.2018.08.003
40. Siqueira PC, Magalhães APR, Pires WC, et al. Cytotoxicity of glass ionomer cements containing silver nanoparticles. *J Clin Exp Dent*. 2015;7(5):e622–e628. doi:10.4317/jced.52566
41. Karkehabadi H, Rahmati A, Abbasi R, et al. Effect of copper oxide nanoparticles and light-emitting diode irradiation on the cell viability and osteogenic/odontogenic differentiation of human stem cells from the apical papilla. *BMC Oral Health*. 2023;23(1):249. doi:10.1186/s12903-023-02916-0
42. Li Y, Carrera C, Chen R, et al. Biofilm-induced degradation of dentin–composite interface subjected to multi-species biofilm challenges. *Acta Biomater*. 2014;10(1):375–383. doi:10.1016/j.actbio.2013.08.034
43. Rojas-Jaimes J, Asmat-Campos D. Cu_2O, ZnO, and Ag/Cu_2O nanoparticles synthesized by biogenic and chemical route and their effect on *Pseudomonas aeruginosa* and *Candida albicans*. *Sci Rep*. 2023;13(1):21478. doi:10.1038/s41598-023-47917-9
44. Garcia-Marin LE, Juarez-Moreno K, Vilchis-Nestor AR, Castro-Longoria E. Highly antifungal activity of biosynthesized copper oxide nanoparticles against *Candida albicans*. *Nanomaterials (Basel)*. 2022;12(21):3856. doi:10.3390/nano12213856
45. Pérez-Díaz MA, Boegli L, James G, et al. Silver nanoparticles with antimicrobial activities against *Streptococcus mutans* and their cytotoxic effect. *Mater Sci Eng C Mater Biol Appl*. 2015;55:360–366. doi:10.1016/j.msec.2015.05.036
46. Farrugia C, Cassar G, Valdramidis V, Camilleri J. Effect of sterilization techniques prior to antimicrobial testing on physical properties of dental restorative materials. *J Dent*. 2015;43(6):703–714. doi:10.1016/j.jdent.2015.03.012
47. Kula Z, Neves CB, Bettencourt A, Oliveira S, Roque JC. Color stability of a composite containing hydroxyapatite, fluorine, and silver fillers after artificial aging. *Appl Sci*. 2025;15(23):12426. doi:10.3390/app152312426
48. Al-Dulaijan YA, AlGhamdi MA, Azmy E, Al-Kholy MRZ, Almulhim KS, Helal MA. Color stability of nanoparticle-modified dental composites. *Appl Sci*. 2023;13(6):3870. doi:10.3390/app13063870

Review

Laser-based management of oral leukoplakia: A narrative review by a study group of the World Federation for Laser Dentistry (WFLD)

Kinga Grzech-Leśniak[1,2,A–F*], Paolo Vescovi[3,A–F*], Georgios Romanos[4,5,B–F], Rafał Wiench[6,A–F], Jakub Fiegler-Rudol[7,A–F], Ilaria Giovannacci[3,D–F], Janina Golob Deeb[2,D–F], Zuzanna Grzech-Leśniak[8,9,A–F], Jacek Matys[10,D–F], Aldo Brugnera Junior[11,12,C–F], Mariusz Szuta[13,C–F], Sajee Sattayut[14,C–F], Praveen Arany[15,B–F], Marco Meleti[3,C–F], Maha Taalab[16,B–F], Josep Arnabat-Dominguez[17,D–F], Alessandro Del Vecchio[18,C–F], Jamil Awad Shibli[19,20,A–F], Maciej Misiołek[21,C–F], Octavi Camps-Font[17,D–F], Akira Aoki[22,A–F], Umberto Romeo[18,C–F], Samir Nammour[23,A–F]

[1] Laser Laboratory, Department of Integrated Dentistry, Faculty of Dentistry, Wroclaw Medical University, Poland
[2] Department of Periodontics, School of Dentistry, Virginia Commonwealth University (VCU), Richmond, USA
[3] Oral Medicine and Oral Surgery Laser Unit, Department of Medicine and Surgery, University of Parma, Italy
[4] Department of Periodontics and Endodontics, School of Dental Medicine, Stony Brook University, USA
[5] Department of Oral Surgery, Implant Dentistry and Oral Medicine, Goethe Dental School, Goethe University, Frankfurt am Main, Germany
[6] Department of Periodontal and Oral Mucosa Diseases, Faculty of Medical Sciences in Zabrze, Medical University of Silesia, Katowice, Poland
[7] University Dental Center, Wroclaw Medical University, Poland
[8] Department of Experimental Dentistry, Faculty of Dentistry, Wroclaw Medical University, Poland
[9] Doctoral School, Faculty of Dentistry, Wroclaw Medical University, Poland
[10] Department of Dental Surgery, Faculty of Dentistry, Wroclaw Medical University, Poland
[11] Basic Optics and Applied Life Sciences, National Institutes of Science and Technology (INCT), São Carlos Institute of Physics (IFSC), University of São Paulo (USP), Brazil
[12] Brugnera and Zanin Institute, Biophotonics Laser Center, Instituto Brugnera e Zanin, São Paulo, Brazil
[13] Department of Oral Surgery, Institute of Dentistry, Faculty of Medicine, Jagiellonian University Medical College, Krakow, Poland
[14] Lasers in Dentistry Research Group, Khon Kaen University, Thailand
[15] Department of Oral Biology, School of Dental Medicine, University of Buffalo, USA
[16] Department of Oral Medicine, Periodontology, Oral Diagnosis, and Oral Radiology, Faculty of Dentistry, Alexandria University, Egypt
[17] Dental School, Faculty of Medicine and Health Sciences, University of Barcelona, Institute of Biomedical Research of Bellvitge (IDIBELL), Barcelona, Spain
[18] Department of Oral and Maxillofacial Sciences, Sapienza University of Rome, Italy
[19] Department of Periodontology, Dental Research Division, Universus Veritas Guarulhos University, Brazil
[20] Department of Oral Medicine, Infection and Immunity, Harvard School of Dental Medicine, Boston, USA
[21] Department of Otorhinolaryngology and Oncological Laryngology, Faculty of Medical Sciences in Zabrze, Medical University of Silesia, Katowice, Poland
[22] Department of Periodontology, Graduate School of Medical and Dental Sciences, Institute of Science Tokyo, Japan
[23] Department of Dental Sciences, Faculty of Medicine, University of Liège, Belgium
* These authors contributed equally to this work.

A – research concept and design; B – collection and/or assembly of data; C – data analysis and interpretation;
D – writing the article; E – critical revision of the article; F – final approval of the article

Dental and Medical Problems, ISSN 1644-387X (print), ISSN 2300-9020 (online) *Dent Med Probl*. 2026;63(5):1289–1302

Cite as
Grzech-Leśniak K, Vescovi P, Romanos G, et al. Laser-based management of oral leukoplakia: A narrative review by a study group of the World Federation for Laser Dentistry (WFLD). *Dent Med Probl.* 2026;63(5):1289–1302. doi:10.17219/dmp/226773

DOI
10.17219/dmp/226773

Copyright
Copyright by Author(s)
This is an article distributed under the terms of the Creative Commons Attribution 3.0 Unported (CC BY 3.0) (https://creativecommons.org/licenses/by/3.0/)

Address for correspondence
Kinga Grzech-Leśniak
E-mail: kinga.grzech-lesniak@umw.edu.pl

Funding sources
None declared

Conflict of interest
None declared

Acknowledgements
None declared

Received on April 4, 2026
Reviewed on April 26, 2026
Accepted on August 3, 2026

Published online on October 30, 2026

Abstract

The aim of the review was to systematically synthesize and critically appraise the available evidence from systematic reviews and meta-analyses evaluating the clinical effectiveness, safety and applicability of laser-based therapies in the management of oral leukoplakia (OL), and to develop evidence-based clinical recommendations of the World Federation for Laser Dentistry (WFLD). The search of PubMed/MEDLINE, Embase, Scopus, and the Cochrane Library was conducted to identify systematic reviews and meta-analyses published between 2016 and 2026. Eligible reviews assessed laser-based interventions for OL and reported clinically relevant outcomes. Methodological quality was evaluated using a laser-adapted nine-domain risk-of-bias assessment tool. Ten reviews were included, comprising systematic reviews, meta-analyses and network meta-analyses. Evaluated modalities included CO_2, erbium-doped yttrium aluminium garnet (Er:YAG), erbium, chromium-doped yttrium, scandium, gallium, and garnet (Er,Cr:YSGG), diode, neodymium-doped yttrium aluminium garnet (Nd:YAG), and potassium titanyl phosphate (KTP) lasers, as well as laser-assisted photodynamic therapy (PDT). Overall, laser-based interventions demonstrated recurrence rates comparable to or lower than those associated with conventional surgery, with favorable postoperative outcomes including reduced pain and improved hemostasis. All included reviews were classified as having a low ($n = 6$) or moderate ($n = 4$) risk of bias according to the study-specific assessment framework, although substantial heterogeneity in laser parameters and outcome reporting was observed. Laser-based therapies represent clinically justified options for the management of OL when appropriately selected and integrated with histopathological assessment, adequate margin control, complete lesion removal, and long-term surveillance. However, current evidence does not demonstrate a consistent reduction in the risk of malignant transformation or definitive superiority of any specific laser modality. Heterogeneity in surgical procedures, outcome definitions and study designs underscores the need for standardized reporting and high-quality prospective studies.

Keywords: recurrence, laser therapy, malignant transformation, oral potentially malignant disorders, leukoplakia

Highlights

- Laser-based therapies are effective and safe for the management of oral leukoplakia, with recurrence rates comparable to or lower than those of conventional surgical approaches.
- No surgical intervention, including laser-based techniques, has been shown to reduce the risk of malignant transformation, which is primarily influenced by lesion biology and patient-related factors.
- Adequate surgical margins, appropriate ablation depth and complete lesion removal are key to reducing recurrence in laser-based treatment.
- This narrative review provides a structured framework for the clinical application of lasers in the management of oral leukoplakia.

Introduction

Oral leukoplakia (OL) is one of the most common oral potentially malignant disorders (OPMDs), defined as a white plaque of questionable risk after the exclusion of other known diseases not associated with an increased risk of cancer.[1–3] Its management should be considered within the broader OPMD framework, encompassing oncologic risk reduction, histopathological risk stratification, adequate surgical management, recurrence prevention, and long-term surveillance. With a global prevalence of 0.1–4.5%, OL represents a significant public health concern due to its potential for malignant transformation into oral squamous cell carcinoma.[2–4] Meta-analytic evidence indicates that OL is associated with significantly increased odds of developing oral cancer (summary odds ratio (*SOR*): 3.35; 95% confidence interval (95% *CI*): 3.21–3.50).[5] Malignant transformation rates vary according to clinical characteristics, anatomical site and lesion subtype, with particularly high rates reported for proliferative verrucous leukoplakia (PVL), which may approach 50%.[3,6,7] Although available management strategies include active surveillance, conventional surgical excision, pharmacological interventions, and laser-based therapies,[8,9] no universally accepted, evidence-based management protocol has yet been established.[10,11]

Laser therapy offers potential advantages over conventional surgery, including improved hemostasis, reduced postoperative morbidity, minimal scarring, and the elimination of the need for sutures, which may prevent distortion of the surgical site and enhance surgical precision, particularly for extensive or multifocal lesions.[12,13] Systems in clinical use include CO_2, erbium-doped yttrium aluminium garnet (Er:YAG), erbium, chromium-doped yttrium, scandium, gallium, and garnet (Er,Cr:YSGG), neodymium-doped yttrium aluminium garnet (Nd:YAG), and diode lasers, each with distinct wavelength-specific tissue interaction properties.[12–14] Several clinical and experimental studies have contributed to our understanding of laser–tissue interactions in OPMDs.[15–17] Despite the increasing availability of laser-based treatments, the evidence remains heterogeneous and methodologically limited. Available systematic reviews suggest that laser-based treatment is associated with lower recurrence rates than conventional surgery, but has no consistent effect on malignant transformation.[12] Core clinical determinants, including lesion characteristics, histopathology and the adequacy of surgical margins, are consistent across treatment modalities, supporting a principle-based rather than parameter-driven approach.[13,18] Several clinically relevant questions remain unresolved: whether laser therapy confers advantages beyond

its technical surgical benefits, whether recurrence is driven primarily by treatment modality or lesion biology, and how surgical margins, ablation depth and surgical procedures should be optimized according to histopathological risk.

Objectives

This narrative review, developed by the World Federation for Laser Dentistry (WFLD) study group through literature synthesis and expert consensus, aims to evaluate the clinical effectiveness, safety and applicability of laser-based treatments in the management of OL and to provide evidence-informed clinical recommendations. The specific objectives are to: (1) evaluate the clinical effectiveness of laser treatments, including lesion resolution, recurrence, symptom control, and malignant transformation risk, in comparison with conventional surgical and non-surgical approaches; (2) identify and compare laser modalities and technical procedures; (3) assess safety profiles, postoperative morbidity, and functional and aesthetic outcomes; (4) appraise methodological quality, heterogeneity and knowledge gaps; and (5) establish an initial framework for consensus-based clinical recommendations to guide standardized and safe use of lasers in OL management.

Methodology

This study was designed as a narrative review supported by an analysis of systematic reviews and meta-analyses. Selected methodological principles from the Joanna Briggs Institute (JBI) umbrella review framework were applied to ensure transparency, and reporting followed the PRISMA (Preferred Reporting Items for Systematic reviews and Meta-Analyses) 2020 guidelines.[19–22] The protocol was registered in the PROSPERO (International Prospective Register of Systematic Reviews) database (registration No. CRD420261287719).

PICO question

In patients with oral leukoplakia, does laser-based surgical treatment (excision, ablation or vaporization), compared with conventional surgery, pharmacological treatment or no intervention, improve lesion resolution, recurrence rates, postoperative morbidity, the risk of malignant transformation, and functional or aesthetic outcomes?

Search strategy and study selection

A structured literature search was conducted in PubMed/MEDLINE, Embase, Scopus, and the Cochrane Library using predefined strategies informed by the PICO framework and combining controlled vocabulary, where applicable, with free-text terms related to OL and laser-based interventions. The search covered studies published from January 1, 2016 to January 31, 2026. Broad review filters were applied, where available, in the respective databases. Eligibility was restricted during screening to systematic reviews and meta-analyses reporting extractable data relevant to OL. Records were screened independently by multiple reviewers in 2 stages: first, title and abstract screening, followed by full-text assessment. Disagreements were resolved through consensus. The complete database-specific search strategies and the number of records retrieved are presented in Table 1.

Table 1. Database search strategies, limits and the number of records retrieved

Database	Search syntax	Filters	Records retrieved, *n*
PubMed	("oral potentially malignant disorder*"[tiab] OR "oral potentially malignant lesion*"[tiab] OR "Leukoplakia, Oral"[MeSH] OR leukoplakia[tiab] OR "Lichen Planus, Oral"[MeSH] OR "oral lichen planus"[tiab] OR "Oral Submucous Fibrosis"[MeSH] OR "oral submucous fibrosis"[tiab]) AND ("Laser Therapy"[MeSH] OR "laser surgery"[tiab] OR laser*[tiab] OR "carbon dioxide laser"[tiab] OR "CO_2 laser"[tiab] OR "Er:YAG"[tiab] OR "Er,Cr:YSGG"[tiab] OR "diode laser"[tiab] OR "Nd:YAG"[tiab]) AND (treatment[tiab] OR therapy[tiab] OR excision[tiab] OR ablation[tiab] OR vaporization[tiab])	review; English; January 1, 2016–January 31, 2026	36
Embase	('oral potentially malignant disorder'/exp OR 'oral potentially malignant disorder*':ti,ab OR 'oral potentially malignant lesion*':ti,ab OR 'leukoplakia':ti,ab OR 'oral lichen planus'/exp OR 'oral submucous fibrosis'/exp) AND ('laser therapy'/exp OR 'laser surgery'/exp OR 'laser*':ti,ab OR 'carbon dioxide laser'/exp OR 'CO_2 laser':ti,ab OR 'er:yag laser'/exp OR 'er,cr:ysgg':ti,ab OR 'diode laser'/exp OR 'nd:yag':ti,ab) AND ('treatment':ti,ab OR 'therapy':ti,ab OR 'excision':ti,ab OR 'ablation':ti,ab OR 'vaporization':ti,ab)	review; English; January 1, 2016–January 31, 2026	41
Scopus	TITLE-ABS-KEY("oral potentially malignant disorder*" OR "oral potentially malignant lesion*" OR "leukoplakia" OR "oral lichen planus" OR "oral submucous fibrosis") AND TITLE-ABS-KEY("laser therapy" OR "laser surgery" OR "laser*" OR "CO_2 laser" OR "carbon dioxide laser" OR "Er:YAG" OR "Er,Cr:YSGG" OR "diode laser" OR "Nd:YAG") AND TITLE-ABS-KEY("treatment" OR "therapy" OR "excision" OR "ablation" OR "vaporization")	review; English; January 1, 2016–January 31, 2026	71
Cochrane Library	("oral potentially malignant disorder" OR "oral potentially malignant disorders" OR "oral potentially malignant lesion" OR "oral potentially malignant lesions" OR "OPMD" OR "leukoplakia" OR "oral leukoplakia" OR "oral lichen planus" OR "oral submucous fibrosis") AND ("laser therapy" OR "laser" OR "lasers" OR "laser treatment" OR "high power laser" OR "dental laser" OR "laser surgery" OR "Er:YAG laser" OR "Er,Cr:YSGG laser" OR "Nd:YAG laser" OR "diode laser" OR "CO_2 laser" OR "carbon dioxide laser")	Cochrane reviews; English; January 1, 2016–January 31, 2026	1

Data extraction

Three reviewers extracted data independently using a standardized, pilot-tested form. Extracted review-level information included study characteristics, patient populations, lesion characteristics, as well as anatomical sites, interventions, comparators, and follow-up periods. Laser-related data, where reported, included the laser system (CO_2, Er:YAG, Er,Cr:YSGG, diode, Nd:YAG, or potassium titanyl phosphate (KTP)), wavelength, power output, energy or radiant exposure, application mode, treatment duration, number of sessions, surgical margins, and ablation or excision depth. For laser-assisted photodynamic therapy (PDT), information on the photosensitizer, light source, wavelength, irradiation parameters, and the number of treatment sessions was also extracted, where available. Outcomes included lesion response or resolution, recurrence, malignant transformation, postoperative pain and complications, bleeding and hemostasis, functional and aesthetic outcomes, patient-reported symptoms, and adverse events. Discrepancies were resolved through consensus, with arbitration by an additional senior reviewer when necessary. Missing information was sought in supplementary materials or by contacting the corresponding authors and was recorded as "not reported" when it could not be retrieved. The extracted data was collated to assess the consistency and clinical applicability of the available evidence and to inform the development of the WFLD clinical recommendations.

Risk of bias and quality assessment

The methodological quality of each included review was assessed independently by 3 reviewers using a structured framework developed for this study, informed by AMSTAR-2 (A MeaSurement Tool to Assess systematic Reviews, version 2) and adapted to incorporate laser-specific domains relevant to reproducibility, technical transparency and clinical interpretation.

The assessment criteria included: (1) description of the laser system and its parameters (wavelength, power, fluence, and application mode); (2) definition of treatment protocols, the number of sessions, and a priori case selection criteria, including lesion subtype, clinical and histopathological features, and patient-related factors; (3) specification of outcomes, including lesion resolution, recurrence, postoperative morbidity, and malignant transformation; (4) inclusion of appropriate comparator groups; (5) transparent inclusion criteria and characterization of the patient population; (6) measures to control bias, including randomization, allocation concealment and blinding; (7) appropriateness and reproducibility of statistical analyses; (8) completeness of outcome and safety reporting, including follow-up duration; and (9) disclosure of funding and conflicts of interest.

Each domain was scored dichotomously (1 = fulfilled, 0 = not fulfilled), yielding a total score of 0–9. Reviews were categorized as having a low (7–9), moderate (4–6) or high (0–3) risk of bias. Disagreements were resolved through discussion or arbitration by a fourth reviewer. The framework was informed by the *Cochrane Handbook for Systematic Reviews of Interventions* and adapted to address heterogeneity in laser-specific reporting.[21]

Consensus development process

The evidence synthesis and consensus process was conducted by the WFLD study group, comprising clinicians and researchers with expertise in oral surgery, oral medicine, oral pathology, laser dentistry, and OPMDs. A structured review of the available evidence was combined with iterative expert discussions focused on clinically relevant principles and their practical implementation. Disagreements were resolved through further discussion until consensus was reached among the contributing experts. When evidence was limited or heterogeneous, clinical statements were intentionally formulated as conditional, principle-based recommendations rather than prescriptive treatment protocols. This evidence-informed and consensus-based approach was consistent with the methodology previously applied in the development of the official WFLD clinical recommendations for the laser-assisted management of other complex oral conditions. The objective was to provide a clinically oriented framework for the safe and appropriate use of lasers in the management of OL.

Results

Study selection

The database search identified 149 records (PubMed, n = 36; Embase, n = 41; Scopus, n = 71; and the Cochrane Library, n = 1). After the removal of 81 duplicates, 68 records underwent title and abstract screening, of which 55 were excluded. The remaining 13 reports were retrieved and assessed for eligibility. Two additional reports were identified through citation searching and assessed for eligibility. Of the 15 full-text reports assessed, 5 were excluded: 2 because they were not systematic reviews or meta-analyses; and 3 because they addressed laryngeal or vocal fold leukoplakia rather than OL. Ultimately, 10 systematic reviews and meta-analyses met the eligibility criteria and were included in the review (Fig. 1).

Risk of bias and quality assessment

Six reviews were classified as having a low risk of bias and 4 as having a moderate risk of bias; none was classified as having a high risk of bias. Reviews categorized as having a low risk of bias generally demonstrated transparent

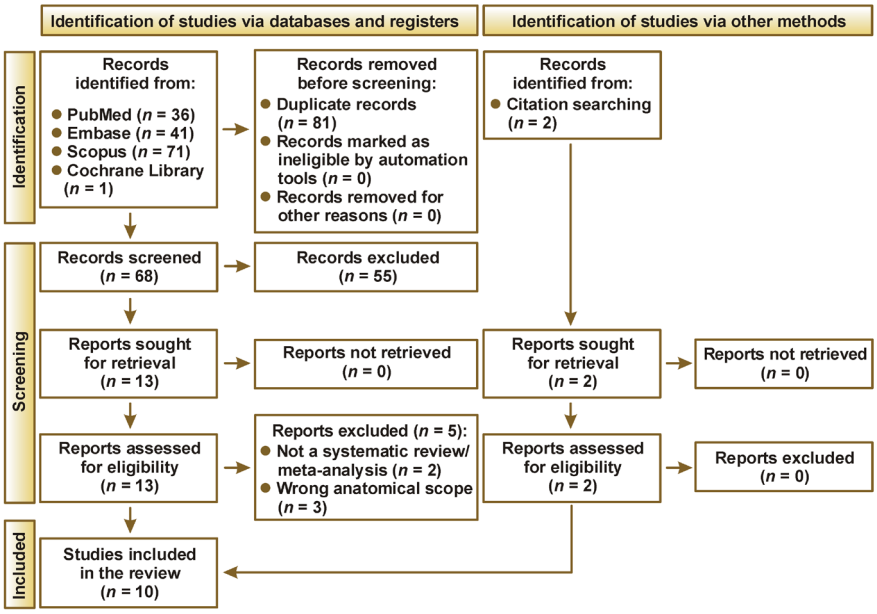

Fig. 1. PRISMA (Preferred Reporting Items for Systematic reviews and Meta-Analyses) 2020 flow diagram illustrating the study selection process

methodology, adequate reporting of intervention parameters, and appropriate statistical analyses.[12,13,23–26] Studies categorized as having a moderate risk of bias showed incomplete reporting of irradiation parameters, insufficient lesion characterization, absent or inadequately defined comparator groups, and limited assessment of potential confounding factors.[27–31] Common limitations across the included reviews encompassed substantial heterogeneity in treatment protocols, inconsistent outcome definitions, limited availability of randomized controlled trials (RCTs), and a potential overlap among primary studies. The extent of overlap among primary studies was not formally quantified. Detailed results are presented in Table 2.

Characteristics of the included reviews

The 10 included reviews evaluated CO_2, Er:YAG, Er,Cr:YSGG, Nd:YAG, diode, and KTP lasers, as well as laser-assisted PDT. Individual reviews included between 11 and 80 primary studies, although not all primary studies specifically addressed OL in reviews with broader eligibility

Table 2. Results of the risk-of-bias assessment

Study	Domain									Total score (0–9)	Risk of bias
	1	2	3	4	5	6	7	8	9		
Abdul 2025[27]	1	1	1	0	1	0	0	1	0	5	moderate
Bhattarai et al. 2024[23]	1	1	1	1	1	1	1	1	1	9	low
Datarkar et al. 2025[13]	1	1	1	1	1	1	1	1	1	9	low
Dong et al. 2019[28]	1	1	1	0	1	0	1	1	0	6	moderate
Gondivkar et al. 2018[24]	1	1	1	1	1	1	1	1	1	9	low
Li et al. 2019[29]	1	1	1	0	1	0	0	1	0	5	moderate
Luo et al. 2024[25]	1	1	1	1	1	1	1	1	1	9	low
Mogedas-Vegara et al. 2016[31]	1	1	1	0	1	0	0	1	0	5	moderate
de Pauli Paglioni et al. 2020[12]	1	1	1	1	1	1	1	1	1	9	low
Proaño-Haro et al. 2021[26]	1	1	1	0	1	1	1	1	1	8	low

Each domain was scored dichotomously (1 = fulfilled, 0 = not fulfilled). Reviews were categorized as having a low (7–9), moderate (4–6) or high (0–3) risk of bias.

criteria.[12,13,23–29,31] The CO_2 laser was the most extensively investigated modality and was evaluated in systematic reviews addressing recurrence, malignant transformation, postoperative outcomes, and comparisons with conventional surgery or other treatment modalities.[12,13,23,28,31] Although some analyses suggested favorable recurrence outcomes following CO_2 laser treatment, the findings were heterogeneous, and no consistent reduction in the risk of malignant transformation compared with conventional treatment was demonstrated.[12,28] Combined laser excision and vaporization were associated with particularly favorable recurrence outcomes in 1 large systematic review and meta-analysis.[23]

Evidence concerning Er:YAG and Er,Cr:YSGG lasers was derived primarily from a network meta-analysis and a limited number of comparative primary studies. These modalities achieved favorable rankings for selected outcomes, including recurrence, intraoperative bleeding and postoperative pain; however, the certainty and generalizability of these findings remained limited.[25] Evidence for diode, Nd:YAG and KTP lasers was comparatively sparse and was generally derived from small subsets of primary studies included in broader reviews.[12,23,25,31]

Three reviews evaluated PDT using photosensitizers such as 5-aminolevulinic acid (ALA), methylene blue (MB), Photofrin, Photosan, temoporfin (mTHPC; Foscan), hematoporphyrin derivatives, and chlorin e6.[24,27,29] Reported response rates varied substantially based on lesion type, photosensitizer, irradiation protocol, and outcome definition, limiting direct comparisons and the extrapolation of findings specifically to OL. The review addressing PVL reported a high pooled recurrence rate and found insufficient evidence that any available treatment reliably prevents recurrence in this particularly aggressive subtype.[26] Overall, substantial heterogeneity in lesion classification, intervention protocols, comparators, follow-up periods, and outcome definitions limited comparability across the included reviews. The characteristics of the included reviews are presented in Table 3.

Discussion

Clinical effectiveness of laser therapies

This narrative review contextualizes laser-assisted interventions within the broader principles governing OPMD management rather than serving as a purely technical review. Across the available evidence, recurrence control, adequate surgical margins, histopathological risk stratification, and long-term surveillance represent more clinically relevant determinants of outcome than the specific laser modality.

Laser-based therapies were most consistently associated with effective intraoperative hemostasis, reduced postoperative morbidity, and recurrence rates comparable to or lower than those observed following conventional surgery.[8,32–34] Potential advantages for the management of extensive or multifocal lesions have been suggested, although these observations are derived predominantly from heterogeneous observational data and therefore remain speculative. Lesion characteristics, dysplasia grade, multifocality, anatomical location, and margin adequacy were identified across multiple reviews as important determinants of recurrence and oncologic outcomes, irrespective of the laser modality used.[12,23,26,31]

Mechanisms of action and tissue interaction

CO_2 lasers (10,600 nm) exhibit high absorption in tissue water, enabling precise superficial ablation with limited peripheral thermal spread, and remain the most extensively studied modality for OL.[13,31,32] Er:YAG (2,940 nm) and Er,Cr:YSGG (2,780 nm) lasers exhibit even greater absorption in water, resulting in narrower thermal damage zones than those associated with CO_2 lasers (median (*Me*): 30.9 μm vs. 72.6 μm), with potential advantages for tissue preservation and healing. However, clinical evidence remains limited.[35–37] Diode (808–980 nm) and Nd:YAG (1,064 nm) lasers exhibit lower absorption in water and deeper tissue penetration, promoting hemostasis while potentially increasing the risk of collateral thermal damage if treatment parameters are not carefully controlled.[38] In anatomically sensitive areas, such as the gingiva and palate, a tangential rather than perpendicular approach may help minimize thermal injury to the periosteum, bone or dental structures.[14,39]

Recurrence rates

A 2024 systematic review and meta-analysis of 80 studies involving 7,614 samples reported a pooled recurrence proportion of approx. 22% for laser-based approaches, with a network meta-analysis indicating that combined protocols (excision followed by vaporization) ranked among the most favorable strategies for reducing recurrence.[23] A 2025 meta-analysis on CO_2 laser treatment reported a trend toward lower recurrence rates compared with other modalities (odds ratio (*OR*): 0.36, 95% *CI*: 0.12–1.04), although this difference did not reach statistical significance ($p = 0.06$).[13] Overall, the available data suggests a possible benefit of laser-assisted treatment in reducing recurrence rates, but the findings remain heterogeneous and inconclusive.

Postoperative outcomes

Laser-based therapies are generally associated with lower pain, improved hemostasis and reduced intraoperative bleeding compared with conventional surgery. An RCT reported significantly greater pain and swelling following cold blade surgery during the first 3 postoperative days

Table 3. Characteristics and key findings of the included systematic reviews and meta-analyses

Study	Study type	Primary studies included, *n*	Interventions	Databases searched	Publication years of included studies	Study designs	Results
Abdul 2025[27]	SR	11	PDT (ALA, MB)	PubMed, Embase, Cochrane Library, Scopus, Web of Science, CINAHL, PsycInfo	2005–2022	clinical studies	• ALA–PDT is an effective and well-tolerated treatment for oral potentially malignant disorders; however, treatment outcomes vary substantially depending on lesion type and biological behavior. • Treatment outcomes are strongly influenced by lesion-specific characteristics, including clinical subtype (e.g., leukoplakia vs. verrucous hyperplasia or erythroleukoplakia), as well as PDT parameters and treatment protocols. • The heterogeneity of the included lesion types limits direct extrapolation of the findings to OL alone, underscoring the need for disease-specific interpretation and individualized treatment strategies. • Standardized protocols and further well-designed studies, with stratification according to lesion type, are required to optimize clinical outcomes.
Bhattarai et al. 2024[23]	SR, MA	80	laser surgery, scalpel surgery, cryosurgery, PDT	Embase, PubMed, Scopus, Web of Science	1968–2024	RCTs, observational studies	• Laser-based surgery was associated with lower recurrence rates of OL than other surgical modalities. • Combined laser excision and vaporization was associated with the most favorable recurrence outcomes. • Higher recurrence rates were correlated with retromolar or multifocal OL, non-homogeneous lesions, older age, female sex, inadequate margins, retrospective study design, and betel quid chewing.
Datarkar et al. 2025[13]	SR, MA	16	CO_2 laser vs. scalpel, cryosurgery, diode laser	PubMed, Scopus, Embase, Web of Science, CENTRAL, PROSPERO, and others	2000–2023	RCTs, non-RCTs	• CO_2 laser demonstrated a statistically non-significant trend toward lower recurrence rates (*OR*: 0.36; $p = 0.06$). • No significant difference in postoperative pain was observed between treatments.
Dong et al. 2019[28]	SR, MA	24	CO_2 laser	Cochrane Library, Embase, PubMed, Web of Science, Scopus	NR (up to 2018)	RCTs, retrospective cohort studies, case–control studies, prospective studies	• A statistically non-significant trend toward a higher risk of malignant transformation was observed in males with homogeneous OL who did not use tobacco or alcohol. • Laser surgery has a limited influence on the risk of malignant transformation. • The available evidence is insufficient to identify risk factors for malignant transformation after CO_2 laser treatment.
Gondivkar et al. 2018[24]	SR	26	PDT (ALA, Photofrin, Photosan, mTHPC, hematoporphyrin derivatives, chlorin e6)	PubMed/MEDLINE, Google Scholar, Embase, ISI Web of Knowledge	1985–2015	RCTs, retrospective cohort studies, case–control studies, prospective studies	• PDT achieved a complete response in 22.58–100% of cases, a partial response in 4–66%, and no response in 0–38.70% of cases involving potentially malignant disorders. • In HNSCC, complete response rates ranged from 16% to 100%. • PDT appears to be effective in the management of oral potentially malignant disorders and HNSCC.
Li et al. 2019[29]	SR	16	PDT (ALA, Photofrin, MB, chlorin e6)	PubMed/MEDLINE, Embase, ISI Web of Knowledge, Ovid, CNKI, Wanfang Data	NR (up to 2018)	clinical studies	• PDT is a useful non-surgical treatment for OL. • The evidence remains insufficient due to the limited number of randomized trials, short follow-up periods and heterogeneous PDT protocols. • Well-designed RCTs with long-term follow-up and standardized parameters are required.
Luo et al. 2024[25]	SR, MA	11	Er:YAG laser, Er,Cr:YSGG laser, CO_2 laser + PDT, surgery	PubMed, Embase, Web of Science, Cochrane Library	1946–2023	RCTs	• Er,Cr:YSGG laser treatment was associated with the lowest estimated recurrence rate among the treatments compared. • Er,Cr:YSGG laser treatment ranked most favorably for recurrence reduction and pain reduction, whereas Er:YAG laser treatment was associated with reduced intraoperative bleeding. • No severe adverse events were reported. • For non-homogeneous OL, Er:YAG, Er,Cr:YSGG, and CO_2 + PDT may represent promising alternatives to surgery. • Further high-quality randomized trials are needed.
Mogedas-Vegara et al. 2016[31]	SR	33	CO_2 laser (including comparisons with cold knife surgery, Nd:YAG laser, KTP laser)	PubMed/MEDLINE	1981–2015	retrospective and prospective clinical studies, comparative studies	• CO_2 laser is the standard treatment approach for OL due to its high efficacy and low morbidity. • Randomized comparative trials evaluating other laser modalities are lacking. • Risk factors for recurrence and malignant transformation remain undefined.
de Pauli Paglioni et al. 2020[12]	SR, MA	36	CO_2 laser, Nd:YAG laser, Er:YAG laser, KTP laser, diode lasers vs. conventional surgery or no control	PubMed/MEDLINE, Scopus, Embase	NR (up to 2019)	RCTs, retrospective cohort studies, case–control studies, prospective studies	• Laser excision of OL may be associated with lower recurrence rates compared with conventional treatment. • No reduction in the risk of malignant transformation has been demonstrated.
Proaño-Haro et al. 2021[26]	SR, MA	12	CO_2 laser	PubMed/MEDLINE, Embase, Web of Science	1985–2020	clinical trials, retrospective and longitudinal observational studies, case series (≥10 patients)	• A global effect MA of pooled proportions demonstrated a recurrence rate of 67.2% (95% *CI*: 48.3–81.8). • The available evidence is insufficient to conclude that any available treatment strategy effectively reduces recurrence in proliferative verrucous leukoplakia.

SR – systematic review; MA – meta-analysis; NR – no restriction; 95% *CI* – 95% confidence interval; PDT – photodynamic therapy; ALA – 5-aminolevulinic acid; MB – methylene blue; mTHPC – meta-tetra(hydroxyphenyl) chlorin; Er:YAG – erbium-doped yttrium aluminium garnet; Er,Cr:YSGG – erbium, chromium-doped yttrium, scandium, gallium, and garnet; Nd:YAG – neodymium-doped yttrium aluminium garnet; KTP – potassium titanyl phosphate; CINAHL – Cumulative Index to Nursing and Allied Health Literature; CENTRAL – Cochrane Central Register of Controlled Trials; PROSPERO – International Prospective Register of Systematic Reviews; CNKI – China National Knowledge Infrastructure; OL – oral leukoplakia; *OR* – odds ratio; HNSCC – head and neck squamous cell carcinoma; RCTs – randomized controlled trials.

($p < 0.05$),[40] while another RCT comparing CO_2 laser, Er:YAG and conventional scalpel surgery demonstrated significantly shorter operative times with laser-based approaches ($p < 0.001$) and less intraoperative bleeding with the CO_2 laser ($p < 0.001$).[37] However, a 2025 meta-analysis found no significant differences in postoperative pain between CO_2 laser treatment and other modalities (standardized mean difference (*SMD*): –0.16, 95% *CI*: –1.37–1.05),[13] reflecting substantial variability among the studies. These findings should be interpreted with caution given the heterogeneity in study designs and the limited availability of high-quality randomized evidence.[14,37,39–42]

Lesion resolution

Complete response rates following laser therapy vary considerably, ranging from approx. 50% to over 90%, depending on lesion characteristics, the degree of dysplasia, multifocality, and treatment modality. A prospective study using a high-power diode laser (808 nm) reported a complete response in 93.5% of cases, with a low recurrence rate during follow-up,[14] while Er:YAG laser treatment demonstrated complete and partial responses in a substantial proportion of lesions, although recurrence remained a concern.[14,35] A retrospective study using a CO_2 laser noted a permanent treatment success rate of 97.8% at 6-year follow-up after complete excision to a depth of ≥1 mm with a 3-mm margin of healthy-appearing tissue. However, the cohort comprised predominantly homogeneous leukoplakias without dysplasia, suggesting that the favorable outcomes may reflect lesion characteristics rather than the technical superiority of the laser modality.[15]

Photodynamic therapy as an adjunctive approach

Photodynamic therapy combines a photosensitizing agent, commonly ALA or MB, a light source operating in the red spectrum (approx. 630–660 nm), and molecular oxygen to generate reactive oxygen species (ROS) that exert cytotoxic effects on dysplastic cells. Systematic reviews have reported substantial heterogeneity in photosensitizers, irradiation parameters, treatment schedules, lesion characteristics, and outcome definitions.[24,27,29] A systematic review addressing OL reported pooled complete and partial response rates of 32.9% and 43.2%, respectively, corresponding to an overall response rate of 76.1%.[29] Ablative fractional laser-assisted PDT achieved an overall positive response rate of 87.5%, including a complete response rate of 62.5%, in a retrospective study with a 3-year follow-up period.[43] Photodynamic therapy with ALA has also demonstrated promising clinical outcomes, suggesting that laser pre-treatment may improve photosensitizer penetration in selected lesions.[34] Nevertheless, the available evidence remains heterogeneous, and these findings do not establish the superiority of any specific photosensitizer, light source or laser-assisted PDT protocol.[24,25,27,29]

Malignant transformation

The available evidence has not demonstrated a consistent or statistically significant difference in malignant transformation rates following laser therapy compared with conventional treatment approaches. Reported rates range from approx. 1% to 15%, with longer follow-up generally associated with higher cumulative rates.[12,32,44–48] Recurrent leukoplakia is associated with an approx. 7-fold higher risk of malignant transformation compared with non-recurrent lesions,[23] highlighting the clinical importance of long-term disease monitoring. Established risk factors include dysplasia severity, lesion heterogeneity, anatomical location, and recurrence status.[28,49,50] The risk of malignant transformation appears to be influenced primarily by lesion biology and patient-related factors rather than the surgical modality employed.

Comparative effectiveness of laser devices

The CO_2 laser has the largest evidence base among the laser modalities used for OL, with studies reporting favorable recurrence control, effective hemostasis and acceptable postoperative outcomes. Nevertheless, the available evidence remains heterogeneous, and neither consistent superiority over other surgical approaches nor a reduction in the risk of malignant transformation has been demonstrated.[12,13,23,28,31]

The Er:YAG laser produces a narrower zone of thermal damage than the CO_2 laser, which may be advantageous for tissue preservation and histopathological assessment.[37] In a retrospective comparative study, Er:YAG treatment was associated with a significantly better clinical outcome than conventional scalpel surgery ($p = 0.015$). However, no significant overall differences were observed among the 5 treatment modalities evaluated.[45] The consistent superiority of Er:YAG laser treatment over CO_2 laser treatment or conventional surgery has not been established in systematic reviews.[12,25,31]

Diode lasers provide effective hemostasis and may facilitate outpatient excision or ablation of OL. However, the available evidence is derived predominantly from small observational or non-comparative studies, and robust conclusions regarding recurrence control and oncologic outcomes cannot be drawn.[14,38,51–53]

Evidence concerning the KTP laser remains limited. A retrospective comparative study reported a lower recurrence rate following KTP laser treatment than after CO_2 laser treatment.[52] However, the available systematic reviews and limited comparative evidence are insufficient to establish the superiority of the KTP laser over the CO_2 laser or other laser modalities.[12,31,52] The selection of a laser modality should therefore be guided by lesion characteristics, anatomical location, the intended surgical procedure, histopathological requirements, and operator experience.

Table 4. Results of studies reporting surgical margin widths and excision depths in relation to the reduction of recurrence of oral leukoplakia (OL)

Study	Lesions evaluated	Peripheral surgical margin width	Depth
Nammour et al. 2017[15]	homogeneous OL	3 mm	minimum 1 mm
Romeo et al. 2020[61]	non-dysplastic OL	≥3 mm	~1 mm
Shivhare et al. 2022[55]	mixed homogeneous and non-homogeneous OL	3–4 mm	ablation: 1 mm excision: 3–5 mm
Vilar-Villanueva et al. 2023[56]	OL	≥3 mm	not specified
Dutra et al. 2026[57]	OL (91 studies included in a scoping review)	≥5 mm recommended	not specified

Technical considerations and optimal parameters

Adequate surgical margin width is a critical determinant of recurrence rates in homogeneous OL, with favorable and sustained outcomes reported even during long-term follow-up.[15] Surgical margins of ≤3 mm have been associated with higher recurrence rates, whereas margins of 3–5 mm may reduce the risk of recurrence.[54–56] However, this relationship varies considerably according to lesion subtype. Proliferative verrucous leukoplakia exhibits high recurrence rates even with surgical margins that exceed 3 mm. In general, a margin extension of 5 mm is considered optimal.[57] For vaporization, a safety margin of approx. 3 mm beyond the clinically visible lesion boundary has been associated with lower recurrence rates ($p < 0.05$) (Table 4).[15,58–61]

Collectively, these findings support lesion-specific surgical planning rather than uniform excision protocols.

Diagnostic utility

Incisional biopsy with histopathological evaluation remains mandatory before any treatment of OL, regardless of the surgical modality used. Laser-induced thermal effects may alter tissue architecture, potentially affecting histopathological interpretation and the assessment of surgical margins. The intraoperative and postoperative clinical advantages of laser surgery, including improved hemostasis and reduced morbidity, are well documented. However, current evidence does not support the diagnostic superiority of lasers over conventional biopsy techniques. These considerations highlight the importance of appropriate surgical technique and wavelength selection when laser-assisted biopsy is performed.[61–65]

Safety and complications

The findings of this review indicate that laser-based therapies for OL are generally well tolerated and associated with low complication rates. Serious adverse events were infrequently reported, with most studies noting minimal postoperative morbidity.[25,32,34] Common transient side effects include mild to moderate pain, swelling and temporary limitation of mouth opening, typically peaking within the first few days after treatment.[48] Wound healing is generally satisfactory, with minimal scarring, although variability in healing time has been reported, with some cases requiring several weeks for complete re-epithelialization.[60] Rare complications, including pyogenic granuloma formation, fibrosis and persistent discomfort have been described.[39,45,60] The reporting of adverse events remains inconsistent across studies, which may limit the accuracy of safety assessments.[12,32,33,46] As expected, no association between surgical modality (laser-based or conventional) and the risk of malignant transformation has been demonstrated. The risk of malignant transformation appears to be influenced by the biological and histological characteristics of the lesions and a history of head and neck cancer.[66] Nevertheless, these findings must be interpreted with caution due to the limited availability of long-term oncologic data (Table 5).[12,32,33,45,67]

Limitations of the evidence

This narrative review confirms that the overall quality of the available evidence remains limited. Substantial clinical and methodological heterogeneity in laser devices, treatment parameters and protocols precludes reliable quantitative synthesis. Outcome definitions, including those for recurrence rates, lesion resolution and malignant transformation, varied considerably, and long-term follow-up was frequently insufficient. The majority of the studies were small, non-randomized and inadequately controlled. These limitations underscore the need for well-designed RCTs with standardized protocols, uniform outcome evaluation and long-term follow-up.

Limitations of the review process

The search was restricted to English-language publications, and gray literature was excluded, introducing a potential risk of language and publication bias. Relevant clinical data was frequently unavailable, preventing subgroup analyses according to dysplasia grade, lesion site or history of exposure to relevant risk factors. Future studies

Table 5. Summary of laser modalities, treatment parameters, clinical effects, and levels of evidence

Laser modality	Wavelength [nm]	Application mode	Commonly reported treatment parameters	Key clinical effects	Level of evidence	Key references
CO_2 laser	10,600	excision, ablation, vaporization	power output: 4–6 W; focused or defocused mode; safety margin: ≥3 mm	most extensively studied laser modality; effective hemostasis and generally favorable postoperative outcomes; varying recurrence outcomes across studies	high	12,13,15,28,31,32,44,47,52
Er:YAG laser	2,940	excision, ablation	pulse energy: ~50 mJ; frequency ~50 Hz; shallow penetration	narrower zone of thermal damage (~30.9 µm); favorable healing; reduced scarring; variable recurrence rates	moderate	12,25,35–37,45
Er,Cr:YSGG laser	2,780	excision, ablation	treatment parameters were variably reported and often grouped with those of Er:YAG lasers	reduced thermal injury; limited recurrence and oncologic outcomes	low to moderate	25,34
Diode laser	808–980	excision, ablation	continuous-wave mode; power output: 1.5–2.0 W	high complete response rates of up to 93.5%; excellent hemostasis; minimal postoperative pain; feasibility of outpatient treatment	moderate	14,38,53,55,60
Nd:YAG laser	1,064	ablation, coagulation	parameters inconsistently reported	deep tissue penetration; effective coagulation; increased risk of collateral thermal damage	low	12,31,33,36,59,62
KTP laser	532	excision, ablation	parameters inconsistently reported	lower recurrence than CO_2 laser treatment in a comparative study; effective vascular control	low	12,31,52
Laser-assisted PDT (ALA–PDT, MB–PDT)	light source-dependent	ablation + PDT	ALA, MB, Photofrin, Photosan, Foscan, hematoporphyrin derivatives, or chlorin e6; irradiation parameters and the number of sessions varied considerably	overall response of approx. 76.1% in a systematic review; a response of 87.5% for ablative fractional laser-assisted PDT; promising outcomes with Waterlase-assisted ALA–PDT, but protocols remained heterogeneous	moderate	24,25,27,29,34,43

The parameters shown are examples reported in individual studies and should not be interpreted as standardized or universally recommended settings. Selection must take into account the device, delivery system, tissue characteristics, and treatment objective.

may benefit from integrating an expert consensus with structured evidence synthesis to minimize subjective interpretation and facilitate the development of clear recommendations based strictly on clinical and histopathological considerations.

Implications for practice, policy and future research

Laser-based therapies are a valid treatment option for selected patients with OL, particularly when lesion extent, multifocality or anatomical constraints limit conventional surgery. Laser excision enables precise lesion removal with effective hemostasis, whereas laser ablation may be considered for superficial or anatomically challenging lesions. The use of lasers does not eliminate the need for histopathological assessment, risk-stratified patient selection or long-term surveillance, all of which remain essential components of OL management. Consensus-based frameworks addressing indications for excision versus vaporization, safety margins, the documentation of laser parameters, and follow-up standards are urgently needed, alongside structured training and credentialing. Future RCTs should compare laser modalities with conventional surgery, incorporate extended follow-up periods, and stratify patients according to dysplasia grade and lesion subtype, with endpoints including recurrence-free survival, malignant transformation and quality of life.

Conclusions

Laser-based management of OL offers surgical precision, tissue preservation and reduced postoperative morbidity, with recurrence rates comparable to or lower than those associated with conventional surgery when adequate surgical margins and complete removal of the lesion to an adequate depth are achieved.

Current evidence does not demonstrate a consistent effect of laser treatment on the risk of malignant transformation in OL, which appears to be influenced by lesion biology and patient-related factors. Clinical management should integrate histopathological findings, lesion characteristics and the patient's individual risk profile, with an emphasis on surgical margin control, case selection and long-term follow-up. Within the limitations of the available evidence, laser-based therapies constitute a clinically justified component of contemporary OL management when applied within a structured framework, encompassing diagnosis, adequate procedures and surveillance.

Table 6. General therapeutic principles for laser-based management of oral leukoplakia (OL)

Principle	Clinical recommendation
Histopathological assessment is mandatory	Histopathological assessment is mandatory before laser treatment. Representative tissue samples should be obtained and evaluated prior to laser excision, ablation or vaporization.
Laser therapy is a technical modality, not a biological modifier	Laser treatment provides surgical advantages (improved hemostasis, precision and reduced morbidity) but does not eliminate field cancerization or the lesion's intrinsic malignant potential.
Patient selection and risk stratification are essential	Treatment planning should consider lesion subtype (homogeneous vs. non-homogeneous), size, anatomical location, severity of dysplasia, multifocality, history of recurrence, history of squamous cell carcinoma of the upper aerodigestive tract, and patient-related risk factors (tobacco use, alcohol consumption, age, and comorbidities).
Recurrence prevention is a primary clinical objective	Complete lesion removal with adequate surgical margins should be prioritized over superficial ablation. Surgical margin width should be determined according to histopathological findings.
Recommended surgical margins (guidance framework)	≥3 mm for lesions without dysplasia; ≥5 mm for lesions with mild to moderate dysplasia; ≥10 mm for lesions with severe dysplasia or carcinoma in situ
Management of suspected or microinvasive carcinoma	Preoperative imaging (e.g., MRI) is recommended. Surgical excision should include margins of ≥1 cm in all directions; lesions involving the gingiva or hard palate may require resection of the underlying bone (osteotomy).
Laser parameters and treatment intent must be documented	Detailed and transparent reporting of the laser wavelength, power output, energy settings, and treatment protocol is essential for reproducibility and clinical interpretation, even when strict standardization is not feasible.

MRI – magnetic resonance imaging.

General principles for the clinical management of oral leukoplakia according to the WFLD study group

Laser-based interventions in OL may serve as: (A) adjuncts to clinical examination; (B) diagnostic support through laser-assisted biopsy; and (C) surgical management with adequate margin control and complete lesion depth ablation control. The consensus-informed clinical principles developed by the WFLD study group are summarized in Table 6.

General therapeutic principles

1. Histopathological assessment is mandatory before laser management. Following histopathological assessment, laser ablation may be considered for appropriately selected lesions.
2. Laser treatment represents a surgical modality rather than a biological modifier. It does not eliminate field cancerization or the intrinsic malignant potential of the lesion.
3. Risk stratification is essential, incorporating lesion subtype, size, location, dysplasia grade, multifocality, history of recurrence, prior squamous cell carcinoma of the upper aerodigestive tract, and patient-related risk factors, including tobacco use, alcohol consumption and relevant comorbidities.
4. Recurrence prevention requires complete lesion removal, with adequate surgical margins tailored to the histopathological risk:
   - ≥3 mm of clinically healthy-appearing marginal mucosa, with complete lesion ablation to an appropriate depth, for lesions without dysplasia;
   - ≥5 mm for lesions with mild to moderate dysplasia;
   - ≥10 mm for lesions with severe dysplasia or carcinoma in situ. When microinvasive carcinoma is suspected, preoperative magnetic resonance imaging (MRI) is recommended. Surgical margins of ≥1 cm are required, and osteotomy should be considered for gingival or palatal localizations.

Safety and operator requirements

Procedures should be performed by clinicians with appropriate training in laser dentistry and OPMD management, in accordance with established laser safety standards. Patients must be informed that laser therapy does not eliminate the need for long-term surveillance.

Trial registration

The study was registered prospectively in the PROSPERO database (registration No. CRD420261287719).

Ethics approval and consent to participate

Not applicable.

Data availability

The datasets generated and/or analyzed during the current study are available from the corresponding author on reasonable request.

Consent for publication

Not applicable.

Use of AI and AI-assisted technologies

AI-assisted tool (Grammarly AI; Superhuman Platform Inc., San Francisco, USA) was used exclusively for language editing and improvement of readability. No AI tools were used for data analysis, interpretation or generation of scientific conclusions. All content was reviewed and approved by the authors.

ORCID iDs

Kinga Grzech-Leśniak https://orcid.org/0000-0002-5700-4577
Paolo Vescovi https://orcid.org/0000-0002-2223-3716
Georgios Romanos https://orcid.org/0000-0002-7745-5957
Rafał Wiench https://orcid.org/0000-0001-5673-7413
Jakub Fiegler-Rudol https://orcid.org/0009-0009-3173-9389
Ilaria Giovannacci https://orcid.org/0000-0001-8157-4046
Janina Golob Deeb https://orcid.org/0000-0002-3189-0136
Zuzanna Grzech-Leśniak https://orcid.org/0000-0001-6109-6809
Jacek Matys https://orcid.org/0000-0002-3801-0218
Aldo Brugnera Junior https://orcid.org/0000-0002-8634-743X
Mariusz Szuta https://orcid.org/0000-0002-7182-4811
Sajee Sattayut https://orcid.org/0000-0001-7111-9381
Praveen Arany https://orcid.org/0000-0002-6116-2340
Marco Meleti https://orcid.org/0000-0002-9111-3224
Maha Taalab https://orcid.org/0000-0003-3586-6747
Josep Arnabat-Dominguez https://orcid.org/0000-0003-1653-8043
Alessandro Del Vecchio https://orcid.org/0009-0002-7768-6074
Jamil Awad Shibli https://orcid.org/0000-0003-1971-0195
Maciej Misiołek https://orcid.org/0000-0002-8476-9153
Octavi Camps-Font https://orcid.org/0000-0001-9991-2226
Akira Aoki https://orcid.org/0000-0002-2504-2894
Umberto Romeo https://orcid.org/0000-0003-2439-2187
Samir Nammour https://orcid.org/0000-0003-0321-9764

References

1. Dunn LA, Ho AL, Pfister DG. Head and neck cancer: A review. *JAMA*. 2026;335(6):531–541. doi:10.1001/jama.2025.21733
2. Villa A, Lodolo M, Ha P. Oncological outcomes of patients with oral potentially malignant disorders. *JAMA Otolaryngol Head Neck Surg*. 2025;151(1):65–71. doi:10.1001/jamaoto.2024.3719
3. Iocca O, Sollecito TP, Alawi F, et al. Potentially malignant disorders of the oral cavity and oral dysplasia: A systematic review and meta-analysis of malignant transformation rate by subtype. *Head Neck*. 2020;42(3):539–555. doi:10.1002/hed.26006
4. Mello FW, Miguel AFP, Dutra KL, et al. Prevalence of oral potentially malignant disorders: A systematic review and meta-analysis. *J Oral Pathol Med*. 2018;47(7):633–640. doi:10.1111/jop.12726
5. Khodadadi M, Khodadadi M. Malignant transformation rate of oral precancerous disorders to oral cancer: Systematic review and meta-analysis of the current evidence. *Front Oral Health*. 2025;6:1673474. doi:10.3389/froh.2025.1673474
6. Pimenta-Barros LA, Ramos-García P, González-Moles MÁ, Aguirre-Urizar JM, Warnakulasuriya S. Malignant transformation of oral leukoplakia: Systematic review and comprehensive meta-analysis. *Oral Dis*. 2025;31(1):69–80. doi:10.1111/odi.15140
7. Fatih MT, Mahmood MK, Garib BT, et al. Malignant transformation of oral leukoplakia and proliferative verrucous leukoplakia and its biomarker predictors: A systematic umbrella review. *Head Neck*. 2026;48(1):246–260. doi:10.1002/hed.70073
8. Lodolo M, Valor J, Villa A. Randomized controlled trials for oral leukoplakia. *Oral Dis*. 2025;31(11):3034–3038. doi:10.1111/odi.15399
9. Gates JC, Abouyared M, Shnayder Y, et al. Clinical management update of oral leukoplakia: A review from the American Head and Neck Society Cancer Prevention Service. *Head Neck*. 2025;47(2):733–741. doi:10.1002/hed.28013
10. Lodi G, Franchini R, Warnakulasuriya S, et al. Interventions for treating oral leukoplakia to prevent oral cancer. *Cochrane Database Syst Rev*. 2016;7(7):CD001829. doi:10.1002/14651858.CD001829.pub4
11. Pentenero M, Sutera S, Lodi G, Bagan JV, Farah CS. Oral leukoplakia diagnosis and treatment in Europe and Australia: Oral medicine practitioners' attitudes and practice. *Oral Dis*. 2023;29(8):3214–3222. doi:10.1111/odi.14301
12. de Pauli Paglioni M, Migliorati CA, Schausltz Pereira Faustino I, et al. Laser excision of oral leukoplakia: Does it affect recurrence and malignant transformation? A systematic review and meta-analysis. *Oral Oncol*. 2020;109:104850. doi:10.1016/j.oraloncology.2020.104850
13. Datarkar A, Shah V, Pandilwar P, Daware S, Datarkar S, Godase P. Is CO_2 laser effective in the surgical management of oral potentially malignant disorders? A systematic review and meta-analysis. *Lasers Med Sci*. 2025;40(1):132. doi:10.1007/s10103-025-04396-w
14. de Arruda JAA, Silva LVDO, Kato CDNAO, et al. Management of oral leukoplakia with an 808-nm high-power diode laser: A single-center experience. *Lasers Med Sci*. 2023;38(1):141. doi:10.1007/s10103-023-03806-1
15. Nammour S, Zeinoun T, Namour A, Vanheusden A, Vescovi P. Evaluation of different laser-supported surgical protocols for the treatment of oral leukoplakia: A long-term follow-up. *Photomed Laser Surg*. 2017;35(11):629–638. doi:10.1089/pho.2016.4256
16. Grzech-Leśniak K. Lasers in dentistry – overview based on FDI policy statement. *Int Dent J*. 2026;76(2):109369. doi:10.1016/j.identj.2025.109369
17. Palaia G, Bellisario A, Pampena R, Pippi R, Romeo U. Oral proliferative verrucous leukoplakia: Progression to malignancy and clinical implications. Systematic review and meta-analysis. *Cancers (Basel)*. 2021;13(16):4085. doi:10.3390/cancers13164085
18. Parker S, Grzech-Leśniak K, Cronshaw M, Matys J, Brugnera AJ, Nammour S. Full operating parameter recording as an essential component of the reproducibility of laser-tissue interaction and treatments. *Adv Clin Exp Med*. 2024;33(6):653–656. doi:10.17219/acem/189795
19. Aromataris E, Stern C, Lockwood C, et al. JBI series paper 2: Tailored evidence synthesis approaches are required to answer diverse questions: A pragmatic evidence synthesis toolkit from JBI. *J Clin Epidemiol*. 2022;150:196–202. doi:10.1016/j.jclinepi.2022.04.006
20. Page MJ, McKenzie JE, Bossuyt PM, et al. The PRISMA 2020 statement: An updated guideline for reporting systematic reviews. *BMJ*. 2021;372:n71. doi:10.1136/bmj.n71
21. Higgins JPT, Thomas J, Chandler J, et al. *Cochrane Handbook for Systematic Reviews of Interventions*. Hoboken, USA: John Wiley & Sons; 2019. doi:10.1002/9781119536604
22. Eriksen MB, Frandsen TF. The impact of patient, intervention, comparison, outcome (PICO) as a search strategy tool on literature search quality: A systematic review. *J Med Libr Assoc*. 2018;106(4):420–431. doi:10.5195/jmla.2018.345
23. Bhattarai BP, Singh AK, Singh RP, et al. Recurrence in oral leukoplakia: A systematic review and meta-analysis. *J Dent Res*. 2024;103(11):1066–1075. doi:10.1177/00220345241266519
24. Gondivkar SM, Gadbail AR, Choudhary MG, Vedpathak PR, Likhitkar MS. Photodynamic treatment outcomes of potentially-malignant lesions and malignancies of the head and neck region: A systematic review. *J Invest Clin Dent*. 2018;9(1). doi:10.1111/jicd.12270
25. Luo R, Wang Y, Li R, et al. Laser therapy decreases oral leukoplakia recurrence and boosts patient comfort: A network meta-analysis and systematic review. *BMC Oral Health*. 2024;24(1):469. doi:10.1186/s12903-024-04179-9
26. Proaño-Haro A, Bagan L, Bagan JV. Recurrences following treatment of proliferative verrucous leukoplakia: A systematic review and meta-analysis. *J Oral Pathol Med*. 2021;50(8):820–828. doi:10.1111/jop.13178
27. Abdul NS. A systematic review on the effectiveness of photodynamic therapy in the treatment of oral precancerous lesions and oral cancers. *J Pharm Bioallied Sci*. 2025;17(Suppl 4):S2862–S2866. doi:10.4103/jpbs.jpbs_1361_25
28. Dong Y, Chen Y, Tao Y, et al. Malignant transformation of oral leukoplakia treated with carbon dioxide laser: A meta-analysis. *Lasers Med Sci*. 2019;34(1):209–221. doi:10.1007/s10103-018-2674-7
29. Li Y, Wang B, Zheng S, He Y. Photodynamic therapy in the treatment of oral leukoplakia: A systematic review. *Photodiagnosis Photodyn Ther*. 2019;25:17–22. doi:10.1016/j.pdpdt.2018.10.023

30. Sattayut S, Srisilapanan P, Patcharanuchat P. Utilizing laser therapy to manage oral potentially malignant disorders in older adults at the primary care level. *Adv Clin Exp Med*. 2024;33(10):1033–1037. doi:10.17219/acem/193604
31. Mogedas-Vegara A, Hueto-Madrid JA, Chimenos-Küstner E, Bescós-Atín C. Oral leukoplakia treatment with the carbon dioxide laser: A systematic review of the literature. *J Craniomaxillofac Surg*. 2016;44(4):331–336. doi:10.1016/j.jcms.2016.01.026
32. Mogedas-Vegara A, Hueto-Madrid JA, Chimenos-Küstner E, Bescós-Atín C. The treatment of oral leukoplakia with the CO_2 laser: A retrospective study of 65 patients. *J Craniomaxillofac Surg*. 2015;43(5):677–681. doi:10.1016/j.jcms.2015.03.011
33. Ishii J, Fujita K, Komori T. Laser surgery as a treatment for oral leukoplakia. *Oral Oncol*. 2003;39(8):759–769. doi:10.1016/S1368-8375(03)00043-5
34. Ou J, Gao Y, Li H, Ling T, Xie X. Application of 5-aminolevulinic acid-mediated Waterlase-assisted photodynamic therapy in the treatment of oral leukoplakia. *Sci Rep*. 2022;12(1):9391. doi:10.1038/s41598-022-13497-3
35. Jurczyszyn K, Kozakiewicz M. Application of texture and fractal dimension analysis to estimate effectiveness of oral leukoplakia treatment using an Er:YAG laser – a prospective study. *Materials (Basel)*. 2020;13(16):3614. doi:10.3390/ma13163614
36. Schwarz F, Maraki D, Yalcinkaya S, Bieling K, Böcking A, Becker J. Cytologic and DNA-cytometric follow-up of oral leukoplakia after CO_2- and Er:YAG-laser assisted ablation: A pilot study. *Lasers Surg Med*. 2005;37(1):29–36. doi:10.1002/lsm.20188
37. Suter VGA, Altermatt HJ, Bornstein MM. A randomized controlled trial comparing surgical excisional biopsies using CO_2 laser, Er:YAG laser and scalpel. *Int J Oral Maxillofac Surg*. 2020;49(1):99–106. doi:10.1016/j.ijom.2019.05.012
38. Romanos G, Nentwig GH. Diode laser (980 nm) in oral and maxillofacial surgical procedures: Clinical observations based on clinical applications. *J Clin Laser Med Surg*. 1999;17(5):193–197. doi:10.1089/clm.1999.17.193
39. Arora KS, Bansal R, Mohapatra S, Verma A, Sharma S, Pareek S. Prevention of malignant transformation of oral leukoplakia and oral lichen planus using laser: An observational study. *Asian Pac J Cancer Prev*. 2018;19(12):3635–3641. doi:10.31557/APJCP.2018.19.12.3635
40. López-Jornet P, Camacho-Alonso F. Comparison of pain and swelling after removal of oral leukoplakia with CO_2 laser and cold knife: A randomized clinical trial. *Med Oral Patol Oral Cir Bucal*. 2013;18(1):e38–e44. doi:10.4317/medoral.17960
41. Grzech-Leśniak K, Wiench R, Shibli JA, et al. Laser therapies as the adjunctive treatment of medication-related osteonecrosis of the jaw: Evidence synthesis and clinical recommendations. Official recommendations of the World Federation for Laser Dentistry (WFLD) and the Polish Society for Laser Dentistry (PTSL) [published online as ahead of print on May 14, 2026]. *Dent Med Probl*. 2026. doi:10.17219/dmp/220709
42. Warnakulasuriya S, Kujan O, Aguirre-Urizar JM, et al. Oral potentially malignant disorders: A consensus report from an international seminar on nomenclature and classification, convened by the WHO Collaborating Centre for Oral Cancer. *Oral Dis*. 2021;27(8):1862–1880. doi:10.1111/odi.13704
43. Yao YL, Wang YF, Li CX, Wu L, Tang GY. Management of oral leukoplakia by ablative fractional laser-assisted photodynamic therapy: A 3-year retrospective study of 48 patients. *Lasers Surg Med*. 2022;54(5):682–687. doi:10.1002/lsm.23534
44. van der Hem PS, Nauta JM, van der Wal JE, Roodenburg JLN. The results of CO_2 laser surgery in patients with oral leukoplakia: A 25 year follow up. *Oral Oncol*. 2005;41(1):31–37. doi:10.1016/j.oraloncology.2004.06.010
45. Monteiro L, Barbieri C, Warnakulasuriya S, et al. Type of surgical treatment and recurrence of oral leukoplakia: A retrospective clinical study. *Med Oral Patol Oral Cir Bucal*. 2017;22(5):e520–e526. doi:10.4317/medoral.21645
46. Schoelch ML, Sekandari N, Regezi JA, Silverman S. Laser management of oral leukoplakias: A follow-up study of 70 patients. *Laryngoscope*. 1999;109(6):949–953. doi:10.1097/00005537-199906000-00021
47. Rodriguez-Lujan A, López-Jornet P, Pons-Fuster López E. Recurrence of oral leukoplakia after CO_2 laser resection: A prospective longitudinal study. *Cancers (Basel)*. 2022;14(21):5455. doi:10.3390/cancers14215455
48. Bagan J, Martorell M, Cebrián JL, et al. Effect of clinical and histologic features on time to malignancy in 224 cases of oral leukoplakia treated by surgery. *Clin Oral Investig*. 2022;26(8):5181–5188. doi:10.1007/s00784-022-04486-x
49. Tenore G, Mohsen A, Fantozzi PJ, et al. Risk assessment for malignant transformation in patients with oral proliferative leukoplakia: A 10-year retrospective cohort study. *Cancers (Basel)*. 2025;18(1):2. doi:10.3390/cancers18010002
50. Pentenero M, Meleti M, Vescovi P, Gandolfo S. Oral proliferative verrucous leucoplakia: Are there particular features for such an ambiguous entity? A systematic review. *Br J Dermatol*. 2014;170(5):1039–1047. doi:10.1111/bjd.12853
51. Lauritano D, Lucchese A, Gabrione F, Di Stasio D, Silvestre Rangil J, Carinci F. The effectiveness of laser-assisted surgical excision of leukoplakias and hyperkeratosis of oral mucosa: A case series in a group of patients. *Int J Environ Res Public Health*. 2019;16(2):210. doi:10.3390/ijerph16020210
52. Lim B, Smith A, Chandu A. Treatment of oral leukoplakia with carbon dioxide and potassium-titanyl-phosphate lasers: A comparison. *J Oral Maxillofac Surg*. 2010;68(3):597–601. doi:10.1016/j.joms.2009.03.028
53. Natekar M, Raghuveer HP, Rayapati DK, et al. A comparative evaluation: Oral leukoplakia surgical management using diode laser, CO_2 laser, and cryosurgery. *J Clin Exp Dent*. 2017;9(6):e779–e784. doi:10.4317/jced.53602
54. Kuribayashi Y, Tsushima F, Sato M, Morita K, Omura K. Recurrence patterns of oral leukoplakia after curative surgical resection: Important factors that predict the risk of recurrence and malignancy. *J Oral Pathol Med*. 2012;41(9):682–688. doi:10.1111/j.1600-0714.2012.01167.x
55. Shivhare P, Haidry N, Kumar A, Parihar A, Singh A, Subramanyam S. Diode laser in the management of leukoplakia – a retrospective study. *Ann Maxillofac Surg*. 2022;12(2):178–184. doi:10.4103/ams.ams_117_22
56. Vilar-Villanueva M, Somoza-Martín JM, Blanco-Carrión A, et al. Importance of the vaporization margin during CO_2 laser treatment of oral leukoplakia: A survival study. *Oral Dis*. 2023;29(7):2689–2695. doi:10.1111/odi.14345
57. Dutra MJ, Araujo IS, Wagner VP, et al. Management of surgical margins in the excision of oral leukoplakia: A scoping review. *Oral Dis*. 2026;32(7):1748–1755. doi:10.1111/odi.70231
58. Vu J, Coleman HG, Palme CE, Riffat F, Schifter M, Zoellner H. Diagnostic utility of microsurgical carbon dioxide laser excision of oral potentially malignant lesions vs incisional biopsy: A retrospective histopathological review. *Oral Surg Oral Med Oral Pathol Oral Radiol*. 2019;127(6):516–525. doi:10.1016/j.oooo.2018.12.010
59. Vivek V, Jayasree RS, Balan A, Sreelatha KT, Gupta AK. Three-year follow-up of oral leukoplakia after neodymium:yttrium aluminum garnet (Nd:YAG) laser surgery. *Lasers Med Sci*. 2008;23(4):375–379. doi:10.1007/s10103-007-0500-8
60. Sagalow ES, Kumar AT, Banoub RG, et al. Recurrence of premalignant oral cavity and oropharynx lesions after pulsed diode laser treatment. *Am J Otolaryngol*. 2022;43(5):103556. doi:10.1016/j.amjoto.2022.103556
61. Romeo U, Mohsen M, Palaia G, Bellisario A, Del Vecchio A, Tenore G. CO_2 laser ablation of oral leukoplakia: With or without extension of margins? *Clin Ter*. 2020;171(3):e209–e215. doi:10.7417/CT.2020.2215
62. Vescovi P, Corcione L, Meleti M, et al. Nd:YAG laser versus traditional scalpel. A preliminary histological analysis of specimens from the human oral mucosa. *Lasers Med Sci*. 2010;25(5):685–691. doi:10.1007/s10103-010-0770-4
63. Merigo E, Clini F, Fornaini C, et al. Laser-assisted surgery with different wavelengths: A preliminary ex vivo study on thermal increase and histological evaluation. *Lasers Med Sci*. 2013;28(2):497–504. doi:10.1007/s10103-012-1081-8
64. Pergolini D, Del Vecchio A, Mohsen M, et al. Histological evaluation of oral soft tissue biopsy by dual-wavelength diode laser: An ex vivo study. *Dent J (Basel)*. 2025;13(6):265. doi:10.3390/dj13060265

65. Palaia G, Renzi F, Pergolini D, et al. Histological ex vivo evaluation of the suitability of a 976 nm diode laser in oral soft tissue biopsies. *Int J Dent*. 2021;2021:6658268. doi:10.1155/2021/6658268
66. Yang SW, Lee YS, Chang LC, Yang CH, Luo CM, Wu PW. Oral tongue leukoplakia: Analysis of clinicopathological characteristics, treatment outcomes, and factors related to recurrence and malignant transformation. *Clin Oral Investig*. 2021;25(6):4045–4058. doi:10.1007/s00784-020-03735-1
67. Rashid A, Warnakulasuriya S. The use of light-based (optical) detection systems as adjuncts in the detection of oral cancer and oral potentially malignant disorders: A systematic review. *J Oral Pathol Med*. 2015;44(5):307–328. doi:10.1111/jop.12218

Review

Efficacy of systemic enzyme therapy as an anti-inflammatory agent when used as monotherapy or in combination with NSAIDs: A systematic review

Ganiga Channaiah Shivakumar[1,A,F], Nishath Sayed Abdul[2,B,C], Mahesh Shenoy[2,C,D], Abdullah Abdulaziz Saeidi[3,C], Vincenzo Ronsivalle[4,C,D], Hande Uzunçıbuk[5,D,E], Gabriele Cervino[4,E,F], Maria Maddalena Marrapodi[6,7,E,F], Giuseppe Minervini[8,E,F]

[1] Department of Oral Medicine and Radiology, People's College of Dental Sciences and Research Centre, People's University, Bhopal, India
[2] Department of Oral Maxillofacial Surgery and Diagnostic Sciences, Faculty of Oral Pathology, College of Medicine and Dentistry, Riyadh Elm University, Saudi Arabia
[3] Department of Oral and Maxillofacial Diagnostic Sciences, College of Dentistry, Taibah University, Medina, Saudi Arabia
[4] Department of Biomedical and Dental Sciences, Morphological and Functional Images, University of Messina, G. Martino Polyclinic, Messina, Italy
[5] Department of Orthodontics, Faculty of Dentistry, Trakya University, Edirne, Turkey
[6] Saveetha Dental College and Hospitals, Saveetha Institute of Medical and Technical Sciences (SIMATS), Chennai, India
[7] Department of Woman, Child and General and Specialist Surgery, University of Campania Luigi Vanvitelli, Naples, Italy
[8] Multidisciplinary Department of Medical-Surgical and Dental Specialties, University of Campania Luigi Vanvitelli, Naples, Italy

A – research concept and design; B – collection and/or assembly of data; C – data analysis and interpretation;
D – writing the article; E – critical revision of the article; F – final approval of the article

Dental and Medical Problems, ISSN 1644-387X (print), ISSN 2300-9020 (online) *Dent Med Probl*. 2026;63(5):1303–1311

Address for correspondence
Giuseppe Minervini
E-mail: giuseppe.minervini@unicampania.it

Funding sources
None declared

Conflict of interest
None declared

Acknowledgements
The authors would like to thank Prof. Luis Eduardo Almeida, a native English speaker and associate professor in the Department of Surgical Sciences at the School of Dentistry, Marquette University (Milwaukee, USA), for reviewing and editing the manuscript to ensure appropriate scientific English.

Received on February 12, 2025
Reviewed on May 12, 2025
Accepted on June 8, 2025

Published online on October 28, 2026

Cite as
Shivakumar GC, Abdul NS, Shenoy M, et al. Efficacy of systemic enzyme therapy as an anti-inflammatory agent when used as monotherapy or in combination with NSAIDs: A systematic review. *Dent Med Probl.* 2026;63(5):1303–1311. doi:10.17219/dmp/206041

DOI
10.17219/dmp/206041

Copyright
Copyright by Author(s)
This is an article distributed under the terms of the Creative Commons Attribution 3.0 Unported (CC BY 3.0) (https://creativecommons.org/licenses/by/3.0/)

Abstract

Systemic enzyme therapy (SET) has emerged as a potential anti-inflammatory intervention, either as monotherapy or in combination with non-steroidal anti-inflammatory drugs (NSAIDs). Despite its increasing clinical application, the comparative efficacy of SET in various inflammatory conditions remains insufficiently explored.

A systematic review was conducted in accordance with the PRISMA (Preferred Reporting Items for Systematic reviews and Meta-Analyses) guidelines to evaluate the effectiveness of SET as an anti-inflammatory therapy. Databases were searched for studies meeting predefined eligibility criteria, including randomized and non-randomized trials. Study characteristics, intervention protocols and outcomes were extracted and analyzed. The risk of bias was assessed using the ROBINS-I (Risk Of Bias In Non-randomized Studies of Interventions) and Cochrane risk-of-bias (RoB) 2.0 tools.

Eleven studies with sample sizes ranging from 30 to 487,372 participants were included. Systemic enzyme therapy demonstrated comparable efficacy to diclofenac in terms of pain relief and functional improvement across various conditions, including joint disorders and temporomandibular disorders (TMD). Combination therapy resulted in significantly greater pain reduction ($p < 0.05$) and improved functional outcomes, as reported in several studies. In most cases, adverse effects were mild, and the safety profile of SET was more favorable than that of NSAIDs. One study reported that the concomitant use of NSAIDs and antihypertensive medications was associated with a 31% increased risk of acute kidney injury during the first 30 days.

Systemic enzyme therapy demonstrated efficacy comparable to that of NSAIDs, with a potentially more favorable safety profile in the management of inflammatory conditions. Combination therapy may provide additional benefits in terms of pain reduction and functional improvement. However, the heterogeneity of study designs and the limited number of large-scale trials warrant further research.

Keywords: systemic enzyme therapy, anti-inflammatory therapy, NSAIDs, combination therapy, pain relief

Highlights

- The study evaluates the efficacy, safety and tolerability of systemic enzyme therapy for inflammatory conditions, particularly temporomandibular disorders and osteoarthritis.
- Systemic enzyme therapy shows efficacy comparable to that of non-steroidal anti-inflammatory drugs and may improve treatment outcomes when used in combination with them.
- Systemic enzyme therapy exhibits multifaceted anti-inflammatory mechanisms, including cytokine modulation, reduced leukocyte migration and promotion of tissue repair.
- Treatment with oral enzyme combinations may offer a safer alternative or adjunct to non-steroidal anti-inflammatory drugs, with potentially fewer gastrointestinal, renal and cardiovascular risks.
- Further high-quality, large-scale randomized controlled trials are needed to confirm these findings, standardize treatment protocols and optimize clinical use.

Introduction

Systemic enzyme therapy (SET) has attracted considerable interest for its potential anti-inflammatory effects, both as monotherapy and as an adjunct to conventional non-steroidal anti-inflammatory drugs (NSAIDs).[1] Systemic enzyme preparations, consisting of combinations of proteolytic enzymes and other active agents, such as trypsin, bromelain and the flavonoid rutin, are thought to act through multiple mechanisms, including fibrinolysis, the reduction of pro-inflammatory cytokines and the promotion of tissue repair.[2] Unlike NSAIDs, which primarily work by inhibiting cyclooxygenase enzymes and thereby reducing prostaglandin synthesis, SET may exert its effects through multiple pathways involving inflammatory mediators, potentially avoiding some of the gastrointestinal and cardiovascular adverse effects associated with chronic use of NSAIDs.[3]

The inflammatory response plays a central role in various acute and chronic conditions, including musculoskeletal injuries and autoimmune disorders. Although widely regarded as a cornerstone of anti-inflammatory therapy, long-term NSAID use is often limited by adverse effects, including gastric ulceration, renal dysfunction and an increased risk of thrombotic events.[4,5] These limitations have prompted interest in complementary or alternative therapies, particularly those that may provide anti-inflammatory benefits with a more favorable safety profile. The proposed systemic absorption of proteolytic enzymes and their potential biochemical activities make SET a possible therapeutic approach for reducing inflammation while potentially minimizing the adverse effects associated with conventional anti-inflammatory medications.[6]

Several recently published studies indicate growing interest in SET for various inflammatory conditions, such as osteoarthritis (OA), rheumatoid arthritis and postoperative inflammation.[7] Preliminary evidence also suggests that SET may act by degrading circulating immune complexes, modulating vascular permeability, and reducing leukocyte adhesion and migration.[8] However, these proposed benefits have not been conclusively established, as inconsistencies in study design, sample size and outcome measures have resulted in conflicting findings regarding the efficacy of SET. Furthermore, questions related to the bioavailability of systemic enzymes and their ability to reach inflammatory sites at therapeutically relevant concentrations continue to limit their widespread adoption in clinical practice.[9–11]

When used in combination therapy with NSAIDs, SET is thought to enhance their anti-inflammatory effect or allow for dose reductions.[9–12] These outcomes could potentially reduce the incidence of adverse events. However, the potential additive or synergistic effects of SET in combination with NSAIDs remain poorly understood, and high-quality evidence is insufficient to draw definite conclusions. Furthermore, the lack of standardized protocols regarding enzyme formulations, dosages and treatment duration complicates direct comparisons across studies and highlights the need for strict evaluation. Given these knowledge gaps, this systematic review aims to critically evaluate the available evidence regarding the efficacy of SET as an anti-inflammatory intervention, both as monotherapy and in combination with NSAIDs.

Material and methods

PECOS framework and PRISMA compliance

The PECOS framework for this review was developed based on the PRISMA (Preferred Reporting Items for Systematic reviews and Meta-Analyses) 2020 reporting guidelines,[13] which ensure transparent and standardized reporting. The framework was defined as follows: Population (P) – patients diagnosed with inflammatory conditions, including joint disorders and temporomandibular disorders (TMD); Exposure (E) – SET administered as monotherapy or in combination with NSAIDs; Comparison (C) – placebo or NSAID treatment; Outcome (O) – reductions in inflammation and pain, improvements in joint mobility, and patient-reported functional scores; Study design (S): randomized controlled trials (RCTs), non-RCTs and cohort studies.

Inclusion and exclusion criteria

The inclusion criteria required studies to investigate patients with inflammatory conditions treated with SET as monotherapy or in combination with NSAIDs. Eligible studies included RCTs, non-RCTs and cohort studies involving human populations. Studies were required to report at least 1 measure of inflammation reduction, pain relief or functional improvement. Only full-text articles published in English were considered, with no restrictions on the year of publication.

Studies involving in vitro or animal models, non-inflammatory conditions or SET formulations that did not include trypsin, bromelain or rutoside were excluded. Reviews, editorials and articles lacking sufficient methodological details or reporting outcomes beyond the scope of this review were also excluded. Conference abstracts were excluded unless they reported sufficient methodological and outcome data. Studies published in languages other than English were not considered.

Database search

A systematic literature search was performed across 6 databases: PubMed; Embase; the Cochrane Library; Scopus; Web of Science; and CINAHL (Cumulative Index to Nursing and Allied Health Literature). The search terms included "systemic enzyme therapy", "anti-inflammatory", "diclofenac", "bromelain", "trypsin", "rutoside", "joint health", "temporomandibular joint", and "inflammation". Boolean operators, such as AND, OR and NOT, were used to refine search results and identify relevant studies. MeSH terms were combined with free-text terms to improve search sensitivity (Table 1).

Data extraction protocol and items

The study used a predesigned template for data extraction. The following information was extracted: study characteristics, such as author names, publication year, country, and study design; population details, including sample size, demographics and the condition being treated; intervention details, such as formulation, dosage and treatment duration; comparator information; and outcome measures, including pain reduction, inflammatory markers, functional scores, and adverse events. Additional information included funding sources, disclosure of conflict of interest and risk-of-bias assessments.

Risk-of-bias assessment

The ROBINS-I (Risk Of Bias In Non-randomized Studies of Interventions)[14] was used to assess the risk of bias in non-randomized studies, including bias due to confounding, selection of participants, classification of interventions, and measurement of outcomes. For RCTs, the Cochrane risk-of-bias (RoB) 2.0 tool[15] was used to evaluate bias arising from the randomization process, deviations from the intended interventions, missing outcome data, and selective reporting. Risk-of-bias assessments were performed independently by 2 reviewers, and any disagreements were resolved through consensus.

Results

Study selection process

A total of 381 records were identified through database searches, of which 46 duplicates were removed before screening. The remaining 335 records were screened for relevance, and none were excluded at this stage. Subsequently, 37 reports could not be retrieved, leaving 298 reports for the assessment of eligibility. Of these, reports were excluded for the following reasons: failure to meet the PECOS eligibility criteria (n = 68); in vitro study design (n = 48); case reports (n = 76); literature reviews (n = 55); and theses (n = 40). Ultimately, 11 studies[16–26] met the eligibility criteria and were included in the final review (Fig. 1).

Table 1. Search strategy used in the systematic review

Database	Search string
PubMed	("systemic enzyme therapy"[MeSH Terms]) AND ("anti-inflammatory agents"[MeSH Terms] OR "diclofenac"[All Fields])) AND ("joint health"[MeSH Terms] OR "temporomandibular joint disorders"[MeSH Terms])
Embase	('systemic enzyme therapy' OR 'bromelain' OR 'trypsin' OR 'rutoside') AND ('anti-inflammatory' OR 'diclofenac') AND ('joint health' OR 'temporomandibular disorders')
Cochrane Library	("systemic enzyme therapy" AND "anti-inflammatory") OR ("bromelain" AND "diclofenac") AND ("joint health" OR "temporomandibular joint")
Scopus	TITLE-ABS-KEY(("systemic enzyme therapy" OR "bromelain" OR "trypsin" OR "rutoside") AND ("anti-inflammatory" OR "diclofenac") AND ("joint health" OR "temporomandibular joint"))
Web of Science	TS=("systemic enzyme therapy" AND "bromelain" OR "trypsin" OR "rutoside") AND ("anti-inflammatory agents" OR "diclofenac") AND ("joint health" OR "temporomandibular joint disorders")
CINAHL	("systemic enzyme therapy" OR "bromelain" OR "trypsin" OR "rutoside") AND ("anti-inflammatory agents" OR "diclofenac") AND ("joint health" OR "temporomandibular joint disorders")

CINAHL – Cumulative Index to Nursing and Allied Health Literature.

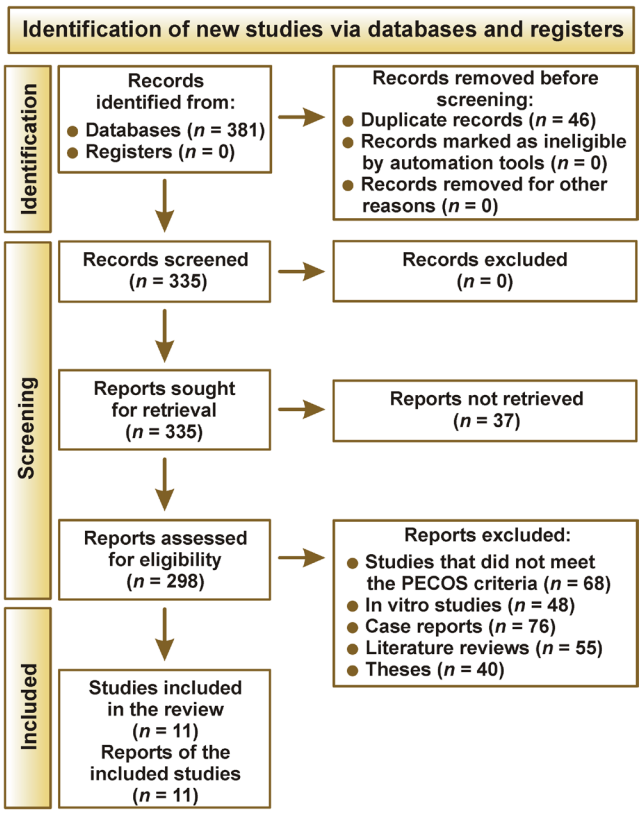

Fig. 1. PRISMA (Preferred Reporting Items for Systematic reviews and Meta-Analyses) flow diagram illustrating the study selection process

Publication year and geographical distribution

The studies covered a wide time span, ranging from 1998[19] to 2020 (Table 2).[18] Regarding geographical distribution, a substantial proportion of studies were conducted in Germany,[16,17,21,22,25,26] reflecting considerable research activity in this country. Other countries represented were India,[18,20] Mexico[19] and the UK.[23] The geographical diversity provided insights into the application of SET across different patient populations and healthcare settings.

Study design

Most studies employed randomized, double-blind, parallel-group designs,[16,19,21,22,25] which are generally considered the gold standard for minimizing bias in clinical trials. A placebo-controlled trial was conducted in 2015,[17] while a retrospective cohort analysis was performed in the UK in 2013.[23] Two studies employed single-blind or comparator-controlled designs,[20,26] with slight variations in methodology tailored to the specific clinical conditions investigated.

Sample size

Sample sizes varied considerably between studies, ranging from small cohorts of 30 participants in India[18,20] to a large retrospective cohort study involving 487,372 participants in the UK.[23] Most of the randomized trials included between 50 and 268 participants,[16,17,19,21,22,25,26] providing a reasonable balance between statistical power and feasibility.

Duration of interventions

Intervention durations and follow-up periods varied from 10 days[20] to a follow-up of 5.9 years in a retrospective study.[23] Most of the randomized trials lasted between 3 and 6 weeks,[16,19,21,22,24,25] while one extended to 12 weeks,[17] and others included additional follow-up assessments.[25,26] These differences in duration reflected variations in the clinical conditions investigated and the study objectives.

Focus areas

The studies primarily focused on joint disorders, particularly those affecting the knee.[16,17,19,21,24–26] One study also investigated hip-related conditions.[22] Two studies targeted TMD, specifically internal derangement and OA of the temporomandibular joint (TMJ).[18,20] Another distinct area of investigation was the risk of acute kidney injury associated with the concomitant use of NSAIDs and antihypertensive medications.[23] The diversity of conditions investigated reflects the broad range of clinical contexts in which SET has been evaluated.

Key findings

Several studies reported that SET demonstrated efficacy comparable to that of diclofenac in reducing pain and inflammation.[16,17,20–22,25,26] Additional findings included a safety profile comparable to that of placebo[17] and long-lasting therapeutic effects even after treatment.[25] The combination of enzymes with diclofenac was associated with improved clinical outcomes, including greater pain reduction, enhanced joint function and improved masticatory function in patients with TMD.[18,20] A large retrospective study reported a 31% increased risk of acute kidney injury associated with triple therapy involving NSAIDs and antihypertensive agents, particularly during the first 30 days.[23] Collectively, these findings suggest that SET is effective and may reduce the risk of adverse effects, particularly when used in combination with conventional anti-inflammatory therapy.

Risk-of-bias assessment

Most RCTs demonstrated a low risk of bias across several key domains, particularly those related to the randomization process, deviations from intended interventions and outcome measurement.[17,18,21,22,25] Additionally, some concerns regarding outcome measurement and selective reporting influenced overall ratings.[19,24,26] Despite these reservations, the vast majority of the RCTs were assessed as having an overall low risk of bias (Fig. 2).

Table 2. Characteristics and key findings of the studies included in the review

Study	Study design	Country	Sample size, *n*	Duration	Focus area	Key findings
Akhtar et al. 2004[16]	randomized, double-blind, parallel-group comparator trial	Germany	103	6 weeks	knee disorders	OEC demonstrated efficacy comparable to that of diclofenac.
Bolten et al. 2015[17]	randomized, double-blind, placebo-controlled comparator trial	Germany	150	12 weeks	knee disorders	OEC demonstrated efficacy comparable to that of diclofenac, with reduced use of rescue medication and a tolerability profile similar to that of placebo.
Gupta et al. 2020[18]	randomized case–control clinical trial	India	30 (15 per group)	14 days	internal derangement of the TMJ	Combination therapy significantly reduced pain and joint sounds and improved chewing ability and mandibular movements. No significant between-group differences were observed in mouth opening.
Herrera 1998[19]	randomized, double-blind, parallel-group comparator trial	Mexico	59	3 weeks	monoarticular gonarthritis (knee)	The LAFI scores and composite symptom scores were comparable between treatment groups at the end of the study. However, the sample size was insufficient to statistically establish equivalence.
Jayachandran and Khobre 2017[20]	randomized, comparator-controlled trial	India	30	10 days	TMJ osteoarthritis	OEC demonstrated efficacy comparable to that of diclofenac. Combination therapy resulted in significantly greater pain reduction ($p < 0.05$) than either treatment alone.
Klein and Kullich 2000[21]	randomized, double-blind, parallel-group comparator trial	Germany	73	3 weeks	knee disorders	OEC demonstrated efficacy comparable to that of diclofenac.
Klein et al. 2006[22]	randomized, double-blind, parallel-group comparator trial	Germany	90	6 weeks	hip disorders	OEC demonstrated efficacy comparable to that of diclofenac regarding the WOMAC domains of pain, stiffness and physical function, the LAFI score, investigator- and patient-reported assessments of efficacy, and responder rates based on pain and physical function.
Lapi et al. 2013[23]	retrospective cohort study with a nested case–control analysis	United Kingdom	487,372	mean follow-up: 5.9 years	risk of acute kidney injury associated with concomitant NSAID and antihypertensive use	Triple therapy involving diuretics, ACE inhibitors/ARBs, and NSAIDs was associated with a 31% increased risk of acute kidney injury, particularly during the first 30 days of treatment.
Roth and Stauder 2001[24]	randomized, double-blind, parallel-group comparator trial (conference poster)	not specified	268	6 weeks	knee disorders	Diclofenac was modestly superior on the LAFI (*MD*: 1.10; 95% *CI*: 0.24–1.96), but the difference remained within the 3-point non-inferiority margin, while 42.9% of participants were excluded from the per-protocol analysis.
Singer et al. 2001[25]	randomized, double-blind, parallel-group comparator trial	Germany	63	3 weeks of treatment followed by a 4-week observation period	knee disorders	OEC demonstrated efficacy comparable to that of diclofenac, with therapeutic effects persisting after the end of treatment.
Tilwe et al. 2001[26]	randomized, single-blind, parallel-group comparator trial	Germany	50	3 weeks of treatment followed by a 4-week observation period	knee disorders	OEC demonstrated overall efficacy comparable to that of diclofenac, with significantly greater improvement in joint tenderness.

ACE – angiotensin-converting enzyme; ARB – angiotensin receptor blocker; *CI* – confidence interval; LAFI – Lequesne algofunctional index; *MD* – mean difference; NSAID – non-steroidal anti-inflammatory drug; OEC – oral enzyme combination; TMJ – temporomandibular joint; WOMAC – Western Ontario and McMaster Universities osteoarthritis index.

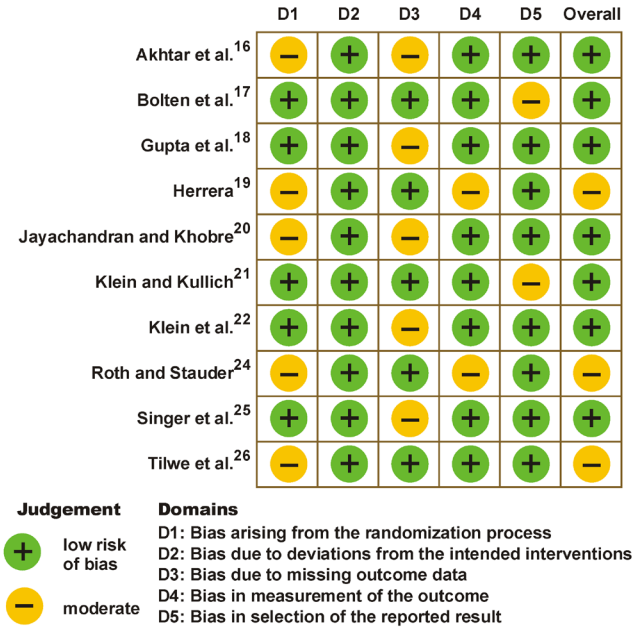

Fig. 2. Risk-of-bias assessment of the randomized controlled trials (RCTs) included in the review using the Cochrane risk-of-bias (RoB) 2.0 tool

The non-randomized study[23] was evaluated as having a moderate risk of bias, primarily due to limitations regarding confounding factors, participant selection and classification of interventions. Other domains, including deviations from the intended interventions and missing outcome data, were assessed as having a low risk of bias. Overall, the study reflected a moderate risk of bias, indicating methodological limitations associated with its design (Fig. 3).

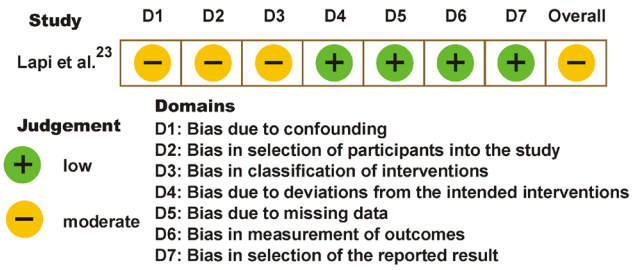

Fig. 3. Risk-of-bias assessment of the non-randomized study included in the review using the ROBINS-I (Risk Of Bias In Non-randomized Studies of Interventions)

Discussion

Inflammatory conditions such as OA are usually treated with NSAIDs.[27–29] Although widely used, long-term NSAID therapy is associated with adverse effects.[30] The evidence suggests that the use of NSAIDs may be linked to the progression of radiographic knee OA.[31] Moreover, NSAIDs can interfere with the natural mechanisms of inflammation resolution, such as tissue healing by inhibiting cyclooxygenase-2 activity, which subsequently suppresses the production of specialized pro-resolving mediators.[32] Systemic enzyme therapy, also referred to as treatment with oral enzyme combinations (OECs), has also been studied as a complementary approach to managing inflammation. Evidence supporting the effectiveness of OECs in OA comes from 9 small clinical studies involving up to 268 patients and a systematic review incorporating a meta-analysis of 6 RCTs comparing OEC therapy with diclofenac in patients with knee OA.[33]

The studies included in this review demonstrated the potential efficacy of SET in the management of inflammation, with several papers reporting outcomes comparable to those of diclofenac and additional benefits in specific clinical contexts. Akhtar et al.[16] and Bolten et al.[17] showed that OECs were as effective as diclofenac in managing knee joint health, with the study by Bolten et al.[17] reporting a more favorable safety profile and reduced need for rescue medication. These findings were consistent with those of Klein and Kullich[21] and Singer et al.,[25] who also reported comparable efficacy, although Singer et al.[25] uniquely highlighted prolonged benefits of OEC therapy after treatment cessation.

Gupta et al.[18] and Jayachandran and Khobre[20] focused on TMD and noted improvements in pain, joint function and other clinical outcomes with combination therapy involving OECs and diclofenac. The outcomes of the studies complemented the broader applications of OECs reported in other investigations. These TMJ-specific findings, however, differed in their clinical focus from studies conducted solely on knee and hip joints. For example, Klein et al.[22] reported comparable efficacy of OECs and diclofenac in hip OA, as assessed using functional indices such as the Western Ontario and McMaster Universities osteoarthritis index (WOMAC) and the Lequesne algofunctional index (LAFI).

Herrera reported findings that differed from the overall trend, as non-inferiority of OECs to diclofenac could not be established, potentially due to the inadequate sample size, although both treatments showed comparable functional results.[19] Lapi et al. investigated a different outcome, focusing not on treatment efficacy but on the increased risk of acute kidney injury associated with combinations of NSAIDs and antihypertensive medications.[23] Their findings highlighted safety concerns associated with NSAID use, although they did not directly establish the comparative safety of OECs reported by Bolten et al.[17]

Tilwe et al.[26] provided further evidence suggesting that OECs were superior to diclofenac in reducing joint tenderness, consistent with the studies by Bolten et al.[17] and Singer et al.[25] Roth and Stauder reported that diclofenac was modestly superior on the LAFI, although the difference remained within the predefined non-inferiority margin.[24] Overall, the majority of studies reported consistent efficacy and safety outcomes, although some discrepancies were observed, mainly due to differences in focus areas and methodological limitations, highlighting the need for more robust trials across various conditions.

The findings of our review, when compared with those of external studies, revealed both similarities and differences in the efficacy and safety of SET and NSAIDs. Bindu et al. highlighted the widespread use of NSAIDs in the management of pain and inflammation, emphasizing their analgesic and anti-inflammatory benefits alongside significant multiorgan adverse effects,[34] which were not comprehensively addressed in our review. Szeto et al. proposed a practical framework for minimizing NSAID-related adverse effects through close patient monitoring and specific prescribing strategies,[35] which were beyond the clinical scope of our review.

Henrotin et al. reported that OECs were as effective as NSAIDs in the management of OA, with fewer adverse effects.[36] These findings are consistent with those of our review, which indicated comparable efficacy of OECs in terms of pain relief and functional outcomes. Furthermore, Ueberall et al. confirmed the comparable effectiveness of OECs and NSAIDs in reducing pain and improving physical function, with significantly more favorable safety and tolerability profiles for OECs than for NSAIDs.[37] These findings were consistent with those of Bolten et al.[17] and other knee OA trials included in our review. Shekhar et al. emphasized the benefits of combination therapy for TMJ osteoarthritis, consistent with our findings suggesting greater effectiveness of OECs combined with NSAIDs compared with NSAIDs alone.[38] Our review and the available external studies reached similar conclusions regarding the efficacy and safety of SET. However, external studies addressed a broader range of safety concerns and provided practical recommendations for NSAID use, highlighting the need for further research in this area.

Limitations

This review was limited by heterogeneity in study designs, intervention durations and outcome measures. Several studies included small sample sizes, had limited statistical power and lacked comprehensive long-term follow-up. Considerable variation in SET dosing protocols and formulations further hindered direct comparisons between studies. Some studies were assessed as having a moderate risk of bias, particularly the non-randomized trial, which may have affected the validity of the findings. Lastly, the lack of uniform reporting standards across studies made it difficult to comprehensively synthesize the available data.

Future implications

Based on the available evidence, SET may be considered a potential adjunct to NSAIDs in the treatment of certain inflammatory conditions for better efficacy and safety. Establishing standardized SET dosing protocols and formulations may improve the consistency of therapeutic outcomes. Large-scale, long-term clinical trials are required to provide more robust evidence of the efficacy and safety of treatment across different patient populations. Furthermore, combination therapies involving SET and NSAIDs should be evaluated to determine optimal treatment regimens and investigate their potential to reduce reliance on conventional anti-inflammatory medications.

Conclusions

Systemic enzyme therapy demonstrated efficacy comparable to that of NSAIDs in several studies, with a potentially more favorable safety profile and a lower incidence of adverse effects. In some studies, combining SET with NSAIDs was associated with greater pain relief and improved functional outcomes compared with NSAID treatment alone. These findings suggest that SET may be a useful therapeutic option for selected inflammatory conditions, particularly when reducing treatment-related adverse effects is a clinical priority. However, the strength of the evidence remains limited by differences in study quality, highlighting the need for additional high-quality clinical trials.

Ethics approval and consent to participate

Not applicable.

Data availability

The analyzed data was obtained from publicly available peer-reviewed studies included in the review.

Consent for publication

Not applicable.

Use of AI and AI-assisted technologies

During the preparation of this manuscript, the authors used DeepL Translator (DeepL SE, Cologne, Germany) for language correction. After its use, the authors thoroughly reviewed, verified and revised all content to ensure accuracy and originality.

ORCID iDs

Ganiga Channaiah Shivakumar https://orcid.org/0000-0001-7572-9873
Nishath Sayed Abdul https://orcid.org/0000-0003-4091-3632
Mahesh Shenoy https://orcid.org/0000-0001-5486-4566
Abdullah Abdulaziz Saeidi https://orcid.org/0000-0002-0822-993X
Vincenzo Ronsivalle https://orcid.org/0000-0003-3059-4981
Hande Uzunçıbuk https://orcid.org/0000-0001-9265-1772
Gabriele Cervino https://orcid.org/0000-0003-4619-4691
Maria Maddalena Marrapodi https://orcid.org/0000-0002-9494-6942
Giuseppe Minervini https://orcid.org/0000-0002-8309-1272

References

1. Chen HS, Cui Y, Zhou ZH, et al.; ARAMIS Investigators. Dual antiplatelet therapy vs alteplase for patients with minor nondisabling acute ischemic stroke: The ARAMIS randomized clinical trial. *JAMA*. 2023;329(24):2135–2144. doi:10.1001/jama.2023.7827
2. Salomon-Zimri S, Pushett A, Russek-Blum N, et al. Combination of ciprofloxacin/celecoxib as a novel therapeutic strategy for ALS. *Amyotroph Lateral Scler Frontotemporal Degener*. 2023;24(3–4):263–271. doi:10.1080/21678421.2022.2119868
3. Kappos L, Fox RJ, Burcklen M, et al. Ponesimod compared with teriflunomide in patients with relapsing multiple sclerosis in the active-comparator phase 3 OPTIMUM study: A randomized clinical trial. *JAMA Neurol*. 2021;78(5):558–567. doi:10.1001/jamaneurol.2021.0405
4. Watanabe H, Morimoto T, Natsuaki M, et al.; STOPDAPT-2 Investigators. Clopidogrel vs aspirin monotherapy beyond 1 year after percutaneous coronary intervention. *J Am Coll Cardiol*. 2024;83(1):17–31. doi:10.1016/j.jacc.2023.10.013
5. Harirforoosh S, Asghar W, Jamali F. Adverse effects of nonsteroidal antiinflammatory drugs: An update of gastrointestinal, cardiovascular and renal complications. *J Pharm Pharm Sci*. 2013;16(5):821–847. doi:10.18433/j3vw2f
6. Pavan R, Jain S, Shraddha, Kumar A. Properties and therapeutic application of bromelain: A review. *Biotechnol Res Int*. 2012;2012:976203. doi:10.1155/2012/976203
7. Hong SJ, Lee SJ, Suh Y, et al.; T-PASS (Ticagrelor Monotherapy in Patients Treated With New-Generation Drug-Eluting Stents for Acute Coronary Syndrome) Investigators. Stopping aspirin within 1 month after stenting for ticagrelor monotherapy in acute coronary syndrome: The T-PASS randomized noninferiority trial. *Circulation*. 2024;149(8):562–573. doi:10.1161/CIRCULATIONAHA.123.066943
8. Nishiyama Y, Kimura K, Otsuka T, et al.; CSPS.com Trial Investigators. Dual antiplatelet therapy with cilostazol for secondary prevention in lacunar stroke: Subanalysis of the CSPS.com trial. *Stroke*. 2023;54(3):697–705. doi:10.1161/STROKEAHA.122.039900
9. Sands BE, Peyrin-Biroulet L, Kierkus J, et al. Efficacy and safety of mirikizumab in a randomized phase 2 study of patients with Crohn's disease. *Gastroenterology*. 2022;162(2):495–508. doi:10.1053/j.gastro.2021.10.050
10. Han MH, Nam JH, Noh E, Lee EK. Gastrointestinal risk of non-steroidal anti-inflammatory drugs and gastroprotective agents used in the treatment of osteoarthritis in elderly patients: A nationwide retrospective cohort study. *Int J Pharmacol Ther*. 2019;57(11):531–541. doi:10.5414/CP203377
11. Zobdeh F, Eremenko II, Akan MA, et al. Pharmacogenetics and pain treatment with a focus on non-steroidal anti-inflammatory drugs (NSAIDs) and antidepressants: A systematic review. *Pharmaceutics*. 2022;14(6):1190. doi:10.3390/pharmaceutics14061190
12. Bai S, Guo W, Feng Y, et al. Efficacy and safety of anti-inflammatory agents for the treatment of major depressive disorder: A systematic review and meta-analysis of randomised controlled trials. *J Neurol Neurosurg Psychiatry*. 2020;91(1):21–32. doi:10.1136/jnnp-2019-320912
13. Page MJ, Moher D, Bossuyt PM, et al. PRISMA 2020 explanation and elaboration: Updated guidance and exemplars for reporting systematic reviews. *BMJ*. 2021;372:n160. doi:10.1136/bmj.n160
14. Igelström E, Campbell M, Craig P, Katikireddi SV. Cochrane's risk of bias tool for non-randomized studies (ROBINS-I) is frequently misapplied: A methodological systematic review. *J Clin Epidemiol*. 2021;140:22–32. doi:10.1016/j.jclinepi.2021.08.022
15. Sterne JAC, Savović J, Page MJ, et al. RoB 2: A revised tool for assessing risk of bias in randomised trials. *BMJ*. 2019;366:l4898. doi:10.1136/bmj.l4898
16. Akhtar NM, Naseer R, Farooqi AZ, Aziz W, Nazir M. Oral enzyme combination versus diclofenac in the treatment of osteoarthritis of the knee – a double-blind prospective randomized study. *Clin Rheumatol*. 2004;23(5):410–415. doi:10.1007/s10067-004-0902-y
17. Bolten WW, Glade MJ, Raum S, Ritz BW. The safety and efficacy of an enzyme combination in managing knee osteoarthritis pain in adults: A randomized, double-blind, placebo-controlled trial. *Arthritis*. 2015;2015:251521. doi:10.1155/2015/251521
18. Gupta P, Naik SR, Ashok L, Poornima R, Shetty R. Combination of trypsin, rutoside, bromelain and diclofenac sodium in the management of internal derangement of temporomandibular joint: A randomized clinical trial. *J Indian Acad Oral Med Radiol*. 2020;32(3):216–221. doi:10.4103/jiaomr.jiaomr_45_20
19. Herrera EG. Phlogenzym in the treatment of a monoarticular painful gonarthritis: Efficacy and tolerance 1998. https://web.archive.org/web/20070207173949/https://www.wobenzym.cz/cdweb/mucos/pittompg.htm. Accessed June 7, 2025.
20. Jayachandran S, Khobre P. Efficacy of bromelain along with trypsin, rutoside trihydrate enzymes and diclofenac sodium combination therapy for the treatment of TMJ osteoarthritis – a randomised clinical trial. *J Clin Diagn Res*. 2017;11(6):ZC09–ZC11. doi:10.7860/JCDR/2017/25771.9964
21. Klein G, Kullich W. Short-term treatment of painful osteoarthritis of the knee with oral enzymes. *Clin Drug Investig*. 2000;19(1):15–23. doi:10.2165/00044011-200019010-00003
22. Klein G, Kullich W, Schnitker J, Schwann H. Efficacy and tolerance of an oral enzyme combination in painful osteoarthritis of the hip: A double-blind, randomised study comparing oral enzymes with non-steroidal anti-inflammatory drugs. *Clin Exp Rheumatol*. 2006;24(1):25–30. PMID:16539815.
23. Lapi F, Azoulay L, Yin H, Nessim SJ, Suissa S. Concurrent use of diuretics, angiotensin converting enzyme inhibitors, and angiotensin receptor blockers with non-steroidal anti-inflammatory drugs and risk of acute kidney injury: Nested case–control study. *BMJ*. 2013;346:e8525. doi:10.1136/bmj.e8525
24. Roth SH, Stauder GM. Oral enzyme therapy (Phlogenzym) in osteoarthritis: Long-term comparative study against diclofenac. Poster presented at: 65th Annual Scientific Meeting of the American College of Rheumatology; November 11–15, 2001; San Francisco, CA.
25. Singer F, Singer C, Oberleitner H. Phlogenzym® versus diclofenac in the treatment of activated osteoarthritis of the knee. A double-blind prospective randomized study. *Int J Immunother*. 2001;17:135–141.
26. Tilwe GH, Beria S, Turakhia NH, Daftary GV, Schiess W. Efficacy and tolerability of oral enzyme therapy as compared to diclofenac in active osteoarthrosis of knee joint: An open randomized controlled clinical trial. *J Assoc Physicians India*. 2001;49:617–621. PMID:11584936.
27. Robbins MS. Diagnosis and management of headache: A review. *JAMA*. 2021;325(18):1874–1885. doi:10.1001/jama.2021.1640
28. Amaechi O, Huffman MM, Featherstone K. Pharmacologic therapy for acute pain. *Am Fam Physician*. 2021;104(1):63–72. PMID:34264611.
29. Ribeiro H, Rodrigues I, Napoleão L, et al. Non-steroidal anti-inflammatory drugs (NSAIDs), pain and aging: Adjusting prescription to patient features. *Biomed Pharmacother*. 2022;150:112958. doi:10.1016/j.biopha.2022.112958
30. Zappavigna S, Cossu AM, Grimaldi A, et al. Anti-inflammatory drugs as anticancer agents. *Int J Mol Sci*. 2020;21(7):2605. doi:10.3390/ijms21072605
31. Bakhshi GD, Rangwala ZS, Chauhan AR. Systemic enzyme therapy in chronic venous disease: A review. *Int J Res Med Sci*. 2021;9(9):2869–2876. doi:10.18203/2320-6012.ijrms20213435
32. Karnam S, Donthi MR, Jindal AB, Paul AT. Recent innovations in topical delivery for management of rheumatoid arthritis: A focus on combination drug delivery. *Drug Discov Today*. 2024;29(8):104071. doi:10.1016/j.drudis.2024.104071
33. Mercer MA, Davis JL, McKenzie HC. The clinical pharmacology and therapeutic evaluation of non-steroidal anti-inflammatory drugs in adult horses. *Animals (Basel)*. 2023;13(10):1597. doi:10.3390/ani13101597
34. Bindu S, Mazumder S, Bandyopadhyay U. Non-steroidal anti-inflammatory drugs (NSAIDs) and organ damage: A current perspective. *Biochem Pharmacol*. 2020;180:114147. doi:10.1016/j.bcp.2020.114147
35. Szeto CC, Sugano K, Wang JG, et al. Non-steroidal anti-inflammatory drug (NSAID) therapy in patients with hypertension, cardiovascular, renal or gastrointestinal comorbidities: Joint APAGE/APLAR/APSDE/APSH/APSN/PoA recommendations. *Gut*. 2020;69(4):617–629. doi:10.1136/gutjnl-2019-319300

36. Henrotin YE, Michlmayr C, Rau SM, Quirke AM, Bigoni M, Ueberall MA. Combination of enzymes and rutin to manage osteoarthritis symptoms: Lessons from a narrative review of the literature. *Rheumatol Ther*. 2022;9(5):1305–1327. doi:10.1007/s40744-022-00472-7
37. Ueberall MA, Mueller-Schwefe GH, Wigand R, Essner U. Efficacy, tolerability, and safety of an oral enzyme combination vs diclofenac in osteoarthritis of the knee: Results of an individual patient-level pooled reanalysis of data from six randomized controlled trials. *J Pain Res*. 2016;9:941–961. doi:10.2147/JPR.S108563
38. Shekhar A, Maddheshiya N, Adit, Rastogi V, Ramalingam K. Anti-inflammatory role of trypsin, rutoside, and bromelain combination in temporomandibular joint osteoarthritis: A systematic review. *Cureus*. 2024;16(1):e51749. doi:10.7759/cureus.51749

Review

Accuracy and reproducibility of photogrammetric measurements in dentistry: A systematic review

Oliwier Wojciech Pioterek[1,A–F], Katarzyna Majka[1,B–D], Jakub Goździewicz[1,B–D], Wiktoria Taurogińska[1,B–D], Barbara Parol[1,C,D], Daria Pozdniakowa[1,C–E], Albert Synal[1,C,D], Aleksander Sowiński[1,C,D], Martyna Piskorz[1,C,D], Mateusz Drążyk[1,D–F], Mateusz Mazurek[1,E,F], Michał Tulski[1,E], Zygmunt Domagała[2,E,F], Maciej Dobrzyński[3,E,F], Paweł Dąbrowski[2,E,F]

[1] Clinical and Dissecting Anatomy Students Scientific Club, Wroclaw Medical University, Poland
[2] Division of Anatomy, Wroclaw Medical University, Poland
[3] Department of Pediatric Dentistry and Preclinical Dentistry, Wroclaw Medical University, Poland

A – research concept and design; B – collection and/or assembly of data; C – data analysis and interpretation; D – writing the article; E – critical revision of the article; F – final approval of the article

Dental and Medical Problems, ISSN 1644-387X (print), ISSN 2300-9020 (online) *Dent Med Probl*. 2026;63(5):1313–1330

Address for correspondence
Oliwier Wojciech Pioterek
E-mail: oliwierpioterek@gmail.com

Funding sources
None declared

Conflict of interest
None declared

Acknowledgements
None declared

Received on March 12, 2025
Reviewed on May 12, 2025
Accepted on May 22, 2025

Published online on September 24, 2026

Abstract

Photogrammetry is a method of acquiring three-dimensional (3D) models by superimposing two-dimensional images. Since the publication of the last systematic review, many new articles concerning its use in dental practice have been published. This study aims to evaluate the accuracy and reproducibility of photogrammetry based on the available literature. Four databases (PubMed®, Web of Science, Google Scholar, and Embase) were searched using the following keywords: "photogrammetry"; "stereophotogrammetry"; "dentistry"; and "tooth implants". The following eligibility criteria were applied: the study had to be published in a reliable journal, specify the type of measurements performed, and describe their accuracy or reproducibility. The Quality Assessment of Diagnostic Accuracy Studies (QUADAS-1) tool was used for the assessment of the risk of bias. The collected data was tabularized and classified into 3 groups based on the type of measurements performed and into 2 subgroups according to accuracy and precision. Forty-four articles were included in the final analysis. The reviewed articles showed that cephalometric measurements based on photogrammetry have high correlation coefficients and are accurate, with measurement errors below 1 mm. Photogrammetry was highly reproducible and more accurate than intraoral scanners (IOS) for assessing implant positions. Measurements of dental arches showed high intraclass correlation coefficients (*ICC*s) and high accuracy, with errors below 0.5 mm. The main limitation of this review is that most of the included studies were conducted in vitro; therefore, it was difficult to evaluate the applicability of photogrammetry in clinical practice. Photogrammetry appears to be a precise and accurate method for performing cephalometric measurements, assessing dental implant positions and measuring dental dimensions. However, further clinical studies are needed to evaluate its practical relevance.

Keywords: dental implants, dental measurements, cephalometry, stereophotogrammetry, three-dimensional models

Cite as
Pioterek OW, Majka K, Goździewicz J, et al. Accuracy and reproducibility of photogrammetric measurements in dentistry: A systematic review. *Dent Med Probl.* 2026;63(5):1313–1330. doi:10.17219/dmp/205471

DOI
10.17219/dmp/205471

Copyright
Copyright by Author(s)
This is an article distributed under the terms of the Creative Commons Attribution 3.0 Unported (CC BY 3.0) (https://creativecommons.org/licenses/by/3.0/)

Highlights

- Photogrammetry is a highly reliable and accurate technique for dental applications, including cephalometric, dental arch and implant position measurements.
- Its effectiveness depends on external conditions, with scanning distance and light intensity identified as significant factors.
- Photogrammetry provides more precise and accurate implant position measurements than intraoral scanners and conventional impressions.
- Commercially available smartphone-based photogrammetry applications can accurately and precisely create digital three-dimensional facial models.
- Photogrammetry enables highly precise dental measurements, with errors below 0.5 mm, comparable to those of conventional techniques.

Introduction

Photogrammetry is an innovative method of obtaining three-dimensional (3D) models that is constantly being developed.[1,2] It has been used in geography and architecture,[3,4] but has now become a part of medicine.[5,6] This technique enables the creation of 3D models from two-dimensional photographs. Images of particular objects are processed using dedicated software, which superimposes photographs taken from different perspectives and creates a 3D mesh with a realistic texture based on the mathematical principle of triangulation (Fig. 1).[2] Such 3D models can later be used to perform measurements or produce 3D prints.[7–9]

The main differences between conventional scanning methods, such as intraoral and extraoral scanners, and photogrammetric methods lie in the process of capturing and processing 3D models. Intraoral scanners (IOS) mainly use laser scanning technology that irradiates an object with a laser beam, which is then reflected back to the scanner, and calculate the angle and distance between the laser, sensor and the scanned object, allowing it to generate a 3D point cloud of the object.[10] Extraoral scanners are based on structured light technology and project a geometric pattern onto the scanned object. A camera then captures the distorted pattern, on the basis of which a 3D model is generated.[11] Photogrammetry, on the other hand, is based solely on photographs captured from multiple angles, which, as mentioned above, are processed to generate a 3D model.[9]

In dentistry, conventional methods, such as IOS, laser scanners and dental impressions obtained using impression trays, are commonly used for taking measurements of the oral cavity and face.[12–15] Photogrammetry has the potential to become a useful tool for the digitization of patients' oral cavity data or an alternative to IOS for determining dental implant positions. Numerous studies have shown that it can be a less expensive alternative to IOS while being as accurate as conventional methods.[16–18] Furthermore, the use of abutments that are screwed onto a patient's implants, functioning as markers for photogrammetric machinery, allows their positions to be captured. Because the abutments are elevated above the gingiva, photogrammetry is not limited by the presence of blood or saliva, as is the case with IOS.[19,20] It is worth noting that this technology, although it has greater potential for capturing dental implant positions, is unable to capture adjacent structures, unlike IOS, which provide direct imaging of the patient's oral cavity and do not require additional steps.[21,22]

Photogrammetry can also be helpful in the digitization of patient information. Studies have shown that the use of photogrammetric techniques can accelerate the process of loading full dental arch prostheses by integrating

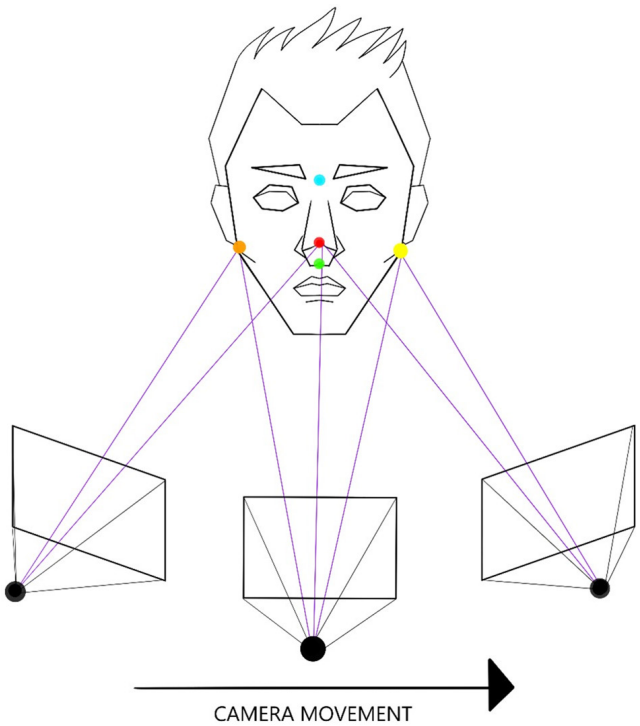

Fig. 1. Graphic depiction of the photogrammetric method

A point in object space, the projective center of the optical system, and the corresponding point in image space lie on a single straight line. Thus, a spatial point can be located at the intersection of 2 rays projected from 2 different camera positions.[9] Original figure was prepared by DP.

photogrammetric 3D models of dental impressions with models obtained from cone beam computed tomography (CBCT).[23,24]

Photogrammetry, when used to measure cephalometric parameters, can accurately predict the values obtained using traditional cephalometric methods, potentially limiting their use to areas of specific interest.[25–27] It also provides a viable approach for objectively assessing changes in facial appearance following dental reconstruction.[28]

There has been a noticeable increase in the number of articles describing the use of photogrammetry in dentistry and maxillofacial surgery in recent years. Authors tend to focus on its application in prosthetic dentistry and anthropological measurements.[16–18]

Since the last systematic review assessing the accuracy and precision of photogrammetry in dentistry was published, many articles on this subject have emerged. Hence, a decision was made to conduct a systematic review that evaluates the use of photogrammetry in dentistry with the aim of improving the understanding and validation of its relevance in dental medicine. This review was structured based on the following PICO question: "How accurate and reliable are photogrammetric techniques, either used alone or compared with traditional methods, in dentistry?"

Material and methods

Eligibility criteria

Based on the Preferred Reporting Items for Systematic reviews and Meta-Analyses (PRISMA) guidelines,[29] a description of the criteria used to assess the eligibility of each study for inclusion in our systematic review was prepared. To be included, an article had to:

- be an original study published in a scientific, peer-reviewed journal;
- be published in English;
- describe the type of dental, prosthodontic or cephalometric measurements performed using a photogrammetric technique;
- describe the accuracy or reproducibility of the above-mentioned measurements.

This systematic review did not include articles for which full study data was unavailable, such as conference abstracts, or articles of uncertain publication status, for example, non-peer-reviewed preprints. Case studies and technical notes were also excluded.

Information sources

At the beginning of December 2023, 4 databases were searched: Embase; Google Scholar; PubMed®; and Web of Science. The first 2,000 articles sorted by relevance in Google Scholar were scoped, as this number has been shown to be sufficient for a systematic review.[30] Although the cited study refers to only the first 200 results, the decision was made to extend the search in order to include studies that might not have been indexed in other databases, considering the novelty of the topic.

Due to the over 12-month time period between the primary search and manuscript submission, additional searches were conducted at the end of February 2025 to incorporate newly reported findings. Re-running searches before manuscript submission is necessary, according to the Cochrane Handbook for Systematic Reviews of Interventions – C37, to identify and incorporate the latest studies into the systematic review.[31]

Search strategy

During the database search, the following queries were used:

- PubMed®:
  - ("photogrammetry"[MeSH Terms] OR "photogrammetry"[All Fields]) AND ("dentistry"[MeSH Terms] OR "dentistry"[All Fields] OR "dentistry s"[All Fields]);
  - ("photogrammetry"[MeSH Terms] OR "photogrammetry"[All Fields]) AND "dental implants"[All Fields];
  - ("photogrammetry"[MeSH Terms] OR "photogrammetry"[All Fields] OR "stereophotogrammetry"[All Fields]) AND ("dentistry"[MeSH Terms] OR "dentistry"[All Fields] OR "dentistry s"[All Fields]);
  - ("photogrammetry"[MeSH Terms] OR "photogrammetry"[All Fields] OR "stereophotogrammetry"[All Fields]) AND "dental implants"[All Fields].
- Embase:
  - ('photogrammetry'/exp OR 'photogrammetry') AND ('dentistry'/exp OR 'dentistry');
  - ('photogrammetry'/exp OR 'photogrammetry') AND ('dental implants'/exp OR 'dental implants');
  - ('stereophotogrammetry'/exp OR 'stereophotogrammetry') AND ('dentistry'/exp OR 'dentistry');
  - ('stereophotogrammetry'/exp OR 'stereophotogrammetry') AND ('dental implants'/exp OR 'dental implants').
- Web of Science:
  - Photogrammetry AND Dentistry (All Fields);
  - Photogrammetry AND Tooth implants (All Fields);
  - Stereophotogrammetry AND Dentistry (All Fields);
  - Stereophotogrammetry AND Tooth implants (All Fields);
- Google Scholar:
  - Photogrammetry AND Dentistry;
  - Photogrammetry AND Tooth implants;
  - Stereophotogrammetry AND Dentistry;
  - Stereophotogrammetry AND Tooth implants.

Searches were not limited by language. We did not use any filters during the database search. For the re-run searches, a publication date filter was applied to include studies published since January 2024.

Considering the novelty of this review's subject and PICO question, "photogrammetry" and "stereophotogrammetry" were used as keywords that would ensure the identification of articles regarding this specific topic, and "dentistry" was used as a broad MeSH and Emtree term allowing the identification of articles within this entire specialty. The keyword "dental implants" was introduced to identify studies regarding dental implant measurements. Although it is included in the "dentistry" MeSH tree, it is not included in the corresponding Emtree hierarchy; therefore, its use was necessary. This search strategy, along with the inclusion of the first 2,000 results from Google Scholar, although more time-consuming, was intended to increase sensitivity by using very broad terms.

Selection process

Four authors (OWP, JG, KM, WT) were responsible for title screening. Each of the 4 authors searched an assigned database: Google Scholar (OWP); Web of Science (JG); Embase (KM); and PubMed® (WT). All authors performed their searches independently. The articles with titles related to the use of photogrammetry in dentistry as a measurement method were collected. Duplicates among the retrieved articles were then removed using Mendeley software (Elsevier, London, UK). Articles retrieved by the other authors were reviewed by OWP, and articles retrieved by OWP were reviewed by JG.

Four authors (OWP, KM, WT, JG) were responsible for screening the abstracts of articles identified in the first step. Each author independently reviewed an equal number of articles, which were assigned in alphabetical order. Using Mendeley software, articles were marked with the tags "included" if accepted and "excluded" if rejected. After the initial evaluation of the abstracts was completed, OWP reviewed the articles assessed by the other authors, and articles assessed by OWP were reviewed by JG.

Data collection

Three authors (KM, WT, JG) were responsible for collecting data from the initially included articles. For this step, we used an Excel spreadsheet in which each paper was evaluated according to the eligibility criteria. Each author collected data independently from an equal number of articles assigned in alphabetical order. The initially collected data was then reviewed by OWP.

Data items

The following data was extracted from each study: population, understood as the group of patients or the type of artificial model used in the study; type of measurements – cephalometric measurement, implant position measurement or dental arch measurement; method of measurement, understood as the technique used to generate the models from which measurements were taken or the technique used to perform direct measurements; and the software used to process photogrammetric data. The accuracy and reproducibility of the measurements were considered the outcomes of the reviewed studies.

Assessment of the risk of bias

Three authors (KM, WT, DP) were responsible for the risk-of-bias assessment of the studies. Each author independently assessed an equal number of studies, which were assigned alphabetically. Each data source was evaluated for risk of bias using the original Quality Assessment of Diagnostic Accuracy Studies (QUADAS-1) tool, which consists of 14 items (Table 1). QUADAS-1 is a validated, evidence-based quality assessment tool.[32,33] Each item was rated as "+", indicating a positive response, or "–", indicating a negative response. The initial assessment was reviewed by OP, and any disagreements were resolved through discussion between the authors.

Effect measures

For the accuracy and reproducibility outcomes, the extracted data showed considerable heterogeneity in the types of effect measures reported. Therefore, all effect measures related to the reproducibility or accuracy of photogrammetric measurements were taken into consideration. Effect measures for reproducibility outcomes included the intraclass correlation coefficient (*ICC*), Pearson's correlation coefficient, root mean square (RMS), mean deviation, and interquartile range. For accuracy, the effect measures included RMS deviation, percentage of measurements within a specified error range, mean deviation, and standard deviation of distances.

Data synthesis

The collected data from each article was then assigned to one of the 3 categories depending on the type of measurement performed: cephalometric measurement (n = 12), dental implant position measurement (n = 18), or dental arch measurement (n = 14), and was further classified according to whether accuracy or reproducibility was assessed.

The data was then sorted and divided into 6 independent groups to properly visualize and describe the synthesized information: cephalometric studies that measured reproducibility; cephalometric studies that measured accuracy; dental implant studies that measured reproducibility; dental implant studies that measured accuracy; dental arch studies that measured reproducibility; and dental arch studies that measured accuracy. A narrative synthesis was performed for each group. Due to the considerable variation in the types of measured effects, a statistical analysis of heterogeneity was not conducted.

Table 1. Items included in the Quality Assessment of Diagnostic Accuracy Studies (QUADAS-1) tool used for the assessment of the risk of bias of studies included in the review

Item	Question
D1	Was the spectrum of patients representative of the patients who will receive the test in practice?
D2	Were selection criteria clearly described?
D3	Is the reference standard likely to correctly classify the target condition?
D4	Is the time period between reference standard and index test short enough to be reasonably sure that the target condition did not change between the two tests?
D5	Did the whole sample or a random selection of the sample, receive verification using a reference standard?
D6	Did patients receive the same reference standard regardless of the index test result?
D7	Was the reference standard independent of the index test (i.e., the index test did not form part of the reference standard)?
D8	Was the execution of the index test described in sufficient detail to permit replication of the test?
D9	Was the execution of the reference standard described in sufficient detail to permit its replication?
D10	Were the index test results interpreted without knowledge of the results of the reference standard?
D11	Were the reference standard results interpreted without knowledge of the results of the index test?
D12	Were the same clinical data available when test results were interpreted as would be available when the test is used in practice?
D13	Were uninterpretable/intermediate test results reported?
D14	Were withdrawals from the study explained?

Results

During the database searches, 4,914 records were initially identified. After title screening for studies describing the use of photogrammetry in dentistry and the removal of duplicates, 490 articles remained. Abstract screening was then conducted, during which 396 papers were excluded, leaving 94 articles. Subsequently, the full texts of the remaining articles were evaluated according to the eligibility criteria. During this phase, 50 articles were excluded, and 44 articles were included in the final review (Fig. 2). Despite meeting the eligibility criteria, 1 study was excluded because of its insufficient sample size – a sample of 6 men and 6 women – which resulted in statistically non-significant findings with high *p*-values for all but one outcome.[34] Therefore, this study, despite meeting the eligibility criteria, did not provide sufficiently informative data regarding the accuracy or reliability of photogrammetric measurements and was excluded, in accordance with the PRISMA explanation and elaboration paper.[29]

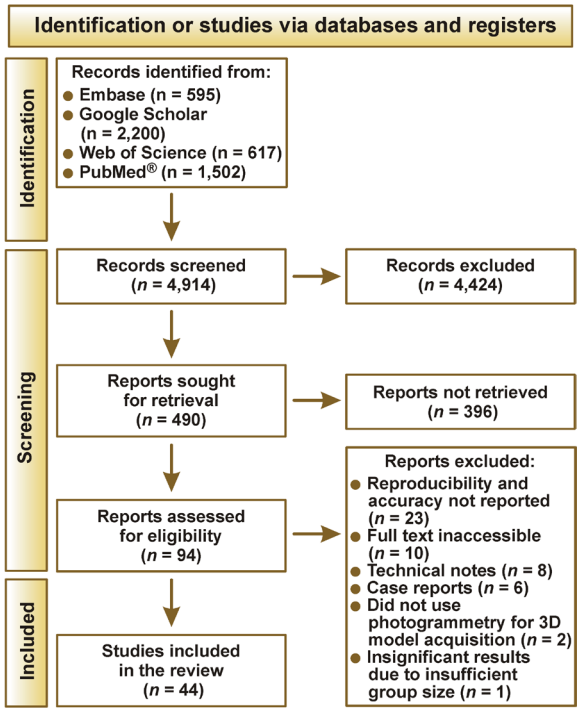

Fig. 2. Study flow diagram based on the Preferred Reporting Items for Systematic reviews and Meta-Analyses (PRISMA) 2020 flow diagram for new systematic reviews that include searches of databases and registers only

Risk of bias

For each study included in this review, the assessment of the risk of bias was conducted and presented graphically, with "+" indicating a positive response and "–"indicating a negative response (Table 2). Most studies received positive ratings for items related to the reference standard and the execution of the index and reference tests (D3–D9), with low-risk ratings ranging from 79.5% for D7 to 97.7% for D4. In contrast, high-risk ratings were more frequent in domains D1 (79.5%), D2 (68.2%), D10 (68.2%), D11 (54.5%), and D12 (52.3%). The highest proportions of high-risk ratings were observed in D13 (95.5%) and D14 (97.7%).

Reproducibility of cephalometric measurements

Seven studies described the reproducibility of photogrammetric measurements in the context of cephalometric measurements (Table 3). All studies described this technique as reproducible, with the exception of a single measurement reported in 1 study – the distance from the incisal edge to the distal canine.[25,28,35–39]

Table 2. Risk-of-bias assessment for each study included in the systematic review

Study	Risk of bias													
	D1	D2	D3	D4	D5	D6	D7	D8	D9	D10	D11	D12	D13	D14
Al-Khatib et al. 2011[64]	–	+	+	+	+	+	–	–	+	+	–	+	–	–
Al-Khatib et al. 2012[63]	+	+	+	+	+	+	+	+	+	+	+	+	–	–
Arapović-Savić et al. 2019[65]	–	–	+	+	+	+	+	+	+	+	+	+	–	–
Artopoulos et al. 2014[40]	–	–	+	+	+	+	+	+	+	–	+	–	–	–
Bergin et al. 2013[60]	–	–	+	+	+	+	+	+	+	+	+	+	–	–
Bratos et al. 2018[45]	–	–	+	+	+	+	+	+	+	–	–	–	–	–
Brons et al. 2013[35]	+	+	+	+	+	+	+	+	+	–	–	+	–	+
Castillo et al. 2018[25]	+	–	+	+	+	+	–	+	–	–	+	+	–	–
Ceinos et al. 2016[36]	–	+	–	+	–	–	–	–	–	–	–	+	–	–
Chaudhary et al. 2024[75]	+	+	+	+	+	+	+	+	–	–	–	–	–	–
Cheng et al. 2024[52]	–	–	+	+	+	+	+	+	+	–	–	–	–	–
Codari et al. 2016[70]	–	–	+	+	+	+	+	+	+	+	+	+	–	–
Di Blasio et al. 2025[43]	–	–	–	+	+	+	+	+	–	–	–	+	–	–
Estibalez-Recasens et al. 2025[56]	+	+	+	+	+	–	–	+	+	+	–	+	–	–
Faria et al. 2025[55]	–	+	+	+	+	+	+	+	+	–	–	–	–	–
Fu et al. 2017[66]	+	+	+	+	+	+	+	+	+	–	+	+	–	–
Goellner et al. 2010[67]	–	–	+	+	+	+	+	+	+	–	–	+	–	–
Hartmann et al. 2025[39]	–	+	+	+	+	+	+	+	+	–	–	–	+	–
Kamel et al. 2022[71]	–	–	+	+	+	–	+	+	+	+	+	–	–	–
Keil et al. 2025[38]	–	+	+	+	+	+	+	+	+	–	–	–	+	–
Lincoln et al. 2016[41]	–	–	+	+	+	+	+	–	+	+	+	–	–	–
Liu et al. 2024[54]	–	–	+	+	+	+	+	+	+	–	–	–	–	–
Ma et al. 2021[46]	–	–	+	+	+	+	+	+	+	+	+	+	–	–
Mahmood et al. 2023[69]	–	–	+	+	+	+	+	+	–	–	+	–	–	–
Mai and Lee 2022[72]	–	+	+	+	+	+	+	+	+	–	–	–	–	–
Örtorp et al. 2005[61]	–	–	+	+	+	+	+	+	+	–	–	–	–	–
Pinto et al. 2024[47]	–	–	+	+	+	+	+	+	+	+	+	+	–	–
Pozzi et al. 2023[53]	–	–	+	+	+	+	+	+	–	+	+	+	–	–

Study	Risk of bias													
	D1	D2	D3	D4	D5	D6	D7	D8	D9	D10	D11	D12	D13	D14
Rangel et al. 2008[73]	–	–	–	+	–	–	+	+	–	–	–	–	–	–
Revilla-León et al. 2021[57]	–	–	+	+	+	+	+	+	+	–	–	–	–	–
Revilla-León et al. 2023[62]	–	–	+	+	+	+	+	+	+	+	+	+	–	–
Revilla-León et al. 2024[48]	–	–	+	+	+	+	–	+	+	–	+	–	–	–
Revilla-León et al. 2025[58]	–	–	+	+	+	+	–	+	+	+	+	–	–	–
Rivara et al. 2016[49]	+	–	+	+	+	+	+	+	+	–	–	+	–	–
Seifert et al. 2024[44]	–	+	+	+	+	+	+	+	+	–	–	+	–	–
Sterenborg et al. 2016[28]	+	+	+	+	+	+	–	+	+	–	+	+	–	–
Sterenborg et al. 2018[37]	+	+	–	–	–	–	–	+	–	–	–	+	–	–
Tohme et al. 2021[51]	–	–	+	+	+	+	+	+	+	+	+	+	–	–
Tohme et al. 2023[50]	–	–	+	+	+	+	+	+	+	–	–	–	–	–
Stuani et al. 2019[17]	–	–	+	+	+	+	–	+	+	–	–	–	–	–
Yang et al. 2023[74]	–	–	+	+	+	+	+	+	+	–	+	–	–	–
Zhou et al. 2024[59]	–	–	+	+	+	+	+	+	+	–	–	–	–	–
Zotti et al. 2022[18]	–	–	+	+	+	+	+	+	+	–	+	–	–	–
Majid et al. 2006[42]	–	–	+	+	+	+	+	+	+	–	–	–	–	–

Table 3. Reproducibility of photogrammetric cephalometric measurements

Study	Population/materials	Technique and software used for measurements	Reproducibility of measurements
Sterenborg et al.[28]	adults	photogrammetry, 3dMDface	Most measurements had a Pearson's correlation coefficient of >0.8. Measurements of the stomion–gnathion and subnasale–gnathion showed lower correlation coefficients, with the lowest values being 0.46 and 0.76, respectively.
Brons et al.[35]	pediatric patients	photogrammetry, 3dMDface	95% of the distances were 0.80 mm or less for intraobserver measurements and below 1.10 mm for interobserver measurements.
Ceinos et al.[36]	adults	photogrammetry, DermaPix	The *ICC* values for intra- and interexaminer facial measurements ranged from 0.732 to 0.976, except for measurements involving the inner part of the dental corridor, for which *ICC* values ranged from 0.598 to 0.914.
Sterenborg et al.[37]	adults	photogrammetry, 3dMDface	All measurements had a Pearson's correlation coefficient of >0.85.
Castillo et al.[25]	adults	photogrammetry, Vectra 3D	The inter- and intraexaminer Pearson's correlation coeffcient for photogrammetry averaged 0.94 and 0.92, respectively.
Hartmann et al.[39]	adults	photogrammetry, Vectra M5, 3D Scanner App	Photogrammetric models generated using smartphones showed higher interobserver reliability for overall landmark-to-landmark deviation, superior alignment and higher volumetric accuracy compared with models generated using the TrueDepth camera.
Keil et al.[38]	mannequin	photogrammetry, Heges 3D, Agisoft Metashape	The lowest precision values for photogrammetry were achieved at 500 lx. Photogrammetry showed the highest precision at 5,000 lx and slightly lower precision at 20,000 lx.

ICC – intraclass correlation coefficient.

The highest Pearson's correlation coefficient was reported in a study evaluating cephalometric measurements in relation to dental measurements. The mean value was 0.94 for interexaminer reliability and 0.92 for intraexaminer reliability, indicating excellent reliability of all measurements made.[25]

Two studies assessed changes in the vertical dimension of occlusion and showed that the photogrammetric technique achieved correlation coefficients above 0.80 for all measurements, indicating good reliability.[28,37]

One study of cephalometric measurements described photogrammetry as having lower precision. Although facial measurements showed inter- and intraoperator *ICC*s ranging from 0.732 to 0.976, indicating good to excellent reliability, the *ICC* values for measurements of the dental corridor ranged from 0.598 to 0.914, indicating lower repeatability. The lowest *ICC* reported for measurements of the dental corridor was observed for the incisal edge – right premolar segment and was 0.732, with a 95% confidence interval (95% *CI*) ranging from 0.285 to 0.915.[36]

Ambient light has a significant influence on the reliability of photogrammetry-based facial models. Keil et al. showed that the photogrammetric method achieved the highest precision at 5,000 lx, slightly lower precision at 20,000 lx, and the lowest precision at 500 lx.[38]

For measurements in a pediatric population, with and without orofacial clefts, 95% of the distances were 0.80 mm or less for intraobserver measurements and below 1.10 mm for interobserver measurements. Statistical analysis showed that the age of the infants and the presence of orofacial clefts did not significantly affect the measurements, indicating that photogrammetry can be a reliable method for soft tissue assessment in infants with and without orofacial clefts.[35]

The 3D Scanner App (v. 2.1.2; Laan Consulting Corp., New York, USA) was also shown to be a reliable method for generating facial 3D models. It demonstrated good to excellent *ICC* values for linear and volumetric measurements. Additionally, photogrammetry-based models showed higher *ICC* values than models generated using TrueDepth camera of an iPhone 14 Pro (Apple Inc., Cupertino, USA).[39]

Accuracy of cephalometric measurements

Seven different studies described the accuracy of photogrammetric measurements in the context of cephalometric measurements (Table 4).[38–44]

A comparative testing study showed photogrammetry to be significantly less accurate than methods such as facial moulage and CBCT scans.[41] The study reported mean percentage differences of 1.067 for photogrammetry, 0.622 for CBCT and 0.482 for facial moulage, indicating that photogrammetry had the largest measurement error among these 3 methods.[41] The results of another comparative study indicated that even though photogrammetry was less accurate than the abovementioned methods, its accuracy was still acceptable, as more than 99% of the measured points in the photogrammetric model specimen were within the clinically acceptable limit of 1 mm compared with the CT scan.[40]

Table 4. Accuracy of photogrammetric cephalometric measurements

Study	Population/materials	Technique and software used for measurements	Accuracy of measurements
Lincoln et al.[41]	mannequins	photogrammetry, 3dMDface	Pairwise comparisons showed differences between the methods, with photogrammetry exhibiting a higher percentage error than the other 2 methods, whereas CBCT and the stone model showed similar percentage errors. Photogrammetry differed significantly from CBCT and the stone model ($p < 0.05$). The greatest differences were observed at the glabella, nasion and palpebrale inferius landmarks, whereas the data for the other points were similar to those obtained using CBCT and the stone model.
Artopoulos et al.[40]	mannequins	photogrammetry, Di3D Capture	More than 99% of the measured points for the photogrammetric specimen were within the clinically acceptable limit of 1 mm compared with the CT scan.
Majid et al.[42]	adults, mannequins	photogrammetry, software not reported	The natural features technique was found to significantly improve the accuracy of non-contact craniofacial anthropometric measurements. In the mannequin test, RMSE values were 0.8 mm and 6.0 mm for the natural features technique and control frame technique, respectively. For human faces, RMSE values were 2.0 mm and 3.0 mm, respectively.
Di Blasio et al.[43]	adults	photogrammetry, Polishape 3D	Measurements were repeatable and remained within the clinically acceptable range of ±1 mm even in the case of roll, pitch and yaw of the head, with the exception of measurements involving the trago.
Seifert et al.[44]	adults	photogrammetry, Polycam, ScandyPro, 3dMDface, EM3D	The mean surface distances for EM3D, Polycam and ScandyPro were 1.46 mm, 1.66 mm and 1.61 mm, respectively. The mean landmark distances for EM3D, Polycam and ScandyPro were 1.45 mm, 1.27 mm and 1.26 mm, respectively. ANOVA showed no significant differences among scanners for any landmark.
Hartmann et al.[39]	adults	photogrammetry, Vectra M5, 3D Scanner App	Smartphone-based approaches using both the TrueDepth camera and photogrammetry exhibited overall landmark-to-landmark distances of ≤2 mm.
Keil et al.[38]	mannequin	photogrammetry, Heges 3D, Agisoft Metashape	Single-camera photogrammetry showed the lowest RMSE values at 5,000 lx, although only random differences were observed compared with 20,000 lx.

CBCT – cone beam computed tomography; CT – computed tomography; RMSE – root mean square error; ANOVA – analysis of variance.

External factors such as ambient light and patient cooperation may influence the accuracy of photogrammetric facial model acquisition. At a light intensity of 5,000 lx, the results were most accurate, whereas at 20,000 lx they were slightly less precise, with the least accurate results observed at 500 lx.[38] Interestingly, patient head positioning affected the accuracy of photogrammetry only slightly. Regardless of head position, all measurements were within the clinically acceptable limit of 1 mm except for the trago.[43]

Two comparative studies tested different methods of acquiring photogrammetry-based facial 3D models. One showed that there were no significant differences between models generated using a smartphone-based TrueDepth camera and those generated using photogrammetry, whereas all of them exhibited overall landmark-to-landmark distances of ≤2 mm.[39] The other study analyzed discrepancies between models generated using different photogrammetry-based smartphone applications and showed no significant differences between them.[44]

Majid et al. proposed a novel photogrammetric technique based on characteristic points of the face, namely the natural features technique.[42] Its accuracy was measured using the root mean square error (RMSE) and was 0.351 mm on the x-axis, 0.381 mm on the y-axis, and 0.843 mm on the z-axis. The method was more accurate than conventional photogrammetry.[42]

Reproducibility of dental implant position measurements

Twelve different studies described the reproducibility of photogrammetric measurements in the context of dental implant positions (Table 5). All of them characterized the technique as reproducible.[45–56]

Table 5. Reproducibility of photogrammetric dental implant position measurements

Study	Population/materials	Technique and software used for measurements	Reproducibility of measurements
Pinto et al.[47]	dental casts	photogrammetry, ICam4D, PIC Dental	Mean RMS repeatability values for the model with 4 implants were 5.18 µm for PIC and 7.01 µm for ICAM. For the model with 6 implants, the corresponding values were 13.88 µm and 8.67 µm.
Tohme et al.[51]	dental casts	photogrammetry, PIC Dental	The mean angular deviation did not differ significantly among the impression techniques and among ISBs within DIOS and DPG. The mean RMS differed significantly among impression techniques ($p < 0.001$) and was lower with DPG (0.014 ±0.013). The mean RMS for 3D deviation within ISBs did not differ significantly for DIOS ($p = 0.615$) or DPG ($p = 0.666$).
Ma et al.[46]	dental casts	photogrammetry, ICam4D	Median precision values were 2.00 µm (*IQR*: 1.65), 36.00 µm (*IQR*: 9.95) and 29.40 µm (*IQR*: 4.80) for the photogrammetry, IOS and CNV groups, respectively. The PG group showed significantly higher precision than the IOS ($p < 0.001$) and CNV groups ($p < 0.001$).
Tohme et al.[50]	dental casts	photogrammetry, PIC Dental	The mean RMS values for 3D deviations of the whole scan body ($p < 0.001$) and the flat angled surface ($p < 0.001$) differed significantly among the techniques and were significantly lower with photogrammetry. Mean global angular deviations also differed significantly among the techniques and were lower with photogrammetric acquisition ($p < 0.001$).
Bratos et al.[45]	dental casts	photogrammetry, iWitnessPRO	For photogrammetry, the grand mean standard error was 26.8 µm (95% *CI*: 18.1–51.4 µm).
Revilla-León et al.[48]	dental casts	photogrammetry, Geomagic	Levene's test showed no significant differences in mean precision among the tested groups ($p = 0.197$).
Rivara et al.[49]	dental casts	photogrammetry, photomodeler, EOS System	The tests showed an average precision of 4 mm for implant positions and less than 1 degree for implant axes.
Cheng et al.[52]	dental casts	photogrammetry, ICam4D	Photogrammetry exhibited the lowest RMS 3D and angular deviations at all implant positions compared with CNV, IOS and MIOS. It also showed lower deviations at the D1 distance than CNV, IOS and MIOS.
Pozzi et al.[53]	dental casts	photogrammetry, PIC Dental	A significantly lower *SD* of the mean 3D deviations was observed with photogrammetry than with IOS (17.7 µm vs. 37.1 µm, $p < 0.0001$). The *SD* of angular measurements was also significantly lower with photogrammetry than with IOS (0.04° vs. 0.14°, $p < 0.0001$).
Liu et al.[54]	dental casts	photogrammetry, PIC Dental	Photogrammetry showed the highest precision for distance and angulation measurements. Its linear, angular and RMS deviation values (9–11 µm, 0.06–0.08°, 8–10 µm, respectively) were significantly lower than those for open tray impression and IOS according to ANOVA.
Faria et al.[55]	dental casts	photogrammetry, PIC Dental	For photogrammetry, no significant differences ($p = 0.075$) were found among the 3 implant distributions evaluated. High precision was observed for all devices analyzed, with no significant differences among them ($p = 0.097$). Overall precision, expressed as RMS, was 12.42 µm (95% *CI*: 11.33–13.50 µm) for photogrammetry.
Estibalez-Recasens et al.[56]	adults	photogrammetry, PIC Dental	For linear measurements, the *M* ±*SD* precision was 14.71 ±12.21 µm. For angular measurements, the *M* ±*SD* precision was 0.072 ±0.064°.

RMS – root mean square; ISBs – intraoral scan bodies; DIOS – digital intraoral scanning; DPG – digital photogrammetry; IOS – intraoral scanners; MIOS – intraoral scanning with splinting; CNV – conventional impression; 95% *CI* – 95% confidence interval; *SD* – standard deviation; *IQR* – interquartile range; *M* – mean.

Five studies comparing the precision of photogrammetry, intraoral scanning and conventional impression techniques for complete arch implant rehabilitation showed photogrammetry to be significantly more precise than the other methods. In the first study, the median precision was 2.00 µm.[46] Another study showed that, in terms of precision, the mean RMS values for 3D deviations of both the entire scan body and the flat angled surface were significantly smaller with photogrammetry. Comparison of the mean global angular deviations yielded similar results.[50] A previous study by the same author compared photogrammetry with IOS and found no differences in angular deviations or the mean RMS values of 3D deviations between the 2 techniques.[51] The most recent studies further demonstrated the superior precision of photogrammetry compared with IOS and conventional impressions.[52–54]

No significant differences in terms of precision were found in a study investigating the impact of changes in scanning distance on the accuracy and reproducibility of photogrammetry.[48]

In a study involving a coordinate-measuring machine (CMM), it was demonstrated that the precision of photogrammetry was similar to that of the CMM.[45] For the groups that used the photogrammetry method, the grand mean for linear measurements was 26.8 µm; however, 2 groups – AvgR-MaxO and MaxR-MaxO – were not included in the calculation due to the limitation of the typodont in simulating living tissues. The precision of angular measurements also showed no significant differences between the groups, with grand means of 0.129° for the x angle and 0.221° for the y angle.[45]

Pinto et al. evaluated the repeatability of various digital acquisition methods for capturing implant positions in prostheses with 4 and 6 implants.[47] The study findings suggested that photogrammetry demonstrated superior repeatability compared with IOS for recording implant locations in complete arch prostheses supported by both 4 and 6 implants, but were less repeatable than laboratory scanners.[47] The most recent findings confirmed that the number of implants did not influence the precision of photogrammetry and that its precision remained very high, with an RMS of 12.42 µm.[55] Additionally, a study by Estibalez-Recasens et al. showed that the in vivo precision of photogrammetry in patients with 6 implants was similarly high.[56] The linear and angular measurements were 14.71 ±12.21 µm and 0.072 ±0.064°, respectively.[56]

Accuracy of dental implant position measurements

Fourteen studies described the accuracy of photogrammetric measurements of dental implant positions (Table 6).[45,46,48,50–54,57–62]

In 5 comparative studies, photogrammetry was shown to have high accuracy.[46,51–54] All of them showed photogrammetry to be more accurate in terms of 3D and angular discrepancies than IOS.[51,53] Additionally, three of them reported higher trueness for photogrammetry than for conventional impressions.[46,52,54]

Two studies compared photogrammetry with conventional impression techniques. In the study by Bergin et al., the mean linear measurement error was 26.2 µm for the conventional impression technique and 28.8 µm for photogrammetry, with no statistically significant difference between the methods.[60] In contrast, Zhou et al. reported greater linear and angular discrepancies for photogrammetry, with mean values of 145 ±196 µm and 0.82 ±0.88°, respectively, which were significantly greater than those obtained with the conventional impression technique.[59]

Interestingly, the study by Örtorp et al. showed that cylinder center-point distortion was smaller with the photogrammetric technique than with the conventional impression technique, whereas angular cylinder distortion was greater with photogrammetry.[61]

Four articles regarding dental implant position measurements described photogrammetry as having lower overall accuracy compared with a CMM. Revilla-León et al. measured the average 3D discrepancy of photogrammetry at 77.6 µm.[57] Their later study confirmed these results, showing a statistically significant difference between the CMM method and photogrammetry, with a trueness difference of 1.8 µm between the systems.[62] Similarly, Bratos et al. conducted a study that showed a mean linear accuracy of 55.2 µm, which was lower than that of the CMM.[45] Additionally, Bergin et al. found the CMM to have higher accuracy than photogrammetry, but the difference was not statistically significant.[60]

Two articles by Revilla-León et al. investigated how scanning distance and the reference point affect the performance of photogrammetry.[48,58] In one study, the authors compared accuracy at 3 different distances.[48] The 30-cm scanning group yielded the most accurate linear measurements, with a linear discrepancy of 17 ±4 µm and an angular discrepancy of 0.17 ±0.02°. Measurements performed at shorter (20 cm) or longer (35 cm) distances were less accurate.[48] In a study investigating the effect of the reference points, it was demonstrated that the selected reference point could also influence the accuracy of photogrammetry.[58] Three groups were created based on the implant used as the reference point: the right first molar, left canine and left first molar. The study revealed differences in linear and angular trueness between the groups, with the first right molar used as a reference point showing the highest trueness values. Despite the differences between the groups, the measured angular and linear discrepancies were 0.01 ±0.01° and 6 ±3 µm, respectively. Therefore, the impact of the observed discrepancies was unlikely to be clinically significant.[58]

Table 6. Accuracy of photogrammetric dental implant position measurements

Study	Population/materials	Technique and software used for measurements	Accuracy of measurements
Tohme et al.[51]	dental casts	photogrammetry, PIC Dental	Mean angular discrepancies differed significantly among the impression techniques ($p < 0.001$). The lowest value was observed with DPG (0.724 ±0.064°), whereas an elevated value was observed with DIOS (1.744 ±0.175°). The mean RMS 3D deviation differed significantly among the impression techniques ($p < 0.001$) and was lower with DPG (0.078 ±0.001) than with DIOS (0.536 ±0.063).
Pozzi et al.[53]	dental casts	photogrammetry, PIC Dental	For 3D deviations, IOS showed a higher mean 3D deviation (ΔEUC) than photogrammetry (52.8 µm vs. 33.4 µm, $p < 0.0001$). For angular deviations, IOS showed a slightly higher mean deviation (ΔANGLE) than photogrammetry (0.28° vs. 0.24°, $p = 0.0022$).
Ma et al.[46]	dental casts	photogrammetry, ICam4D	The median of trueness was 24.45 (*IQR*: 0.73), 43.45 (*IQR*: 6.17) and 28.70 (*IQR*: 7.90) µm for the photogrammetry, IOS and CNV groups, respectively. The photogrammetry group showed significantly higher trueness than the IOS ($p < 0.001$) and CNV groups ($p = 0.033$).
Bergin et al.[60]	dental casts	photogrammetry, iWitnessPRO	The average measurement error was 26.2 µm (95% *CI*: 15.9–36.6) for the conventional method and 28.8 µm (95% *CI*: 24.8–32.9) for photogrammetry. Overall measurement accuracy did not differ significantly between the conventional and photogrammetric methods.
Tohme et al.[50]	dental casts	photogrammetry, PIC Dental	The 3D deviation of the whole scan body was significantly lower with photogrammetry and higher with digital scanning. The mean RMS for 3D deviations of the flat angled surface was significantly lower with digital scanning and higher with photogrammetry ($p < 0.001$). The mean global angular distortion was lower with photogrammetry and higher with digital scanning ($p < 0.001$).
Revilla-León et al.[57]	dental casts	photogrammetry, ICam4D	Photogrammetry showed significantly greater y-axis distortion and a larger 3D discrepancy than all CNV and IOS groups ($p = 0.004$). The y-axis discrepancy for photogrammetry was 73.7 µm, and the 3D discrepancy was 77.6 µm.
Bratos et al.[45]	dental casts	photogrammetry, iWitnessPRO	The grand mean of accuracy of linear measurements for photogrammetry was 55.2 µm (95% *CI*: 8.8–130.8 µm). Angular measurements showed a similar patter to linear measurements.
Revilla-León et al.[48]	dental casts	photogrammetry, Geomagic	At a scanning distance of 20 cm, the linear discrepancy was 25 ±4 µm and the angular discrepancy was 0.15 ±0.01°. At 30 cm, the corresponding discrepancies were 17 ±4 µm and 0.17 ±0.02°. At 35 cm, they were 27 ±6 µm and 0.19 ±0.01°, respectively.
Revilla-León et al.[58]	dental casts	photogrammetry, PIC Dental	A linear discrepancy of 6 ±3 µm and an angular discrepancy of 0.01 ±0.01° were reported.
Örtorp et al.[61]	dental casts	photogrammetry, Zeiss Prismo VAST	Photogrammetry reproduced the x-axis and 3D parameters more accurately than the plaster technique when cylinder centre-point distortion was assessed. Angular cylinder distortion was greater with photogrammetry than with the impression technique.
Revilla-León et al.[62]	dental casts	photogrammetry, PIC Dental	Photogrammetry showed an overall scanning accuracy value of 20.15 ±25.41 µm.
Cheng et al.[52]	dental casts	photogrammetry, ICam4D	Photogrammetry showed lower RMS 3D discrepancies at all implant positions, reduced RMS 3D bias at implant positions #7 and #3, and lower angular bias at implant positions #7, #5 and #3. However, photogrammetry showed larger linear errors for the D3 and D4 distances.
Zhou et al.[59]	dental casts	photogrammetry, ICam4D	The overall *M* ±*SD* distance deviation for photogrammetry was 149 ±196 µm, and the angular deviation was 0.82 ±0.88°. Using 150 µm as the clinically acceptable error range, 69.7% of distance deviations were below 150 µm.
Liu et al.[54]	dental casts	photogrammetry, PIC Dental	The linear, angular and RMS trueness values for photogrammetry (31–39 µm, 0.22–0.28°, 20–23 µm) were significantly lower ($p < 0.001$) than those for open tray impression and IOS.

Reproducibility of dental arch dimension measurements

The reproducibility of dental arch dimension measurements was reported in 7 studies (Table 7).[17,18,63–67] Two of them reported *ICC* values above 0.90 for all measurements performed,[18,65] indicating excellent reliability.[68] Four studies indicated good agreement or values ranging from good to excellent, depending on the measurement, with *ICC* values varying from 0.71 to 0.998.[63,64,66,67] One study reported lower reproducibility, with a repeatability coefficient of 0.474.[17]

One of the studies measured validity and reliability using crown widths and selected dental arch dimensions.[63] The *ICC* values varied between both measurements – the mean *ICC* was 0.88 for crown widths, whereas the mean *ICC* for dental arch dimensions was 0.97.[63] A similar range of *ICC* values (0.879–0.998) was reported in a study that focused on measuring the mesiodistal crown diameter, arch width and arch perimeter.[66]

Table 7. Reproducibility of photogrammetric dental arch dimension measurements

Study	Population/materials	Technique and software used for measurements	Reproducibility of measurements
Arapović-Savić et al.[65]	dental casts	photogrammetry, OP4D	Correlation coefficients were close to 1 for all measurements.
Zotti et al.[18]	dental casts	photogrammetry, 3DF Zephyr Free	*ICC* was 0.99 for each pair of measurements, indicating almost perfect agreement between the 2 measurements.
Goellner et al.[67]	adults	photogrammetry, ARAMIS	*ICC*s ranged from "good" (0.71 at 3 N) to "optimal" (0.98 at 18 N).
Stuani et al.[17]	dental casts	photogrammetry, 3DF Zephyr Free	The precision between the digital model measurements showed a repeatability coefficient of 0.474.
Fu et al.[66]	dental casts	photogrammetry, MeshLab	The intrarater *ICC*s ranged from 0.879 to 0.998 for the digital measurements, indicating good intrarater reliability.
Al-Khatib et al.[64]	adults	photogrammetry, software not reported	Precision was generally high, with all *ICC* values >0.80.
Al-Khatib et al.[63]	dental casts	photogrammetry, Australis software	The mean *ICC* was 0.88 for crown widths and 0.97 for dental arch dimensions.

The widest range of *ICC* values was observed in a study focused on evaluating tooth displacement under a low horizontal tensile force (≤18 N), with the lowest *ICC* value of 0.71 at a force of 3 N and the highest value of 0.98 at a force of 18 N.[67]

Good reliability, with all *ICC* values >0.80, was reported in the study focused on investigating tooth size and dental arch dimensions in Malays using a stereophotogrammetric system.[64]

Two studies compared photogrammetric measurements obtained using 3D scanning systems and confirmed their high reproducibility.[18,65] The first study reported *ICC* values at 0.99 for each pair of measurements obtained with photogrammetry, indicating almost perfect agreement between the 2 measurements.[18] The second study noted similarly high *ICC* values for different measurements, including mesiodistal widths of individual teeth, mesiodistal widths of two-teeth segments, and intercanine and intermolar distances in both the maxilla and mandible, with correlations close to 1 in all cases and the lowest *ICC* value being 0.9737.[65] These studies indicated excellent reproducibility of photogrammetry.

In contrast to all the abovementioned studies, 1 study reported low reproducibility of photogrammetric measurements, with a repeatability coefficient of 0.474.[17]

Accuracy of dental arch dimension measurements

Thirteen studies evaluated the accuracy of photogrammetry in comparison with various measurement methods (Table 8).[17,18,63–66,69–75]

Three studies found no statistically significant differences between the results when photogrammetry was compared with other reliable measurement techniques.[64,66,69] When photogrammetric measurements were compared with those performed on dental casts using calipers, the statistical analysis showed no significant differences between the 2 methods except for the lower arch perimeter. Additionally, photogrammetric measurements showed clinically acceptable accuracy, with differences between measurements of less than 0.5 mm.[64,66,69] This was further confirmed by 3 other studies that investigated the accuracy of the photogrammetric technique and demonstrated clinically acceptable accuracy, with errors below 0.5 mm.[18,65,74]

A study by Kamel et al. compared the accuracy of photogrammetry and an extraoral scanner in assessing the marginal fit of crowns.[71] The findings showed no statistically significant difference between the 2 methods, and the accuracy of photogrammetry was deemed to be clinically acceptable, with discrepancies below 120 μm.[71]

Two studies that compared photogrammetric measurements with measurements performed on plaster impressions reported differences between the methods.[63,73] One study observed differences in measurements involving the second premolars, canines and arch perimeter when comparing values obtained using calipers and photogrammetry, with photogrammetry showing larger discrepancies. However, all measurements remained within a clinically acceptable error range of less than 0.5 mm.[63] The most recent study by Chaudhary et al. showed no statistically significant differences between measurements made on gypsum models and photogrammetric digital models for intercanine distances and distances from the first premoral to the first molar in both quadrants.[75] Additionally, there was no significant difference in the volumetric comparison.[75]

One study assessed photogrammetry against measurements obtained using CBCT.[70] No statistically significant differences were noted between the results obtained using 3D dentofacial imaging and the CBCT reference, except for a single distance.[70]

An analysis of different approaches to facial scanning concluded that the use of extraoral markers significantly enhanced the accuracy of 3D dentofacial images obtained using photogrammetry.[72]

Table 8. Accuracy of photogrammetric dental arch dimension measurements

Study	Population/materials	Technique and software used for measurements	Accuracy of measurements
Arapović-Savić et al.[65]	dental casts	photogrammetry, OP4D	For the mesiodistal widths of individual teeth, the mean error was <0.2 mm. For the mesiodistal widths of two-tooth segments, errors were approx. 0.2 mm. For intercanine and intermolar distances in both the maxilla and mandible, errors were <0.3 mm, with a mean value of 0.2741 mm. The recorded differences were considered clinically negligible.
Yang et al.[74]	adults, dental casts	photogrammetry, PhotoCatch	The majority of reconstructed points fell within the ±0.2 mm error range. The reported values were 80.9 µm ±3.1% for an f/2.5 lens with a polarizer and 82.4 µm ±2.7% for an f/5.6 lens with a polarizer.
Mahmood et al.[69]	dental casts	photogrammetry, Agisoft Metashape	The mean differences between measurements ranged from –0.042 mm to 0.355 mm, were clinically acceptable (<0.5 mm) and were not statistically significant ($p > 0.05$).
Zotti et al.[18]	dental casts	photogrammetry, 3DF Zephyr Free	For the various superimpositions, the *M* ±*SD* differences between the 2 meshes were –0.02 ±0.077 mm for photogrammetry vs. dental extraoral laboratory scanner and 0.009 ±0.087 mm for photogrammetry vs. IOS, indicating good agreement among models obtained using the different acquisition methods.
Mai and Lee[72]	adults	photogrammetry, Di3D Capture	The 3D positional discrepancy was 0.959 mm (*SD*: 0.043) for tooth-based matching and 0.078 mm (*SD*: 0.041) for marker-based matching. Occlusal angle deviation was 3.187° (*SD*: 0.147) for tooth-based matching and 0.955° (*SD*: 0.350) for marker-based matching. Dental midline deviation was 0.393 mm (*SD*: 0.257) for tooth-based matching and 0.054 mm (*SD*: 0.074) for marker-based matching.
Rangel et al.[73]	adults	photogrammetry, 3dMDface	The average distance between the matched datasets was 0.35 mm (*SD*: 0.32 mm), indicating acceptable agreement between the datasets.
Kamel et al.[71]	dental casts	photogrammetry, 3DF Zephyr Free	The mean marginal gap obtained using photogrammetric scanning was 99.6 ±28.3 µm.
Stuani et al.[17]	dental casts	photogrammetry, 3DF Zephyr Free	The accuracy of digital model measurements was characterized by an *SD* of ±0.171 mm.
Fu et al.[66]	dental casts	photogrammetry, MeshLab	The mean differences between measurements ranged from 0.011 mm to 0.402 mm. The mean differences between measurements obtained by photogrammetry and on dental casts were not significant, except for the lower arch perimeter. All differences were regarded as clinically acceptable (<0.5 mm).
Al-Khatib et al.[64]	adults	photogrammetry, software not reported	Most of the mean differences between calliper and photogrammetric measurements were not statistically significant ($p > 0.05$). The differences ranged from 0.02 mm to 0.2 mm.
Codari et al.[70]	adults	photogrammetry, Vectra 3D	The median distance between ROI point clouds was 0.59 mm (0.43–0.73 mm). The median percentage of corresponding points was 86.1% (81.6–92.1%).
Al-Khatib et al.[63]	dental casts	photogrammetry, Australis software	A high degree of validity was observed, with a mean difference of <0.5 mm between direct and indirect measurements.
Chaudhary et al.[75]	dental casts	photogrammetry, 3DF Zephyr Free	Statistical analysis showed no significant differences between photogrammetric and gypsum models in the C–C distance, the distance between the mesial marginal ridge of the first premolar and the distal marginal ridge of the first molar in the first and second quadrants, or volumetric measurements.

ROI – region of interest.

Discussion

The findings suggest that photogrammetry may be a promising measurement method in dentistry for assessing cephalometric measurements, dental implant positions and dental arch dimensions. However, further studies are needed to provide robust evidence of its clinical utility before its routine implementation in dental practice can be recommended.

In the case of cephalometric measurements, it should be noted that indirect measurements, such as 3D face scans, can be more precise than direct methods, such as measurements performed using calipers. Direct measurements can comprise soft tissues or trigger muscle reflexes, such as blinking, resulting in reduced accuracy.[76] Photogrammetric reconstructions, being non-contact, do not have this disadvantage.

Additionally, once a photogrammetric 3D scan of a patient's face is acquired, the generated digital model can be stored on a computer, similarly to 3D models reconstructed from CT scans.[77] Therefore, measurements can be taken from the model without the patient's presence. This feature may be particularly useful in situations requiring repeated measurements and when integration with other digital 3D models is needed (Fig. 3).

The reviewed articles reported that photogrammetry is also a reliable method for soft tissue measurements in pediatric patients, regardless of the children's age or the presence of orofacial clefts. This may make it a valuable tool for dentists, who often face difficulties when performing

uncomfortable but necessary measurements of the face, dental arches and other structures in children.

Photogrammetric measurements of dental arches are reliable, with high *ICC* values of up to 0.99 reported in most studies. However, one study showed low precision. The majority of studies indicated that the discrepancies between photogrammetric measurements and standard methods were not statistically significant and that the measurement errors were acceptable, with values below 0.5 mm.

Given the high accuracy and reproducibility of photogrammetry, plaster dental arch models can be accurately digitized using this technique. Therefore, after further research into the capabilities and limitations of photogrammetry, especially in clinical settings, this method may become a potential alternative to more expensive extraoral scanners in the future. Additionally, because of its relatively low cost, photogrammetry can be used by students to obtain 3D dental casts, as the technique primarily requires appropriate photographic acquisition skills.[78] Photogrammetry may also be useful for teaching purposes when a university cannot afford expensive scanners, enabling students to learn digital dental workflows during their training. However, the limitations of this technique should be considered; for example, direct scanning of gingiva is not possible.

Photogrammetry appears to be a highly reproducible technique for measuring dental implant positions in terms of both linear and angular measurements.[50–54] Studies indicate that photogrammetry is more accurate than IOS but less accurate than the CMM.[45,51,53,57,60,62] In the case of dental impressions, the results are inconclusive.[59–61] Additionally, it was shown that working conditions, such as the distance between the camera and the scanned object, have a significant impact on measurement accuracy.[48]

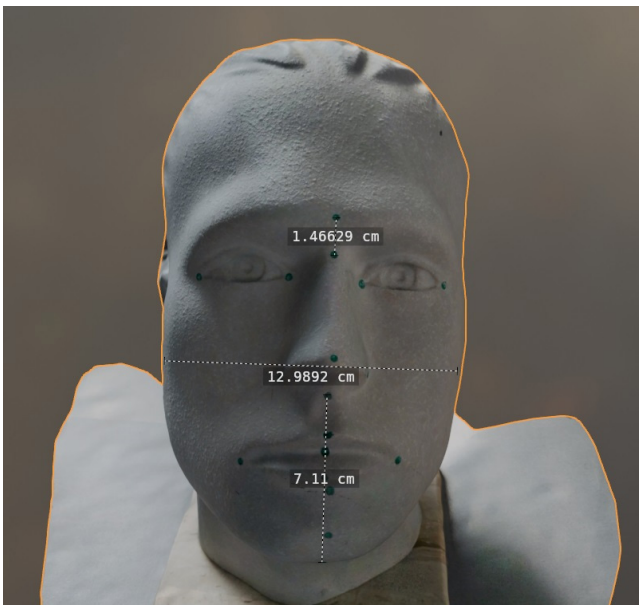

Fig. 3. Exemplary photogrammetric 3D digital model of a mannequin's face with cephalometric landmarks and distances between the glabella and nasion, the left and right masseters, and the subnasale and menton measured in cm

The three-dimensional photogrammetric digital model was created using Polycam software (Polycam Inc., San Francisco, USA) and measured using Blender software (Blender Studio, Amsterdam, the Netherlands). Original figure was prepared by OWP.

Even though photogrammetry demonstrated superior repeatability compared with IOS for capturing implant positions in prostheses, some evidence suggests that its precision, unlike that of laboratory scanners, decreases as the number of implants increases. This may indicate that photogrammetry is a practical option for cases involving fewer implants, but for more complex full-arch reconstructions, laboratory-based techniques might offer better reliability.[79] Clinicians may consider combining techniques, using photogrammetry for its non-invasive and efficient workflow while relying on laboratory scanners when greater precision across multiple implants is necessary.[24]

The higher accuracy of photogrammetry compared with IOS for recording dental implant positions may be attributed to the fact that photogrammetry is less affected by the presence of blood and saliva.[19,20] However, because the photogrammetric method used for implant position measurement relies on reference markers, the resulting 3D digital model does not capture the surrounding soft tissues. In this context, integrating both methods may be advantageous.

Integrating photogrammetry with other methods of 3D scanning, such as IOS and CBCT, can provide complementary information and enable the creation of virtual patient models; therefore, these combined techniques can be utilized in treatment planning and diagnosis. This approach may help to deliver immediate complete arch implant-supported fixed interim and definitive prostheses in suitable patient groups, thereby reducing the time required to produce these prostheses.[80–82]

The use of photogrammetry in clinical practice, particularly for implant-supported prostheses, requires careful consideration of specific conditions, especially the scanning distance. Although in a reviewed study it was confirmed that 30-cm distance provided the greatest accuracy, the optimal distance may vary depending on the environmental conditions, such as brightness and shadowing.[48,83] This is an important limitation of photogrammetry that requires further research to determine the specific conditions under which images should be taken.

In addition to its efficacy, photogrammetry is also a non-invasive, painless, comfortable, and quick method, which represents an important advantage for a diagnostic tool.[84] These characteristics are particularly attractive in pediatric dentistry, where patients are often less willing to cooperate during dental procedures.[85] To obtain a high-quality photogrammetric 3D model, the patient should remain as still as possible during the acquisition of consecutive images, as blurred pictures can decrease measurement accuracy.[86] This, in the context of working with children, may pose a challenge for the operator.

Regarding the ALARA (as low as reasonably achievable) principle, photogrammetry has an advantage over X-ray-based imaging techniques. It can be used for cephalometric measurements instead of CT scans or radiographic examinations and, potentially in the future, for measurements of dental arch dimensions as an alternative to CBCT. These findings are especially important for pregnant women and children, as they are particularly vulnerable to radiation.[72,87] However, it is important to consider that photogrammetry can capture only the surface of an object, unlike CBCT, which can be used to reconstruct structures located within the human body, such as the inferior alveolar canal.[88]

Although creating photogrammetric facial models and taking dental implant position measurements are relatively straightforward processes, digitization of dental arches requires an additional step. First, an impression must be taken, on the basis of which a physical model of the dental arches is prepared; this model can subsequently be scanned and digitized using photogrammetry. For dental implants, this technique captures only their positions, without the surrounding tissues, unlike IOS. Therefore, the digitization of the gingiva and implant positions in edentulous patients requires the combination of these methods. These are important limitations of photogrammetry, as they can potentially prolong scanning time and require more effort from the operator compared with conventional methods.

Other limitations of photogrammetry in dentistry require further research, including the establishment of standardized measurement conditions, such as appropriate lighting. From a pediatric perspective, the need for patient to remain still may be problematic. The potential reductions in precision in more complex reconstructions involving larger numbers of implants should also be considered, suggesting that photogrammetry may currently have a complementary rather than replacement role relative to laboratory scanners.

It is also important to acknowledge that this review is based mostly on ex vivo studies using artificial models. Therefore, its results cannot be directly extrapolated to clinical practice. Overall, the high accuracy and reproducibility reported for photogrammetry suggest that it may be a useful tool for performing cephalometric measurements, recording implant positions and measuring dental arches under laboratory conditions; however, its effect on clinical outcomes remains undetermined.

Conclusions

Photogrammetry has proved to be a precise and accurate method for cephalometric measurements, recording the position of dental implants and measuring dental arch dimensions. Its reliability is comparable to that of other established methods currently used in dentistry, such as IOS and traditional casts. In some cases, particularly when compared to IOS, photogrammetry showed superior outcomes. Moreover, photogrammetry may be more economically viable than other techniques.

Photogrammetry is a promising method with considerable potential in dentistry. However, it should be noted that only one of the reviewed studies was conducted in a clinical setting; therefore, photogrammetry cannot yet be considered the preferred method for the measurements discussed in this review. To assess this limitation, photogrammetric techniques should be further evaluated in clinical settings, particularly in view of the promising results obtained in laboratory conditions. We hope that this research will provide useful information and encourage clinicians to further investigate the applicability of photogrammetry in dental practice.

Ethics approval and consent to participate

Not applicable.

Data availability

Not applicable.

Consent for publication

Not applicable.

Use of AI and AI-assisted technologies

Not applicable.

ORCID iDs

Oliwier Wojciech Pioterek https://orcid.org/0009-0000-7896-9266
Katarzyna Majka https://orcid.org/0009-0002-7497-4265
Jakub Goździewicz https://orcid.org/0009-0003-4507-3043
Wiktoria Taurogińska https://orcid.org/0009-0009-8169-1520
Barbara Parol https://orcid.org/0009-0004-8956-4378
Daria Pozdniakowa https://orcid.org/0009-0001-4685-447X
Albert Synal https://orcid.org/0009-0007-3185-4374
Aleksander Sowiński https://orcid.org/0009-0008-0457-338X
Martyna Piskorz https://orcid.org/0009-0005-8542-5052
Mateusz Drążyk https://orcid.org/0009-0004-6594-7112
Mateusz Mazurek http://orcid.org/0009-0008-0066-6087
Michał Tulski https://orcid.org/0009-0001-3867-5850
Zygmunt Domagała https://orcid.org/0000-0002-2317-1932
Maciej Dobrzyński https://orcid.org/0000-0003-2368-1534
Paweł Dąbrowski https://orcid.org/0000-0001-6016-9201

References

1. Champion EM, ed. *Virtual Heritage: A Guide*. London, UK: Ubiquity Press; 2021. doi:10.5334/bck
2. Schenk T. *Introduction to Photogrammetry*. Columbus, OH: The Ohio State University; 2005.
3. Luhmann T. Close range photogrammetry for industrial applications. *ISPRS J Photogramm Remote Sens*. 2010;65(6):558–569. doi:10.1016/j.isprsjprs.2010.06.003
4. Valença J, Júlio ENBS, Araújo HJ. Applications of photogrammetry to structural assessment. *Exp Tech*. 2017;36(5):71–81. doi:10.1111/j.1747-1567.2011.00731.x
5. Mitchell HL. Applications of digital photogrammetry to medical investigations. *ISPRS J Photogramm Remote Sens*. 1995;50(3):27–36. doi:10.1016/0924-2716(95)91288-u

6. Talevi G, Pannone L, Monaco C, et al. Evaluation of photogrammetry for medical application in cardiology. *Front Bioeng Biotechnol*. 2023:11:1044647. doi:10.3389/fbioe.2023.1044647
7. Barbero-García I, Lerma JL, Mora-Navarro G. Fully automatic smartphone-based photogrammetric 3D modelling of infant's heads for cranial deformation analysis. *ISPRS J Photogramm Remote Sens*. 2020;166:268–277. doi:10.1016/j.isprsjprs.2020.06.013
8. Malian A, Azizi A, van den Heuvel FA. MEDPHOS: A new photogrammetric system for medical measurement. Paper presented at: XXth ISPRS Congress; July 12–23, 2004; Istanbul, Turkey. https://www.isprs.org/proceedings/XXXV/congress/comm5/papers/571.pdf. Accessed April 16, 2025.
9. Alshawabkeh Y, Douglas K, Matarya M, Khrisat B. Combined photogrammetric techniques and computer vision: 2D–3D recording of Gharissa, Jordan. *J Archit Conserv*. 2011;17(2):77–92. doi:10.1080/13556207.2011.10785090
10. Kihara H, Hatakeyama W, Komine F, et al. Accuracy and practicality of intraoral scanner in dentistry: A literature review. *J Prosthodont Res*. 2020;64(2):109–113. doi:10.1016/j.jpor.2019.07.010
11. Jacobs L, Dvorak J, Cornelius A, Zameroski R, No T, Schmitz T. Structured light scanning artifact-based performance Study. *Manuf Lett*. 2023;35:873–882. doi:10.1016/j.mfglet.2023.07.014
12. Bohner LOL, De Luca Canto G, Marció BS, Laganá DC, Sesma N, Tortamano Neto P. Computer-aided analysis of digital dental impressions obtained from intraoral and extraoral scanners. *J Prosthet Dent*. 2017;118(5):617–623. doi:10.1016/j.prosdent.2016.11.018
13. Burzynski JA, Firestone AR, Beck FM, Fields HW, Deguchi T. Comparison of digital intraoral scanners and alginate impressions: Time and patient satisfaction. *Am J Orthod Dentofacial Orthop*. 2018;153(4):534–541. doi:10.1016/j.ajodo.2017.08.017
14. Flügge TV, Schlager S, Nelson K, Nahles S, Metzger MC. Precision of intraoral digital dental impressions with iTero and extraoral digitization with the iTero and a model scanner. *Am J Orthod Dentofacial Orthop*. 2013;144(3):471–478. doi:10.1016/j.ajodo.2013.04.017
15. Cunha J, Fernandes GVO, Fernandes JCH, Lopes PC, Rio R. The interference of age and gender on smile characterization analyzed on six parameters: A clinical-photographic pilot study. *Medicina (Kaunas)*. 2023;59(3):595. doi:10.3390/medicina59030595
16. Silvester CM, Hillson S. A critical assessment of the potential for structure-from-motion photogrammetry to produce high fidelity 3D dental models. *Am J Phys Anthropol*. 2020;173(2):381–392. doi:10.1002/ajpa.24109
17. Stuani VT, Ferreira R, Manfredi GGP, Cardoso MV, Sant'Ana ACP. Photogrammetry as an alternative for acquiring digital dental models: A proof of concept. *Med Hypotheses*. 2019;128:43–49. doi:10.1016/j.mehy.2019.05.015
18. Zotti F, Rosolin L, Bersani M, Poscolere A, Pappalardo D, Zerman N. Digital dental models: Is photogrammetry an alternative to dental extraoral and intraoral scanners? *Dent J (Basel)*. 2022;10(2):24. doi:10.3390/dj10020024
19. Agustín-Panadero R, Peñarrocha-Oltra D, Gomar-Vercher S, Peñarrocha-Diago M. Stereophotogrammetry for recording the position of multiple implants: Technical description. *Int J Prosthodont*. 2015;28(6):631–636. doi:10.11607/ijp.4146
20. An H, Mickesh GJ, Cho D, Sorensen JA. Effect of finish line location and saliva contamination on the accuracy of crown finish line scanning. *J Prosthodont*. 2023;33(1):86–94. doi:10.1111/jopr.13658
21. Emam M, Ghanem L, Abdel Sadek HM. Effect of different intraoral scanners and post-space depths on the trueness of digital impressions. *Dent Med Probl*. 2024;61(4):577–584. doi:10.17219/dmp/162573
22. Farag EAA, Rizk A, Ashraf R, Emad Eldin F. Effect of the scanner type on the marginal gap and internal fit of two monolithic CAD/CAM esthetic crown materials: An in vitro study. *Dent Med Probl*. 2025;62(6):1131–1137. doi:10.17219/dmp/185895
23. Bolandzadeh N, Bischof W, Flores-Mir C, Boulanger P. Multimodal registration of three-dimensional maxillodental cone beam CT and photogrammetry data over time. *Dentomaxillofac Radiol*. 2013;42(2):22027087. doi:10.1259/dmfr/22027087
24. Rico JP, Brinkmann JCB, Martin MC, et al. Digital impression taking for maxillary full-arch restoration with immediate loading: A case report. *J Oral Implantol*. 2021;48(2):125–132. doi:10.1563/aaid-joi-d-20-00117
25. Castillo JC, Gianneschi G, Azer D, et al. The relationship between 3D dentofacial photogrammetry measurements and traditional cephalometric measurements. *Angle Orthod*. 2018;89(2):275–283. doi:10.2319/120317-825.1
26. Dindaroğlu F, Kutlu P, Duran GS, Görgülü S, Aslan E. Accuracy and reliability of 3D stereophotogrammetry: A comparison to direct anthropometry and 2D photogrammetry. *Angle Orthod*. 2016;86(3):487–494. doi:10.2319/041415-244.1
27. Tofangchiha M, Esfehani M, Eftetahi L, Mirzadeh M, Reda R, Testarelli L. Comparison of the pharyngeal airway in snoring and non-snoring patients based on the lateral cephalometric study: A case–control study. *Dent Med Probl*. 2023;60(1):121–126. doi:10.17219/dmp/154776
28. Sterenborg BAAM, Maal TJJ, Vreeken RD, Loomans BAC, Huysmans MCDNJM. 3D facial effects of a simulated dental build-up. *J Esthet Restor Dent*. 2016;28(6):397–404. doi:10.1111/jerd.12228
29. Page MJ, Moher D, Bossuyt PM, et al. PRISMA 2020 explanation and elaboration: Updated guidance and exemplars for reporting systematic reviews. *BMJ*. 2021:n160. doi:10.1136/bmj.n160
30. Haddaway NR, Collins AM, Coughlin D, Kirk S. The role of Google Scholar in evidence reviews and its applicability to grey literature searching. *PLoS One*. 2015;10(9):e0138237. doi:10.1371/journal.pone.0138237
31. Lefebvre C, Glanville J, Briscoe S, et al. Chapter 4: Searching for and selecting studies. In: Higgins JPT, Thomas J, Chandler J, et al., eds. *Cochrane Handbook for Systematic Reviews of Interventions version 6.5.1*. Cochrane; 2025. https://www.cochrane.org/authors/handbooks-and-manuals/handbook/current/chapter-04. Accessed April 16, 2025.
32. Whiting P, Rutjes AWS, Reitsma JB, Bossuyt PMM, Kleijnen J. The development of QUADAS: A tool for the quality assessment of studies of diagnostic accuracy included in systematic reviews. *BMC Med Res Methodol*. 2003;3(1):25. doi:10.1186/1471-2288-3-25
33. Whiting PF, Weswood ME, Rutjes AWS, Reitsma JB, Bossuyt PNM, Kleijnen J. Evaluation of QUADAS, a tool for the quality assessment of diagnostic accuracy studies. *BMC Med Res Methodol*. 2006;6(1):9. doi:10.1186/1471-2288-6-9
34. Lavorgna L, Cervino G, Fiorillo L, et al. Reliability of a virtual prosthodontic project realized through a 2D and 3D photographic acquisition: An experimental study on the accuracy of different digital systems. *Int J Environ Res Public Health*. 2019;16(24):5139. doi:10.3390/ijerph16245139
35. Brons S, van Beusichem ME, Maal TJJ, et al. Development and reproducibility of a 3D stereophotogrammetric reference frame for facial soft tissue growth of babies and young children with and without orofacial clefts. *Int J Oral Maxillofac Surg*. 2013;42(1):2–8. doi:10.1016/j.ijom.2012.07.006
36. Ceinos R, Tardivo D, Bertrand MF, Lupi-Pegurier L. Inter- and intra-operator reliability of facial and dental measurements using 3D-stereophotogrammetry. *J Esthet Restor Dent*. 2016;28(3):178–189. doi:10.1111/jerd.12194
37. Sterenborg BAAM, Maal TJJ, Vreeken R, Loomans BAC, Huysmans MCDNJM. The facial effects of tooth wear rehabilitation as measured by 3D stereophotogrammetry. *Dent J*. 2018;73:105–109. doi:10.1016/j.jdent.2018.04.014
38. Keil PU, Beuer F, Unkovskiy A, Atay E, Jennes ME. Influence of ambient light on the accuracy of different face scanning methods: An in-vitro study. *BMC Oral Health*. 2025;25(1):229. doi:10.1186/s12903-025-05594-2
39. Hartmann R, Weiherer M, Nieberle F, et al. Evaluating smartphone-based 3D imaging techniques for clinical application in oral and maxillofacial surgery: A comparative study with the Vectra M5. *Oral Maxillofac Surg*. 2025;29(1):29. doi:10.1007/s10006-024-01322-2
40. Artopoulos A, Buytaert JAN, Dirckx JJJ, Coward TJ. Comparison of the accuracy of digital stereophotogrammetry and projection moiré profilometry for three-dimensional imaging of the face. *Int J Clin Oral Maxillofac Surg*. 2014;43(5):654–662. doi:10.1016/j.ijom.2013.10.005
41. Lincoln KP, Sun AYT, Prihoda TJ, Sutton AJ. Comparative accuracy of facial models fabricated using traditional and 3D imaging techniques. *J Prosthodont*. 2016;25(3):207–215. doi:10.1111/jopr.12358
42. Majid Z, Chong A, Setan H, Ahmad AB, Rajion ZA. Natural features technique for non-contact three dimensional craniofacial anthropometry using stereophotogrammetry. *Arch Orofac Sci*. 2006;1:42–50. https://aos.usm.my/docs/Vol_1/42_50_majid.pdf. Accessed April 16, 2025.

43. Di Blasio M, Minervini G, Segù M, et al. An in-vivo study on the effect of head orientation in the measurement of anthropometric points in stereophotogrammetry. *Minerva Dent Oral Sci*. 2025;73(6):343–351. doi:10.23736/s2724-6329.24.04852-6
44. Seifert LB, Beyer M, Czok V, et al. Comparative accuracy of stationary and smartphone-based photogrammetry in oral and maxillofacial surgery: A clinical study. *J Clin Med*. 2024;13(22):6678. doi:10.3390/jcm13226678
45. Bratos M, Bergin JM, Rubenstein JE, Sorensen JA. Effect of simulated intraoral variables on the accuracy of a photogrammetric imaging technique for complete-arch implant prostheses. *J Prosthet Dent*. 2018;120(2):232–241. doi:10.1016/j.prosdent.2017.11.002
46. Ma B, Yue X, Sun Y, Peng L, Geng W. Accuracy of photogrammetry, intraoral scanning, and conventional impression techniques for complete-arch implant rehabilitation: An in vitro comparative study. *BMC Oral Health*. 2021;21(1):636. doi:10.1186/s12903-021-02005-0
47. Pinto RJ, Casado SA, Chmielewski K, Caramês JM, Marques DS. Accuracy of different digital acquisition methods in complete arch implant-supported prostheses: An in vitro study. *J Prosthet Dent*. 2024;132(1):172–177. doi:10.1016/j.prosdent.2023.07.008
48. Revilla-León M, Gómez-Polo M, Drone M, et al. Impact of scanning distance on the accuracy of a photogrammetry system. *J Dent*. 2024;142:104854. doi:10.1016/j.jdent.2024.104854
49. Rivara F, Lumetti S, Calciolari E, Toffoli A, Forlani G, Manfredi E. Photogrammetric method to measure the discrepancy between clinical and software-designed positions of implants. *J Prosthet Dent*. 2016;115(6):703–711. doi:10.1016/j.prosdent.2015.10.017
50. Tohme H, Lawand G, Chmielewska M, Makhzoume J. Comparison between stereophotogrammetric, digital, and conventional impression techniques in implant-supported fixed complete arch prostheses: An in vitro study. *J Prosthet Dent*. 2023;129(2):354–362. doi:10.1016/j.prosdent.2021.05.006
51. Tohme H, Lawand G, Eid R, Ahmed KE, Salameh Z, Makzoume J. Accuracy of implant level intraoral scanning and photogrammetry impression techniques in a complete arch with angled and parallel implants: An in vitro study. *Appl Sci*. 2021;11(21):9859. doi:10.3390/app11219859
52. Cheng J, Zhang H, Liu H, Li J, Wang HL, Tao X. Accuracy of edentulous full-arch implant impression: An in vitro comparison between conventional impression, intraoral scan with and without splinting, and photogrammetry. *Clin Oral Implants Res*. 2024;35(5):560–572. doi:10.1111/clr.14252
53. Pozzi A, Agliardi E, Lio F, Nagy K, Nardi A, Arcuri L. Accuracy of intraoral optical scan versus stereophotogrammetry for complete-arch digital implant impression: An in vitro study. *J Prosthodont Res*. 2023;68(1):172–180. doi:10.2186/jpr.jpr_d_22_00251
54. Liu M, Fu XJ, Lai HC, Shi JY, Liu BL. Accuracy of traditional open-tray impression, stereophotogrammetry, and intraoral scanning with prefabricated aids for implant-supported complete arch prostheses with different implant distributions: An in vitro study. *J Prosthet Dent*. 2024;132(3):602.e1–602.e9. doi:10.1016/j.prosdent.2024.06.006
55. Faria JC, Sampaio-Fernandes MA, Oliveira SJ, Malheiro R, Sampaio-Fernandes JC, Figueiral MH. Precision of photogrammetry and intraoral scanning in full-arch implant rehabilitation: An in vitro comparative study. *Appl Sci*. 2025;15(3):1388. doi:10.3390/app15031388
56. Estibalez-Recasens M, Serrano-Granger C, Santamaría-Laorden A, Andreu-Vázquez C, Orejas-Pérez J. Precision of stereophotogrammetry in complete arch implant recordings: A clinical study. *J Prosthet Dent*. 2025;133(5):1242–1249. doi:10.1016/j.prosdent.2024.12.021
57. Revilla-León M, Att W, Özcan M, Rubenstein J. Comparison of conventional, photogrammetry, and intraoral scanning accuracy of complete-arch implant impression procedures evaluated with a coordinate measuring machine. *J Prosthet Dent*. 2021;125(3):470–478. doi:10.1016/j.prosdent.2020.03.005
58. Revilla-León M, Gómez-Polo M, Drone M, et al. Influence of implant reference on the scanning accuracy of complete arch implant scans captured by using a photogrammetry system. *J Prosthet Dent*. 2025;133(1):252–257. doi:10.1016/j.prosdent.2024.01.008
59. Zhou Y, You L, Fan Z. Accuracy of implant abutment level digital impressions using stereophotogrammetry in edentulous jaws: An in vitro pilot study. *BMC Oral Health*. 2024;24(1):1167. doi:10.1186/s12903-024-04888-1
60. Bergin JM, Rubenstein JE, Mancl L, Brudvik JS, Raigrodski AJ. An in vitro comparison of photogrammetric and conventional complete-arch implant impression techniques. *J Prosthet Dent*. 2013;110(4):243–251. doi:10.1016/s0022-3913(13)60370-4
61. Örtorp A, Jemt T, Bäck T. Photogrammetry and conventional impressions for recording implant positions: A comparative laboratory study. *Clin Implant Dent Relat Res*. 2005;7(1):43–50. doi:10.1111/j.1708-8208.2005.tb00046.x
62. Revilla-León M, Rubenstein J, Methani MM, Piedra-Cascón W, Özcan M, Att W. Trueness and precision of complete-arch photogrammetry implant scanning assessed with a coordinate-measuring machine. *J Prosthet Dent*. 2023;129(1):160–165. doi:10.1016/j.prosdent.2021.05.019
63. Al-Khatib AR, Rajion ZA, Masudi SM, Hassan R, Townsend GC. Validity and reliability of tooth size and dental arch measurements: A stereo photogrammetric study. *Aust Orthod J*. 2012;28(1):22–29. doi:10.2478/aoj-2012-0004
64. Al-Khatib AR, Rajion ZA, Masudi SM, Hassan R, Anderson PJ, Townsend GC. Tooth size and dental arch dimensions: A stereophotogrammetric study in Southeast Asian Malays. *Orthod Craniofac Res*. 2011;14(4):243–253. doi:10.1111/j.1601-6343.2011.01529.x
65. Arapović-Savić M, Savić M, Umićević-Davidović M, Arbutina A, Nedeljković N, Glišić B. A novel method of photogrammetry measurements of study models in orthodontics. *Srp Arh Celok Lek*. 2019;147(1–2):10–16. doi:10.2298/sarh180419074a
66. Fu X, Peng C, Li Z, Liu S, Tan M, Song J. The application of multi-baseline digital close-range photogrammetry in three-dimensional imaging and measurement of dental casts. *PLoS One*. 2017;12(6):e0178858. doi:10.1371/journal.pone.0178858
67. Goellner M, Schmitt J, Karl M, Wichmann M, Holst S. Photogrammetric measurement of initial tooth displacement under tensile force. *Med Eng Phys*. 2010;32(8):883–888. doi:10.1016/j.medengphy.2010.06.004
68. Bobak CA, Barr PJ, O'Malley AJ. Estimation of an inter-rater intra-class correlation coefficient that overcomes common assumption violations in the assessment of health measurement scales. *BMC Med Res Methodol*. 2018;18(1):93. doi:10.1186/s12874-018-0550-6
69. Mahmood RSH, Hamandi SJ, Al-Mahdi AH. Creating a digital 3D model of the dental cast using structure-from-motion photogrammetry technique. *Int J Online Biomed Eng*. 2023;19(03):4–17. doi:10.3991/ijoe.v19i03.36289
70. Codari M, Pucciarelli V, Tommasi DG, Sforza C. Validation of a technique for integration of a digital dental model into stereophotogrammetric images of the face using cone-beam computed tomographic data. *Br J Oral Maxillofac Surg*. 2016;54(5):584–586. doi:10.1016/j.bjoms.2016.01.019
71. Kamel M, Elkady A, Ghanem I. Marginal fit of PMMA CAD/CAM crowns fabricated by using photogrammetry scanning method (an invitro study). *Egypt Dent J*. 2022;68(4):3537–3544. doi:10.21608/edj.2022.146431.2164
72. Mai HN, Lee DH. Effects of artificial extraoral markers on accuracy of three-dimensional dentofacial image integration: Smartphone face scan versus stereophotogrammetry. *J Pers Med*. 2022;12(3):490. doi:10.3390/jpm12030490
73. Rangel FA, Maal TJJ, Bergé SJ, et al. Integration of digital dental casts in 3-dimensional facial photographs. *Am J Orthod Dentofacial Orthop*. 2008;134(6):820–826. doi:10.1016/j.ajodo.2007.11.026
74. Yang B, Schinke J, Rastegar A, Tanyeri M, Viator JA. Cost-effective full-color 3D dental imaging based on close-range photogrammetry. *Bioengineering (Basel)*. 2023;10(11):1268. doi:10.3390/bioengineering10111268
75. Chaudhary S, Kumar S, Aggarwal R, et al. Evaluation of the accuracy of digital models generated using photogrammetry. *Cureus*. 2024;16(12):e75448. doi:10.7759/cureus.75448
76. Gašparović B, Morelato L, Lenac K, Mauša G, Zhurov A, Katić V. Comparing direct measurements and three-dimensional (3D) scans for evaluating facial soft tissue. *Sensors (Basel)*. 2023;23(5):2412. doi:10.3390/s23052412
77. Martín del Rey A, Hernández Pastora JL, Rodríguez Sánchez G. 3D medical data security protection. *Expert Syst Appl*. 2016;54(C):379–386. doi:10.1016/j.eswa.2016.02.001
78. Jankiewicz J, Mazurek M, Gajda-Janiak A, et al. Can we make anatomical specimen last forever? Technical note on photogrammetry. *Med J Cell Biol*. 2023;11(4):108–113. doi:10.2478/acb-2023-0018

79. Ebeid K, Nouh I, Ashraf Y, Cesar PF. Accuracy of different laboratory scanners for scanning of implant-supported full arch fixed prosthesis. *J Esthet Restor Dent*. 2022;34(5):843–848. doi:10.1111/jerd.12918
80. Habib S, Motiwala MA, Khan FR. Does the sagittal root position of maxillary anterior teeth affect the decision making on immediate implants in the anterior maxilla? A CBCT-based study. *Dent Med Probl*. 2024;61(1):65–70. doi:10.17219/dmp/133072
81. Clozza E. Intraoral scanning and dental photogrammetry for full-arch implant-supported prosthesis: A technique. *Clin Adv Periodontics*. 2023;14(4):244–249. doi:10.1002/cap.10269
82. Wang J, Wu YL, Ma J, Wu F, Li DH. A novel technique for implant-supported fixed complete rehabilitation based on a dynamic virtual patient. *J Dent*. 2023;137:104649. doi:10.1016/j.jdent.2023.104649
83. Pojda D, Tomaka AA, Luchowski L, Tarnawski M. Integration and application of multimodal measurement techniques: Relevance of photogrammetry to orthodontics. *Sensors (Basel)*. 2021;21(23):8026. doi:10.3390/s21238026
84. Ey-Chmielewska H, Chruściel-Nogalska M, Frączak B. Photogrammetry and its potential application in medical science on the basis of selected literature. *Adv Clin Exp Med*. 2015;24(4):737–741. doi:10.17219/acem/58951
85. Baier K, Milgrom P, Russell S, Mancl L, Yoshida T. Children's fear and behavior in private pediatric dentistry practices. *Pediatr Dent*. 2004;26(4):316–321. PMID:15344624.
86. Sieberth T, Wackrow R, Chandler JH. Motion blur disturbs – the influence of motion-blurred images in photogrammetry. *Photogramm Rec*. 2014;29(148):434–453. doi:10.1111/phor.12082
87. Shaw P, Duncan A, Vouyouka A, Ozsvath K. Radiation exposure and pregnancy. *J Vasc Surg*. 2011;53(1 Suppl):28S–34S. doi:10.1016/j.jvs.2010.05.140
88. Issa J, Kulczyk T, Rychlik M, Czajka-Jakubowska A, Olszewski R, Dyszkiewicz-Konwińska M. Artificial intelligence versus semi-automatic segmentation of the inferior alveolar canal on cone-beam computed tomography scans: A pilot study. *Dent Med Probl*. 2024;61(6):893–899. doi:10.17219/dmp/175968

Review

Silver diamine fluoride for the treatment of dental caries: A comprehensive review of the literature

Mehmood Asghar[1,2,A–D], Ros Anita Omar[2,A,C,E,F], Rosiyah Yahya[3,4,A,C,E,F], Adrian Ujin Yap[5,6,A,C,E,F], Muhammad Amber Fareed[7,8,A,E,F]

[1] Basic Dental Sciences Department, Army Medical College, National University of Medical Sciences (NUMS), Rawalpindi, Pakistan
[2] Department of Restorative Dentistry, Faculty of Dentistry, Universiti Malaya, Kuala Lumpur, Malaysia
[3] Department of Chemistry, Faculty of Science, Universiti Malaya, Kuala Lumpur, Malaysia
[4] Centre for Ionics Universiti Malaya, Department of Physics, Faculty of Science, Universiti Malaya, Kuala Lumpur, Malaysia
[5] Department of Dentistry, Ng Teng Fong General Hospital and Faculty of Dentistry, National University Health System (NUHS), Singapore
[6] National Dental Research Institute Singapore, National Dental Centre Singapore and Duke-NUS Medical School, Singapore Health Services, Singapore
[7] Department of Clinical Sciences, College of Dentistry, Ajman University, United Arab Emirates
[8] Center for Medical and Bio-Allied Health Sciences Research, Ajman University, United Arab Emirates

A – research concept and design; B – collection and/or assembly of data; C – data analysis and interpretation;
D – writing the article; E – critical revision of the article; F – final approval of the article

Dental and Medical Problems, ISSN 1644-387X (print), ISSN 2300-9020 (online) *Dent Med Probl*. 2026;63(5):1331–1345

Address for correspondence
Ros Anita Omar
E-mail: anitaomar@um.edu.my

Funding sources
This study was supported by a research grant awarded to Ros Anita Omar by Universiti Malaya, Kuala Lumpur, Malaysia (grant No. GPF010E-2019).

Conflict of interest
None declared

Acknowledgements
The authors would like to thank Ajman University for providing support for the article processing fee.

Received on June 17, 2025
Reviewed on July 10, 2025
Accepted on October 13, 2025

Published online on October 30, 2026

Abstract

Silver diamine fluoride (SDF) is an aqueous solution of silver (Ag^+) and fluoride (F^-) ions stabilized by ammonia. It is regarded by the World Health Organization (WHO) as a safe, efficacious and cost-effective pharmacological agent for the minimally invasive management of dental caries. The Ag^+ ions in SDF mainly exert an antibacterial effect, while the F^- ions remineralize dental tissues. Recently, SDF has also been approved by the US Food and Drug Administration (FDA) for desensitization. The main advantages of SDF over other treatment options are its shorter application time, ease of application and no need for anesthesia. Furthermore, it is suitable for individuals with physical or mental disabilities, non-ambulatory patients, and elderly patients, as it can also be applied by dental nurses, hygienists and healthcare workers. Various studies have confirmed the efficacy of SDF in arresting and preventing coronal and root caries, desensitizing teeth, and disinfecting root canals, highlighting its potential to reduce the global healthcare and economic burden associated with untreated dental caries. The aim of this review is to provide an updated overview of SDF properties and its use in the minimally invasive management of dental caries.

Keywords: dental caries, minimally invasive dentistry, remineralization, silver diamine fluoride

Cite as
Asghar M, Omar RA, Yahya R, Yap AU, Fareed MA. Silver diamine fluoride for the treatment of dental caries: A comprehensive review of the literature. *Dent Med Probl.* 2026;63(5):1331–1345. doi:10.17219/dmp/212537

DOI
10.17219/dmp/212537

Copyright
Copyright by Author(s)
This is an article distributed under the terms of the Creative Commons Attribution 3.0 Unported (CC BY 3.0) (https://creativecommons.org/licenses/by/3.0/)

Highlights

- Silver diamine fluoride provides a minimally invasive and cost-effective approach to arresting and preventing dental caries, particularly in children and older adults.
- Anticaries effects of silver diamine fluoride involve silver-mediated antibacterial activity, fluoride-driven remineralization and protection against dentinal collagen degradation.
- In addition to caries management, silver diamine fluoride reduces dentin hypersensitivity, while its applications in hypomineralized teeth, endodontics and periodontal care require further clinical validation.
- Black staining of treated carious tissue remains the main aesthetic limitation and may affect acceptance among patients, parents and clinicians.
- Potassium iodide, capping agents and nanosilver formulations show potential for reducing staining; however, reliable long-term stain prevention without compromising therapeutic efficacy has yet to be established.

Introduction

Dental caries is a global health problem that affects billions of people worldwide.[1–3] Despite significant advancements in preventive dental care, untreated dental caries is still regarded as one of the most prevalent yet preventable diseases worldwide.[4] According to the Global Burden of Disease Study 2017, over 532 million children and 2.3 billion adults were affected by dental caries in 2017.[5] Dental caries remains a childhood disease affecting a subset of children in both developed and developing countries.[6] Similarly, root caries is a prevalent condition that affects over one-third of the global elderly population.[7]

Traditionally, dental caries is managed using a surgical approach that involves removing the damaged tooth structure and replacing it with a suitable restorative material. However, this is a destructive process that inevitably results in the removal of healthy tooth structure. The so-called surgical approach is a short-term solution and has become financially unsustainable globally.[8] Hence, the trend is shifting toward a minimally invasive approach in which attempts are made to remineralize dental tissues using various antibacterial agents such as chlorhexidine (CHX), calcium phosphate, casein phosphopeptide–amorphous calcium phosphate, and fluoridated compounds such as sodium fluoride (NaF) varnish.[9–15] Among these, silver diamine fluoride (SDF) has recently gained popularity as a potent, efficacious and cost-effective antibacterial and remineralizing agent.

Silver diamine fluoride has been clinically used to arrest cavitated dentin lesions and prevent new cavities.[16,17] In addition, clinicians have used it to manage early childhood caries, root caries, and pit and fissure caries, as well as for desensitization.[18] Silver diamine fluoride has also been utilized as a root canal disinfectant and has been suggested as a treatment for dental erosion and a dye to detect carious lesions.[19] In 2021, the World Health Organization (WHO) added SDF to its Model List of Essential Medicines for the management of dental caries in children and adults.[20]

Silver diamine fluoride has become the center of attention for clinicians and researchers. A recent bibliometric analysis has shown that the research interest regarding the use and clinical efficacy of SDF has increased exponentially from 2016 to 2021.[21] Therefore, this review aimed to provide comprehensive, updated information regarding the multipronged clinical use of SDF as a non-invasive and cost-effective agent to combat the global burden of dental caries and other preventable dental issues, such as dentin hypersensitivity, molar hypomineralization and gum disease. The review also discusses the adverse effects and toxicity-related issues of SDF and provides an overview of the various strategies used to overcome its inherent tooth-staining potential.

Material and methods

The SANRA (Scale for the Assessment of Narrative Review Articles) reporting guidelines were used in this study to enhance methodological transparency and scientific rigor.[22] This involved identifying a clear research objective, documenting the literature search strategy and conducting a thematic synthesis of findings from the included studies.

As this was a narrative review, this study did not follow a methodology of a systematic review. This may have introduced selection bias, resulting in limitations related to the availability and quality of the published studies. A comprehensive search was conducted in 3 databases, namely PubMed, Scopus and Web of Science, up to August 2025. The review focused on studies that provided information on the composition, mechanism of action, clinical applications, and adverse effects of SDF. Only full-text research articles of all types or review articles related to the clinical efficacy, chemistry or safety of SDF were included. Editorials were excluded, and case reports and non-English articles were cited only when no other evidence was available. Furthermore, an additional search was performed for articles that discussed patients', parents' and healthcare professionals' views regarding the clinical acceptability of SDF owing to its tooth-staining effect. The keywords used for the database search are provided in Table 1.

Table 1. Keywords used to search digital databases

Database	Search string	Search fields	Results, *n*
PubMed	(silver diamine fluoride OR diamine silver fluoride OR silver fluoride OR silver compounds OR ammoniacal silver nitrate) AND (caries prevention OR caries arrest OR tooth sensitivity OR dentinal hypersensitivity OR molar incisor hypomineralization OR root canal irrigant)	all fields	724
Web of Science	(silver diamine fluoride OR diamine silver fluoride OR silver fluoride OR silver compounds OR ammoniacal silver nitrate) AND (caries prevention OR caries arrest OR tooth sensitivity OR dentinal hypersensitivity OR molar incisor hypomineralization OR root canal irrigant)	all fields	584
Scopus	(ALL ((silver diamine fluoride OR diamine silver fluoride OR silver fluoride OR silver compounds OR ammoniacal silver nitrate)) AND TITLE-ABS-KEY (caries arrest OR caries prevention OR hypersensitivity OR hypomineralization))	all fields/title, abstract, keywords	43

Results

Using the predefined search strategy, a total of 1,351 articles were retrieved from the selected databases. Screening for duplicate records resulted in the removal of 1,045 papers. The remaining 306 articles underwent title and abstract screening, leaving 213 papers for full-text review. A thematic narrative synthesis of the included studies was performed based on the themes of chemical composition, clinical efficacy and uses, adverse effects, and aesthetic concerns related to SDF. A PRISMA (Preferred Reporting Items for Systematic reviews and Meta-Analyses) flow diagram presenting the process of study selection, screening and full-text retrieval is presented in Fig. 1.

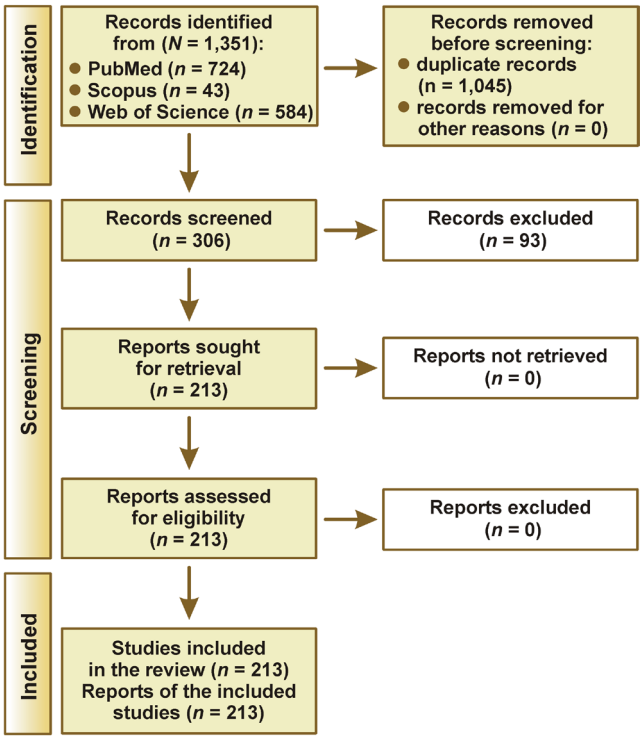

Fig. 1. Flowchart illustrating the review process according to the updated PRISMA (Preferred Reporting Items for Systematic reviews and Meta-analyses) guidelines

Silver compounds in dentistry

Silver compounds have been used in medicine and dentistry since the 1800s, owing to their antibacterial and caries-preventive properties. In dentistry, the use of silver compounds dates back to the 1840s, when silver nitrate ($AgNO_3$) was used for a variety of dental restorative and preventive purposes.[23] Some of the silver compounds used in dentistry are discussed in the following sections.

Silver nitrate

Silver nitrate was the first silver compound to be used in dentistry.[23] Metallic silver (Ag^0) is relatively inert chemically. However, silver particles in an aqueous solution of $AgNO_3$ exist in ionic form and exert a bactericidal effect. Silver ions (Ag^+) are highly reactive species that have a high affinity for binding to bacterial proteins, thereby causing structural changes in the bacterial cell walls and membranes.[24] Klein et al. evaluated $AgNO_3$ and other preventive materials for their effects on artificial caries.[25] The results of their study showed that $AgNO_3$ could significantly reduce the progression of caries compared with no treatment.[25] However, the use of $AgNO_3$ gradually declined, mainly due to its potential to cause tooth staining and the introduction of fluoride compounds with improved properties.[26,27]

Ammoniacal silver nitrate

In an effort to enhance the stability and antibacterial efficacy of $AgNO_3$, Percy Howe combined $AgNO_3$ with ammonia to form ammoniacal silver nitrate, also known as Howe's solution (HS) – $AgNH_3NO_3$.[23] The silver ions in HS were shown to be able to penetrate the affected enamel and dentin and exert their antibacterial effect. As a result, HS became popular as a cavity-sterilizing agent and was also advocated for the treatment of endodontic problems, even though its efficacy had not been clinically proven at that time.[26]

In a clinical study involving ground sections of human and dog teeth, Zander and Smith showed that HS penetrated dentin tissue, despite the presence of a calcified barrier.[28] In addition, less pulpal damage was observed when ammoniacal silver nitrate was applied directly to the exposed pulp than when it was applied to a carious lesion.[23]

Silver fluoride

Silver fluoride (AgF) was introduced in order to combine the antibacterial effect of silver ions with the remineralization potential of fluoride ions. Various in vitro studies have documented the ability of AgF to inhibit the growth of *Streptococcus mutans* in biofilms, inhibit the metabolic activity of dental plaque, and reduce the depth of carious lesions.[25,29,30]

An in vivo study conducted by Craig et al. demonstrated the ability of AgF to inhibit occlusal and proximal caries in primary molars.[31] Green indicated that AgF, with or without the addition of stannous fluoride (SnF_2), was able to inhibit the initial progression of carious lesions in permanent teeth.[32] Despite its efficacy, the effect of AgF is short-lived due to its unstable chemical nature. Therefore, subsequent studies were aimed at enhancing the stability of AgF. This resulted in the incorporation of ammonia into AgF to form SDF, which possesses superior chemical and light stability.

Table 2 summarizes the historical advancements in the use of silver compounds for caries management in dentistry that led to the development and clinical use of SDF. As this review focuses primarily on SDF, this compound will be discussed in greater detail in a separate section.

Silver diamine fluoride

Silver diamine fluoride is a topical solution containing diamine silver and fluoride ions. The compound has been shown to be more stable and undergo less oxidation than silver fluoride.[33] The first use of SDF for caries prevention dates back to the 1960s and 1970s in Japan, where it was used to arrest primary carious lesions.[34] The use of SDF remained mostly limited to Japan for many decades until it was recommended for use among schoolchildren in Brazil in the 20th century.[23]

Over the past decade, interest in the use of SDF for the prevention and management of dental caries has increased.[35] In addition, SDF is considered a safe, efficacious, non-invasive, and cost-effective option for caries management, with the potential to support the achievement of the WHO global oral health goals for 2020.[35] Subsequently, WHO included SDF as an "essential dental medicine" in the *Global strategy and action plan on oral health 2023–2030*.[36] Various in vitro and clinical studies have shown the efficacy of SDF in preventing and arresting caries and its superiority over other preventive agents.[37–41]

Knight et al. conducted a series of in vitro tests between 2005 and 2009 and showed the efficacy of SDF in arresting and preventing caries.[42,43] In 2014, the US Food and Drug Administration (FDA) approved SDF in the USA for preventing dentinal hypersensitivity.[34,44] However, it has also been used off-label as a caries-preventive and caries-arresting agent. Since its approval by the FDA, there has been considerable interest worldwide in the use of SDF for the non-surgical management of dental caries.

Chemical structure and composition

Chemically, SDF is an aqueous solution of AgF stabilized by the addition of ammonia.[45–47] Physically, SDF is a colorless solution with a molecular mass of 160.98 g/mol.[48] Overall, SDF has an alkaline pH. However, its alkalinity varies from one product to another. Various studies have shown that the pH of SDF remains stable for up to 180 days.[49–51] Asghar et al. measured the pH of 38% SDF (FAgamin) for up to 90 days.[52] Their results showed that the mean pH of SDF was 7.73 ±0.02 after the first hour of measurement, while the mean pH on day 90 was 7.70 ±0.01, indicating minimal time-dependent changes.[52] However, once the cap is opened, there is a risk of light-induced reduction of the Ag^+ ions in SDF. Hence, care should be taken to prevent direct exposure to light during SDF use and storage.

The chemical structure of SDF is presented in Fig. 2, while its composition is outlined in Table 3.

Mechanism of action

Several mechanisms of action have been proposed for SDF based on the effects of its silver and fluoride ions (Fig. 3).

Table 2. Historical advancements in the use of silver compounds for caries management

Period	Advancements in the use of silver compounds
Up to 1900	initial use of $AgNO_3$ in the management of caries
1917	Howe's solution ($AgNH_3NO_3$) developed and used until the 1950s
1970s–1990s	use of AgF, alone or in combination with SnF_2, in Western Australia
1970s	SDF developed and introduced in Japan with the support of the Central Pharmaceutical Affairs Council of the Ministry of Health and Welfare
1980s	SDF recommended for young children in Brazil, China and Argentina
2000s	randomized controlled clinical trials on SDF and other preventive treatments addition of silver particles to restorative materials and the use of silver nanoparticles
2014	SDF approved by the FDA as a desensitizing device
2015	first commercial SDF product introduced in the USA (Advantage Arrest; Elevate Oral Care)

$AgNO_3$ – silver nitrate; AgF – silver fluoride; SnF_2 – stannous fluoride; FDA – U.S. Food and Drug Administration.

Table 3. Composition of silver diamine fluoride (SDF)

Component	Percentage [%]	Concentration of SDF [%]	Concentration [ppm]
Silver	24–27	38	255,000
		30	200,000
		12	80,000
Fluoride	5–6	38	44,800
		30	35,400
		12	14,150
Ammonia	7.5–11	–	
Deionized water	62.5	–	

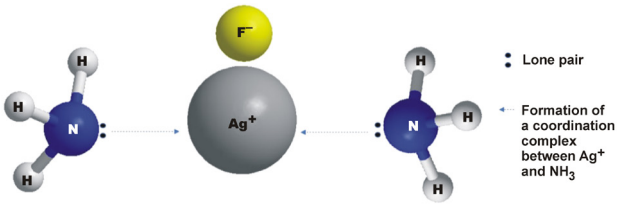

Fig. 2. Chemical structure of silver diamine fluoride (SDF)

NH_3 – ammonia.

Antibacterial action

Silver ions

As SDF is an aqueous solution, silver ions are continuously released from SDF into the oral environment and can exist in 3 oxidation states: silver ions (Ag^+); divalent silver ions (Ag^{2+}); and trivalent silver ions (Ag^{3+}).[53] It has been shown that among these 3 states, only Ag^+ possesses sufficient stability to exert an antibacterial effect.[54] Silver ions in SDF combine with the sulfhydryl groups of bacterial proteins and deoxyribonucleic acid (DNA), resulting in altered hydrogen bonding and inhibition of respiratory processes, DNA unwinding, cell division, and cell wall synthesis.[24,55] In an in vitro study, Knight et al. showed that dentin surfaces treated with SDF had significantly less growth of *S. mutans* than those in the control group.[42] Similarly, Chu et al. observed that the application of SDF to dentin resulted in considerably fewer bacterial colony-forming units (CFU) of *S. mutans* and *Actinomyces naeslundii*, two of the most commonly found bacterial species in root dentin caries.[56,57]

The silver ions in SDF prevent biofilm formation by reacting with functional and structural bacterial proteins, particularly those containing thiol groups (–SH), resulting in bacterial cell death.[46,58] Silver ions in SDF have also been shown to inhibit collagen degradation and the enzymatic activity of matrix metalloproteinases (MMPs).[37] Furthermore, silver ions bind to bacterial cell membranes, leading to membrane leakage and rupture, and can also cause DNA mutations that lead to bacterial cell death.[47,59] Finally, Ag^+ can infiltrate the hydroxyapatite (HA) crystals that form on the tooth surface following SDF application and reduce bacterial adhesion.[60]

Another aspect of the antibacterial efficacy of SDF is the cariostatic reaction between tooth components and SDF. It has been shown that the fluoride ions (F^-) released from SDF can penetrate dentin to a depth of 50–100 µm and provide a bacteriostatic effect.[18,61] Similarly, high concentrations of F^- in SDF inhibit bacterial biofilm formation by binding to bacterial cellular components and affecting their enzymatic activity related to carbohydrate metabolism.[33]

Fluoride ions

At high concentrations, fluoride ions have been shown to exert a bacteriostatic effect by binding to bacterial cellular components. The formation of hydrogen fluoride following the application of SDF results in increased bacterial cell membrane permeability coupled with the inhibition of plaque-dependent bacterial metabolism.[62] Furthermore, fluoride ions inhibit non-metal enzymes such as phosphatases, thereby preventing acid production by dental plaque.[47]

A summary of the mechanisms of action of SDF is provided in Table 4.

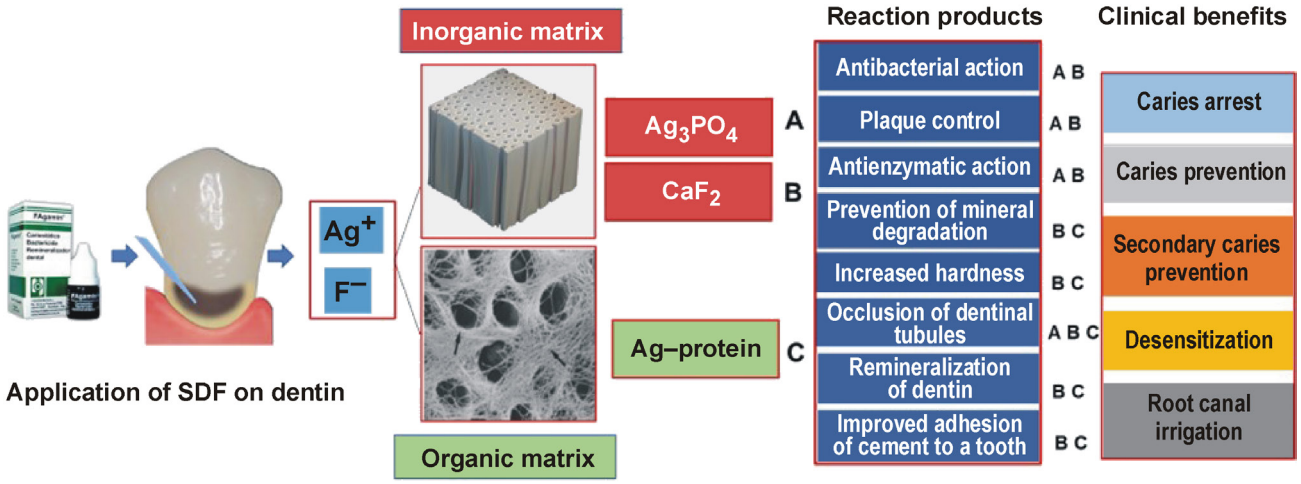

Fig. 3. Multipronged mechanisms of action of silver diamine fluoride (SDF)

Ag_3PO_4 – silver phosphate; CaF_2 – calcium fluoride.

Table 4. Mechanisms of action of silver diamine fluoride (SDF)

Mechanism of action	Key findings	Cited articles
Silver ions	antibacterial action: • binding to bacterial proteins and DNA • altering hydrogen bonding • inhibiting bacterial respiratory processes • preventing bacterial cell wall synthesis, cell division and DNA unwinding biofilm and enzyme inhibition: • reacting with bacterial proteins, particularly those containing thiol groups (–SH), causing cell death • inhibiting the enzymatic activity of MMPs, preventing collagen degradation reduced bacterial adhesion: • infiltrating HA crystals on the tooth surface after application, reducing bacterial adhesion	24,37,42,46,47,53–60
Fluoride ions	remineralization and bacteriostatic effects: • penetrating dentin up to 50–100 µm and exerting a bacteriostatic effect • promoting the formation of FHA crystals, which strengthens enamel and dentin metabolic inhibition: • inhibiting bacterial biofilm formation • preventing acid production by binding to bacterial cellular components and affecting bacterial metabolism	18,33,47,61,62

MMP – matrix metalloproteinase; HA – hydroxyapatite; FHA – fluorohydroxyapatite.

Effect of silver diamine fluoride on dental tissues

Enamel

The enamel remineralization potential of SDF has been attributed to the presence of a high concentration of fluoride ions and its alkaline pH. Similarly, the antibacterial effect results from the high concentration of Ag^+ ions in SDF.[63] It has been shown that the application of SDF results in the formation of calcium fluoride (CaF_2), fluorohydroxyapatite (FHA), Ag^0, and other silver compounds.[23,64] Although CaF_2-like globules form due to the high F^- ion concentration in SDF, they have been found to be easily washed away by saliva, water or other media in which the samples are stored.[63] Similarly, FHA formation occurs due to the reaction of HA with F^- ions in SDF.

Li et al. evaluated and compared the penetration of Ag^+ ions into primary enamel and dentin tissues.[65] Their results showed that Ag^+ ions penetrated vertically into the enamel surface, followed the direction of the enamel rods, and then penetrated demineralized dentin. The extent of silver penetration was found to be dependent on the degree of demineralization. It has been shown that there was considerable variability in the depth of penetration of Ag^+ ions into the tooth structure, with a mean penetration depth of 744.7 ±448.7 µm.[65] In contrast, as reported in a literature review by Shah et al., Suzuki et al. showed that silver ions were mainly deposited on the enamel surface and could penetrate up to 20 µm, while fluoride ions could diffuse up to 25 µm beneath the enamel.[18,66] Similar results were reported by Akyildiz et al., who showed that SDF could penetrate up to 25 µm into enamel.[67] This considerable difference in the reported penetration depths may be due to the differences in the types of dental tissues used for analysis, such as primary and permanent dental tissues.

Dentin

Previous studies have shown that the application of SDF on dentin results in a significant reduction in demineralization. Furthermore, higher concentrations of Ca^{2+} and PO_4^{3-} ions have been observed in the outer 25 µm of carious dentin treated with SDF compared to demineralized control specimens.[57] This indicated that SDF was able to promote remineralization in the previously demineralized dentin specimens. Mei et al. also showed that SDF could inhibit MMPs, an effect attributed to the high pH of SDF, thereby preventing degradation of the dentinal organic matrix.[68] The authors of the study observed the formation of dense granules on the dentin surface following SDF application, which were ascribed to extrafibrillar mineral deposition. It has also been shown that the hardness of the dentinal surface following SDF application was higher than that of the underlying tissue.[37] The alkaline pH of SDF tends to provide a favorable environment for cross-linking between minerals and collagenous proteins, thereby preventing the degradation of the exposed fibers.[44]

In addition, fluoride ions have been shown to protect the dentinal collagen structure in 2 main ways.[68] First, fluoride ions promote remineralization through the formation of FHA. The newly formed apatite crystals cover and protect the underlying collagen fibers from damage. Mei et al. used an immunolabelling technique and observed that SDF-treated dentin had more intact type I collagen than water-treated lesions.[39] The second proposed mechanism of protection of the dentinal organic matrix is the inhibition of MMPs. Mei et al. compared $AgNO_3$ and AgF and demonstrated that AgF was a much stronger inhibitor of MMP-2, MMP-8 and MMP-9.[68] Similarly, Kato et al. showed that 200 ppm of fluoride could completely inhibit the active and inactive forms of MMP-2 and MMP-9.[69] It has been proposed that the high electronegativity of F^- ions prevents the binding of zinc and calcium ions to MMPs,thereby preventing their activation.[69]

Clinical uses

Caries arrest and prevention

Dental caries in primary teeth

Silver diamine fluoride is most commonly used as a fluoride-based agent for caries arrest and prevention.[33] Zhi et al. showed that the annual application of 38% SDF or the use of a flowable, high-fluoride-releasing glass ionomer cement (GIC) had comparable caries-arresting potential. However, the rate of caries arrest with SDF increased when the agent was applied twice a year.[40]

In 2002, a 30-month clinical trial conducted by Chu et al. in Chinese preschool children showed that the annual application of 38% SDF was more effective in arresting dentin caries in primary anterior teeth than 5% NaF varnish applied every 3 months.[16] Caries excavation before the application of SDF provided no significant benefits.[16] A meta-analysis by Rosenblatt et al. reported prevented fractions of 96.1% for caries arrest and 70.3% for caries prevention with SDF, compared with 21.3% and 55.7%, respectively, with NaF varnish.[46]

Llodra et al. conducted a 36-month clinical trial to assess the caries-arresting potential of SDF in primary and permanent molars.[70] The results showed that the application of SDF every 6 months was effective in arresting caries in both primary and permanent teeth.[70] Yee et al. demonstrated that a single application of 38% SDF was effective in arresting caries in the primary teeth of schoolchildren.[38]

Braga et al. compared the effectiveness of SDF with other non-invasive measures: the cross-tooth brushing technique (CTT) and sealing with GIC for arresting dental caries in erupting permanent molars.[71] After 3 and 4 months of treatment, 10% SDF demonstrated significantly higher caries-arresting potential than CTT and GIC sealants.[71] Similarly, dos Santos et al. compared the caries-arresting potential of 30% SDF with GIC used as an interim restorative treatment (IRT) in schoolchildren aged 5–6 years.[72] The results showed that SDF was 1.73% more effective in arresting caries than IRT.[72]

In 2020, a randomized clinical trial (RCT) by Mabangkhru et al. investigated the caries-arresting efficacy of 38% SDF and 5% NaF in Thai children aged 3–5 years.[73] Both treatment options were applied every 6 months. At the end of 1 year, the caries arrest rate with 38% SDF was 35.7%, compared with 20.9% for 5% NaF ($p < 0.001$). Furthermore, the appearance of the children's teeth following SDF treatment did not affect parental acceptability.[73]

In 2022, Satyarup et al. conducted a randomized controlled trial to compare the efficacy of 38% SDF (Group 1) with the atraumatic restorative technique (ART) (Group 2) in schoolchildren. The results showed that after 9 months, the mean survival rate (± standard error (*SE*)) of the teeth in Group 1 was significantly higher (76.7 ±0.21) than that in Group 2 (62.2 ±0.28). Hence, SDF was shown to be more effective at arresting caries than ART in schoolchildren.[74]

Dental caries in adults

Tan et al. compared the efficacy of 4 different treatment protocols for preventing root caries among older adults who had at least 5 teeth with exposed sound root surfaces.[75] The following treatment groups were used in the study: placebo and oral hygiene instructions (OHI); OHI + 1% CHX application every 3 months; OHI + 5% NaF application every 3 months; and OHI + annual application of 38% SDF. Compared with the placebo and OHI groups, the prevented fractions for root caries were 71%, 64% and 57% for SDF, NaF and CHX varnish, respectively. The prevented fraction for root caries with the combination of annual SDF application and OHI was significantly higher than those of the other treatment groups.[75]

Similarly, Zhang et al. demonstrated the caries-arresting potential of different treatment options in community-dwelling older adults.[76] The treatment groups included annual OHI (Group 1), OHI + annual SDF application (Group 2), and OHI + SDF + oral health education program twice a year (Group 3). After a 24-month follow-up, the mean numbers of arrested root caries surfaces in Groups 1, 2 and 3 were 0.04, 0.28 and 0.33, respectively, with Group 3 demonstrating significantly greater caries-arresting potential than the other 2 groups.[76]

In 2016, Li et al. investigated the efficacy of 38% SDF in arresting root caries among community-dwelling adults in Hong Kong, China.[77] The following 3 groups were tested: soda water (control); annual SDF application; and annual SDF application immediately followed by the application of potassium iodide (KI). Tooth color changes were measured using PANTONE color plates. After a 30-month follow-up, the caries arrest rates in Groups 1, 2 and 3 were 45%, 90% and 93%, respectively (χ^2 test; $p < 0.01$). It was concluded that the annual application of SDF, regardless of adjunctive KI application, was effective in arresting root caries in adults.[77] Interestingly, it was also shown that the application of KI following SDF treatment was ineffective in mitigating long-term SDF-mediated tooth staining. Additionally, Mitchell et al. showed that the probability of arresting an active root caries lesion with SDF was 91.6% after 18 months of treatment.[78]

Management of tooth sensitivity

Silver diamine fluoride has been shown to be effective in minimizing dentinal hypersensitivity. It has been demonstrated that the application of SDF results in the formation of compounds such as silver phosphate (Ag_3PO_4) and CaF_2, which form a squamous surface layer, occlude the exposed dentinal tubules and prevent hypersensitivity.[34] In 2014, SDF was cleared for use by the FDA for the management of dentin hypersensitivity.

In a multi-center study, Castillo et al. compared the efficacy of 38% SDF with that of a placebo (sterile water).[79] In their study, 129 subjects with at least 1 tooth sensitive to air-drying were recruited from 2 different sites, and

pain levels before and after treatment were measured using a 100-mm visual analog scale (VAS). At both sites, SDF was shown to significantly reduce dentin sensitivity (–35.8 ±27.7 and –23.4 ±21, respectively) after 7 days, compared with VAS scores of 0.4 ±16.2 and –5.5 ±18.1 for the control group at both sites. The authors concluded that SDF was a clinically effective option for managing tooth sensitivity.[79]

In another study, Craig et al. evaluated the efficacy of an SDF/KI-based commercial product compared with that of an oxalic acid-based product in reducing dentinal sensitivity.[80] Tooth sensitivity was measured in 19 study subjects at baseline and 7 days after treatment using a VAS. It was shown that the SDF/KI-based product could significantly reduce dentin hypersensitivity compared with the oxalic acid-based product 1 week after treatment (p = 0.00134). The SDF/KI-based product was recommended as a potential option for managing dentin hypersensitivity.[80]

Molar incisor hypomineralization

Dental hypomineralization is a congenital defect that mainly affects the permanent first molars and incisors.[81] This condition is characterized by the appearance of well-demarcated, chalky white or brown opacities. Histologically, these opacities appear porous and are located in the deeper parts of the enamel. Children with this condition experience severe tooth hypersensitivity, as their teeth are more prone to wear and dentinal exposure. The application of SDF to these teeth has been shown to effectively reduce sensitivity and arrest the lesions.

An RCT by Ballikaya et al. compared the effects of SDF and silver-modified atraumatic restorative treatment (SMART) sealants for the treatment of initial carious lesions in molars affected by molar incisor hypomineralization (MIH).[82] The results showed that SDF and SMART had comparable short-term effectiveness in preventing dental caries in MIH-affected molars.[82]

Similarly, a study by Saad et al. compared the effectiveness of SMART with that of conventional restorations and fluoride varnish application in moderately hypomineralized and severely hypomineralized molars.[83] Their results demonstrated that both SDF and fluoride varnish had a significant and comparable effect on the reduction of hypersensitivity in hypomineralized molars.[83]

Endodontic irrigant and inter-appointment medication

Silver diamine fluoride has also been investigated as a root canal disinfectant and irrigant. In 2010, Hiraishi et al. studied the efficacy of 3.8% SDF and 5.25% sodium hypochlorite (NaOCl) in penetrating dentin and neutralizing *Enterococcus faecalis* biofilms.[84] It was shown that 3.8% SDF and 5.25% NaOCl were equally effective at disrupting the bacterial biofilm compared with NaCl. The authors also observed silver deposits on 66.5% of the radicular dentin, which penetrated up to 40 µm at 72 h after SDF treatment.[84]

In another ex vivo study, Mathew et al. compared the antibacterial action of 3.8% SDF and 2% CHX against *E. faecalis* for endodontic purposes using single-rooted teeth.[85] Their results showed an absence of CFU in specimens treated with SDF and CHX 24 h after treatment, compared with a CFU count of 3.8×10^7 for the negative control (0.9% sterile saline). The authors concluded that SDF could be used as an endodontic antibacterial agent. However, one limitation of this study was the short duration of antibacterial testing.[85]

In contrast, Al-Madi et al. demonstrated that NaOCl was more effective in disrupting bacterial biofilm than SDF or CHX.[86] The study investigated the antibacterial potential of 3.8% SDF as a root canal irrigant compared with 2% CHX, using NaOCl and saline as positive and negative controls, respectively. Single-rooted teeth without anatomical or structural deformities were treated with SDF and CHX, and confocal laser scanning microscopy (CLSM) was used to evaluate the live-to-dead ratio of *E. faecalis* biofilms. After a 10-minute exposure to the treatment solutions, NaOCl had the highest live-to-dead percentage among all treatment groups. Furthermore, SDF had a significantly higher live-to-dead ratio than CHX and saline.[86]

Management of dental erosion

Dental erosion is the chemical loss of dental tissues due to non-bacterial acids.[87] Dental erosion can lead to the exposure of dentinal tubules, resulting in hypersensitivity and the development of carious lesions. Silver diamine fluoride has been shown to be an excellent antierosive agent owning to its remineralization potential. The compound reacts with tooth minerals to form Ag^0 and silver chloride on the tooth surface, which may contribute to its antierosive effect.[39,88] A study demonstrated the formation of silver-containing HA on enamel following SDF treatment.[63] Similarly, another laboratory-based study showed that SDF could effectively reduce erosion of enamel and dentin.[19]

Treatment of gingivitis

Owing to its high Ag^+ ion concentration, SDF possesses excellent antibacterial properties. Hence, it can also be used for the treatment of gingival problems. In 2020, Rams et al. evaluated the antibacterial efficacy of 19% SDF and 38% SDF against various periodontal pathogens.[89] Their results showed that SDF exhibited significant in vitro antibacterial efficacy against putative periodontal pathogens cultured from severe lesions.[89] Similarly, a case report by Lim and Yang demonstrated that SDF treatment was effective in the management of gingival hyperplasia due to its anti-inflammatory properties.[90]

A summary of the clinical uses of SDF is presented in Table 5.

Table 5. Summary of the clinical uses of silver diamine fluoride (SDF)

Clinical use	Key findings	References
Caries arrest and prevention	SDF is a more effective caries-arresting and preventive agent than fluoride varnish in preschool children. Its efficacy in arresting caries increases with more frequent application. A single annual application of SDF is effective in arresting root caries in older adults. It is a superior caries-arresting agent compared with atraumatic restorative treatment in school settings.	16,33,38,40,70–78
Dentin hypersensitivity	SDF effectively reduces tooth sensitivity by forming a layer of compounds that occlude exposed dentinal tubules. Its use was cleared by the FDA for this purpose in 2014.	34,79,80
Molar incisor hypomineralization	SDF application effectively reduces hypersensitivity and arrests lesions associated with this congenital defect.	81–83
Endodontic irrigant and inter-appointment medication	SDF has been investigated as a root canal disinfectant and irrigant. Studies have shown varying results, with some finding it as effective as NaOCl in disrupting bacterial biofilms, while others have found NaOCl to be superior.	84–86
Management of dental erosion	As a potent remineralizing agent, SDF may exert an antierosive effect by reacting with tooth minerals to form metallic silver and other compounds on the tooth surface.	19,39,63,87,88
Treatment of gingivitis	Due to its high concentration of silver ions, SDF exhibits excellent antibacterial properties and has been used to treat gingival problems.	89,90

NaOCl – sodium hypochlorite.

Safety

Although SDF contains high concentrations of Ag^+ and F^- ions, 1 drop of 38% SDF has been shown to contain 2.24 mg of F^-, compared with 11.3 mg of F^- in a typical dose of 0.25 mL of 5% NaF. Hence, the annual or biannual application of SDF does not pose a safety or toxicity risk.[91]

During the process of obtaining the FDA approval, the median lethal dose (LD_{50}) for 38% SDF was found to be 520 mg/kg by the oral route and 380 mg/kg by the subcutaneous route. One drop of SDF has an approximate volume of 25 µL and contains 9.5 mg of the active ingredient, which is sufficient for treating 5 teeth. If SDF is administered to a child weighing only 10 kg, the administered dose would be 0.95 mg/kg of body weight. Therefore, the safety margin of SDF for a child weighing 10 kg would be calculated as 380 mg/kg LD_{50} or 0.95 mg/kg dose, corresponding to an approx. 400-fold safety margin.[27] In fact, the administered dose is much lower. Vasquez et al. showed that the maximum total dose required to apply 38% SDF to 3 teeth was 2.37 mg.[92] Therefore, approx. 400 applications of 38% SDF, equivalent to 1 g of silver, would be required to result in silver poisoning.[47]

Adverse effects

No long-term adverse effects of SDF have been reported in the literature.[47] According to the results of 9 RCTs in which SDF was applied to multiple teeth for caries arrest and prevention, the only side effect observed was the appearance of mild, painful, white lesions on the oral mucosa, which disappeared within 48 h.[27,40] In a randomized controlled trial by Milgrom et al., the most commonly reported adverse effects following SDF application were mild diarrhea and headache.[93] However, these symptoms resolved within 48 h of SDF treatment. Similarly, the gingival response to SDF has been shown to be minimal.[93]

In a RCT by Zheng et al., it was shown that there were no short- (1-day) or long-term (1-year) adverse effects of SDF application to primary anterior teeth, such as swelling, irritation or bleaching.[94] A RCT by Castillo et al. reported mild erythema in some survey participants during the first 24 h following SDF application.[78] However, Horst et al. recommend the application of a coating agent on the mucosa opposite the teeth to which SDF will be applied.[27] Due to the high concentration of silver ions present in SDF, it must not be used in patients who have an allergy to silver.[47]

Aesthetic concerns

Parental aesthetic concerns regarding SDF treatment

Despite its excellent efficacy, ease of application and cost-effectiveness, the use of SDF remains limited by its potential to cause black staining of teeth and to stain clothing and countertops.[27,33,34,46,95] While this staining is an indication of the successful anticaries effect of SDF, it is also an aesthetic concern for many patients.[96]

The exact cause of SDF-mediated tooth staining is not fully understood. However, according to Lou et al., silver ions react at the surface of enamel to form Ag_3PO_4, CaF_2 and Ag^0.[97] The resulting Ag_3PO_4 is brownish in color and gradually turns black, staining the teeth. Similarly, in the case of dentin, silver ions react with proteins present within dentin to form a silver protein complex, in addition to Ag_3PO_4 and CaF_2, which further contributes to the staining mechanism.[98] Tooth staining occurs 2 min after the application of SDF, and a visually discernible color change occurs within 5 min.[99]

A graphical summary of the proposed mechanism of SDF-mediated tooth staining is shown in Fig. 4.

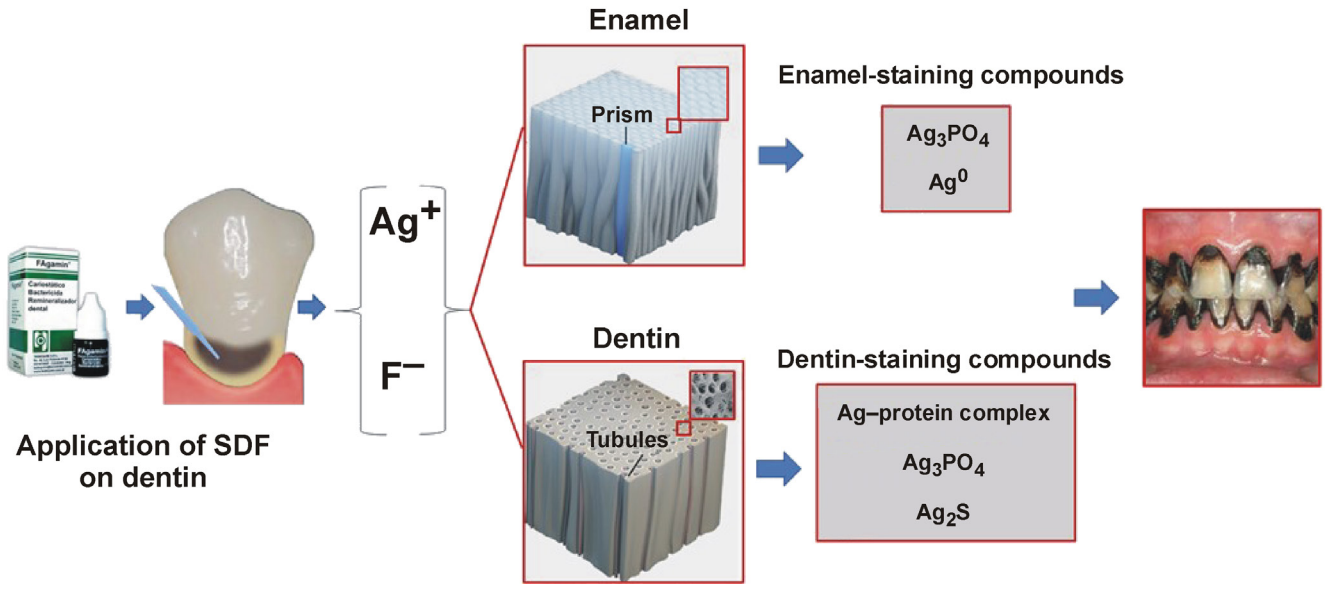

Fig. 4. Proposed mechanism of tooth staining caused by the application of silver diamine fluoride (SDF)

Ag_2S – silver sulfide; Ag^0 – metallic silver.

A survey by Crystal et al. was conducted to evaluate parental acceptance of SDF staining.[100] Only 29.7% of the parents found SDF-mediated tooth staining acceptable on anterior teeth. Furthermore, parental acceptability was likely to be higher for posterior teeth than for anterior teeth.[100] These findings were summarized by Gordon, who noted that parental acceptance of SDF staining was higher when children's teeth were located in less visible areas of the mouth.[101] It has also been shown that parents tend to be more accepting of SDF use on primary teeth than on permanent teeth.[102]

Alshammari et al. conducted a cross-sectional study in Saudi Arabia in which a total of 222 parents were asked for their opinions regarding SDF staining after viewing before-and-after photographs.[103] The results showed that parents considered SDF-mediated staining of anterior teeth unacceptable, with 90% of them strongly refusing treatment. Similarly, in the case of posterior teeth, 28.4% of parents refused the treatment, while 68.5% of them strongly refused SDF treatment due to aesthetic concerns.[103] Likewise, a cross-sectional study conducted by Bagher et al. investigating parental acceptance of SDF use on their children's primary and permanent teeth showed that only 2 (1.9%) of the 104 parents found SDF treatment acceptable, while 46 (44.2%) considered the treatment strongly unacceptable.[104]

On the other hand, Magno et al. concluded that the parental acceptance of SDF treatment was not affected by its staining potential.[105] Instead, the findings of the study showed that clinicians were more concerned about the staining effect of SDF than parents.[105] Similar results were obtained by Mabangkhru et al.,[73] while Duangthip et al. reported that the overall parental acceptance of the staining potential of SDF was 71%.[106]

Dental professionals' aesthetic concerns regarding SDF treatment

Various studies have documented dental professionals' concerns about the tooth-staining potential of SDF. In a survey of US Pediatric Dentistry Residency Program directors, 91.8% of the respondents believed that parental concerns regarding SDF staining were the main impediment to its widespread clinical use.[107]

Similarly, a survey of registered dental hygienists conducted by Chhokar et al. revealed that 56% of the respondents believed that patients or their guardians would object to SDF-mediated staining of carious teeth.[108] In 2019, another survey of US pediatric dentists demonstrated that only 33% of the respondents agreed or strongly agreed with the application of SDF to primary teeth in the aesthetic zone. Interestingly, only 14.3% of dentists agreed or strongly agreed with SDF application to permanent teeth in the aesthetic zone.[109]

Methods to reduce silver-mediated tooth staining associated with SDF

Various techniques have been employed to reduce the staining of teeth caused by SDF.

Potassium iodide

Knight et al. incorporated KI into SDF and demonstrated its effectiveness in reducing tooth staining.[43] Potassium iodide reacts with silver ions to form silver iodide (AgI), a creamy white mixture that deposits on the surface of the tooth and cosmetically masks the staining effect. However, other studies have shown that the effect of KI is only temporary, and black staining of the teeth still occurs over

time.[27,110] Miller et al. evaluated the staining associated with SDF and SDF + KI after the placement of a GIC restoration.[111] The results showed that there was no statistically significant difference in the staining between the control and experimental groups.[111] Similarly, Zhao et al. compared discoloration around restoration margins in teeth that were treated with either SDF or SDF followed by KI and then restored with GIC.[112] The results of their study showed that despite the reduction in staining in the SDF + KI group, perceptible staining still occurred around the restoration margins.[112] Furthermore, a radomized clinical trial by Li et al. revealed that the immediate application of KI to the teeth following SDF application could not eliminate long-term black staining.[77]

Recently, Detsomboonrat et al. investigated the effect of incorporating different concentrations of KI into SDF on its tooth-staining potential.[113] The results of their study showed that the inclusion of KI into SDF resulted in a concentration-dependent reduction in tooth staining. However, the color change in the specimens treated with SDF + KI was minimal over the following 14 days. The study did not describe long-term effects of the incorporation of KI into SDF on its ability to minimize tooth staining.[113]

Glutathione biomolecule

Sayed et al. added 20% glutathione (G) to SDF to reduce its staining potential.[110] Glutathione is a biomolecule that coats silver particles and prevents them from forming clusters. As a result, the particles do not agglomerate, thereby reducing the black staining of teeth. It was observed that the overall color change in specimens treated with 20% G + SDF, with or without light exposure, was greater than that in the control group (SDF) and the SDF + KI group. Similarly, G-modified SDF was more effective in preventing staining in enamel than in dentin specimens. The authors of the study evaluated color changes over 14 days only, which is insufficient to establish the long-term staining potential of a silver-based solution.[110]

Similarly, Gupte et al. compared the staining potential of enamel specimens treated with 38% SDF, SDF application followed by 10% KI, and SDF containing 20% (w/v) G at 4 different timepoints: 1, 7 and 14 days, as well as 1 month after treatment.[114] Their results showed that while KI could effectively reduce SDF-mediated staining, G-modified SDF lacked the ability to prevent long-term enamel staining. In another study, Kamble et al. compared the tooth discoloration potential of 38% SDF following the incorporation of KI and the G biomolecule.[115] Their results showed that while KI could effectively reduce SDF-mediated staining in primary molar specimens, glutathione could also be used as an alternative.[115]

Capping agents

Capping agents have also been used to overcome the staining potential of SDF. Their ability to encapsulate Ag^+ ions prevents the formation of silver compounds that cause tooth staining. In a laboratory study, Asghar et al. incorporated 4 different capping agents in 30% SDF, namely tannic acid (TA), G, carboxymethyl chitosan (CM), and gallic acid (GA) at 3 different concentrations: 5%; 10%; and 15% (w/v). The study results showed that capping agents could reduce SDF-mediated staining of dentin specimens. However, the stain-reducing effect was observed to be more dependent on the type of capping agent than on its concentration. It was shown that TA and G biomolecules produced the greatest reduction in dentin staining following SDF treatment among all capping agents tested. Hence, the incorporation of capping agents could be an effective method to overcome SDF staining and enhance its clinical use.[116]

Silver nanoparticles

Another approach to reducing SDF-associated staining involves the use of nanosilver-based formulations. Silver nanoparticles (AgNPs) exhibit enhanced, size-dependent antimicrobial activity compared with conventionally used silver products and SDF. In addition, AgNPs have also been shown to be safe for use inside the human body at low concentrations.[117] Osorio et al. demonstrated the role of silver ions in reducing collagen degradation and inhibiting the enzymatic activity of MMPs.[118] Similarly, Espíndola-Castro et al. showed that nanosilver fluoride resulted in significantly less staining compared with SDF.[119]

Comparable results were obtained by Sayed et al., who demonstrated that tooth staining caused by the application of nanosilver was significantly reduced compared with that caused by SDF and SDF + KI. However, one problem associated with AgNPs is their inherent tendency to aggregate after reduction, leading to reduced antibacterial efficacy and the development of tooth stains over time. Hence, further research is required to identify modifications or alternatives to SDF that minimize color change.[120]

The aggregation of AgNPs in an ionic environment, such as the oral cavity, tends to occur rapidly.[121] This can be prevented by coating AgNPs to stabilize them electrostatically.[122] Yin et al. used polyethylene glycol (PEG), a synthetic polyether, as a capping and stabilizing agent to prepare fluoride-containing AgNPs.[123] The results of their study showed that these AgNPs not only possessed good antibacterial properties but also minimized tooth staining compared with 38% SDF. However, information regarding the remineralization efficacy of these AgNPs and their concentration-dependent effects on tooth staining was not available.[123]

Currently, no alternative to or modification of SDF can eliminate the black staining of teeth associated with its use. The clinical application of SDF could be considerably enhanced if its staining effect were eliminated. This can be achieved with the use of capping agents. Capping agents are amphiphilic molecules comprising a polar head and a non-polar hydrocarbon-based tail. The tail interacts with the surrounding medium, while the head reacts with

metal atoms.[124] The addition of capping agents to metallic solutions tends to result in the coating of metal ions, thereby preventing them from forming reduction products that subsequently cause tooth staining.

Conclusions

Silver diamine fluoride has diverse dental applications that make this topical treatment option an excellent, cost-effective, non-invasive therapeutic agent for managing carious lesions, treating dentin hypersensitivity and enamel hypomineralization, performing endodontic irrigation and disinfection, and providing periodontal treatment.

Despite its clinical efficacy, the use of SDF is limited by its potential to cause silver-mediated staining of carious tooth structure, which raises aesthetic concerns. Various approaches to addressing this problem, including the use of capping agents, KI application after SDF treatment, and alternatives to SDF such as AgNPs, have been used with varying degrees of success. However, to date, the staining problem has not been fully resolved. Hence, there is a need to further explore SDF modifications or non-staining alternatives with similar or improved efficacy.

Ethics approval and consent to participate

Not applicable.

Data availability

Not applicable.

Consent for publication

Not applicable.

Use of AI and AI-assisted technologies

Not applicable.

ORCID iDs

Mehmood Asghar https://orcid.org/0000-0002-5554-4449
Ros Anita Omar https://orcid.org/0000-0002-5664-3019
Rosiyah Yahya https://orcid.org/0000-0002-9846-5206
Adrian Ujin Yap https://orcid.org/0000-0003-0361-6209
Muhammad Amber Fareed https://orcid.org/0000-0001-8440-0092

References

1. Tomczyk J, Olczak-Kowalczyk D, Turska-Szybka A, Studnicki M. Oral health behaviors and tooth decay at the age of 12 and 15–18 years in Poland. *Dent Med Probl*. 2025;62(1):13–22. doi:10.17219/dmp/184054
2. Grzesiak-Gasek I, Dębska-Łasut K. Occurrence of dental caries, the prevalence of hygiene and dietary habits, and the influence of the workout session on the selected parameters of saliva in youth swimmers. *Dent Med Probl*. 2026;63(1):51–63. doi:10.17219/dmp/187213
3. Mazur M, Ndokaj A, Brugnoli I, Francescangeli M, Moubayidin T, Jedliński M. Insect flour and dental caries: Friends or foes? *Dent Med Probl*. 2025;62(1):9–12. doi:10.17219/dmp/196883
4. Manton DJ. Child dental caries – a global problem of inequality. *EClinicalMedicine*. 2018;1:3–4. doi:10.1016/j.eclinm.2018.06.006
5. Bernabe E, Marcenes W, Hernandez CR, et al.; GBD 2017 Oral Disorders Collaborators. Global, regional, and national levels and trends in burden of oral conditions from 1990 to 2017: A systematic analysis for the global burden of disease 2017 study. *J Dent Res*. 2020;99(4):362–373. doi:10.1177/0022034520908533
6. Edelstein BL. Pediatric caries worldwide: Implications for oral hygiene products. *Compend Contin Educ Dent*. 2005;26(5 Suppl 1):4–9. PMID:17036538.
7. Griffin SO, Griffin PM, Swann JL, Zlobin N. Estimating rates of new root caries in older adults. *J Dent Res*. 2004;83(8):634–638. doi:10.1177/154405910408300810
8. González-Gil D, Flores-Fraile J, Vera-Rodríguez V, Martín-Vacas A, López-Marcos J. Comparative meta-analysis of minimally invasive and conventional approaches for caries removal in permanent dentition. *Medicina (Kaunas)*. 2024;60(3):402. doi:10.3390/medicina60030402
9. Brookes ZLS, Bescos R, Belfield LA, Ali K, Roberts A. Current uses of chlorhexidine for management of oral disease: A narrative review. *J Dent*. 2020;103:103497. doi:10.1016/j.jdent.2020.103497
10. Borompiyasawat P, Putraphan B, Luangworakhun S, Sukarawan W, Techatharatip O. Chlorhexidine gluconate enhances the remineralization effect of high viscosity glass ionomer cement on dentin carious lesions in vitro. *BMC Oral Health*. 2022;22(1):60. doi:10.1186/s12903-022-02098-1
11. Alyahya Y. A narrative review of minimally invasive techniques in restorative dentistry. *Saudi Dent J*. 2024;36(2):228–233. doi:10.1016/j.sdentj.2023.11.005
12. Grohe B, Mittler S. Advanced non-fluoride approaches to dental enamel remineralization: The next level in enamel repair management. *Biomater Biosyst*. 2021;4:100029. doi:10.1016/j.bbiosy.2021.100029
13. Geeta RD, Vallabhaneni S, Fatima K. Comparative evaluation of remineralization potential of nanohydroxyapatite crystals, bioactive glass, casein phosphopeptide-amorphous calcium phosphate, and fluoride on initial enamel lesion (scanning electron microscope analysis) – an in vitro study. *J Conserv Dent*. 2020;23(3):275–279. doi:10.4103/JCD.JCD_62_20
14. de Oliveira PRA, Barreto LSC, Tostes MA. Effectiveness of CPP-ACP and fluoride products in tooth remineralization. *Int J Dent Hyg*. 2022;20(4):635–642. doi:10.1111/idh.12542
15. Kooshki F, Fatemi SM, Darvishghaderi S, Vahedi P. Comparison of the effects of fluoride varnish containing silver nanoparticles and conventional fluoride varnish on the surface microhardness of tooth enamel. *Dent Med Probl*. 2024;61(2):241–247. doi:10.17219/dmp/151702
16. Chu CH, Lo EC, Lin HC. Effectiveness of silver diamine fluoride and sodium fluoride varnish in arresting dentin caries in Chinese preschool children. *J Dent Res*. 2002;81(11):767–770. doi:10.1177/0810767
17. Gao SS, Zhao IS, Hiraishi N, et al. Clinical trials of silver diamine fluoride in arresting caries among children: A systematic review. *JDR Clin Trans Res*. 2016;1(3):201–210. doi:10.1177/2380084416661474
18. Shah S, Bhaskar V, Venkatraghavan K, Choudhary P, Trivedi K. Silver diamine fluoride: A review and current applications. *J Adv Oral Res*. 2014;5(1):25–35. doi:10.1177/2229411220140106
19. Ainoosah SE, Levon J, Eckert GJ, Hara AT, Lippert F. Effect of silver diamine fluoride on the prevention of erosive tooth wear in vitro. *J Dent*. 2020;103S:100015. doi:10.1016/j.jjodo.2020.100015
20. World Health Organization. World Health Organization Model List of Essential Medicines: 22nd List (2021). Geneva, Switzerland: World Health Organization; 2021. https://www.who.int/publications/i/item/WHO-MHP-HPS-EML-2021.02. Accessed August 30, 2025.
21. Jiang CM, Duangthip D, Chan AKY, Tamrakar M, Lo ECM, Chu CH. Global research interest regarding silver diamine fluoride in dentistry: A bibliometric analysis. *J Dent*. 2021;113:103778. doi:10.1016/j.jdent.2021.103778
22. Baethge C, Goldbeck-Wood S, Mertens S. SANRA – a scale for the quality assessment of narrative review articles. *Res Integr Peer Rev*. 2019;4(1):5. doi:10.1186/s41073-019-0064-8
23. Peng JJ, Botelho MG, Matinlinna JP. Silver compounds used in dentistry for caries management: A review. *J Dent*. 2012;40(7):531–541. doi:10.1016/j.jdent.2012.03.009

24. Lansdown ABG. Silver I: Its antibacterial properties and mechanism of action. *J Wound Care*. 2002;11(4):125–130. doi:10.12968/jowc.2002.11.4.26389
25. Klein U, Kanellis MJ, Drake D. Effects of four anticaries agents on lesion depth progression in an in vitro caries model. *Pediatr Dent*. 1999;21(3):176–180. PMID:10355008.
26. Gao SS, Zhao IS, Duffin S, Duangthip D, Lo ECM, Chu CH. Revitalising silver nitrate for caries management. *Int J Environ Res Public Health*. 2018;15(1):80. doi:10.3390/ijerph15010080
27. Horst JA, Ellenikiotis H, Milgrom PM; UCSF Silver Caries Arrest Committee. UCSF protocol for caries arrest using silver diamine fluoride: Rationale, indications, and consent. *J Calif Dent Assoc*. 2016;44(1):16–28. PMID:26897901.
28. Zander HA, Smith HW. Penetration of silver nitrate into dentin II. *J Dent Res*. 1945;24(3–4):121–128. doi:10.1177/00220345450240030101
29. Thibodeau EA, Handelman SL, Marquis RE. Inhibition and killing of oral bacteria by silver ions generated with low intensity direct current. *J Dent Res*. 1978;57(9–10):922–926. doi:10.1177/00220345780570091901
30. Oppermann RV, Rölla G. Effect of some polyvalent cations on the acidogenicity of dental plaque in vivo. *Caries Res*. 1980;14(6):422–427. doi:10.1159/000260485
31. Craig GG, Powell KR, Cooper MH. Caries progression in primary molars: 24-month results from a minimal treatment programme. *Community Dent Oral Epidemiol*. 1981;9(6):260–265. doi:10.1111/j.1600-0528.1981.tb00342.x
32. Green E. A clinical evaluation of two methods of caries prevention in newly-erupted first permanent molars. *Aust Dent J*. 1989;34(5):407–409. doi:10.1111/j.1834-7819.1989.tb00696.x
33. Greenwall-Cohen J, Greenwall L, Barry S. Silver diamine fluoride – an overview of the literature and current clinical techniques. *Br Dent J*. 2020;228(11):831–838. doi:10.1038/s41415-020-1641-4
34. Seifo N, Cassie H, Radford JR, Innes NPT. Silver diamine fluoride for managing carious lesions: An umbrella review. *BMC Oral Health*. 2019;19(1):145. doi:10.1186/s12903-019-0830-5
35. Patel J, Anthonappa RP, King NM. Silver diamine fluoride: A critical review and treatment recommendations. *Dent Update*. 2019;46(7):626–632. doi:10.12968/denu.2019.46.7.626
36. World Health Organization. Global strategy and action plan on oral health 2023–2030. https://www.who.int/publications/i/item/9789240090538. Accessed August 30, 2025.
37. Mei ML, Ito L, Cao Y, Lo ECM, Li QL, Chu CH. An ex vivo study of arrested primary teeth caries with silver diamine fluoride therapy. *J Dent*. 2014;42(4):395–402. doi:10.1016/j.jdent.2013.12.007
38. Yee R, Holmgren C, Mulder J, Lama D, Walker D, van Palenstein Helderman W. Efficacy of silver diamine fluoride for arresting caries treatment. *J Dent Res*. 2009;88(7):644–647. doi:10.1177/0022034509338671
39. Mei ML, Chu CH, Low KH, Che CM, Lo ECM. Caries arresting effect of silver diamine fluoride on dentine carious lesion with *S. mutans* and *L. acidophilus* dual-species cariogenic biofilm. *Med Oral Patol Oral Cir Bucal*. 2013;18(6):e824–e831. doi:10.4317/medoral.18831
40. Zhi QH, Lo ECM, Lin HC. Randomized clinical trial on effectiveness of silver diamine fluoride and glass ionomer in arresting dentine caries in preschool children. *J Dent*. 2012;40(11):962–967. doi:10.1016/j.jdent.2012.08.002
41. Lo EC, Chu CH, Lin HC. A community-based caries control program for pre-school children using topical fluorides: 18-month results. *J Dent Res*. 2001;80(12):2071–2074. doi:10.1177/00220345010800120901
42. Knight GM, McIntyre JM, Craig GG, Mulyani, Zilm PS, Gully NJ. An in vitro model to measure the effect of a silver fluoride and potassium iodide treatment on the permeability of demineralized dentine to *Streptococcus mutans*. *Aust Dent J*. 2005;50(4):242–245. doi:10.1111/j.1834-7819.2005.tb00367.x
43. Knight GM, McIntyre JM, Craig GG, Mulyani, Zilm PS, Gully NJ. Inability to form a biofilm of *Streptococcus mutans* on silver fluoride- and potassium iodide-treated demineralized dentin. *Quintessence Int*. 2009;40(2):155–161. PMID:19365897.
44. Zhao IS, Gao SS, Hiraishi N, et al. Mechanisms of silver diamine fluoride on arresting caries: A literature review. *Int Dent J*. 2018;68(2):67–76. doi:10.1111/idj.12320
45. Burgess JO, Vaghela PM. Silver diamine fluoride: A successful anticarious solution with limits. *Adv Dent Res*. 2018;29(1):131–134. doi:10.1177/0022034517740123
46. Rosenblatt A, Stamford TCM, Niederman R. Silver diamine fluoride: A caries "silver-fluoride bullet". *J Dent Res*. 2009;88(2):116–125. doi:10.1177/0022034508329406
47. Contractor IA, MS G, MD I. Silver diamine fluoride: Extending the spectrum of preventive dentistry, a literature review. *Pediatr Dent J*. 2021;31(1):17–24. doi:10.1016/j.pdj.2020.12.005
48. National Center for Biotechnology Information. PubChem compound summary for CID 161820, silver diammine fluoride. https://pubchem.ncbi.nlm.nih.gov/compound/Silver-diammine-fluoride. Accessed August 30, 2025.
49. Mei ML, Chu CH, Lo ECM, Samaranayake LP. Fluoride and silver concentrations of silver diammine fluoride solutions for dental use. *Int J Paediatr Dent*. 2013;23(4):279–285. doi:10.1111/ipd.12005
50. Crystal YO, Rabieh S, Janal MN, Rasamimari S, Bromage TG. Silver and fluoride content and short-term stability of 38% silver diamine fluoride. *J Am Dent Assoc*. 2019;150(2):140–146. doi:10.1016/j.adaj.2018.10.016
51. Yan IG, Zheng FM, Yin IX, Sun IG, Lo ECM, Chu CH. Stability of silver and fluoride contents in silver diamine fluoride solutions. *Int Dent J*. 2023;73(6):840–846. doi:10.1016/j.identj.2023.05.001
52. Asghar M, Omar RA, Yap AU, Bano NZ, Yahya R, Azzahari AD. Impact of capping agent incorporation on pH stability of silver diamine fluoride: An in vitro analysis. *Life and Science*. 2025;6(2):266–273. doi:10.37185/LnS.1.1.901
53. Marx DE, Barillo DJ. Silver in medicine: The basic science. *Burns*. 2014;40 Suppl 1:S9–S18. doi:10.1016/j.burns.2014.09.010
54. Lansdown ABG. Silver in health care: Antimicrobial effects and safety in use. *Curr Probl Dermatol*. 2006;33:17–34. doi:10.1159/000093928
55. Youravong N, Carlen A, Teanpaisan R, Dahlén G. Metal-ion susceptibility of oral bacterial species. *Lett Appl Microbiol*. 2011;53(3):324–328. doi:10.1111/j.1472-765X.2011.03110.x
56. Van Houte J, Jordan HV, Laraway R, Kent R, Soparkar PM, DePaola PF. Association of the microbial flora of dental plaque and saliva with human root-surface caries. *J Dent Res*. 1990;69(8):1463–1468. doi:10.1177/00220345900690080301
57. Chu CH, Mei L, Seneviratne CJ, Lo ECM. Effects of silver diamine fluoride on dentine carious lesions induced by *Streptococcus mutans* and *Actinomyces naeslundii* biofilms. *Int J Paediatr Dent*. 2012;22(1):2–10. doi:10.1111/j.1365-263X.2011.01149.x
58. Kędziora A, Speruda M, Krzyżewska E, Rybka J, Łukowiak A, Bugla-Płoskońska G. Similarities and differences between silver ions and silver in nanoforms as antibacterial agents. *Int J Mol Sci*. 2018;19(2):444. doi:10.3390/ijms19020444
59. Slawson RM, Lee H, Trevors JT. Bacterial interactions with silver. *Biol Met*. 1990;3(3–4):151–154. doi:10.1007/BF01140573
60. Chen W, Liu Y, Courtney HS, et al. In vitro anti-bacterial and biological properties of magnetron co-sputtered silver-containing hydroxyapatite coating. *Biomaterials*. 2006;27(32):5512–5517. doi:10.1016/j.biomaterials.2006.07.003
61. Shimooka S. On the penetration of silver nitrate and ammoniacal silver fluoride into microstructure of the sound dentin [in Japanese]. *Shigaku*. 1972;59(6):534–566. PMID:4500827.
62. Koo H. Strategies to enhance the biological effects of fluoride on dental biofilms. *Adv Dent Res*. 2008;20(1):17–21. doi:10.1177/154407370802000105
63. Yu OY, Mei ML, Zhao IS, Li QL, Lo ECM, Chu CH. Remineralisation of enamel with silver diamine fluoride and sodium fluoride. *Dent Mater*. 2018;34(12):e344–e352. doi:10.1016/j.dental.2018.10.007
64. Caslavska V, Moreno EC, Brudevold F. Determination of the calcium fluoride formed from in vitro exposure of human enamel to fluoride solutions. *Arch Oral Biol*. 1975;20(5–6):333–339. doi:10.1016/0003-9969(75)90023-0
65. Li Y, Liu Y, Psoter WJ, et al. Assessment of the silver penetration and distribution in carious lesions of deciduous teeth treated with silver diamine fluoride. *Caries Res*. 2019;53(4):431–440. doi:10.1159/000496210
66. Suzuki T, Nishida M, Sobue S, Moriwaki Y. Effects of diammine silver fluoride on tooth enamel. *J Osaka Univ Dent Sch*. 1974;14:61–72. PMID:4535096.

67. Akyildiz M, Sönmez IS. Comparison of remineralising potential of nano silver fluoride, silver diamine fluoride and sodium fluoride varnish on artificial caries: An in vitro study. *Oral Health Prev Dent*. 2019;17(5):469–477. doi:10.3290/j.ohpd.a42739
68. Mei ML, Lo ECM, Chu CH. Arresting dentine caries with silver diamine fluoride: What's behind it? *J Dent Res*. 2018;97(7):751–758. doi:10.1177/0022034518774783
69. Kato MT, Bolanho A, Zarella BL, Salo T, Tjäderhane L, Buzalaf MAR. Sodium fluoride inhibits MMP-2 and MMP-9. *J Dent Res*. 2014;93(1):74–77. doi:10.1177/0022034513511820
70. Llodra JC, Rodriguez A, Ferrer B, Menardia V, Ramos T, Morato M. Efficacy of silver diamine fluoride for caries reduction in primary teeth and first permanent molars of schoolchildren: 36-month clinical trial. *J Dent Res*. 2005;84(8):721–724. doi:10.1177/154405910508400807
71. Braga MM, Mendes FM, De Benedetto MS, Imparato JCP. Effect of silver diammine fluoride on incipient caries lesions in erupting permanent first molars: A pilot study. *J Dent Child (Chic)*. 2009;76(1):28–33. PMID:19341576.
72. dos Santos VE, de Vasconcelos FMN, Ribeiro AG, Rosenblatt A. Paradigm shift in the effective treatment of caries in schoolchildren at risk. *Int Dent J*. 2012;62(1):47–51. doi:10.1111/j.1875-595X.2011.00088.x
73. Mabangkhru S, Duangthip D, Chu CH, Phonghanyudh A, Jirarattanasopha V. A randomized clinical trial to arrest dentin caries in young children using silver diamine fluoride. *J Dent*. 2020;99:103375. doi:10.1016/j.jdent.2020.103375
74. Satyarup D, Mohanty S, Nagarajappa R, Mahapatra I, Dalai RP. Comparison of the effectiveness of 38% silver diamine fluoride and atraumatic restorative treatment for treating dental caries in a school setting: A randomized clinical trial. *Dent Med Probl*. 2022;59(2):217–223. doi:10.17219/dmp/143547
75. Tan HP, Lo ECM, Dyson JE, Luo Y, Corbet EF. A randomized trial on root caries prevention in elders. *J Dent Res*. 2010;89(10):1086–1090. doi:10.1177/0022034510375825
76. Zhang W, McGrath C, Lo ECM, Li JY. Silver diamine fluoride and education to prevent and arrest root caries among community-dwelling elders. *Caries Res*. 2013;47(4):284–290. doi:10.1159/000346620
77. Li R, Lo ECM, Liu BY, Wong MCM, Chu CH. Randomized clinical trial on arresting dental root caries through silver diammine fluoride applications in community-dwelling elders. *J Dent*. 2016;51:15–20. doi:10.1016/j.jdent.2016.05.005
78. Mitchell C, Gross AJ, Milgrom P, Mancl L, Prince DB. Silver diamine fluoride treatment of active root caries lesions in older adults: A case series. *J Dent*. 2021;105:103561. doi:10.1016/j.jdent.2020.103561
79. Castillo JL, Rivera S, Aparicio T, et al. The short-term effects of diammine silver fluoride on tooth sensitivity: A randomized controlled trial. *J Dent Res*. 2011;90(2):203–208. doi:10.1177/0022034510388516
80. Craig GG, Knight GM, McIntyre JM. Clinical evaluation of diamine silver fluoride/potassium iodide as a dentine desensitizing agent. A pilot study. *Aust Dent J*. 2012;57(3):308–311. doi:10.1111/j.1834-7819.2012.01700.x
81. William V, Messer LB, Burrow MF. Molar incisor hypomineralization: Review and recommendations for clinical management. *Pediatr Dent*. 2006;28(3):224–232. PMID:16805354.
82. Ballikaya E, Ünverdi GE, Cehreli ZC. Management of initial carious lesions of hypomineralized molars (MIH) with silver diamine fluoride or silver-modified atraumatic restorative treatment (SMART): 1-year results of a prospective, randomized clinical trial. *Clin Oral Investig*. 2022;26(2):2197–2205. doi:10.1007/s00784-021-04236-5
83. Saad AE, Alhosainy AY, Abdellatif AM. "Evaluation of Silver Diamine Fluoride Modified Atraumatic Restorative Treatment (SMART) on hypomineralized first permanent molar" – a randomized controlled clinical study. *BMC Oral Health*. 2024;24(1):1182. doi:10.1186/s12903-024-04860-z
84. Hiraishi N, Yiu CKY, King NM, Tagami J, Tay FR. Antimicrobial efficacy of 3.8% silver diamine fluoride and its effect on root dentin. *J Endod*. 2010;36(6):1026–1029. doi:10.1016/j.joen.2010.02.029
85. Mathew VB, Madhusudhana K, Sivakumar N, Venugopal T, Reddy RK. Anti-microbial efficiency of silver diamine fluoride as an endodontic medicament – an ex vivo study. *Contemp Clin Dent*. 2012;3(3):262–264. doi:10.4103/0976-237X.103615
86. Al-Madi EM, Al-Jamie MA, Al-Owaid NM, Almohaimede AA, Al-Owid AM. Antibacterial efficacy of silver diamine fluoride as a root canal irrigant. *Clin Exp Dent Res*. 2019;5(5):551–556. doi:10.1002/cre2.222
87. Imfeld T. Dental erosion. Definition, classification and links. *Eur J Oral Sci*. 1996;104(2(Pt 2)):151–155. doi:10.1111/j.1600-0722.1996.tb00063.x
88. Zheng FM, Yan IG, Duangthip D, Gao SS, Lo ECM, Chu CH. Silver diamine fluoride therapy for dental care. *Jpn Dent Sci Rev*. 2022;58:249–257. doi:10.1016/j.jdsr.2022.08.001
89. Rams TE, Sautter JD, Ramírez-Martínez GJ, Whitaker EJ. Antimicrobial activity of silver diamine fluoride on human periodontitis microbiota. *Gen Dent*. 2020;68(5):24–28. PMID:32857044.
90. Lim GXD, Yang J. Effect of silver diamine fluoride on hyperplastic gingivitis in an adult with intellectual disability – a case report. *Spec Care Dentist*. 2022;42(1):73–79. doi:10.1111/scd.12633
91. Crystal YO, Niederman R. Silver diamine fluoride treatment considerations in children's caries management. *Pediatr Dent*. 2016;38(7):466–471. PMID:28281949.
92. Vasquez E, Zegarra G, Chirinos E, et al. Short term serum pharmacokinetics of diammine silver fluoride after oral application. *BMC Oral Health*. 2012;12:60. doi:10.1186/1472-6831-12-60
93. Milgrom P, Horst JA, Ludwig S, et al. Topical silver diamine fluoride for dental caries arrest in preschool children: A randomized controlled trial and microbiological analysis of caries associated microbes and resistance gene expression. *J Dent*. 2018;68:72–78. doi:10.1016/j.jdent.2017.08.015
94. Zheng FM, Yan IG, Duangthip D, Lo ECM, Gao SS, Chu CH. Caries prevention using silver diamine fluoride: A 12-month clinical trial. *Int Dent J*. 2023;73(5):667–673. doi:10.1016/j.identj.2022.12.005
95. Kaur M, Shahid S, Karpukhina N, Anderson P, Wong FSL. Characterization of chemical reactions of silver diammine fluoride and hydroxyapatite under remineralization conditions. *Front Oral Health*. 2024;5:1332298. doi:10.3389/froh.2024.1332298
96. Sayed M, Nikaido T, Abdou A, Burrow MF, Tagami J. Potential use of silver diammine fluoride in detection of carious dentin. *Dent Mater J*. 2021;40(3):820–826. doi:10.4012/dmj.2020-308
97. Lou YL, Botelho MG, Darvell BW. Reaction of silver diamine fluoride with hydroxyapatite and protein. *J Dent*. 2011;39(9):612–618. doi:10.1016/j.jdent.2011.06.008
98. Mei ML, Ito L, Cao Y, Li QL, Lo ECM, Chu CH. Inhibitory effect of silver diamine fluoride on dentine demineralisation and collagen degradation. *J Dent*. 2013;41(9):809–817. doi:10.1016/j.jdent.2013.06.009
99. Surendranath P, Krishnappa S, Srinath S. Silver diamine fluoride in preventing caries: A review of current trends. *Int J Clin Pediatr Dent*. 2022;15(Suppl 2):S247–S251. doi:10.5005/jp-journals-10005-2167
100. Crystal YO, Janal MN, Hamilton DS, Niederman R. Parental perceptions and acceptance of silver diamine fluoride staining. *J Am Dent Assoc*. 2017;148(7):510–518. doi:10.1016/j.adaj.2017.03.013
101. Gordon NB. Silver diamine fluoride staining is acceptable for posterior primary teeth and is preferred over advanced pharmacologic behavior management by many parents. *J Evid Based Dent Pract*. 2018;18(1):94–97. doi:10.1016/j.jebdp.2018.01.001
102. Almarwan M, Almawash A, AlBrekan A, Albluwi S. Parental acceptance for the use of silver diamine fluoride on their special health care-needs child's primary and permanent teeth. *Clin Cosmet Investig Dent*. 2021;13:195–200. doi:10.2147/CCIDE.S307190
103. Alshammari AF, Almuqrin AA, Aldakhil AM, Alshammari BH, Lopez JNJ. Parental perceptions and acceptance of silver diamine fluoride treatment in Kingdom of Saudi Arabia. *Int J Health Sci (Qassim)*. 2019;13(2):25–29. PMID:30983942.
104. Bagher SM, Sabbagh HJ, AlJohani SM, Alharbi G, Aldajani M, Elkhodary H. Parental acceptance of the utilization of silver diamine fluoride on their child's primary and permanent teeth. *Patient Prefer Adherence*. 2019;13:829–835. doi:10.2147/PPA.S205686
105. Magno MB, da Silva LP, Ferreira DM, Barja-Fidalgo F, Fonseca-Gonçalves A. Aesthetic perception, acceptability and satisfaction in the treatment of caries lesions with silver diamine fluoride: A scoping review. *Int J Paediatr Dent*. 2019;29(3):257–266. doi:10.1111/ipd.12465
106. Duangthip D, Fung MHT, Wong MCM, Chu CH, Lo ECM. Adverse effects of silver diamine fluoride treatment among preschool children. *J Dent Res*. 2018;97(4):395–401. doi:10.1177/0022034517746678
107. Nelson T, Scott JM, Crystal YO, Berg JH, Milgrom P. Silver diamine fluoride in pediatric dentistry training programs: Survey of graduate program directors. *Pediatr Dent*. 2016;38(3):212–217. PMID:27306245.
108. Chhokar SK, Laughter L, Rowe DJ. Perceptions of registered dental hygienists in alternative practice regarding silver diamine fluoride. *J Dent Hyg*. 2017;91(4):53–60. PMID:29118084.

109. Antonioni MB, Fontana M, Salzmann LB, Inglehart MR. Pediatric dentists' silver diamine fluoride education, knowledge, attitudes, and professional behavior: A national survey. *J Dent Educ*. 2019;83(2):173–182. doi:10.21815/JDE.019.020
110. Sayed M, Matsui N, Hiraishi N, Nikaido T, Burrow MF, Tagami J. Effect of glutathione bio-molecule on tooth discoloration associated with silver diammine fluoride. *Int J Mol Sci*. 2018;19(5):1322. doi:10.3390/ijms19051322
111. Miller MB, López LA, Quock RL. Silver diamine fluoride, potassium iodide, and esthetic perception: An in vitro pilot study. *Am J Dent*. 2016;29(5):248–250. PMID:29178735.
112. Zhao IS, Mei ML, Burrow MF, Lo ECM, Chu CH. Effect of silver diamine fluoride and potassium iodide treatment on secondary caries prevention and tooth discolouration in cervical glass ionomer cement restoration. *Int J Mol Sci*. 2017;18(2):340. doi:10.3390/ijms18020340
113. Detsomboonrat P, Thongmak P, Lertpayab P, Aiemsri W, Sooampon S. Optimal concentration of potassium iodide to reduce the black staining of silver diamine fluoride. *J Dent Sci*. 2022;17(1):300–307. doi:10.1016/j.jds.2021.03.014
114. Gupte M, Saraf T, Jawdekar A, Khare S, Tiku A. A comparative analysis of staining propensity of SDF, SDF with potassium iodide and SDF with glutathione biomolecule on demineralized enamel: An in-vitro study. *Int J Appl Dent Sci*. 2021;7(3):297–301. doi:10.22271/oral.2021.v7.i3e.1314
115. Kamble AN, Chimata VK, Katge FA, Nanavati KK, Shetty SK. Comparative evaluation of effect of potassium iodide and glutathione on tooth discoloration after application of 38% silver diamine fluoride in primary molars: An in vitro study. *Int J Clin Pediatr Dent*. 2021;14(6):752–756. doi:10.5005/jp-journals-10005-2076
116. Asghar M, Yahya R, Yap AUJ, Azzahari AD, Omar RA. Incorporation of green capping agents to reduce silver-mediated dentine staining. *Caries Res*. 2022;56(3):149–160. doi:10.1159/000525505
117. Pauksch L, Hartmann S, Rohnke M, et al. Biocompatibility of silver nanoparticles and silver ions in primary human mesenchymal stem cells and osteoblasts. *Acta Biomater*. 2014;10(1):439–449. doi:10.1016/j.actbio.2013.09.037
118. Osorio R, Osorio E, Aguilera FS, Medina-Castillo AL, Toledano M, Toledano-Osorio M. Silver improves collagen structure and stability at demineralized dentin: A dynamic-mechanical and Raman analysis. *J Dent*. 2018;79:61–67. doi:10.1016/j.jdent.2018.10.003
119. Espíndola-Castro L, Rosenblatt A, Galembeck A, Monteiro G. Dentin staining caused by nano-silver fluoride: A comparative study. *Oper Dent*. 2020;45(4):435–441. doi:10.2341/19-109-L
120. Sayed M, Hiraishi N, Matin K, Abdou A, Burrow MF, Tagami J. Effect of silver-containing agents on the ultra-structural morphology of dentinal collagen. *Dent Mater*. 2020;36(7):936–944. doi:10.1016/j.dental.2020.04.028
121. Campisi S, Schiavoni M, Chan-Thaw CE, Villa A. Untangling the role of the capping agent in nanocatalysis: Recent advances and perspectives. *Catalysts*. 2016;6(12):185. doi:10.3390/catal6120185
122. Murphy A, Galon R, Jaiswal AK, Jaiswal S. An investigation on effect of capping agent on silver nanoparticles antibacterial activity. *J Food Chem Nanotechnol*. 2020;6(4):189–196. doi:10.17756/jfcn.2020-0101
123. Yin IX, Yu OY, Zhao IS, et al. Inhibition of dentine caries using fluoride solution with silver nanoparticles: An in vitro study. *J Dent*. 2020;103:103512. doi:10.1016/j.jdent.2020.103512
124. Gulati S, Sachdeva M, Bhasin KK. Capping agents in nanoparticle synthesis: Surfactant and solvent system. *AIP Conf Proc*. 2018;1953(1):030214. doi:10.1063/1.5032549

Review

Subsite-resolved molecular and epigenetic characterization of oral tongue squamous cell carcinoma: A systematic review and in silico genome-wide DNA methylation analysis

Bacem Othman[1,2,3,A–D,F], Omid Moztarzadeh[1,3,E,F], Lukas Hauer[1,E,F]

[1] Department of Stomatology, University Hospital Pilsen, Faculty of Medicine in Pilsen, Charles University, Pilsen, Czech Republic
[2] Biopticka Laboratory, Pilsen, Czech Republic
[3] Department of Anatomy, Faculty of Medicine in Pilsen, Charles University, Czech Republic

A – research concept and design; B – collection and/or assembly of data; C – data analysis and interpretation;
D – writing the article; E – critical revision of the article; F – final approval of the article

Dental and Medical Problems, ISSN 1644-387X (print), ISSN 2300-9020 (online) *Dent Med Probl*. 2026;63(5):1347–1361

Address for correspondence
Omid Moztarzadeh
E-mail: omid.moztarzadeh@lfp.cuni.cz

Funding sources
None declared

Conflict of interest
None declared

Acknowledgements
None declared

Received on August 2, 2026
Reviewed on August 30, 2026
Accepted on September 25, 2026

Published online on October 30, 2026

Abstract

Tongue squamous cell carcinoma (TSCC) arises predominantly in a human papillomavirus (HPV)-negative context, which shifts its pathogenesis away from the viral oncogene pathways involved in head and neck cancer.

Tongue-attributable literature was systematically reviewed in accordance with the Preferred Reporting Items for Systematic Reviews and Meta-Analyses (PRISMA) 2020 guidelines, and integrated with a primary genome-wide DNA methylation analysis of 112 SCC samples profiled using Illumina Infinium arrays, with comparisons against normal mucosa and SCCs arising at other head and neck subsites. The reported genes were functionally annotated using PANTHER, consolidated into interpretable thematic clusters, and assessed for evidence of druggability and methodological quality. The findings were synthesized narratively according to the functional theme, with the experimental system specified for each finding.

Fifty of the 197 extracted records could be confidently assigned to the tongue, while the remaining 147 were retained as an oral cavity comparator. Tongue SSC was distinguished by methylation and expression markers rather than by *PAX5* promoter methylation. Methylation was specifically associated with the tongue, together with a seven-gene expression signature (*MTFR1*, *C8orf33*, *OTUD6B*, *NUDCD1*, *PRKC1*, *ANO1*, and *PIK3CA*) derived from an HPV-associated comparator set.

Tongue SCC diverges from SCCs arising at other oral cavity subsites along an epigenetic rather than a mutational axis. Heterogeneity within TSCC reflects multiple molecular routes converging on a limited number of shared functional endpoints.

Limitations of the evidence: Human series were small and mostly retrospective; most study designs were preclinical and therefore provided indirect evidence; HPV, p53 and p16 ascertainment was incomplete; patient-tissue microRNA profiling relied on a single 50-pair series; and no outcomes were reported in a form that permitted data pooling.

Keywords: methylation, tongue squamous cell carcinoma, transcription factors, epigenetics, pseudogenes

Cite as
Othman B, Moztarzadeh O, Hauer L. Subsite-resolved molecular and epigenetic characterization of oral tongue squamous cell carcinoma: A systematic review and in silico genome-wide DNA methylation analysis. *Dent Med Probl.* 2026;63(5):1347–1361. doi:10.17219/dmp/240335

DOI
10.17219/dmp/240335

Copyright
Copyright by Author(s)
This is an article distributed under the terms of the Creative Commons Attribution 3.0 Unported (CC BY 3.0) (https://creativecommons.org/licenses/by/3.0/)

Highlights

- Genome-wide DNA methylation profiling revealed promoter methylation differences in tongue squamous cell carcinoma (TSCC) at loci also affected by rearrangements in fusion-positive oral cancer.
- Integrated systematic review and in silico analysis identified 19 genes shared between fusion-partner events and promoter hypermethylation across tumor subsets.
- Functional classification of 280 unique gene symbols into 13 consolidated PANTHER protein classes showed pathway-level convergence in TSCC.
- Convergent methylation targets highlight potential biomarkers for early diagnosis and prognosis in TSCC, although none has yet been validated against clinical endpoints.

Introduction

Squamous cell carcinoma (SCC) of the oral tongue is one of the most common malignancies of the oral cavity, and outcomes remain poor once the disease is locally advanced, recurrent or metastatic. Unlike SCC of the oropharynx, oral tongue SCC (OTSCC) is overwhelmingly human papillomavirus (HPV)-negative; therefore, its molecular pathogenesis must be sought outside the viral oncogene pathways that dominate much of the head and neck cancer literature.[1] Tongue tumors are nevertheless often grouped with SCCs arising at other oral cavity subsites, or with head and neck squamous cell carcinoma (HNSCC) as a whole.

The divergence from the oropharynx merits explanation on anatomical grounds, since the two subsites lie within a few centimeters of each other. Transforming papillomavirus infection depends on the access of virions to basal keratinocytes. The reticulated, discontinuous epithelium of the tonsillar and base-of-tongue crypts provides direct access to these cells, without the need for antecedent injury. In contrast, the oral tongue is covered by a continuous keratinizing stratified squamous epithelium overlying an intact basement membrane and a dense lamina propria. Access to the basal compartment at this subsite therefore depends on tissue injury. The crypt epithelium is further embedded in lymphoid tissue characterized by a locally tolerogenic immune milieu, which is permissive of viral persistence. Persistence at the oral tongue is correspondingly uncommon, and the detection of viral DNA at this subsite frequently reflects transient viral carriage.

Carcinogenesis at the oral tongue is dominated instead by tobacco- and alcohol-related field changes and, in a distinct subset of young never-smokers, by an etiology that remains unexplained. The practical consequence for the present synthesis is that p16 immunohistochemistry has no validated role as a surrogate marker of viral causation at this subsite.

Treating OTSCC, particularly non-HPV-related disease, presents significant therapeutic challenges. Conventional chemotherapeutic agents (cisplatin, paclitaxel, docetaxel, carboplatin, gemcitabine, fluorouracil, methotrexate, oxaliplatin, and doxorubicin) demonstrate limited efficacy as monotherapies, and are therefore often used in combination with immune checkpoint inhibitors (ICIs) (pembrolizumab, nivolumab, cemiplimab, atezolizumab, durvalumab, ipilimumab, camrelizumab, and toripalimab) or agents targeting epidermal growth factor receptor (EGFR) and vascular endothelial growth factor (VEGF) signaling (cetuximab, afatinib, erlotinib, bevacizumab, sorafenib, and lenvatinib), depending on the relevant biomarker profile, including positive immunohistochemical markers or the detection of *FGF3*/*FGF4* amplification.[2–5]

Still, no recurrent gene fusion has been reported in tongue-attributable series, and the fusion events available for comparison in this review derive from oral SCC records in which the tongue was not identified as a separate subsite. Denominators are unavailable for either group; therefore, no comparison of fusion frequency by subsite is made in this review.

Genetic alterations more broadly are sparsely reported in the tongue-restricted literature. Given this paucity of evidence, we reasoned that epigenetic mechanisms, and DNA methylation in particular, might account for a disproportionate share of TSCC pathogenesis.

Two research questions therefore structure the synthesis that follows. The first asks how the molecular profile of TSCC compares with that of SCC arising at other oral cavity subsites, and whether this comparison identifies alterations that are genuinely distinctive to the tongue. The second asks what accounts for the molecular heterogeneity observed within TSCC itself, and what contributions microRNAs, long non-coding RNAs, and pseudogenes make to this heterogeneity.

Methods

Systematic review

Protocol and vetted studies

This systematic review was conducted and is reported in accordance with the Preferred Reporting Items for Systematic Reviews and Meta-Analyses (PRISMA) 2020 statement. The review addressed which somatic, germline and

epigenetic alterations, and which consequent changes in gene and protein expression, have been reported in TSCC, and how these findings differ according to the experimental system in which they were generated. Eligibility was framed using a PECO (Population, Exposure, Comparator, and Outcome)-type structure adapted for molecular research. The population comprised SCC arising in the tongue, whether studied as human tumor tissue, patient-derived material, cell lines of tongue origin, or experimentally induced tongue carcinoma in animal models. The exposure was any reported molecular alteration, including somatic mutation, germline variant, copy number alteration, gene fusion, promoter or genome-wide methylation change, histone modification, differential mRNA, microRNA, long non-coding RNA or circular RNA expression, and differential protein expression or post-translational modification. The comparator, where present, was non-neoplastic tongue or oral mucosa, paired surgical margin tissue, premalignant lesions, or a less aggressive counterpart cell line or subline. Outcomes were the identity of the altered gene or gene product, the direction of the alteration, its functional consequence where tested, its association with clinical or pathological variables, and its reported druggability.

Studies were eligible if they reported original molecular data attributable to OTSCC and identified at least one gene, gene product or defined genomic region. Exclusion from the review altogether was applied to purely methodological work without disease-specific findings and to records without an available English full text. Ineligibility for the tongue cluster, as distinct from exclusion from the review, was applied to records without primary data, such as narrative reviews, editorials and conference abstracts without an accompanying dataset, to records on malignancy arising outside the tongue, and to records on non-neoplastic material. Records of these three kinds were retained in the comparator cluster as the oral-cavity and head and neck background for interpretation of tongue-attributable findings. Comparator records were never counted toward tongue-specific evidence and are identified as comparator at every point of use. No restriction was placed on sample size or study design. Records published before 2005 were not retrieved. The PRISMA 2020 flow diagram is shown in Fig. 1.

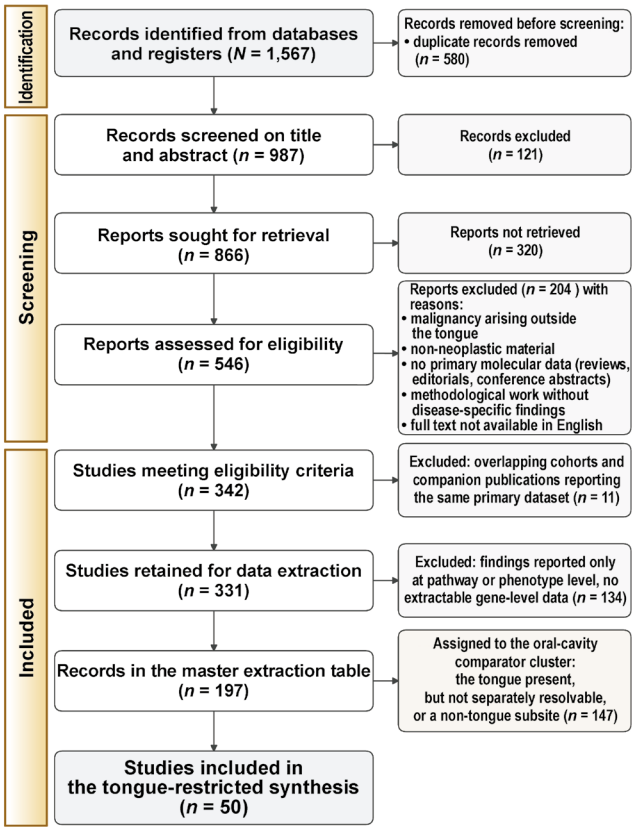

Fig. 1. PRISMA 2020 flow diagram for study identification, screening and inclusion

Search strategy and study selection

Electronic search was performed in Scopus, the Web of Science, Ovid, and PubMed from 2005 to 2025. The search combined controlled vocabulary with free-text terms across anatomical site, histology and molecular alteration. The anatomical block included tongue, oral tongue, lingual and their variants; the histological block included squamous cell carcinoma, carcinoma, and the abbreviations TSCC, OTSCC, SCCOT, OSCC and HNSCC; the molecular block included mutation, methylation, copy number, amplification, deletion, gene expression, microRNA, long non-coding RNA, proteomic, transcriptomic, exome and genome sequencing. Blocks were combined with AND, and terms within blocks with OR. The reference lists of retrieved articles and of relevant reviews were hand-searched, and forward citation tracking was performed on studies retained at full-text stage.

Title-and-abstract screening and full-text assessment were performed independently by two reviewers (B.O. and O.M.), with disagreement resolved by discussion against the eligibility criteria. Formal risk-of-bias instruments were not applied. The included literature is predominantly laboratory-based molecular work, for which no validated instrument of this kind exists. Methodological confidence was recorded instead at extraction as 3 items: the design category of the study; the presence or absence of an internal comparator; and the presence or absence of orthogonal validation of the reported alteration.

The search yielded 1,567 records. After the removal of duplicates, 987 records were screened on title and abstract, of which 866 were sought for retrieval. Of these, 546 reports were obtained and assessed against the full eligibility criteria, leaving 342 studies meeting the criteria, of which 331 were retained after resolution of overlapping cohorts and companion publications reporting the same primary dataset. Of these 331 studies, 197 reported gene-level molecular data in a form permitting structured extraction and constitute the master extraction table on

which the synthesis is based; the remaining 134 reported findings only at pathway or phenotype level and were not extracted. Fifty of the 197 extracted records reported findings attributable to the tongue and constitute the tongue cluster analyzed; the remaining 147 constitute the oral-cavity comparator cluster.

Data extraction and classification of the study design

Data were extracted into a purpose-built master table using a standardized form piloted on a random sample of 10 studies. The following items were recorded for every included study: first author and year; study design; anatomical site and histological type as reported by the authors; number of patients, specimens or cell lines; HPV status; p53 status; p16 status; whether immunohistochemistry was performed and for which targets; the genetic or molecular method used; the class of molecular alteration; the output gene or genes; the key molecular findings in narrative form; the nature of the biological material as primary, control or secondary; and the digital object identifier of the source publication. Where a study reported findings for more than one anatomical site or experimental system, each was recorded separately so that site- and system-specific attribution was preserved. Extraction was performed by two reviewers (B.O. and O.M.).

Since the interpretive weight of a molecular finding depends on the system in which it was generated, every study was assigned to one or more of 4 design categories. Human tissue studies analyzed primary patient material, including retrospective and prospective cohorts, paired tumor and margin designs, tissue microarrays, liquid biopsy and patient-derived organoids. In vitro studies used established or patient-derived cell lines, three-dimensional (3D) organotypic cultures, extracellular vesicle preparations or cell-free systems. In vivo studies used genetically engineered mouse models, chemically induced carcinogenesis such as 4-nitroquinoline 1-oxide (4NQO) exposure, subcutaneous or orthotopic xenografts, syngeneic implantation, or non-murine animal systems. In silico studies analyzed public repositories such as The Cancer Genome Atlas (TCGA) or the Gene Expression Omnibus (GEO), or performed meta-analysis, network reconstruction or predictive modelling without generating primary data. All applicable categories were retained.

Tongue cluster and oral-cavity comparator

The cohort was defined by the authors as tongue squamous cell carcinoma (TSCC, OTSCC or SCCOT); the tumors were induced in, or the tissue sampled from, the tongue in an animal model; a specific finding was reported for the tongue subsite within a larger oral cavity or head and neck cohort; or the experimental material was a cell line of documented tongue origin. Cell lines accepted as tongue-derived were SCC-4, SCC-9, SCC-15, SCC-25, HSC-3, CAL-27, SAS, Tca8113, UM1 and UM2, together with the murine MOC-L and MTCQ series derived from carcinogen-induced tongue tumors. Carcinomas of the base of tongue and of the tonsil were classified as oropharyngeal and excluded from the tongue cluster, because their etiology, HPV association and molecular profile diverge substantially from those of the oral tongue. Carcinomas of the gingivobuccal complex, gingiva, buccal mucosa, floor of mouth, larynx, esophagus and salivary glands were likewise excluded.

Studies of oral cavity or head and neck SCC in which tongue tumors were present but not separately resolvable were not discarded. They were assigned to a comparator cluster and retained as the oral-cavity control against which tongue-specific findings were read, allowing alterations distinctive to the tongue to be distinguished from those general to oral squamous carcinogenesis. Findings drawn from the comparator cluster are identified as such wherever they appear and are never presented as tongue-specific evidence.

Functional annotation of output genes

All genes and gene products recorded in the extraction table were consolidated into a single non-redundant list and submitted to the PANTHER classification system for assignment to protein class. Gene symbols were reconciled against current HGNC nomenclature before submission, and symbols reported under superseded or non-standard forms were mapped to their approved equivalents, while the original designation was preserved in the extraction table. Annotation returned 308 gene assignments across 84 protein classes. A single symbol may receive more than one class assignment, so the 308 assignments correspond to a smaller number of distinct symbols. The removal of duplicate assignments and of symbols not reconcilable to current HGNC nomenclature left 280 unique gene symbols. The largest single category was Unknown, comprising 62 genes for which PANTHER returned no assignment, followed by transmembrane signal receptors (15), non-receptor serine/threonine protein kinases (12) and a residual Unclassified category (10), with a further 34 classes containing a single gene each. Since a synthesis organized around 84 classes would be neither readable nor interpretable, and because many classes are functionally adjacent, the PANTHER output was used as the basis for a smaller number of functional themes. Genes returned as Unknown or Unclassified were assigned to a theme based on the function attributed to them in the source study.

Transcription factors and transcriptional regulators were treated as a distinct analytical focus. They were distributed across 12 separate PANTHER classes – homeodomain, DNA-binding, basic helix-loop-helix, C2H2 zinc finger, winged helix/forkhead, Rel homology, HMG box, P53-like, Runt, basic leucine zipper and zinc finger transcription

factors, together with transcription cofactors – comprising 38 gene assignments and forming the single largest functional grouping once the dispersal across classes is reversed. This dispersal is an artefact of the PANTHER structural taxonomy, and the classes were reconsolidated for synthesis so that transcriptional regulation could be assessed as a coherent axis.

Druggability annotation

Each study was classified according to whether druggability was addressed and at what level of evidence. Pharmacological testing, in which a defined compound was administered to a biological system and an effect measured; target nomination, in which a gene or pathway was proposed as actionable without experimental testing; and no assessment. For studies in the first category, the compound, its molecular target, the system in which it was tested, and the direction of the observed effect were recorded, together with any result running counter to the expected pharmacological direction.

Fusion-partner gene set used as the genetic comparator

The genetic comparator shown in Fig. 2 is a gene set where no fusion calling was performed de novo for this review. Fusion transcripts recorded for fusion-positive oral squamous cell carcinoma were split into their constituent 5' and 3' partner genes. Partner symbols were reconciled to the current HGNC nomenclature, so that genes altered by rearrangement and genes altered by promoter methylation occupy one symbol space. Fusion counts carry no denominator in this design and are not used to estimate fusion frequency at any subsite. Comparison against the methylation output is made at the level of gene identity alone.

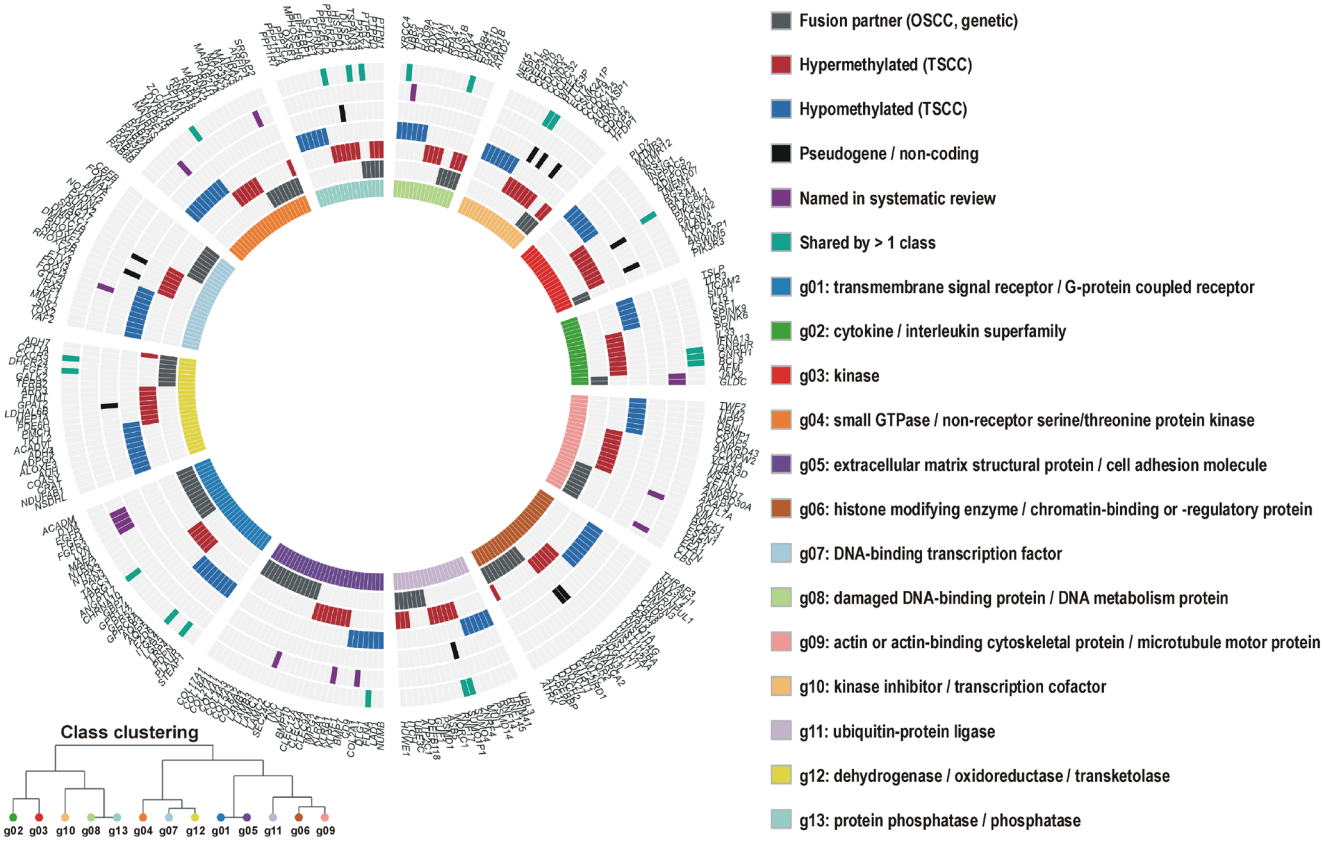

Fig. 2. Convergence of genetic and epigenetic alteration on shared functional classes in tongue squamous cell carcinoma (TSCC)

Each radial sector represents one gene symbol (n = 280). Fusion transcripts detected in fusion-positive oral SSC were split into their constituent partner genes, so that genes altered by rearrangement and genes altered by methylation occupy the same symbol space and can be compared directly. Sectors are grouped into 13 PANTHER protein classes and separated by gaps. Concentric rings indicate, from the center outward: (1) PANTHER class, color-coded as in the key; (2) presence as a fusion partner in fusion-positive oral SCC, which serves as the genetic comparator; (3) promoter hypermethylation in fusion-negative, mutation-negative TSCC; (4) promoter hypomethylation in the same tumors; (5) annotation as a pseudogene or non-coding transcript; (6) the gene is also named in the systematic-review gene set; and (7) the gene is assigned to more than one PANTHER class, in which case only its first class in cluster order is shown. Pale grey denotes the absence of that feature. Gene symbols are set radially outside the outermost ring. The inset dendrogram orders the 13 classes by Ward D2 clustering (Euclidean distance) of their alteration-mode composition – the proportion of each class's entries contributed by fusion, hypermethylation and hypomethylation, together with class size – so that classes group by how they are altered; membership-based clustering was not informative because the 13 gene sets are almost entirely disjoint. Nineteen genes carry both a fusion partner mark and a hypermethylation mark (*ADH7*, *ATAD2*, *ATRX*, *CXCR5*, *ERBB4*, *HUWE1*, *ITCH*, *P2RX4*, *PTPN1*, *PTPRD*, *PTPRN2*, *PTPRZ1*, *RAD51B*, *RAD51D*, *SRGAP2*, *TFDP1*, *TFDP2*, *TIAM1*, and *UBE3C*), identifying loci disrupted genetically in one tumor group and epigenetically in the other. No gene was both a fusion partner and hypomethylated. Methylation calls derive from Infinium array IDAT files retrieved from the Gene Expression Omnibus and processed.

In silico genome-wide DNA methylation analysis

Dataset selection

In addition to the systematic review, a primary bioinformatic analysis of genome-wide DNA methylation was performed to characterize epigenetically OTSCC from OSCC. Raw intensity data (IDAT) files for Illumina Infinium methylation arrays were retrieved from the Gene Expression Omnibus (GEO). Every contributing series, and the disposition of every array within it, is listed at sample level in Supplementary Table S2. That table records, for each array, the GEO series, the GSM accession, the array platform, the anatomical subsite, the tumor or normal status, the sex and the age where deposited, the sentrix slide and position, and the final analytical group. Series were selected in preference to processed beta matrices so that preprocessing could be harmonized across submissions, and in preference to mixed head and neck cohorts so that the tongue could be resolved as a discrete subsite. The largest contribution was GSE79556 (n = 83; GSM2098204–GSM2098286), a single-institution series of comprehensively annotated OTSCCs profiled on the HumanMethylation450 BeadChip (GPL13534). This was supplemented by 6 oral tongue carcinoma arrays from GSE210443 (GSM6430352, 6430354, 6430356, 6430358, 6430360 and 6430362), profiled on the higher-resolution MethylationEPIC BeadChip (GPL21145) covering approximately 850,000 loci, which extends coverage beyond the 450K design and provides a platform-independent check on the principal cohort.

Samples were eligible where the array was generated from primary, treatment-naive human tissue; where raw IDAT files were available so that preprocessing could be harmonized across series; and where the anatomical subsite was stated unambiguously in the sample metadata. Arrays from cell lines, from recurrent or post-treatment specimens, and from samples whose subsite could not be determined were not used. Within the tongue group, only cases negative for recurrent driver gene fusions and for recurrent somatic driver mutations were analyzed, so that methylation change could be examined in tumors not otherwise accounted for by a genetic driver; fusion-positive OSCC cases were retained separately as the genetic-driver comparator and accessioned in Supplementary Table S2 with their series of origin, their platform and their subsite as deposited. Anatomical group and series of origin are not orthogonal in this design. GSE79556 contributes oral tongue carcinoma only.

Preprocessing

The IDAT files were imported in R with the minfi package using read.metharray.exp, retaining the red and green channel intensities without prior transformation. Since the contributing series span 2 generations of the Infinium platform, arrays were harmonized before any quantitative comparison: HumanMethylation450 (450K) and MethylationEPIC (EPIC) data were combined using combineArrays, which reduces the feature set to the probes present on both designs, and all downstream analysis was restricted to that common set. Background correction and dye-bias equalization were performed with single-sample Noob (ssNoob), which is applied independently to each array and is therefore the appropriate choice when data from different platforms and different submission batches are to be merged; array-dependent methods such as standard Noob or SWAN were avoided for this reason. Methylation was expressed as beta values, defined as the ratio of methylated to total (methylated plus unmethylated plus 100) signal, for description and visualization, and as M values, the base-two logit of beta, for all statistical testing, since M values are approximately homoscedastic across the methylation range whereas beta values are not.

Normalization

Following ssNoob, between-array normalization was performed by functional normalization (preprocessFunnorm) using the first two principal components of the internal control probes as covariates. Functional normalization was preferred to quantile-based methods, because the comparison of interest is between tumor and normal tissue, where global methylation differences are expected to be genuine and quantile normalization would suppress them. Residual Infinium type I / type II design bias was then corrected with beta-mixture quantile normalization (BMIQ). The effect of each normalization step was inspected on density plots of the beta distribution, on multidimensional scaling plots of the 1,000 most variable positions, and on the control probe metrics, both before and after correction.

Probe filtering

Probes were removed, in order, where the detection p-value exceeded 0.01 in any sample; where fewer than 3 beads contributed in more than 5% of samples; where the probe interrogates a non-CpG site; where the probe overlaps a known single nucleotide polymorphism at the target CpG or the single-base extension position at a minor allele frequency of at least 0.05, using dropLociWithSnps; where the probe has been reported as cross-reactive or multi-mapping in the published masking lists for the 450K and EPIC arrays; and where the probe maps to a sex chromosome, since sex was not the exposure of interest and unbalanced sex distribution across groups would otherwise contribute spurious signal. Samples were excluded where the mean detection p-value exceeded 0.01 across all probes, or where more than 1% of probes failed detection.

Batch correction and cell composition

As the samples derive from independent GEO submissions processed in different laboratories, on 2 array generations and across multiple slides, batch effect is the dominant technical risk in this design and was addressed. Sources of unwanted variation were first quantified by singular value decomposition against the available technical and biological covariates, testing the association of each principal component with series of origin, array platform, sentrix slide and sentrix position, alongside analytical group, sex and age. Correction was then applied to M values with ComBat, using series of origin as the batch variable and including the analytical group in the model matrix so that the biological contrast was protected from removal; slide was modelled as a nested second batch term where singular value decomposition indicated residual slide-associated variance. Correction was verified by repeating the decomposition on the adjusted matrix and by re-examining the multidimensional scaling plot. ComBat removes variance attributable to the batch variable, and it cannot recover a biological effect where the biological group and the batch are collinear. In this design the tongue carcinoma group derives almost entirely from one series on one platform, so analytical group and series of origin are close to structurally confounded for the tongue against other subsites contrasts. The tongue against normal mucosa contrast is not affected to the same degree, since normal and tumor arrays are contributed within series. Since solid tumor and mucosal samples are cellular mixtures, epithelial, fibroblast and immune cell fractions were estimated by reference-based deconvolution with the hierarchical EpiDISH procedure and included as covariates in the differential methylation model, so that differences in tumor purity and immune infiltrate are not read as methylation differences.

Quality control

Quality control was applied at 3 points. Before preprocessing, the median methylated and unmethylated intensities of each array were plotted and arrays falling below the conventional threshold were flagged; the 17 Illumina control probe categories, covering bisulphite conversion for both Infinium chemistries, staining, extension, hybridization, target removal, specificity and negative controls, were inspected on the standard qcReport. After preprocessing, genotypic sex was predicted from the median total intensity of the X and Y chromosomes and compared with the sex recorded in the sample metadata, with discordant arrays excluded (Supplementary Table S3). The 65 (450K) or 59 (EPIC) SNP-targeting rs probes were used to check for unrecognized duplicate samples across the contributing series, since overlapping patient material between public submissions would otherwise inflate significance; any pair exceeding a genotype correlation of 0.90 was reduced to a single representative array. After filtering, the beta distribution of every retained array was inspected for bimodality, and arrays with distorted distributions were removed.

Differential methylation and functional mapping

Differentially methylated positions were identified by fitting a linear model to the batch-corrected M values with *limma*, using an analytical group term and adjusting for age, sex and the estimated cell fractions, with empirical Bayes moderation of the variance estimates. Three contrasts were specified. The 1st set tongue carcinoma against normal tongue and oral mucosa. The 2nd set tongue carcinoma against carcinoma of other oral cavity subsites, namely gingivobuccal, buccal, gingival, palatal and floor-of-mouth carcinoma, and this contrast addresses the review question directly. The 3rd set tongue carcinoma against carcinoma of head and neck subsites outside the oral cavity, namely oropharyngeal, laryngeal and sinonasal carcinoma, and it is reported as a secondary comparison. Positions were considered significant at a Benjamini-Hochberg adjusted p-value below 0.05 together with an absolute mean beta difference greater than 0.3, a threshold chosen to exclude changes too small to be biologically meaningful or reliably measurable on array platforms. Differentially methylated regions were called with DMRcate using a Gaussian kernel bandwidth of 1,000 base pairs and a scaling factor of 2, requiring at least three constituent CpGs and a region-level false discovery rate below 0.05. Probes were annotated to genes and to genomic context (TSS1500, TSS200, 5' UTR, first exon, gene body, 3' UTR; island, shore, shelf, open sea) using the manufacturer manifest, and gene-level hypermethylation or hypomethylation was assigned where concordant differentially methylated positions fell within the promoter region, defined as TSS1500, TSS200, the 5' UTR or the first exon. Genes unique to tongue carcinoma after comparator filtering were clustered with PANTHER and mapped onto the same functional themes as the review, and set against the fusion-driven alterations reported in oral cavity carcinoma, so that genetic and epigenetic routes to the disruption of each functional axis could be compared directly.

Software

All analysis was performed in R version 4.3.2 using Bioconductor release 3.18, with *minfi* 1.48.0 for import, preprocessing and quality control; the IlluminaHumanMethylation450kanno.ilmn12.hg19 and IlluminaHumanMethylationEPICanno.ilm10b4.hg19 annotation packages; wateRmelon 2.8.0 for BMIQ; *sva* 3.50.0 for ComBat; EpiDISH 2.18.0 for cell type deconvolution; limma 3.58.1 for differential testing; DMRcate 2.16.0 for region calling; and missMethyl 1.36.0 for probe-number-corrected enrichment testing.

Results

Oral tongue squamous cell carcinoma

Composition and study disposition

Of the 197 records held in the master extraction table, 50 reported molecular findings attributable to the tongue with confidence and were retained for synthesis. The remaining 147 records were assigned to the oral-cavity comparator cluster. These comprised oral-cavity or head and neck cohorts in which tongue tumors were present, but not separately resolvable; carcinomas of non-tongue subsites (gingivobuccal, gingival, buccal pouch, oropharyngeal and tonsillar, laryngeal, esophageal and salivary gland); malignancies of other organs; non-neoplastic studies of the tongue or oral cavity; and narrative reviews without primary data. Records of these kinds were ineligible for the tongue cluster and were retained as a comparator.

Distribution of study designs

Twenty-eight studies used in vitro systems, whether established or patient-derived cell lines, 3D organotypic cultures or extracellular vesicle preparations; 21 included an in vivo component, most often 4NQO carcinogenesis in genetically modified mice, but also subcutaneous and orthotopic xenografts, syngeneic implantation, a rat carcinogenesis model and a zebrafish embryo model; 14 analyzed human tongue tissue in retrospective cohorts or paired tumor-margin designs; and 9 were wholly or partly in silico. Several studies spanned more than one category, and the strongest reports combined human tissue with functional validation. Human cohorts were generally small: the largest tongue-specific series were 93 OSCCs with tongue-stratified analysis,[6] 68 early-stage TSCC primary tumors,[7] 60 TSCC specimens[8] and 50 tumor-margin pairs,[9] while genome-wide methylation profiling of oral tongue carcinoma was performed on only 6 paired tissue-saliva samples before validation against TCGA.[10]

Molecular alterations by functional axis

The p53 axis, cell-cycle control and replicative immortality

Alterations converging on p53 were reported across every study design. A germline family study combined with an Mdm4 knock-in mouse showed that the *MDM4* p.T454M substitution paradoxically increases p53 activity and produces telomere shortening and bone marrow failure, with TSCC and acute myeloid leukemia occurring in affected family members.[11] In murine tongue tumor cell lines derived from 4NQO-treated transgenic animals, a missense *TP53* mutation in the DNA-binding domain co-occurred with miR-211 upregulation in the most metastatic line.[12] Conditional mouse genetics established that p53 loss is permissive as inducible K-rasG12D combined with Trp53 deficiency and PPP6C (PP6) deletion produced tongue carcinoma in situ within approx. 2 weeks, through enhanced ERK-ELK1-FOS and AKT-4EBP1 signaling, DNA double-strand breaks and NF-kappaB activation,[13] while K14-CreERtam-driven K-rasG12D with conditional p53 loss drove oral and tongue carcinoma via mTOR pathway activation.[14]

Downstream cell-cycle effectors were addressed mainly in vitro. In the tongue-derived SCC-9 line, eugenol modulated p21, p27 and cyclin D1 to impose G0/G1 arrest while downregulating *MMP1* and *MMP3*[15]; the parallel silencing of p16 (*CDKN2A*) and p21 by *EZH2* is described with the chromatin evidence. Replicative immortality was addressed in a pan-cancer sequencing survey of 1,230 tumors across 60 types, which placed TSCC among the TERT-high tumor types with promoter mutation frequencies of at least 15%, and showed *TERT* promoter and *ATRX* mutations to be mutually exclusive.[16]

Receptor tyrosine kinase, kinase and phosphatase signaling

Receptor-proximal signaling was interrogated almost entirely in cell line systems. Triple inhibition of FAK, ErbB-family receptors and AXL in 2D and 3D spheroid cultures of head and neck cancer lines including tongue carcinoma downregulated Axl, FAK and N-cadherin while restoring E-cadherin, reversing the mesenchymal phenotype.[17] Focal adhesion kinase (PTK2) showed progressive overexpression across the successive stages of 4NQO-induced rat tongue carcinogenesis, making it one of the few kinases with staged in vivo evidence.[18] In CAL-27-derived clones, de novo integrin alphaVbeta3 expression conferred multidrug resistance through loss of Src phosphorylation at Y418, with ILK and integrin beta5 knockdown used to dissect the mechanism; the Src inhibitors dasatinib and PP2 reproduced.[19]

PI3K-AKT input was reported through 2 distinct upstream mechanisms. Sp1 overexpression in tongue cancer cell lines transcriptionally repressed PTEN through an HDAC1-dependent mechanism, increasing AKT phosphorylation and migratory capacity,[20] while in TSCC tissue and matched cell lines the long non-coding RNA *LINC00152* sponged miR-193b-3p to activate PI3K/AKT signaling.[21] The loss of the secreted MAPK modulator *CHRDL1* in CAL-27 cells and patient tissue activated ERK1/2, p38 and JNK to drive epithelial-mesenchymal transition, and its re-expression suppressed pulmonary colonization in a tail-vein metastasis model.[22] *FOXO4* was downregulated and under negative control by peroxiredoxin-1 in tongue tissue, cell lines and a 4NQO mouse model, with proximity ligation used to demonstrate the interaction.[23] In head and neck cancer lines including tongue lines with mouse xenograft validation, the BH3-mimetic gossypol reduced Bcl-2 and ErbB2, inhibited *ERK1/2* and *AKT*, and activated p38 and JNK.[24]

Developmental signaling: Wnt, Notch, Hedgehog and Hippo

Wnt/beta-catenin was the most frequently implicated developmental pathway. In APCmin/+ and Patched+/– mice studied alongside human tongue tissue, APC mutation activated Wnt/beta-catenin signaling and the normal Shh- and JAG2-mediated negative feedback was lost in established carcinoma.[25] A zebrafish embryo model combined with the tongue carcinoma line SAS showed that loss of LZAP raises nuclear beta-catenin through inhibitory phosphorylation of *GSK3*.[26] In SCC-9 transfectants, the balance between plakoglobin and beta-catenin governed Bcl-2 expression and therefore apoptotic threshold, with concomitant changes in N-cadherin and alpha-catenin.[27] The secreted Wnt antagonist *SFRP1* was downregulated in TSCC on combined GEO and TCGA mining with RT-PCR, Western blot, immunohistochemical and animal validation.[28]

Notch signaling behaved inconsistently between model systems. Stable transfection of the intracellular Notch1 domain into Tca8113 tongue carcinoma cells suppressed growth and induced apoptosis and cell-cycle arrest, with accompanying changes in beta-catenin, p21WAF1/CIP1, p53, Skp2 and Bcl-2, supporting a tumor-suppressive role.[29] In contrast, whole-exome and transcriptome sequencing of 68 early-stage TSCC tumors found *NOTCH1* somatically amplified and overexpressed with an inactivating mutation rate of only 4 per cent, and gamma-secretase inhibition with shRNA knockdown supported an oncogenic role.[7] Hippo pathway disruption produced the most rapid tumor phenotype recorded in any included model: tongue-specific Mob1a/b knockout mice developed carcinoma in situ by two weeks and invasive carcinoma by four weeks through *YAP1* hyperactivation; *YAP1* activation was detectable in human precancerous tongue dysplasia where it correlated with reduced survival, and both siRNA and pharmacological *YAP1* inhibition blocked tumor onset.[30]

Adhesion, epithelial–mesenchymal transition and invasion

Epithelial–mesenchymal transition was consistently reported, but studied almost exclusively in cell lines and paired-line comparisons. HMGA2 overexpression in the SCC-15 line and in TSCC tissue drove EMT with Twist and vimentin upregulation and E-cadherin loss.[31] In paired cell lines established from a primary tongue lesion and its nodal metastasis, vimentin overexpression maintained the mesenchymal phenotype and in vivo tumorigenicity, with reciprocal loss of keratins K13, K14 and K15.[32] The comparison of the high-invasion UM1 and low-invasion UM2 TSCC lines identified downregulation of MTUS1/ATIP3a, which normally restrains ERK1/2 signaling, with downstream Snai2 (SLUG) and vimentin induction.[33] Hypoxia contributed directly: cobalt chloride treatment of OTSCC cells induced *FNDC3B* through HIF-1alpha, and FNDC3B knockdown suppressed the EMT and metastatic phenotype.[34]

RNA sequencing across five increasingly invasive SCC-9-derived lines identified *PIGG* and *SLC8B1* as novel metastasis markers and nominated MYH14, ANGPTL4, PPARD and ENPP1 as interactome-predicted druggable hits, although no compound was tested.[35] Multi-omic profiling of extracellular vesicles from the primary SCC-9 line and its metastatic LN1 derivative identified 7 hub proteins – *ALDH7A1*, *CAD*, *CANT1*, *GOT1*, *MTHFD1*, *PYGB*, and *SARS* – whose low abundance correlated with reduced survival on public database validation.[36] In SCC-25 cells, *TTLL12* overexpression protected tubulin from nitrotyrosine-induced dysfunction and enhanced survival, and nocodazole proved more effective than paclitaxel in this regard.[37]

Copy number architecture

Only one study characterized genome-wide copy number in a purely tongue-derived resource. Microarray profiling of copy number and expression across 18 OTSCC cell lines identified high-level amplifications at 6q12-q14, 9p24, 11p12-p13, 11q13 and 14q24, and nominated *CD109*, *MYO6*, *JAK2*, *CD274*, *TRAF6*, *CD44*, *FADD*, and *CTTN* as amplified candidate targets.[38]

Chromatin regulation and DNA methylation

Polycomb-mediated repression was addressed by3 studies with divergent results, and the direction of effect depended on the model. In tongue cancer tissue, cell lines and xenografts, *EZH2* overexpression silenced p16, p21 and E-cadherin through *H3K27* trimethylation and modulated CD44, and the *EZH2* inhibitor DZNep combined with 5-fluorouracil produced tumor suppression.[39] In direct contrast, tamoxifen-regulated conditional *EZH2* knockout in the tongue epithelium of 4NQO-treated mice increased the incidence of invasive carcinoma and high-grade neoplasia, a context-dependent result carrying an explicit cautionary implication for EZH2-directed therapy.[40] BMI1 overexpression in tongue basal stem cells of 4NQO-treated KrTB transgenic mice increased tumor severity and drove glycolytic reprogramming, with coordinate changes in *SOX9*, *HIF1A*, *MMP9*, *INHBB*, and *MYOF*.[41]

Methylation studies were the most tongue-specific body of evidence in the dataset. Genome-wide profiling of 6 paired oral tongue carcinoma tissue and saliva samples using the MethylationEPIC array, validated against the TCGA oral tongue cohort, identified 25,890 differentially methylated CpG sites and 6 salivary hypermethylated genes – *A2BP1* (*RBFOX1*), *ANK1*, *ALDH1A2*, *GFRA1*, *TTYH1* and *PDE4B* – each achieving diagnostic accuracy of at least 0.800 by area under the curve (AUC).[10]

Methylation-based enhancer and transcription factor binding site analysis of SCC of the oral tongue identified master regulator transcription factors activated in association with invasiveness, metastasis, EMT and poor prognosis, and others downregulated in association with tumor suppression, although individual factors were not enumerated.[42] Within a 93-patient oral SCC cohort analyzed by MS-MLPA, PAX5 promoter methylation was specifically associated with the tongue subsite, while WT1, *MSH6* and GATA5 methylation carried prognostic weight across the cohort.[6]

Metabolic reprogramming, hypoxia and ferroptosis

Metabolic findings clustered around glycolysis and the hypoxic response and were derived predominantly from transgenic mouse models. The BMI1 tongue stem cell model coupled transcriptomic and metabolomic evidence of glycolytic shift with induction of *SLC2A1* (*GLUT1*), *PKM*, *LDHA* and *HK2*.[41] Caveolin-2 upregulation in intratumoral nerves of 4NQO-treated global and cell-type-specific Cav2 knockout mice drove tumor-nerve crosstalk together with metabolic reprogramming, assessed by orthotopic implantation and metabolic profiling.[43] A bioinformatic analysis with immunohistochemical validation in 60 TSCC specimens identified the ferroptosis-related prognostic genes *CA9*, *TNFAIP3* and *NRAS*, enriched for ECM-receptor interaction and IL-17 signaling.[8]

Immune, inflammatory and neural microenvironment

Microenvironmental findings were reported almost entirely from in vivo systems. Loss of the endoribonuclease N4BP1 in 4NQO-treated knockout mice arrested early carcinogenic transformation and prevented tumor formation altogether, against an 86% tumor incidence in wild-type animals, with CCL2 and GM-CSF implicated by single-cell and bulk transcriptomic profiling.[44] Dietary sodium nitrite induced a macrophage-mimicry phenotype switch in TSCC cells through a *CREB1–CD68* axis that promoted lymphatic metastasis, and a CREB1-specific inhibitor reversed the effect.[45] In syngeneic murine tongue carcinoma lines carrying complex p53 alterations, oncogenic miR-134 was associated with low E-cadherin, and the model was used to test cisplatin combined with anti-PD-L1 blockade.[46] Papillomavirus infection with MmuPV1 synergized with 4NQO exposure to produce invasive tongue carcinoma in both immunodeficient and immunocompetent mice, establishing viral oncogene activity as a cofactor.[47]

Non-coding RNA regulation

Non-coding RNA findings were distributed across every tier of evidence and were exclusively microRNA- and long non-coding RNA-mediated; no pseudogene or circular RNA evidence was recovered from tongue-attributable studies. The strongest microRNA evidence came from in vivo work. In K14-EGFP-miR-211 transgenic mice exposed to 4NQO, miR-211 suppressed TCF12 and thereby induced *FAM213A*, an axis corroborated against TCGA.[48] The same microRNA reappeared alongside miR-196b in murine tongue tumor cell lines derived from 4NQO-treated animals, where miR-211 was highest in the most metastatic line and co-occurred with a DNA-binding-domain TP53 missense mutation, and where cisplatin treatment reduced miR-196b expression in xenografts.[12] In syngeneic murine tongue carcinoma, miR-134 behaved as an oncogenic microRNA associated with low E-cadherin expression.[46]

Two microRNA axes were linked directly to treatment response. In a multicenter TSCC cohort with in vitro and in vivo validation, a BRCA1–miR-593-5p–MFF axis regulated mitochondrial fission and cisplatin sensitivity, and was significantly associated with both cisplatin response and survival.[49] In a 3D organotypic invasion model using the highly invasive HSC-3 line and SCC-15, combined with laser-capture microdissection, mass spectrometry proteomics and miRNA microarray, miR-498 and miR-940 acted through focal adhesion and ECM-receptor interaction pathways alongside 67 differentially expressed proteins.[50] Moreover, miR-124-3 and miR-769 target-gene networks converged ECM-receptor interaction, focal adhesion, protein digestion/absorption, and AGE-RAGE signaling.[51]

Patient-tissue profiling was limited to a single series. Comparison of 50 tongue tumors against paired marginal tissue found miR-184 and miR-378 upregulated and miR-497 and miR-506 downregulated, with miR-103 additionally differentially expressed.[9] On the long non-coding RNA side, LINC00152 sponged miR-193b-3p in TSCC tissue and matched cell lines to activate PI3K/AKT signaling,[21] and integrated competing-endogenous-RNA network analysis of TCGA and GEO TSCC data identified 15 differentially expressed mRNAs, 1 microRNA and 2 long non-coding RNAs of prognostic relevance, resolving TSCC into basal and differentiated molecular subtypes, the differentiated subtype being associated with lower alcohol exposure and better overall survival.[52]

Mixed OSCC cohorts have described a TP53-linked set comprising miR-34a, miR-99a, miR-143, miR-373, miR-380-5p and miR-504, with miR-99a acting through AKT/mTOR[53]; a diagnostic panel of miR-21, miR-125b-2*, miR-138, miR-155, miR-184 and miR-205[54]; downregulation of let-7a, let-7d, let-7f and miR-16 with variable upregulation of miR-29b, miR-142-3p, miR-144, miR-203, miR-223 and miR-1275[55]; and a *CDK2AP1* (DOC1)-directed set of miR-21-5p, miR-23b-3p, miR-26b-5p, miR-93-5p and miR-155-5p.[56] The only circular RNA evidence anywhere in the extraction table is likewise from the comparator cluster, where circRNA-102450 sponges miR-1178 in OSCC.[57] Only miR-184 is common to the tongue-specific and comparator lists, which indicates that the microRNA literature has not been resolved by subsite. One microRNA

acts on many transcripts, and one transcript is acted on by many microRNAs, so a measured effect on a named pathway does not establish selective control of that pathway through the microRNA concerned.

Subsite- and age-stratified expression analyses

Two secondary analyses addressed the tongue explicitly as a distinct subsite. A meta-analysis of 8 public microarray datasets with TCGA survival validation identified a tongue-specific gene set comprising *MTFR1*, *C8ORF33*, *OTUD6B*, *NUDCD1*, *PRKC1*, *ANO1*, and *PIK3CA*, distinguishing it from the HPV-associated set of *RPP25*, *NUDCD2* and *NOVA1*.[58] Multi-omic analysis of 127 TCGA cases comparing younger with older patients and tongue with other oral sites found distinct pathway activation by age and subsite across *Rap1*, *PI3K-Akt*, *MAPK*, *cGMP-PKG*, *JAK-STAT*, and *PD-L1/PD-1* signaling, without nominating individual driver genes.[59] A separate paired-tissue study of 35 tongue and floor-of-mouth carcinomas profiled the metallothionein family, finding *MT1A*, *MT1X*, *MT3*, and *MT4* downregulated and *MT1F* upregulated; *MT1G* downregulation carried the worst prognosis, *MT1X* upregulation was restricted to non-metastatic cases and *MT3* upregulation was linked to nodal metastasis.[60]

Translation, biomarkers and reporting quality

Druggability and pharmacological validation

Fourteen of the 50 retained studies tested a compound experimentally, and all did so in cell lines, xenografts or genetically modified mice. Agents with a defined molecular target included the EZH2 inhibitor DZNep with 5-fluorouracil,[39] gamma-secretase inhibition for NOTCH1,[7] siRNA and pharmacological YAP1 inhibition,[30] rapamycin against mTOR in the K-ras/p53 mouse,[14] a CREB1 inhibitor,[45] the EGFR tyrosine kinase inhibitor EKB-569 (pelitinib) used to suppress radiation-induced NF-kappaB activation across 74 pathway molecules in SCC-4 and SCC-9 cells,[61] the combination of the FAK inhibitor Y15 with afatinib and an Axl inhibitor,[17] and the BH3-mimetic gossypol.[24] The natural compound eugenol was tested in SCC-9 with a normal keratinocyte comparator.[15] Chemotherapy and immunotherapy were tested as modulated endpoints. Cisplatin sensitivity in the BRCA1-miR-593-5p-MFF axis,[49] cisplatin with anti-PD-L1 in the syngeneic murine model,[46] and nocodazole against paclitaxel in the TTLL12 context.[37] Two pharmacological results ran counter to expectation: Src inhibition with dasatinib or PP2 reproduced, not reversed integrin alphaVbeta3-mediated multidrug resistance in CAL-27 clones,[19] and EZH2 knockout increased.[40] The remaining 36 studies proposed therapeutic targets without pharmacological testing.

Biomarker discovery

A proliferation- and mitosis-linked panel comprising *CDK1*, *CCNA2*, *TOP2A*, *SENP1* and *MAD2L1* has been proposed as a candidate biomarker set shared between OTSCC and esophageal SCC.[62] Four of the 5 are canonical cell-cycle and mitotic effectors – cyclin-dependent kinase 1, cyclin A2, topoisomerase II alpha, and the mitotic checkpoint component *MAD2L1*. Yet, none of these markers has been validated as a surrogate endpoint. Across the retained evidence, no proposed biomarker – the six-gene salivary hypermethylation panel,[10] the seven-gene tongue-specific expression signature,[58] the 7 extracellular vesicle hub proteins,[36] or the ferroptosis-related trio *CA9, TNFAIP3* and *NRAS*[8] – has been shown to predict a clinical endpoint prospectively, to change in response to therapy in a manner tracking outcome, or to have been tested in an independent validation cohort of adequate size. The single exception in terms of clinical correlation, though not of surrogacy, is the BRCA1–miR-593-5p–MFF axis, which was associated retrospectively with both cisplatin response and survival in a multicenter TSCC cohort.[49] The distinction matters for trial design. Bioinformatic studies nominated the *CDK1*, *CCNA2*, *TOP2A*, *SENP1*, and *MAD2L1* panel as candidate biomarkers. No study has evaluated the panel as a surrogate endpoint, and no evidence of surrogacy exists for it.

Reporting of HPV, p53 and p16 status

Ascertainment of viral and surrogate marker status was poor across the tongue-restricted evidence base. The HPV status was not reported in the large majority of retained studies, and where viral involvement was addressed directly it was through the murine surrogate MmuPV1.[47] The p53 status was formally characterized in only a minority, principally the germline MDM4 family study,[11] the murine tongue line series[12] and the conditional Trp53 models.[13,14] p16 was more often measured as a downstream target of epigenetic silencing than as an HPV surrogate.[39] This pattern reflects the predominance of laboratory over clinical designs in tongue-specific work and precludes any synthesis stratified by viral status at this subsite.

In silico genome-wide DNA methylation analysis

Supplementary Table S1 gives, for each contrast, the number of samples retained after quality control, the number of probes retained after filtering, the number of significant differentially methylated positions, the number of significant differentially methylated regions, the split of those calls into hypermethylated and hypomethylated, the range of mean beta differences, and the range of Benjamini-Hochberg adjusted *p*-values.

Gene-level output was restricted to promoter-region calls was then intersected with the fusion-partner gene set.

Nineteen gene symbols carry both a fusion-partner assignment and a promoter hypermethylation call in tongue carcinoma: *ADH7*; *ATAD2*; *ATRX*; *CXCR5*; *ERBB4*; *HUWE1*; *ITCH*; *P2RX4*; *PTPN1*; *PTPRD*; *PTPRN2*; *PTPRZ1*; *RAD51B*; *RAD51D*; *SRGAP2*; *TFDP1*; *TFDP2*; *TIAM1*; and *UBE3C*. No gene symbol carries both a fusion-partner assignment and a promoter hypomethylation call.

Discussion

Fusion frequency at this subsite has not been established. No denominator by sample number is available for the tongue or for the comparator subsites. The wider genetic literature at this subsite is correspondingly sparse. Across 50 tongue-attributable studies, not one recurrent somatic driver was reported consistently, and the only genome-wide copy number resource specific to the tongue was a panel of 18 cell lines.[38] An absence of this kind is not itself evidence of an epigenetic mechanism, but it makes the hypothesis worth testing.

Two earlier studies addressed the molecular characteristics of oral tongue carcinoma specifically, and the position of the present work relative to them should be stated explicitly. Krishnan et al. profiled 52 oral tongue tumors with matched controls on the 450K array and derived a minimal signature of 16 differentially methylated regions, validated against the head and neck cohort of TCGA. Their comparator was matched normal tissue, and their question was tumor against normal within one subsite. Wang et al. integrated gene expression profiles across multiple oral tongue cohorts and reported expression characteristics attributed to the subsite. Their evidence is transcriptomic and carries no methylation component. Neither study set oral tongue carcinoma against carcinoma of other oral cavity subsites profiled on the same platform. Neither placed methylation output alongside the gene set disrupted by rearrangement in fusion-positive oral cancer.

Transcription regulations compound the landscape

The evidence should be read in order of how directly each finding functions as a comparison. The most direct is PAX5 promoter methylation, which was associated with the tongue subsite within a single 93-patient oral SCC cohort analyzed on one platform[6]: the tongue and non-tongue cases were drawn from the same series and assayed identically, so the subsite contrast is internal to the study. Two further findings establish a tongue-specific signature without benchmarking it against other non-tongue subsites in the same material. The seven-gene expression set – *MTFR1*, *C8ORF33*, *OTUD6B*, *NUDCD1*, *PRKC1*, *ANO1*, and *PIK3CA* – was distinguished from an HPV-associated comparator set,[58] and the six-gene salivary hypermethylation panel – *A2BP1*, *ANK1*, *ALDH1A2*, *GFRA1*, *TTYH1*, and *PDE4B* – was validated against the TCGA oral tongue cohort, that is, against more tongue tumors.[10] Both are informative about the tongue; neither settles whether the signature is peculiar to it. The OTSCC-specific amplifications at 6q12-q14, 9p24, 11p12-p13, 11q13 and 14q24 add structural characterization of the same type.[38] Only 50 of the 197 extracted records resolved the tongue as a separate subsite, and of those, the number that placed the tongue alongside another oral-cavity subsite in the same experiment is smaller still.

The transcriptional regulators recurring across the retained evidence are *TP53*, *FOXO4*, *HIF1A*, *SOX9*, *CREB1*, *TCF12*, *Twist*, *Snai2*, *PAX5*, *WT1*, and *GATA5*, together with the unnamed master regulators identified by methylation-based enhancer analysis.[42] They appear in the p53 axis, in EMT, in the hypoxic and metabolic response, in the immune microenvironment and in the methylation findings alike. Heterogeneity in TSCC operates at the level of the individual factor, while convergence operates at the level of the output: many different transcriptional inputs, a few shared functional endpoints. *CREB1* driving macrophage mimicry,[45] *TCF12* suppressed by miR-211,[48] *SOX9* and *HIF1A* induced downstream of BMI1[41] and Snai2 induced on loss of *MTUS1*[33] are unrelated events that nonetheless terminate in proliferation, invasion or metabolic shift. The p53 pathway remained the most frequently implicated axis overall, and TERT promoter mutation recurred at a defined frequency of at least 15% in a pan-cancer survey that included TSCC among the TERT-high types.[16] Yet *TP53* status itself was characterized in a minority of retained studies, and conditional mouse genetics indicates that p53 loss is permissive.[13,14]

NOTCH1 provides the clearest instance of genuine biological heterogeneity. Forced expression of the intracellular Notch1 domain suppressed growth in Tca8113 cells,[29] while in 68 early-stage TSCC tumors *NOTCH1* was amplified and overexpressed with an inactivating mutation rate of only 4%, and both gamma-secretase inhibition and shRNA knockdown supported an oncogenic role.[7] These are not contradictory measurements of the same quantity: one is a gain-of-function experiment in an immortalized line, the other an observation in primary human tumors with loss-of-function validation. The direction of *NOTCH1* effect depends on the context in which it is assayed, and that context-dependence is a property of the biology, not an artefact of the literature. The same lesson attaches to EZH2, where overexpression in xenografts and conditional knockout in mice produced opposite phenotypes.[39,40]

Whether any of these is modified by viral status cannot be determined. Human papillomavirus was not reported in most retained studies, p16 was more often measured as a target of epigenetic silencing than as a viral surrogate, and the only direct interrogation of viral oncogene activity at this subsite used a murine papillomavirus, where

infection acted as a cofactor with chemical carcinogen exposure.[47] Harmonized HPV, p53 and p16 ascertainment is the single most straightforward improvement available to future tongue-specific studies.

Non-coding RNA and the missing arms of competing-endogenous-RNA regulation

Non-coding RNA regulation feeds into the same axes implicated by protein-coding evidence. *LINC00152* sponging miR-193b-3p activates PI3K/AKT[21]; miR-211 acts through TCF12 on a transcriptional axis[48]; miR-498 and miR-940 act through focal adhesion and ECM-receptor interaction[50]; miR-134 tracks E-cadherin loss[46]; and the BRCA1–miR-593-5p–MFF axis acts on mitochondrial fission and cisplatin sensitivity.[49] This last is the only microRNA finding in the tongue-restricted evidence with a demonstrated clinical correlate, and it is the natural candidate for prospective evaluation. That candidacy is candidacy for prospective evaluation as a correlate, and not for microRNA-directed therapy. Target multiplicity is the obstacle. A single microRNA represses many transcripts simultaneously, and any therapeutic manipulation of it acts on the whole target set. A single transcript is in turn repressed by several microRNAs, so removal of one leaves the others in place. Consequences at the remaining targets are unmeasured in every microRNA study retained here, and no microRNA-directed agent has been tested in TSCC in any retained record. The biological role of these microRNAs and their therapeutic potential are accordingly treated as separate claims throughout, and the second does not follow from the first.

Two gaps deserve comment, because they bear directly on the second research question. First, patient-tissue microRNA profiling in the tongue rests on a single 50-pair series,[9] whereas the oral-cavity comparator literature contains several larger microRNA panels, of which only miR-184 overlaps with the tongue-specific list. The reasonable inference is that the microRNA literature has not been resolved by subsite, not that the tongue lacks microRNA involvement. Second, pseudogenes and circular RNAs were absent from the tongue-attributable evidence entirely, the sole circular RNA finding anywhere in the extraction table coming from the comparator cluster.[57]

Translational and druggability implications

The translational position is unfavorable. Only 14 of the 50 retained studies tested a compound at all. The remaining 36 nominated targets without testing them. Against that background, the two counter-expectation results carry disproportionate weight as cautionary evidence for trial design. Src inhibition with dasatinib or PP2 reproduced and conditional *EZH2* knockout increased the incidence of invasive carcinoma.[40] Both involve agent classes in active clinical development, and both indicate that the direction of pharmacological effect at this subsite cannot be assumed from target biology established elsewhere. The methylation panels occupy a different translational niche: salivary detection with AUC of at least 0.800 points toward non-invasive diagnosis and surveillance.[10] However, no marker at this subsite has been validated as a surrogate endpoint, and prognostic association should not be reported as though it were.

Limitations

As an in silico study, tongue arrays derive predominantly from a single GEO series on a single platform, so analytical group and series of origin are close to collinear for the subsite contrasts. ComBat protects the biological term specified in the model matrix, and it cannot separate a biological effect from a technical one where the two are collinear. Results from the subsite contrasts are therefore reported as exploratory. A definitive test requires tongue and non-tongue oral carcinomas profiled within one series, in one laboratory, on one array generation, with subsite recorded in the deposited metadata. Further, the comparator cluster is heterogeneous by construction. It contains oral cavity and head and neck cohorts without subsite resolution, carcinomas of non-tongue subsites, and non-neoplastic material. Comparisons drawn against it are comparisons against a literature, not against a matched control series, and they carry the reporting practices of that literature with them. Design category, internal comparator and orthogonal validation were recorded instead, and these 3 items carry the whole weight of methodological appraisal here.

Moreover, array-based methylation measurement covers a fixed probe set and returns no information outside it, so promoter regions absent from the common 450K and EPIC feature set are unassessed. Tongue-attributable microRNA evidence from patient tissue rests on one series of 50 tumor-margin pairs, so subsite-resolved microRNA conclusions remain provisional. The HPV, p53 and p16 status were unreported in the majority of retained studies, which precludes any stratification of the synthesis by viral status.

Conclusions

Relative to SCC arising elsewhere in the oral cavity, OTSCC lacks recurrent somatic driver, and recurrent fusion events. Wherever studies resolved the tongue as a separate subsite, they returned tongue-specific methylation and expression markers, and methylation is accordingly the most promising axis on which to test divergence of TSCC from SCC at other oral-cavity subsites. The evidence assembled here does not establish that divergence. Within TSCC, heterogeneity arises less from variation at the level of individual genes than from multiple distinct

molecular routes converging on a small number of shared functional endpoints. Long non-coding RNAs contribute through competing-endogenous-RNA networks that feed into the same PI3K–AKT, p53 and EMT axes implicated by protein-coding evidence. Pseudogenes and circular RNAs were absent from the reviewed literature. Transcription factor disruption funnels into cell-cycle control, hypoxic-metabolic reprogramming and EMT.

On the present evidence, OTSCC is best described as a subsite carrying a candidate epigenetic signature. Designation as a distinct entity should follow a comparison of subsites profiled within one series, in one laboratory, on one array generation. That comparison has not yet been reported, and the present work does not supply it.

Ethics approval and consent to participate

Not applicable.

Data availability

The datasets supporting the findings of the current study, including all supplementary materials, are available from the corresponding author on reasonable request.

Consent for publication

Not applicable.

Use of AI and AI-assisted technologies

Not applicable.

ORCID iDs

Bacem Othman https://orcid.org/0009-0006-5567-6771
Omid Moztarzadeh https://orcid.org/0000-0002-4768-2382
Lukas Hauer https://orcid.org/0000-0001-6639-2690

References

1. Grajewski L, Greiner A, Wurschi G, et al. Challenges in recurrent head and neck squamous cell cancer treatment: Systematic review and meta-analysis comparing efficacy and toxicity between post-operative and definitive IMRT-based reirradiation. *Clin Transl Radiat Oncol*. 2025;56:101061. doi:10.1016/j.ctro.2025.101061
2. Silva JP, Pinto B, Monteiro L, Silva PM, Bousbaa H. Combination therapy as a promising way to fight oral cancer. *Pharmaceutics*. 2023;15(6):1653. doi:10.3390/pharmaceutics15061653
3. Astsaturov I, Cohen RB, Harari PM. EGFR-targeting monoclonal antibodies in head and neck cancer. *Curr Cancer Drug Targets*. 2006;6(8):691–710. doi:10.2174/156800906779010191
4. Teng Z, Teng L, Xie J. IAPs in cancers: Molecular mechanisms, clinical prognostic value, and translational therapeutic potential. *J Transl Med*. 2026;24(1):143. doi:10.1186/s12967-025-07640-7
5. Kong S, Zhang J, Wang L, et al. Mechanisms of low MHC I expression and strategies for targeting MHC I with small molecules in cancer immunotherapy. *Cancer Lett*. 2025;611:217432. doi:10.1016/j.canlet.2024.217432
6. Ribeiro IP, Caramelo F, Marques F, et al. WT1, MSH6, GATA5 and PAX5 as epigenetic oral squamous cell carcinoma biomarkers – a short report. *Cell Oncol (Dordr)*. 2016;39(6):573–582. doi:10.1007/s13402-016-0293-5
7. Upadhyay P, Nair S, Kaur E, et al. Notch pathway activation is essential for maintenance of stem-like cells in early tongue cancer. *Oncotarget*. 2016;7(31):50437–50449. doi:10.18632/oncotarget.10419
8. Zhu H, Tao Y, Huang Q, et al. Identification of ferroptosis-related genes as potential biomarkers of tongue squamous cell carcinoma using an integrated bioinformatics approach. *FEBS Open Bio*. 2022;12(2):412–429. doi:10.1002/2211-5463.13348
9. Ghffari M, Asadi M, Shanaehbandi D, et al. Aberrant expression of miR-103, miR-184, miR-378, miR-497 and miR-506 in tumor tissue from patients with oral squamous cell carcinoma regulates the clinical picture of the patients. *Asian Pacific J Cancer Prev*. 2020;21(5):1311–1315. doi:10.31557/APJCP.2020.21.5.1311
10. Rapado-González Ó, Costa-Fraga N, Bao-Caamano A, et al. Genome-wide DNA methylation profiling in tongue squamous cell carcinoma. *Oral Dis*. 2024;30(2):259–271. doi:10.1111/odi.14444
11. Toufektchan E, Lejour V, Durand R, et al. Germline mutation of *MDM4*, a major p53 regulator, in a familial syndrome of defective telomere maintenance. *Sci Adv*. 2020;6(15):eaay3511. doi:10.1126/sciadv.aay3511
12. Chen YF, Liu CJ, Lin LH, et al. Establishing of mouse oral carcinoma cell lines derived from transgenic mice and their use as syngeneic tumorigenesis models. *BMC Cancer*. 2019;19(1):281. doi:10.1186/s12885-019-5486-7
13. Kishimoto K, Kanazawa K, Nomura M, et al. Ppp6c deficiency accelerates K-ras^{G12D}-induced tongue carcinogenesis. *Cancer Med*. 2021;10(13):4451–4464. doi:10.1002/cam4.3962
14. Raimondi AR, Molinolo A, Gutkind JS. Rapamycin prevents early onset of tumorigenesis in an oral-specific K-ras and p53 two-hit carcinogenesis model. *Cancer Res*. 2009;69(10):4159–4166. doi:10.1158/0008-5472.CAN-08-4645
15. Issa H, Loubaki L, Al Amri A, et al. Eugenol as a potential adjuvant therapy for gingival squamous cell carcinoma. *Sci Rep*. 2024;14(1):10958. doi:10.1038/s41598-024-60754-8
16. Killela PJ, Reitman ZJ, Jiao Y, et al. TERT promoter mutations occur frequently in gliomas and a subset of tumors derived from cells with low rates of self-renewal. *Proc Natl Acad Sci U S A*. 2013;110(15):6021–6026. doi:10.1073/pnas.1303607110
17. Lucarini V, Angiolini V, Nardozi D, et al. In vitro synergistic effect of AXL, FAK and ErbB receptors inhibitors for head and neck cancer. *Biol Direct*. 2025;20(1):77. doi:10.1186/s13062-025-00668-1
18. Xia J, Lv N, Hong Y, et al. Increased expression of focal adhesion kinase correlates with cellular proliferation and apoptosis during 4-nitroquinoline-1-oxide-induced rat tongue carcinogenesis. *J Oral Pathol Med*. 2009;38(6):524–529. doi:10.1111/j.1600-0714.2008.00728.x
19. Stojanović N, Brozovic A, Majhen D, et al. Integrin αvβ3 expression in tongue squamous carcinoma cells Cal27 confers anticancer drug resistance through loss of pSrc(Y418). *Biochim Biophys Acta*. 2016;1863(8):1969–1978. doi:10.1016/j.bbamcr.2016.04.019
20. Kou XX, Hao T, Meng Z, Zhou YH, Gan YH. Acetylated sp1 inhibits PTEN expression through binding to PTEN core promoter and recruitment of HDAC1 and promotes cancer cell migration and invasion. *Carcinogenesis*. 2013;34(1):58–67. doi:10.1093/carcin/bgs336
21. Li X, Rui B, Cao Y, Gong X, Li H. Long non-coding RNA LINC00152 acts as a sponge of miRNA-193b-3p to promote tongue squamous cell carcinoma progression. *Oncol Lett*. 2020;19(3):2035–2042. doi:10.3892/ol.2020.11293
22. Wu Q, Zheng Z, Zhang J, et al. Chordin-like 1 regulates epithelial-to-mesenchymal transition and metastasis via the MAPK signaling pathway in oral squamous cell carcinoma. *Front Oncol*. 2022;12:862751. doi:10.3389/fonc.2022.862751
23. Lu Y, Shen Y, Li L, et al. Clinicopathological significance of FOXO4 expression and correlation with Prx1 in head and neck squamous cell carcinoma. *Anal Cell Pathol (Amst)*. 2021;2021:5510753. doi:10.1155/2021/5510753
24. Benvenuto M, Mattera R, Masuelli L, et al. (±)-Gossypol induces apoptosis and autophagy in head and neck carcinoma cell lines and inhibits the growth of transplanted salivary gland cancer cells in BALB/c mice. *Int J Food Sci Nutr*. 2017;68(3):298–312. doi:10.1080/09637486.2016.1236077
25. Schneider FT, Schänzer A, Czupalla CJ, et al. Sonic hedgehog acts as a negative regulator of {beta}-catenin signaling in the adult tongue epithelium. *Am J Pathol*. 2010;177(1):404–414. doi:10.2353/ajpath.2010.091079

26. Lin KY, Kao SH, Lai CM, et al. Tumor suppressor Lzap suppresses Wnt/β-catenin signaling to promote zebrafish embryonic ventral cell fates via the suppression of inhibitory phosphorylation of glycogen synthase kinase 3. *J Biol Chem*. 2015;290(50):29808–29819. doi:10.1074/jbc.M115.669309
27. Li L, Chapman K, Hu X, Wong A, Pasdar M. Modulation of the oncogenic potential of β-catenin by the subcellular distribution of plakoglobin. *Mol Carcinog*. 2007;46(10):824–838. doi:10.1002/mc.20310
28. Yu M, Wu G, Chen Y, Wang H, Gao Y, Wang A. Bioinformatic screening and experimental analysis identify SFRP1 as a prognostic biomarker for tongue squamous cell carcinomas. *Arch Oral Biol*. 2020:104587;110. doi:10.1016/j.archoralbio.2019.104587
29. Duan L, Yao J, Wu X, Fan M. Growth suppression induced by Notch1 activation involves Wnt-β-catenin down-regulation in human tongue carcinoma cells. *Biol Cell*. 2006;98(8):479–490. doi:10.1042/BC20060020
30. Omori H, Nishio M, Masuda M, et al. YAP1 is a potent driver of the onset and progression of oral squamous cell carcinoma. *Sci Adv*. 2020;6(12):eeay3324. doi:10.1126/sciadv.aay3324
31. Zhang H, Tang Z, Deng C, et al. HMGA2 is associated with the aggressiveness of tongue squamous cell carcinoma. *Oral Dis*. 2017;23(2):255–264. doi:10.1111/odi.12608
32. Paccione RJ, Miyazaki H, Patel V, et al. Keratin down-regulation in vimentin-positive cancer cells is reversible by vimentin RNA interference, which inhibits growth and motility. *Mol Cancer Ther*. 2008;7(9):2894–2903. doi:10.1158/1535-7163.MCT-08-0450
33. Zhao T, He Q, Liu Z, Ding X, Zhou X, Wang A. Angiotensin II type 2 receptor-interacting protein 3a suppresses proliferation, migration and invasion in tongue squamous cell carcinoma via the extracellular signal-regulated kinase–Snai2 pathway. *Oncol Lett*. 2016;11(1):340-344. doi:10.3892/ol.2015.3898
34. Zhong Z, Zhang H, Hong M, et al. FNDC3B promotes epithelial–mesenchymal transition in tongue squamous cell carcinoma cells in a hypoxic microenvironment. *Oncol Rep*. 2018;39(4):1853–1859. doi:10.3892/or.2018.6231
35. Pérez-Valencia JA, Prosdocimi F, Cesari IM, et al. Angiogenesis and evading immune destruction are the main related transcriptomic characteristics to the invasive process of oral tongue cancer. *Sci Rep*. 2018;8(1):2007. doi:10.1038/s41598-017-19010-5
36. Busso-Lopes AF, Carnielli CM, Winck FV, et al. A reductionist approach using primary and metastatic cell-derived extracellular vesicles reveals hub proteins associated with oral cancer prognosis. *Mol Cell Proteomics*. 2021;20:100118. doi:10.1016/j.mcpro.2021.100118
37. Xue L, Zeng Y, Fang C, Cheng W, Li Y. Effect of TTLL12 on tubulin tyrosine nitration as a novel target for screening anticancer drugs in vitro. *Oncol Lett*. 2020;20(6):340. doi:10.3892/ol.2020.12203
38. Järvinen AK, Autio R, Kilpinen S, et al. High-resolution copy number and gene expression microarray analyses of head and neck squamous cell carcinoma cell lines of tongue and larynx. *Genes Chromosomes Cancer*. 2008;47(6):500–509. doi:10.1002/gcc.20551
39. Li Z, Wang Y, Qiu J, et al. The polycomb group protein EZH2 is a novel therapeutic target in tongue cancer. *Oncotarget*. 2013;4(12):2532–2549. doi:10.18632/oncotarget.1503
40. Baquero J, Tang XH, Scognamiglio T, Gudas LJ. EZH2 knockout in oral cavity basal epithelia causes more invasive squamous cell carcinomas. *Carcinogenesis*. 2021;42(12):1485–1495. doi:10.1093/carcin/bgab091
41. Baquero J, Tang XH, Galke D, et al. Exogenous BMI1 expression aggravates oral squamous cell carcinomas in tongue epithelia. *Neoplasia*. 2025;62:101146. doi:10.1016/j.neo.2025.101146
42. Okano LM, Maciel da Fonseca LM, Erthal ID, Malta TM. Epigenomic integrative analysis pinpoint master regulator transcription factors associated with tumorigenesis in squamous cell carcinoma of oral tongue. *Genet Mol Biol*. 2023;46(2):e20220358. doi:10.1590/1678-4685-GMB-2022-0358
43. Zhang Z, Wang C, Sun Z, et al. CAV2-expressing nerves induce metabolic switch toward mitochondrial oxidative phosphorylation to promote cancer stemness. *Nat Commun*. 2026;17(1):203. doi:10.1038/s41467-025-66914-2
44. Song Y, Sun R, Ji J, et al. N4BP1 is essential for the development of oral cancer via controlling both cancer cells and immune microenvironment. *Cell Death Dis*. 2026;17(1):23. doi:10.1038/s41419-025-08229-0
45. Lu X, Lin W, Zheng J, et al. Sodium nitrite orchestrates macrophage mimicry of tongue squamous carcinoma cells to drive lymphatic metastasis. *Br J Cancer*. 2025;132(4):340–353. doi:10.1038/s41416-024-02923-0
46. Chen YF, Chang KW, Yang IT, Tu HF, Lin SC. Establishment of syngeneic murine model for oral cancer therapy. *Oral Oncol*. 2019;95:194–201. doi:10.1016/j.oraloncology.2019.06.026
47. Wei T, Buehler D, Ward-Shaw E, Lambert PF. An infection-based murine model for papillomavirus-associated head and neck cancer. *mBio*. 2020;11(3):e00908–e00920. doi:10.1128/mBio.00908-20
48. Chen YF, Yang CC, Kao SY, Liu CJ, Lin SC, Chang KW. MicroRNA-211 enhances the oncogenicity of carcinogen-induced oral carcinoma by repressing TCF12 and increasing antioxidant activity. *Cancer Res*. 2016;76(16):4872–4886. doi:10.1158/0008-5472.CAN-15-1664
49. Fan S, Liu B, Sun L, et al. Mitochondrial fission determines cisplatin sensitivity in tongue squamous cell carcinoma through the BRCA1–miR-593-5p–MFF axis. *Oncotarget*. 2015;6(17):14885–14904. doi:10.18632/oncotarget.3659
50. Korvala J, Jee K, Porkola E, et al. MicroRNA and protein profiles in invasive versus non-invasive oral tongue squamous cell carcinoma cells in vitro. *Exp Cell Res*. 2017;350(1):9–18. doi:10.1016/j.yexcr.2016.10.015
51. Avram EG, Moatar IA, Miok V, et al. Gene network analysis of the transcriptome impact of methylated microRNAs on oral squamous cell carcinoma. *Adv Clin Exp Med*. 2022;31(11):1231–1242. doi:10.17219/acem/151911
52. Li Z, Jiang C, Yuan Y. TCGA based integrated genomic analyses of ceRNA network and novel subtypes revealing potential biomarkers for the prognosis and target therapy of tongue squamous cell carcinoma. *PLoS One*. 2019;14(5):e0216834. doi:10.1371/journal.pone.0216834
53. Manikandan M, Magendhra Rao AK, Arunkumar G, Rajkumar KS, Rajaraman R, Munirajan AK. Down regulation of miR-34a and miR-143 may indirectly inhibit p53 in oral squamous cell carcinoma: A pilot study. *Asian Pacific J Cancer Prev*. 2015;16(17):7619–7625. doi:10.7314/apjcp.2015.16.17.7619
54. Manikandan M, Magendhra Rao AK, Rajkumar KS, Rajaraman R, Munirajan AK. Altered levels of miR-21, miR-125b-2*, miR-138, miR-155, miR-184, and miR-205 in oral squamous cell carcinoma and association with clinicopathological characteristics. *J Oral Pathol Med*. 2015;44(10):792–800. doi:10.1111/jop.12300
55. Manikandan M, Magendhra Rao AK, Arunkumar G, et al. Oral squamous cell carcinoma: microRNA expression profiling and integrative analyses for elucidation of tumourigenesis mechanism. *Mol Cancer*. 2016;15:28. doi:10.1186/s12943-016-0512-8
56. Stabile R, Cabezas MR, Verhagen MP, et al. The deleted in oral cancer (DOC1 aka CDK2AP1) tumor suppressor gene is downregulated in oral squamous cell carcinoma by multiple microRNAs. *Cell Death Dis*. 2023;14(5):337. doi:10.1038/s41419-023-05857-2
57. Ando T, Kasamatsu A, Kawasaki K, et al. Tumor suppressive circular RNA-102450: Development of a novel diagnostic procedure for lymph node metastasis from oral cancer. *Cancers (Basel)*. 2021;13(22):5708. doi:10.3390/cancers13225708
58. Reddy RB, Khora SS, Suresh A. Molecular prognosticators in clinically and pathologically distinct cohorts of head and neck squamous cell carcinoma – a meta-analysis approach. *PLoS One*. 2019;14(7):e0218989. doi:10.1371/journal.pone.0218989
59. Prostakishina EA, Dampilova TD, Kononova LA, et al. Molecular landscape of oral cancer in young adults. *Russ J Genet*. 2023;59(11):1190–1201. doi:10.1134/S1022795423110108
60. Brazão-Silva MT, Rodrigues MF, Eisenberg AL, et al. Metallothionein gene expression is altered in oral cancer and may predict metastasis and patient outcomes. *Histopathology*. 2015;67(3):358–367. doi:10.1111/his.12660
61. Aravindan N, Thomas Jr. CR, Aravindan S, Mohan AS, Veeraraghavan J, Natarajan M. Irreversible EGFR inhibitor EHB-569 targets low-LET γ-radiation-triggered rel orchestration and potentiates cell death in squamous cell carcinoma. *PLoS One*. 2011;6(12):e29705. doi:10.1371/journal.pone.0029705
62. Gumedag C, Atay S. Integrated analysis identifies CCNA2 as a candidate diagnostic and prognostic biomarker in oral tongue squamous cell carcinoma. *J Appl Oral Sci*. 2026;34:e20250618. doi:10.1590/1678-7765-2025-0618

Dental

and Medical Problems

